PRELIMINARY SUBSYSTEM DESIGNS

for the

ASSURED CREW RETURN VEHICLE

(ACRV)

FINAL REPORT

Vols. I-III

Department of Aerospace Engineering
Pennsylvania State University
University Park, PA

NASA/USRA University Advanced Design Program
1990 Annual Summer Conference
NASA Lewis Research Center
June 11-15, 1990

PENNSTATE

PRELIMINARY SUBSYSTEM DESIGNS

for the

ASSURED CREW RETURN VEHICLE

(ACRV)

Final Report Vol. I

Department of Aerospace Engineering
Pennsylvania State University
University Park, PA

NASA/USRA University Advanced Design Program
1990 Annual Summer Conference
NASA Lewis Research Center
June 11-15, 1990

PENNSTATE

ABSTRACT

This report comprises a series of design studies concerning the Assured Crew Return Vehicle (ACRV) for Space Station *Freedom*. Study topics, developed with the aid of NASA/Johnson Space Center's ACRV Program Office, include: a braking and landing system for the ACRV, ACRV growth options, and the design impacts of the ACRV's role as a medical emergency vehicle.

Four alternate designs are presented for the ACRV braking and landing system. Options presented include: ballistic and lifting body reentries; the use of high-lift, high-payload aerodynamic decelerators, as well as conventional parachutes; landing systems designed for water landings, land landings, or both; and an aerial recovery system. All four design options presented combine some or all of the above attributes, and all meet performance requirements established by the ACRV Program Office.

Two studies of ACRV growth options are also presented. Use of the ACRV or a similarly designed vehicle in several roles for possible future space missions is discussed, along with the required changes to a basic ACRV to allow it to perform these missions optimally. The outcome of these studies is a set of recommendations to the ACRV Program Office describing the vehicle characteristics of the basic ACRV which lend themselves most readily to be adapted for use in other missions.

Finally, the impacts on the design of the ACRV due to its role as a medical emergency vehicle were studied and are presented herein. The use of the ACRV in this manner will impact its shape, internal configuration, and equipment. This study included: the design of a stretcher-like system to transport an ill or injured crew member safely within the ACRV; the compilation of a list of necessary medical equipment and the decisions on where and how to store it; and recommendations about internal and external vehicle characteristics which will ease the transport of the ill or injured crewman and allow for swift and easy ingress/egress of the vehicle.

This report is divided into three volumes. Volume I contains the four braking and landing proposals, volume II contains the two growth options studies, and volume III contains the single medical mission impact study.

INTRODUCTION

Since the beginning of the manned space program, NASA has been dedicated to the design philosophy of assured crew return capability (ACRC). This philosophy has meant that every manned program in NASA's history has had some method of returning the astronauts safely to Earth in the event of a failure of the primary return system. The commitment to ACRC continues in the design of Space Station *Freedom*. The primary return method for the Space Station's crew is the NSTS, but NASA has foreseen the need for a dedicated, space-based return vehicle at *Freedom* to act as a "lifeboat" in at least three circumstances: 1) a catastrophic event occurs on the Space Station, the crew is forced to evacuate immediately, and the Shuttle is not at *Freedom*, 2) there is a medical emergency which exceeds the capability of the Space Station's facilities, and the Shuttle cannot respond in time; and 3) the NSTS is forced to halt flights for any reason, meaning it is not available to resupply or transport the Station's crew. NASA has begun the design of the Assured Crew Return Vehicle (ACRV) to meet these contingencies.

Through USRA's Advanced Design Program, Penn State became associated with the ACRV Program Office at Johnson Space Center in 1989. Prior to the 1989-90 academic year, several ACRV design topics were identified by Penn State faculty and ACRV Program Office personnel. During the past academic year, forty-nine seniors in Penn State's Aerospace Engineering Department were divided into seven project groups and pursued three of these topics: the design of a braking and landing system for the ACRV, the investigation of ACRV growth options, and the investigation of the ACRV's role as a medical emergency vehicle and how this impacts its overall design. This report comprises the seven individual final reports of the project groups

VOLUME I

ACRV BRAKING AND LANDING

For the purposes of this investigation, the braking and landing system of the ACRV was defined as those devices and vehicle characteristics which slow the vehicle upon atmospheric reentry and allow it to land safely on the Earth's surface. This did not necessarily include a propulsion system for a deorbit burn or an attitude control system, but some of the project groups felt it necessary to examine these systems also.

The braking and landing system of a reentry craft provides an interesting design challenge due to the large variety of alternatives available to the designers. It also involves some of the most important design decisions, since this system may impose size, shape, and weight constraints on the vehicle's other systems.

The project groups had certain restrictions imposed on their design by the ACRV System Performance Requirements Document (SPRD). This document, written by the ACRV Program Office, was developed to provide guidelines for the ACRV design, but was intentionally left as vague as possible to allow for the maximum creativity on the part of the designers. Some of the more important requirements are:

1. The fully constructed ACRV must be able to be launched in the Shuttle payload bay.

2. In its role as a medical emergency vehicle, the ACRV system (including recovery forces) must be able to deliver the returning astronauts to a suitable medical care facility on the ground within twenty-four hours of the decision to leave the Space Station. Of this time, no more than six hours may be spent in transit. This allows for up to eighteen hours to be spent on orbit waiting for an appropriate reentry window.

3. Reentry accelerations must be limited to four g's for all crew members. Impact accelerations and total impulses upon landing must be limited to fifteen g's and three g-seconds for healthy crewmembers, and ten g's and two g-seconds for an ill or injured crewmember.

4.   The ACRV must be able to be operated by a deconditioned crew.

5.   To maximize the reliability of the system, proven "off-the-shelf" hardware should be used

whenever possible.

Four of the seven student project groups did preliminary and detailed designs of an ACRV braking

and landing system. The four final project reports for these groups are presented in the following sections.

The Braking and Landing System
for the Assured Crew Return Vehicle

Pennsylvania State University
Aerospace 401B

Group Arbutiski

Group Members: Thomas B. Arbutiski
                  James H. Galasso
                  William J. Mowry
                  Melissa Paoline
                  Christine A. Perry
                  Daniel C. Vergano

Prepared for Dr. Helton and Dr. Thompson

30 April 1990

ABSTRACT

A long term manned facility in space must include provisions for the safety of the crew. The resolution of this need was the design of an Assured Crew Return Vehicle, the ACRV. This report focuses on the braking and landing system of the ACRV. This subsystem of the ACRV was divided into three phases. The Phase I analysis showed that the use of a tether to aid in the reentry of the ACRV was infeasible due to cost and efficiency. Therefore, a standard rocket would be used for reentry. It was also found that the continental United States was an achievable landing site for the ACRV. The Phase II analysis determined the L/D of the vehicle to be 1.8, thus requiring the use of a lifting body for reentry. It was also determined that shuttle tiles would be used for the Thermal Protection System. In addition, a parachute sequence for further deceleration was included, namely a ringslot drogue chute, a pilot chute, and finally a ringsail main parachute. This sequence was found to be capable of slowing the vehicle to a descent velocity of 9-10 m/s, which is the required velocity for aerial recovery. The Phase III analysis proved that a Sikorsky CH-53E helicopter is capable of retrieving the ACRV at 5.5 km altitude with minimal g-forces induced on the ACRV and minimal induced moments on the helicopter upon hookup. The helicopter would be modified such that it could stabilize the ACRV close to the bottom of helicopter and carry it to the nearest designated trauma center.

TABLE OF CONTENTS

LIST OF FIGURES

LIST OF TABLES

ACRONYMS AND NOMENCLATURE

Acronyms:
ACRV - Assured Crew Return Vehicle
CERV - Crew Emergency Return Vehicle
DME - Distance Measuring Equipment
SPRD - Systems Performance Requirements Document
TPS - Thermal Protection System
TRD - Tether Released Deployment
VOR - Very High Frequency Omni-directional Radio

Nomenclature:

C_D Coefficient of drag

C_L Coefficient of lift

D Drag

D_b Drag of vehicle

F_p Parachute opening force

L Lift

m Mass

m_a Apparent mass of parachute

m_b Mass of vehicle

q Dynamic pressure

$V_{(o)}$ Initial velocity

Δ Ballistic parameter

γ Flight path angle

ϕ_{opt} Optimum banking angle

Θ Flight path angle

v

INTRODUCTION

Space Station Freedom (SSF) is one of NASA's latest projects,
with the goal of establishing a permanent manned presence in space.
As with all of NASA's programs, crew safety is of the utmost
importance. To guarantee the safety of SSF's crew, NASA has begun
to search for a vehicle that will return the astronauts to Earth in
the event of an emergency. This vehicle has been given the name:
Assured Crew Return Vehicle (ACRV). The specifications for the
design of the ACRV are given in the Systems Performance Requirements
Document (SPRD).

To begin the analysis of the design, the requirements listed
below were examined to determine which were most important for this
application.

1) Crew training for operating the ACRV would be kept at
   a minimum.

2) The maximum g-loading on the vehicle cannot be greater
   than 4.

3) The time required for the vehicle to reach a health
   facility from SSF must be under 6 hours.

4) Heating of the vehicle must be minimized.

5) To ensure reliability, system components should not
   be excessively complex.

6) The weight of the system should be minimized.

One of the major subsystems of the ACRV is the braking and
landing system, which is the focus of this report. The main
objective of this system is to enable the crew to leave SSF and
reach the ground without violating any specifications listed in the

1

SPRD.

In order to simplify the analysis of the braking and landing system, three definite phases have been defined. They are:

1) Phase I - From SSF departure to a point just beyond maximum heating

2) Phase II - From a point just beyond maximum heating to an altitude of 5.5 km

3) Phase III - From a 5.5 km altitude to a landing on Earth.

Having defined these distinct phases, each phase can be analyzed separately. The results of each phase can then be combined to form a complete design that ~~obeys~~ *satisfies* the limitations and restrictions dictated by the SPRD.

(2.0) Phase I

Phase I in the braking and landing design of the ACRV is
defined as the time from vehicle release from SSF to the 100 km
altitude at reentry. Phase I concepts were examined for three
reasons. They were: assessment of potential landing sites and
lateral range requirements arising from SSF orbital track,
assessment of potential for propellent mass reduction, and analysis
of requirements for beginning reentry conditions to occur.

The analysis of orbital mechanics addressed these concerns as
well as some numerical analysis of certain concepts. It is desired
to identify trends in Phase I operations which could benefit the
braking and landing system design.

(2.1) Mass Reductions in Propellent Use

Two vehicle transfer concepts were examined for Phase I: a
conventional rocket propelled transfer and a tether released
deployment (TRD) along a reentry path. As a baseline approach, a
Hohmann-like transfer from a circular SSF orbit to some lower
altitude (100 km) was contrasted with a tethered deployment from
SSF. The propellent considered was bipropellent N_2O_4-MMH with
an Isp of 300 seconds [Agrawal, 1986]. This propellent was chosen
for two reasons. The first consideration was the reliability of a
hypergolic propellent; the second was the common use of the
propellent. The Hohmann-like transfer was used solely for
analytical purposes; it is not necessarily the best transfer
approach for this application.

The rocket propelled transfer proceeds as follows. After

3

separation from SSF, the ACRV uses a braking burn to set itself onto a transfer orbit with a periapsis at a 100 km altitude. At periapsis, the ACRV performs another braking burn to align itself with the proper flight path angle to begin reentry.

The analysis of the conventional rocket propelled reentry showed that relatively little propellent was used in placing the vehicle on its transfer orbit. The major use of propellent involves the flight path velocity angle change at periapsis.

The TRD proceeds as follows. After separation from SSF, the gravity gradient experienced by the tethered ACRV and SSF system causes the tether to unreel. Due to the higher velocity experienced by the ACRV at a lower altitude it begins to swing ahead of SSF. When sufficient tether has unreeled, the tether is stopped, and the system begins to experience pendulum-like librations. The ACRV is released from the tether at the lowest point of the swing to proceed onto its own transfer orbit which has a periapsis located at 100 km altitude. All of this occurs without the use of any propellent. Like the rocket transfer, a burn is made at this point to align the ACRV along the desired reentry conditions.

The TRD needed to behave satisfactorily in four areas for the purposes of the Phase I braking and landing system. First, it was desirable for the tether not to exceed 150 kg mass, which limited it to approximately 50 km in length. Second, tether deployment time was required to be under one hour or one-third of the allowable flight time of the ACRV [SPRD]. Third, deployment swing should not exceed a 65 degree in-plane swing or the tether would go slack [Tethers in Space Handbook]. Finally, a propellent savings near 10%

4

over the propellent cost of the conventional rocket propelled transfer was desired to offset the mass of a deployer and logistical costs associated with a new technology.

Tether length was found to be approximately 44 km (see Appendix 1), which met one of the criteria. With very minimal damping, libration during deployment reached a maximum of 45 degrees which met the third requirement. The time for deployment to reach 44 km was found to be 45 minutes with 10 additional minutes for the ACRV to swing into the required location. This met the second criteria.

Propellent use was analyzed in a manner similar to the conventional rocket. The conventional rocket was found to arrive at the reentry point with a velocity of 7.932 km/s while the TRD ACRV has a velocity of 7.912 km/s (see Appendix 1). Figure 1 depicts the results of this analysis. There is a definite mass reduction arising from the TRD, which increases as inclination angle is decreased. For the ACRV, this reduction amounts to approximately 4%, which is 240 kg of propellent. The principal reason for this low savings is that the magnitude of the propellent needed for a flight path angle change exceeds the transfer mass by a great deal. This does not meet the criteria for placement into the ACRV braking and landing system. Table 1 summarizes the results of the TRD. A full treatment of the analysis is given in Appendix 1.

(2.2) Reentry Concerns

Since the TRD failed to meet the criteria, it was decided to use a conventional rocket propelled transfer and maneuver of the ACRV into the reentry alignment described in the Phase II section.

5

A propellent mass of about 300 kg of N_2O_4-MMH was found to be needed for the entire maneuver (see Figure 2). This mass represents about 3% of the total mass of the ACRV. Transfer time was a little over 45 minutes (see Appendix 1).

(2.3) Groundtrack Analysis

Due to mission time constraints, it may be necessary for the ACRV to cover considerable distances in its descent to a landing site. From successful *computational* analysis of lifting body reentry characteristics in Phase II ~~by a computer program~~, it is possible to estimate a maximum vehicle range in all directions ~~using~~ *by* integrat~~ion~~ *ing* of *the* equations for lateral range [Hankey, p.28].

Since NASA has stated that the ACRV can remain at SSF up to eighteen hours from the time of an emergency, the space station will have passed over approximately 75% of its orbital corridor (see Figure 2). In the worst case, 12.5% of the uncovered area would fall in the region of the United States where the landing site is anticipated to be located. Therefore, a worst case footprint centered at the landing site and stretching 15 degrees south *in latitude* and 45 degrees east and west ~~latitude~~ *longitude*, respectively, was investigated. Orbital maneuvers by an ACRV occurring early in the 18 hour time limit are not considered, in order to conserve propellent.

(2.4) Summary of Phase I

In general, it was necessary to examine the Phase I impact on the ACRV braking and landing system in order to look for required

6

vehicle abilities and potential area for mass reductions. No attempt was made to perform an analysis of the likely inclination change at SSF separation or propellent requirements needed for a second deorbit opportunity. These problems were deemed to be beyond the scope of this analysis. It was found that the conditions in Phase I matched very well with the requirements for Phase II with regard to entry velocity, inclination angle, and propellent use.

(3.0) Phase II

For the analysis of Phase II, the deceleration of the vehicle will be studied in two stages, the upper stage and the lower stage. The upper stage encompasses deceleration during initial reentry to a point beyond maximum heating. The lower stage includes deceleration during the remaining flight.

(3.1) Upper Stage Deceleration

To decelerate the vehicle during reentry, it was decided to modify the L/D for a lifting body trajectory. An analysis of the reentry of a vehicle was achieved using a computer code developed to model the entry of a vehicle into the atmosphere from 100 km. To accomplish this, the equations of motion of a vehicle in two dimensions were integrated using a fourth-order Runge-Kutta method (see Appendix 2). From this simulation, the effects of varying the following parameters were studied:

1) The initial velocity at 100 km

2) The initial flight path angle

3) The ballistic parameter

4) The lift to drag ratio.

After varying each parameter, with the others held constant, an optimal trajectory for the ACRV was achieved. To determine this optimal trajectory, the problems facing a vehicle reentering the atmosphere were examined.

When designing the braking and landing system of an ACRV, the problems of g-loading on the crew and the heating at the stagnation point on the vehicle were given primary concern. The maximum

8

g-loading was limited to 4 g's, a specification made in the SPRD [p. 21]. As specified, the limit of decelerations are: 4 g's in the x-direction, 1 g in the y-direction, and 0.5 g's in the z-direction. These directions are shown in Figure 3 with reference to the orientation of a crew member. With these limits placed on the g-loadings of the vehicle, some limits on the heating of the vehicle were determined.

(3.2) Thermal Protection Systems

Initially in the design of this vehicle, two types of thermal protection systems (TPS) were considered. First, the use of an ablation shield was examined. This type of shield protects the vehicle by slowly disintegrating and dissipating much of the energy that would normally increase the temperature of the vehicle. The ablation shield has been proven effective in the Mercury, Gemini, and Apollo programs and was considered at the onset of this project.

The second type of TPS was the tile used on the space shuttle. These tiles, known as Orbiter LI-2200 tiles, have a maximum temperature limit of about 1,925 degrees Kelvin and can be used only once [NASA Conceptual Design of a CERV, 1989]. A maximum convective heating was set using Stefan's Law to convert the temperature to a convective heat rate. By calculating the heat rate in the program, the use of tiles could be proven feasible if the convective heating was low enough. The maximum convective heating on the vehicle would have to be less than 620,000 Watts/meter at the stagnation point. This would permit the use of the single-use tiles. The temperature at the other points was assumed to be less than that at the

9

stagnation point.

(3.3) Additional Concerns

Further study of the heating on the vehicle can be done once a shape is established. With the heating and deceleration problems identified, other concerns for the ACRV during reentry were addressed. Problems that were forseen in Phase II were:

1) The final velocity at the end of Phase II

2) The maximum lateral and longitudinal range of the ACRV

3) The amount of time required for reentry.

The first problem listed above was of major concern due to a need for a deceleration system to be deployed at an altitude of 10 km. This altitude of 10 km would allow the vehicle to slow down enough for aerial recovery at a 5.5 km altitude. In order to decrease the extent of the deployment system, the Mach number at 10 km should be as low as possible.

The second problem facing the ACRV would be its range. From the analysis of the ground track of SSF in Phase I, the ACRV would need to either burn fuel for a flight path angle change in its orbit or use its lifting characteristics to execute a banking turn to increase its lateral glide distance. Establishing a sufficient lateral range is vital if a landing site in the continental United States is desired. Therefore, since as little propellent as necessary should be carried by the ACRV, the L/D of the ACRV should provide enough range to reach the United States mainland. With the range of the vehicle being directly related to its L/D, more consideration was given to using a lifting body for the ACRV.

The last problem in the ACRV design for Phase II was that of time. In the SPRD, specifications define the maximum amount of time allowable for various missions. The worst case, the medical mission, limits the time from deorbit to landing at a trauma center to 6 hours. From the analysis of Phase I, a Hohmann transfer from SSF to an altitude of 100 km requires 45 minutes. By limiting the reentry from deorbit to arrival at the health facility to approximately 1 hour, about 4 hours will be left for recovery and transport of the ACRV and its crew. Thus, the time required for the vehicle to pass through Phase II should be about 1 hour.

Summarizing the three problems, five objectives were set for Phase II:

1) Limit the g-loading to 4 g's in the x-direction

2) Minimize the convective heating rate

3) Slow the ACRV to a subsonic velocity before the 10 km altitude

4) Maximize the lateral and longitudinal range of the vehicle

5) Allow the vehicle approximately 1 hour to reenter.

By using the above five criteria to analyze the trajectory of an ACRV, some characteristics of an ACRV could be determined; these include:

1) The L/D of the vehicle

2) The ballistic parameter of the vehicle

3) The minimum radius of the vehicle at its stagnation point.

Finally, the computer simulation was repeatedly run to find the appropriate characteristics.

To conduct this study, each of the four parameters: initial velocity, initial flight path angle, ballistic parameter, and L/D

11

were varied while the others were held constant. The default values
of the variables which were held constant were defined in a baseline
configuration:

V(o), initial velocity, 6.5 km/s

γ(o), initial flight path angle, -1.0 degrees

Δ, ballistic parameter, 370.0

C_L, lift coefficient, 0.6.

With the baseline configuration set, each parameter was varied to
measure its effect on achieving each of the five objectives. The
range of the variations of the parameters was kept to what was
characteristic of reentry vehicles that are obtainable at the
present time. The range of each of the parameters is listed below:

V(o) from 5.0 km/s to 10 km/s at 0.5 km/s steps

γ(o) from -5 degrees to 5 degrees at 0.1 degree steps

Δ from 135 kg/m^2 to 1481 kg/m^2 at 14.8 kg/m^2 steps

C_L from 0.1 to 0.8 in steps of 0.1

From this analysis, the results that show a highly measurable effect
on the vehicle's performance are plotted in Figures 4 through 16 and
listed in Tables 2 through 5. After close examination, the
appropriate range for each parameter was chosen.

The effects of changing the deorbit velocity are shown in Table
2. The reentry velocity effects on g-loading (Figure 4), Mach
number (Figure 5), vehicle range (Figure 6), and deorbit time
(Figure 7) were analyzed by the previously mentioned numerical
integration of the trajectory equations. The results indicated that
a deorbit velocity between 7.5 km/s to 8.0 km/s was sufficient to
fulfill all the study objectives.

12

With the range of velocities found by the study above, an analysis was done to determine the velocity the ACRV would naturally have as it reached deorbit. A Hohmann transfer was used from SSF to an altitude of 100 km. The velocity at perigee of the transfer was found to be approximately 7.9 km/s. Since the desired range was from 7.5 km/s to 8.0 km/s and the velocity at the end of the Hohmann transfer was 7.9 km/s, the velocity range for the ACRV to reenter the atmosphere was set from 7.8 km/s to 8.0 km/s. This allows for an uncertainty of ±0.1 km/s in the deorbit velocity.

Because the range of deorbit velocities has been determined, optimum values of the flight path angle can be calculated. The results are shown in Table 3. Only the maximum g-loading and the convective heating rate seem to be significantly affected by the variation. As seen in Figure 8, the maximum g-loading reaches a minimum when the deorbit flight path angle is close to zero degrees with the same result occuring for the convective heating rate. Therefore a flight path angle close to zero degrees is desired to minimize the g-loading and the heating. The range determined for the ACRV was set at -0.5 degrees to 0.5 degrees.

When designing a reentry vehicle, the ballistic parameter plays a major role in its performance. The effects of varying the ballistic parameter are presented in Table 4. For all the ballistic parameters, except for the highest one, the Mach numbers are subsonic at a 10 km altitude. Thus, the Mach number data was not plotted because it seemed insignificant, except when the ballistic parameter is 1,481 kg/m^2.

Maximum g-loading seems to be a strong function of the

13

ballistic parameter as depicted in Figure 10. In order for the g-loading to be less than 4.0, ballistic parameters greater than or equal to 83 kg/m^2 are desired. This limit, however, was just a first approximation. The convective heat rate is shown in Figure 11 to increase as the ballistic parameter increases. Therefore, a high ballistic parameter could cause a high heating rate. The effect of the ballistic parameter on the range of the ACRV is presented in Figure 12. This range is important if the vehicle needs to glide a large distance during reentry. The reentry time is found to increase almost proportionally to the ballistic parameter (Figure 11). From these results, a moderate ballistic parameter in the range of 200 to 600 kg/m^2 is desired.

The final parameter, the C_L of the vehicle, was varied to allow for an L/D of 0.25 to 3.0. The results of this part of the study are shown in Table 5. Three significant trends were observed. First, in Figure 14, the maximum g-loading is shown to greatly increase for L/D's lower than approximately 0.75, which eliminates a ballistic trajectory. In Figure 15, the heating approachs a minimum when the L/D was greater than or equal to one. The range appears to be directly proportional to the L/D of the reentry vehicle, as seen in Figure 16. By examining the results of this data, an L/D in the range of 1.0 to 3.0 appears feasible.

With this range of L/D selected, research was initiated to determine the appropriate values of the L/D. For high L/D lifting bodies, the C_D can reach a maximum of about 0.4, and the C_L can reach a maximum of about 1.0. Using these limits, the simulation developed was used to achieve the five objectives stated

14

previously. When repeated simulations were conducted, the results of the previous analyses were validated for the C_D and C_L limits. At this point in the design, the vehicle was determined to have an L/D greater than 1.0.

Because this indicated that the ACRV should be a lifting body, an ablation shield for the ACRV was ruled out due to the instabilities that an ablation shield would create. In using this thermal protection system, the shield ablates and causes particles to be released into the flow around the vehicle. This affects the Reynold's number of the vehicle and will result in the shifting of the transition points. Because of this, the use of an ablation shield was rejected. Since this type of TPS was not acceptable, it was determined that shuttle tiles would be used.

Shuttle tiles have several advantages. These advantages include availability, utility, and the prevention of instabilities caused by an ablation shield. Thus, shuttle tiles were selected for use in the design.

Due to the use of the tiles, an additional requirement was that the maximum convective heating rate should be 620,000 Watt/m^2. With this limit defined, the computer simulation was repeated to find the optimal L/D of the vehicle. In all the simulations run, the stagnation point radius was set at 0.5 meters. It was observed that heating became the most important problem.

Table 6 shows the performance of a reentry vehicle with a C_D=0.4, a flight path angle of -0.5 degrees, and a ballistic parameter of 370 kg/m^2. Varying the C_L and the initial velocity allowed determination of an appropriate L/D and a range of initial

15

velocities for the vehicle.

From the results presented in Table 6, the major concern was found to be the heating of the vehicle. When the L/D of the vehicle increases, the maximum heating decreases. While this indicated a good reason to make the L/D as high as possible, raising the L/D results in a longer reentry time. Therefore, the L/D of the vehicle could be increased, but the time for reentry had to be watched closely.

From the preliminary design done for the ACRV, the required time for reentry was set to approximately 1 hour. An analysis was done on the time needed for a Hohmann transfer from SSF's orbit to an altitude of 100 km; this period was found to be about 45 minutes. Because the time for the Hohmann transfer was shorter than originally thought, the time required for reentry was allowed to be a maximum of 2.5 hours for the simulation. With this increase in the reentry time allowed, higher L/D's for the vehicle can be used. By examining the results in Table 6, an L/D of 2.0 will allow the vehicle to reenter safely with respect to heating for a deorbit velocity between 7.8 km/s and 8.1 km/s. The only drawback to using this L/D is that the reentry time begins to exceed 2.5 hours. Because of this, an L/D for the vehicle was chosen to be 1.8. A compromise for the value of L/D was made between the range of reentry velocities allowable and the time required for reentry.

The L/D of 1.8 would allow the vehicle to reenter over a range of deorbit velocities and still allow for the use of shuttle tiles. From the results in Table 6, the velocity range can be between 7.85 km/s and 8.1 km/s. The time required for reentry for this velocity

16

range is between 1.16 and 2.32 hours. While the time does begin to get large, an optimum trajectory for the deorbit velocity would be 7.9 km/s. This design allows for an uncertainty in the deorbit velocity and flight path angle. The envelope for an ACRV with $C_D=0.4$, $C_L=0.72$, a ballistic parameter of 370 kg/m², and a minimum nose radius of 0.5 m would be:

Deorbit velocity: 7.85 km/s $\leq$ V(o) $\leq$ 8.10 km/s

Flight path angle: -0.5 degrees $\leq$ γ(o) $\leq$ 0.5 degrees.

By using this design, the performance of the vehicle would be as follows:

1) Maximum g-loading less than 1.28

2) Maximum convective heating rate less than 620,000 kg/m²

3) Mach number at 10 km altitude less than 0.5

4) Range of the vehicle greater than 20,000 km

5) Time needed for reentry less than 2.4 hours.

Since this performance meets the criteria for an ACRV, the characteristics stated before were used for the final design of the vehicle.

With an L/D of 1.8, the ACRV would have an added bonus of a greater lateral range. To determine the lateral range, the equation derived by Hankey was used with Δy being the lateral range:

$$\Delta y_{max} = \frac{(L/D)^2 \, V_c}{g \cdot \cot \phi_{opt}}$$

The optimum banking angle can be found by using:

$$\cot \phi_{opt} = 5.2 \sqrt{1 + 0.106 \, (L/D)^2}$$

Using an L/D of 1.8 and a bank angle of 40 degrees, the lateral range of the vehicle was found to be about 3,355 km. When this distance is translated into latitude, it allows the vehicle to reach

17

an additional 30 degrees of latitude. This range becomes useful for the groundtrack of SSF. Because the highest latitude of the groundtrack is 28 degrees, a maximum latitude for an ACRV with an L/D of 1.8 would be about 60 degrees. This allows for most of the continental United States to be covered. Due to the lateral range of this vehicle and its performance, the design of the ACRV will allow the vehicle to be slowed by its own aerodynamic characteristics.

(3.4) Lower Stage Deceleration

For the lower stage of Phase II, it has been determined that:

1) An L/D of approximately 1.8 will be used

2) A lifting body trajectory will be used

3) The deceleration device deployment Mach number will be 0.5. Because it was found that a lifting body trajectory will be used and a subsonic Mach number would be achieved, several deceleration devices initially considered for the lower stage of Phase II were eliminated. Such devices include ballutes, Hemisflo, and Hyperflo parachutes (see Table 7).

Upon further analysis, the following sequence of events has been adopted. At a 10 km altitude, a ringslot parachute could be deployed as a drogue, if necessary. The function of the drogue chute is to initially slow the vehicle, stabilize it, and provide attitude control. This parachute would be ejected by means of a mortar ejection system. It is this type of system that is frequently used when extraction by a pilot chute device is not feasible [Recovery Systems Design Manual, 1978].

18

The second parachute, a pilot chute, would be used to extract the main parachute. A pilot parachute may be a conventional ringslot, of the ribbon and ribless guide surface types, or a specialized design with ribs and vanes to ensure good opening reliability [Recovery Systems Design Manual, 1978]. The factors which affect the pilot chute's stability include the distance from the main parachute and the chute size and type. These factors for this design have yet to be determined. The pilot chute would extract the main parachute, a ringsail parachute.

The ringsail parachute is required to have a total surface area of 2,410 m² to ensure a descent velocity of 9 to 10 m/s at a 5.5 km altitude, which is the required descent velocity for the planned aerial recovery. The use of a ringsail parachute is advantageous due to its past performance in the Apollo missions and because it is easily modified with vanes, reefing, and porosity. A search for modified designs of these parachutes has not been performed, but it will be necessary to modify the ringsail parachute with vanes to create a forward velocity, thereby simplifying the aerial recovery. For our analysis, though, these parachutes are assumed to be unreefed with little porosity. This is because porosity causes a reduction in the drag coefficient of the parachute, and reefing ensures better stability of the parachute. In addition, the main parachute should be connected to the vehicle at three points, not only for stability but also for support during aerial recovery.

Determination of the parachute opening forces was attempted after a preliminary analysis of system terminal velocities (see Appendix 3), and estimation of the required parachute sizes was

performed (see Table 8). When solved using a numerical method, such as Runge-Kutta, the following equations would generate the opening forces, velocity, deceleration, filling time, and altitude [AIAA Aerodynamic Deceleration Systems Conference, 1970].

$$\text{Parachute Force:} \quad F_p = C_D Sq + V\dot{m}_a + (m_a + m_p)\dot{V} + W_p \sin\Theta$$

$$\text{Change in Altitude:} \quad \dot{z} = V\sin\Theta$$

$$\text{Acceleration:} \quad \dot{V} = -(F_p + D_b + W_b \sin\Theta)/m_b$$

$$\text{Change in Flight Path Angle:} \quad \dot{\Theta} = -(g\cos\Theta)/V$$

By including parachute characteristics into the program, such as surface area, drag coefficient, filling time, and system weight, the particular system could be checked for feasibility. Results would provide analytical verification of preliminary estimations of filling time, deceleration, and operational altitude.

(3.5) Summary of Phase II

In summary, the performance of an ACRV designed with the characteristics of: an L/D=1.8, a ballistic parameter of 370 kg/m^2, and a nose radius greater than or equal to 0.5 m will meet the performance criteria set for the ACRV. The performance of an ACRV with an L/D=1.8 has been found to:

1) Limit the maximum g's to 1.5

2) Limit the maximum convective heat rate to less than 620,000 W/m^2

3) Obtain a Mach number of 0.5 at an altitude of 10 km

4) Have a lateral range large enough to reach a large part of the continental United States

5) Allow the vehicle to reach the surface of the Earth from SSF in less than ~~about~~ 3.0 hours.

Since these attributes surpass the criteria set earlier, this ACRV design will allow the vehicle to slow via aerodynamic effects as a consequence of the shape. Because this design also uses shuttle tiles, an existing technology, the protection of the vehicle from high temperatures is assumed. A lifting body with the characteristics listed above should be found and utilized ~~since~~ because it meets the requirements of the SPRD and allows for the use of an existing thermal protection system. If this is done, the evidence presented here would allow for most of the braking to be done by the vehicle itself and require no other deceleration system except in preparation for aerial recovery.

The preparation for aerial recovery involves using a system of parachutes deployed from the top of the vehicle. In order of deployment they are: a ringsail drogue chute, a pilot chute, and a ringsail main parachute. This would slow the ACRV to approximately 10 m/s, which is the preferred velocity for the aerial recovery.

21

(4.0) Phase III

The final area of investigation is the recovery and transportation of the ACRV to a trauma center. The ACRV has gone through the deceleration phase and its descent rate has been reduced to approximately 10 m/s at an altitude of 5,500 m. In approximately 8.5 minutes the ACRV will land either on land or water. This section will evaluate the landing/recovery possibilities and explain the analysis for the chosen recovery system.

(4.1) Ground Landing

A ground landing has many positive attributes, but as with any design, there are negative tradeoffs. Ground landing ideas were evaluated to compare positive and negative attributes.

One of the first ideas evaluated was the possibility of an SSF crew member acting as a pilot in order to control the ACRV for a ground landing. This idea was eliminated due to the requirement in the SPRD stating that the crew must be minimally trained [SPRD, p.39].

The next idea includes the use of onboard and ground control flight systems as used in the first ground landing of the U.S.S.R. Space Shuttle, Buran. This plan was eliminated due to the high cost of onboard equipment and the large number of personnel necessary to accomplish this mission.

Positive attributes to a ground landing include ability to select a landing site that would be close to a trauma center and ease of recovery in comparison with a water landing. These attributes were considered important factors and would be integrated

22

into the final recovery design as were some of the positive

attributes of a water landing.

(4.2) Water Landing

In general, the complexity of a water landing is much less than

that of a ground landing. Water landings have been successfully

performed in the past. While targeting a landing zone remains a

problem, terrain will not be a concern, therefore minimal flight

control systems are needed.

Disadvantages of a water landing are weather conditions and the

recovery operations, which need naval support. In the 1960's as

many as 20 naval destroyers and one aircraft carrier were involved

in recovery operations [NASA Manned Spaceflight Center, 1962].

Terrain may not be a concern, but bad weather conditions at sea will

be a major concern. Reentry will be dependent on avoiding harsh

weather conditions if an effective water landing is to be

considered. Since weather conditions play an important role in

recovery operation effectiveness, all naval and recovery vehicles

have to be reliable in all weather conditions.

The best attribute of a water landing is the safety of the ACRV

and its crew. This positive aspect of a water landing was

integrated into the final design/recovery system, which consists of

both the positive attributes of a ground and water landing. The

recovery will take place over water, but the ACRV will not normally

land in the water. As aerial recovery system has been designed that

will catch the ACRV and carry it to a trauma center. This is the

recovery system that is the simplest, safest, and most cost

23

~~efficient~~. *effective*

(4.3) Aerial Recovery

The idea for this recovery system came from similar missions in the 1960's that involved Lockheed C-130H's with Fulton Star Recovery Equipment (see Figure 17). For this system, each JHC-130H was equipped with two 4.42 meter tines, hinged forward to form a V-shaped fork on the nose of each aircraft. The object to be recovered was attached to a 152.4 meter line which was connected to a Helium balloon. The JHC-130H would snag the recovery line in flight with the nose fork, and the cable was hooked and placed into a winch. The recovered object could then be loaded into the aircraft through the rear door.

Some problems existed with this system that made it inappropriate for the recovery of the ACRV. The slowest recovery speed for the JHC-130H is 62.6 m/s [Marshall, 1988]. Recovery of the ACRV would have to be at high speeds, and a system would have to be designed to stabilize the ACRV against a spin rate of less than 5 rotations per minute while being winched into the rear of the aircraft. The limitation of 5 rotations per minute is a requirement listed in the SPRD. Another problem is that the clear cargo volume of the JHC-130H is 12.2x3x2.7 meters. If the ACRV is wider than the dimensions of the cargo hold, a system would have to be designed to stabilize the ACRV outside the aircraft. The problem that terminated the possibility of the Fulton Star Recovery System was the weight limitations. The average weight of the ACRV is between 5,443 kg and 6,804 kg. The maximum allowable weight for the

24

internal payload of the Fulton Star Recovery System in the JHC-130H is 227.27 kg. Thus, the Fulton Star Recovery System was rejected for the aerial recovery.

Though the JHC-130H is incapable of carrying the ACRV after retrieving it, there is at least one aircraft that is able to carry the ACRV. This aircraft is the Sikorsky CH-53E Super Stallion Helicopter.

(4.4) Chosen Aerial Retrieval Aircraft

An aircraft was required that had the capabilities of being used in all weather conditions and that had the power to catch and carry a 6804 kg payload. The Sikorsky CH-53E Super Stallion Helicopter is a heavy-duty, multi-role, search and rescue/transport helicopter that has many advantages that make it the perfect aerial recovery vehicle for the ACRV (see Figure 18). More information on the CH-53E is supplied in Appendix 4.

Possibly one of the most important features of the CH-53E is that it has a mid-air refueling capability. Not only will the helicopter be able to remain in the air for extended periods of time (up to 2076 km unrefuelled), but the pilots will also be trained for mid-air refueling. The pilots of the CH-53E's must become proficient at this activity. So, if a catching device were designed and placed in the area of the refuelling prod, the pilot could maneuver the helicopter such that it could catch a trailing chute on the ACRV and retrieve the ACRV. To design such a system it is required to be able to predict the behavior of the helicopter when it catches the ACRV.

(4.5) Stability and Control

Information was obtained from Sikorsky Aircraft that permitted
a stability and control analysis to be performed (see Appendix B).
The worst loading and moment condition would be after the aerial
retrieval was completed and the helicopter has increased power to
decelerate the ACRV's vertical descent and forward velocity. The
descent rate from the Phase II design is 10 m/s.

Two programs were written to calculate the forces the
helicopter would experience during deceleration. The first program
assumed the cable attached to the ACRV was directly underneath the
center of gravity of the helicopter. The ACRV was assumed to be
6000 kg. The helicopter's center of gravity was assumed to be at
the 164 water line, and the helicopter could remain parallel to the
ground (see Figure 19 and Table 10). The results of this program
are presented in Figures 27 through 30. When the helicopter retards
the motion of the ACRV, the cable will swing forward. The distance
is travels forward is shown in Figure 27. Figure 28 demonstrates
how the tension in the cable increases as the helicopter
decelerates. Induced moments about the center of gravity produced
as the load swings forward (during deceleration) or aft (during
acceleration) are shown in Figure 29 and 30. These figures were
compared to the maximum nose down moment the helicopter can
control. The maximum nose down moment calculated is 172,180 N-m.
The helicopter would be able to decelerate at approximately 10.5
m/s^2 without losing control (see Figure 29). This corresponds to
an angle of approximately 46 degrees (see Figure 30).

The program described above simulated a load directly under the

26

center of gravity. As the helicopter is flying, the center of
gravity moves due to fuel expenditure. The second program
calculates the induced moments as the load is moved along the
horizontal axis away from the center of gravity (see Appendix 5).
These results can be seen in Figure 31. This program also assumes
the flight to be horizontal at all times. Figure 31 is a
performance chart used to determine the maximum required power for
retarding the ACRV's motion. If the helicopter is using power to
control the induced moment, then it is power lost for lifting
abilities. Therefore, if the pilot can pitch the aircraft as the
load swings forward, then the power required to control the induced
moment will be minimized. The minimization of the moment control is
dependent upon the deceleration and location of the load with
respect to the center of gravity. As the pilot pitches the
helicopter, the controls of the helicopter will provide the pilot
with a sense of the effect of the load of the ACRV on the
helicopter.

The recovery zone will be limited to 5,455.92 meters. The
service ceiling for the helicopter is 5,638.8 meters, and the rate
of climb for the CH-53E is approximately 30.5 m/s. A "no-go zone"
has been determined at which the pilot will not attempt an aerial
recovery (see Figure 22); this altitude has been established at
335.3 meters. From Figure 29, the helicopter could decelerate up to
10.5 m/s^2 with no factor of safety. Using the constant
acceleration equation:

$$V_r^2 = V_o^2 + 2a(\triangle y)$$

yields a stopping distance of 58.73 meters, which provides a

comfortable margin of safety. Multiplying by a factor of safety of
3.0 gives a stopping distance of 183 meters. This distance was then
added to a 152.4 meter safety zone measured from sea level.

An important note at this stage is that the helicopter is
capable of accelerating 10.24 m/s² with a gross estimated weight
of 68,000 lbs, which includes the ACRV weight. This acceleration
(or deceleration for downward flight) is less than the maximum
allowable deceleration to maintain helicopter moment control (see
Figure 29). This means that the helicopter does not have enough
power available to lose induced moment control with a load
connection of ±1.22 meters from the horizontal center of gravity
location. It does have the power to retard the vertical descent
short of 61 meters. If the pilot is unable to connect by an
altitude of 335.3 meters, then the pilot will follow the ACRV down
to a water landing and then hookup to the ACRV and transport it to
the nearest trauma center.

(4.6) Aerial Recovery

The next area investigated was the aerial connection. A system
had to be designed that would not induce any unnecessary moments on
the helicopter. The simplest design was a hook and cable system.

A Kevlar cable would be attached to the ACRV in three
locations, one forward and two aft, for in-flight stability. The
cables would splice together and climb up through the main parachute
to the pilot chute. At the pilot chute, the cable would circle the
circumference of the chute, and attach to itself very similar to a
lasso. This would enable any device to catch the pilot chute, and

28

if a force was applied, the pilot chute would close itself and the cable around the device.

At first, the hook device was placed underneath the helicopter, but the pilot could not see the hookup, and the downwash from the main rotor blades could adversely effect the pilot chute and hookup. An idea was developed that would put the hooking device away from the downwash of the main rotor blades and also in the visual vision range of the pilot. By placing the hooking device at the end of the fueling probe, it would satisfy these conditions. The refueling probe can withstand a 454 kg load at the tip, so a hook-cable system could be attached just behind the refueling probe tip, with a 45.4 kg breakaway string (see Figure 21). The CH-53E will be able to refuel during flight since the hook-cable system would be attached behind the refueling probe tip. When the hook catches the pilot chute, the pilot can retard the motion of the helicopter enough to allow the string to break, and the hook and cable will fall away from the helicopter. The ACRV will then be connected to the helicopter by the Kevlar cable.

At this stage the hookup forces are negligible. The helicopter will have matched the descent rate of the ACRV at 10.4 m/s and will have a slight forward velocity compared to the forward drift of the ACRV parachute system. Figure 23 shows how the helicopter could hookup to the ACRV. The angle the cable makes with the vertical will not be as great as in the fifth position of Figure 23. Both the helicopter and the ACRV are descending at 10.4 m/s. The loads will gradually increase as the pilot increases power to retard the motion, as discussed earlier.

29

(4.7) Flight Stability

The next step will be to arrest the verical descent and hover the helicopter. This will be done to winch the ACRV closer to the helicopter for flight stability. It would be difficult to stabilize the ACRV during flight if it was permitted to hang below the helicopter while supported only by the cable. To eliminate this, the four CH-53E's will be equipped with winches to raise the ACRV close to the bottom of the helicopter. After the ACRV is winched under the helicopter, three pressure jacks will be extended to the ACRV from the helicopter bottom. They will apply reverse pressure against the tension of the cable and stabilize the ACRV for flight (see Figures 24 and 25).

Only four helicopters are considered necessary for this mission. The helicopters will all have Very High Frequency Omni-directional Radio (VOR) receivers that will track the ACRV by using a VOR emitter located in the ACRV. They will also be equipped with Distance Measuring Equipment (DME) which will allow each helicopter to locate the exact position of the ACRV. They will also be equipped with g-meters to monitor the deceleration rates during hookup. With this equipment and the help of ground tracking stations and a USAF E-3 Sentry or Navy E-2 Hawkeye (see Appendix 6), the helicopters could be waiting for the ACRV. The helicopters will form a diamond pattern in the direction of the ACRV's flight. A helicopter will be on the right side, and one on the left side of the entry direction, one will be forward of the entry window, and one will be short of the entry window, all of which are at an altitude of 5,500 meters. This will enable the four helicopters to

30

cover the entrance zone for quick recovery.

The only people specially trained for this mission are the helicopter crews. Extensive additional training will not be necessary because they will already be active search/rescue crews. The crews of the ground tracking and the military AWACS are professionally trained. Thus, the aerial recovery system will not require highly specialized equipment or extraordinary technological developments.

When not in use, the helicopters could be used as modified search/rescue helicopters until they are needed for the aerial recovery. Furthermore, the helicopters can fit into Air Force C-5's for quick transport anywhere in the country. Special crews can be reserved and rotated throughout the years to remain proficient at the task of aerial recovery.

(4.8) Aerial Scenario

The following is a scenario to show the simplicity of this design. An emergency takes place on SSF and eight people must be evacuated. The possible landing zone is the Gulf of Mexico, and the reentry window is eight hours away. Crews are flown in to Hurlbert AFB, Florida, a USAF E-3 Sentry from Randolph AFB is detailed for air control, and a KC-135 refueling plane is detailed from Pensacola Naval Air Station. The four CH-53E's are stationed at Hurlbert AFB, Florida. Both Johnson Space Center and Kennedy Space Center ground tracking crews are put on full watch. The KC-135 and E-3 form into a holding pattern at 10,000 meters in the Gulf of Mexico and in the general vicinity of reentry for the ACRV at 5,500 meters. The four

helicopters refuel and receive word from Johnson Space Center that due to strong tailwinds, the ACRV will be 161 km downrange of the first estimated reentry window. The helicopters go to the area and wait in the diamond pattern. The E-3 spots the ACRV on radar at 10,000 meters and provides coordinate information to the helicopter pilots. The forward diamond helicopter establishes visual contact at 5,300 meters and attempts the hookup. Hookup is established and vertical descent is retarded in 61 vertical meters from the location of the hookup. The ACRV is winched up to the helicopter and is braced by the pressure jacks. The pilot goes to maximum power for maximum duration of velocity to Panama City Trauma Center, Florida. The trauma center was previously alerted, and the technical personnel are on hand for extraction of ACRV crew members. The helicopter hovers over the trauma center helipad and lowers the ACRV to the pad. The ACRV is detached and the crew is extracted.

At this point the ACRV is retrieved from the trauma center's helipad and returned to a designated location.

(4.9) Summary of Phase III

The analysis of the data received from Sikorsky Aircraft Company shows that the aerial recovery system using a modified Sikorsky CH-53E could easily catch the ACRV during its descent and transport it to a trauma center. The success of its mission is completely dependent on the tracking accuracy of ground and air units. The ACRV will not be within the flight envelope of the helicopter for very long, and it is essential to be as close as possible to the ACRV at 5,500 meters, which is 305 meters below the

32

CH-53E's service ceiling. Parachutes could be designed for slower descent rates, but proximity of the helicopters to the ACRV at 5,300 meters altitude will prove to be the most important factor in the aerial recovery system.

(5.0) CONCLUSIONS

The final design of the ACRV's braking and landing system has achieved the goals set for it. In Phase I a simple analysis of the ground track established a criterion for which the ACRV would have a sufficient lateral range to reach landing sites within the continental United States. In addition, a comparison between a tether released deployment and conventional rockets for reentry proved the latter to be more efficient. It was determined that 300 kg of the propellent N_2O_4-MMH would be needed for the reentry of a 6,000 kg vehicle.

The Phase II analysis yielded a preferred L/D determination of 1.8, thus assuring the utilization of a lifting body trajectory. In addition, the deceleration device deployment Mach number of 0.5 was achieved at an altitude of 10 km. At this altitude, a ringslot drogue, a pilot, and a ringsail main parachute would be deployed in that order thereby sufficiently decreasing the descent velocity of the vehicle to 9-10 m/s at an altitude of 5.5 km.

In Phase III, the aerial recovery will be performed with a modified Sikorsky CH-53E Super Stallion helicopter such that a hooking device will catch the trailing parachute on the ACRV, to which a Kevlar cable is connected. A winch will raise the ACRV by the Kevlar cable to the underside of the helicopter. At that time, pressure jacks will be extended from the base of the helicopter to the ACRV. The jacks will apply a slight force to the ACRV which will serve to stabilize the ACRV in a fixed location below the helicopter. The CH-53E will then transport the ACRV directly to a trauma center. By using this design, the ACRV will meet all the

requirement listed in the SPRD.

FUTURE CONSIDERATIONS

For Phase II, several considerations still need to be addressed. The mortar ejection system was chosen because of its proven record. There are other ejection devices that may prove to be more effective, such as a drogue deployment gun, a tractor rocket, or a telescoping catapult gun.

Another consideration involves choosing an exact pilot chute design which includes the vanes, the distance between the pilot chute and the main chute, and the chute size and type. Also, the modification of the main parachute to include reefing and porosity could be investigated. The characteristics of parachute materials such as nylon, rayon, polyester, fabrics, and Kevlar should be analyzed. In addition, determination of the exact location of the points of connection between the vehicle and the main parachute should be calculated.

For Phase III, there are also areas that should be investigated further. The only aircraft examined for this mission was the Sikorsky CH-53E Super Stallion. It is the most powerful helicopter adapted for search/rescue missions. Another aircraft may be more practical and efficient. The Bell/Boeing Vertol V-22 Osprey (see Figure 26) may be able to handle the forces and moments induced upon hookup. The V-22 could then tilt its rotors forward for additional speed to the trauma center. A modified Fulton Star Recovery System may also be developed that would enable modern jets to recover the ACRV.

The hook and breakaway cable could be further studied. The cable may need to have a breaking strenth greater than 100 lbs, or

36

the design of a release mechanism may be required.

The winch will also have to be further evaluated. A winch may be found that can winch the ACRV up while the helicopter is still in forward flight. This will reduce the forces on the helicopter and helps reduce the flight time to the trauma center.

Another area of investigation is the backup system for the aerial recovery. If the aerial recovery is not successful, or if something goes awry, an abort system should be available for use. The helicopter would then retrieve the ACRV from the water.

(7.0) ACKNOWLEDGMENTS

We would like to thank the following people for their assistance with the material in the report. Without their help this report would not have been possible. From Pennsylvania State University: Dr. Robert Melton, Dr. Roger Thompson, Dr. Barnes McCormick, Dr. Mark Maughmer, Mike Ross, and Jay Burton. From Boeing, Don Eastman, and from Sikorsky Aircraft, Dr. David Jenney.
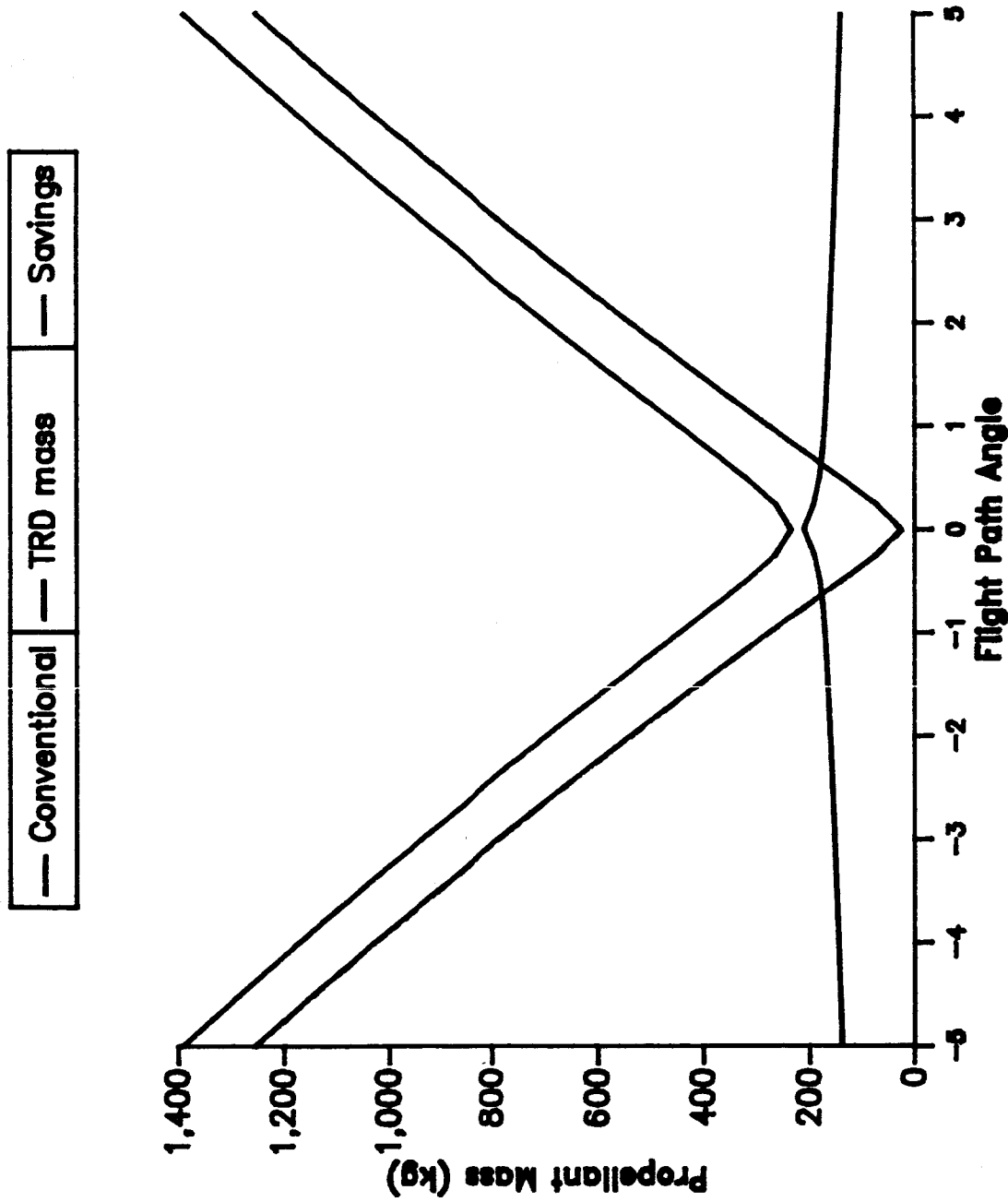
Fig. 1: Propellent Mass vs. Reentry Flight Path Angle

FIGURE 2: 18 HOUR OVERFLIGHT OF SSF
WITH WORST CASE UNCOVERED AREA
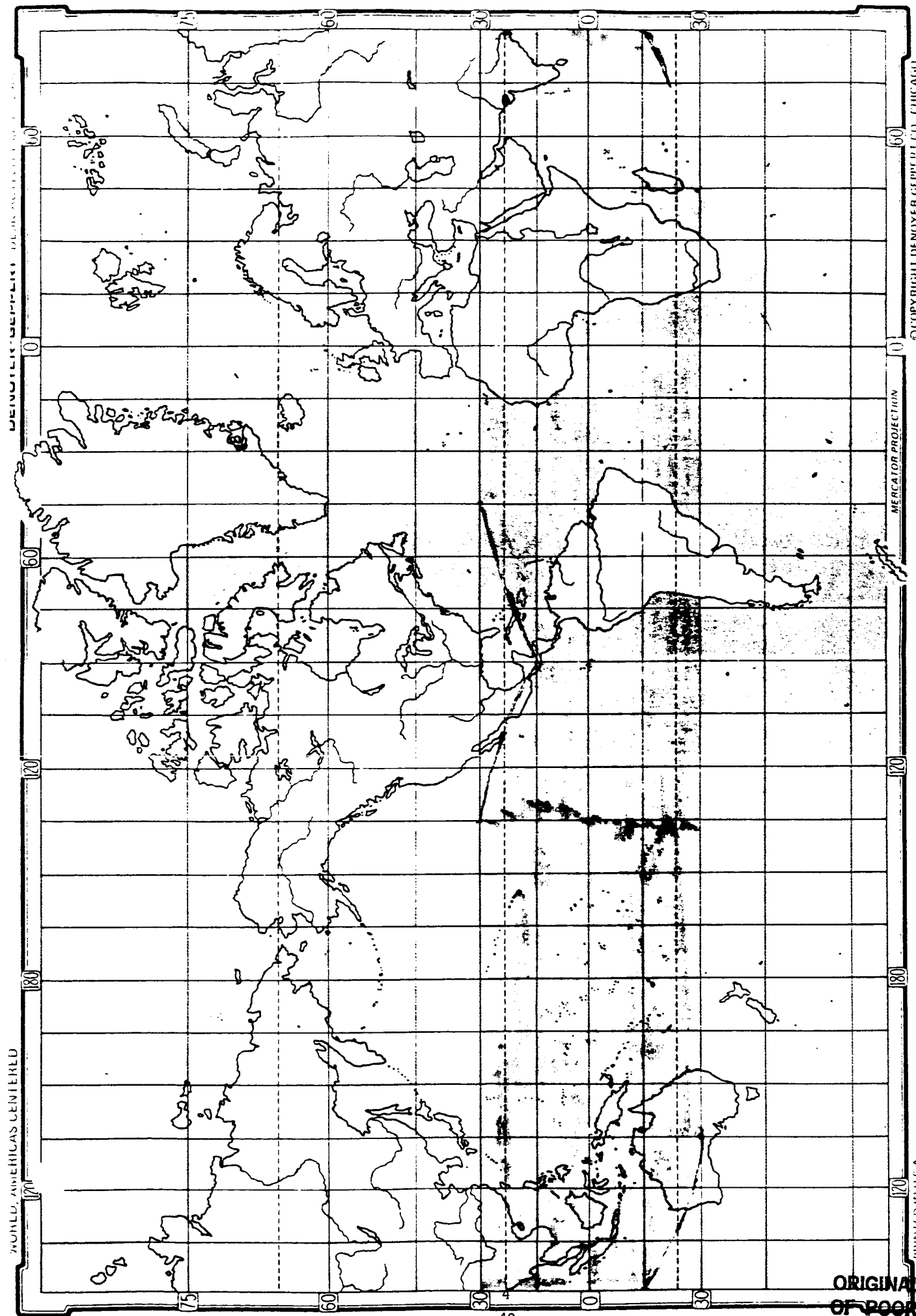
- UNCOVERED AREA

- COVERED AREA
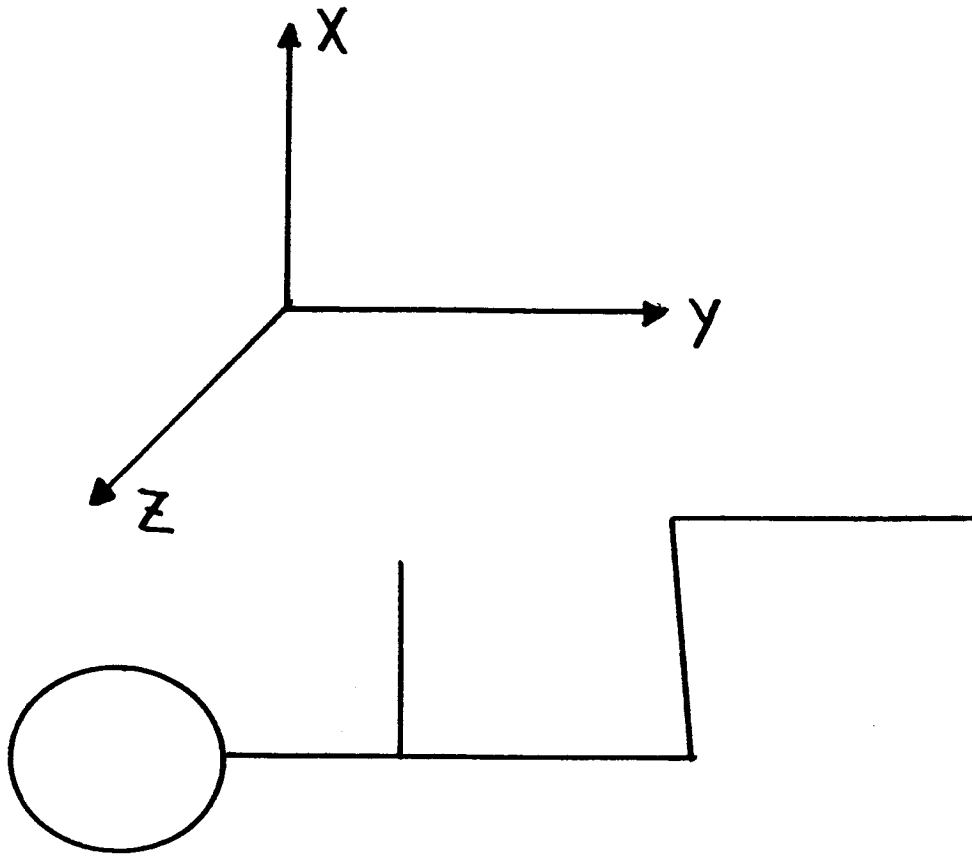
FIGURE 3: ~~BODILY~~ Body COORDINATE DIRECTIONS

[REF: JAY BURTON]

41
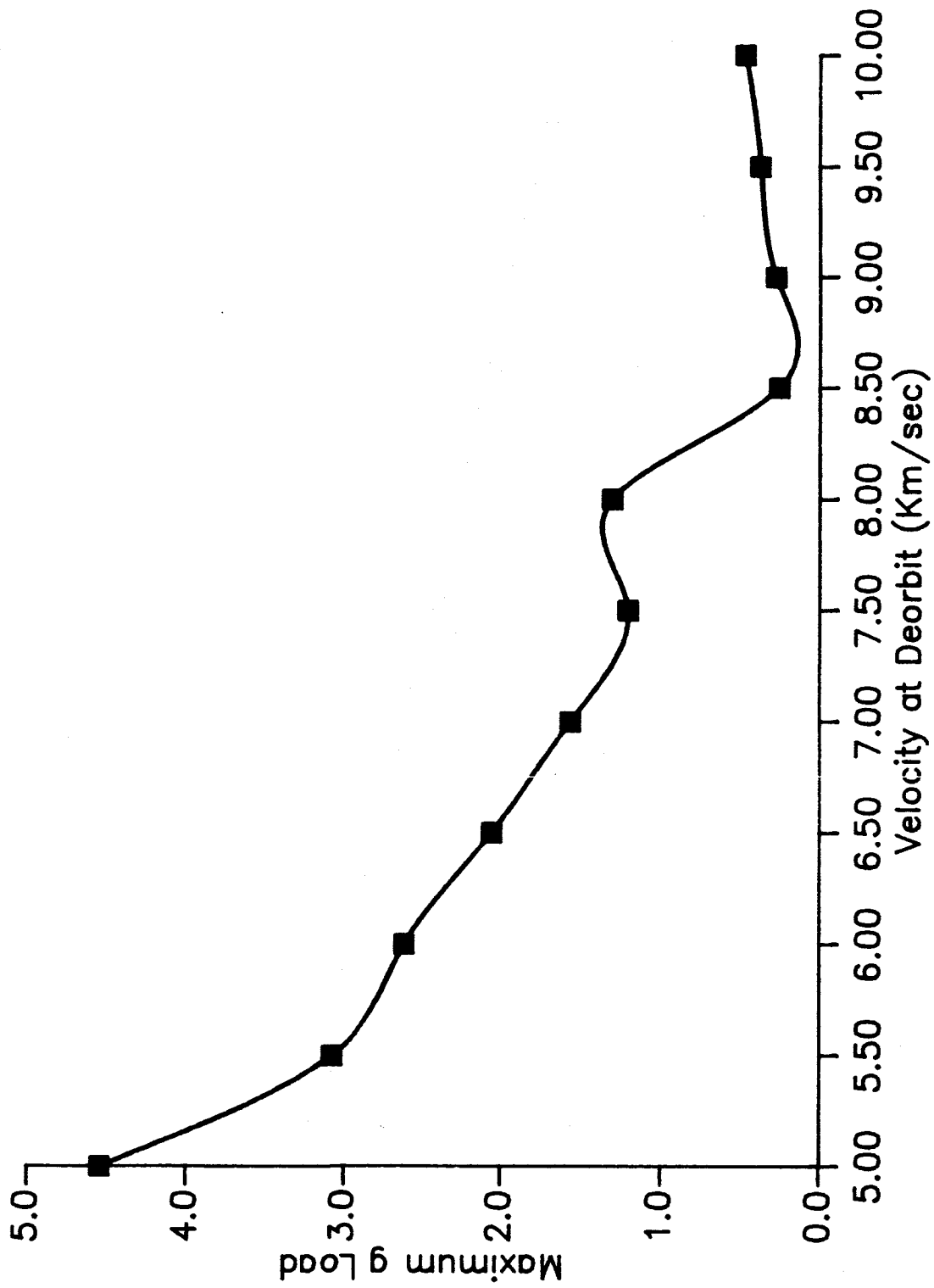
Fig. 4: Maximum g loading as a function of Deorbit Velocity
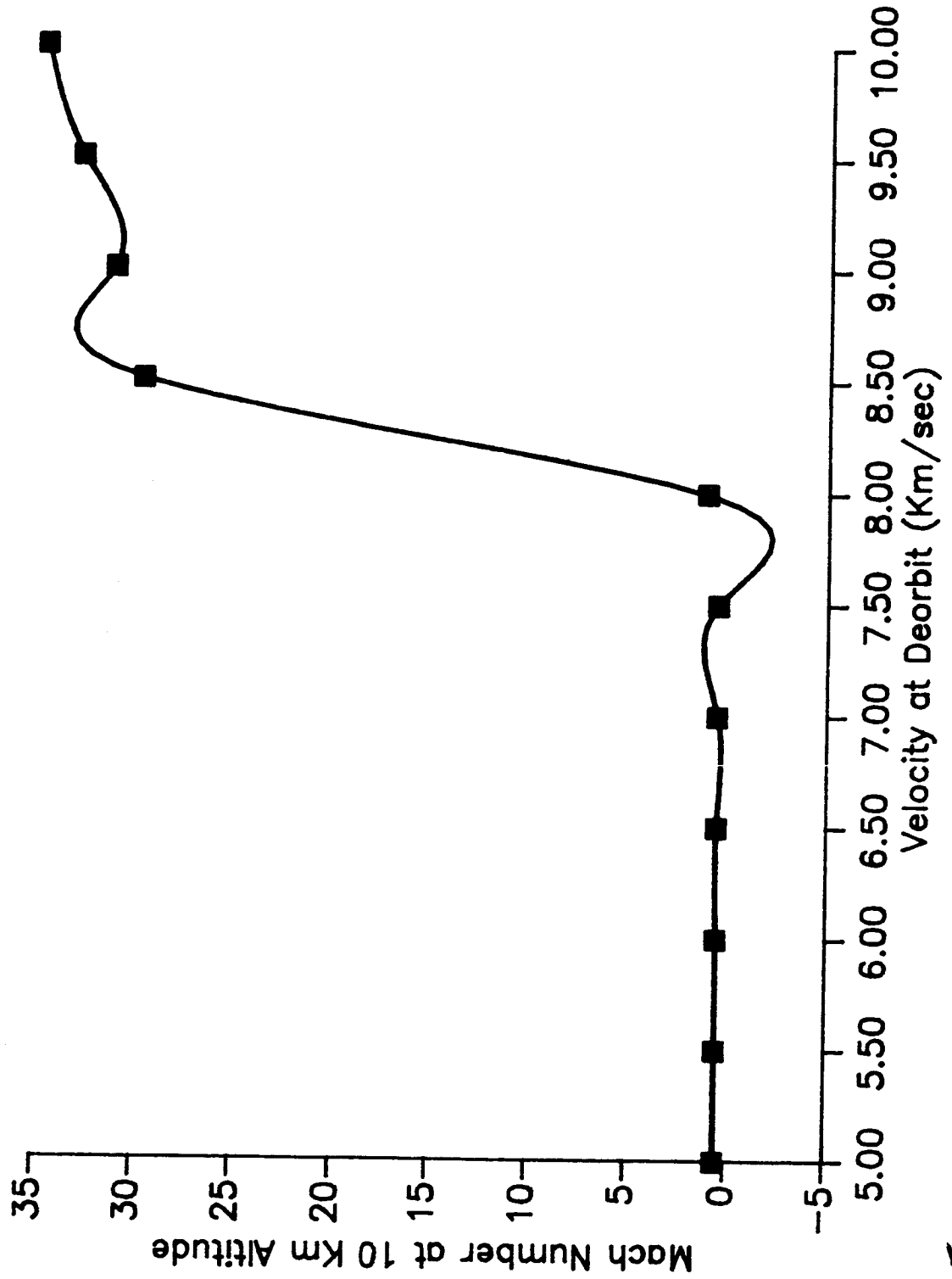
Fig. 5: Mach Number at 10 Km. altitude as a function of Deorbit Veloctiy
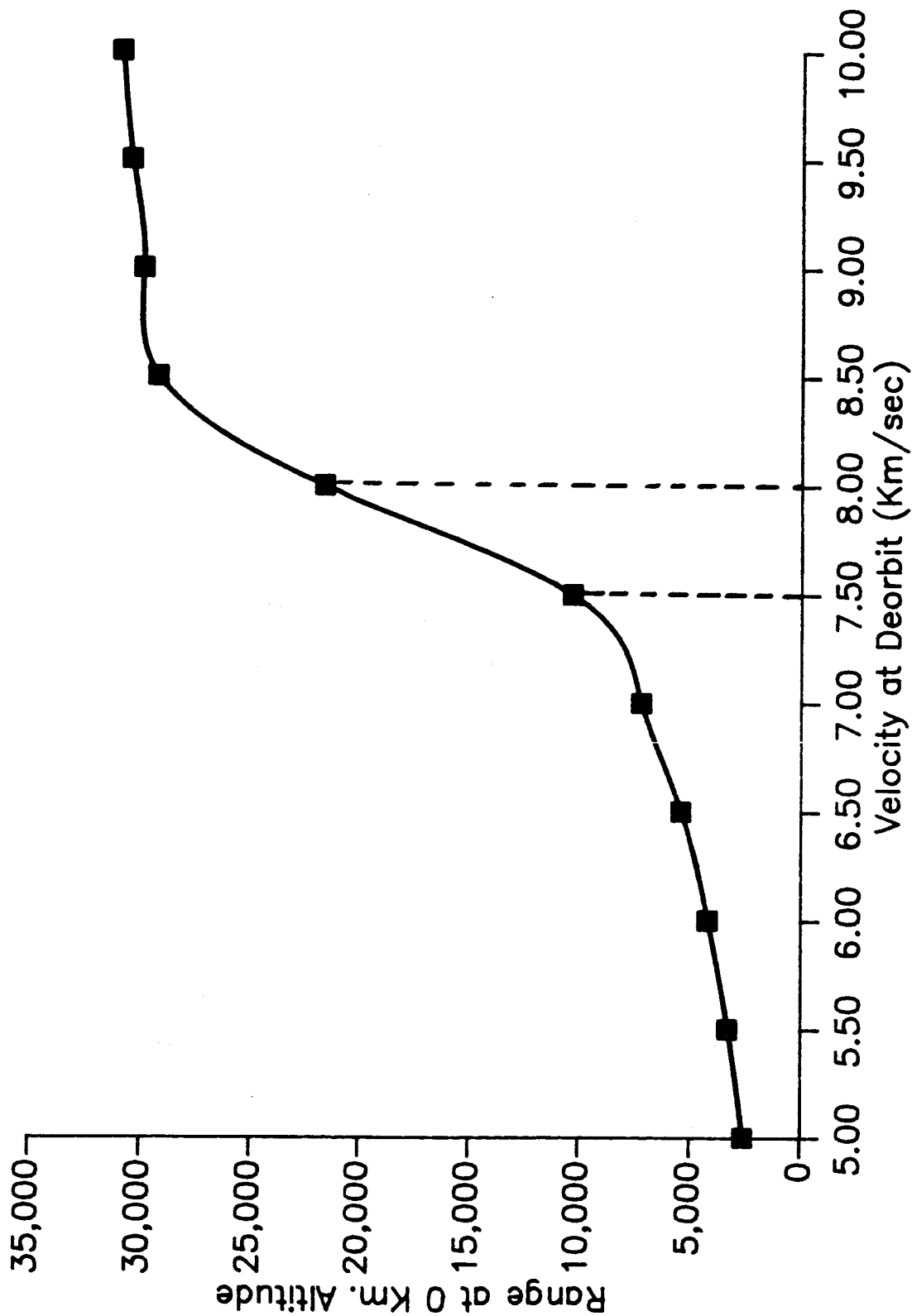
Fig.6: Maximum Range as a function of deorbit velocity
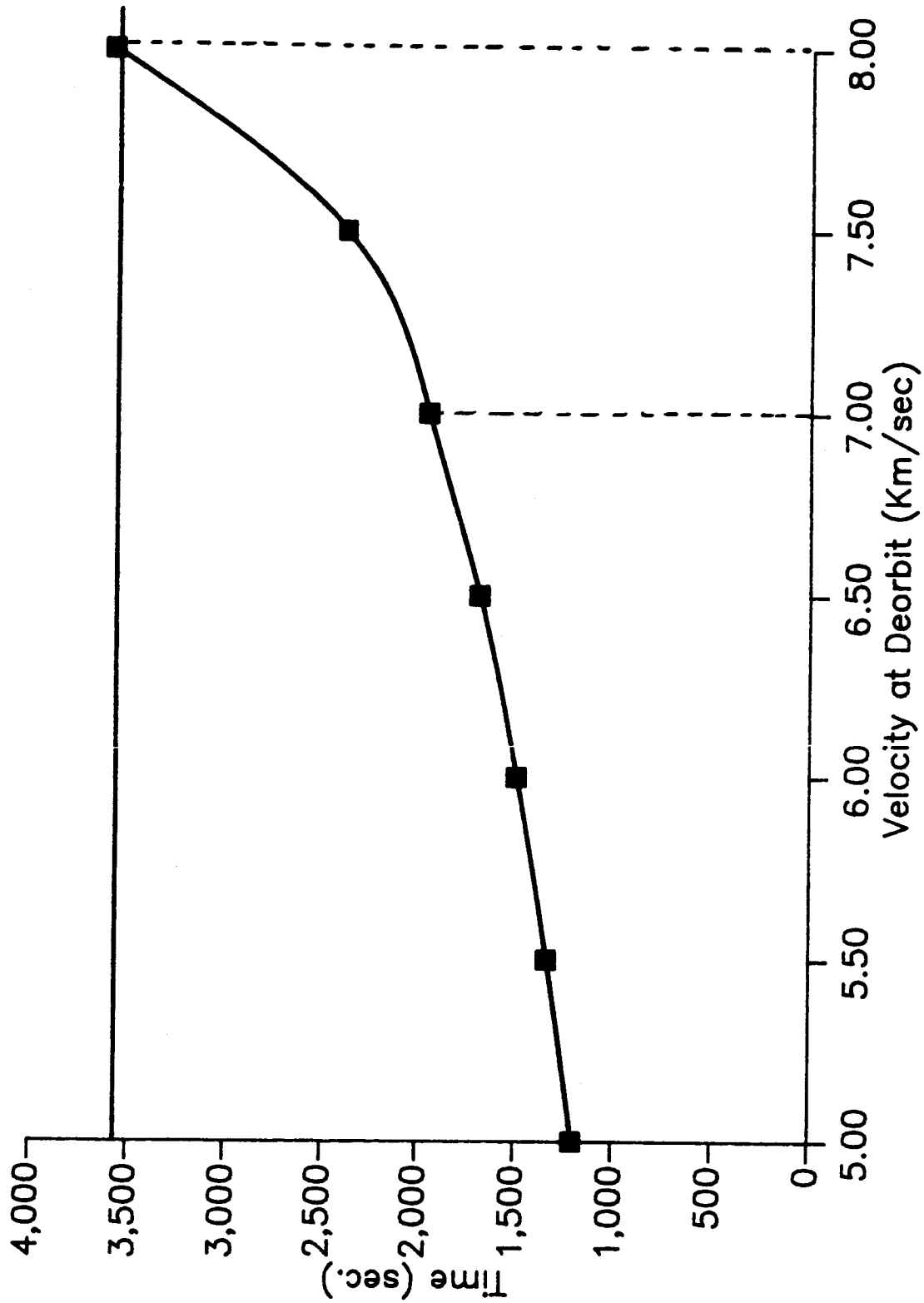
Fig. 7: Reentry time as a function of deorbit velocity

45
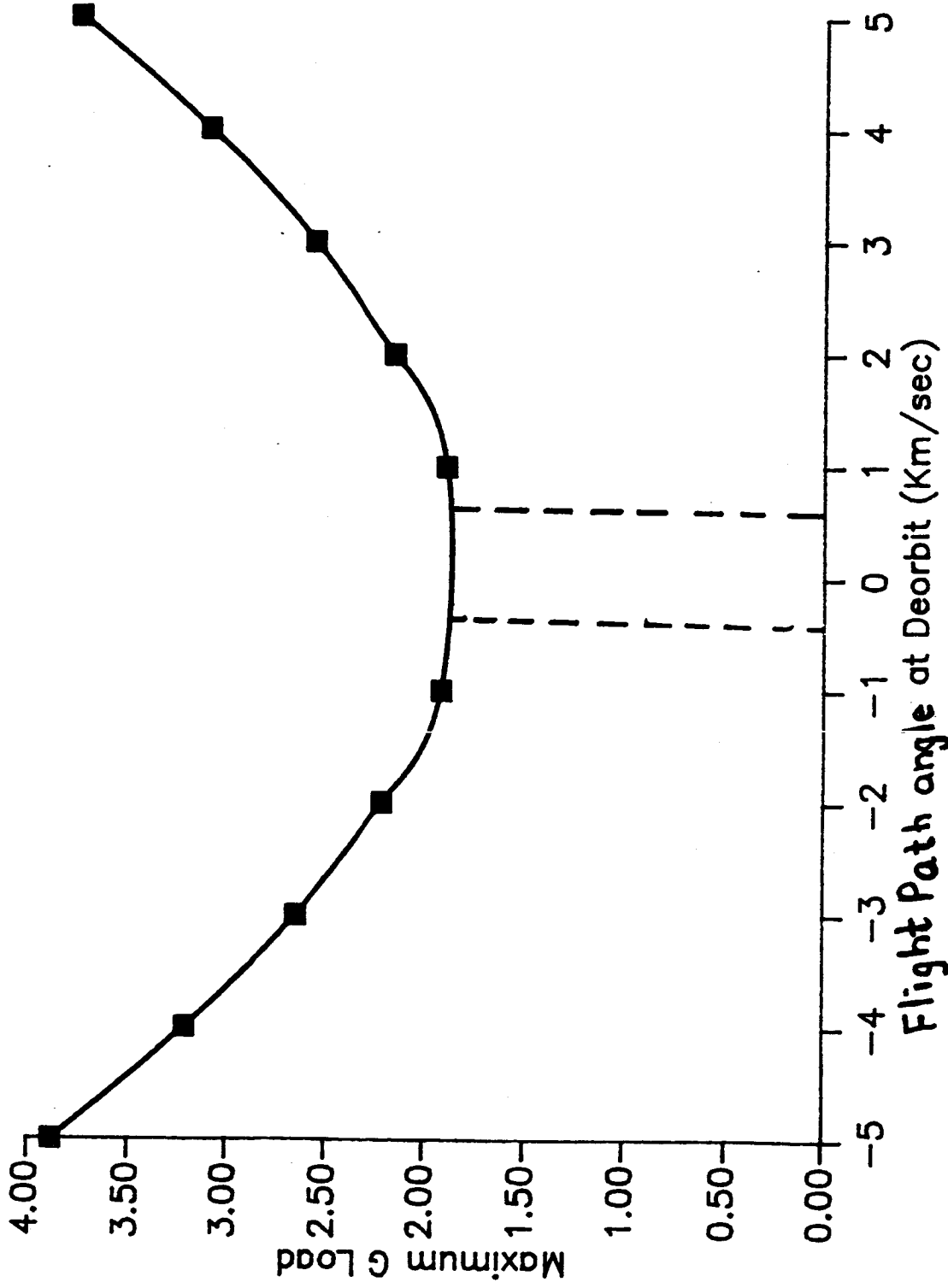
Fig. 8: Maximum G loading vs. deorbit Flight Path angle

Fight Path Angle at Deorbit (Degrees)
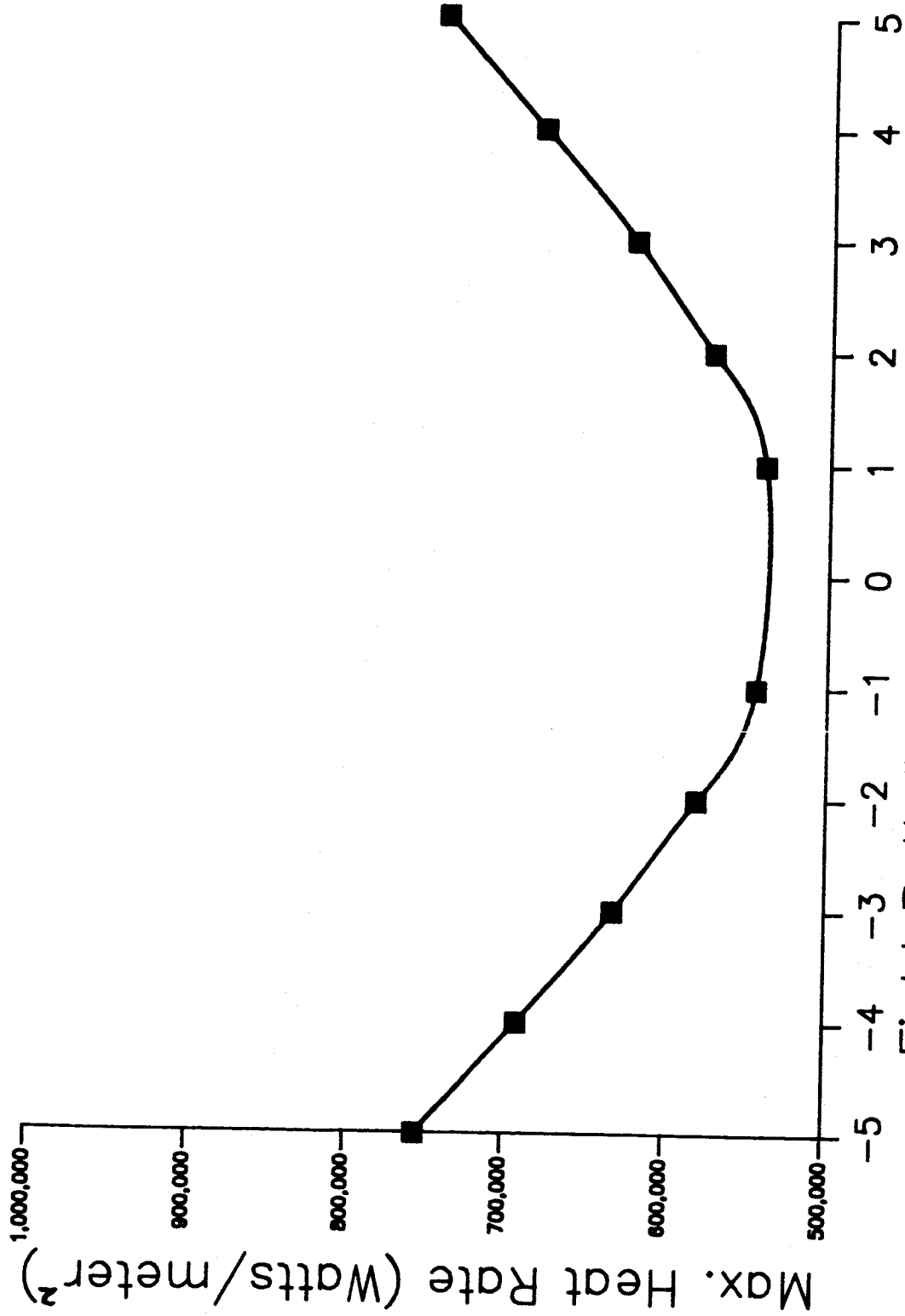
Fig. 9: Maximum Heat Rate vs. Deorbit Flight Path Angle

Max. Heat Rate (Watts/meter²)
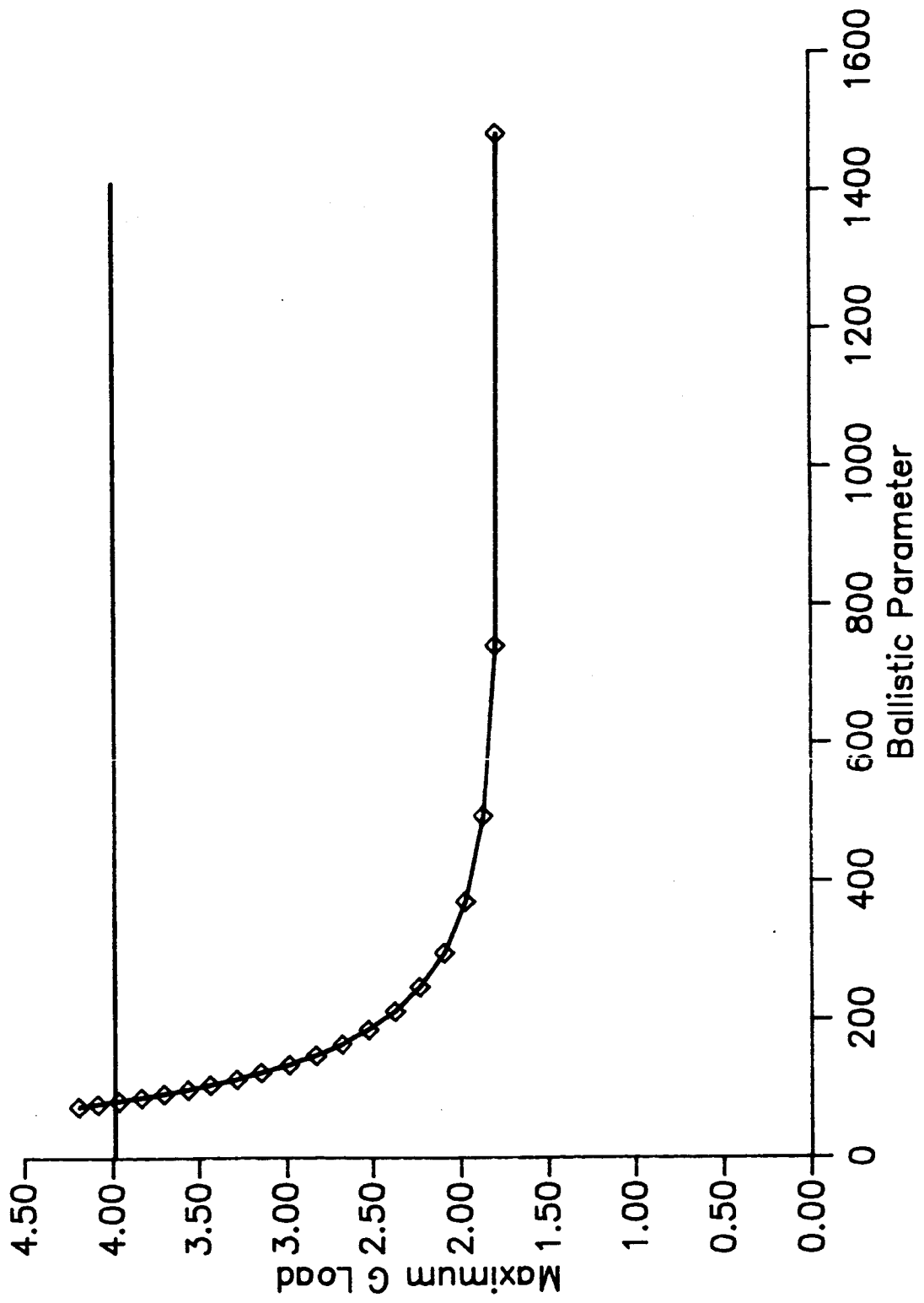
Fig. 16: Maximum G loading as a function of ballistic parameter
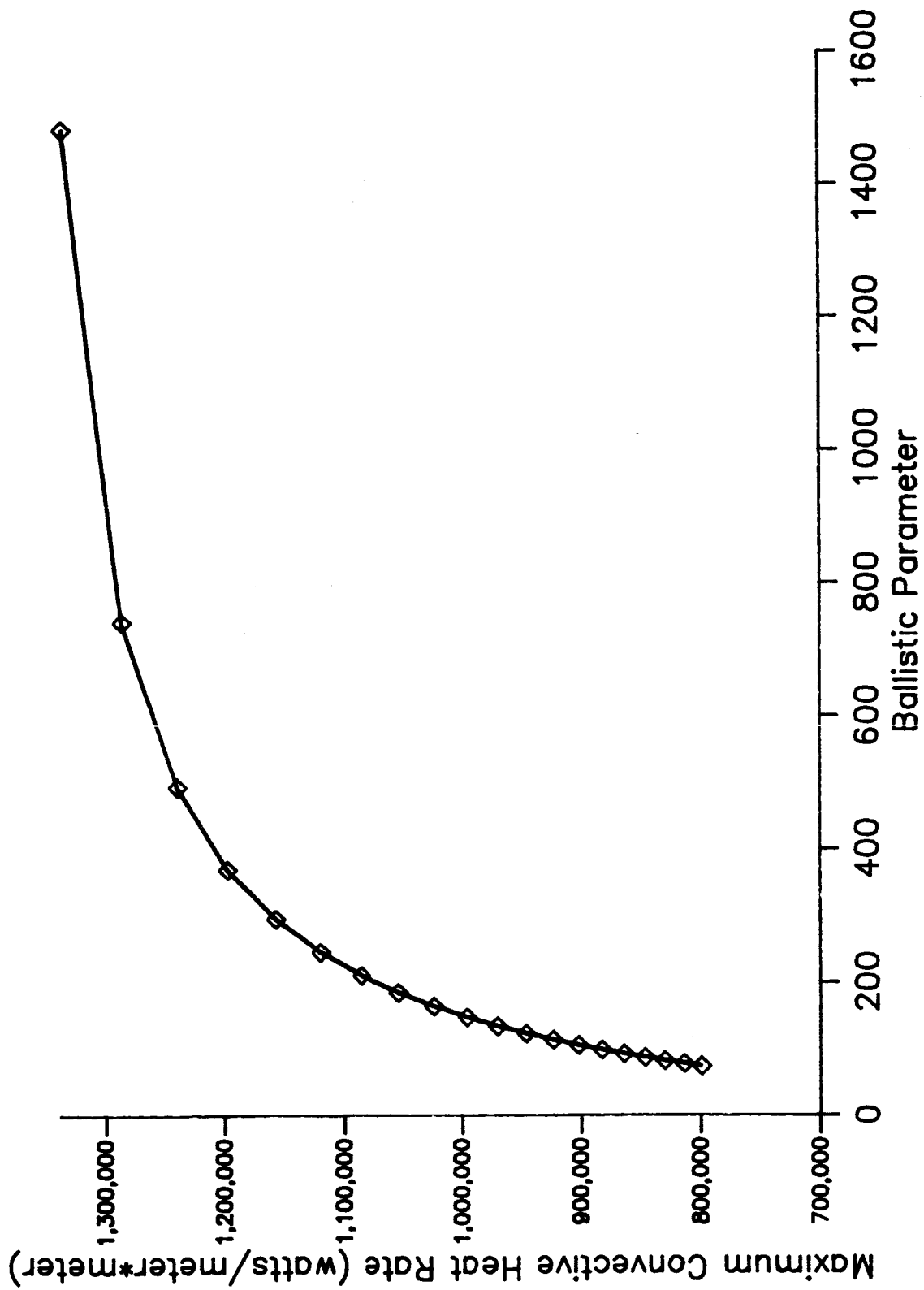
Fig. II: Maximum convective heat rate as a function of ballistic parameter
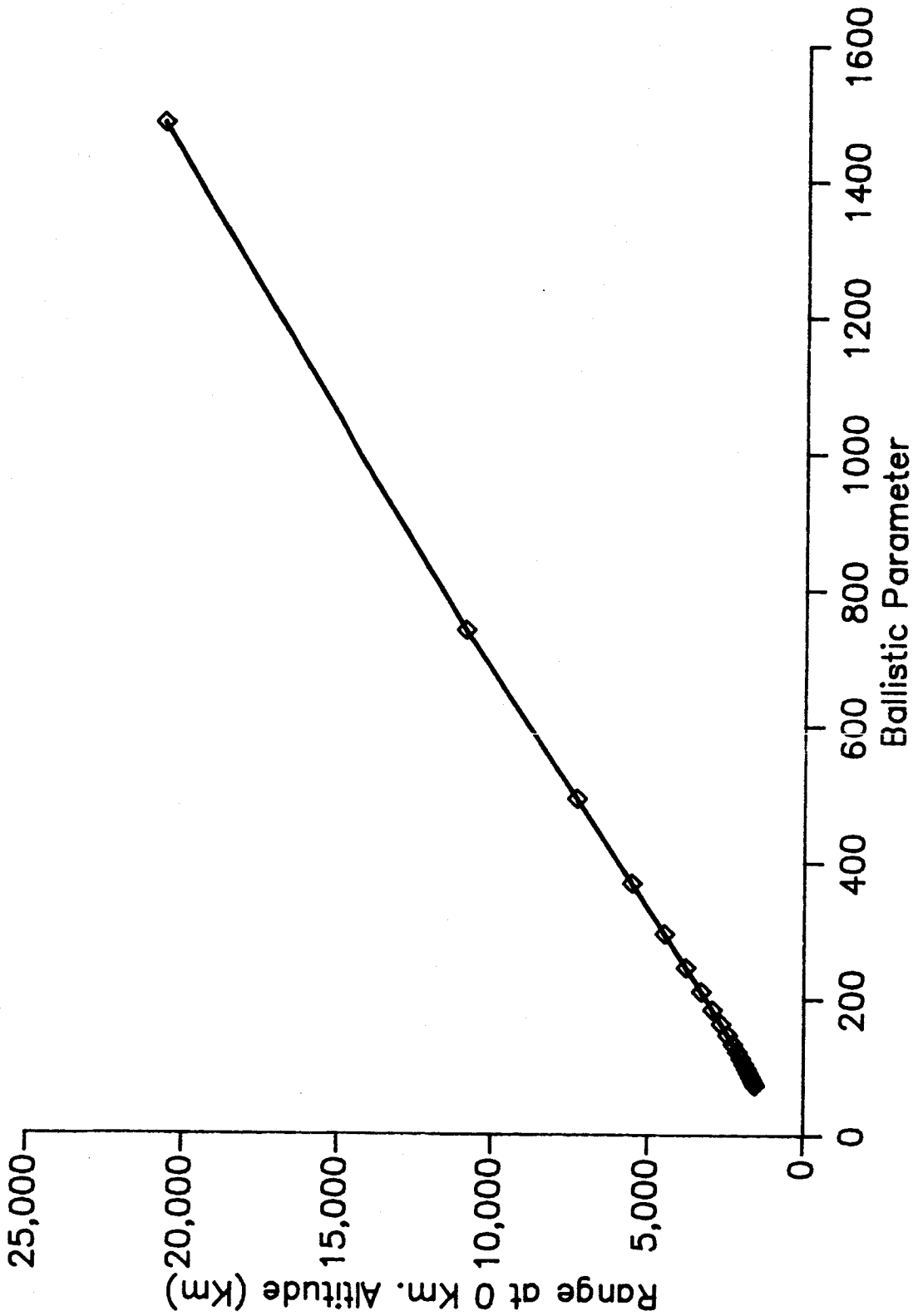
Fig. 12: Maximum range as a function of ballisitic parameter
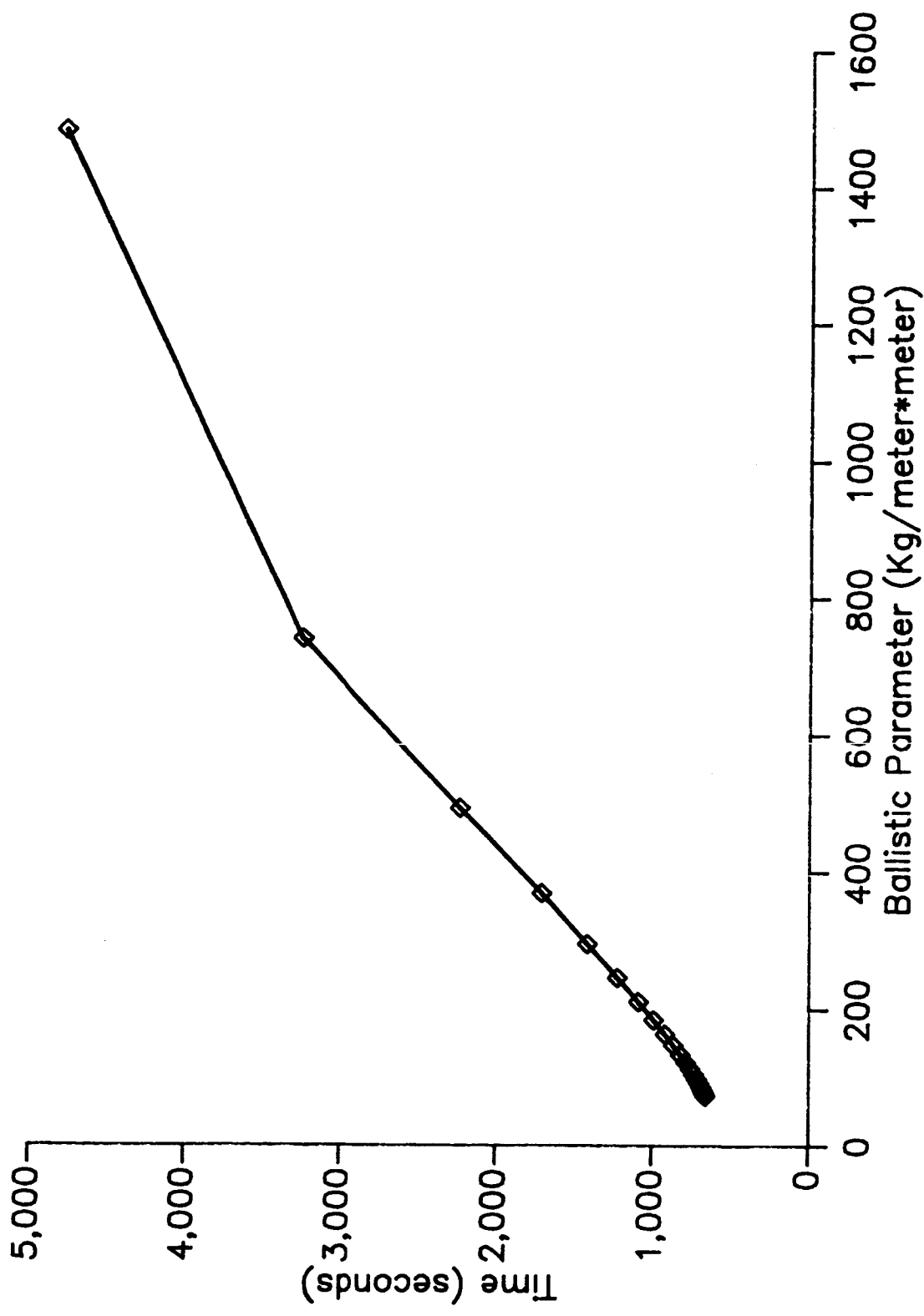
Fig. *13*: Reentry time as a function of ballistic paramter
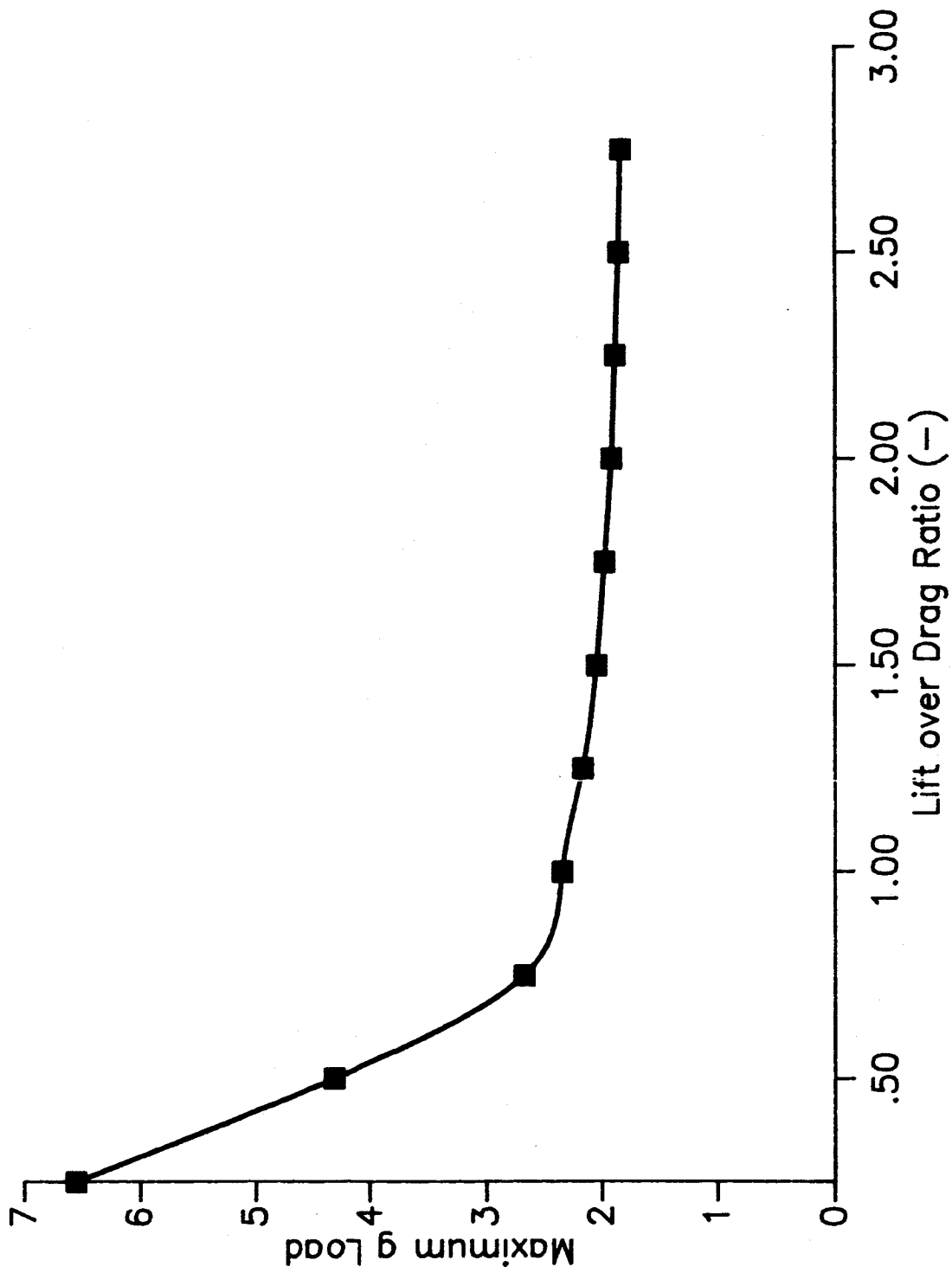
Fig.14: Maximum G Loading vs. Lift over Drag ratio
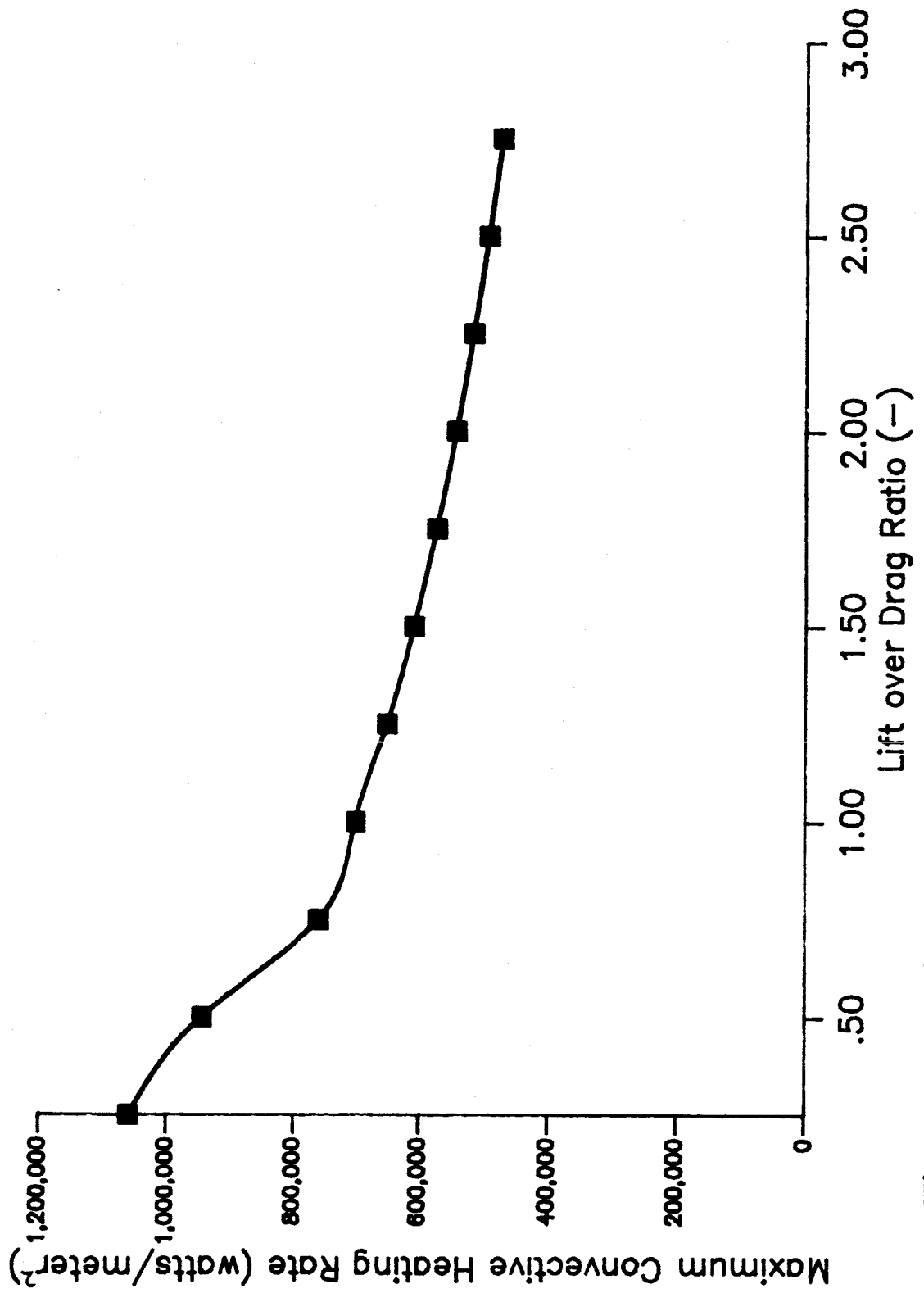
Fig. *15:* Maximum convective heat rate vs. Lift over Drag

53
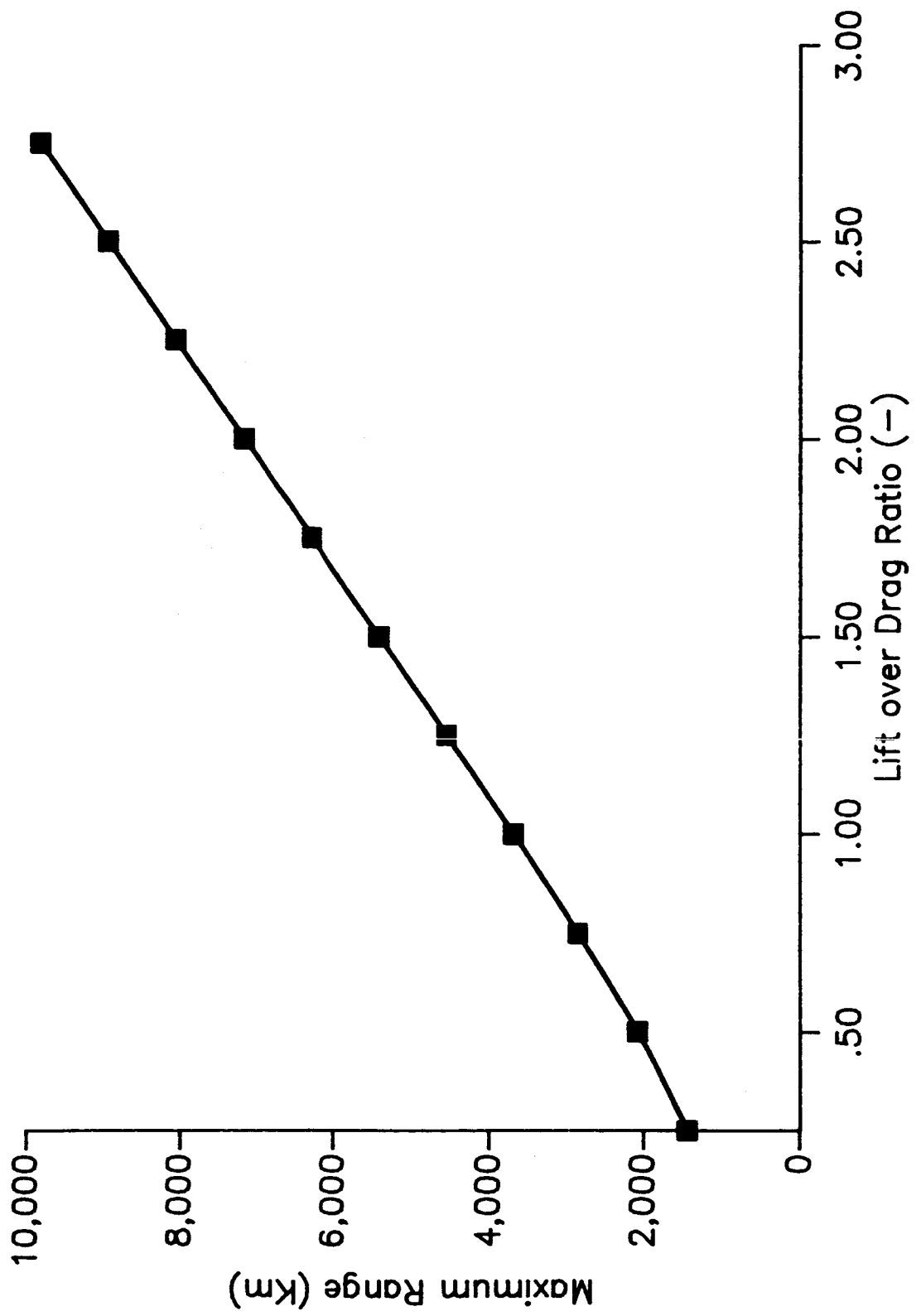
Fig. 16: Maximum Range as a function of Lift over Drag ratio

54
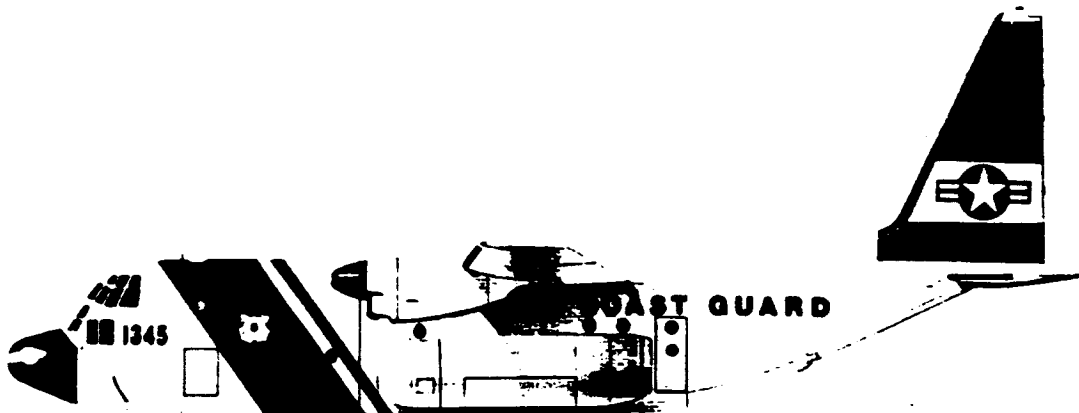
First customer for a search-and-rescue variant of the Hercules was the US Coast Guard, 12 modified C-130Bs being ordered from 1958 as **Lockheed R8V-1G** aircraft, becoming **SC-130B** aircraft before the first deliveries in 1959. Later redesignated **HC-130B**, they featured additional crew posts and two scanner stations offering an unrestricted field of view. Space was provided for 74 stretchers. The basic avionics of the transport version were retained, including the APS-59 nose radar.

On 8 December 1964 Lockheed flew the first HC-130H, a rescue variant powered by Allison T-56-A-15s. Forty-three were ordered for the USAF Air Rescue Service and the Coast Guard have received 23 aircraft, with deliveries continuing. The HC-130H was ordered for a variety of work focusing on the recovery of downed aircrew but also including duties related to the space programme. The HC-130H carried additional equipment and two 6814-litre (1,800-US gal) fuel tanks in the cargo hold. Externally it mounted a large blister above the forward fuselage containing the Cook Electric re-entry tracking system for use in conjunction with the Gemini spacecraft. The most remarkable feature, however, is the Fulton recovery system: two 4.42-m (14.5-ft) nose-mounted tines are normally stowed back along the fuselage, but hinge forward to make a V-shaped fork. The aircraft

also carries recovery kits, including rafts and helium balloons. The latter, when inflated, carry aloft a 152-m (500-ft) line which is attached to a body harness. Flying at 122 kts (225 km/h, 140 mph) into wind the HC-130 snags the line with its recovery yoke, snatching the maximum 227-kg (500-lb) load from the surface. The balloon breaks away at a weak link and the rescued person or load is winched into the aircraft, the line being grapnelled to allow recovery into the cargo bay. Teflon lines from nose to fin and wingtips deflect the wire from the propellers in the event of a missed approach. The US Coast Guard's HC-130s do not usually operate with the Fulton gear. Four USAF HC-130Hs were subsequently converted for space capsule recovery as the **JHC-130H** version.

To cope with the increased rescue demands of the Vietnam War an additional 20 HC-130Hs were built but with outer wing pods for inflight-refuelling of helicopters. Designated **HC-130P**, these aircraft worked most successfully with the Sikorsky HH-3E to save many lives. The last rescue Hercules is the **HC-130N** which differs from earlier models in having advanced direction-finding equipment but without the Fulton gear and additional fuel tanks. Fifteen were delivered to the USAF from 1969, and with the earlier types these equip 10 squadrons across the world.

This Lockheed HC-130B serves with the US Coast Guard.
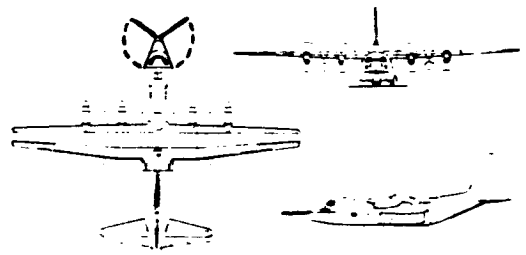
Lockheed HC-130P with Fulton gear (now rarely carried)

This RAF Woodbridge-based HC-130P of the 67th ARRS, US Air Force, is seen refuelling an HH-3 during a deployment to Keflavik, Iceland. The 67th ARRS is responsible for Europe-wide combat rescue.

The US Coast Guard operates a large fleet of HC-130 Hercules for rescue and patrol missions. This HC-130H does not carry the Fulton recovery system, in common with most current examples.

Specification: Lockheed HC-130H Hercules
Origin: USA
Type: rescue and recovery aircraft
Powerplant: four 3362-ekW (4,508-eshp) Allison T56-A-15 turboprop engines
Performance: maximum speed 325 kts (602 km/h, 374 mph) at 30,000 ft (9145 m); initial rate of climb 1,900 ft (579 m) per minute; service ceiling 33,000 ft (10060 m); range with maximum payload and reserve fuel 3792 km (2,356 miles)
Weights: empty 32936 kg (72,611 lb); maximum take-off 70307 kg (155,000 lb)
Dimensions: span 40.41 m (132 ft 7 in); length 30.73 m (100 ft 10 in); height 11.66 m (38 ft 3 in); wing area 162.16 m² (1,745.5 sq ft)
Armament: none

F IGURE 17 :   Lockheed HC-130 Hercules
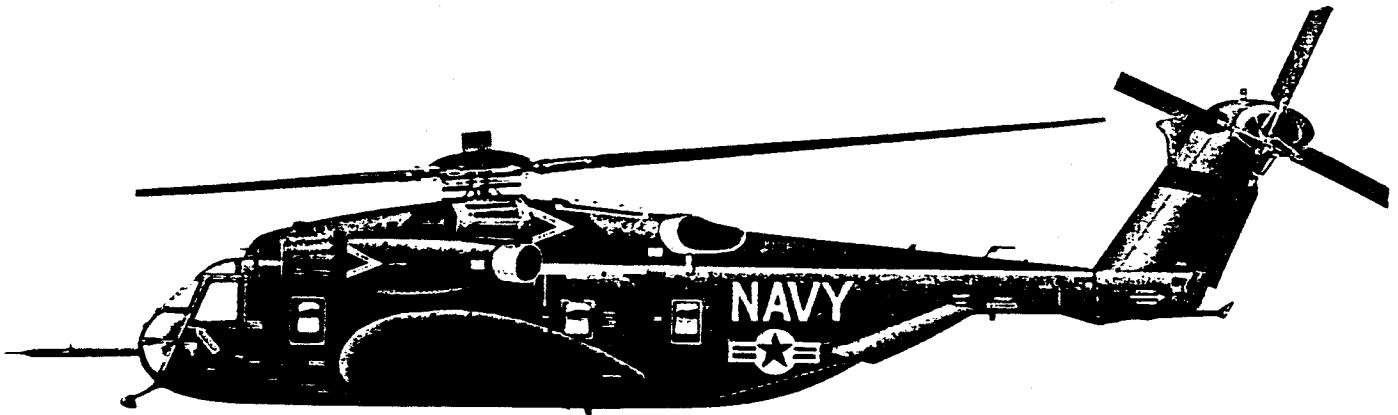
Although both the US Navy and Marine Corps had gained good service in heavy transport and minesweeping roles from the Sikorsky CH-53D and RH-53D, it was clear by the early 1970s that an even more capable helicopter could be built to fulfil such tasks. In 1973 the Sikorsky S-65 was selected for development, and in May of that year the construction of two **YCH-53E** prototypes was initiated, the first of them flying on 1 March 1974. The first of two pre-production aircraft flew on 13 December 1980, and initial production deliveries of the **Sikorsky CH-53E Super Stallion** to Marine Corps squadron HMH-464, at New River, North Carolina, began on 16 June 1981. The US Navy plans to procure ultimately at least 300 of these helicopters, and about 100 had been delivered in mid-1986. By comparison with the CH-53D, the new helicopter has a lengthened fuselage, three turboshaft engines, an increased diameter seven-blade main rotor and an uprated transmission, giving double the lift capability of the twin-turbine H-53s with only 50 per cent more engine power. With a single-point cargo hook rated at 16329 kg (36,000 lb), the CH-53E is suitable for combat tasks such as lifting battle-damaged aircraft from carrier decks, or the support of mobile construction battalions, and for vertical onboard delivery has

an internal cargo load of 13608 kg (30,000 lb).

Further capability enhancement for the mine countermeasures helicopter was explored first with a prototype, initially designated **CH/MH-53E**, which was a conversion from a pre-production CH-53E and flown for the first time on 23 December 1981. Early evaluation by the US Navy resulted in the construction of a pre-production aircraft, then designated **MH-53E** and named **Sea Dragon**, which was flown on 1 September 1983. Since then the Navy has stated its requirement for at least 57 of these aircraft and the first production example was scheduled for delivery during 1986. The MH-53E is easily identified externally by its enlarged sponsons containing additional fuel and allowing the helicopter to operate for up to six hours on station; it is also equipped with an inflight-refuelling probe and, at the hover, can refuel by hose from a surface vessel. Extended capability is provided by duplicated digital automatic flight-control systems and automatic tow couplers which allow automatic approach to and departure from the hover. Export versions of the CH-53E and MH-53E are being offered by Sikorsky under the respective designations **S-80E** and **S-80M**.

A Sikorsky MH-53E Sea Dragon of the US Navy.
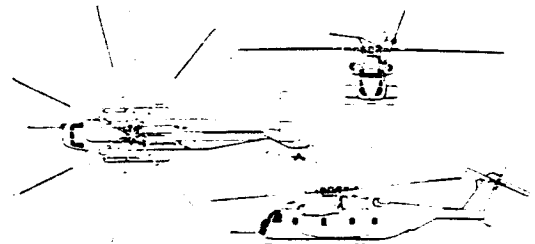
Sikorsky CH-53E Sea Stallion Super

Two CH-53E Super Stallions of the US Marine Corps, refuelling from a KC-130T Hercules. The CH-53E differs from earlier variants in having three engines and an uprated transmission.

Specification: Sikorsky CH-53E Super Stallion
Origin: USA
Type: heavy-duty multi-role helicopter
Powerplant: three 3266-kW (4,380-shp) General Electric T64-GE-416 turboshaft engines
Performance: maximum speed 170 kts (315 km/h; 196 mph) at sea level; cruising speed at sea level 150 kts (278 km/h; 173 mph); initial climb rate 2,500 ft (762 m) per minute; service ceiling 18,500 ft (5640 m); unrefuelled self-ferry range 2076 km (1,290 miles)
Weights: empty 15071 kg (33,226 lb); maximum take-off, internal payload 31638 kg (69,750 lb) and external payload 33339 kg (73,500 lb)
Dimensions: main rotor diameter 24.08 m (79 ft 0 in); length, rotors turning 30.19 m (99 ft 0.5 in); height, tail rotor turning 8.6 m (28 ft 5 in); main rotor disc area 455.37 m² (4,901.68 sq ft)
Armament: none, but there are suggestions that AIM-9 Sidewinders might be provided to give a self-defence capability

Figure 18: Sikorsky S-65 (CH-53E/MH-53E)

REAR VIEW

LEFT SIDE VIEW
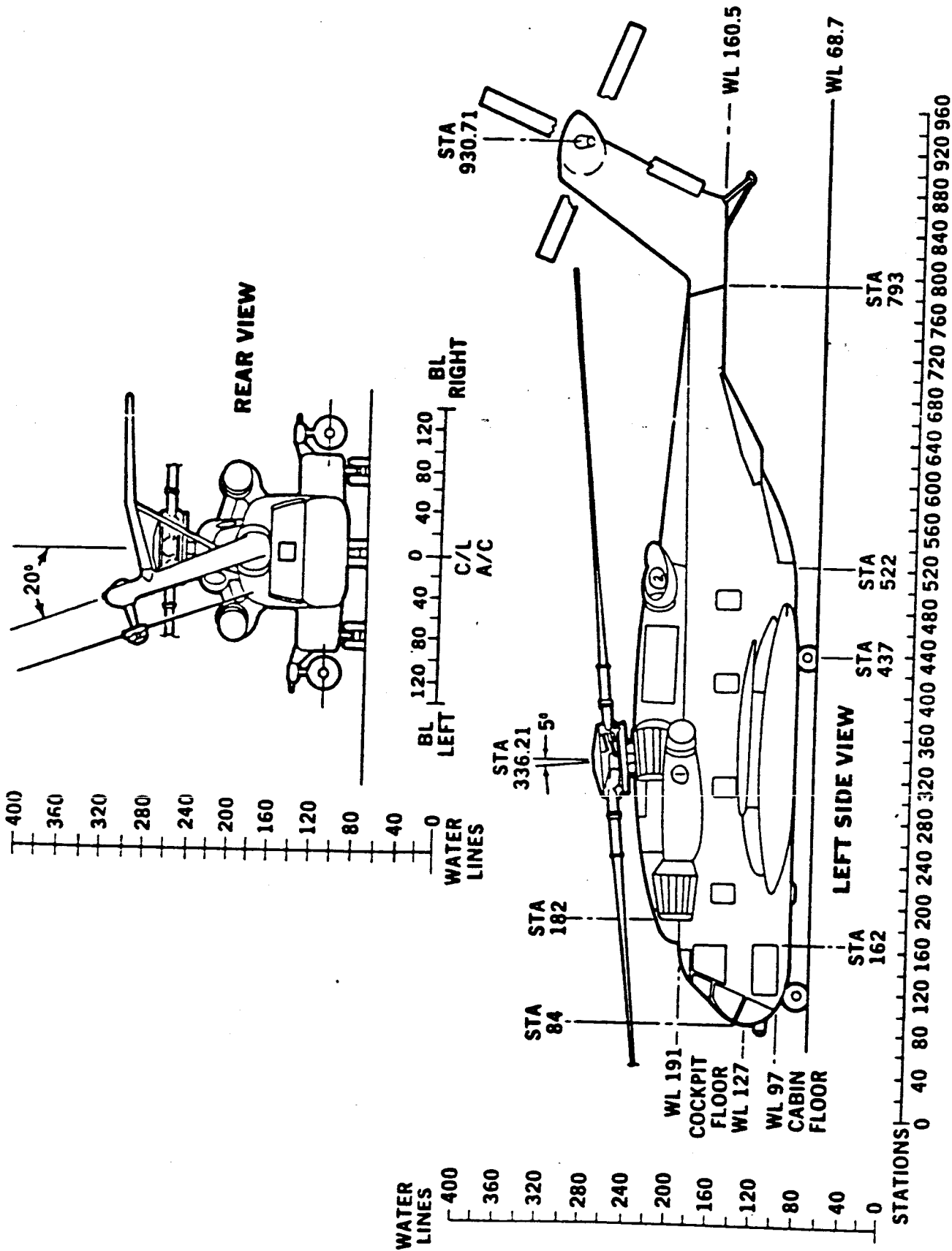
Fig. 19 STATIONS, WATERLINES, AND BUTTLINES
CH-53E

57

INDUCED MOMENT ARMS CAUSED BY LOAD:
UNDERNEATH OF CG

FORWARD OF CG

AFT OF CG

DECELERATION

HELICOPTER FLOOR

CG

θ
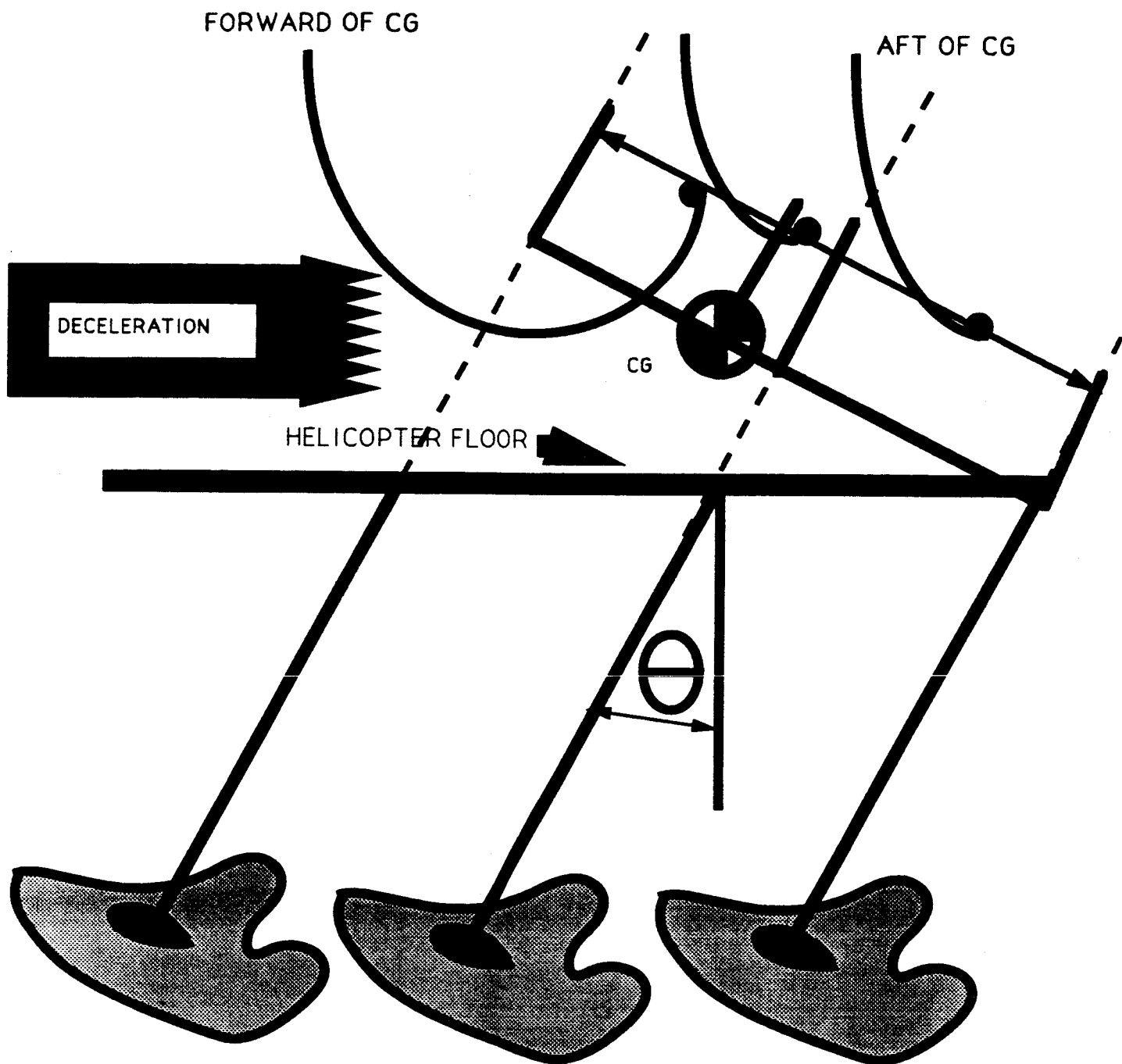
FIGURE 20. INDUCED MOMENT CAUSED BY
DECELERATION AND MOMENT ARM

58

Sikorsky
CH-53E

Drogue → Chute

Main Chute

Escape Vehicle
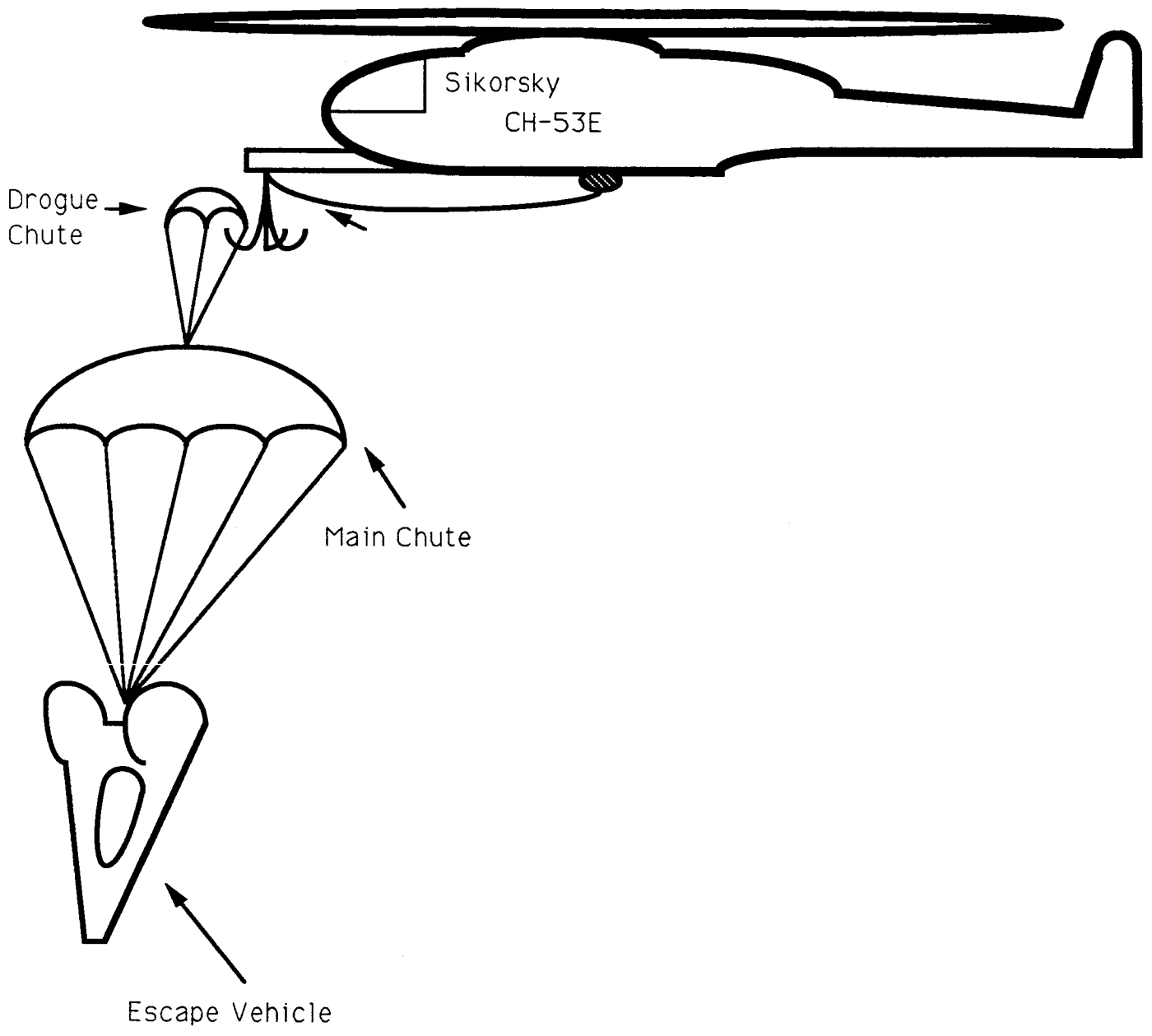
Figure21:Air-to-Air Hook-up Configuration

SERVICE CEILING OF CH-53E

34 FT/S

PICK-UP ZONE

18,500 feet

600 Feet

NO GO (192.7 feet at
Zone   -3ft/second**2)

500 feet Safety Zone

Water
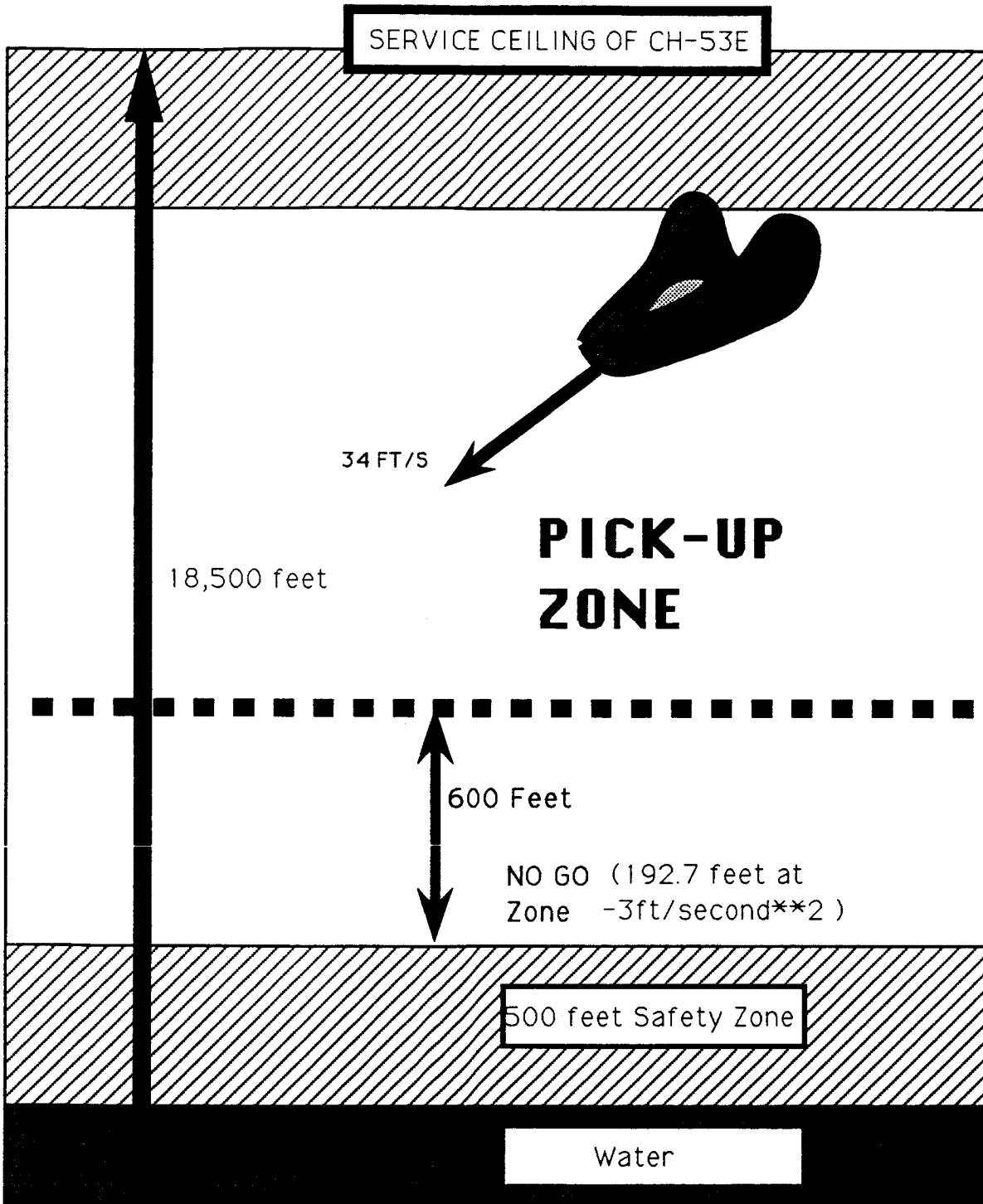
FIGURE 22: Service Ceiling
of CH-53E

5.

1.

2.

4.

3.
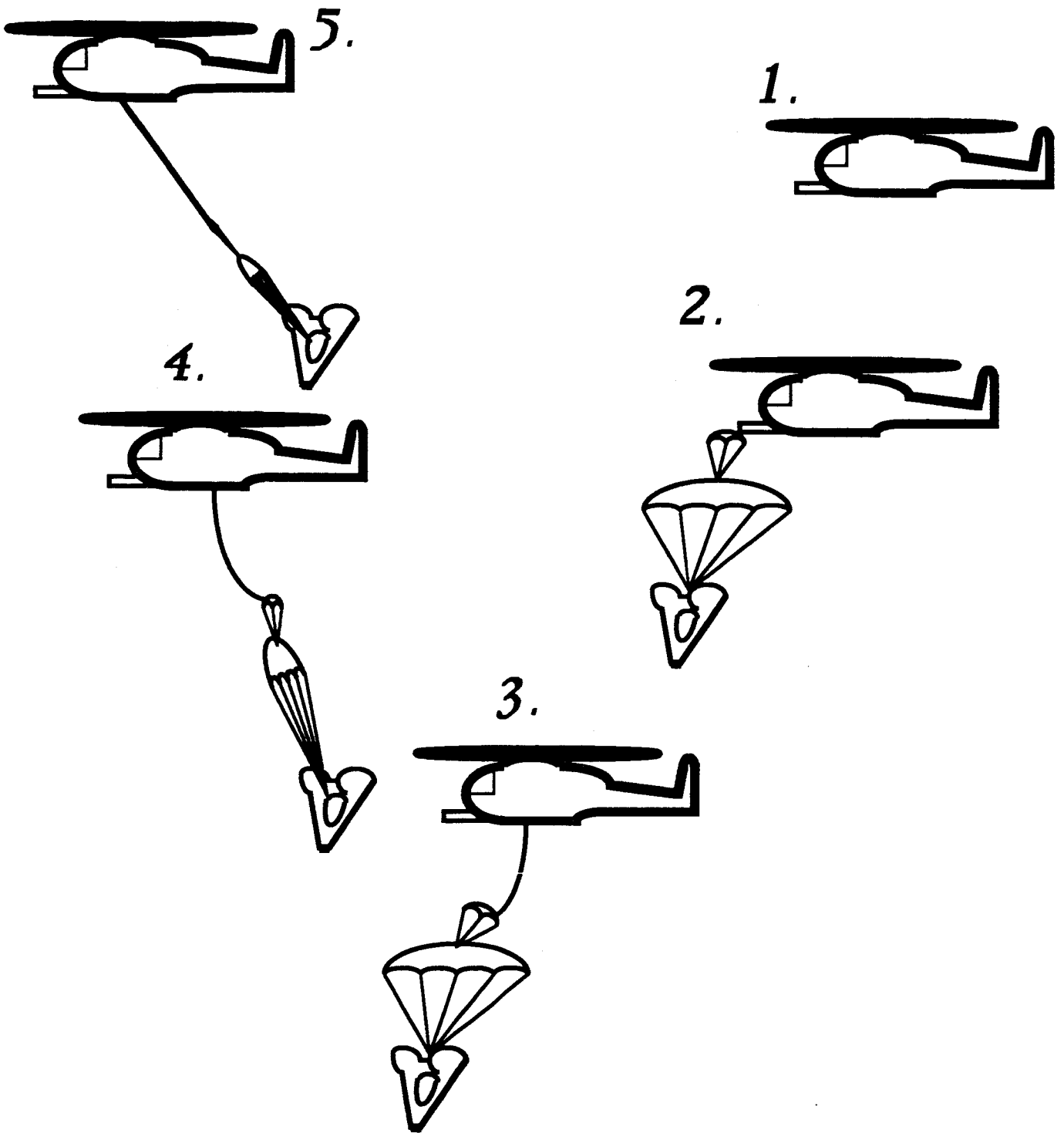
Figure 23: AIR-TO-AIR HOOK-UP
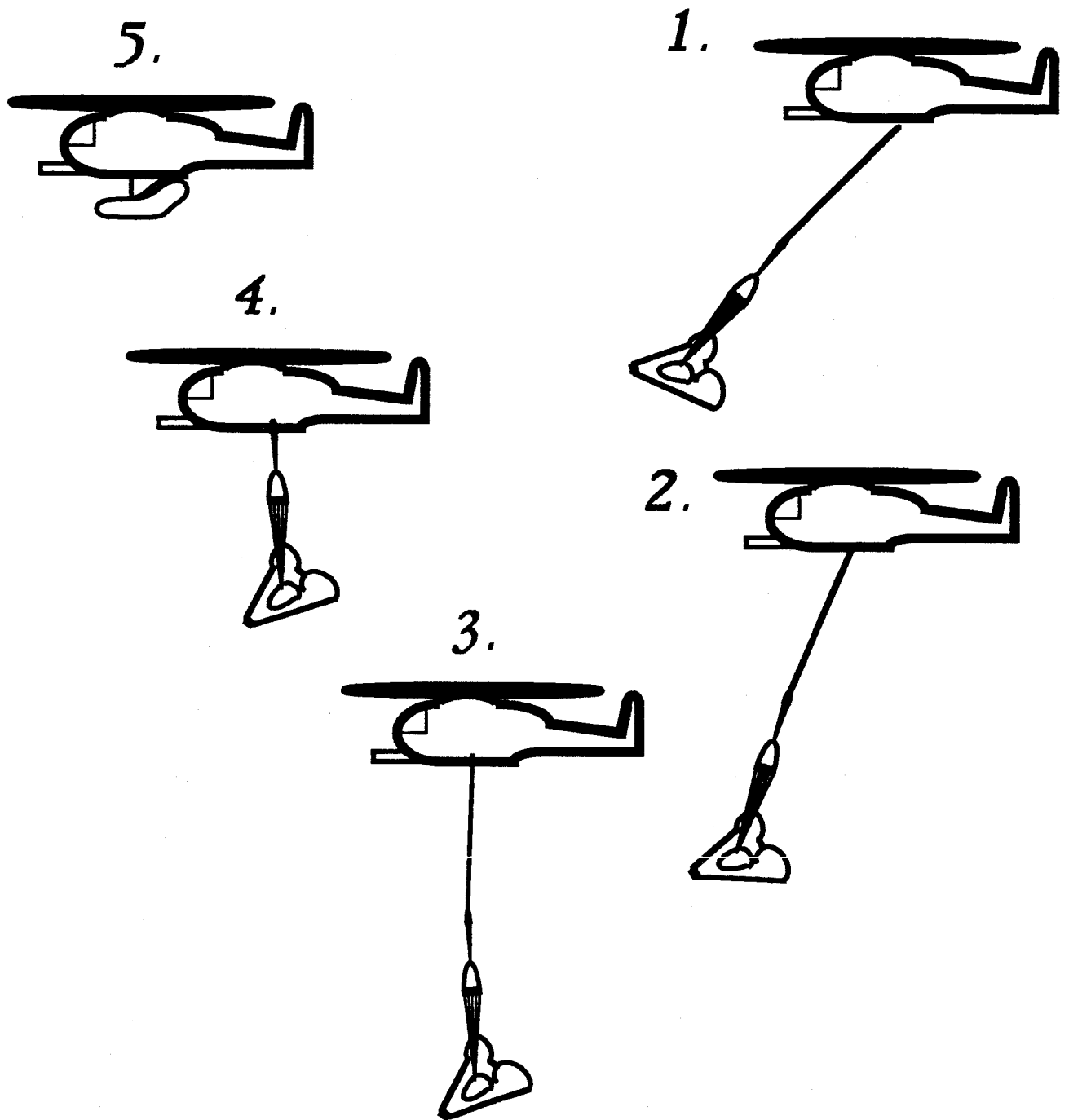
Figure 24: Deceleration to hover and Retraction of ACRV

WINCH

SECURELY
FASTENED TO
HELICOPTER
FLOOR

HELICOPTER FLOOR

PRESSURE
JACKS
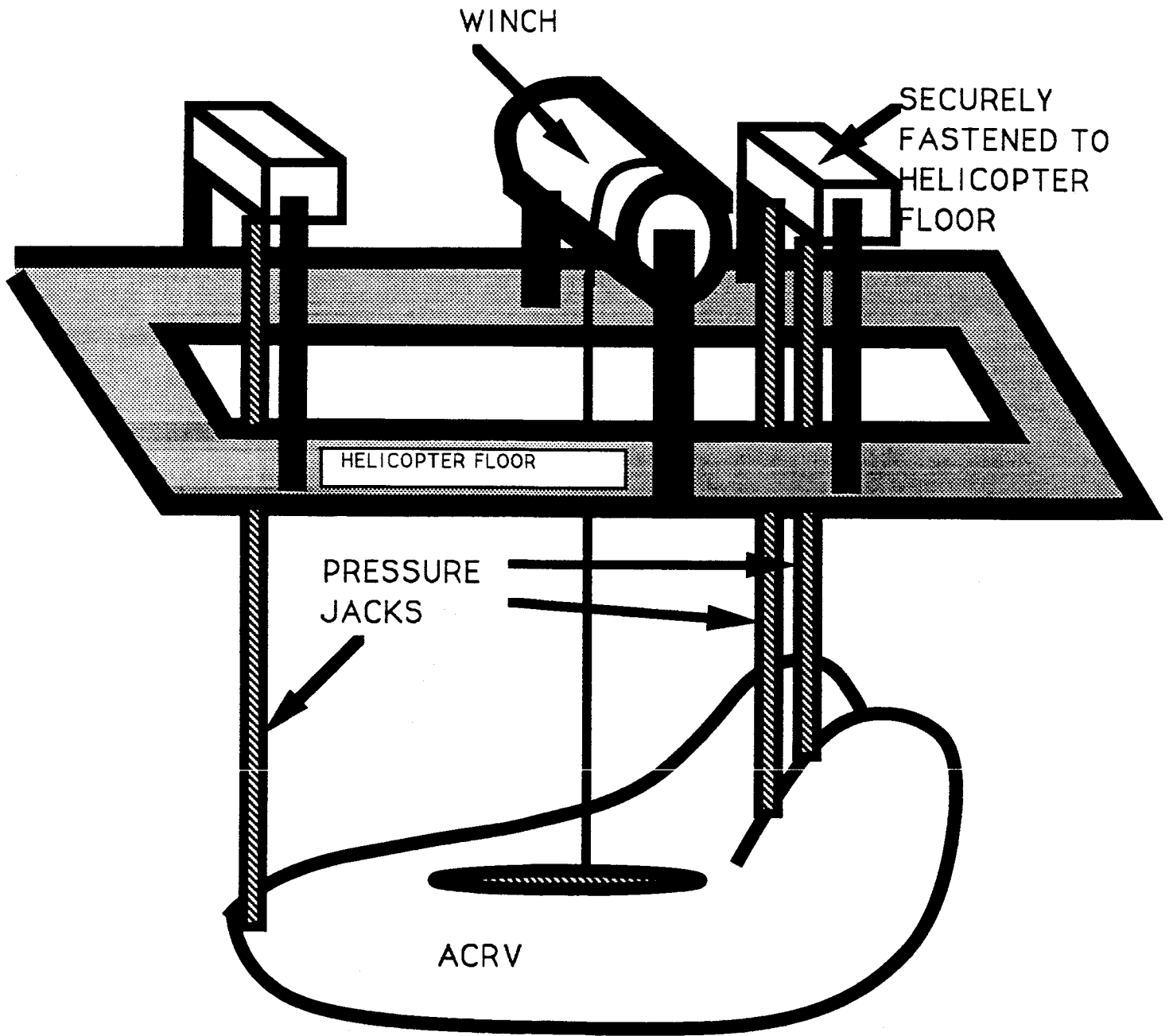
ACRV

FIGURE 25: STABILITY IN FLIGHT BY
PRESSURE JACKS AGAINST ACRV TO OPPOSE
TENSION FROM WINCH
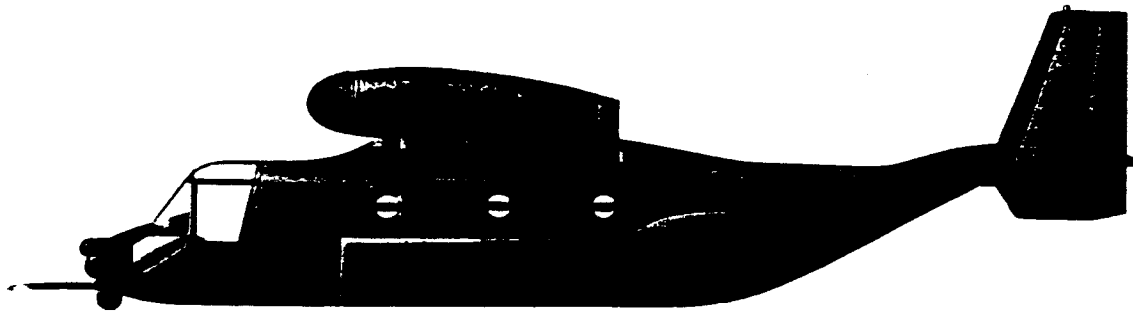
Bell/Boeing V-22 Osprey as it is expected to appear in US Marine Corps service.

The basic helicopter has in its normally accepted configuration (with either a single main rotor and anti-torque tail rotor or twin counter-rotating rotors to overcome torque) two major shortcomings, its comparatively low forward speed and high operating costs. Many manufacturers have explored means of overcoming these disadvantages, to give improved performance and lower operating costs to an aircraft with the helicopter's VTOL capability, but there is not the space here to ... of V ... ... apph ... to the problem. However, Bell has been working for almost 40 years on tilt-rotor systems and as early as 18 December 1958 demonstrated with its second Model 200 prototype (US Army designation XV-3), that it was possible to take off or land vertically with twin rotors that could be tilted progressively forward to act as propellers for horizontal flight. Continuing research and development by Bell led to the company's Model 301, US Army designation XV-15, which is a twin tilt-rotor research aircraft powered by two 115.6 kW (1,550 shp) Lycoming LTC1K-4K turboshaft

engines. The first of the two XV-15 research prototypes was flown on 3 May 1977 and they have since demonstrated helicopter forward speeds of up to 100 kts (185 km/h; 115 mph), and with the rotors tilted fully forward, horizontal flight cruising speeds of 301 kts (558 km/h; 347 mph).

Bell teamed up with Boeing Vertol to submit a design proposal for the US government's Joint Services Advanced Vertical Lift Aircraft (JVX), and on 26 April 1983 the team was awarded a contract covering the preliminary design phase. Based on the XV-15 techniques, the **Bell/Boeing Vertol JVX,** which has since been designated **V-22 Osprey,** is a twin-engine tilt-rotor aircraft for deployment by all US armed services for amphibious assault carrying up to 24 troops, and suitable also for such roles as combat SAR, electronic warfare and special operations. If a go ahead for full scale development is given during 1985, Bell and Boeing Vertol have estimated that a first flight will be made during August 1987, with initial entry into service following in 1991.

Specification: Bell/Boeing Vertol JVX
Origin: USA
Type: tilt-rotor multi-role aircraft
Powerplant: two General Electric T64-GE-717 turboshaft engines, each with a maximum power rating of 3620 kW (4,855 shp)
Performance: (provisional) maximum cruising speed 261 kts (483 km/h; 300 mph), range with pilot and 24 troops 740 km (460 miles) at 3,000 ft (915 m)
Weights: (provisional) maximum take-off VTOL 19,867 kg (43,800 lb), maximum take-off STOL 24,948 kg (55,000 lb)
Dimensions: (provisional) rotor diameter, each 11.58 m (38 ft 0 in), width overall 25.76 m (84 ft 6 in), length 17.32 m (56 ft 10 in), height, rotors in take-off position 6.15 m (20 ft 2 in), rotor disc area, total 210.72 m² (2,268.24 sq ft)
Armament: nose-mounted 12.7-mm (0.5-in) multi-barrel machine-gun

Bell/Boeing V-22 Osprey

This impression shows the V-22 in its intended role of assault transport. The type will be well suited to Marine Corps operations, providing rapid and versatile transport from ship to shore.

FIGURE 26: BELL/BOEING V-22 OSPREY
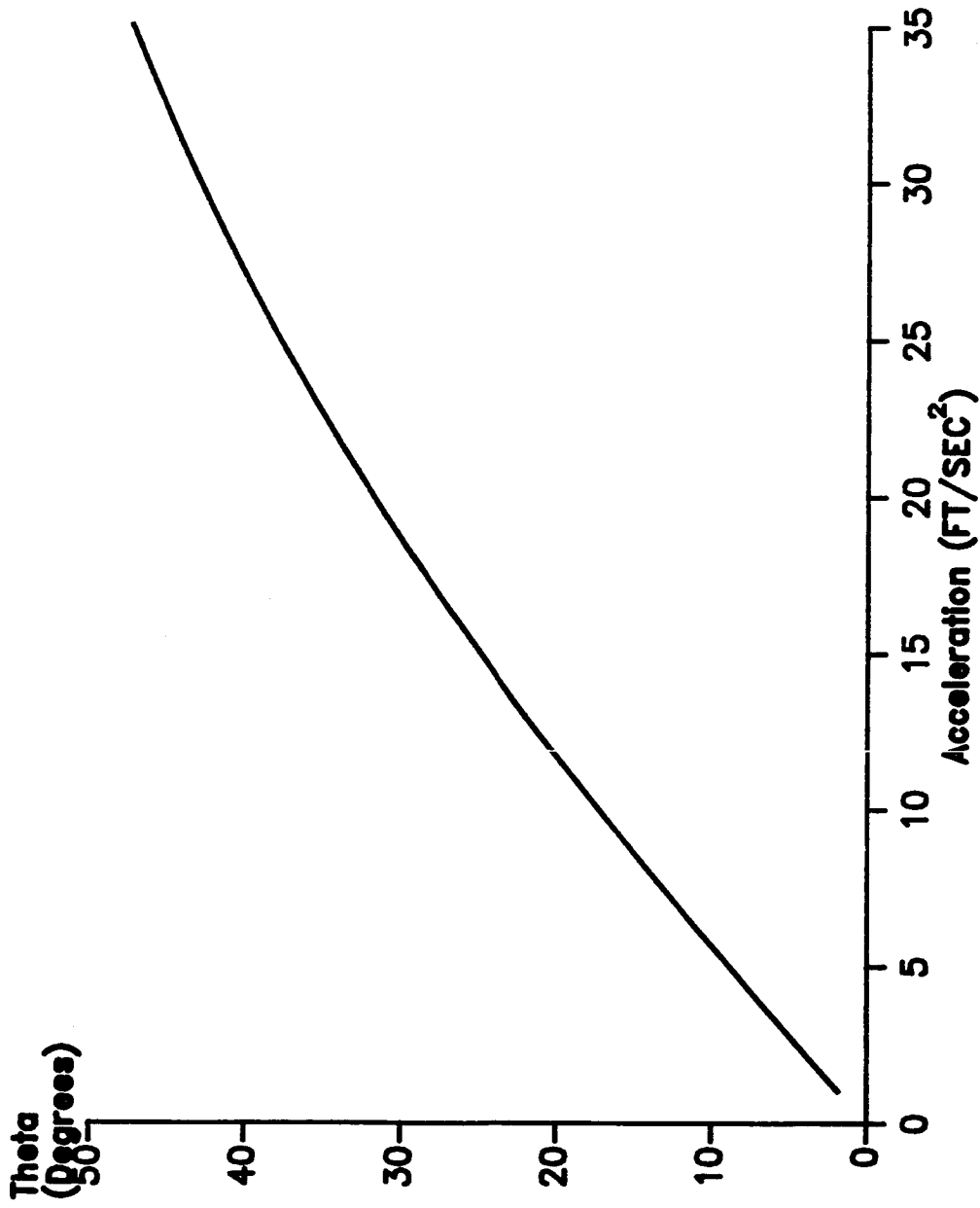
Figure 27: Angle between the Vertical and Cable vs. Acceleration
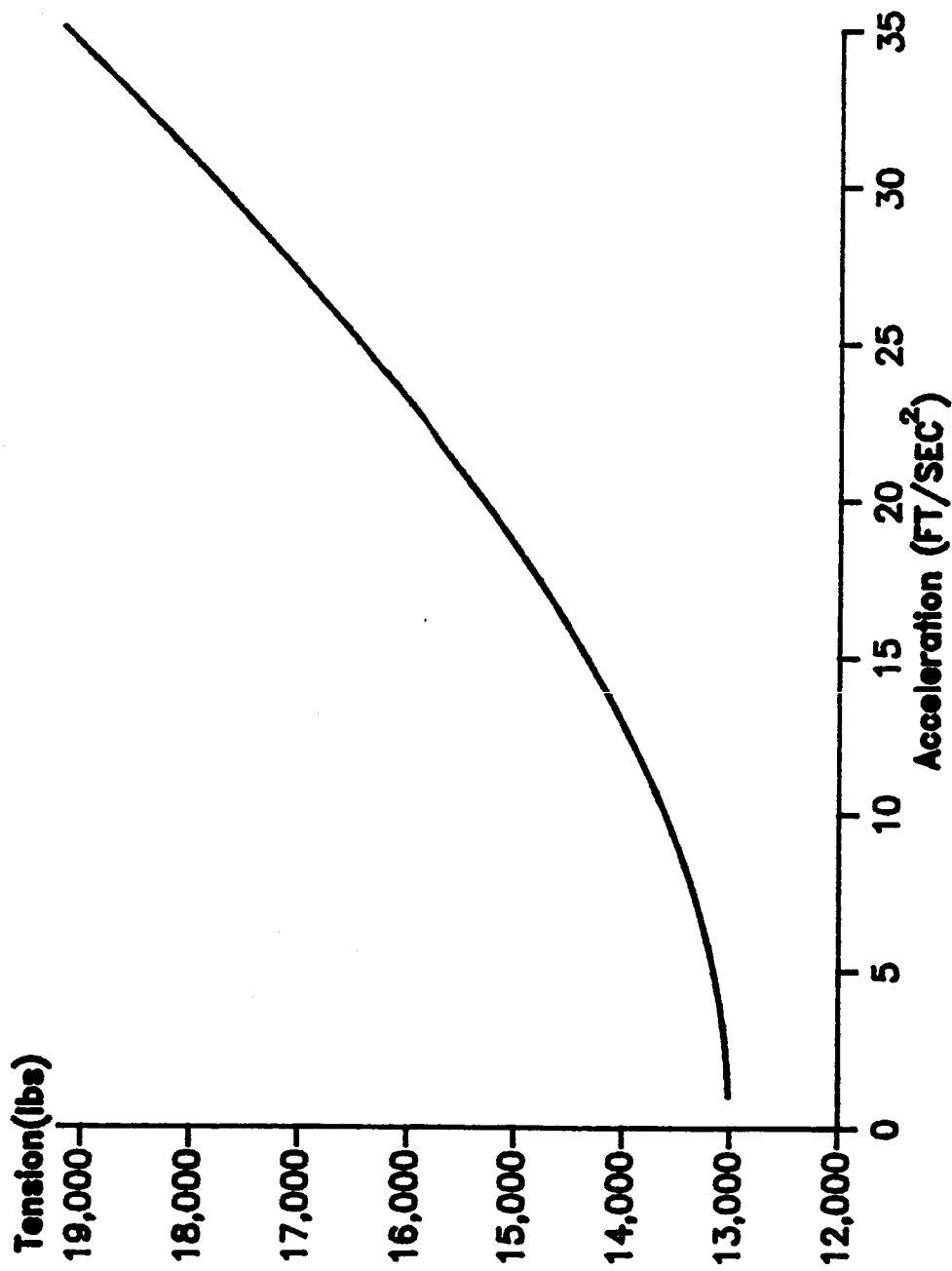
Figure 28:   Tension in the Cable
             vs. Acceleration

66
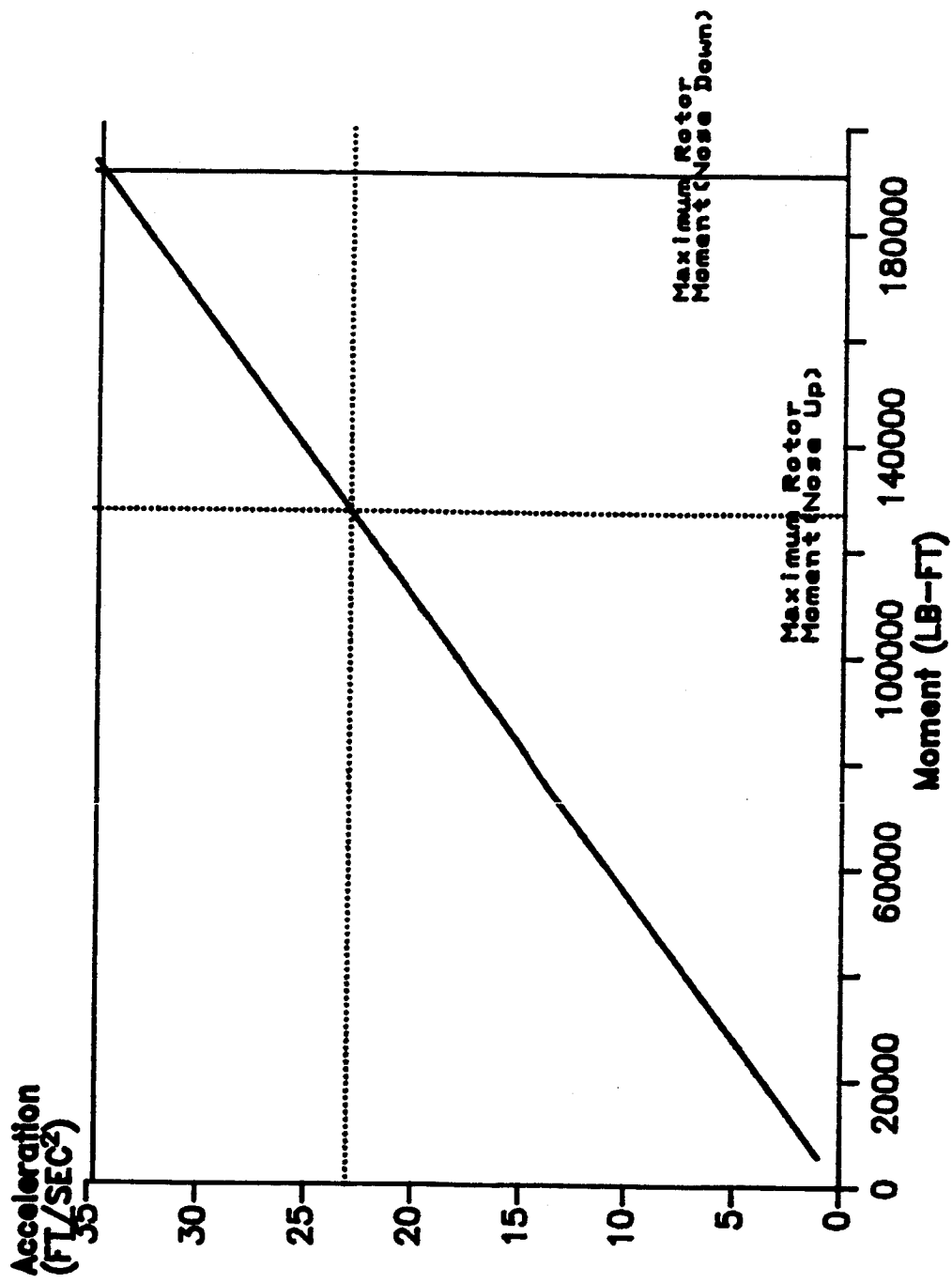
Figure 29: Helicopter Acceleration vs. Moment about CG
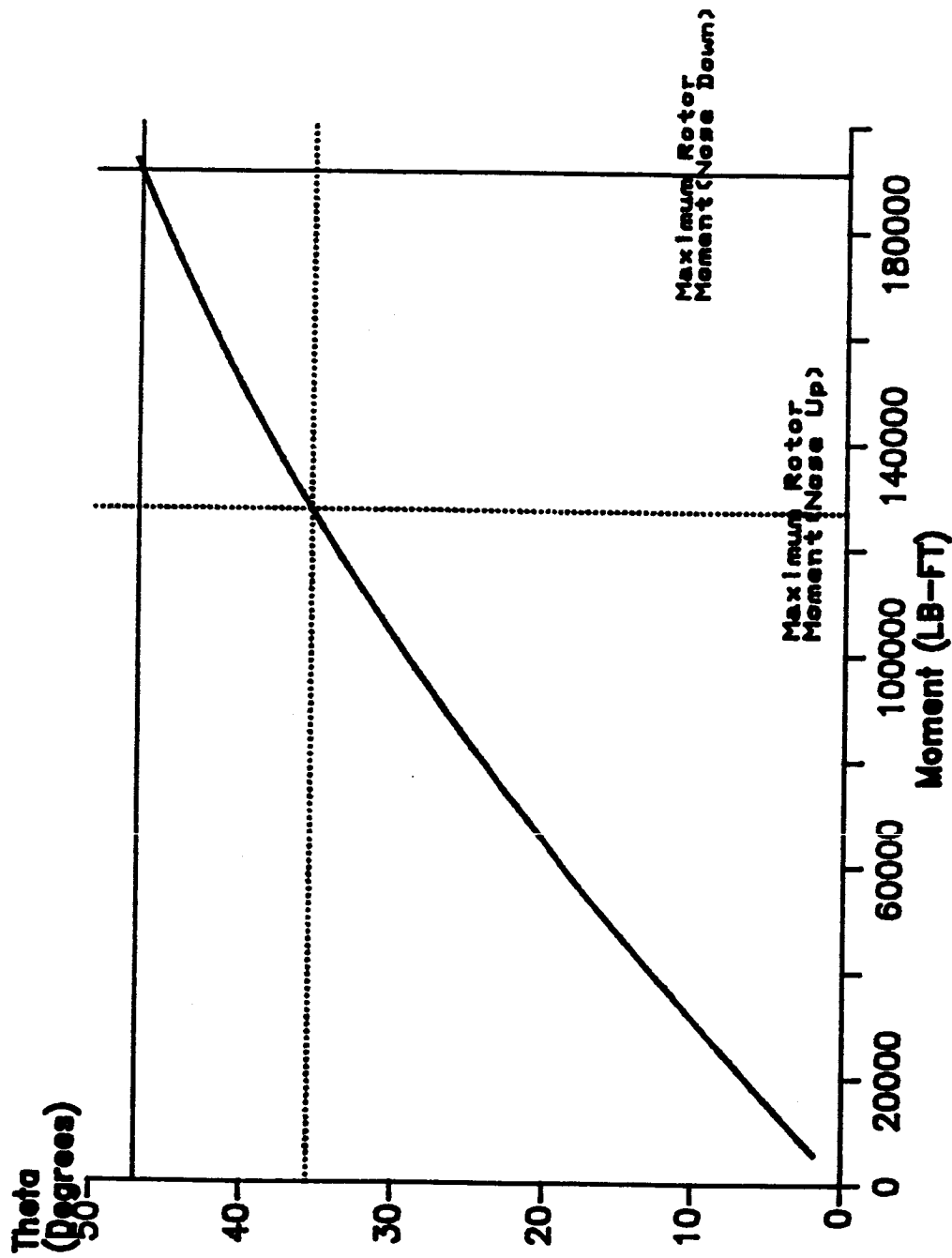
FiGURE 30: Angle between the Vertical and Cable vs. Moment about CG
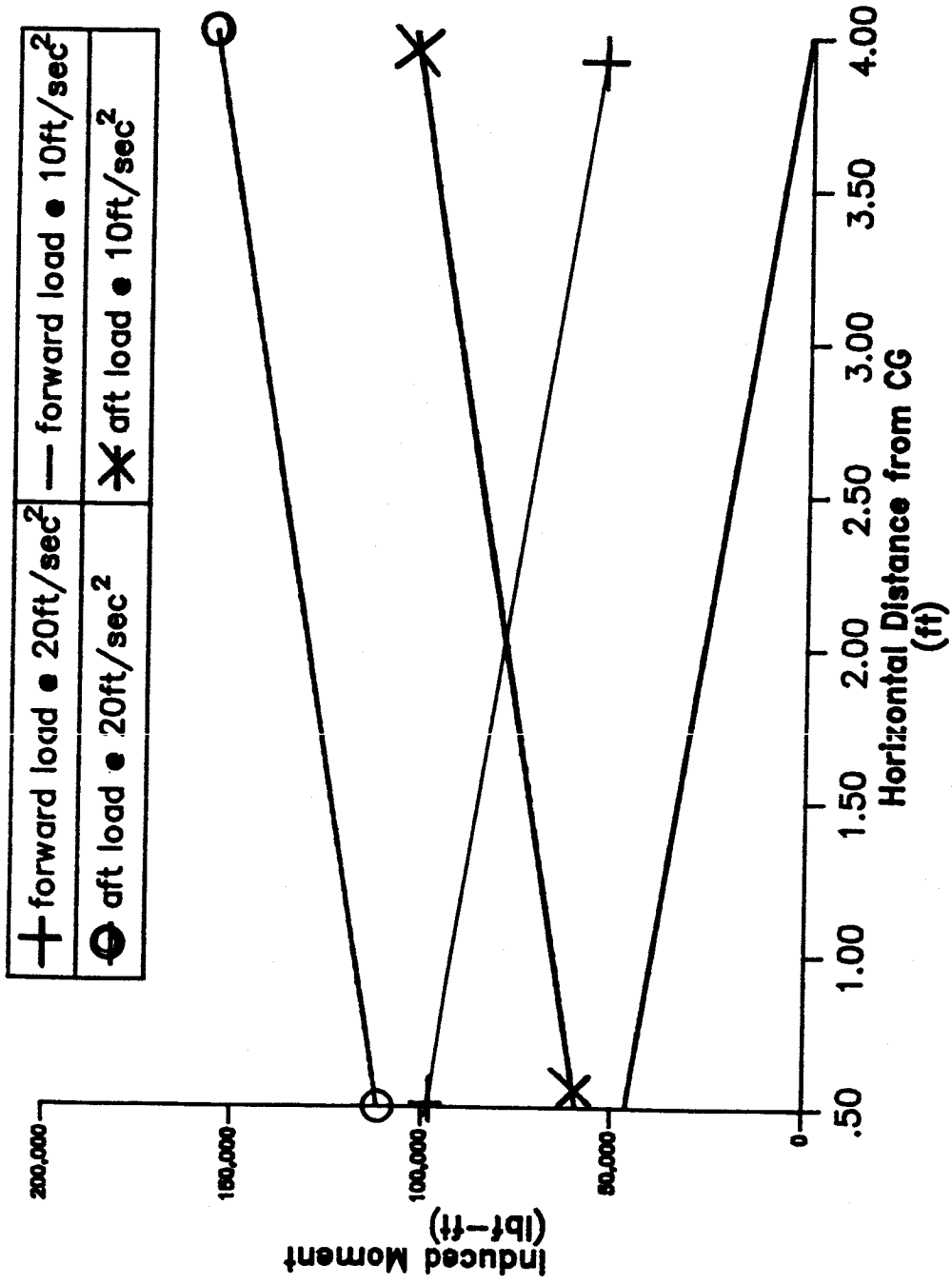
FIGURE 31: Induced Moments caused by Helicopter Deceleration plotted against distance away from CG Location (forward & aft)

69

Table 1. Tether released deployment characteristic summary

Factor	Criteria	Result
Length	under 50 km	44 km
Time	under 1 hour	55 minutes
Librations	under 65 degrees	maximum at approximately 45 degrees
Propellent Savings	over 10%	maximum of 4%

Table 2. Performance of baseline vehicle at
different deorbit velocities

Initial Velocity (km/s)	Max g Loading (g's)	Maximum Heating (Watt/m²)	Mach Number (-)	Range Obtained (km)	Time (sec.)
5.00	4.54	507016.19	0.52	2601.22	1202.37
5.50	3.07	514626.25	0.52	3307.41	1337.53
6.00	2.60	573051.63	0.52	4212.40	1495.09
6.50	2.05	609663.31	0.52	5431.07	1690.65
7.00	1.56	607643.25	0.52	7210.61	1854.98
7.50	1.20	534699.25	0.52	10318.81	2383.88
8.00	1.30	350007.50	1.11	21733.19	3599.18
8.50	0.25	389129.81	29.69	29281.21	3599.18
9.00	0.27	455087.50	31.19	29850.39	3599.18
9.50	0.37	522639.19	32.90	30516.25	3599.18
10.00	0.47	592984.00	34.82	30989.28	3599.18

Table 3. Perofornance of baseline vehicle at different deorbit
flight path angles

Inclination at 100 km (degrees)	Max g Loading (g's)	Maximum Heating (Watt/m²)	Mach Number (-)	Range Obtained (km)	Time (seconds)
-5.00	3.88	753840.19	0.46	6317.45	2121.74
-4.00	3.21	681100.00	0.46	6532.66	2155.33
-3.00	2.65	632243.88	0.46	6750.04	2189.52
-2.00	2.21	580816.94	0.46	6975.43	2226.52
-1.00	1.92	544133.56	0.46	7194.62	2258.91
1.00	1.90	539951.94	0.46	7638.01	2327.09
2.00	2.16	573678.38	0.46	7854.56	2362.08
3.00	2.57	622801.44	0.46	8058.40	2392.07
4.00	3.11	680693.63	0.46	8252.40	2422.67
5.00	3.77	743123.44	0.46	8425.17	2449.26

Table 4. Performance of baseline vehicle with different
ballistic parameters

Ballistic Parameter (kg/m²)	Max g Loading (g's)	Maximum Heating (Watt/m²)	Mach Number (-)	Range Obtained (km)	Time (seconds)
1481.48	1.80	1338045	4.1228	20829	4796
740.74	1.81	1287521	0.5487	10891	3242
493.83	1.88	1241111	0.5342	7319	2228
370.37	1.98	1198376	0.5167	5539	1707
296.30	2.10	1157762	0.5023	4484	1412
246.91	2.24	1120509	0.4824	3793	1220
211.64	2.38	1085974	0.4669	3302	1084
185.19	2.53	1054011	0.4499	2942	987
164.61	2.69	1024331	0.4326	2666	913
148.15	2.84	996406	0.4171	2448	858
134.68	2.99	970841	0.4029	2275	814
123.46	3.15	946782	0.3894	2134	779
113.96	3.29	924058	0.3764	2017	751
105.82	3.44	902925	0.3646	1921	728
98.77	3.57	883312	0.3535	1839	710
92.59	3.71	864535	0.3431	1768	694
87.15	3.84	847133	0.3336	1707	681
82.30	3.97	830429	0.3248	1653	671
77.97	4.09	814531	0.3166	1608	662
74.07	4.20	800002	0.3091	1568	655

Table 5. Performance of baseline vehicle with different L/D´s

L/D (-)	Max g Loading (g´s)	Maximum Heating (Watt/m^2)	Mach Number (-)	Range (km)	Time (seconds)
0.25	6.56	1059901.00	0.74	1449.60	453.15
0.50	4.33	943800.63	0.69	2085.94	662.50
0.75	2.68	760690.06	0.64	2866.70	902.64
1.00	2.35	700582.94	0.60	3702.17	1156.38
1.25	2.17	651085.94	0.55	4558.54	1424.31
1.50	2.05	609663.31	0.52	5431.07	1690.65
1.75	1.98	574273.50	0.49	6310.70	1874.58
2.00	1.92	544133.56	0.46	7194.62	2258.81
2.25	1.89	517774.56	0.44	8083.57	2538.84
2.50	1.86	494697.56	0.42	8966.49	2802.57
2.75	1.84	474190.56	0.40	9856.62	3098.90

Table 6. Performance of different L/D´s at different
deorbit velocities

Initial Velocity (km/s)	L/D (-)	Max g Loading (g´s)	Maximum Heating (Watt/m^2)	Mach Number (-)	Range (km)	Time (seconds)
7.80	1.50	1.29	711166	0.5173	15260	3032
	1.60	1.31	690027	0.5064	16247	3231
	1.70	1.31	669616	0.4968	17238	3436
	1.80	1.24	650978	0.4852	18230	3634
	1.90	1.27	632551	0.4689	19234	3836
	2.00	1.25	615580	0.4625	20237	4040
7.85	1.50	1.32	681070	0.5168	16727	3221
	1.60	1.28	656170	0.5082	17820	3437
	1.70	1.29	638198	0.4965	18909	3651
	1.80	1.28	624106	0.4854	20004	3862
	1.90	1.23	608241	0.4688	21084	4073
	2.00	1.23	591658	0.4627	22169	4287
7.90	1.50	1.30	656106	0.5166	18796	3483
	1.60	1.27	635769	0.5061	20056	3721
	1.70	1.26	618260	0.4966	21272	3951
	1.80	1.25	598450	0.4850	22500	4180
	1.90	1.24	584985	0.4691	23729	4409
	2.00	1.25	570156	0.4625	24949	4638

Table 6. (continued)

Initial Velocity (km/s)	L/D (-)	Max g Loading (g's)	Maximum Heating (Watt/m²)	Mach Number (-)	Range (km)	Time (seconds)
7.95	1.50	1.31	629820	0.5174	21880	3874
	1.60	1.28	618860	0.5061	23394	4144
	1.70	1.27	601200	0.4963	24857	4404
	1.80	1.28	580678	0.4851	26323	4660
	1.90	1.25	569328	0.4689	27779	4920
	2.00	1.26	557350	0.4626	29210	5176
8.00	1.50	1.29	625307	0.5169	28734	4736
	1.60	1.29	600762	0.5058	30719	5063
	1.70	1.26	593990	0.4967	32625	5380
	1.80	1.26	577568	0.4854	34490	5687
	1.90	1.27	558763	0.4690	36278	5986
	2.00	1.26	546462	0.4626	38012	6281
8.05	1.50	1.27	638127	0.5168	42006	6395
	1.60	1.27	620257	0.5059	43630	6678
	1.70	1.28	601488	0.4967	45376	6974
	1.80	1.26	585698	0.4848	46887	7236
	1.90	1.26	576338	0.4689	48389	7501
	2.00	1.27	562008	0.4624	50140	7797
8.10	1.50	1.30	659033	0.5167	50171	7411
	1.60	1.29	641006	0.5058	51981	7717
	1.70	1.27	625710	0.4968	54123	8062
	1.80	1.24	607915	0.4848	56030	8375
	1.90	1.24	596569	0.4690	57878	8682
	2.00	1.26	587924	0.4626	59712	8980
8.15	1.50	1.27	684108	0.5174	56863	8242
	1.60	1.30	670369	0.5058	58643	8545
	1.70	1.30	653970	0.4968	60469	8850
	1.80	1.24	640366	0.4851	62259	8980
	1.90	1.27	626514	2.3547	64011	8980
	2.00	1.26	613473	6.4068	65745	8980
8.20	1.50	1.30	714539	0.5171	31470	8810
	1.60	1.31	700568	0.5064	63284	8980
	1.70	1.32	687936	2.6894	65045	8980
	1.80	1.24	672604	7.2928	66728	8980
	1.90	0.94	662712	11.3458	67800	8980
	2.00	0.81	656193	14.5266	68510	8980

Table 7. Deceleration Devices

Device	Description	Advantages	Disadvantages
Conventional Rocket	-Rocket	-Experience	-Propellent requirements
Aeroshields	-Flexible/ rigid drag brakes	-Thermal protection abilities	-Weight -Insufficient data
Rearbody Ballute	-Balloon type inflatable parachute	-Stable in upper atmosphere -No propellent	-Not good for reentry due to shock impingment
Forebody Ballute	-Balloon type inflatable parachute	-Stable -Operational for 0.5<M<6.0 -Highly reliable -Reduces atmosphere heating -Drag modulator -Low cost -No unique subsystem needed	-Weight -Shock impingment
Rotornet	-Flexible spinning disk	-Can be large without increas- ing overall system weight	-Violent and spiral divergence -Traveling wave flutter causing rotation
20-degree Conical Parachute	-Drogue parachute	-Used with Space Shuttle solid rocket boosters	-Excessive weight
Hemisflo	-Supersonic drogue	-Stable -Reduced oscillation -Applicable for 1.5<M<2.5	
Hyperflo	-Spersonic drogue	-Applicable for M=4.0	
Parafoil	-Inflatable wing	-Lightweight -Good performance	

Table 8. size of parachutes for requiring velocities

Altitude Change (km)	Parachute	Velocity Change (m/s)	Required Surface Area (m²)	Diameter (m)
10 to 9	Ringslot	146.6 to 90.76	60.95	8.8
9 to 5.5	Ringsail	90.76 to 9.50	2408.7	55.4

Table 9. Apollo Earth Landing System [Ref. West, 1973]

Supersonic drogue parachutes deployed at: 7.3 km
Main parachutes (ringsail) deployed at: 3.4 km
Full inflation of main parachutes at: 2.7 km
Apollo's total altitude distance for deceleration to 9.8 m/s: 4.6 km
ACRV's total altitude distance for deceleration to 9.5 m/s: 4.5 km

Table 10. Estimated Mission Gross Weight/Center of Gravity

	Weight	Horizontal Arm	Lateral Arm	Vertical Arm
Weight Empty	33,519	374.2	2.6	192.2
Fixed Useful Load	1,674	262.6	-8.6	133.2
Basic Weight	35,193	368.9	2.1	189.4
Crew (4)	800	157.1	0.0	135.8
Operating Weight	35,993	364.2	2.0	188.2
Full Fuel (986 Gal.)	6,705	313.7	0.0	176.8
Gross Weight - Full Fuel	42,698	356.3	1.7	176.8
Single-Point Load	22,050	356.0	0.0	140.0
Gross Weight	64,748	356.2	1.1	164.3

Note: Above weights include refueling probe single-point
        suspension system

76

Table 11. Miscellaneous Data

<u>Transmission Limits</u>
    MAX, 10 min.   137% Q or 13,140 hp.
    MIL, 30 min.   121% Q or 11,570 hp.
    NRP, Continuous   100%

<u>Load Factors</u>

<u>Gross Weight</u>	<u>Positive</u>	<u>Negative</u>
46,500 lbs	3.00	-0.50
68,750 lbs (internal load)	2.20	-0.33
73,500 lbs (external load)	2.09	-0.00

<u>Refueling Probe</u>
    Design Limit Loading Conditions
        (a) Axial load, 1000 lbs tension combined with a radial load
            of 1000 lbs applied at the probe tip.
        (b) Axial load, 2000 lbs compression applied at probe tip.

<u>Main Rotor Lift and Head Moments</u>
    Hub Moment Constant 191,520 in-lb/deg Max Longitudinal Flapping
        12 degrees forward
         8 degrees aft

    Main Rotor Head Moment (maximum)
      -191,000 ft-lb (nose down)
       127,000 ft-lb (nose up)

    Maximum Rotor Lift Steady-State
      Approximately 139,000 lbs lift at 11,000 horsepower

    Location of Main and Tail Rotor Hub Reference Points

	<u>Main Rotor</u>	<u>Tail Rotor</u>
FS	336.215	930.711
WL	259.265	289.005
BL	0.0	80.361

(10.0) REFERENCES

AIAA Aerodynamic Deceleration Systems Conference, An Investigation of Parachute Opening Loads, and a New Engineering Method for Their Determination, Dayton, Ohio, 14-16 September 1970.

AIAA 9th Aerodynamic Deceleration and Balloon Technology Conference, A Collection of Technical Papers, Albuquerque, New Mexico, 7-9 October 1986.

Andrews, D. and Bloetscher, F. "Aerobraked Orbital Transfer Vehicle Definition," AIAA Aerospace Sciences Meeting, 12-15 January 1981.

Carleton, W. and Anderson C. "The Characteristics of Several Hyperflo Drogue Parachutes in the Wake of the Full-Scale SV-5D Vehicle at Supersonic Mach Numbers," Arnold Engineering Development Center, Air Force Systems Command, Arnold Air Force Station, TN, January, 1966.

Ewing, E., Bixby, H., and Knacke, T. Recovery Systems Design Guide, Government Printing Office, Washington, D.C., 1978.

Hankey, Wilbur. Reentry Aerodynamics, AIAA Education Series, Washington, D.C., 1988.

Knacke, T. Parachute Recovery Systems Design Manual, Aerosystems Department, Naval Weapon Center, July 1985.

Loh, W. Re-entry and Planetary Entry Physics and Technology II Dynamics, Physics, Radiation, Heat Transfer, and Ablation, Springer-Verlay, New York, 1968.

Marshall, Chris, The Defenders, Oriole Publishing, New York, 1988.

NASA Engineering Directorate Advanced Programs Office, "A Conceptual Design Study of a Crew Emergency Return Vehicle," August, 1988.

Reichenau, David. "Investigation of a Ballute Behind the Martin SV-5D Vehicle at Mach Numbers from 0.6 to 2.6," Defense Technical Information Center, Cameron Station, Alexander, Virginia, 10 March 1966.

Sims, Leland. "The Effects of Design Parameters and Local Flow Fields on the Performance of Hyperflo Supersonic Parachutes and High Dynamic Pressure Parachute Concepts," Air Force Systems Command, Wright-Patterson Air Force Base, OH, October, 1965.

West, Robert B. "Apollo Experience Report - Earth Landing System," Government Printing Office, Washington, D.C., 1973.

Theory

A few of the concepts used in this report that deal with the analysis of tether applications are presented here.

The fundamental force affecting tethered satellites is the gravity gradient force arising from the difference in radius between two masses that are separated by some vertical distance and connected by a tether [NASA, 2-1 to 2-10]. The higher mass experiences a larger centrifugal force than the lower, which conversely experiences a greater gravitational force. This is because the tension in the tether causes the two masses to travel with the same angular velocity as the system's center of gravity, which is the only point where the two forces balance.

This gravity gradient force is given by [NASA 2-7]:

$$Fgg = \mu m \left[\frac{(r + L)^3 - r^3}{r^3 (r + L)^2} \right]$$ (A1.1)

where μ is the Earth's gravitational parameter, m is the end satellite mass, r is the radius of the center of gravity, and L is the tether length. This force governs the tension felt in the tether as well as the force accelerating it while it deploys.

The equations of motion for the simple case of the "dumbbell satellite" are given by [Bergamaschi, 106]:

$$\theta'' + \frac{2L'\theta'}{L} + 3n^2 \theta = -\frac{2nL'}{L}$$ (A1.2)

79

$$\phi'' + \frac{2L'\phi'}{L} + 4n^2\phi = 0 \qquad (A1.3)$$

where Θ is the offset angle from the local vertical in the orbit plane, ϕ is the out of plane offset angle, n is the mean orbit motion, and the apostrophes designate differentiation with respect to time. These equations are used in this paper to analyze the motions of the TRD system.

There are a few assumptions regarding the Keplerian orbit that the vehicle follows. They are that the vehicle travels with the same orbital angular velocity as the SSF, that it has the same flight path angle as the SSF until release, and finally, that perturbation effects will be negligible. It should be kept in mind that a circular SSF orbit, which is central to the analysis, is an assumption in the first place.

Analysis Methodology

The analysis of TRD behavior is divided into three parts. The first part is a comparison using Keplerian orbital mechanics of a conventional rocket-propelled reentry to a TRD reentry, both involving Hohmann-Like transfers to an orbit of 100 nmiles (185km). Depending on the final velocity desired, different efficiencies result. The Hohmann transfer is selected as the model transfer simply as a baseline approach and also due to its efficiency and simplicity [Bates, 163-166]. The orbit of SSF is approximated as a circle of 6775.5 km radius.

The libration and time of deployment for the model TRD are evaluated in the next part of the analysis. *Numerically* Solving equations (1), (2), and (3) in a fourth-order Runge-Kutta scheme was *an available means* to predict these values. These are important effects in consideration of the ACRV time limit as well as SSF impact of a TRD system.

Lastly, an analysis of tether tension and estimated mass and diameter were

completed for a Kevlar 29 tether. These values are important in discussions of SSF effects and reel sizes.

Conventional Rocket Propelled Transfer

The equations governing the Hohmann-like transfer of a conventional rocket orbit are:

$$a_t = \frac{(r_1 + r_2)}{2} \tag{A1.4}$$

$$v_{t1} = \sqrt{2(\epsilon + \frac{\mu}{r_1})} \qquad\qquad v_{t2} = \sqrt{2(\epsilon + \frac{\mu}{r_2})} \tag{A1.5}$$

$$v_1 = \sqrt{\frac{\mu}{r_1}} \tag{A1.6}$$

$$\delta v = |(v_{t1} - v_1)| + |(v_2 - v_{t2})| \tag{A1.7}$$

$$m_p = 5000 \ (1 - e^{\frac{\delta v}{I_{sp}*g}}) \ \text{kilograms} \tag{A1.8}$$

$$\tau = \pi \sqrt{\frac{a_t^3}{\mu}} \tag{A1.9}$$

Tether Released Deployment

The calculation of orbital velocities required for a TRD was done in two parts. The first involved calculating the required length of a tether that would be able to deposit the ACRV onto an orbit whose perigee was located at 6469 km, which equals the 100 nmi entry height. This requires the assumption that the center of gravity of the TRD system will remain within or very close to SSF. The space station is expected to have an approximate mass of 250,000 kg, which is much larger than that of the 5000 kg ACRV [NASA, 3-117].

81

Tether length was determined using the orbital equations in a computer program which is included in the appendix [Bates, Chapter 1]. The release velocity that takes the place of v_1 and v_{t1} is calculated by taking the product of the relative velocity of an object traveling with SSF's angular velocity of 1.13203×10^{-3} rad/sec and a radial distance for the ACRV of the quantity (6775.5 - L) km. This velocity can also be called v_{t1}.

Knowing this radius, (6775.5 - L) km, and velocity, v_{t1}, a radius of perigee can be calculated for the sudden release of the tethered ACRV at some distance from SSF. Equation 5 is first used to calculate the transfer orbit's energy. The semi-major axis is then calculated by:

$$a = -\frac{\mu}{2\varepsilon} \qquad (A1.10)$$

Angular momentum is found from:

$$h = (6775.5 - L)\, v_{t1}\, \cos\beta \qquad (A1.11)$$

where β, the flight path angle, is zero at the instant of release since the ACRV is traveling in a circular motion up to that point. The Semi-Latus Rectum, p, is determined by:

$$p = \frac{h^2}{\mu} \qquad (A1.12)$$

The radius of perigee, r_p, can then be calculated by

$$r_p = \frac{p}{1 + \sqrt{\frac{1-p}{a}}} \qquad (A1.13)$$

where the target $r_p = r_2 = 6563$ km.

A tether length was determined by this method using the program already mentioned. As part of this analysis, the final transfer velocity, v_{t2}, was

calculated by equation 5.

The second part of these calculations involved placing this v_{t_2} into equations 9 and 1 of the first program, as mentioned in the report, for comparison to the rocket reentry. This is analogous to the ACRV deploying by tether for some distance, being released and coasting until it reaches the perigee of this coasting orbit, and finally firing a retrorocket in order to slow for some reentry velocity. Note that this analysis presents a worst case length possible within a certain range of entry velocities for which a longer tether would result in a smaller radius of perigee and reentry occurring without any propellant at all.

Total time was found by

$$\tau = \tau_{TRD} + \pi \sqrt{\frac{a^3}{\mu}} \tag{A1.14}$$

Tether Libration Analysis

In order to more fully understand the motions of the TRD, Equations (1), (2), and (3) were parameterized into a fourth-order Runge-Kutta scheme [Ferziger, 79], which is listed in the appendix of the report. The libration model equations, Equations (2) and (3), are parameterized as

$$x'(1) = \theta' \qquad x'(2) = -2(\frac{L'\theta}{L\cos\theta} + \frac{nL'}{L\cos\theta}) - 3n^2\theta \tag{A1.15}$$

$$x'(3) = \phi' \qquad x'(4) = -2(\frac{L'\phi}{L\cos\theta} + 2n^2\phi) \tag{A1.16}$$

where $x(1) = \theta$

$x(2) = \theta'$

$x(3) = \phi$

$x(4) = \phi'$

while the gravity-gradient acceleration [Ref NASA, 2-6] is given by dividing Equation (1) by the mass term and parameterizing

$$x''(5) = L' \qquad x''(6) = \frac{\mu[(r + L\cos\theta)^3 - r^3]}{r^3 (r + L\cos\theta)^2}$$
(A1.17)

Starting conditions were pulled from a report [NASA MSC, 35] for a Space Shuttle TRD. These conditions were

$$\text{Length}(0) = 1 \text{ km} \qquad \text{Velocity } (0) = 3 \text{ m/s}$$

They were incorporated into the Runge-Kutta program, which echo checks the two values.

Tether Mass Properties

Equation (1) gives a straightforward method to estimate the tension present in a tether of length L. The determination of tether mass and diameter needed to accept this tension can be accomplished using some material properties [Martin Marietta, 2-7] of Kevlar 29:

$$So = 6.92*10^8 \text{ N/m}^2 \quad (F.S. = 4) \quad \text{density} = 1493 \text{ kg/m}^3$$

which for a tension, P:

$$\text{Area} = \frac{P}{So}$$
(A1.18)

$$\text{where Area} = \pi r^2$$
(A1.19)

Tether mass and diameter is given below.

Tether Mass Properties

Tension	667.5 N
Area	$9.646*10^{-7} \text{ m}^2$
Diameter	0.001108 m
Mass	50.26 kg

Appendix 2 - Computer Simulation for a Reentry Vehicle

Nomenclature

c	constant
C_D	coefficient of drag
C_L	coefficient of lift
D	drag
g	gravitational constant (9.80665 m/s^2)
h	altitude
L	lift
m	mass
$\dot{Q}$	convective heating rate
R	radial height
R_n	nose radius
S	wetted area
V	velocity
W	weight
α	inclination angle
Δ	ballistic parameter
ρ	density

This program was designed to simulate the reentry of a vehicle through the Earth's atmosphere. By doing this simulation, the trajectory of various types of vehicles could be studied. To do the simulation, the equations of motion of an entry vehicle as determined by Hankey [Hankey, 1988, p.25] are given by:

$$\frac{V\dot{\alpha}}{g} = \frac{L}{W} - \left[1 - \frac{V^2}{gR}\right]\cos\alpha \qquad (A2.1)$$

$$-\frac{\dot{V}}{g} = \left(\frac{D}{W}\right) + \sin\alpha \qquad (A2.2)$$

$$\dot{R} = \dot{h} = V\sin\alpha \qquad (A2.3)$$

By integrating these equations with a fourth-order Runge-Kutta method, different trajectories can be studied.

In the studies done thus far, the area of the vehicle, S, was found by taking into consideration the dimensions of the shuttle bay and that the shuttle should be able to carry two ACRV's at once. For this simulation, S was set to 20.25 m^2. The mass of the reentry vehicle was given as 6,000 kg.

$$\Delta = \frac{mg}{C_D S} \qquad (A2.4)$$

$$C_D = \frac{mg}{\Delta S} \qquad (A2.5)$$

With this defining the C_D, the C_L can then be varied to achieve a different L/D. Thus, by varying the C_L, different types of vehicles with different L/D's can be simulated in reentry.

To calculate the convective heating rate at the stagnation point, the Sutton Graves equation was used.

86

C-2

$$\dot{q}_{s,conv} = c \ (R_n)^{-.5} \ (\rho)^{.5} \ (V)^3 \qquad\qquad (A2.6)$$

where $c = 1.74153 \times 10^{-4} \ kg^{.5}/m$.

```
CCCCCCCCCCCCCCCCCCCCCCCCCCCCCCCCCCCCCCCCCCCCCCCCCCCCCCCCCCCCCCCCCCCCC
C                                                                   C
C     PROGRAM: INTEGRATION BY RK4                                    C
C                                                                   C
C     AUTHOR: DAN VERGANO & JIM GALASSO   AERSP 401B SPRING 1990     C
C     PENNSYLVANIA STATE UNIVERSITY                                  C
C                                                                   C
C     DESCRIPTION:  THIS PROGRAM IS DESIGNED TO INTEGRATE ODE'S      C
C                   USING A RUNGE-KUTTA METHOD                       C
C                   OF NUMERICAL INTEGRATION. THE RESULTS OF BOTH    C
C                   WILL BE COMPARED IN THE FINAL OUTPUT.            C
C                                                                   C
C                   THE RK4 PORTION WORKS AS FOLLOWS.  AFTER         C
C                   RECEIVING THE INITIAL VALUES, THE PROGRAM CALLS  C
C                   THE RUNGE-KUTTA ROUTINE KMAX TIMES. THE RUNGE-   C
C                   KUTTA ROUTINE INTEGRATES THE FUNCTION IN  4      C
C                   STEPS EACH INVOLVING A FUNCTION CALL AND A TEMPORARY
C                   VARIABLE VALUE FOR EVERY VARIABLE BEING INTEGRATED
C                   WHICH IS PLACED IN THE NEXT STEPS FUNCTION CALL. C
C                   AS PART OF THE 4TH STEP VALUES ARE CALCULATED    C
C                   FOR THAT TIME STEP.                              C
C                                                                   C
C                                                                   C
C     VARIABLE LIST:                                                 C
C              X - ARRAY OF DIMENSION NDIM CONTAINING X VALUES       C
C           XDOT - ARRAY OF DIMENSION NDIM CONTAINING X DERIVATIVES
C           NDIM - NUMBER OF ODE'S TO BE INTEGRATED                  C
C              H - INTEGRATION TIME STEP                             C
C           TEMP - ARRAY HOLDING ALL VALUES FOR LATER COMPARISION C
C         YSTAR1 - TEMPORARY VALUE (X+H/4 STEP) IN RK4 ROUTINE       C
C         YSTAR2 - TEMPORARY VALUE (X+H/3 STEP) IN RK4 ROUTINE       C
C         YSTAR3 - TEMPORARY VALUE (X+H/2 STEP) IN RK4 ROUTINE       C
C           TIME - HOLDS TIME STEP, NOT USED IN THIS PROBLEM         C
C                                                                   C
C                                                                   C
C                                                                   C
C     SUBROUTINES:                                                   C
C              F - FUNCTION CONTAINING ODE'S                         C
C           RK4A - SUBROUTINE WHICH PERFORMS RUNGE-KUTTA METHOD      C
C           VINH - DENSITY PRODUCING SUBROUTINE                      C
C_____C
         DIMENSION X(9), XDOT(9), TEMP(10)
         DIMENSION YSTAR1(9), YSTAR2(9), YSTAR3(9)
        DOUBLE PRECISION DENS,TIME,INCLIN,H,X,TEMP,XDOT,YSTAR1, YSTAR2
     *                   ,YSTAR3,CL,CD,LD
         EXTERNAL F
       CL = 0.10
       CD = 0.10
       LD = CL/CD
C ******SET INITIAL CONDITIONS******ECHO CHECK*******
C ====>  INITIAL APPROACH ANGLE (DEGREES)
         INCLIN = 2.5
C ******INITIAL APPROACH ANGLE CONVERTED TO RADIANS*****
 X(1) = INCLIN/180*3.14159
C ===========>  INITIAL VELOCITY (KM/S)
         X(2) = 7.0
C ===========>  INITIAL RADIUS (KM)
         X(3) = 6478.000
```

```
                   WRITE (6,'(///)')
 20                FORMAT (10X,A60,/)
                   WRITE(6,20) '***** INITIAL CONDITIONS OF VEHICLE AT 100 KM ALTI
         *TUDE *****'
                   WRITE(6,'(A30,F5.2)') 'INCLINATION ANGLE (DEGREES): ',INCLIN
                   WRITE(6,'(A30,F6.3)') 'VELOCITY (KM/SEC):            ',X(2)
                   WRITE(6,'(A30,F5.2)') 'LIFT TO DRAG RATIO:          ',LD
 C >>>INSERT TIME STEP HERE (S)<<<
                   H =  0.500
 C     ===========>  NDIM = # OF EQ.S INTEGRATED
                   NDIM = 3
 C         **TIME VAR. ADDED IN CASE OF FUTURE USE OF PROGRAM**
                   TIME = 0.0
 C  %%%%%%%%%%%%  DENS -} INITIAL DENSITY, DUMMY VARIABLE
                   DENS = 0.0
 C  %%%%%%%%%%%%     KMAX = # OF ITERATIONS TO PERFORM
                   KMAX =  8000
 C         ********           KMAX *  H  = FINAL TIME   (SEC)
 C
 C   *******BEGIN SIMULATION LOOP*********
                   FLAG = 0
                   TEMP(5) = 0
                   TEMP(10) = 0
 800               FORMAT (3X,A12,4X,A8,4X,A8,4X,A16,3X,A12)
 810               FORMAT (7X,A5,7X,A8,6X,A4,12X,A4,12X,A5)
                   WRITE(6,800) 'ACCELERATION','VELOCITY','ALTITUDE','RANGE TRAVEL
         *ED','TIME ELAPSED'
                   WRITE(6,810) '(G S)','(KM/SEC)','(KM)','(KM)','(SEC)'
                   DO 100 K = 1, KMAX
 C   *******START RK4 ROUTINE AND STORES VALUES IN TEMP ARRAY***
                   CALL RK4A(X,XDOT,F,H,NDIM,YSTAR1,YSTAR2,YSTAR3,CL,CD)
                     TEMP(1)=(-XDOT(2)*1000/9.80665*(1+LD*LD)**(1./2.))
                     TEMP(2)=X(2)
                     TEMP(4)= X(3)-6378
                     TEMP(5)=(1./2.)*XDOT(2)*SIN(XDOT(1))*(H)*(H)+
         *              X(2)*COS(X(1))*H + TEMP(5)
                     TIME = TIME + H
                     FLAG = FLAG + 1
                     IF (TEMP(1).GT.TEMP(10)) THEN
                       TEMP(10) = TEMP(1)
                     ENDIF
                     IF (FLAG.EQ.10) THEN
                       WRITE(6,900) TEMP(1),TEMP(2),TEMP(4),TEMP(5),TIME
                       FLAG = 0
                     ENDIF
                     IF (TEMP(4).LE.0) THEN
                       WRITE(6,*) '*****  SURFACE OF EARTH REACHED!!! *****'
                       GOTO 500
                     ENDIF
 900               FORMAT (6X,F5.2,8X,F8.4,4X,F8.3,6X,F10.3,6X,F8.2)
 100        CONTINUE
 500         WRITE(6,'(A40,F6.2)') 'MAXIMUM ACELERATION IN SIMULATION (GS)'
         *      ,TEMP(10)
        END
         SUBROUTINE RK4A(X,XDOT,F,H,NDIM,YSTAR1,YSTAR2,YSTAR3,CL,
         *      CD)
 C
 C ###################################################################
```

```fortran
C #     INTEGRATES A SET OF 1ST ORDER DIFFERENTIAL EQUATIONS BY A    #
C #     FOURTH ORDER RUNGE-KUTTA METHOD.                             #
C #                                                                  #
C #     AUTHOR: DAN VERGANO          ALGORITHM: DR. L. LONG   PSU    #
C #                                                                  #
C ###################################################################
          DIMENSION X(NDIM),XDOT(NDIM), YSTAR1(NDIM)
          DIMENSION YSTAR2(NDIM), YSTAR3(NDIM)
         DOUBLE PRECISION X,XDOT,YSTAR1,YSTAR2,YSTAR3, H,CL,CD
          EXTERNAL F
C ********BEGINS ROUTINE**********
          CALL F(XDOT,X,NDIM,CL,CD)
          DO 250 I = 1, NDIM
           YSTAR1(I) = X(I) + .25*H*XDOT(I)
250       CONTINUE
          CALL F(XDOT,YSTAR1,NDIM,CL,CD)
          DO 300 I = 1, NDIM
           YSTAR2(I) = X(I) + .3333*H*XDOT(I)
300       CONTINUE
          CALL F(XDOT, YSTAR2, NDIM,CL,CD)
          DO 350 I = 1, NDIM
           YSTAR3(I) = X(I) + .5*H*XDOT(I)
350       CONTINUE
          CALL F(XDOT, YSTAR3, NDIM,CL,CD)
          DO 400 I = 1, NDIM
           X(I) = X(I) + H*XDOT(I)
400       CONTINUE
         RETURN
         END
C ####################################################################
C #                                                                  #
C # FUNCTION CONTAINS ODE'S FOR REENTRY  DYNAMIC MODEL               #
C #     FROM HANKEY, "REENTRY AERODYNAMICS"                          #
C #_____#
          SUBROUTINE F(XDOT,X,NDIM,CL,CD)
          DOUBLE PRECISION X,XDOT,A, R, CL, CD, W, S, DENS
          DIMENSION X(NDIM), XDOT(NDIM)
          DATA A,DENS/.0098, 0.01/
          DATA  W, S/ 98.0,.02091 /
C
C  INSERT VINH MODEL DENSITY HERE, POSSIBLE CALL SUBROUTINE
              R = X(3)
                  CALL VINH(R,DENS)
C
C   ***********  SYSTEM OF 3 1ST ORDER EQ.S   ***********
C
          XDOT(1) = A*((CL*S*.5*DENS*X(2)*X(2))/W -(1-X(2)*X(2)/(A*R)
     *              )*COS(X(1)))/X(2)
          XDOT(2) = -A*((CD*S*.5*DENS*X(2)*X(2))/W+SIN(X(1)))
          XDOT(3) = X(2) * SIN(X(1))
          RETURN
          END
          SUBROUTINE VINH(R,DENS)
C #################################################################
C #                                                              #
C #  DENSITY BY VINH MODEL W/ EXPONENTIAL MODEL BELOW 50 KM#
C #                                                              #
C #################################################################
```

```
DOUBLE PRECISION R,  PI, RI, ALPHA, ENTH, TEMP, A, DENS
      A = R - 6378
   IF (A.GT.207) THEN
    RI = 6632.0
    PI =    0.1149
    ALPHA = 0.1190323
    ENTH =   13.8588
    TEMP =   11.9322
    GO TO 100
   END IF
   IF (A.GT.175) THEN
    RI = 6568.0
    PI =    0.468
    ALPHA = 0.1596875
    ENTH =   21.8982
    TEMP =   19.9577
    GO TO 100
   END IF
   IF (A.GT.164) THEN
    RI = 6548.0
    PI =    0.7932
    ALPHA = 0.3054545
    ENTH =   45.7107
    TEMP =   43.6648
    GO TO 100
   END IF
   IF (A.GT.107) THEN
    RI = 6488.0
    PI =   59.3000
    ALPHA = 0.592524
    ENTH = 432.8391
    TEMP = 424.4544
    GO TO 100
   END IF
   IF (A.GT.91) THEN
    RI = 6477.0
    PI = 450.4000
    ALPHA = 0.1189286
    ENTH = 128.4549
    TEMP = 126.467
    GO TO 100
   END IF
   IF (A.GT.80.0) THEN
    RI = 6463
    PI = 7726.000000
    ALPHA = .1545455
    ENTH = 197.97
    TEMP =   0.0
    GO TO 100
   END IF
   IF (A.GT.50.0) THEN
    RI =   6445
    PI = 149750.0000
    ALPHA = -0.1296385
    ENTH =-124.1549
    TEMP =-126.078
    GO TO 100
   END IF
```

```
          ALPHA =-.13961702
            DENS = 1391978200.000*EXP(ALPHA*A)
          GO TO 200
100       DENS = (1/(1+ENTH*(R-RI)/6378))**(1/ALPHA)
          DENS = DENS*(1/(1+TEMP*(R-RI)/6378))*PI
200       RETURN
          END
```

Appendix 3 - Parachute Design Method

Determination of the size of a parachute is mainly dependent on the terminal velocity of the parachute. At the terminal velocity, the drag of the parachute is equal to the weight of the vehicle. This relationship is given by:

$$C_{Do} \, S_o \, \tfrac{1}{2} \, \rho_\infty \, V^2 = M_v \, g \qquad (3.1)$$

This analysis was performed using the ARDC model of the atmosphere to determine the temperature and density at a given altitude.

Example Calculation for a Ringslot Parachute:

At an altitude of 9 km:

$$\rho_\infty = 0.3807 \text{ kg/m}^3$$

$$T_\infty = 227.8 \text{ K}$$

So the speed of sound, a, is found using:

$$\sqrt{a = \gamma \, R \, T_\infty}$$

$$\gamma = 1.4$$

$$R = 287 \text{ N·m/kg·K}$$

Given a Mach number of 0.3, the diameter of the parachute can be calculated as follows:

Velocity: $V = M \, a = 0.3 \, (302.54 \text{ m/s}) = 90.76 \text{ m/s}$

Weight of vehicle = 57,824 N

Then:

$$C_{Do} \, S_o \, \tfrac{1}{2} \, \rho_\infty \, V^2 = 57,824 \text{ N}$$

$$C_{Do} = 0.605 \text{ for a ringslot parachute}$$

93

$$S_O = \frac{(57,824 \text{ N}) (2)}{(0.605) (0.3807 \text{ kg/m}^3) (90.76 \text{ m/s})^2} = 60.95 \text{ m}^2$$

Finally, the diameter of the parachute, D_O, can be calculated. For this example:

$$D_O = \sqrt{\frac{4 \, S_O}{\pi}} = 8.8 \text{ m}$$

Appendix 4 - Engine Performance of CH-53E at different altitudes

The next four pages contain figures that show the variation of shaft horsepower with altitude for the CH-53E helicopter. Shaft horsepower is plotted as a function of the true airspeed in knots.

CH-53E

FORWARD FLIGHT PERFORMANCE

BASIC CONFIGURATION   100 % R^e N^r

STANDARD TEMP

SEA LEVEL
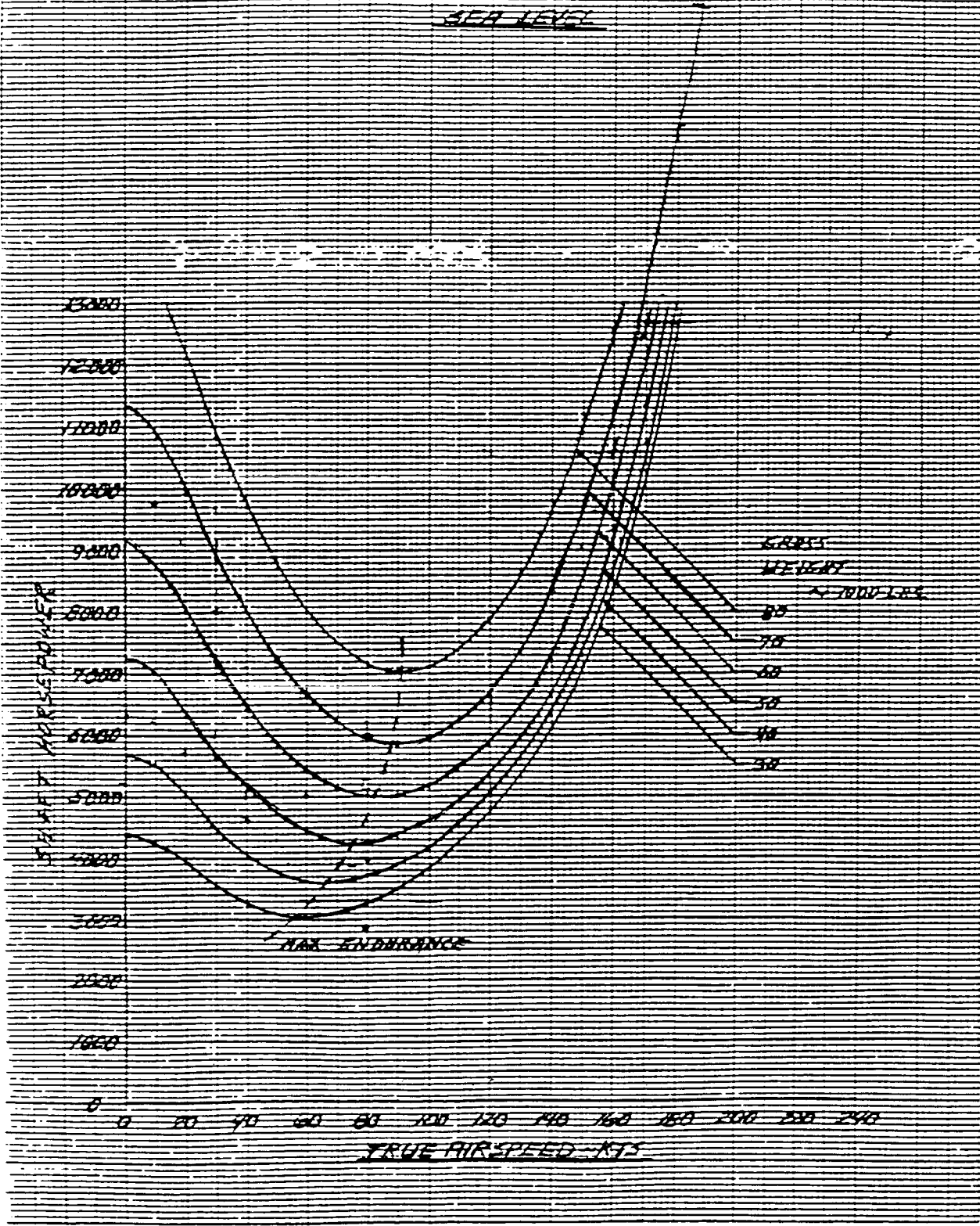
GROSS
WEIGHT
~ 1000 LBS

85
70
60
50
40
30

MAX ENDURANCE

TRUE AIRSPEED ~ KTS

96

FORWARD FLIGHT PERFORMANCE

BASIC CONFIGURATION   100% N_r

STANDARD TEMP

2000 FT

GROSS
WEIGHT
~ 1000 LBS

80
70
60
50
40
30

MAX ENDURANCE

138000
120000
110000
100000
90000
80000
70000
60000
50000
40000
30000
20000
10000
0

0   20   40   60   80   100   120   140   160   180   200   220   240

TRUE AIRSPEED ~ KTS

CH-53E
FORWARD FLIGHT PERFORMANCE
BASIC CONFIGURATION   100% NR
STANDARD TEMP
40000 FT

GROSS
WEIGHT
~ 1000 LBS
90
70
60
50
40
30

SHAFT HORSEPOWER
13000
12000
11000
10000
9000
8000
7000
6000
5000
4000
3000
2000
1000
0

MAX ENDURANCE

0   20   40   60   80   100   120   140   160   180   200   220   240
TRUE AIRSPEED ~ KTS

98
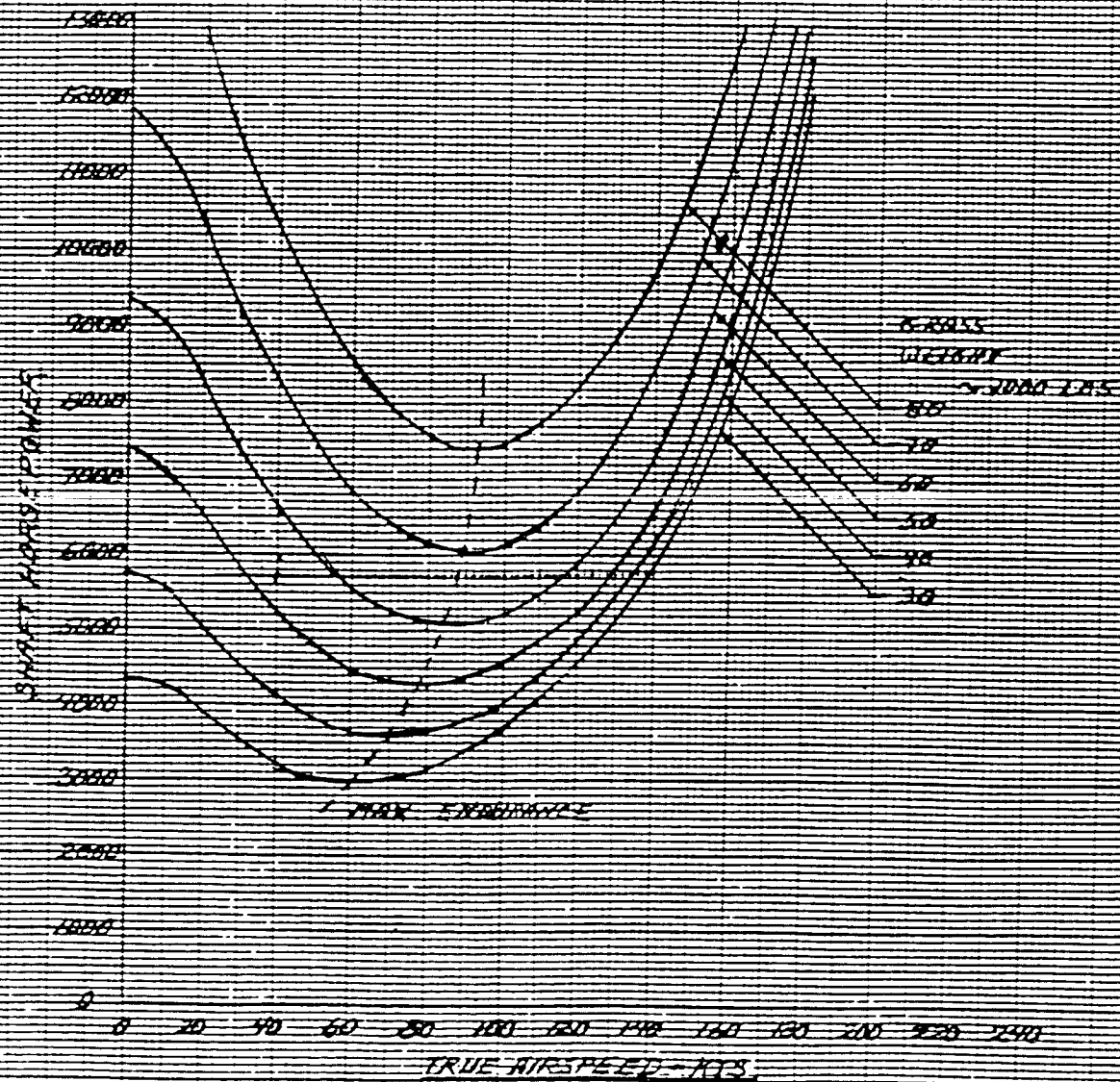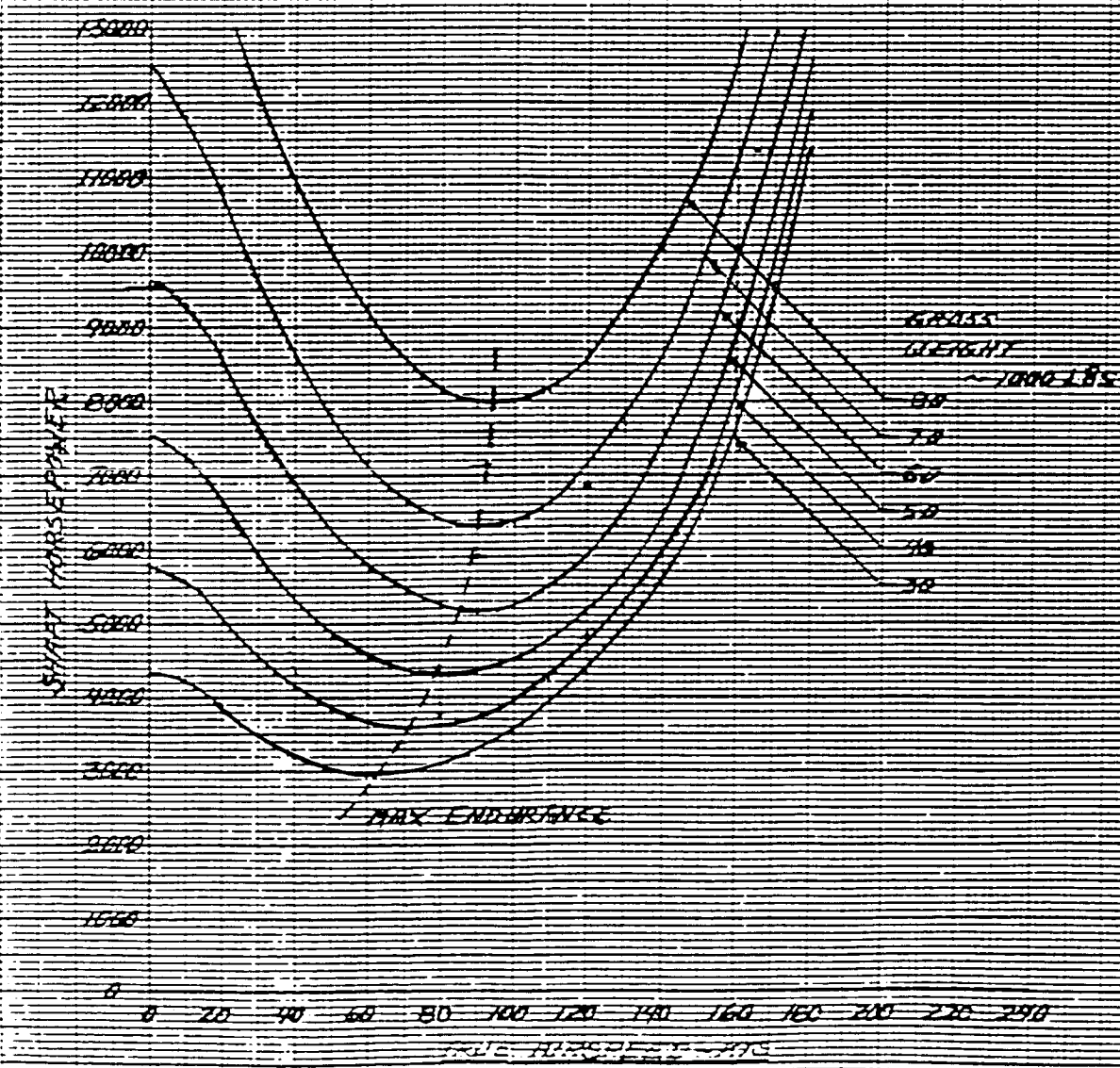
ORIGINAL PAGE IS
OF POOR QUALITY

CH-53E

FORWARD FLIGHT PERFORMANCE

BASIC CONFIGURATION   100% NR

STANDARD TEMP

6000 FT

SHAFT HORSEPOWER

GROSS
WEIGHT
~ 1000 LBS

MAX ENDURANCE

TRUE AIRSPEED ~ KTS
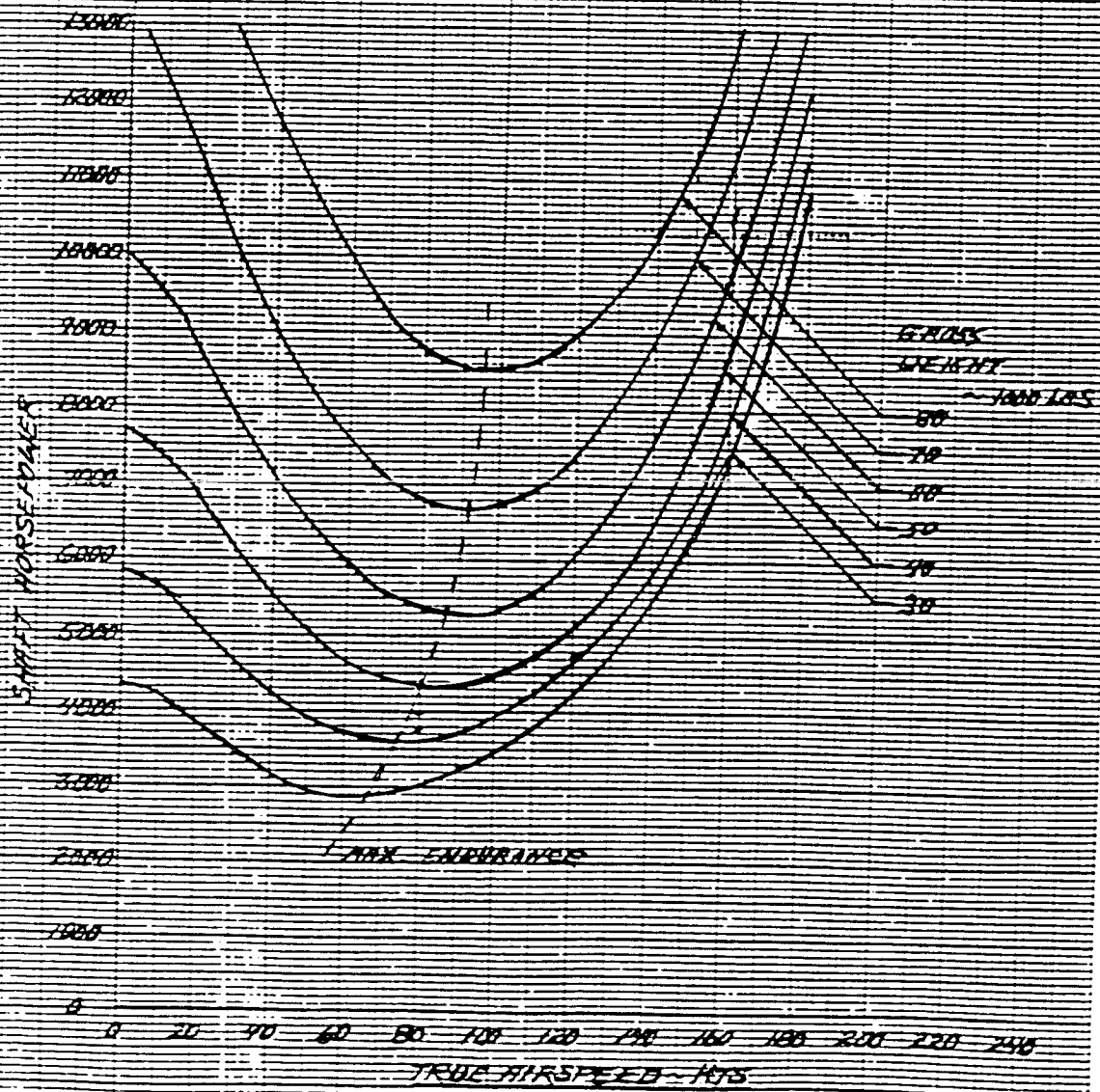
Appendix 5 - Hookup Force and Moment Analysis

To determine the forces and moments induced on the CH-53E helicopter upon hookup of the ACRV, the following data and programs were used.

1. CENTER OF GRAVITY LIMITS

A. INTERNAL LOAD

   (1) Forward - Sta. 342.0 up to 60,000 lb. gross weight
             - Sta. 343.9 @ 69,750 lb gross weight
   (2) Aft   - Sta. 367.0 up to 35,000 lb. gross weight
             - Sta. 366.6 @ 46,500 lb. gross weight
             - Sta. 366.0 @ 56,000 lb. up to 68,000 gross weight
             - Sta. 365.0 @ 69,750 lb gross weight

B. EXTERNAL LOAD

   (1) Forward - Sta. 342.0 up to 60,000 lb. gross weight
             - Sta. 343.9 @ 69,750 lb. gross weight
             - Sta. 347.5 @ 73,500 lb. gross weight
   (1) Aft   - Sta. 367.0 up to 35,000 lb. gross weight
             - Sta. 366.6 @ 46,500 lb. gross weight
             - Sta. 366.0 @ 56,000 up to 68,000 lb gross weight
             - Sta. 363.4 @ 73,500 lb gross weight
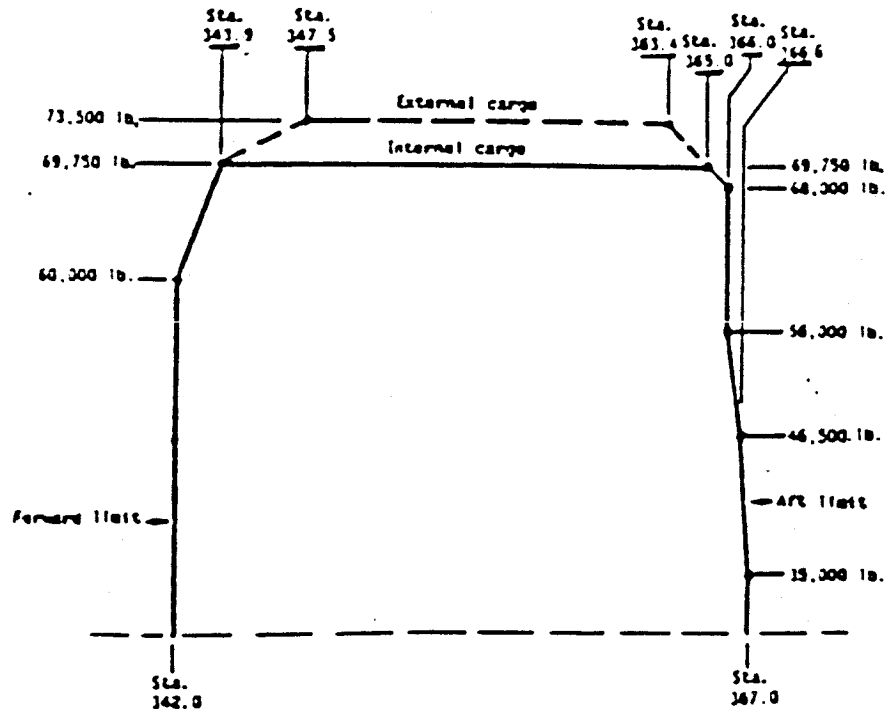
NOTE: There is a linear c.g. limit taper between the c.g. datum points shown above. The C.G. limits are in accordance with the directive in Reference II-1.

2. Gross Weight Limitations
      Flight - Internal cargo 69,750 lb
             - External cargo 73,500 lb
      Landing 69,750 lb

```
*********************************************************************
*                                                                   *
*      THIS PROGRAM WAS DESIGNED FOR THE FINAL DESIGN ANALYSIS IN AERSP  *
*      401D AT THE PENNSYLVANIA STATE UNIVERSITY. THIS PROGRAM ASSUMES   *
*      THE WEIGHT OF THE ACRV IS 13000 LBS, ITS CENTER OF GRAVITY AT THE *
*      164 WATERLINE POSITION OF A SIKORSKY CH53-E HELICOPTER, AND THAT  *
*      THE CABLE IS LOCATED DIRECTLY BELOW THE HELICOPTER'S CENTER OF    *
*      GRAVITY.  THIS PROGRAM CALCULATES THE TENSION IN THE CABLE, THE   *
*      ANGLE THE CABLE TAKES WITH THE VERTICAL, THE MOMENTARM THE        *
*      SWING CREATES, AND THE MOMENT THE SWING INDUCES UPON THE HELI-    *
*      COPTER.                                                          *
*                                                                   *
*********************************************************************
       REAL THETA,TENSON,MOMENT,MOMARM,SIN,ATAN,COS,AX
       OPEN(UNIT=10,FILE='WOIDATA')
       AX=1
       DO 10 I=1,35
       THETA=ATAN(AX/32.2)
       TENSON=13000/COS(THETA)
       MOMARM=SIN(THETA)*164/12
       MOMENT=MOMARM*TENSON
       THETA=THETA*57.29577951
       WRITE(10,100)AX
       WRITE(10,105)TENSON
       WRITE(10,110)THETA
       WRITE(10,120)MOMENT
100    FORMAT(1X,'DECELERATION = ',F15.5)
105    FORMAT(1X,'TENSION = ',F15.5)
1      FORMAT(1X,'THETA = ',F15.3)
       FORMAT(1X,'MOMENT = ',F15.5/)
       AX=AX+1
10     CONTINUE
       STOP
       END
```

```
*********************************************************************
*                                                                   *
*     WRITTEN BY WILLIAM JAMES MURRAY                                *
*                190-53-5554                                         *
*                                                                   *
*********************************************************************
```

```
**************************************************************************
**                                                                      **
**        THIS PROGRAM WAS DESIGNED FOR THE FINAL DESIGN ANALYSIS IN AERSP **
**     401S AT THE PENNSYLVANIA STATE UNIVERSITY. THIS PROGRAM ASSUMES   **
**     THE WEIGHT OF THE ACRV IS 13000 LBS, ITS CENTER OF GRAVITY AT THE **
**     164 WATERLINE POSITION ON A SIKORSKY CH53-E HELICOPTER. THIS      **
**     PROGRAM CALCULATES INDUCED MOMENTS CAUSED BY THE DECELERATION     **
**     OF THE HELICOPTER WHEN THE ACRV IS NOT DIRECTLY BENEATH THE CG.   **
**     IT CALCULATES THE MOMENTS IF THE LOAD IS EITHER FORWARD OR AFT    **
**     OF THE CG. ANY NEGATIVE MOMENTS FROM THIS PROGRAM MEANS THE ANGLE **
**     HAS MADE THE MOMENT ARM GO ON THE OTHER SIDE OF THE CG.           **
**                                                                      **
**************************************************************************
      REAL THETA,TENSON,MOMNTA,MOMNTF,MOARMA,MOARMF,SIN,ATAN,COS,AX,D
      OPEN(UNIT=10,FILE='401DATA')
      WRITE(*,*)'WHAT IS THE DISTANCE THE LOAD IS AWAY FORM THE CG(FT)?'
      READ(*,*) D
      DO 20 Z=0.5,0, .5
      AX=Z
      DO 10 I=1,35
      THETA=ATAN(AX/32.2)
      TENSON=13000/COS(THETA)
**************************************************************************
**                                                                      **
**        EQUATIONS FOR MOMENT ARM WITH LOAD FORWARD AND AFT OF CG       **
**                                                                      **
**************************************************************************
      MOARMF=COS(THETA)*(Z+164/12/TAN(THETA))-(164/12/SIN(THETA))
      MOARMA=SQRT(((164/12)**2+(164/12/TAN(THETA))**2)+COS(THETA)*(Z-164/
     &12/TAN(THETA))
      MOMNTF=MOARMF*TENSON
      MOMNTA=MOARMA*TENSON
      THETA=THETA*57.29577951
      WRITE(10,100)AX
      WRITE(10,105)TENSON
      WRITE(10,110)THETA
      WRITE(10,120)MOMNTF
      WRITE(10,130)MOMNTA
100   FORMAT(1X,'DECELERATION = ',F15.3)
105   FORMAT(1X,'TENSION = ',F15.3)
110   FORMAT(1X,'THETA = ',F15.3)
120   FORMAT(1X,'MOMENT INDUCED WITH LOAD FORWARD OF CG = ',F15.3)
130   FORMAT(1X,'MOMENT INDUCED WITH LOAD AFT OF CG = ',F15.3/)
      AX=AX-1
10    CONTINUE
20    CONTINUE
      STOP
      END
**************************************************************************
**                                                                      **
**     WRITTEN BY WILLIAM JAMES MUARY (814) 867-5074                     **
**                     193-56-2654                                      **
**                                                                      **
**************************************************************************
```

103

Appendix 6 - Additional Aircraft Information

In addition to the information presented in the description of Phase III in the report the following pages are provided. The aircraft for which additional material is provided are the Grumman E-2 Hawkeye, the Boeing EC-137D/E-3 Sentry, and the Boeing KC-135E and KC-135R.
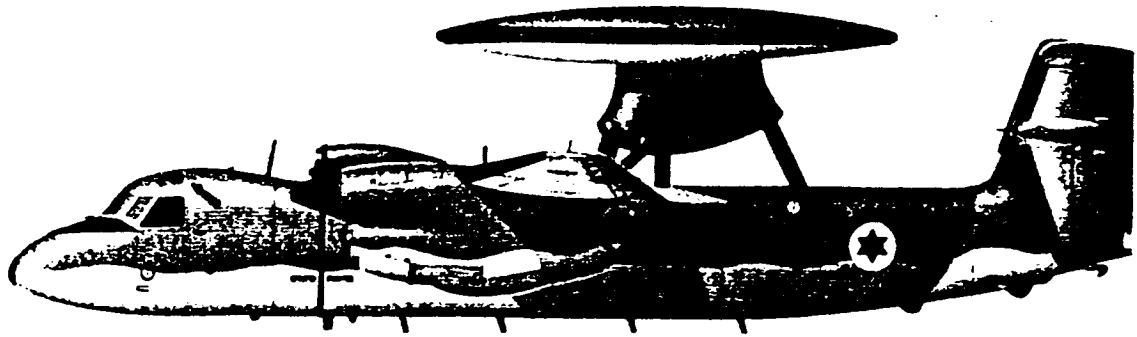
First flown as long ago as 21 October 1961, the **Grumman E-2 Hawkeye** has demonstrated a remarkable ability to keep pace with developments in the airborne early warning field, being perhaps a classic example of cramming a quart into a pint pot. In its latest guise as the **E-2C**, it is infinitely superior to the original **E-2A** model which entered service with Navy AEW squadron VAW-11 at the beginning of 1964 and which played an important role in controlling Navy strike packages during the Vietnam War.

Early AEW-dedicated aircraft such as the Grumman TBF Avenger and Grumman WF-2 Tracer were adequate for the time, but were unable to cope with more than a handful of targets at once. It gradually became clear, therefore, that some form of computerization was required if radar systems operators were to take full advantage of all information at their disposal. However, it was not until the late 1950s that miniaturization of computers reached the stage at which it was possible to install such devices in an airframe small enough for operation from Navy carriers.

What resulted was the **W2F-1** (E-2A from late 1962) Hawkeye, instantly recognizable by the pancake-shaped dorsal radome which housed the antenna for the General Electric APS-96 surveillance radar. Including prototypes and test specimens, a total of 59 E-2As was built and delivered to the US Navy between 1962 and 1967, most being later modified to **E-2B** standard through installation of a Litton L-304 general-purpose computer. A few E-2Bs remain operational with the Navy early in 1986.

Further upgrading of the avionics systems led to the appearance of the E-2C model, perhaps the most significant change entailing fitment of rather more capable General Electric APS-120 radar, since replaced by the even more effective APS-125. Attention was also paid to improving data-processing capability to a point where the aircraft is capable of automatically tracking more than 250 targets at any given time, whilst also controlling 30 or more interceptions.

Flown for the first time in prototype form on 20 January 1971, the E-2C became operational with VAW-123 aboard the USS *Saratoga* in the autumn of 1974 and variants of the type now equip most Navy AEW squadrons. In addition, small quantities have also been purchased by Egypt (4), Israel (4), Japan (8) and Singapore (4) whilst production continues for the US Navy, which plans to buy no fewer than 102, later examples benefiting from installation of the recently-developed APS-138 surveillance radar.

Specification: Grumman E-2C Hawkeye
Origin: USA
Type: airborne early warning and control aircraft
Powerplant: two 3661-ekW (4 910-ehp) Allison T56-A-425 turboprop engines
Performance: maximum speed 325 kts (602 km/h; 374 mph), cruising speed for maximum range 269 kts (499 km/h; 310 mph); service ceiling 30,800 ft (9390 m), patrol endurance 6 hours, maximum ferry range 2583 km (1,605 miles)
Weights: empty 17265 kg (38.063 lb), maximum take-off 23556 kg (51,933 lb)
Dimensions: span 24 56 m (80 ft 7 in); length 17 54 m (57 ft 6 75 in), height 5 58 m (18 ft 3 75 in), wing area 65 03 m² (700 sq ft)
Armament: none

A Grumman E-2C of the Israeli air force.
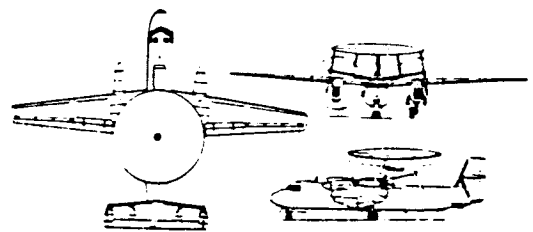
Grumman E-2C Hawkeye
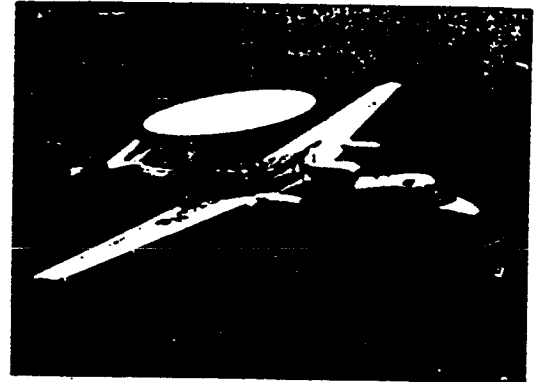
A Grumman E-2C Hawkeye of VAW-126 is shown during a Pacific fleet deployment on board USS Constellation as a part of CVW-9. The Hawkeye provides Fleet airborne early warning cover.

This E-2C of VAW-124 'Bear Aces' is seen landing back on an Atlantic Fleet carrier. The Hawkeye's turboprop powerplants confer great economy and endurance.

Grumman E-2 Hawkeye
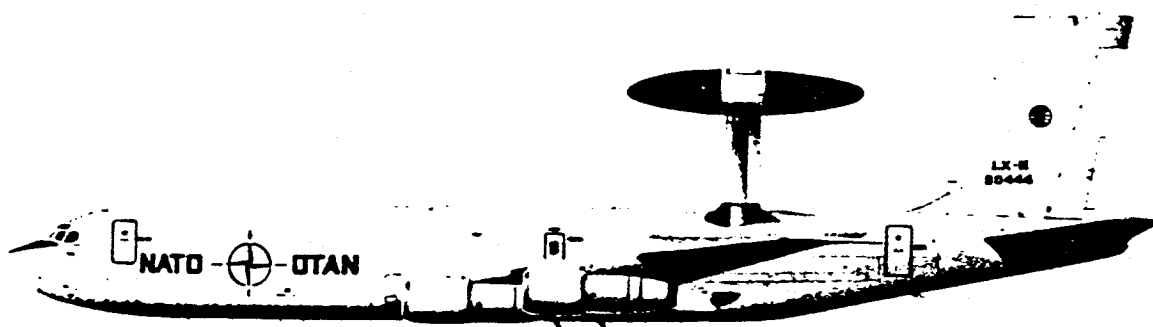
Boeing E-3A Sentry of the NATO Airborne Early Warning Force, based at Geilenkirchen, West Germany.

One of the most vital roles fulfilled by the Model 707 airframe is that of the USAF's and NATO's Airborne Warning And Control System (AWACS) aircraft, which carries the designation **Boeing E-3 Sentry** It is, in effect, an airborne radar station serving also as a command, control and communications (C³) centre. Operating in three dimensions it s regarded as survivable under wartime conditions, as it is highly resistant to jamming, and in addition to the C³ function provides long-range surveillance over all terrains.

On 23 July 1970 the Boeing Aerospace Company, previously concerned only with missiles and space, became prime contractor integrator for the AWAC System, proposing the Model 707-320B as its carrier and recommending that the aircraft be powered by eight TF34 engines, a choice later changed back to four TF33 turbofans to save cost. Under the designation **EC-137D** two prototypes evaluated competing radar systems proposed by Hughes Aircraft and Westinghouse, the latter finally being named winner. The most notable external feature of these aircraft is the 9 14-m (30-ft) diameter rotodome pylon-mounted above the rear fuselage, which streamlines the back-to-back antennas for the radar and IFF. In January 1973 the USAF authorized development of the AWACS, designating these aircraft E-3 and later naming them Sentry. The first USAF **E-3A** was delivered to TAC's 552nd AWAC

Wing on 24 March 1977, and the force of 34 was completed in 1985. NATO's 18 Luxemburg-registered multi-national crew E-3As were delivered from 22 January 1982 to 25 April 1985.

The USAF's first 24 Sentries were equipped to **Core E-3A** standard, which provides pulse-Doppler radar, a CC-1 computer, nine situation display consoles (SDCs), two auxiliary display units (ADUs) and 13 communication links. These 24 aircraft are in the process of updating to **E-3B** standard with the secure Joint Tactical Information Distribution System (JTIDS), faster CC-2 computer, some maritime reconnaissance capability and other equipment. The remaining 10 USAF and 18 NATO aircraft, designated **Standard E-3A**, have maritime (overwater) reconnaissance capability plus the JTIDS and CC-2 computer. Under modifications started in 1984 the 10 USAF Standard E-3As are being updated to **E-3C** configuration, gaining five more SDCs, additional UHF radios and provision for Have Quick anti-jamming improvements.

Five **E-3A/Saudi** AWACS have been contracted for the Royal Saudi Air Force, with initial deliveries planned for 1986. Like the tanker transports on order for this air arm under the designation KE-3A, they are powered by 9979-kg (22,000-lb) thrust CFM International CFM56-2 turbofan engines

Specification: Boeing E-3A Sentry
Origin: USA
Type: airborne early-warning and C³ aircraft
Powerplant: four 9525-kg (21,000-lb) thrust Pratt & Whitney TF33-100/100A turbofan engines
Performance: maximum speed 460 kts (853 km/h; 530 mph), operating ceiling 29,000 ft (8840 m), loiter time on station 1609 km (1,000 miles) from base 6 hours, maximum endurance on internal fuel 11 hours
Weights: maximum take-off 147418 kg (325,000 lb)
Dimensions: span 44 42 m (145 ft 9 in), length 46 61 m (152 ft 11 in), height 12 73 m (41 ft 9 in), wing area 283 35 m² (3,050 0 sq ft)
Armament: none

Boeing E-3A Sentry

The carriage of the large rotodome is clearly seen here, on each side of the scanning radar and the IFF antenna. The E-3 design was based upon the Model 707 airframe.

E-3s now serve in some numbers, most in USAF service having been updated to E-3B or E-3C standard as better equipment has become available to the AWACS force.

Boeing EC-137D/E-3 Sentry
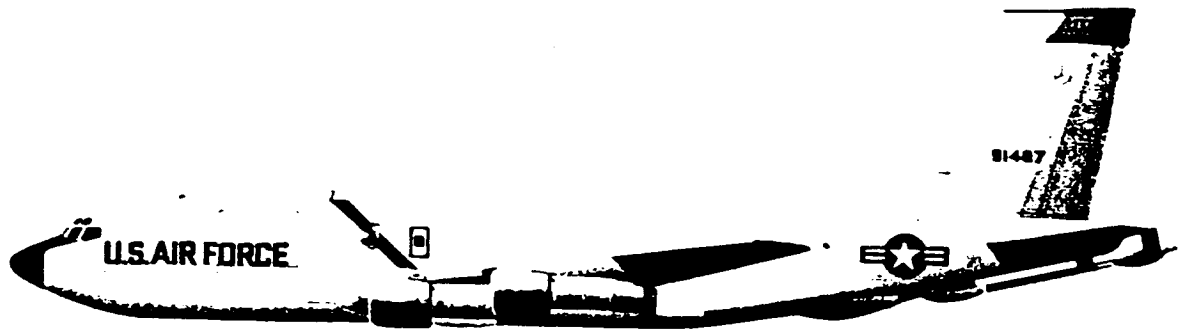
Boeing KC-135E Stratotanker of the 108th ARS, 126th ARW, Illinois Air National Guard.

Modern performance requirements for fighter/interceptor aircraft are an antithesis to range, yet the policy of major air forces to react quickly when needed in a far distant policing role demands unprecedented range. It is a constantly growing demand, one which makes the requirement for inflight-refuelling tankers increase by leaps and bounds, and it is important for an air arm to get the maximum utilization from its existing fleet.

When production of Boeing KC-135 tankers for the US Air Force ended a total of 724 had been built, of which about 650 remain in use. It was decided to ensure they would remain operational into the next century, the major requirement being replacement of the underwing skin. This task, started in 1975, has progressed steadily and by mid-1985 more than 500 KC-135s had benefited from this modification which should extend service life by some 27,000 hours. It was followed by a programme to re-engine Air National Guard and Air Force Reserve KC-135s with JT3D engines (civil equivalent of the TF33). These powerplants were removed and refurbished from ex-commercial Boeing 707s acquired by the USAF, and at the same time the KC-135s gain also tail units, engines pylons and cowlings

from the Model 707s. Simultaneously new brakes and anti-skid units are installed and, upon completion of the work, the aircraft are redesignated **KC-135E**

Far more comprehensive is the programme to update the main tanker fleet with the 9979-kg (22,000-lb) thrust CFM International F108-CF-100 turbofan (equivalent to the civil CFM56-2B-1), existing contracts covering 108 conversions. With this powerplant revision comes also an APU to give self-start capability; more advanced autopilot, avionics, controls and displays on the flight deck; strengthened main landing gear incorporating anti-skid units; revised hydraulic/pneumatic systems; and an enlarged tailplane. Redesignated **KC-135R** on completion of this update, the first example was redelivered to SAC's 384th Air Refueling Wing at McConnell AFB, Wichita in July 1984. Improved capability enables the KC-135R to operate from shorter runways (civil airports if necessary) and to transfer more fuel, to an extent that two can cover the workload of three KC-135A tankers. In addition to KC-135R conversions for the USAF, Boeing received a contract to modify seven of the 11 remaining French C-135F tankers to this same standard

Specification: Boeing KC-135R
Origin: USA
Type: inflight-refuelling tanker/cargo transport aircraft
Powerplant: four 9979-kg (22,000-lb) thrust CFM International F108-CF-100 turbofan engines
Performance: average cruising speed 460 kts (853 km/h; 530 mph) between 30,500 and 40,000 ft (9300 and 12190 m), able to transfer 150 per cent more fuel than the KC-135A at a radius of 4627 km (2,875 miles)
Weight: maximum take-off 146284 kg (322,500 lb); maximum fuel-load 92210 kg (203,288 lb)
Dimensions: span 39.88 m (130 ft 10 in); length 41.53 m (136 ft 3 in); height 12.70 m (41 ft 8 in); wing area 226.03 m² (2,433.0 sq ft)
Armament: none

Boeing KC-135R Stratotanker
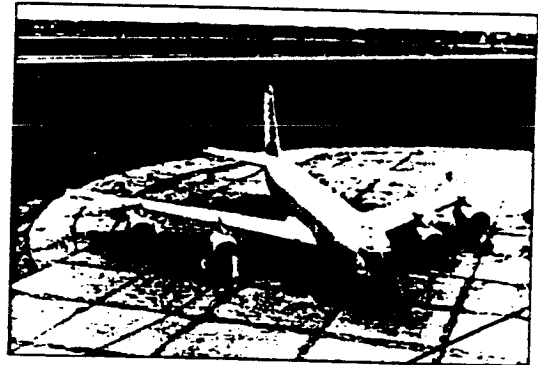
An early KC-135R shows the large high-bypass ratio CFM F108 turbofans which have replaced the thirsty J57s. Fuel receiving capability has also been added.

The whole first-line KC-135 fleet will eventually be re-engined, giving a planned service life into the 21st century. This example is from the 384th ARW at McConnell AFB.

Boeing KC-135E and KC-135R

107

ASSURED CREW RETURN VEHICLE

BRAKING AND LANDING SYSTEMS

DETAILED DESIGN

FINAL REPORT

APRIL 19, 1990

GROUP MEMBERS: ANDREW BIDDLE
BRETT BUSHEY
DAWN GABRIEL
MICHAEL KLINE
WILLIAM LANE
KEVIN SCHUREK
JOSEPH STONE

ABSTRACT

A braking and landing system for Space Station Freedom's Assured Crew Return Vehicle (ACRV) is developed. The subsystems considered in this design are the ACRV shape, the thermal protection system (TPS), the deceleration system, and the landing system. ~~After a cost analysis~~, An eight-man ACRV is chosen over two-, four-, and six-man designs. An L/D of 1.0 allows the ACRV to complete its mission, providing adequate cross-range and decreased g loads. The shape selected for the ACRV is the M2-F3 configuration. The M2-F3 provides several advantages: 1) it offers an acceptable L/D of 1.2 and a high volumetric efficiency 2) a tested prototype already exists 3) it can incorporate "off-the-shelf" hardware and 4) a large base of test data for the M2 series has been compiled over many years. An ablative thermal protection system (TPS) is preferred for use with the ACRV because of its relatively low cost and the ease with which it can be integrated with the M2-F3 shape. The lower heat shield of the ACRV will be expendable, being detached upon approach to landing to allow for the deployment of the landing system. A parafoil gliding parachute comprises the primary deceleration system. The parafoil offers the advantages of a tested 10,000 lb. payload, maneuverability, easy fabrication methods, low loads ~~forces~~, and a final vertical velocity of less than 15 ft/sec. The sailwing auxiliary lifting surface is considered as a possible secondary deceleration system. It offers a very light weight, a simple design, and increased control and stability for the M2-F3; however, its development has been very limited. An air cushion landing system (ACLS) enables the ACRV to withstand adverse landing conditions on both land and water. It incorporates a three-segmented triangular shape that offers simplicity, maintainability, and ease of integration with the surface of the M2-F3. The material most appropriate to the ACLS is chosen to be Kevlar-polyurethane, because of its physical properties, easy fabrication, and low cost.

ASSURED CREW RETURN VEHICLE

BRAKING AND LANDING SYSTEMS

DETAILED DESIGN

FINAL REPORT

APRIL 19, 1990

GROUP MEMBERS: ANDREW BIDDLE
BRETT BUSHEY
DAWN GABRIEL
MICHAEL KLINE
WILLIAM LANE
KEVIN SCHUREK
JOSEPH STONE

TABLE OF CONTENTS

LIST OF TABLES

LIST OF FIGURES

LIST OF SYMBOLS AND NOMENCLATURE

Symbols

cg = center of gravity

d = clearance height

g = gravitational acceleration at sea level

h = altitude above sea level

q = local heating rate

q_o = stagnation point heating rate

$\bar{q}_o$ = stagnation point heating rates dimensionless with respect to maximum heating rate at vehicle pullout

A = surface area

A_c = cushion area

AR = aspect ratio

C_D = drag coefficient

C_L = lift coefficient

C_d = discharge coefficient

Hp = horsepower

L/D = lift-to-drag ratio

P_c = air cushion pressure

P_j = trunk pressure

Q_j = air flow rate

S = perimeter of trunk

V = velocity of flow through cushion perimeter

V_E = velocity at entry into Earth's atmosphere

v

ΔV = change in velocity

W = weight of vehicle

α = angle of attack

γ_E = flight path angle at entry into Earth's atmosphere

ρ = air density at sea level

Subscripts

max = maximum values

Nomenclature

ACLS = air cushion landing system

ACRV = Assured Crew Return Vehicle

FRSI = felt reusable surface insulation

HRSI = high temperature reusable surface insulation

LRSI = low temperature reusable surface insulation

NASA = National Aeronautics and Space Administration

NSTS = National Space Transportation System

RCC = reinforced carbon-carbon

RCS = reaction control system

SAS = stability augmentation system

TPS = thermal protection system

I. INTRODUCTION

The purpose of this paper is to describe the design of a braking and landing system for the Space Station's Assured Crew Return Vehicle (ACRV). The ACRV will 1) serve as a transport to Earth in the event of a grounding of the National Space Transportation System (NSTS), 2) provide a safe and fast means for evacuation of the space station crew of 8 in the event of a station catastrophe, and 3) provide for fast transportation of a critically injured or ill crew-member to a ground-based medical facility.

The process of the design involved considering each of the different subsystems comprising the ACRV braking and landing system: the ACRV shape, the deceleration system, the thermal protection system, and the landing system. Extensive research into each of these topics was performed, during which many alternatives were considered.

After comparing each of the alternatives to mission and cost criteria, the most feasible system was chosen: the M2-F3 lifting body would be used as the Assured Crew Return Vehicle shape. It provides a hypersonic lift-to-drag ratio of about 1.0, which was judged to be sufficient for the ACRV to carry out its mission. The deceleration system will include a parafoil gliding parachute that will enable the craft to glide to a predetermined landing site. An air cushion landing system will be utilized because it will enable the ACRV to land on a number of surfaces, including land and water, even in adverse conditions.

In this report, each of the alternatives considered in

1

designing each subsystem will be reviewed. The evaluation of
their utility will also be summarized, and a final design of the
braking and landing system will be presented.

II. DEFINITION OF LIFT-TO-DRAG RATIO

The ACRV will need some lifting capability in order to assure an ability to land at a predesignated point, to meet NASA specifications limiting reentry deceleration, and to have a wide range of acceptable reentry trajectories to follow.

In the event of an emergency medical mission, it will be imperative that the ACRV have the ability to land at a predetermined landing site, close to a trauma center if possible. NASA performance requirements for the medical mission specify the interval of time between the decision for a medical evacuation of an injured crew member and his arrival at an Earth-based medical facility to be no more than 24 hours. Further restrictions limit the period of time between departure from the Space Station and arrival at the facility to be no more than six hours. Also, the maximum time from entrance into the ACRV to landing is to be limited to only three hours (13:11-12). In order to complete this mission, a lifting capability is essential for the ACRV.

The ability to produce lift gives a reentry vehicle a greater crossrange maneuvering capability. Stated simply, a larger crossrange gives a ~~vehicle~~ _pilot_ the means to maneuver/ _a vehicle_ ~~from its entry point, through the atmosphere,~~ _over_ a greater lateral distance to a preselected landing site. The vehicle can thus travel to a specific landing site from a greater number of orbits. For example, for a spacecraft with orbital inclination angles between 28° and 90° (the Space Station will have an inclination of 28.5°), a return to the continental US is possible from approximately 50% of the orbits in this range if the spacecraft has a hypersonic L/D

3

of 1.0. This percentage increases to 62% if the craft has an L/D greater than 1.8; however, even if a craft has a lift-to-drag ratio of 1.8, it may be necessary to delay reentry up to as many as seven hours to achieve landing at certain locations within the continental US. As L/D increases, the number of orbits from which return to the US is possible increases rapidly as maximum time to achieve touchdown decreases. If a spacecraft has a lift-to-drag ratio of 2.5, it would be possible to achieve continental touchdown from more than 80% of possible orbits in the range of inclination of $0°$ to $90°$ with a maximum return interval of only five hours (18:42-44). In addition, a higher L/D has been found to increase the frequency of access to candidate landing sites during daylight hours (41:115)

The ACRV will also need some lifting capability in order to meet NASA specifications that limit reentry deceleration to four g's (13:21). This becomes apparent when one compares the Mercury and Apollo spacecraft. A capsule with L/D = 0.0, the Mercury spacecraft underwent an acceleration of 7.7 g's upon reentry (43:133). On the other hand, the Apollo capsule, with an L/D of 0.5 (40:43), experienced reentry accelerations of only 3 g's (8:1)

Another advantage of having some lifting capability is its relationship to a given vehicle's entry corridor. For a given L/D and C_D, maximum acceleration encountered upon reentry is a function of both the entry angle γ_E and entry velocity V_E (42:124). For return from a near-earth orbit, V_E is approximately constant at 26,000 ft./sec; therefore, the values of γ_E that give

4

acceptable levels of acceleration define the lower boundary of the entry corridor, or range of possible entry trajectories. The upper boundary of the corridor is defined by an entry angle at which a reentry vehicle would deflect off the earth's atmosphere instead of reentering. In general, a narrower corridor could mean longer times to earth landing. For a given amount of fuel, there will be only a given amount of ΔV available to the craft to move it into its reentry trajectory. If the corridor is small, it may take the craft longer to achieve proper orbital position for a boost onto the return trajectory, A wider entry corridor would mean time saved in return; always, ~~helpful~~ a critical component a in medical emergencies.

One method of effectively increasing entry corridor boundaries is to use lift. The curved path of a lifting body in reentry allows a lifting vehicle with a set load limit to enter at a steeper angle than a vehicle with no lift and the same load limit (40:36-37). In Figure 1, ~~shows~~ is shown the effect of increasing lift on entry corridor for a craft with a 12 g limit.

After considering these arguments, a hypersonic L/D of approximately 1.0 has been chosen as sufficient to enable the ACRV ~~vehicle~~ to perform its mission correctly within the time constraints specified by NASA. Vehicles with L/D's greater than 1.0 were not considered to be appropriate for the ACRV design because of volume constraints and current technology. This matter will be discussed more in depth in the following section.

5

III. SHAPE CONFIGURATION

Shape configurations considered for the ACRV were evaluated on several criteria that satisfied the requirements of the NASA specifications manual. The first constraint was that the ARCV have a medium-range L/D of one or greater. This allowed for a large enough cross-range capability for selection of more than one continental U.S. landing site, for a reentry load factor of less than 4 g's, and for a minimal reentry flight path angle. Other constraints were the Space Shuttle cargo bay size (15 ft. diameter and 60 ft. length) and the NASA specification ACRV mass limit ≤ on the (15,000 lbs). The internal volume required to house the crew and necessary subsystems also limited the selection of the ACRV configuration. The aerodynamic characteristics of the shape configuration through the hypersonic, transonic, and subsonic regions of the flight trajectory were also evaluated. Other criteria affecting the ACRV shape selection were the life cycle, costs of production, and other braking and landing applications.

In order to further define the ACRV shape configuration, the shapes were evaluated against several more criteria, the first of these being the difficulty in the development of the shape into an operational ACRV. Also considered with this is the ease of the process of manufacturing of the shape configuration. Another criterion which greatly affects the decision of the ACRV shape is the intent to use "off-the-shelf" hardware. Stability and control of the ACRV until landing is also a concern in the design parameters. Finally, actual test data from models and prototypes would lead to an operational ACRV.

6

Based on the above criteria and mission needs, a shape configuration was selected.

A. Waverider

The concept of a waverider relies on the fact that the body rides on the shock wave created by the leading edge of the wings. It also differs from conventional aircraft in that the wings are not slender, and that the primary lift is generated from the lower surface rather than the upper surface (44: 10/2). This allows the waverider to operate in the Mach range of 3 to 12 (44: 10/1), which corresponds to reentry Mach numbers. The waverider has a high L/D ratio in the range of 7 to 9 (18:19). This high L/D ratio would allow the ACRV to reenter the Earth's atmosphere at smaller angles of attack. It would also allow the deceleration forces experienced by the ACRV to be less than 2 g's, and gives the waverider a greater selection of possible landing sites. Although the waverider shape, Figure 2, seems to be a good choice for the ACRV configuration, it does have some undesirable characteristics that prevent it from being a viable option. At high Reynolds numbers, the L/D ratio is relatively high, but as the Reynolds number decreases, a large decay in the L/D ratio occurs due to the increasing viscous effects (39:13/7). This also corresponds to a decreased Mach number, at which the waverider is no longer riding on a shock wave. Therefore, it would not be able to develop the necessary lift characteristics at subsonic velocities. A possible solution to this problem is the implementation of some type of parachute system. This system would provide the necessary lift at these lower velocities and would be used to land the ACRV with the

designed landing gear. A problem encountered with parachute deployment is that the velocity at which the ACRV will be traveling is too great (Mach 3 or greater). Another disadvantage is that the waverider shape has a relatively low volumetric efficiency associated with the high L/D characteristics (see Figure 3). This would not allow sufficient space for the crew and necessary subsystems. Due to the wing structure dimensions of the waverider, aspect ratio = 1.2 (39:13/17), there would be difficulty fulfilling the ~~Space Shuttle bay constraints~~ size constraints for the Shuttle bay. In considering the geometry of a waverider, the planforms are often complex and involve numerical methods for the optimization of the best shape (25:1463).

B. Winged Body

Winged bodies are essentially lifting bodies with various wing shapes. A possible winged body for the mission, shown in Figure 4, features 73° to 78° highly swept delta wings. These delta forms are the best candidates for transitional flight. Stability can be maintained throughout the entire range of angle of attack, and therefore can be used effectively for atmospheric deceleration techniques. High L/D values, from 1.5 to 4.5, are inherent for winged body structures, which increase range and landing site possibilities (20:31). Delta wing body concepts, with a combination of leading-edge and trailing edge flaps, provide longitudinal trim and control over the entire angle of attack range. Limitations that eliminate the winged body as a possible ACRV configuration are its extended wing span, which could not be easily confined in the Space Shuttle cargo bay, its poor internal volume

for crew and subsystems, and its lack of actual prototype testing.

C. Pod Lifting Body

A lifting body structure bridges the gap between the winged body and capsule forms. A lifting body may be easily designed to fit within the Shuttle bay for launch. The ratio of internal volume to external surface area is not nearly as efficient as a capsule form; however, the ~~area considerations~~ *volometric dimensions* necessary to accommodate an eight person crew and subsystems are possible with a lifting body. Examples of two shapes that were considered are: a thick/blunt delta wing, and a "bobsled" configuration (Figure 5). Trailing edge controls would provide static trim and stability (27:21). Such forms of supersonic gliders would decelerate by reentry into the atmosphere at high angles of attack, as do the winged body forms. Transitional flight is attained by recovery to a smaller angle of attack for sustained flight and maneuverability. A sailwing feature may be an applicable design enhancement to increase glide and range in the lower atmosphere. The sailwing feature basically consists of extendible booms and flexible ribbed wings which are spread from the main body. This possible design consideration has received intensive study and evaluation and will be discussed in depth later in this report. Sailwings would increase the typical lifting body L/D values which range from 0.8 to 2.4, (33:40-82).

1. Flared Cylinder

Shown in Figure 6 is the flared cylinder reentry vehicle configuration. This design incorporates a simple-geometry approach of a cylinder with a 16° half-angle blunted tip and 10°

9

flared aft body. The hypersonic L/D for this vehicle is in the range of 0.8 to 1.1 (12:83). A disadvantage to this approach is the fact that the body has only been optimized for the hypersonic region of flight. Studies by Lockheed (12:89) show that this L/D drops significantly with lower Mach numbers, necessitating some form of parachute recovery system. This system would have to be deployed at a high Mach number and could result in failure. Based on wind tunnel data, the dimensions of a 6-man ACRV would have a length of 22 ft., an outside diameter of 7 ft., a crew compartment diameter of 6 ft., and a vehicle mass of around 15000 lbs. An advantage of this vehicle configuration is the simple geometry used in the design which would be relatively easy to manufacture. The volumetric efficiency of the flared cylinder is 0.11 (12:85) and the internal volume is 430 ft^3. This presents a rather limited space for the crew and necessary subsystems, and until other braking and landing options being considered are implemented, this vehicle design presents too little volume. Another factor limiting the flared cylinder is its lack of aerodynamic control surfaces. The only control surface on the vehicle is a flap on the underside of the flared aft body used to control the center of gravity trim (12:90). Due to this fact, the vehicle would be unable to make any adjustments in the lateral direction and would be more or less on a straight path approach leaving little room for error. The heating rates experienced by the vehicle are around 200 Btu./ft^2-sec. at peak points and would require a strong thermal protection system (12:147). One of the greatest factors limiting the use of the flared cylinder as an ACRV is that there has been no prototype built to scale. All data

has come from wind tunnel tests done on scale models. This type of data cannot take into account the large scale effects of a full scale vehicle, nor can other problems that may occur be tested and corrected.

2. M2-F3

Shown in Figure 7 is the M2-F3 reentry vehicle configuration developed by NASA-Ames. This design incorporates a half cone structure using a 13° half-angle cone with blunted tip and flared aft-body. The control surfaces on the rear portion of the body consist of: two upper flaps used to control the pitch of the vehicle, two lower flaps used for transonic and subsonic flight, two rudders to control the yaw and act as speed brakes, and a central fin. The central fin is the main distinction between the M2-F2 and the M2-F3 configurations and helps to keep the flow from separating over the two fins containing the rudders (50:4). The overall dimensions of an 8-man M2-F3 configuration yield an estimated length of 31 ft. and a span of 13 ft. (Figure 8). These specifications are based on studies done by Syverston et al(Ref. 49) on variations of 2,6,and 10-man M2-F2 configurations. The M2-F3 also contains four hydrogen peroxide thrusters on the aft portion of the vehicle that act as a Reaction Control System (RCS). The RCS would work in conjunction with the control surfaces of the M2-F3 to help with a smooth transfer from orbital conditions to a flight region where the vehicle could be flown using only its control surfaces (21:2), to help maintain stability through different phases of the flight, and to dampen any oscillatory motion (28:14). Based on the dimensions of the M2-F3, the mass of the vehicle is approximately 14,500 lbs.

(49:912). The volumetric efficiency of the M2-F3 is around 0.09 (12:89) and gives around 115 ft^3 per ~~man~~ person (49:913). This allows ample room in the vehicle for the necessary subsystems and a crew of eight. Shown in Figures 9 and 10 are the L/D's for the M2 at hypersonic (Mach = 20) and subsonic (Mach = 0.25) velocities respectively. These results show an advantage in that as the velocity of the vehicle decreases, the maximum L/D increases from 1.2 to 3.1 and additional lift is created. Another advantage lies in the incorporation of a stability augmentation system (SAS) in the M2-F3 configuration. Using the SAS biases the control surfaces as a function of the Mach number thus allowing for limited pilot control of the vehicle (23:226). Problems existed in the SAS; ~~in that,~~ when the vehicle reached subsonic velocities, the system did not perform satisfactorially (23:226). A solution to this problem would be to implement the entry guidance system used on the Space Shuttle. This system is based upon a drag deceleration profile (25:442). By applying different drag profiles for each segment of the landing and linking these profiles together, a desired analytical landing approach can be formulated. Then, as the vehicle descends, the level of the drag profile is adjusted to the analytical drag profile (25:442). This system is currently being used on the Space Shuttle and has had satisfactory flight results (25:447). The use of "off-the-shelf" hardware of the vehicle design and Space Shuttle computer command abilities also make the M2-F3 an attractive option. The biggest advantage to the M2-F3 configuration is that an actual prototype has been built and tested at supersonic speeds. This allows for correlation between actual test data and wind tunnel results. It

12

also creates a model in which unforeseen problems, not visible during wind tunnel testing, can be solved. Another advantage lies in the fact that the development costs of the prototype to operational vehicle would be low. In conducting flight tests of the M2-F3 it was also found that the vehicle yielded a high tolerance to turbulence (28:40). One disadvantage to this configuration was the steep flight path required on the approach to landing, which could be difficult for a deconditioned pilot returning from the Space Station (23:225). Another disadvantage was, that at subsonic speeds, the vehicle handling abilities became difficult (28:41). These disadvantages could be solved with the addition of a gliding deceleration system.

3. HL-10

The HL-10 is a lifting body similar to the M2-F3 configuration (see Figure 11) with a hypersonic L/D in the range of 1.1 to 1.3. Instead of the half cone structure, the HL-10 uses a positive camber structure to the vehicle design. Although it offers many of the same advantages of the M2-F3 configuration, such as acceptable cross-range, "off-the shelf" hardware, and a tested prototype, it does possess disadvantages that prevent it from being a viable option. One negative aspect is the volume efficiency, which tends to give less than 90 cubic feet per man. This is not acceptable for the ACRV concept. Another disadvantage is that the reentry g-level experienced by the crew members is around 6 g's (50:6). Also, the dimensions of the HL-10 for an eight-man crew would far exceed the Space Shuttle cargo bay constraints since the wing span for just a one-man HL-10 is over 15 ft. (see Figure 11).

4. SV-5P

The SV-5P, shown for a one-man crew in Figure 12, has
similar characteristics to the above mentioned lifting bodies and
incorporates improvements from flight test data provided by the
M2-F3 and HL-10 prototypes (50:7). The design approach differs
from the above two in that a negative camber design is used.
Compared to the other lifting bodies, the SV-5P offers a slightly
higher volume efficiency and contains eight movable control
surfaces offering better control at subsonic speeds. It also has
the advantage of featuring the same "off-the-shelf" hardware as
the M2-F3 and HL-10. A disadvantage to this shape is that the
reentry g levels are between -2 and 5, yielding g-levels greater
than 4 (50:7), which exceeds the maximum established by mission
requirements. Another disadvantage lies in the development of an
eight-man SV-5P. This configuration's wingspan would exceed
shuttle cargo bay constraints.

D. Capsule

The capsule shape considered as a possible ACRV has similar
aerodynamic characteristics to that of the Apollo spacecraft but
has a shape similar to that of a cylinder (see Figure 13).
Capsule shapes have an L/D in the range of 0.0 to 0.5 (10:130).
These shapes may be referred to as ballistic. This shape does have
positive aspects that make it a possible shape consideration. The
design of the shape itself is simple and could be conceived from
previous flight data bases. Another point of consideration is that
the capsule design has very good volume efficiency (see Figure 3)
for crew and subsystems and could comply with the Space Shuttle

14

bay volume and mass specifications. Disadvantages lie in the fact that the L/D ratio is considered to be too low to fulfill mission requirements. Also, the capsule shape would reenter at a higher angle of attack, which would lead to high Mach numbers, necessitating strong thermal protection. Another disadvantage of the low L/D is the limited crossrange capability (see Figure 14) which would lead to a fewer number of possible landing sites for a given orbit. The only means of controlling the capsule is by changing the angle of attack by center of gravity displacement. There are possibilities with the application of a parachute system, but most of the landings of capsules are water landings due to the high impact loads, and this limits accessibility for rescue.

In comparing the various vehicle configurations with mission requirements and vehicle parameters, the M2-F3 reentry configuration best accomplishes these goals. The M2-F3 offers an acceptable hypersonic L/D of 1.2 and an increasing L/D with lower Mach number. This allows for a crossrange of around 700 n. mi., various possible landing sites, and a maximum 2 g reentry deceleration. Proposed dimensions of the vehicle result in suitable volumetric efficiency, and internal volume per man is within acceptable limits. Dimensions also allow for suitable Shuttle cargo bay volume and mass constraints. It also incorporates "off-the shelf" hardware and has an extensive data base that has been compiled. The greatest advantage of the M2-F3 over most of the other vehicle configurations is the existence of a prototype model that has been tested in the supersonic range. This allows for the solution of "bugs" in the vehicle design that

15

could not be observed in wind tunnel tests. The design goal of
the M2 project was to accomplish an unpowered horizontal landing
(23:224). The disadvantages of a high approach angle and
difficult handling abilities at low Mach numbers could be solved
with the addition of a gliding deceleration system to be discussed
later in this report. This system could create higher L/D's at
the lower Mach numbers allowing for a less severe (approach) landing
angle. With the implementation of newer and more powerful
computer systems, the Space Shuttle entry guidance system could
readily control the vehicle from deorbit to landing with very
little pilot intervention. In studies conducted on the cost vs.
the number of crew for an ACRV, the development cost of a 6-man to
8-man ACRV was ~~relatively~~ approximately the same (9:1). Therefore, a
recommendation for two 8-man ACRV's would eliminate the
possibility of having to recover two ACRV's in the case of total
evacuation of the Space Station and would also allow evacuation of
the entire Space Station in the event one of the ACRV's is
disabled.

IV. THERMAL PROTECTION SYSTEM

The ACRV must have some form of thermal protection system (TPS) that will enable it to withstand the extreme heating characteristic of an entry into the Earth's atmosphere. Results of a theoretical analysis of the M2 configuration's aerodynamic heating are presented, as well as a discussion of materials under consideration for the ACRV's TPS. Heating data for the M2-F3 configuration is not available, but the data for the M2 configuration is considered sufficient for the purposes of this design.

A. Reentry Heating

Upon reentry from a near-Earth orbit, the ACRV may follow one of the three lift-modulated trajectories shown in Figure 15. The trajectories require angles of attack from 0° to almost 45°. The vehicle will most likely follow the L/D_{max} trajectory, as it gives the greatest lateral range. Freestream Reynolds numbers, based on a vehicle length of 31 ft. (9.4 m) are shown at points along the $L/D=1$ trajectory, as well as stagnation point heating rates, $\overline{q}_0$. These were made dimensionless with respect to maximum heating rate at pullout, which occurs at an altitude of 75 km, as shown (45:3).

Syverston et al (Ref. 49) performed an analysis of the reentry heating of the M2. Figure 16 is a plot of the vehicle's maximum stagnation point heating rates, q_0, as a function of L/D, during an entry from a near-earth orbit. The stagnation point of the M2 is located at or near the vehicle's nose. It is evident that q_0 decreases with increasing angle of attack

17

α. In addition to the heating data, the expected radiation

equilibrium temperature for an emissivity of 0.9 ~~are~~ ˡˢ also shown

(49:904). This number is significant in that it is close ~~the~~ ᵗᵒ the

value of emissivity calculated for the Space Shuttle TPS tiles of

0.71 to 0.9 and allows easy comparison of this data with the Space

Shuttle's TPS data(51:5).

Another important quantity to be considered is the integrated

heat load, the total amount of heat energy expected to be

transferred to the vehicle during reentry. This quantity is very

important in planning the amount of material to be used in an

ablative TPS. The stagnation point heat loads are shown in

Figure 17 (49:904).

In order to design the complete TPS, heating distributions

about the entire vehicle must also be known. Syverston et al

(Ref. 49) performed a theoretical analysis of the longitudinal

heating distribution over the M2 configuration. The results of

the analysis are shown in Figure 18, which gives the ratio of

local heating rate, q, to stagnation point heating rate, q_o, as a

function of distance along the bottom center-line of the body.

Distributions are shown for $\alpha = 0^o$, $\alpha = 12^o$ (at L/D_{max}), and

$\alpha = 45^o$ (at C_{Lmax}) (49:905).

Figure 18 shows that the relative local heating of the lower

surface is reduced by a factor of 8 to 10 as pitch is changed from

0° to 45°. A decrease in heating due to an increase in angle of

attack is surprising, in that this behavior is opposite that seen

at the stagnation point (Figure 16). The variation in lower

surface heating with angle of attack is shown in Figure 19. The

18

figure presents the maximum heating rate and equilibrium wall

temperature as functions of L/D and α for the shoulder point,

where the bottom surface of the M2 becomes conical. This is the

point of highest heating on the lower surface. Figure 19 clearly

shows the variation in lower surface heating and how it is

opposite that of the stagnation point. Also shown in Figure 20 is

the integrated heat load for the shoulder point (49:905-906).

The ACRV TPS should be designed to protect against heating

characteristic of flight at maximum L/D, or $\alpha = 12^O$, which

provides the greatest range for the vehicle.

B. Thermal Protection System

Three main types of TPS were considered for the ACRV. They

were 1) hot (radiative) metallic structures, 2) ablators, and 3)

ceramic tiles and reinforced carbon-carbon (RCC). The last two

materials are grouped together because they comprise the majority

of the TPS of the Space Shuttle. In choosing the TPS, it was

assumed that the structural temperature limit, or backface

temperature limit, will be 350^OF. The performance of materials

like aluminum and graphite/epoxy degrades significantly above this

temperature. After an intense study, an ablative TPS was chosen

as the most suitable for use with the ACRV.

Hot metallic structures have been used for many years in

aerospace applications, giving engineers a great deal of

experience in their use. The X-15 used Inconel alloy X-750 on

both its aerodynamic and radiative surfaces to temperatures of

1150^OF. Shingles made from Rene 41 were placed on the sidewalls

of the Mercury and Gemini capsules. They withstood temperatures

up to 1700°F. The columbium rocket nozzles used in the Apollo

engines were designed for service up to 2400°F (30:234-235).

Use of these alloys on the nose of the ACRV is impossible, as

Figure 16 shows stagnation point temperatures over 3000°F, but

they may be used on the ACRV's lower surface, where temperatures

are below 2500°F at L/D_{max} (Figure 19).

Hot metallic structures were not seriously considered for use

in the ACRV TPS for a number of reasons: 1) they are heavier than

ceramic tiles, 2) the metallic panels must provide for expansion

and contraction without buckling and distortion of aerodynamic

surfaces, 3) the large number of parts, including clips, beams,

standoffs, brackets, and fasteners, that are needed for

installation presents a high degree of manufacturing complexity,

4) attachment to curved substructures presents a problem, and 5)

thermal structural analysis of the effects of stress, thermal

cycling, and creep for the various panel geometries is a very

difficult, costly, and time-consuming task (31:1189).

A table of Space Shuttle TPS materials is shown in Table 1.

Listed are the material compositions and the temperature ranges

these materials can withstand. A primary advantage of utilizing

these materials is their reusability.

The tiles, both high and low temperature reusable surface

insulation (HRSI and LRSI), are made from pure silica fiber and

are coated with a high emittance layer of glass. The tile acts as

both a radiator, for the dissipation of heat, and an insulator, to

block heating of the orbiter's structure. The structure is

characterized by ⌀ stiffened aluminum panels and honeycomb sandwich structures. Two types of tile of varying density are used on the orbiter: the 9-lb/ft^3 LI-900 and the 22-lb/ft^3 LI-2200. LI-2200 is used in areas that require higher structural strength. As is evident from Table 1, the tiles can withstand temperatures up to 2300°F (31:1189).

Reinforced carbon-carbon (RCC) is used on the Shuttle areas that are subjected to the highest temperatures during reentry, the wing leading edge and the nose cap (31:1192). As is evident from Table 1, RCC can withstand temperatures up to 3000°F; however, its density is very high (90 to 100 lb/ft^3) (17:1065).

Looking at Figure 16, it becomes clear that RCC cannot be used for the nose cap of the ACRV, as temperatures encountered at L/D$_{max}$ are well above 3000°F. Figure 19 shows that this material can be used on the lower surface of the vehicle. However, the RCC's very high density makes it a poor choice, as the TPS would become extraordinarily heavy if this material were used on the entire lower surface.

It appears that ablative materials must be used on the nose cap of the ACRV, because they have been proven to withstand temperatures in excess of 3000°F ~~characteristic of the stagnation point~~ (17:1067). The rest of the ACRV lower surface, from the shoulder point to the rear, may be covered with either ceramic tiles or an ablative material.

Figure 19 indicates that if flight at L/D$_{max}$, and hence maximum range, is desired, the maximum temperatures encountered would be very close to the

2300°F-limit of the HRSI. If the vehicle is flown at an L/D = 0.8, the maximum temperatures encountered on the lower surface would be about 2000°F, and ceramic tiles could be used. However, the lateral range of the ACRV would be reduced from about 950 miles to 500 miles, a substantial loss. Fortunately, part of this lost range could be recovered with a simple maneuver suggested by Syverston et al (Ref. 49). The vehicle could fly at the α giving L/D = 0.8 until the point of maximum heating is past (h ≈ 75 km as shown in Figure 15). The ACRV would then pitch to the attitude for maximum L/D, extending range without increasing maximum heating rates. In this case, pitching to L/D = 1.2 after flying at L/D = 0.8 would *increase the to* ~~supply a~~ range ~~of~~ about 750 miles. A trajectory of this sort would enable *the* use of ~~the~~ ceramic tiles on the lower surface of the ACRV, with a small sacrifice of cross range.

Integrating a ceramic tile TPS with the M2 shape poses problems, however. The HRSI tiles can run as thick as 4 to 6 in., as they do on the Space Shuttle's body flap's lower surface, where temperatures exceed 2000°F (11:24). Looking at Figure 19, it becomes evident that, at maximum L/D, the maximum lower surface equilibrium temperature is about 2200°F or, with trajectory adjustment, 2000°F. If the ceramic tiles are to be used at this point at all, they must be at least 6 in. thick.

The problem with using tiles of this size on the ACRV becomes clear when looking at Figure 21. This figure shows the curvature of the M2's lower surface at the shoulder point and how the

22

six-in. tiles would appear if they were employed there. Assuming a vehicle span of 13 ft. and length of 31 ft., the radius at this point would be about 2.75 ft., as shown. Assuming some means could be found to attach the flat-surfaced tiles to the highly curved surface, tile gaps on the order of 1.5 in. would be produced at a point on the vehicle critical to thermal protection.

Gap fillers are available. For this high-temperature application, only pillow-type gap fillers could be considered. These consist of an envelope of ceramic fabric that is stuffed with a resilient fiber batt and sewed together with quartz thread. Use of these fillers for this purpose would probably be impossible, however, as published reports discuss filling gaps only on the order of 0.2 in. Also, the pillow type fillers can only withstand temperatures up to 2000°F for a single mission (31:1192).

Tiles of lower width could be used, but the tiles are *ceramic*. This material is very brittle, has little tolerance for stress concentrations, and has a large scatter in material properties (31:1191). Using thinner tiles with the required six-in. thickness would decrease the structural stability of each tile considerably, making them more susceptible to failure. Granted, the six-in. ~~thick~~ tile thickness is not required over the entire underside of the ACRV, but this example does illustrate the problems with using ceramic tiles on a highly curved surface.

In order to integrate the tiles with the ACRV shape, they would have to be fabricated in curved or angled shapes. This would increase both the manufacturing expense and structural complexity of the tiles.

Another problem with using a ceramic tile TPS is its integration with the ACRV's landing system. As will be covered later in detail in this report, the preferred landing system for this vehicle is an Air Cushion Landing System (ACLS), which consists of a flexible trunk into which compressed air is driven. If a ceramic tile TPS is used, the ACLS trunk fabric will have to be deployed through doors in the tile surface, as shown by the shaded areas in Figure 22.

Clearly, a large number of doors are required, but an even larger problem would be the hinging of the doors. Obviously, the hinges cannot lie at the tile surface because of the extreme temperature they would encounter there, ruling out the possibility of the doors opening out as in Figure 22. Placing the hinges inside, on the primary structure of the ACRV, would enable the doors to open inwards and protect the hinges but would also require a large clearance, reducing the amount of usable volume in the spacecraft. Also, tile thicknesses could run as high as 6 in., so that a large clearance between the door tiles and the surrounding tiles would be necessary to allow the doors to swing open. One possible solution would be the use of a mechanical or hydraulic system to lower the doors clear of the surrounding tiles and then swing them open; however, this also offers mechanical complexity and reduced vehicle volume. Still another solution to the landing gear problem would be to make the lower surface tiles expendable and to discard the entire lower surface upon approach to landing; however, using the tiles in this manner is not cost effective, as their reusability, an advantage gained through great expense, would be wasted.

24

As has been shown, use of either the ceramic tiles or hot radiative structures with this vehicle have substantial drawbacks. An ablative TPS, designed with expendable sections for easy deployment of the landing system, seems to be the best choice for use with the ACRV. A good example of an ablative TPS, and one which is considered suitable for the ACRV, is that which was employed to protect the Apollo command module (CM) during its reentry at lunar return velocities.

The Apollo TPS made up the entire outer shell of the CM and consisted of an ablator bonded to a substructure constructed from brazed stainless-steel sandwich panels. The ablative material used was AVCO 5026-39G. It consists of an epoxy novalic resin reinforced with quartz fibers and phenolic microballoons. Its density is 31 lb/ft^3. AVCO 5026-39G was applied to the substructure in the following manner: a phenolic honeycomb was first bonded to the stainless-steel shell with HT-424 adhesive, and then the ablator was inserted into each individual honeycomb cell with a hypodermic device (37:4).

Figure 23 shows how the ablator thickness varied with location on the CM and the corresponding surface temperatures encountered during reentry. Note how the stagnation point temperature of 5000°F was at least 1000°F higher than the maximum temperature expected to be encountered at the ACRV's stagnation point (Figure 16). Also note how the ablator is its thickest at the stagnation point. There, the heat load was at its maximum and required an ablator thickness of 2.7 in. (37:5).

A closer view of the structure at the stagnation point, and also a point on the windward side of the CM, is presented in

Figure 24. Section B-B, which cuts through the leeward side where the heating rates were lower, shows an ablator thickness of only 0.7 in. At both section A-A and B-B, the space between the stainless steel substructure and the CM's pressurized aluminum cabin is shown to have been filled with a low density (3.5 lb/ft^3) fibrous insulation, TG15000. This insulation acted to reduce heat transfer between the two structures (37:5). At the ablator-substructure interface, the maximum temperature encountered was $600^{\circ}F$. The insulation kept the aluminum pressure vessel structure under $200^{\circ}F$, well within material limits (37:2).

Stainless-steel was chosen for the heat shield substructure because of its higher melting point, providing for at least partial protection of the CM in the event of a localized loss of ablator. The stainless-steel alloy PH14-8MO was used because it exhibited good fracture toughness throughout a wide temperature range (37:13).

As mentioned earlier, the Apollo TPS was designed for protection of the CM at lunar return velocity. This velocity, approximately 36,000 fps, is much higher than the entry velocity characteristic of a return from earth orbit (26,000 fps); thus, the Apollo TPS was designed to withstand heating rates and loads much higher than those expected to be encountered during ACRV entry. The Apollo TPS was designed to accommodate heating rates up to 1030 $BTU/sec\text{-}ft^2$, about ten times the expected stagnation point heating rates for the ACRV (Figure 16), and heat loads up to $45x10^3$ BTU/ft^2 (47:186). This number refers to the total heat load for

26

the entire vehicle. It is lower than those corresponding to the ACRV's stagnation point at L/D_{max} (Figure 17); however, at the shoulder point (Figure 20) and the rest of the lower surface, heat loads never appear above 20×10^3 BTU/ft^2.

Basically, the thermal environment the ACRV will encounter upon reentry is not as severe as that met by the Apollo CM; therefore, the ablative TPS of the ACRV is not expected to require as much ablator per square foot. The thickness of the stainless-steel substructure may also be much less.

Because of the unavailability of specific information, it was not possible to define the size and structure of the heat shield required for the ACRV. No simple relationships between local heat loads and heating rates and required ablator thickness were located. Also, proper design of the substructure would require knowledge of the specific aerodynamic loads on the ACRV and the type of structure the vehicle itself will have. A rough weight estimate can be made, however, if the type of TPS to be used is very similar to the Apollo CM's.

The weight of the CM TPS was 1700 lb (37:14). The TPS covered the entire vehicle. Assuming CM dimensions of 11.7 ft. by 12.8 ft. (22:66), then the TPS covered an area of approximately 460 ft^2. The ACRV dimensions of 31 ft. by 13 ft. would suggest a total vehicle surface area of approximately 900 ft^2, about twice that of the CM. Noting from the previous discussions that the Apollo vehicle was designed for heat loads roughly twice those to be encountered by the ACRV, one could roughly estimate the weight of an ablative TPS for the ACRV to be 2000 lb. The weight could

27

probably be reduced if light, reusable protective materials, like those in Table 1, were used on the cooler, less curved parts of the vehicle, such as the upper surface.

Integration of the lower-surface ACRV heat shield with a landing system can be easily accomplished by making it expendable. Upon approach to landing, light explosives could be used to detach the heat shield from the ACRV as in the two cases in Figure 25. Special care would have to be taken in designing the explosive sequence and magnitudes and the vehicle attitude at which the detachment takes place to insure the shield does not strike the ACRV. Once the shield is detached, the ACLS or any other type of landing system may be deployed.

Of course, making the lower heat shield expendable will limit the number of landing sites open to the ACRV. Approach to landing will only be made over water or unpopulated areas.

From both an economic and engineering standpoint, the ablative heat shield is the best candidate for use with the ACRV. Although much heavier than a ceramic system, the ablative TPS is mechanically much simpler, and therefore, less costly to develop.

V. DECELERATION SYSTEM

Because one of the purposes of the ACRV is to provide transportion in the event of a medical emergency, a deceleration system is needed that will satisfy the following criteria:

1) limiting deceleration g's to 4.0 in the x direction (13:21)

2) limiting impact g's to 10.0 in the x direction (13:21)

3) limiting the time to six hours for departure from the space station to arrival at the medical facility (13:11)

4) allowing alternative landing sites (13:9).

Methods of achieving a controlled descent were examined that best met these criteria. These methods include the use of conventional parachutes, gliding parachutes, and the sailwing auxiliary lifting surface.

A. Conventional Parachutes

In the past, the Mercury, Gemini and Apollo capsules all used parachutes for deceleration. In particular, the Apollo capsule used one 16.5 ft. diameter drogue parachute and two 85.5 ft. diameter ringsail parachutes (29:9). The parachute system kept the capsule reentry below 4 g's through descent and 10 g's at impact with water (8:1). This system fits the ACRV requirements except that the system does not provide any lateral control for the choice of landing site. Also, this system is restricted to a water landing since tests of a land landing of the Apollo capsule exceeded the prescribed g's (8:2).

29

B. Gliding Parachutes

After examining several types of parachute systems, a gliding parachute system appears to best meet the needs of the ACRV in regard to payload, descent velocity, g limits and fabrication. Also, a gliding system will allow a greater choice in landing sites. Control of the landing site can reduce the elapsed time of flight by landing near a major health care facility. The systems that are examined include paragliders, parawings and parafoils.

A paraglider (shown in Figure 26) is a triangular planform wing which contains a rigid support along the center. The paraglider is also referred to as a single-keel parawing. Although the paraglider was successfully tested with a Mercury capsule, other tests have verified that the paragliding system can not presently accomodate the weights of 10,000 to 20,000 lbs. as are predicted for the ACRV(7:6).

The twin-keel parawing (shown in Figure 27) which is also referred to as the "Rogallo" wing, was found to perform better than the paraglider (35:1). The twin-keel parawing consists of two triangular panels which are connected to opposite sides of a rectangular panel with two keels at the connection points.

To date, the twin-keel parawing has only been tested with payloads up to 6000 lbs(35:1). With this payload, the parawing was successful at achieving a steady glide despite canopy damage and was capable of limiting the maximum g's to below 4.0 (35:10). The parawing system, however, requires a four-stage reefing sequence for deployment (35:11). This reefing sequence would require a complex control system and would be subject to many opportunities for failure. For this reason, the twin-keel

parawing deceleration system was not chosen.

The final gliding parachute that has been examined is the ram-air inflated parafoil. The parafoil consists of an upper and lower surface connected by longitudinal webs as shown in Figure 28. The cross-sectional shape is a standard airfoil shape with the leading edge open for inflation.

Pioneeer Aerospace Corporation and Marshall Space Flight Center are currently researching parafoil systems with the goal of obtaining a deceleration system for a 60,000 lb. payload. As an intermediate step, wind tunnel and drop tests of a 10,000 lb. payload have been completed. During these drop tests, the parafoil achieved a steady gliding state despite minor canopy and suspension line damage (2:102). The parafoil system, in comparison to the parawing, only requires a two-stage reefing sequence (2:102). The purpose of the reefing sequence is to reduce the peak loads created during deployment.

A maximum vertical velocity of 12 ft/s has been established for the proposed landing system. This velocity and a proposed vehicle weight of 10,000 to 20,000 lbs. are being used to determine the parafoil wing span and a deceleration system weight. This information is shown graphically in Figures 29 and 30. According to the estimates in Figure 29, the parafoil wing span should be at least 300 ft.(1:56). Figure 30 shows that the parafoil system weight, which includes a drogue parachute, is between 700 and 1300 lbs. (1:56). These estimates were based on a linear fit of the data, and therefore, do not account for constant weight components such as control systems, steering, sensors and computers. For this reason, the parafoil system weights of actual

31

drop tests are used to estimate the weight between 1500 and 2000 lbs.

The deployment sequence will consists of five stages which are 1) deployment and reefing of the drogue parachute, 2) deployment and reefing of the parafoil, 3) a flare maneuver, 4) full gliding state and 5) touchdown (1:20). Table 2 shows the anticipated velocity components for each stage.

The purpose of the flare maneuver is to position the payload for landing and to decrease the touchdown velocity. This maneuver eliminates the need for retro rockets. The flare effectively increases the L/D at low angles of attack (3:30A). This maneuver can be accomplished with trailing edge deflection at 60 to 80 ft. above ground level with the use of pyrotechnic retractors and cutters (1:56-58).

Two different drop tests were examined for velocity and load estimations. The first parafoil has a span of 322 ft. with 7 cells and a payload of 10,450 lbs. The second parafoil has a span of 598 ft. with 27 cells and a payload of 11,864 lbs. An estimate of the g force for each case is determined by dividing the load by the mass of the vehicle. The drop test data and estimated g forces are shown in Table 3. For these cases, the peak g's are below 4.0 even for the cases of premature disreef (5:1990). This data also shows that an increase in span creates a significant decrease in the descent velocity (5:1990). Overall, this data indicates that a vertical velocity of 15 ft/s and forces less than 4 g's are feasible.

Since the wing loading is found to be maximum at the leading edge, the strongest suspension lines, 1000 lb. Kevlar cord, are

32

needed at the leading edge (4:111). Over the leading 40% of the chord, the strength of the lines can be gradually decreased to 400 lb. Kevlar which can then be used throughout the remainder of the chord (4:111). The load across the span displays an elliptical behavior. The minimum load is experienced at the tips and the maximum at the center of the span (3:31A). Again, the suspension lines can be adjusted with the highest strength cord at the center.

The canopy is constructed of nylon fabric, and the risers are made of nylon webbing (2:62). These materials are already in fabrication and have been successfully used for conventional parachutes.

After analyzing these different parachute systems, the parafoil system was found to most effectively meet the criteria of g limits, mission time and landing sites; however, the sailwing auxiliary lifting surface was also seriously considered for use in the ACRV's braking system, and is described below.

C. Sailwing Auxiliary Lifting Surface

The lifting body shape represents a vast improvement in reentry capability over ballistic bodies; however, its flying qualities are still severely limited. Several types of auxiliary lifting surfaces may offer improved landing performance, such as increased control and stability and decreased sink rate. In particular, the sailwing concept is ideally suited to satisfy these requirements.

The efficiency necessary for a lifting body reentry vehicle intensifies the penalties in weight, space, and cost that many

auxiliary lifting surfaces have. The sailwing, however, offers several unique characteristics including light weight, simplicity, and very good aerodynamic performance.

A sailwing is a semi-flexible, high aspect ratio wing. This wing is stowed prior to extension in a small body cavity. The space requirements are minimized for the rigid leading edge spar and wing material. The wing may be extended from behind an expendable cover by deploying small solid rocket thrusters mounted at the wing tips. Figure 31 roughly visualizes the application of sailwings to the M2-F2 lifting body configuration.

As presently envisioned, the vehicle will reenter the atmosphere and descend to approximately 50,000 feet. Deceleration to subsonic flight may be accomplished with the help of a drogue chute. The vehicle will then be maneuvered through a near zero-g trajectory for a few seconds, allowing deployment of the sailwings. The vehicle may then fly a normal glider landing to a preselected site. Figure 32 shows a comparison of the M2-F2, the M2-F2 with sailwings, and another lifting body (CC-1) with sailwings. Lift coefficient is much greater for a given glide path angle, with deployment of the sailwings. It should be noted here that although the CC-1 shows an even greater performance in the figure, the lifting body does not fit the needs of the braking and landing system. Poor flight performance and shape considerations negated any positive contribution of the sailwings with the CC-1 lifting body shape. Figure 32 describes a nominal landing weight of 8000 lbs. and a reference area of 160 feet (48:14). This data is a scaled down version of the vehicle envisioned in the project objectives; however, it does show a

34

relative improvement and should therefore be considered valid for any weight and size of the vehicle.

An important aspect to take into consideration in the braking and landing system is the rate of sink. This is the time required to descend from a given altitude, and the minimum speed attainable before touchdown. With the use of sailwings, an approximate 75% reduction in the sink rate and a 25% reduction in landing speed is possible (36:42). Also, the velocity for minimum sink rate is reduced, as are angles of attack. Figure 33 shows this sailwing performance improvement for the M2-F2 lifting body, presenting rate of sink verses velocity at sea level. A decrease in rate of sink is necessary for the air cushion landing system that is described in this report.

The aerodynamic characteristics of the sailwing are also positive in comparison to a rigid wing of similar dimensions. The sailwing will effectively gain an increase in camber as load is increased and dynamic pressure is constant. This essentially increases the lift curve slope, the maximum lift, and static stability. In fact, the lift capability and lift-to-drag ratios are nearly doubled over the plain M2-F2 lifting body aerodynamic characteristics. This equates to a performance gain and a percentage of gross weight loss when comparing the sailwing and a rigid wing of similar dimensions. The estimated sailwing weight penalty is shown in Figure 34.

Some other problems of a simple lifting body shape are also alleviated with the use of sailwings. Inherent to a plain M2-F2 lifting body shape without sailwings are weak low-speed dynamic damping, low directional stability, and low roll damping.

35

Although the sailwing auxiliary lifting surface does not completely reduce these effects, the addition of an aft auxiliary horizontal wing will further improve the performance. The M2-F3 lifting body shape being studied has this added feature of stability.

Possible flutter of the sail is also a concern. This may occur if a zero g trajectory was not used during deployment. Loss of lift and high pitching moments may also occur if this flutter exists in the sailwings during flight.

High dynamic pressures will also create problems due to internal loads in the wings. Special venting to the aft interior of the sailwing may reduce this problem. Filleting of the wing will add an effective porosity to the wing in a controlled manner, allowing a reduction in internal loads but a minimal increase in the sink rate.

Several important performance and stability tests of an M2-F2 lifting body model were analyzed at Princeton University in a 4 ft. by 5 ft. subsonic wind tunnel. The testing was done at a dynamic pressure of 15 psf.

Due to the large percentage lift contribution of the lifting body relative to the comparably small sailwings, the M2-F2 model with sailwing features does not have a large stall effect or leveling off of the lift curve at large angles of attack.

The effect of wing location was tested at four positions (MID, AFT, AFT I, AFT II), each position progressively rearward on the model. The wing location does not have a pronounced effect on pitching moment in the tests. Figure 35 shows a nearly exact data correlation for the four sailwing locations on the body, as lift

36

coefficient increment is plotted relative to the angle of attack. These results present the large stability and control gains of sailwing features, regardless of rearward body position.

Both the parafoil and sailwing braking system offer several advantages; therefore, both are considered good candidates for use with the ACRV. Presently, the parafoil system is favored because, as discussed above, prototypes have ~~recently~~ been built and successfully tested *recently*, giving designers a good database to work from. Development of the sailwing lifting concept has been limited. Perhaps both systems could be used together with the ACRV; the parafoil would act as a primary system and the sailwing would offer redundancy.

VI. LANDING SYSTEMS

For the ACRV mission, a landing system must be employed to minimize impact forces that would occur during landing for crew safety. In order to minimize the g forces, a high glide path will be taken to ensure a safe landing and not a straight drop to the landing site. Systems that have been deployed on spacecraft have been conventional aircraft landing gear as on the Space Shuttle, strut-shock absorbers and thrusters as on the Apollo lunar module, impact landings on water with parachute systems as with the Apollo program, and mid-air recovery systems of drones. The landing system for the ACRV will have the ability to land at as many locations as possible for a medical emergency mission. A land landing provides quick access to medical facilities and a water landing provides immediate return in the event of a Space Station evacuation. The landing system of the ACRV will be designed to be a small percentage of the ACRV total weight.

A. Conventional Aircraft Landing Gear

Conventional aircraft landing gear systems consist of a set of nose gear located forward of the ACRV's cg and two sets of main gear located aft. Each set contains two wheels, pneumatic shock absorption systems, extension/retraction mechanisms, and hydraulic brake systems. Conventional aircraft landing gear systems can only land on prepared surfaces and typically weigh five percent of the aircraft gross weight (14:312). This system is inappropriate for the ACRV since it may not be possible to land on a prepared surface.

B. Strut-Shock Absorbers and Thrusters

Strut-shock absorbers and thrusters offer little application to the ACRV due to the weight of the strut-shock absorber and the additional thruster system required. The thruster would be located on a lower surface of the ACRV and would require additional structural support, fuel and oxidizer, and system components. Floatation devices would also be required for a water landing. Therefore, strut-shock absorbers and thrusters ~~will~~ *would* provide excessive weight ~~which could be minimized~~ *that would be eliminated* with the use of a different landing system.

C. Skid Landing Systems

Skid landing systems are low-weight, low-cost, easy-maintenance systems which can only land on soft surfaces. This landing system consists of three skids, one located forward of the ACRV's cg and two located aft. Even though the skid lacks maneuverability on the ground, this problem may be overcome with a small retractable wheel in each skid. The small wheel creates disadvantages by increasing weight to 4.7 percent of the vehicle gross weight which increases both cost and maintenance (14:309). Thus, the skid landing system is inappropriate for water and airstrip landings.

D. Ski Landing Systems

Ski landing systems are similar to skids but incorporate a larger ground contact area. Skis are commonly used for landings on snow and ice, and can be adapted for operation on other

39

surfaces by incorporating a wheel into the ski (14:309). This
system has disadvantages in that it is mainly designed for arctic
conditions. The ACRV will not be exposed to these conditions
since the orbital inclination of the Space Station is 28.5°.
Cross-range capability of the ACRV will not enable the vehicle to
reach these areas from that orbit.

E. Mid-Air Recovery Systems

Mid-air recovery systems incorporate a deceleration system,
such as a parachute, and a grappling device intended for
helicopter retrieval. The mid-air recovery system has been tested
and "proven costly from the point of view of damage, loss and
logistical complexity" (6:605-606). Hence, this system was no
longer considered in the research.

F. Air Cushion Landing System

The Air Cushion Landing System (ACLS) provides an alternative
to the landing systems previously considered. The ACLS provides
the ACRV with the ability to land on surfaces such as concrete,
water, sand, snow, rough land with _small_ tree stumps, high grass and
muddy fields (15:12-5). The ACLS mainly consists of an inelastic
or elastic trunk fit to the lower surface of the vehicle. A
general example of this is shown in Figure 36. An inelastic trunk
is fabricated from materials resembling reinforced nylon which do
not stretch, whereas an elastic trunk stretches. A variety of
shapes may be used, ranging from an oval shape to a pear shape to
a rectangular shape. The trunk inflates through the use of a
compressor unit. Air flows through the lower surface of the trunk

creating a clearance height over the ground (typically one inch).
The air, when in ground effect, creates a pressure within the
trunk cavity which supports the vehicle. The clearance height
reduces the friction between the trunk and the ground, and
increases maneuverability.

1. Testing

The ACLS has been tested on aircraft ranging from the
2,400 pound Bell LA-4 to the 41,000 pound de Havilland Buffalo CC-
115 (designated the XC-8A for testing). See Figure 37.

a. Test Results of the LA-4

The LA-4 was tested in three stages by Bell Aerospace.
The first stage consisted of static ground tests in which the ACLS
equipped LA-4 was pulled over various surfaces for baseline data
on drag, brake effectiveness, and engine-cushion pressure
characteristics with the pull force (6:421). Taxi tests were
performed over paved surfaces and grass. These tests showed that
the test craft could be operated in positive control with a safe
turning radius superior to the conventional tricycle gear of the
LA-4. The testing continued over sand, long and short grass, and
snow with performance altered only by the relative friction of the
surface (6:422). The next step of this stage was an obstacle
course set up with tree stumps, ditches, multi-leveled formations.
The course was successfully negotiated at speeds up to 30 mph. No
unusual trunk wear was noticed in these tests (6:422).

The next stage was a series of flight tests to determine
the landing characteristics of the ACLS. These tests showed that
the ACLS flight performance and handling were comparable to
conventional gear on paved surfaces and better on unprepared

surfaces.

The final tests determined its capability for over-water flight and damage tolerance. Low and high speed taxi tests were performed on Lake Erie in six to twelve inch choppy water and were very successful. The aircraft was able to takeoff in 650 feet and land in about 450 feet. The damage tests were done by physically damaging the trunk allowing air to escape. With a 350 sq. in. hole, the ACLS was able to maintain a constant air pressure under the vehicle (6:423).

b. Test Results of the XC-8A

This study began from considering the LA-4 a scaled model of the XC-8A to predict actual power requirements, trunk size, and cushion pressure. Wind tunnel tests and vertical drop tests were done on a 1/10 and 1/4 scale models of the XC-8A. Figure 38 shows the vertical peak loads as a function of descent rate at varying pitch angles. These results show an acceptable range of loading which is comparable to conventional gear (26:96). With a maximum velocity of 12 ft/s, the ACLS can land at a higher vertical velocity than conventional aircraft landing gear which land at 10 ft/s. The longitudinal decelerations of the 1/10 scale model did not exceed 0.25 g's for any landing on hard surfaces with a maximum forward velocity of 83 mph (6:485). The 1/10 model was also tested by adjusting the height of the braking system. It was found that increasing the height resulted in an increase in the horizontal acceleration up to a height of twelve inches and any further increase in height resulted in no increase in the deceleration which peaked at 0.35 g's, Figure 39.

2. Designing

In designing an air cushion landing system, the following parameters must be considered:

1) the shape

2) the material

3) the cushion pressure, P_c (psfg)

4) the clearance height, d (in)

5) the flow rate required to the trunk, Q_j (ft^3/s)

6) the horsepower of the fan unit, Hp.

These parameters ~~was~~ *were* analyzed and determined based on the M2-F3 configuration. Figure 36 locates these parameters on a diagram of the standard ACLS configuration.

a. Shape of the ACLS Trunk

The ACLS shape must contain a large cushion area to distribute the weight of the spacecraft, have a high width to length ratio to minimize the cushion perimeter (which reduces the trunk airflow) ~~thus decreasing required horsepow~~er, and lie away from the spacecraft's center of gravity to provide roll and pitch restoring moments (16:262). The three cushion planforms shown in Figure 40 are the most commonly used for ACLS test vehicles. These planforms have been successfully tested; however, NASA has developed a segmented trunk concept which simplifies fabrication, cost, production, and maintainability due to simple, repeated geometries with no compound curvature (32:66). Figure 41 shows the trunk planform of the NASA test vehicle designed for a 5,500 lb. load. If trunk damage occurs, only the affected segment would need to be replaced ~~not affecting the other segments~~. The ACLS design will incorporate the segmented trunk concept to better fit

43

the M2-F3's curved underside. The M2-F3 design would permit a pear shaped trunk, but a three-segmented trunk design would provide cost savings in production due to the simplified design. The trunk will be designed in the shape of an isoceles triangle with the tip pointing forward. Since each segment of the trunk will have an independent air valve, the ACLS will implement a roll and pitch control system by increasing or decreasing air flow to a particular segment, Figure 42.

b. Materials

The material for the ACLS trunk must provide a controlled shape when inflated, strength and high tear resistance, ability to sustain damage without catastrophic failure, air containment and retraction elasticity. Various materials that have been used in ACLS trunk development include: natural rubber, Spandex, butyl, neoprene, polyurethane, teflon, hypalon, viton, nylon, Kevlar, and silicone rubber. A fabric is used to control shape and provide strength, and rubber is used for retraction. These materials are combined to form a composite material.

i. Elastic

Elastic trunks are constructed from a wound nylon tire cord placed between layers of natural rubber. By varying the number of coils per inch, each section of the trunk will be able to expand by the amount necessary (from 0% to 300%). Orifices are molded into this composite and cured into a homogeneous sheet.

ii. Inelastic

Inelastic trunks are more cost efficient than elastic trunks because inelastic trunks are fabrics with a polymer sealer. Two types of inelastic trunk materials are neoprene-

coated nylon and Kevlar-polyurethane fabrics. The nylon-neoprene trunk may be stitched and molded to the desired trunk shape. The Kevlar-polyurethane trunk is produced through the use of a mold. The mold is first sprayed with coats of polyurethane and the Kevlar fabric is then laid over the mold before the polyurethane dries.

The orifice zone for the two inelastic materials are made differently. For the nylon-neoprene trunk, the holes are drilled through the brake treads at an inward angle of 45°. The Kevlar-polyurethane trunk makes use of the natural porosity of the material. This is done by covering this region with tape in a checker board fashion and lightly spraying it with more polyurethane.

iii. Material Comparisons

An advantage of the elastic trunk is that it retracts to the vehicle surface when the air flow is turned off. An elastic trunk is more complicated than an inelastic trunk and "is an order of magnitude more expensive than an inelastic trunk. Other one-piece trunks, both molded and stitched (to shape), are at least two or three times more expensive than the segmented trunk" (32:62,66). "An inelastic trunk which is manually stowed should prove best for ... emergency landing systems and crew escape capsules" (6:567). The most advantageous option would seem to be an inelastic trunk constructed of Kevlar-polyurethane.

c. Trunk Cross-Sectional Shape

The trunk dimensions can be found through the use of a computer program which simulates the unloaded inelastic trunk cross-section, and the loaded inelastic trunk cross-section. The

unloaded or free trunk shape occurs prior to the touchdown phase of flight when the vehicle is entirely supported by the air cushion and no load is transferred to the ground. The loaded trunk cross-section occurs while the trunk is partly flattened by the ground and is transmitting forces through the thin layer of air. The program is provided by Digges (6:262-290) whose theory is the basis for the ACLS design. The programs are coded in FORTRAN 66 and understanding sections of the code is difficult. Since the current design did not delve into the exact location of the ACLS trunk on the M2-F3, only rough estimates were used in locating the attach points needed to run the program. As a result, indecipherable output was obtained from the programs. The programs are listed in Appendix I for reference.

d. Deployment of ACLS Trunk

An additional covering is necessary to protect and isolate the ACLS trunk from the force of the explosive charges necessary to detach the ablative thermal protection system. The trunk will be joined at one location on the main structure and the other on the hinged section, Figure 43. Three of these sections will be positioned on the underside of the M2-F3 in a triangular configuration using a series of assembly tubes. This concept would allow the minimum change of structure to the vehicle.

e. Braking System

A braking system is necessary to bring the vehicle to a stop on land in an appropriate distance with a safe deceleration rate. There are two types of braking techniques used in the ACLS system: skid braking and suction braking.

Skid braking is comprised of six brake pillows which are

46

embedded within the trunk near the rear section of the vehicle, Figure 44, and are inflated separately from the trunk. The outer portion of the pillow is a replaceable skid material which consists of steel impregnated butyl pads and ~~are~~ *is* similar to tire treads. Testing on these brake pads show that if braking is initiated below 50 knots, 50 landings can be made before replacement is necessary with *a* deceleration rate of around 0.3 g's (38:6).

The cushion of air which supports the vehicle may be altered to create a vacuum which pulls the vehicle to the ground, thus decelerating the ACRV (See Figure 45). This would require an additional compressor unit to create this vacuum ~~and~~ *which would* increase the weight of the ACRV.

f. Determination of Cushion and Trunk Pressures

The cushion pressure within the trunk cavity which supports the vehicle can be determined by

$$P_c = W/A_c \tag{1}$$

where:　　W = weight of the vehicle,

A_c = cushion area under the vehicle.

The trunk pressure, P_j, is related to the cushion pressure by the dynamic response of the system (6:62). A low P_c/P_j ratio gives a rigid trunk increasing the impact load while a high P_c/P_j ratio results in a more deformable trunk. The ACLS must withstand the impact forces in the acceptable range and be rigid enough to deflect obstacles. Since the landing site depends on the type of the mission, a P_c/P_j ratio of 0.5 is recommended so that the ACLS could land on water or land.

g. Determination of Flow Rate and Horsepower Required

47

To determine the flow rate, Q_j, into the trunk, the perimeter of the trunk, S, and the clearance height, d, are needed. The cushion perimeter is the distance around a tangent to the lower surface of the trunk, see Figures 36 and 46. The clearance height is the height of the air flow between the trunk and the landing surface. The flow rate Q_j can be found from Currey (15:12-25).

$$Q_j = V \, S \, d \, C_d \qquad (2)$$

where: V = flow velocity exiting the cushion perimeter,

           S d = effective cross-sectional area of the flow,

           C_d = the discharge coefficient.

In this design, C_d will be considered to be equal to 1.0, the ideal case. The flow velocity, V, may be found by applying Bernoulli's equation to the flow field, refer to Appendix II. The result is

$$V = S \, d \, \sqrt{(2 \, P_c)/\rho} \qquad (3)$$

where: P_c = cushion pressure(psfg)

           ρ = density of air at STP (lbf s^2/ft^4).

Subsequently, the horsepower for driving the fan is given by

$$Hp = (Q_j \, P_c)/550 \qquad (4)$$

All of these equations may be combined to get the horsepower as a function of weight, cushion area, perimeter of the trunk, and clearance height.

$$Hp = S \, d \, (W/A_c)^{1.5} \, (2/\rho)^{0.5} \qquad (5)$$

Table 4 lists values calculated in the areas of interest with the weight of the ACRV varying between 10,000 and 15,000 pounds. The parameters found to change the horsepower the most are the

clearance height and the cushion area. The perimeter does not change as much as the area for a given change in dimensions of the triangular base. Using an average value for the weight of 12,500 lbf and a clearance height of 0.75 to 1.00 in., the horsepower for the two areas ranges from 163.57 Hp to 263.69 Hp. The LA-4 required a horsepower of 44 and the XC-8A needed 1,080 Hp (6:265). A power requirement of 160 to 270 Hp would be the approximate range for the compressor.

VII. CONCLUSIONS

Having considered the proposed subsystems and discussions presented in this report, a design for the braking and landing system of the ACRV has been developed. An eight-man ACRV is preferred because a cost analysis has shown that having two of the vehicles docked at the Space Station will provide improved levels of redundancy without a substantial increase in cost relative to two-, four-, and six-man designs. The braking and landing sequence proposed consists of a reentry, during which the ACRV will use lift to reduce deceleration loads and maneuver through the atmosphere, and then deployment of a parachute system that will enable the vehicle to glide to a land landing.

An L/D of 1.0 for the reentry vehicle will be sufficient to provide for a quick return to Earth as required by the emergency medical mission. In comparing the various vehicle configurations with mission requirements and vehicle parameters, the M2-F3 reentry configuration best satisfies the criteria. The M2-F3 offers an acceptable hypersonic L/D of 1.2 and an increasing L/D with decreasing Mach number. This allows for a crossrange of around 700 n. mi., various possible landing sites, and a maximum 2 g reentry deceleration. Dimensions of the vehicle result in acceptable volumetric efficiency *and* are suitable for Shuttle cargo bay volume and mass constraints. The vehicle also incorporates "off-the shelf" hardware and has an extensive data base *on performance characteristics* that has been compiled. The greatest advantage of the M2-F3 over most of the other vehicle configurations is the existence of a prototype model that has been tested in the supersonic range. With the

50

implementation of newer and more powerful computer systems, the
Space Shuttle entry guidance system could readily control the
vehicle from deorbit to landing with very little pilot
intervention (to provide for use by a deconditioned crew).

Of the three forms of thermal protection systems (TPS)
considered, an ablative TPS was chosen to be the most appropriate
for use with the ACRV. Hot radiative (metallic) surfaces were
ruled out because of their structural complexity. Ceramic tiles
were not chosen because of obvious difficulties that would be
encountered when trying to integrate them with the highly curved
lower surface of the M2-F3 lifting body. It is assumed that the
TPS will be similar to that used on the Apollo command module,
consisting of an ablator bonded to a stainless-steel substructure.
Insulation between the substructure and the main airframe of the
ACRV must be provided. The heat shield on the lower surface of
the ACRV will have to be expendable. It will detach from the
vehicle via explosive charges upon approach to landing. This will
allow for the deployment of the air cushion landing system. Total
TPS weight is estimated to be 2,000 lbs.

After examining several deceleration systems, both the ram-
air inflated parafoil and the sailwing appear to satisfy the established
criteria. The parafoil itself is estimated to have a span of 300
ft. and a weight between 1,500 and 2,000 lbs. A two-stage reefing
sequence is required to keep the g forces below 4.0. The parafoil
system will be constructed of typical nylon fabric, nylon webbing
and Kevlar cord. This system will enable the vehicle to glide to
a predetermined landing site with a vertical velocity of less than
15 ft/s. The sailwing system offers several characteristics that

warrant its use, including light weight, simplicity and good aerodynamic performance. The wing will be extended from behind an expendable cover by deploying small solid rocket thrusters mounted at the wing tips to allow a normal glider landing. Since more testing has been conducted on the parafoil system, it will be used as the primary deceleration system (Figure 47) with the sailwing as a secondary system (Figure 48).

The landing system will be an air cushion landing system (ACLS). Testing on aircraft has shown that the ACLS is an effective landing system for all types of surfaces, land or water. Also, the ACLS ~~shows~~ *has been shown to be* reliable since it can sustain damage and still function properly. From these tests, a pitch attitude of 12° was shown to be the optimum for limiting vertical loads below 1 g with a descent rate of 12 ft/sec. The shapes considered for the ACLS were an oval, pear shape, and a segmented shape. A three-segmented shape was chosen due to the ease of integration with the M2-F3, *low* cost of fabrication, and the simple design. The segments will be triangular and will be equipped with a roll and pitch sensor. Several materials were compared (inelastic and elastic) and the inelastic material of Kevlar-polyurethane was chosen because of simple construction and the advantageous property of porosity. Analyses of various trunk sizes were carried out to find an acceptable range of reqirements for the ACLS to meet. The horsepower varies from 160 to 270 Hp. This corresponds to an estimated vehicle weight of 12,500 lbf and a cushion area ranging from 145 ft^2 to 125 ft^2, respectively.

The design presented is feasible and economical because the ACRV will be constructed of "off-the-shelf" hardware with proven

52

designs and materials. The parafoil braking system requires further testing to become completely operational. The ACLS is a reliable and versatile landing system which has been proven to be weight-effective. A weight estimate needs to be completed for the ACLS presented in this report. Additional information regarding the parafoil and air cushion landing system is available from the respective sources listed in the Reference section on the following pages.

REFERENCES

1. "Advanced Recovery Systems Study for the Next Generation
    Space Transportation System." NAS8-36631, June 10, 1987.

2. "Advanced Recovery Systems Study for the Next Generation
    Space Transportation System." NAS8-36631, February 1989.

3. "Advanced Recovery Systems Study for the Next Generation
    Space Transportation System." NAS8-36631, May 1989.

4. "Advanced Recovery Systems Study for the Next Generation
    Space Transportation System." NAS8-36631, August 1989.

5. "Advanced Recovery Systems Study for the Next Generation
    Space Transportation System." NAS8-36631, January 1990.

6. Air Cushion Landing Systems Conference. December 1972.
    Tennessee: University of Tennessee Space Institute, 1973.

7. "Application of Gliding Paracutes to the Space Station Crew
    Emergency Return Vehicle." NASA JSC-22820. December,
    1987.

8. Benson, Harold. "Land Impact of the Apollo Command Module."
    AIAA Aerodyanmic Decelerator Conference. September 14-16,
    1970. New York: American Institute of Aeronautics and
    Astronautics, 1970.

9. "CERV Program Cost Estimates." NASA Document No. C-89-
    0060.1A.

10. Collins, Michael. Liftoff: The Story of the American
    Adventure in Space. New York: Grove Press, 1988.

11. Cooper, Paul A. and Paul F. Halloway. "The Shuttle Tile Story."
    Astronautics and Aeronautics. V. 19, No. 1, January 1,
    1981.

12. "Crew Emergency Return Vehicle." Lockheed Proprietary Data
    LMSC-F24365.

13. "Crew Emergency Return Vehicle System Performance Requirements
    Document." NASA JSC-31017. November, 1988.

14. Currey, Norman S. Aircraft Landing Gear Design: Principles
    and Practices. AIAA   Education Series: American
    Institute of Aeronautics and Astronautics, 1988.

15. Currey, Norman S. Landing Gear Design Handbook. Georgia:
    Lockheed-Georgia Co., 1982.

16. Digges, Kennerly H., "Theory of an Air Cushion Landing System for Aircraft." AFFDL-TR-71-50, June 1971.

17. Dotts, Robert J., Donald M, Curry, and Donald J. Tillian, "Orbiter Thermal Protection System." NASA-CP-2343, pt.2. June 1983.

18. Draper, Alfred C. and Melvin L. Buck. "Hypervelocity Entry Configurations." Proceedings of Retardation and Recovery Symposium. May, 1963. Dayton: United States Air Force, 1963.

19. Earl, T. D., "Air Cushion Landing Gear Applications Study." NASA-CR-159002, April 1979.

20. Foster, Gerald V. "Exploratory Investigation at Mach Number of 2.01 of the Longitudinal Stability and Control Characteristics of a Winged Reentry Vehicle Configuration." NASA TM X-178. 1959.

21. Gamble, J.D. and J.C. Young. "The Development and Application of Aerodynamic Uncertainties in the Design of the Entry Trajectory and Flight Control System of the Space Shuttle Orbiter." AIAA Paper 82-1335. AIAA Ninth Atmospheric Flight Mechanics Conference, San Diego, CA, August 9-11, 1982. New York: American Institue of Aeronautics and Astronautics, 1982.

22. Gatland, Kenneth. The Encyclopedia of Spaceflight in Color. The Macmillian Company: New York, 1967.

23. Gentry, Jerauld R., "Lifting Body Flight Test." The Society of Experimental Test Pilots. Lancaster, CA, Vol. 5, 1968.

24. Hankey, W.L. and G.A. Elliot. "Hypersonic Lifting Body Optimization." Journal of Spacecraft and Rockets. Vol. 5. December 1968.

25. Harpold, J.C. and D.E. Gavert. "Space Shuttle Entry Guidance Performance Results." Journal of Spacecraft and Rockets. Vol. 6, December 1983.

26. Hildebrandt, L.H. and K.H. Digges. "Summary of the Air Cushion Landing System on the de Havillard Buffalo Aircraft." Canadian Aeronautics and Space Journal, March 1974.

27. Jackson, Charlie M., Jr. and Roy V. Harris, Jr. "Investigation of Mach Number of 1.99 of Two Series of Blunted Delta Wing Models with Several Cross-sectional Shapes for Angles of Attack from 0 deg. to 90 deg." NASA TM X-543. 1961.

28. Kempel, Robert W., et. al., "Flight Evaluation of M2-F3 Lifting Body Handling Qualities at Mach Numbers from 0.30 to 1.61."

29. Knacke, T.W. "Technical-Historical Development of Parachutes and Their Applications Since World War I." AIAA 9th Aerodynamic Decelerator and Balloon Technology Conference. October 7-9, 1986. New York: American Institute of Aeronautics and Astronautics, 1986.

30. Korb, L. J. and H. M. Clancy, "The Shuttle Orbiter Thermal Protection System: A Material and Structural Overview." Proceedings of 26th National SAMPE Symposium, Los Angeles, CA, Vol. 26, April 1989.

31. Korb, L. J., G. A. Morant, R. M. Calland, and C. S. Thatcher, "The Shuttle Orbiter Thermal Protection System." American Ceramic Society Bulletin, Vol. 60, No. 11, 1981.

32. Lee, E. G. S., "Experimental and Analytical Studies of Advanced Air Cushion Landing Systems." NASA-CR-3476.

33. McDevitt, John B. and Rakich, John V. "The Aerodynamic Characteristics of Several Thick Delta Wings at Mach Numbers to 6 and Angles of Attack to 50 deg." NASA TM X-162. 1960.

34. Moeller, J. H., "Free Flight Investigation of Large All-Flexible Parawings and Performance Comparison with Small Parawings. Final Report." NASA-CR-66918, March 1970.

35. Moeller, J.H. and E.M. Linhart. "Parawing Technology for Spacecraft Land Landing – A Progress Report." AIAA Aerodynamic Decelerator Conference. September 14-16, 1970. New York: American Institute of Aeronautics and Astronautics, 1970

36. Ormiston, R. A., "The Sailwing Lifting Body Concept." Princeton University. February 1968.

37. Pavlosky, James E. and Leslie St. Leger. "Apollo Experience Report – Thermal Protection Subsystem." NASA TN D-7564. January, 1974.

38. Perez, David J. and Major William A. Benner. <u>Development of</u> <u>an Air Cushion Landing System</u>. AIAA Paper 73-812. AIAA 5th Aircraft Design, Flight Test and Operations Meeting, St.Louis, MO., August 6-8, 1973.

39. Pike, J. "Experimental Results From Three Cone-Flow Waveriders."<u>Hypersonic Boundary Layers and Flow Fields.</u> London: Technical Editing and Reproductions, Ltd., 1968.

40. Purser, Paul E., Maxime A. Faget, and Norman F. Smith.. <u>Manned</u> <u>Spacecraft: Engineering Design and Operation.</u> New York: Fairchild Publications, 1964.

41. Reding, J.P. and H.O. Svendsen. "Lifting Reentry Rescue Vehicle Configuration." <u>AIAA Atmospheric Flight</u> <u>Mechanics</u> <u>Conference</u>. AIAA Paper 88-4342. 1988.

42. Regan, Frank J. <u>Re-entry Vehicle Dynamics.</u> New York: American Institute of Aeronautics and Astronautics, 1984.

43. <u>Results of First US Manned Orbital Spaceflight-February 20,</u> <u>1962.</u> Washington: US Government Printing Office, 1962.

44. Seddon, J. and A. Spence. "The Use of Known Flow Fields as an Approach to the Design of High Speed Aircraft." <u>Hypersonic</u> <u>Boundary Layers and Flow Fields.</u> London: Technical Editing and Reproductions, Ltd., 1968.

45. Seegmiller, H. Lee, "Convective Heat Transfer to the Ames M2 and M2-F2 Lifting Entry Vehicles." NASA-TM-X-1691, December 1963.

46. Spearman, Leroy M. "Supersonic Aerodynamic Characteristics of Some Reentry Concepts for Anlges of Attack to 90 deg." NASA TM N86-16243. 1985.

47. Strouhal, G., D.M. Curry, and J.M. Janney. "Thermal Protection System Performance of the Apollo Command Module." <u>AIAA/ASME</u> <u>Seventh Structures and Materials Conference</u>. April 18-20, 1966, Cocoa Beach, FL. New York: American Institute of Aeronautics and Astronautics, 1966.

48. Sweeney, T. E., "Exploratory Sailwing Research at Princeton." Princeton University. Report 578. December 1961.

49. Syverston, C. A., B. L. Swenson, J. L. Anderson, and G. C. Kenyon, "Some Considerations of the Performance of a Maneuverable, Lifting-Body, Entry Vehicle." <u>Advances in</u> <u>the Astronautical Sciences</u>, Vol. 16, Part 1, 1963.

50. Thompson, M.O. and B.A. Peterson. "Lifting-Body Flight Test Program."<u>The Society of Experimental Test Pilots</u>. Vol. 8, Lancaster, CA. September 1966.

51. Throckmorton, D. A., "Benchmark Aerodynamic Heat Transfer Data from the First Flight of the Space Shuttle Orbiter." AIAA-82-0003, January 1982.

Table 1. Orbiter TPS materials (Korb, Morant, pg. 1188)

Material generic name	Material temp. capability. °C (°F)*	Material comp	Areas of orbiter	Material generic name	Material temp. capability. °C (°F)*	Material comp	Areas of orbiter
Reinforced carbon-carbon (RCC)	to 1650 (3000)	Pyrolized carbon-carbon. coated with SiC	Nose cone. wing leading edges. forward external tank separation panel	Low temperature reusable surface insulation (LRSI)	400–650 (750–1200)	SiO₂ tiles. borosilicate glass coating	Upper wing surfaces. tail surfaces. upper vehicle sides. OMS pods
High temperature reusable surface insulation (HRSI)	650–1260 (1200–2300)	SiO₂ tiles. borosilicate glass coating with SiB₄ added	Lower surfaces and sides. tail leading and trailing edges. tiles behind RCC	Felt reusable surface insulation (FRSI)	to 400 (750)	Nylon felt. silicone rubber coating	Wing upper surface. upper sides. cargo bay doors. sides of OMS pods

*100 missions: higher temperatures are acceptable for a single mission

ORIGINAL PAGE IS OF POOR QUALITY

Table 2. Trajectory points (NAS8-36631/June 1987, pg. 20)

EVENT	ELAPSED TIME, s	ALTITUDE, ft	VELOCITY, VERTICAL, ft/s	VELOCITY, HORIZ., ft/s
INITIATE RECOVERY (DEPLOY DROGUE)	0.0	17000	604	0
DISREEF DROGUE, 1st REEFED STAGE	6.5	13520	410	0
DISREEF DROGUE, 2nd REEFED STAGE	14.0	10980	268	0
RELEASE DROGUE AND DEPLOY PARAFOIL	22.5	8690	186	0
DISREEF PARAFOIL, 1st REEFED STAGE	37.5	6580	156	102
DISREEF PARAFOIL, 2nd REEFED STAGE	44.5	5690	82	89
INITIATE FLAP RELEASE	50.0	5410	47	53
FULL GLIDE	58.0	5000	31	86
INITIATE FLARE MANEUVER	248.5	60	25	75
TOUCHDOWN	252.5	0	<15	<35

Table 3. Drop test data and estimated g forces
(NAS8-36631/Feb. 1989, pp. 74 and 114)

event	velocity (ft/s)	Q (psf)	load (lbs)	g's
322 ft. parafoil with 7 cells with payload of 10,450 lbs.				
parafoil line stretch	194.8	33	25173	2.4
1st peak load	163	23.6	29108	2.8
disreef	93.5	9.4	12000	1.2
2nd peak load	83.8	6.3	18959	1.8
parafoil glide	62.8	5.1	9188	0.9
touchdown	65.8	4.4	-----	---
598 ft. parafoil with 27 cells and payload of 11,864 lbs.#				
parafoil line stretch		27.4	33863	2.9
1st peak load		28.3	36964	3.1
1st disreef	*	27.6	32411	2.7
	**	6.5	9069	0.8
2nd peak load	*	26.7	42472	3.6
	**	5.4	13413	1.1
2nd disreef		3.4	9774	0.8
touchdown		6.0	-----	---

velocity data not available

* right side premature disreef

** left side normal disreef

TABLE 4. RESULTS OF HORSEPOWER CALCULATIONS (Varying Weight,
Cushion Size, and Clearance Height).

Weight (lbf)[*]	Clearance Height d(in)	Perimeter s(ft)	Cushion Area $A(ft^2)$	Horespower (Hp)
10,000	0.5	60	125	97.26
	1.0	60	125	194.53
	0.5	62	145	78.03
	1.0	62	145	156.06
12,500	0.75	60	125	203.91
	1.00	60	125	263.69
	0.75	62	145	163.57
	1.00	62	145	218.10
15,000	0.5	60	125	178.70
	1.0	60	125	357.40
	0.5	62	145	143.35
	1.0	62	145	286.70

[*] $\rho = 0.002377$ lbf s^2/ft^4
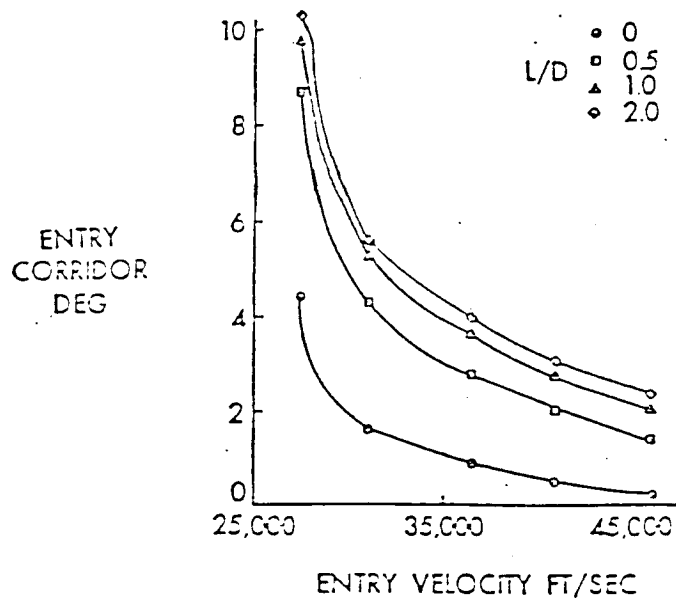
Figure 1. Effect of L/D on entry corridor (Purser, Pg. 37)
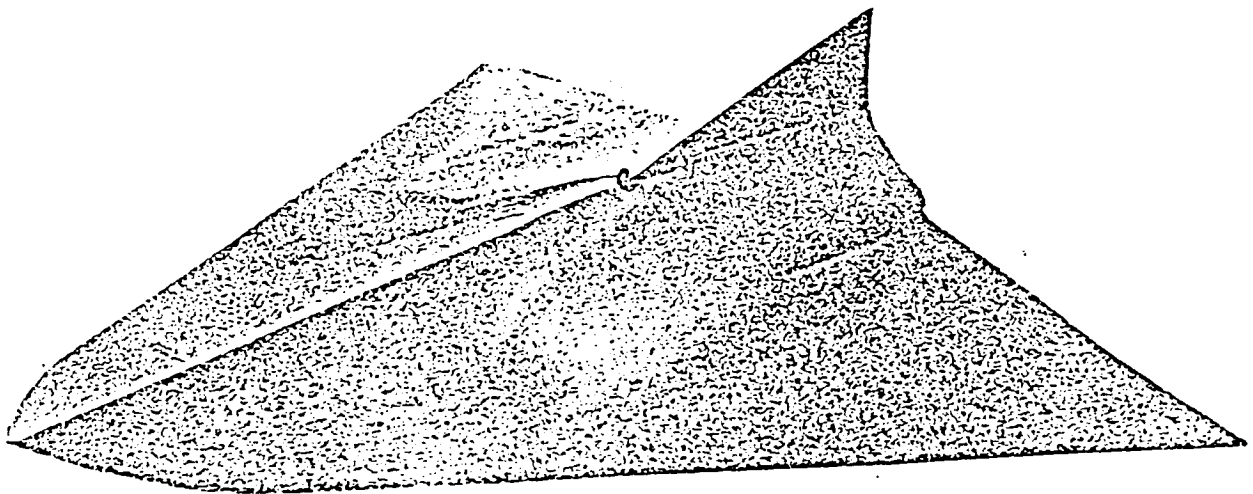
Figure 2. Model of waverider (Draper and Buck, pg. 20)

63
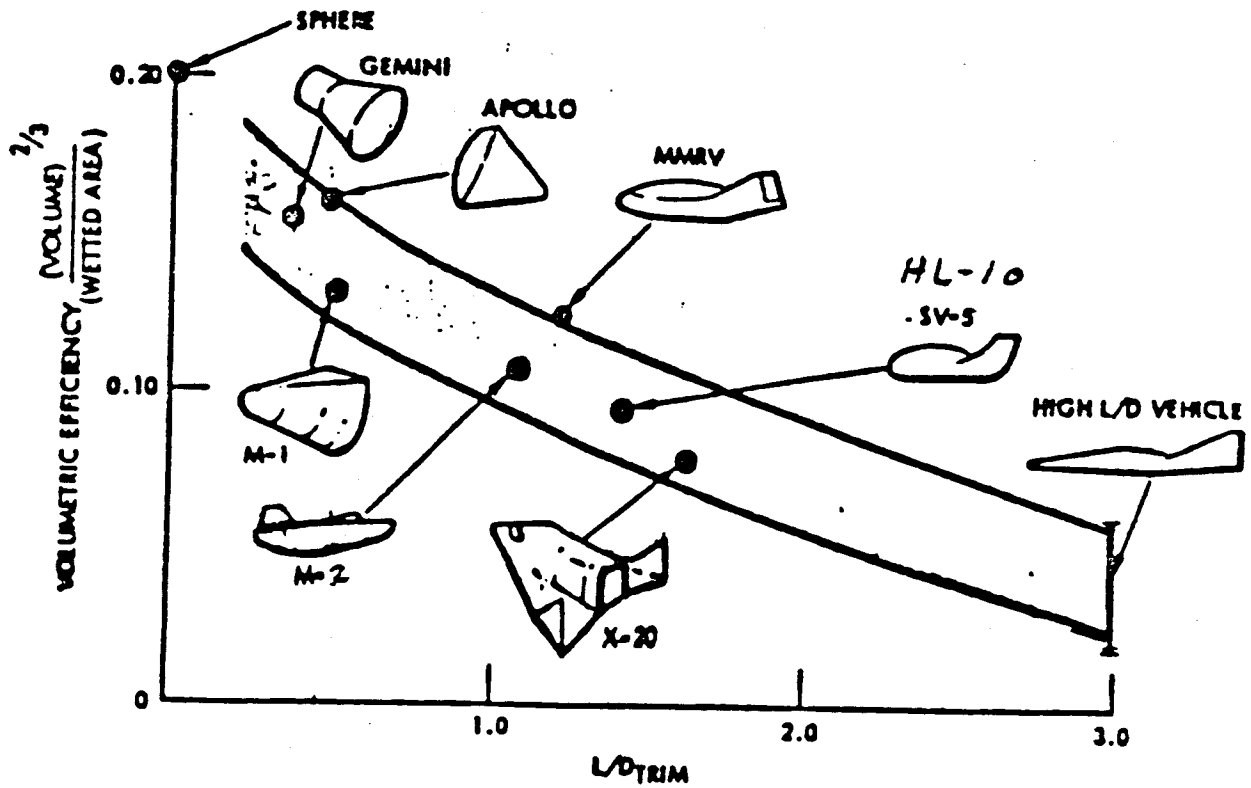
Figure 3. Comparisons of Reentry Vehicles (Lockheed, pg. 89)
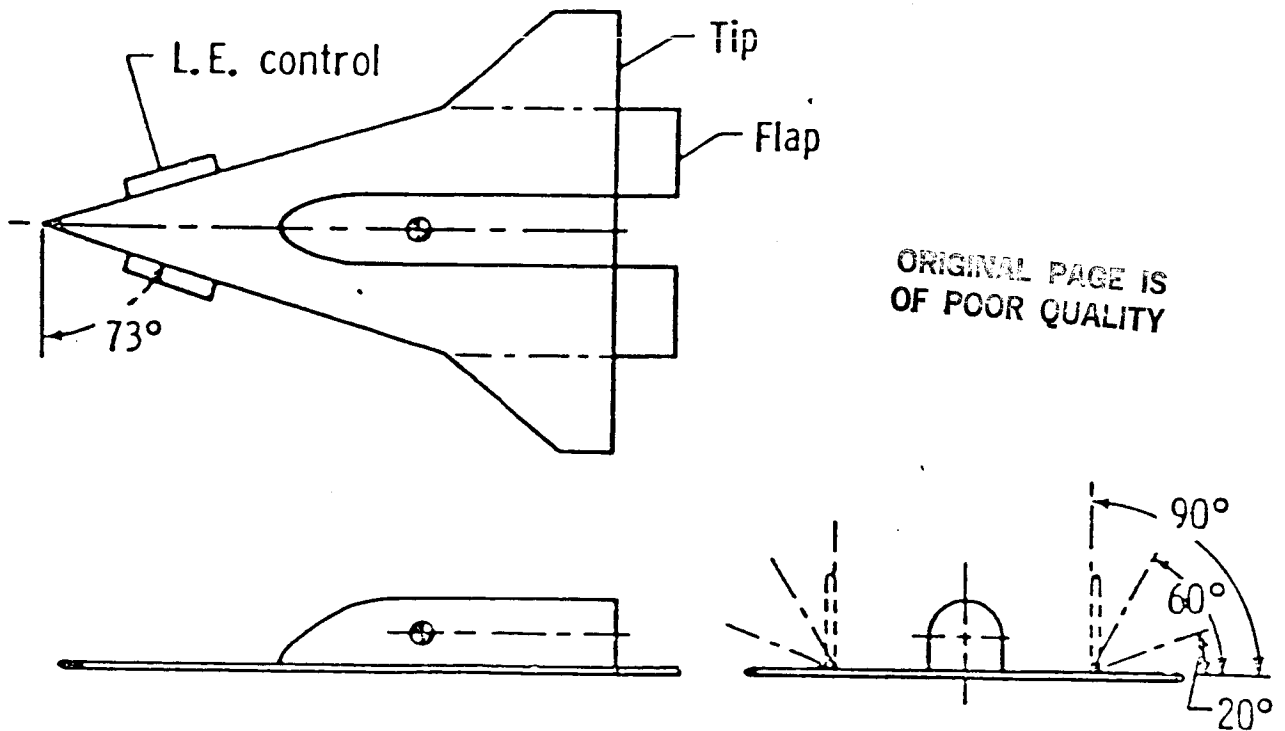
Figure 4. Modified delta wing model (Spearman, pg. 8)
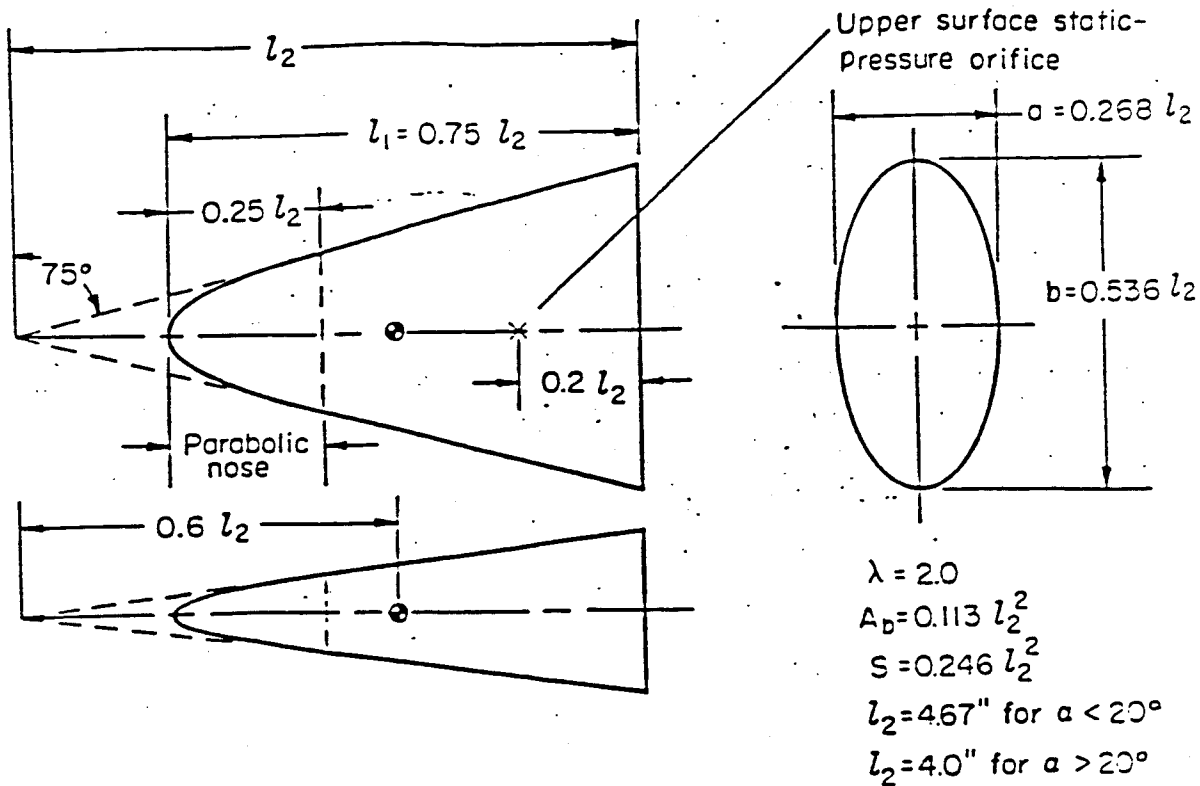
Figure 5. Pod lifting body geometry (McDevitt and Rakich, pg. 10)
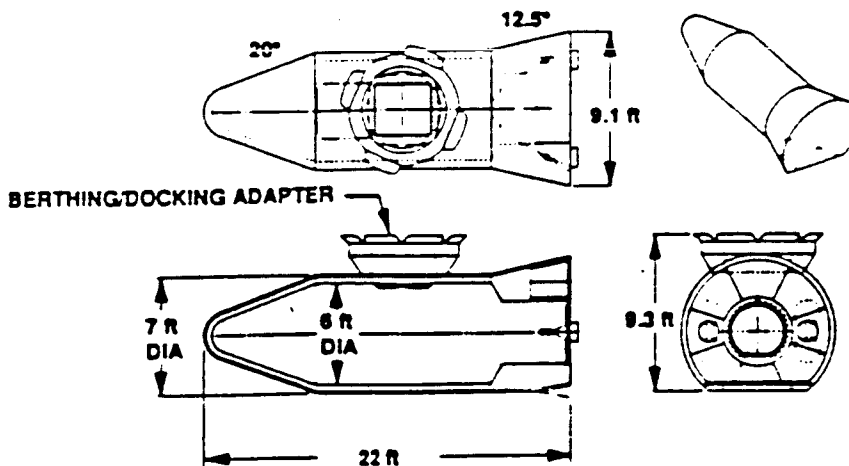
Figure 6. Flared cylinder configuration
(Reding and Svendsen, pg. 118)
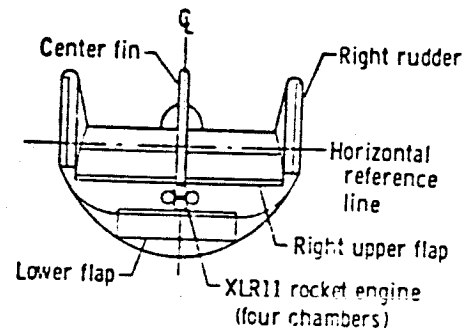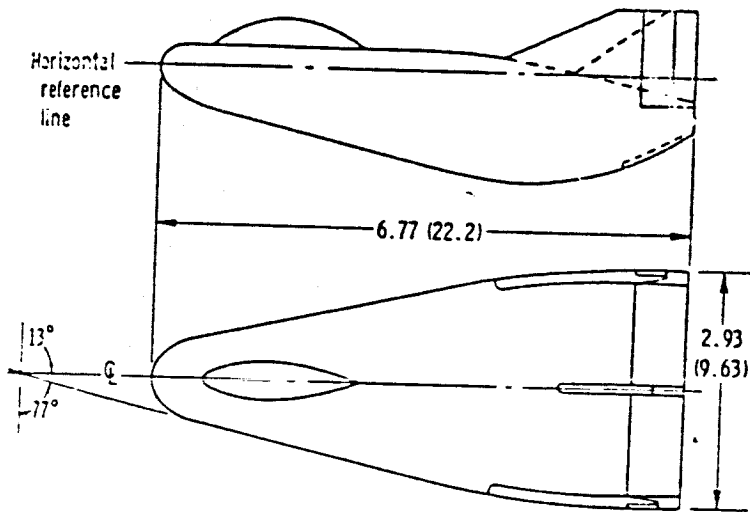
Figure 7. M2-F3 lifting body vehicle (Kemple, et. al., pg. 5)
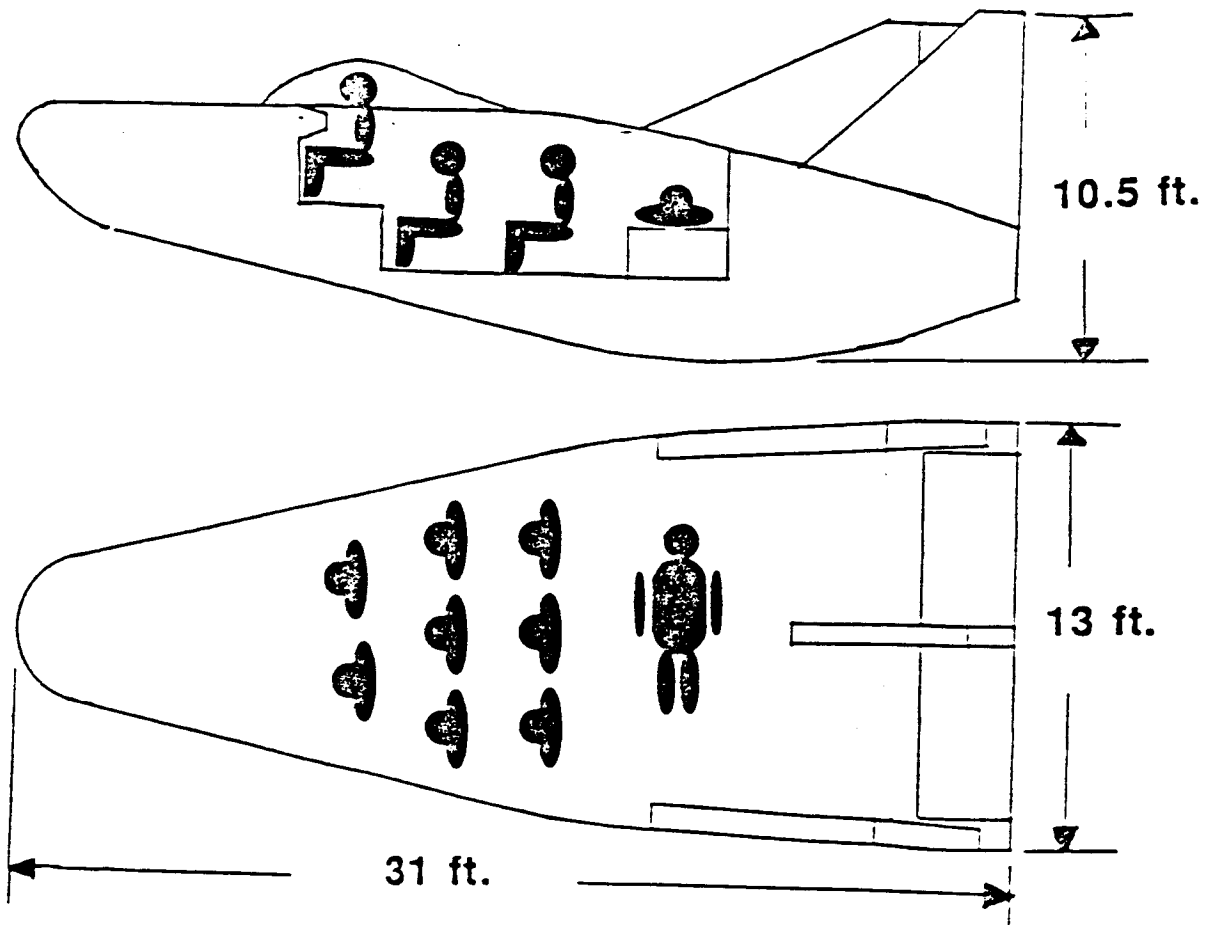
Hypersonic L/D   1.2
Internal volume   115 ft³/man
Volumetric efficiency   .0 9
Weight   14,500 lbs.

Figure 8. Eight-man M2-F3 configuration drawing
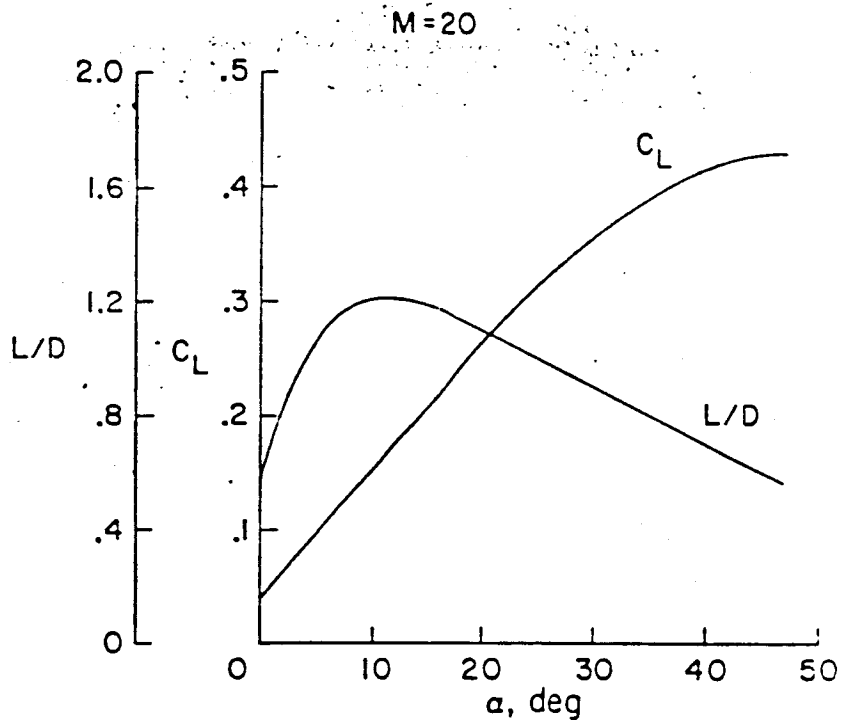
Figure 9. Aerodynamic characteristics of M2 at Mach 20
(Syvertson, et. al., pg. 903)

ORIGINAL PAGE IS
OF POOR QUALITY
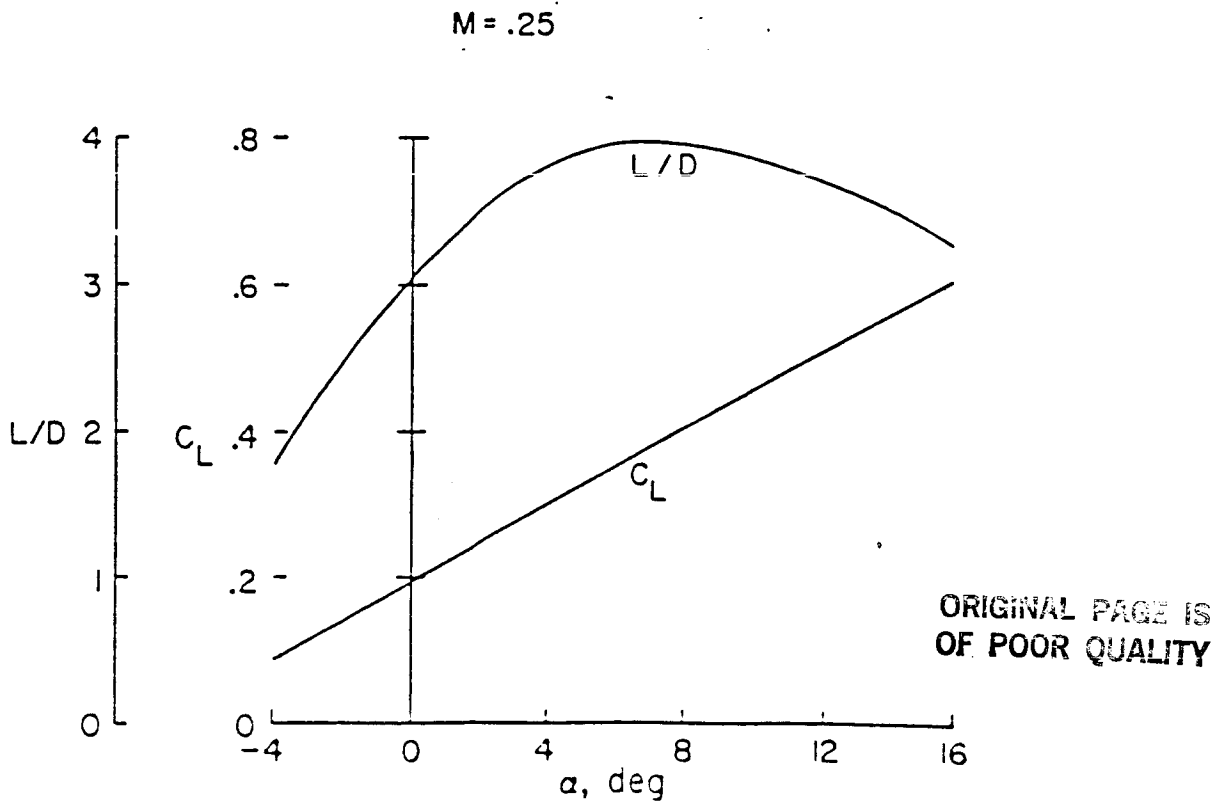
Figure 10. Aerodynamic characteristics of M2 at Mach .25
(Syvertson, et. al., pg. 903)

HL-10

Length 22 ft 2 in.

Width 15 ft 1 in.

Propulsion: XLR-11 8,000 lb thrust rocket engine

Air-launched from B-52
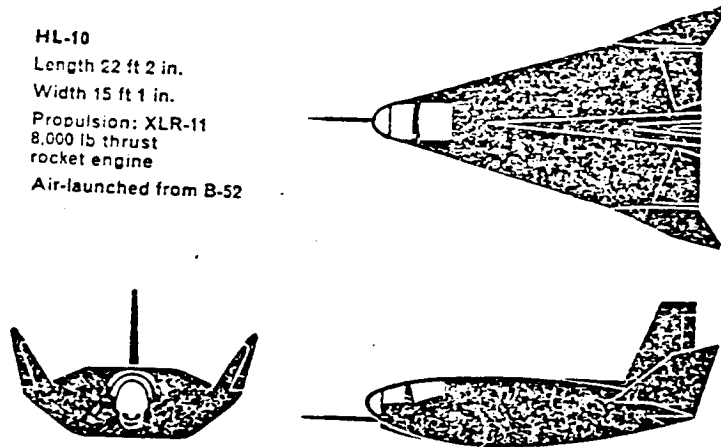
Figure 11. HL-10 lifting body planform (Gatland, pg. 166)

SV-5P

Length 24 ft 6 in.

Width 13 ft 8 in.

Propulsion: XLR-11 8,000 lb thrust rocket engine

Air-launched from B-52
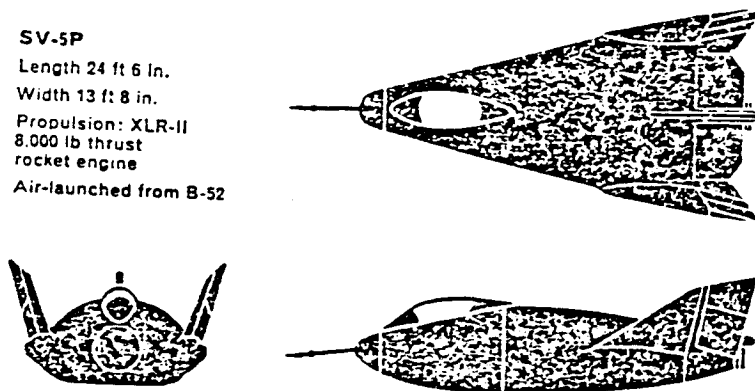
Figure 12. SV-5P lifting body planform (Gatland, pg. 166)
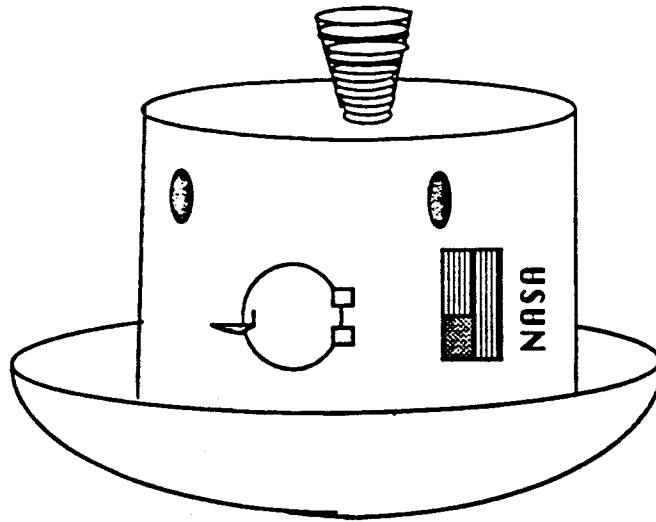
Figure 13. Sketch of capsule
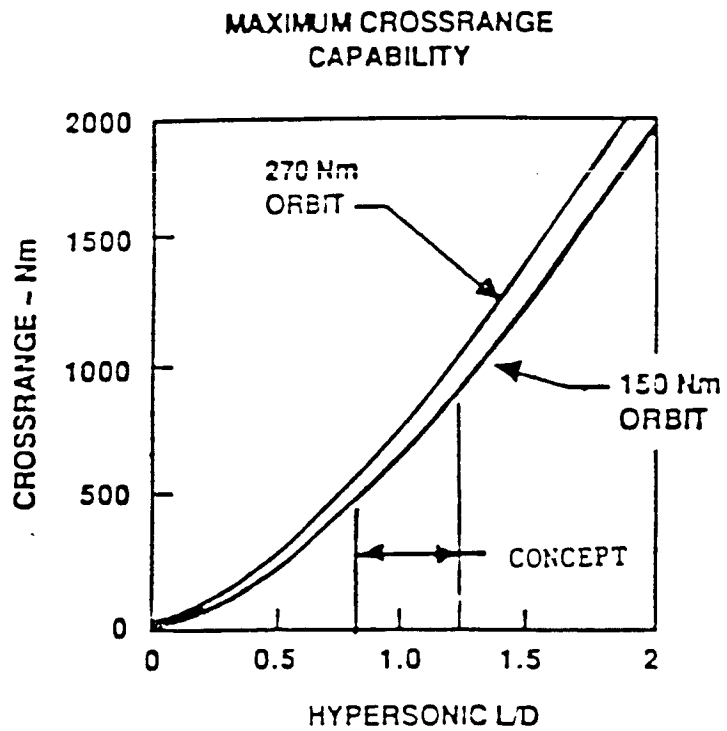
Figure 14. Maximum crossrange capability
(Reding and Svendsen, pg.118)
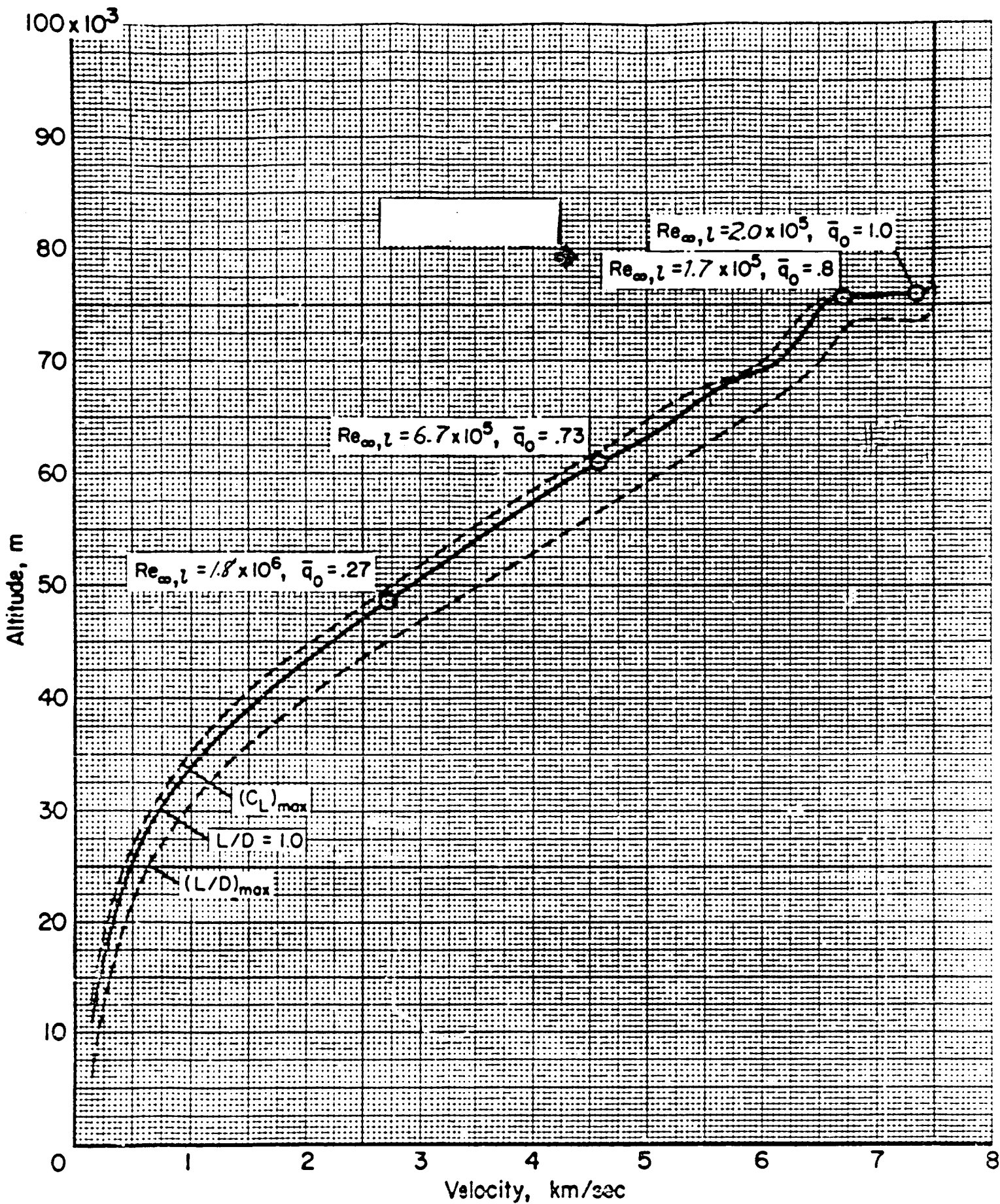
Figure 15. ACRV entry trajectories (Seegmiller, pg. 27)

The chart shows Altitude, m (vertical axis, 100×10^3 at top down to 0) versus Velocity, km/sec (horizontal axis, 0 to 8).

Curve labels:
- $Re_{\infty, l} = 2.0 \times 10^5$, $\bar{q}_0 = 1.0$
- $Re_{\infty, l} = 1.7 \times 10^5$, $\bar{q}_0 = .8$
- $Re_{\infty, l} = 6.7 \times 10^5$, $\bar{q}_0 = .73$
- $Re_{\infty, l} = 1.8 \times 10^6$, $\bar{q}_0 = .27$
- $(C_L)_{max}$
- $L/D = 1.0$
- $(L/D)_{max}$
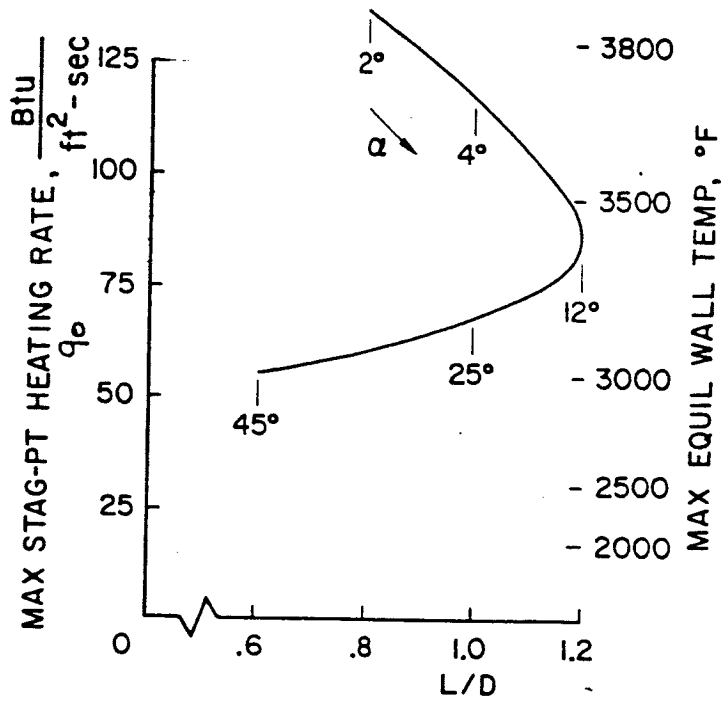
Figure 16. M2 stagnation point heating rate
(Syverston, et. al., pg. 903)
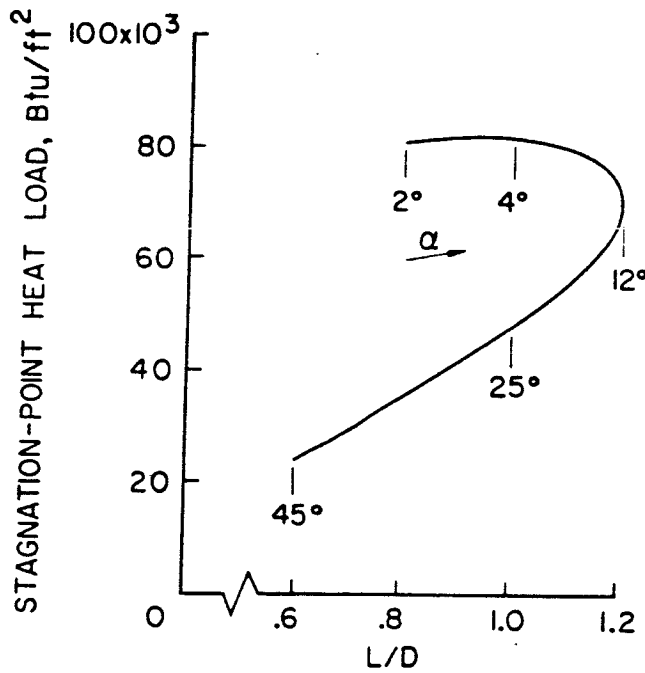
Figure 17. M2 stagnation point heat load
(Syverston, et. al., pg. 904)
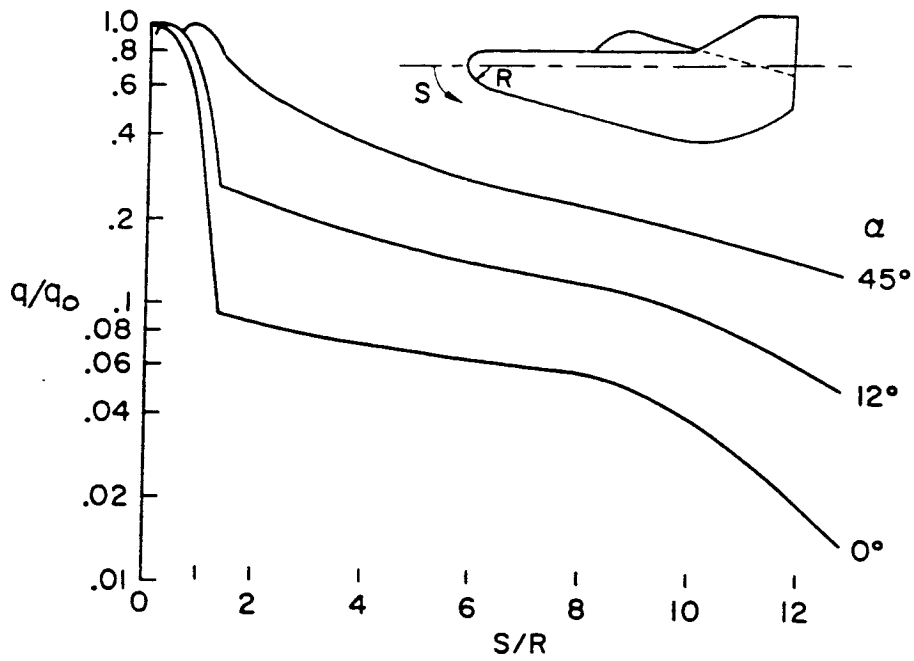
Figure 18. M2 theoretical longitudinal heating distribution
(Syverston, et. al., pg. 905)
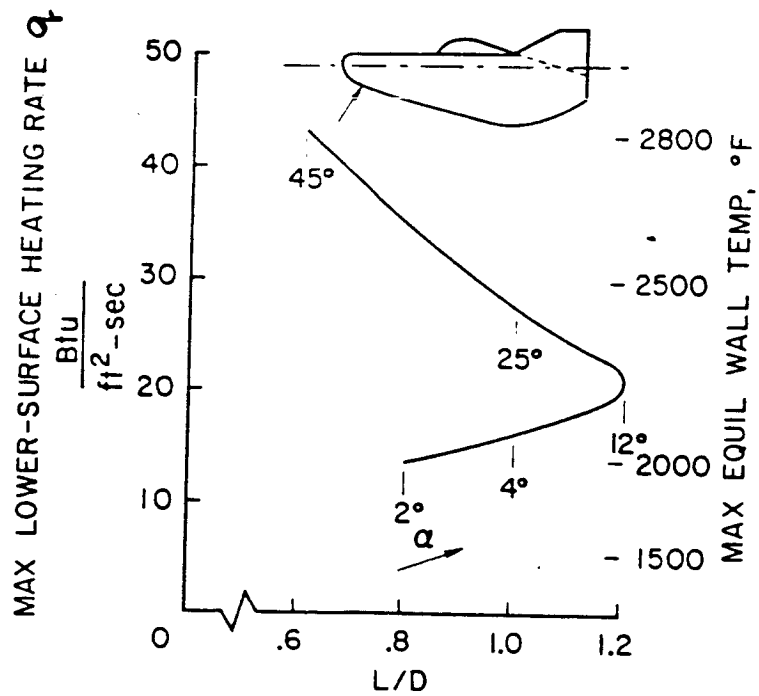
Figure 19. M2 maximum lower surface heating rate
(Syverston, et. al., pg. 906)
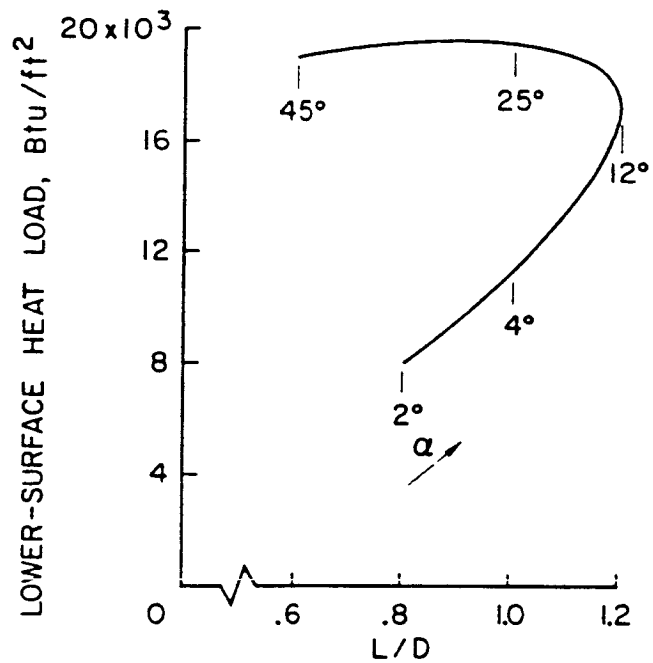
Figure 20. M2 lower surface heating load
(Syverston, et. al., pg. 907)
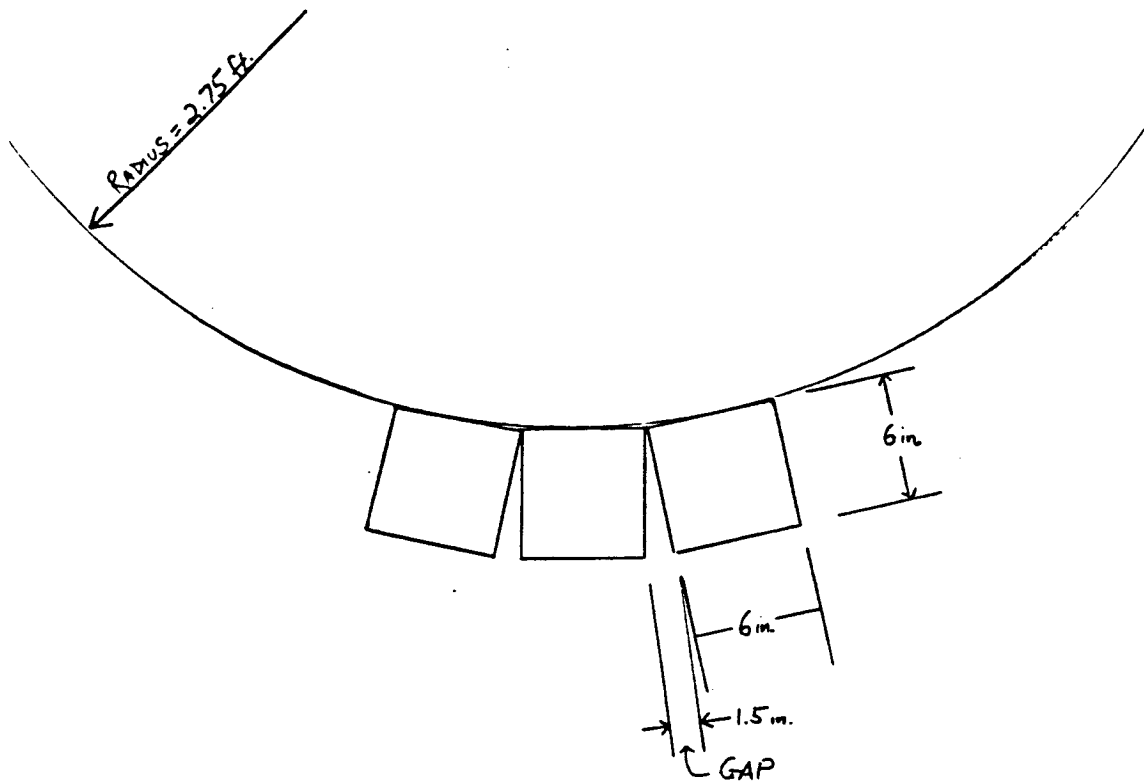
Figure 21. 6 in. tile configuration at vehicle shoulder point
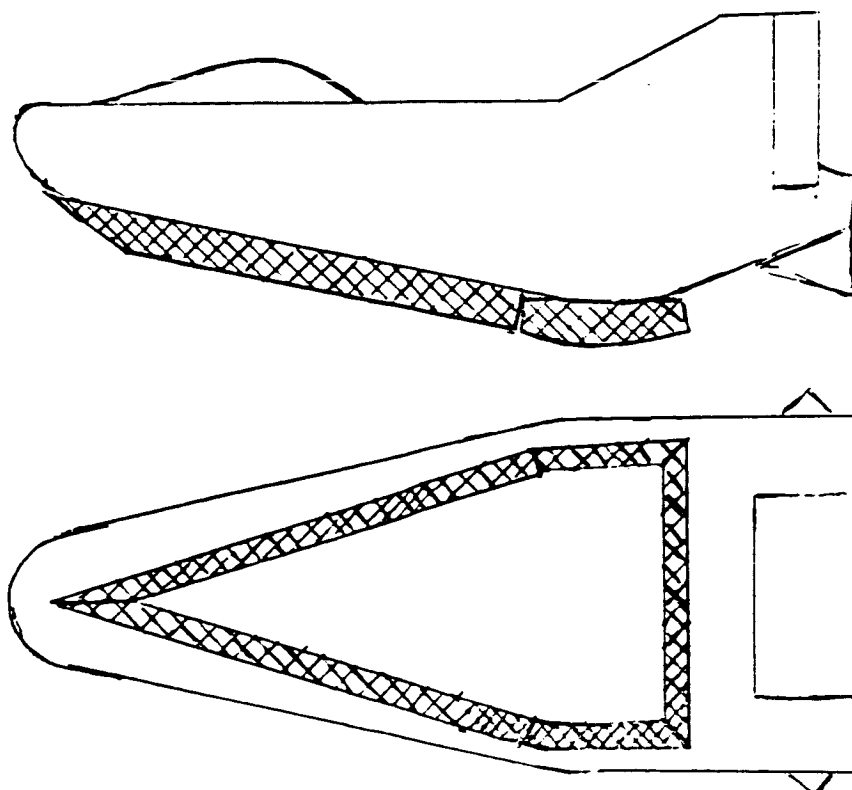
Figure 22. Landing gear door configuration necessary for ACLS
deployment
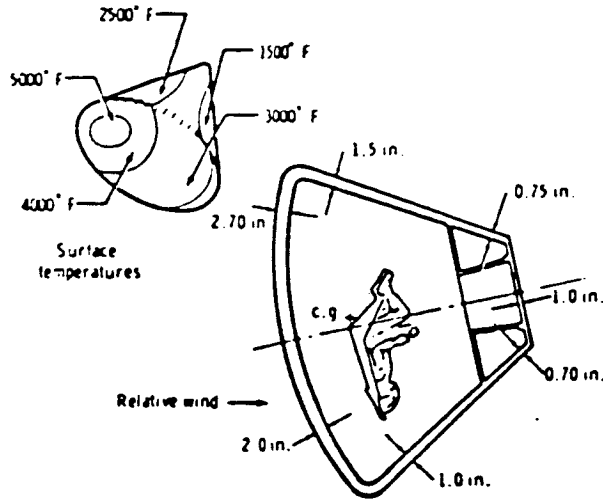
Figure 23. Apollo Command Module ablator thickness
(Pavlosky and St. Leger, pg. 4)
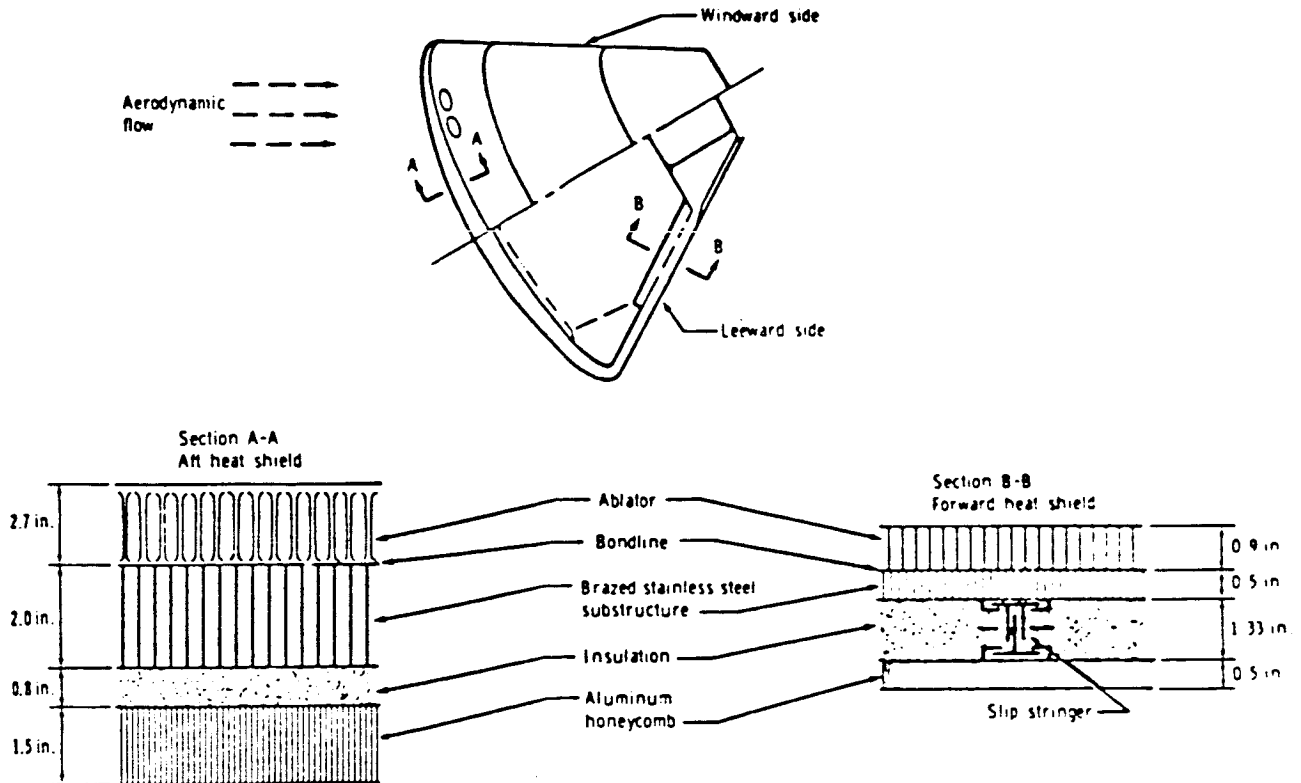
Figure 24. Structural arrangement of Apollo TPS
(Pavlosky and St. Leger, pg. 5)

76
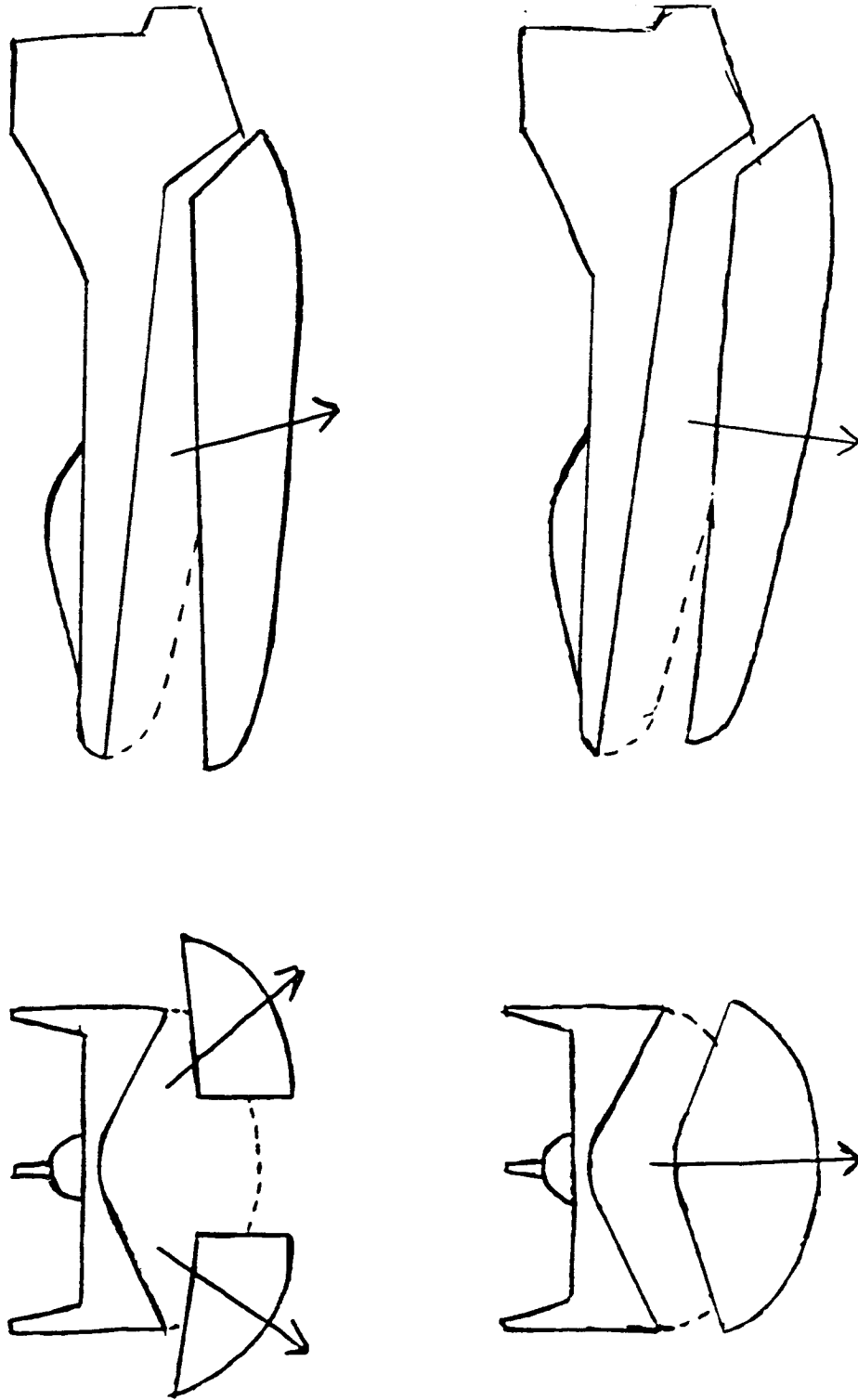
Figure 25. Two cases of expendable ablative shield detachment
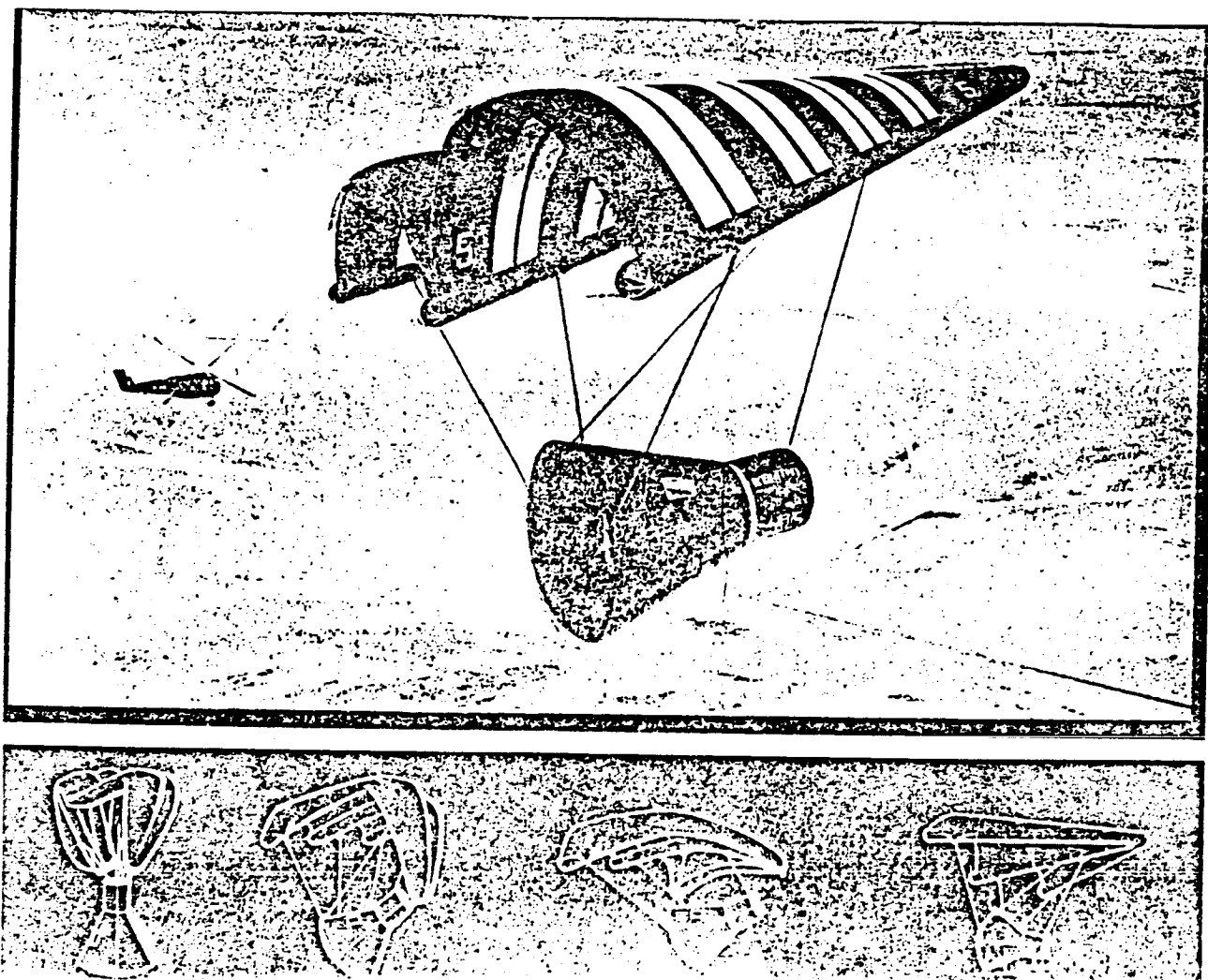
Figure 26. Paraglider (single-keel parawing) (Application of
Gliding Parachutes, pg. 21)
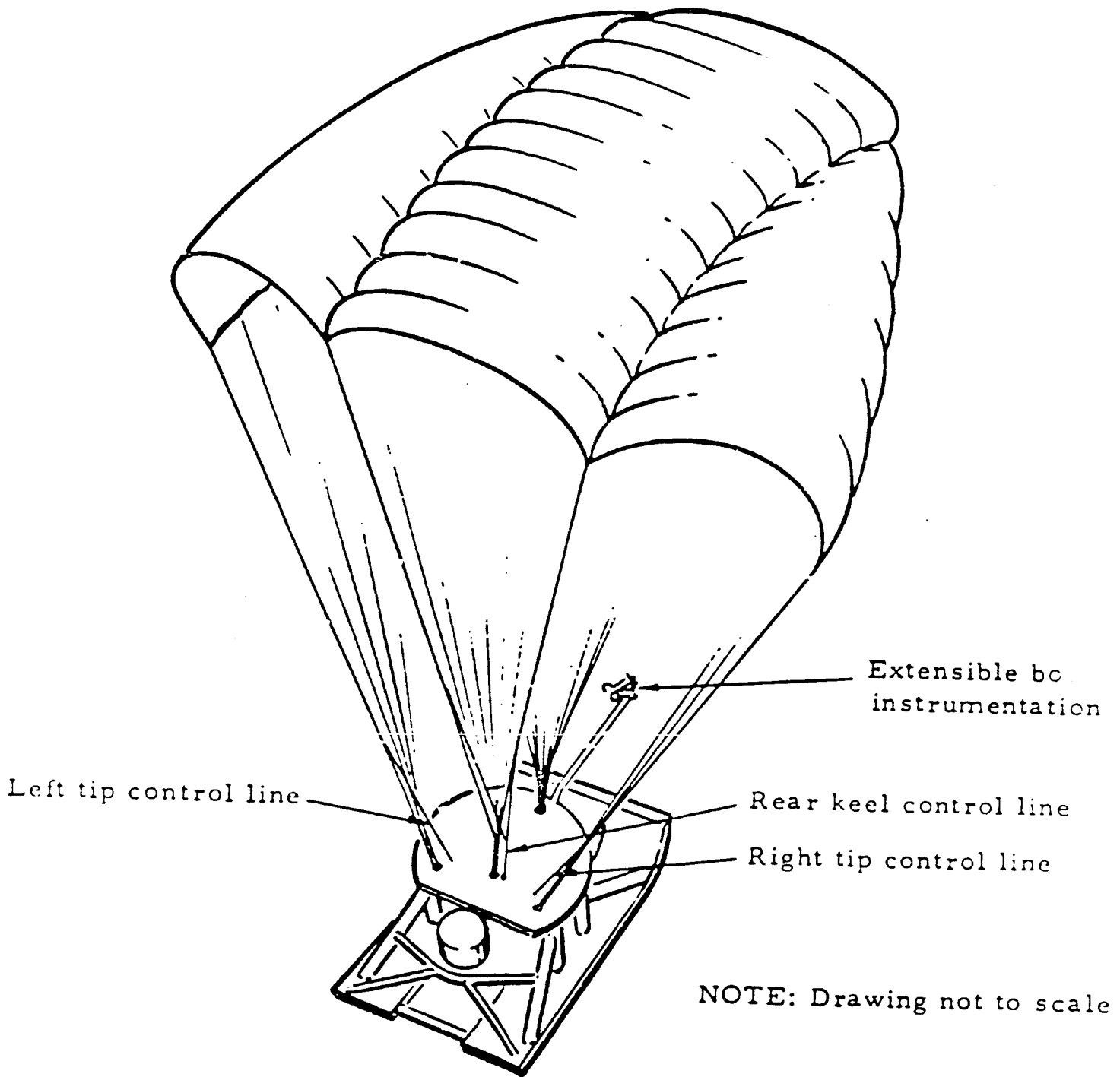
Figure 27. Twin-keel parawing (Moeller, pg. 12)
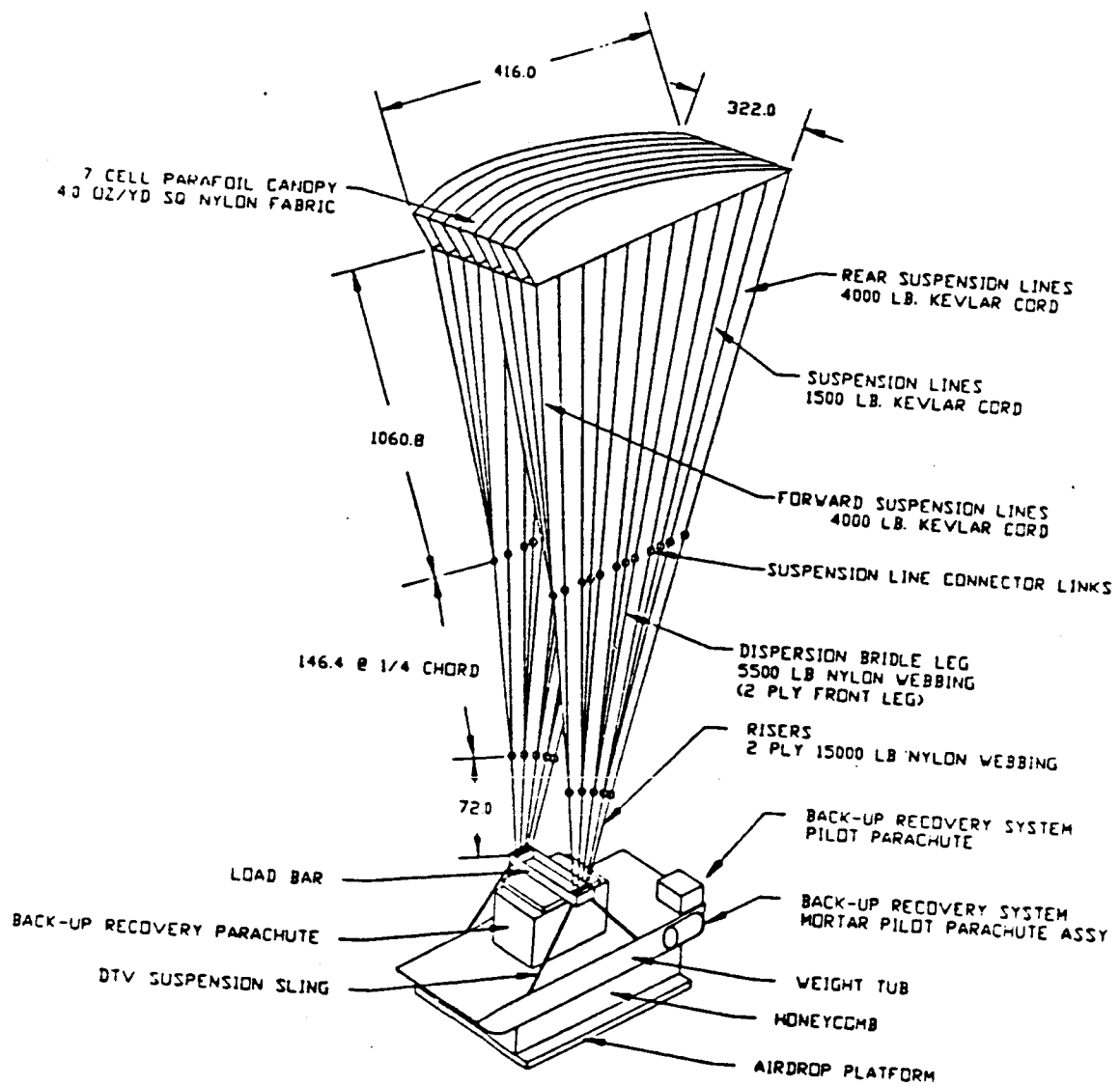
Figure 28. Ram-air inflated parafoil (ARS Feb. 1989, pg. 62)

Parafoil span as a function of payload and vertical velocity
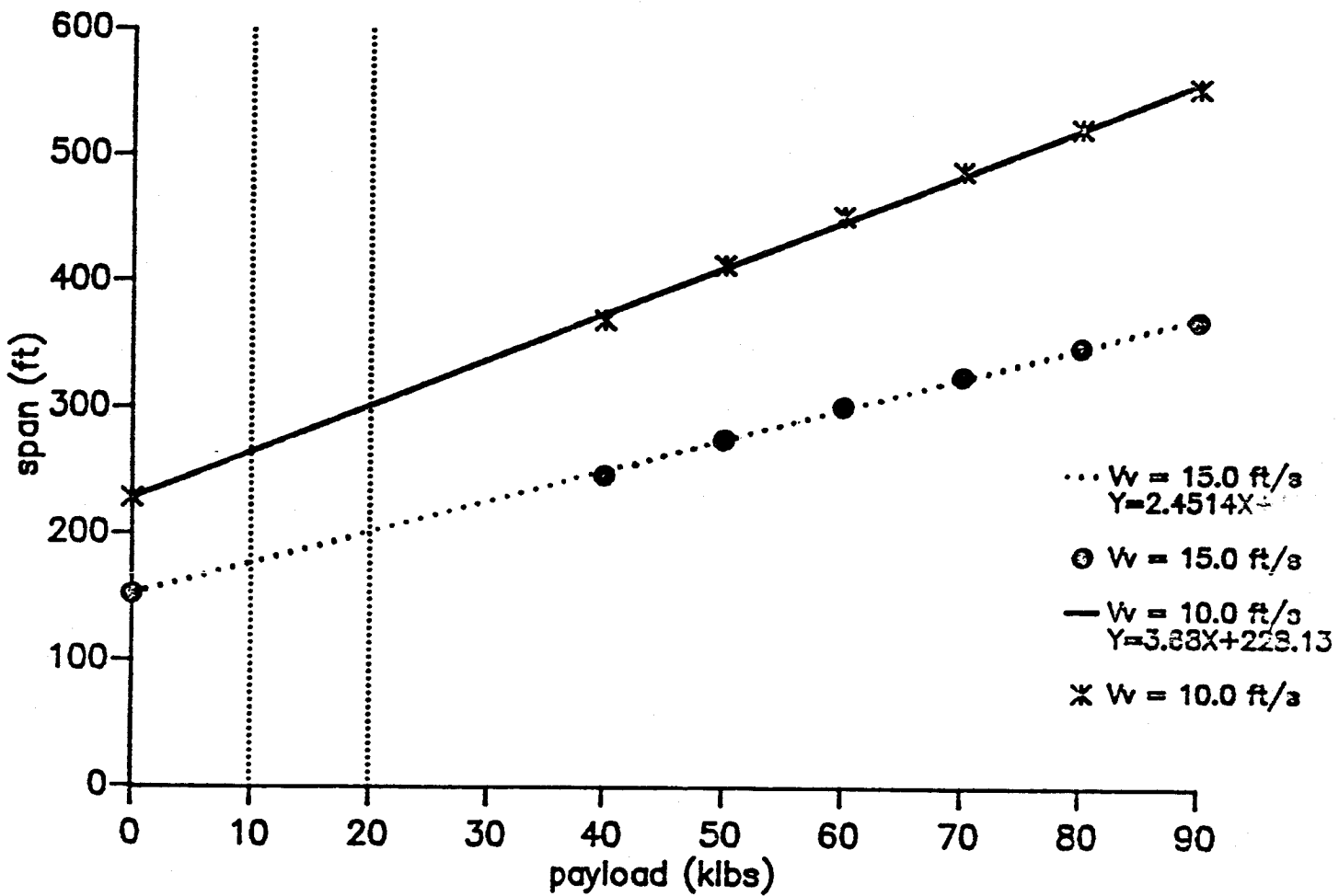
Figure 29. Parafoil span (ARS June 1987, pg. 56)

Parafoil weights as a function of payload and vertical velocity (including drogue weight)
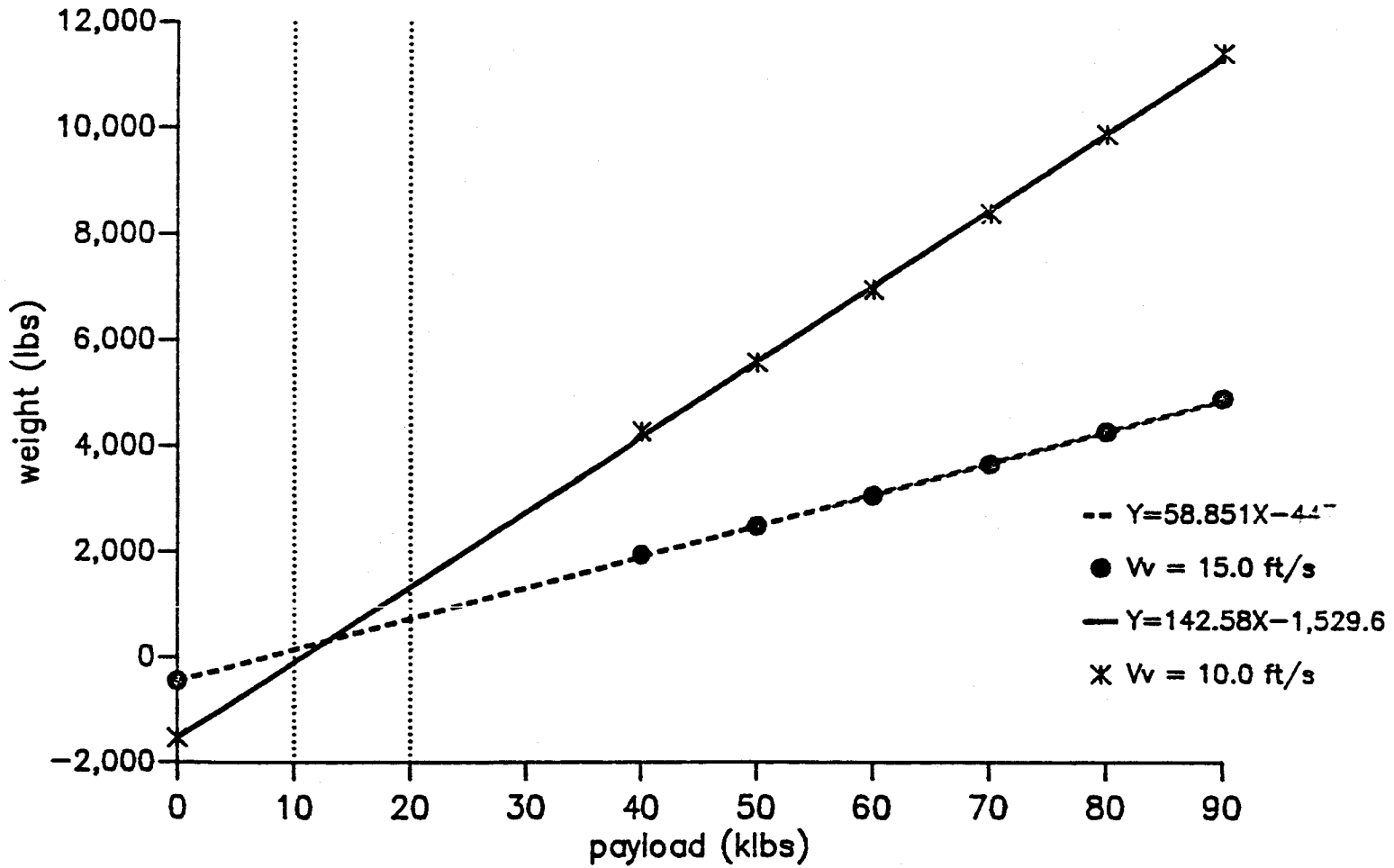
Figure 30. Parafoil weight (ARS June 1987, pg. 56)
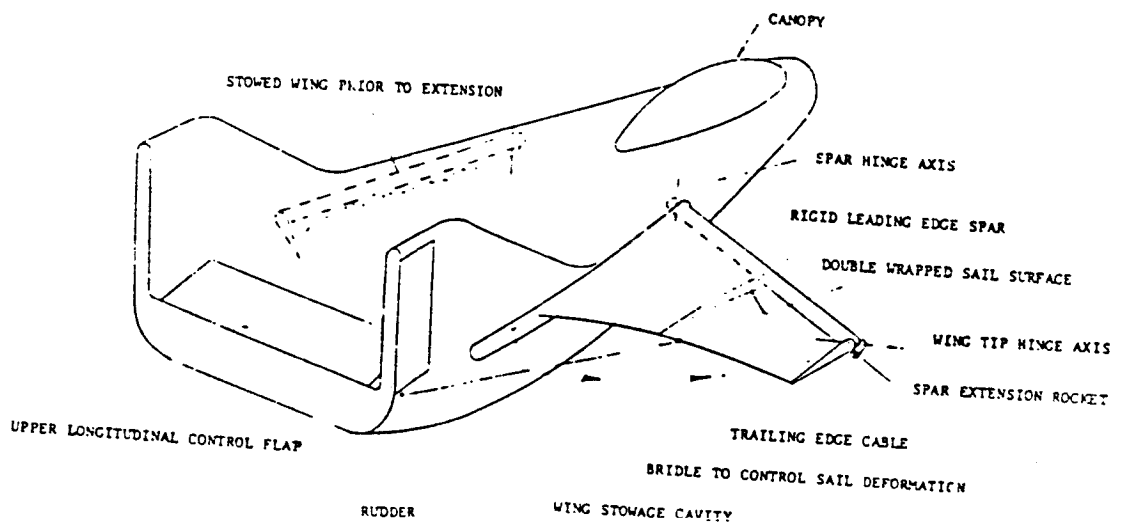
Figure 31. M2-F2 sailwing configuration (Ormiston, pg. 10)
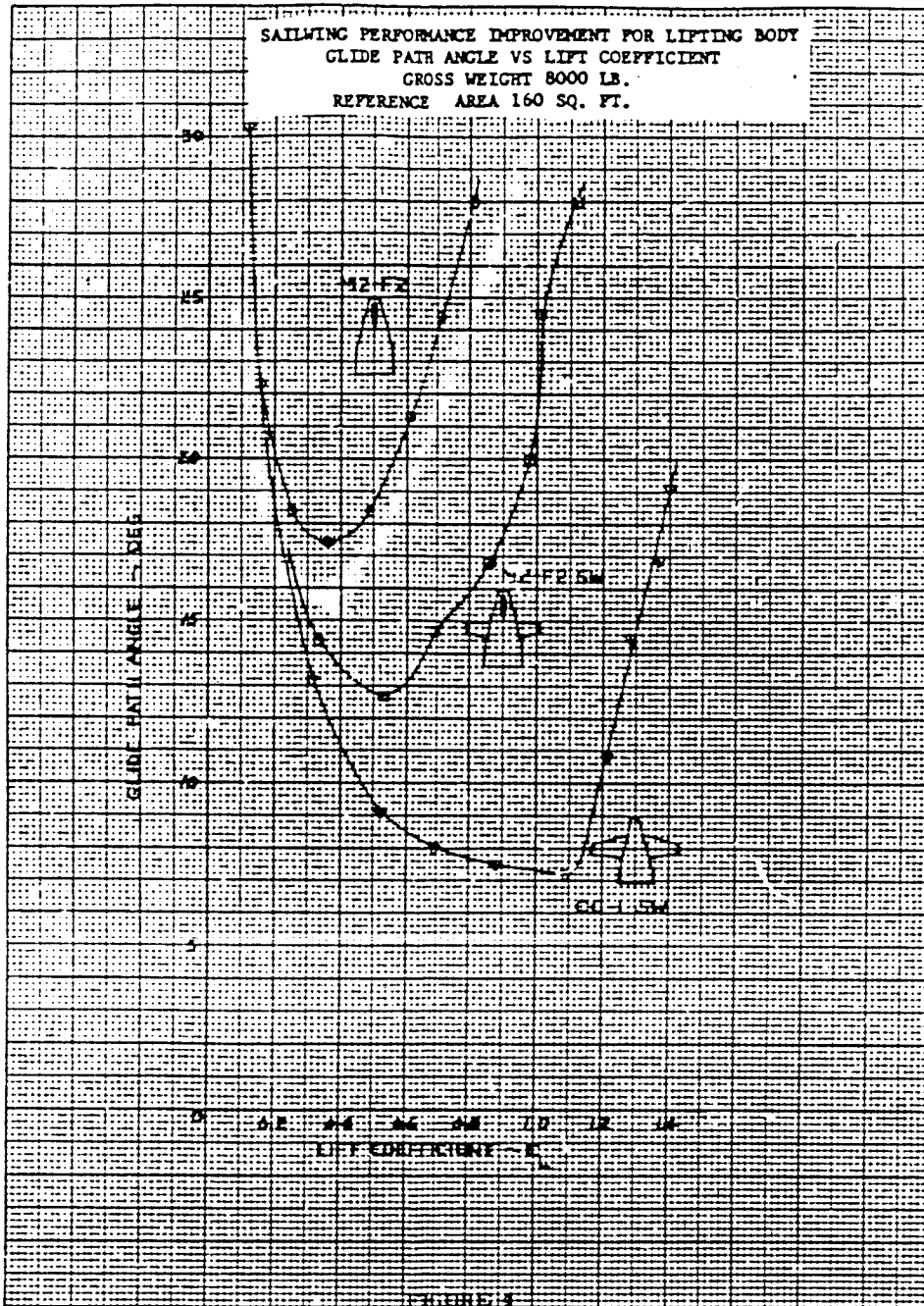
Figure 32. Sailwing performance improvement for M2-F2
(Ormiston, pg. 14)
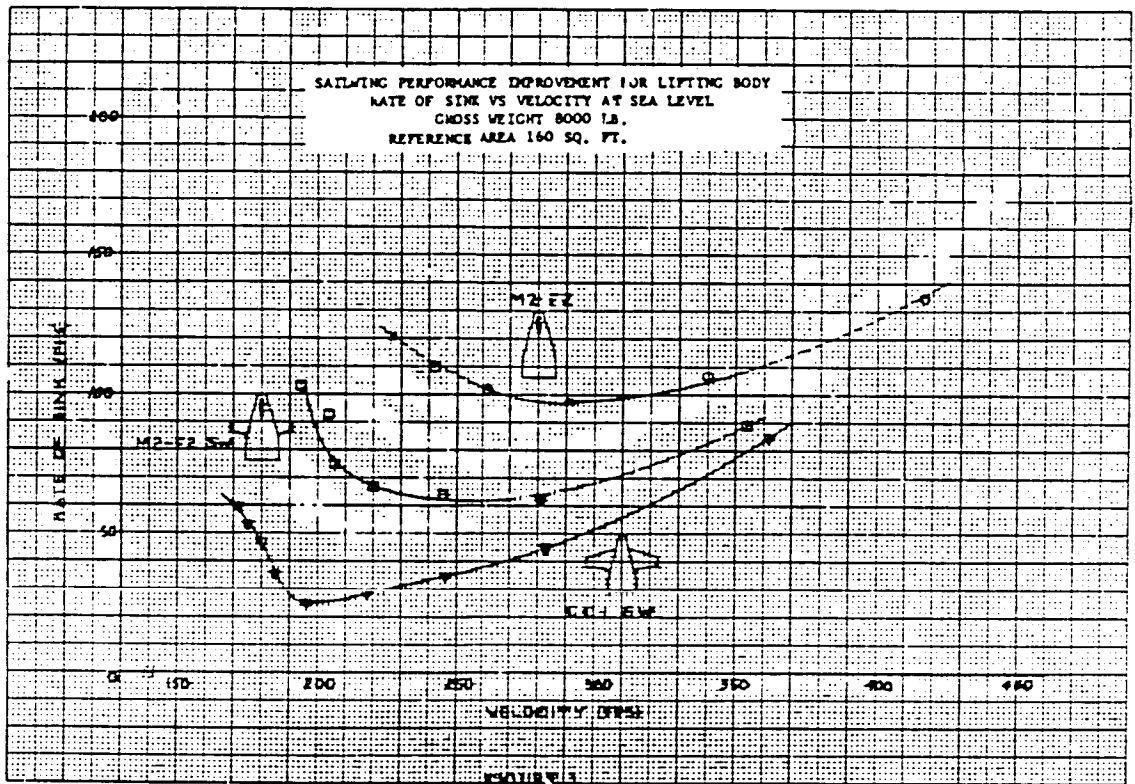
Figure 33. Sailwing performance improvement for M2-F2
(Ormiston, pg. 13)
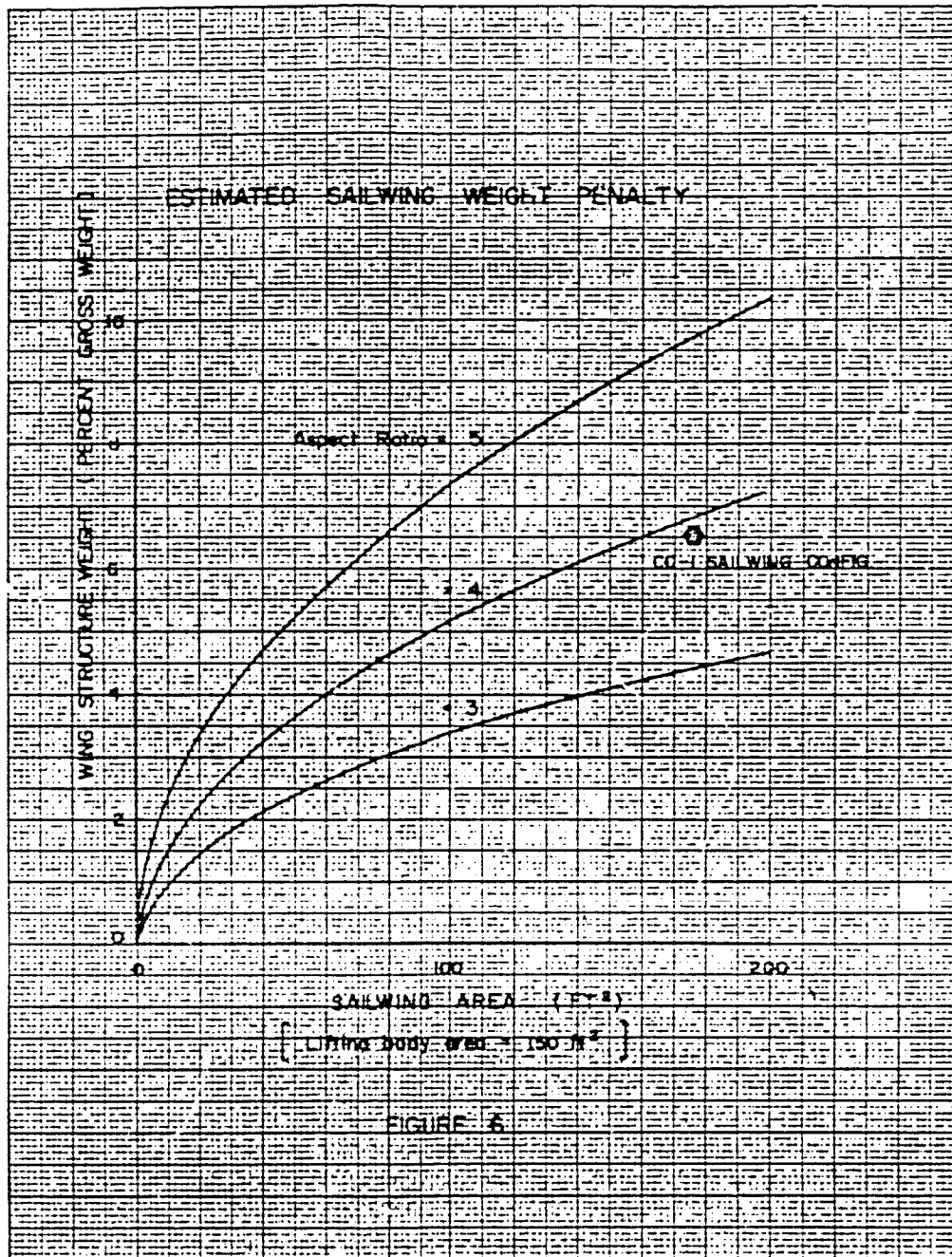
Figure 34. Estimated sailwing weight penalty (Ormiston, pg. 22)
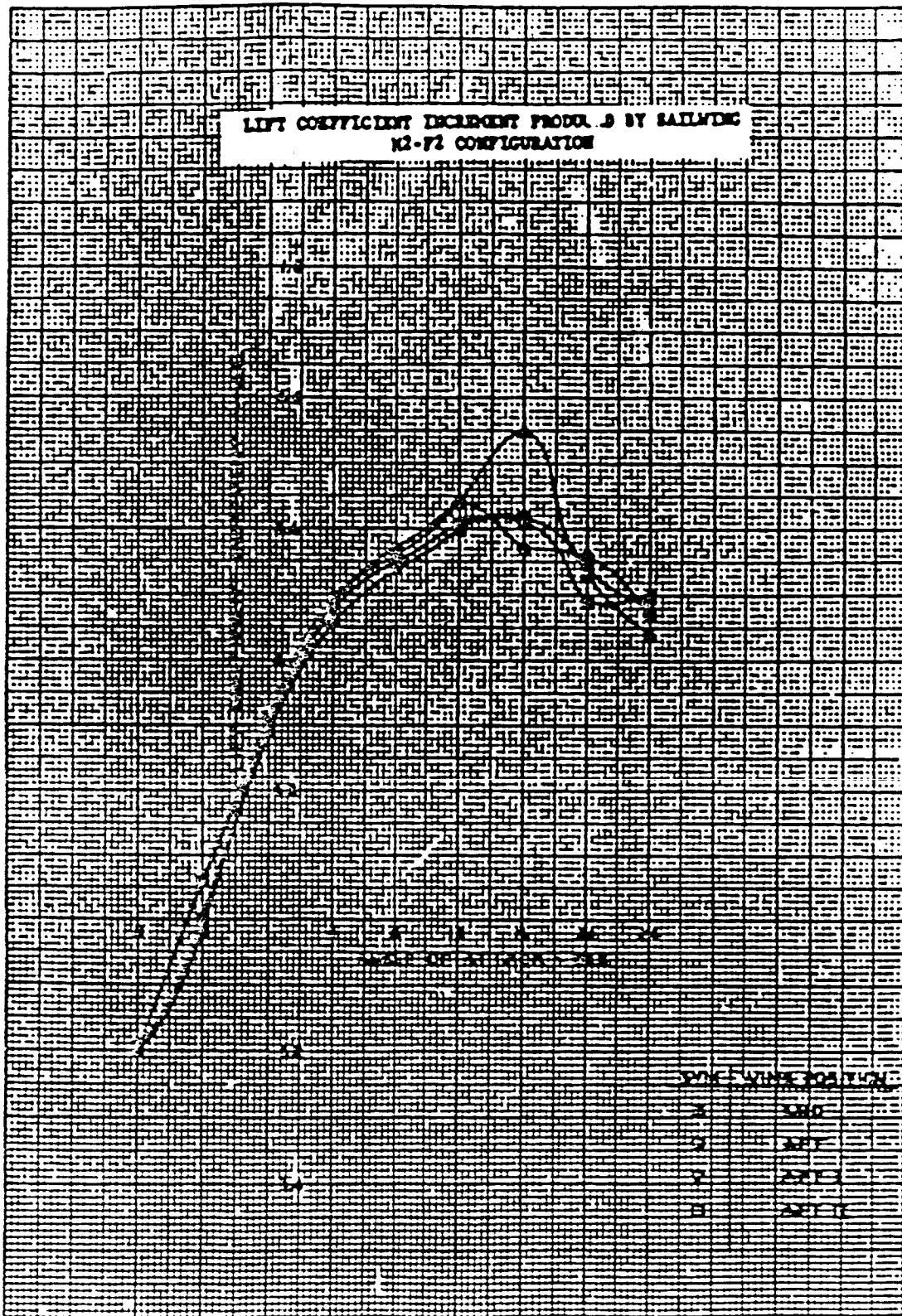
Figure 35. Lift coefficient increment produced by sailwing
(Ormiston, pg. 50)
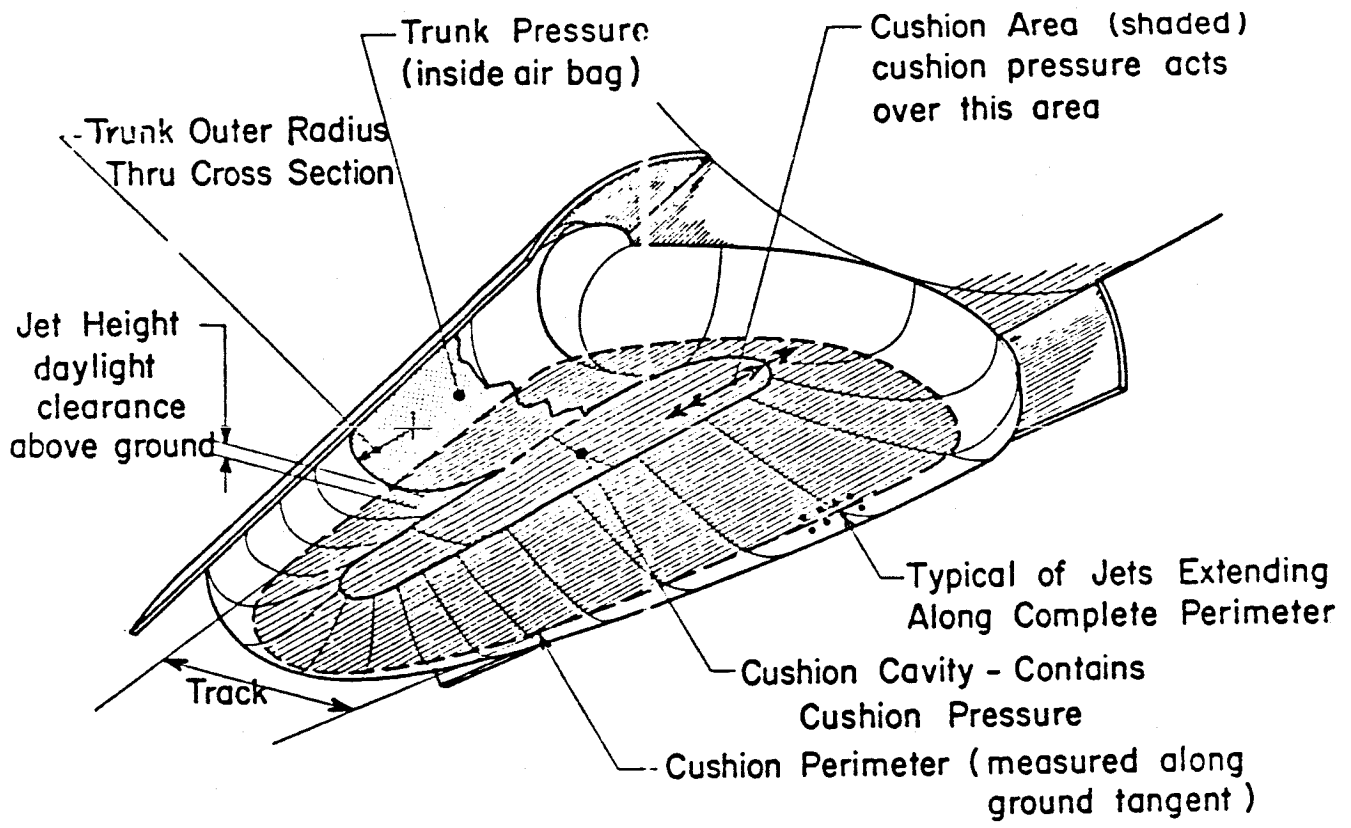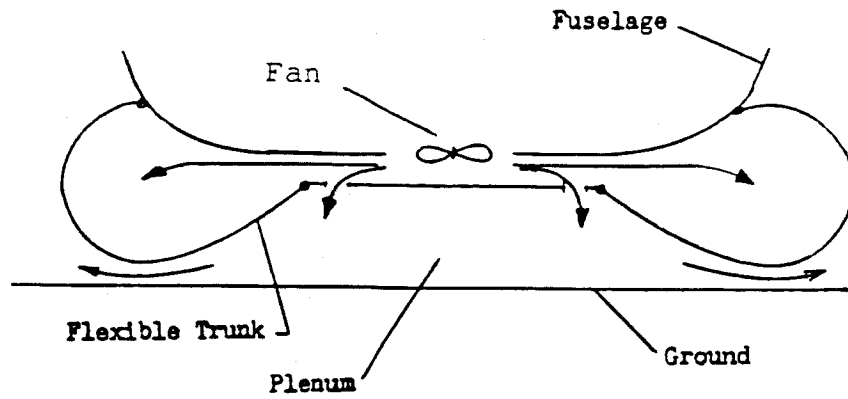
Figure 36. Standard ACLS configuration
(ACLS Conference, pp. 227 and 574)

88
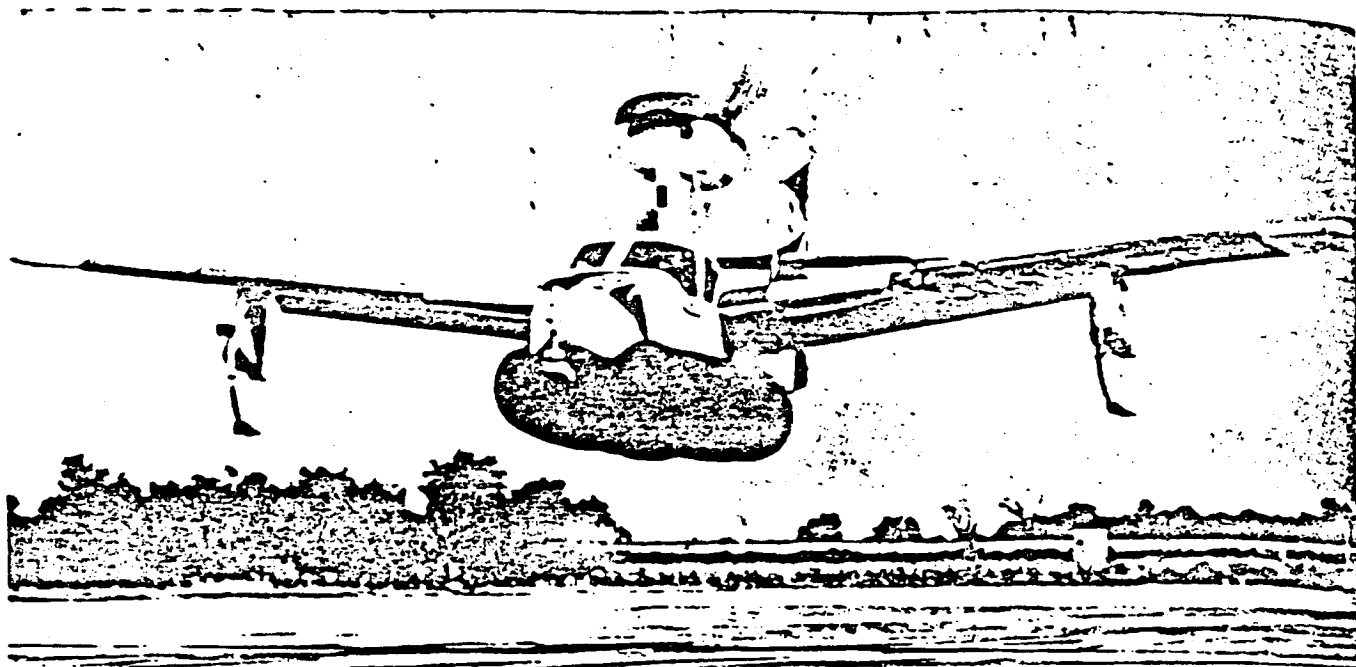
a) LA-4 with ACLS
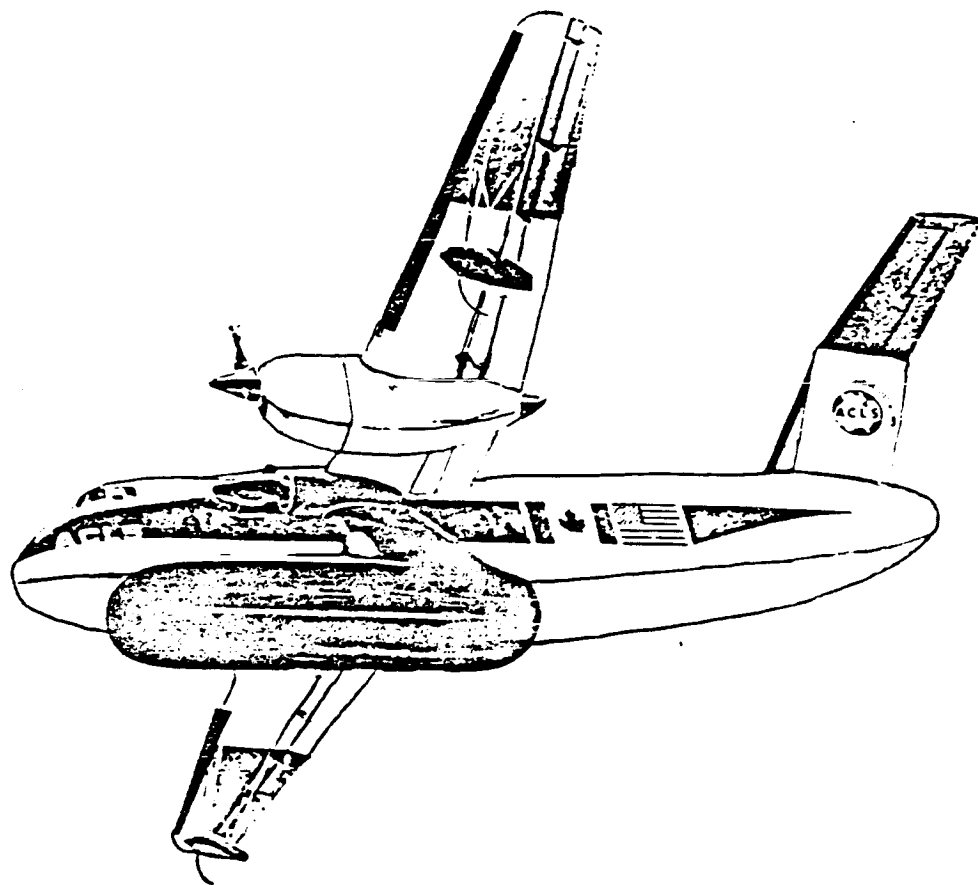
b) XC-8A with ACLS

Figure 37. ACLS testcraft (ACLS Conf., pp. 437 and 572)

Figure 38. Peak landing loads vs. descent rate
(ACLS Conf., pg. 469)
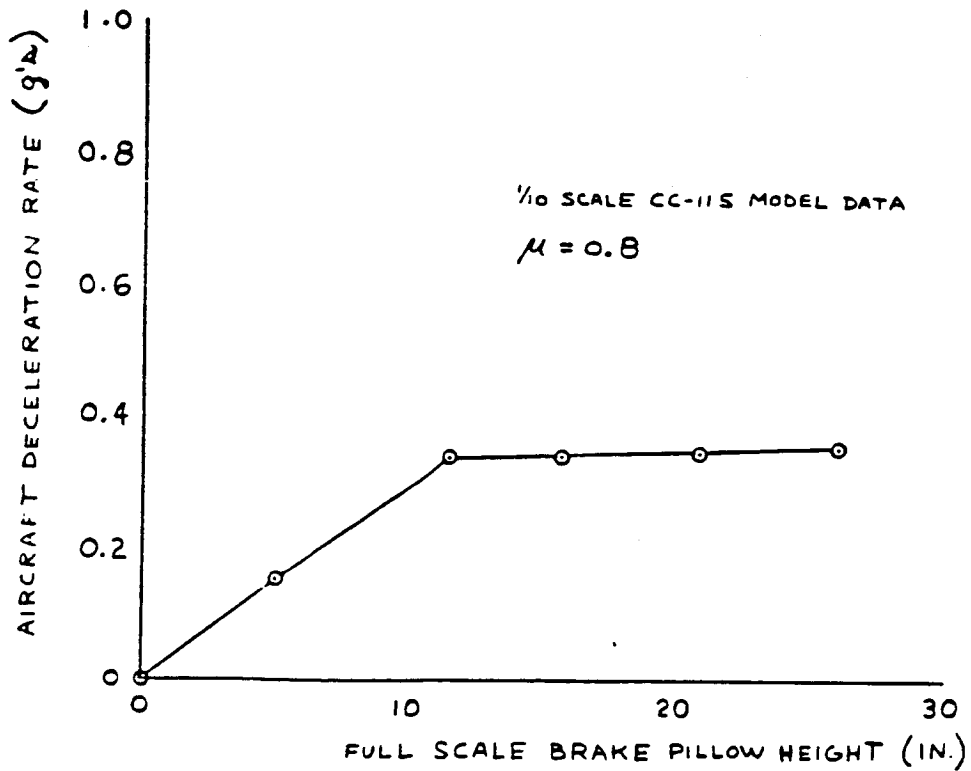
Figure 39. Effects of brake height on deceleration
(ACLS Conf., pg. 575)
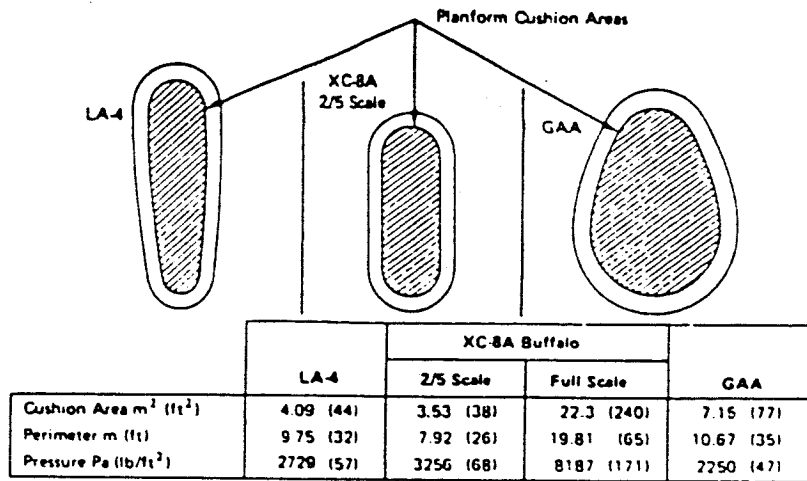
Figure 40. Air cushion planform comparison   (Earl, pg. 8)

	LA-4	XC-8A Buffalo		GAA
		2/5 Scale	Full Scale	
Cushion Area m² (ft²)	4.09 (44)	3.53 (38)	22.3 (240)	7.15 (77)
Perimeter m (ft)	9.75 (32)	7.92 (26)	19.81 (65)	10.67 (35)
Pressure Pa (lb/ft²)	2729 (57)	3256 (68)	8187 (171)	2250 (47)

0.953 (0.375) DRILL
13 HOLES 20.3 cm
APART EXCEPT AT ENDS
TOLERANCES 10.2 (4.0)
NONCUMULATIVE

10.2 (4.0)   20.3 (8.0)

10.2 (4.0)   20.3 (8.0)

12.7 (5.0)

0.953 (0.375)
DRILL 22 HOLES
ALL 20.3 cm APART
EXCEPT AT ENDS
TOLERANCES
NONCUMULATIVE

20.3 (8.0)

86.4 (34)

304.8 (120)

0.953 (0.375)
DRILL 5 HOLES
ACCORDING TO
LAYOUT ABOVE

426.7 (168)

(ALL TRUNK ENDS)
TOLERANCES
NONCUMULATIVE

0.953 (0.375)
DRILL 16 HOLES
20.3 cm APART
EXCEPT AT ENDS
TOLERANCES
NONCUMULATIVE

0.953 (0.375)
DRILL 7 HOLES
20.3 cm APART
EXCEPT AT ENDS
TOLERANCES
NONCUMULATIVE

20.3 (8.0)

10.2 (4.0)

10.2 (4.0)

20.3 (8.0)

121.9 (48)
243.8 (96)

ORIGINAL PAGE IS
OF POOR QUALITY

NOTE: DIMENSIONS IN CM (IN.)

Figure 41. NASA test vehicle trunk design (Lee, pg. 61)

91

Intake   Intake

Roll & Pitch
Control Sensor

Stagnation
Chamber

Fan

Control
Valve

Trunk

Stagnation
Chamber

Fan

Control
Valve

Intake

Trunk

Intake

Control
Valve

Roll & Pitch
Control Sensor
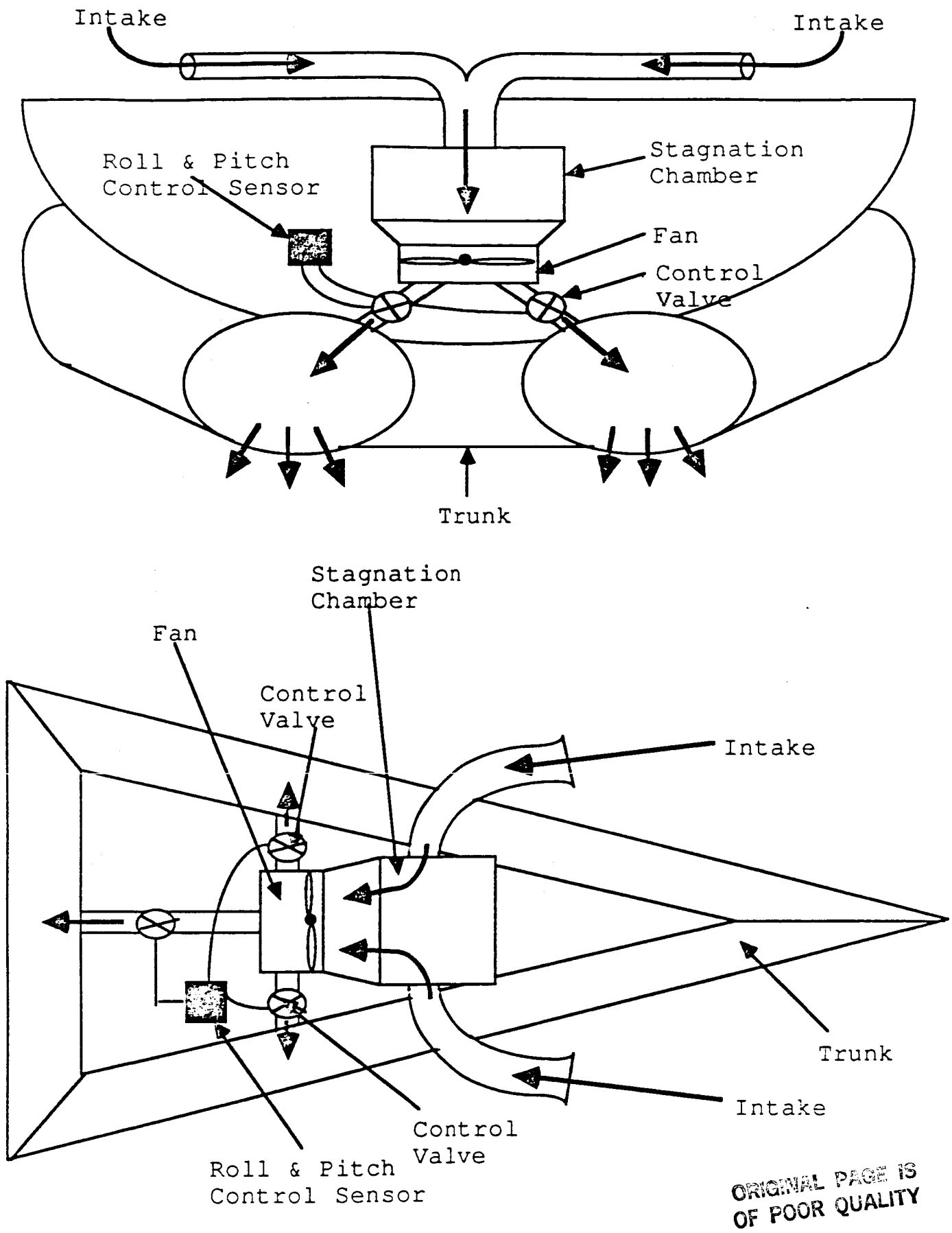
Figure 42. Roll and pitch control system for the ACLS trunk

STOWED POSITION
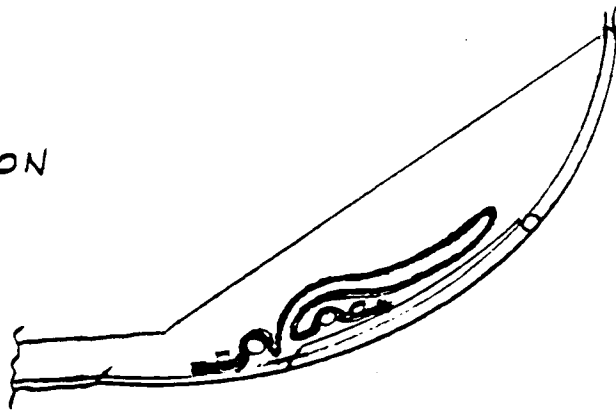
AIR FLOW SYSTEM
POWERED ON
AND FLOW VALVES
OPENED
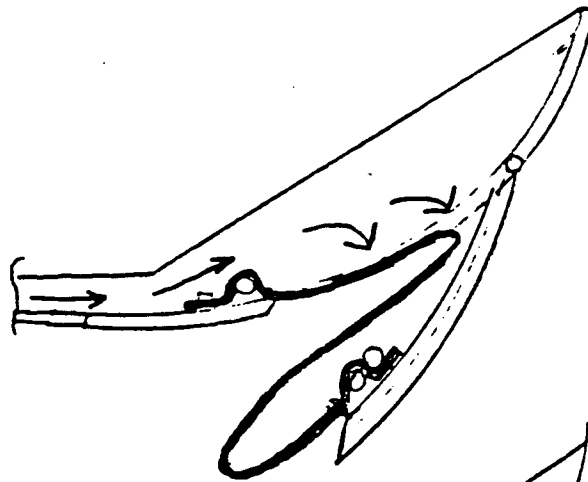
TRUNK IN
FULLY DEPLOYED
AND OPERATIONAL
POSITION

P_c

P_j

P_a
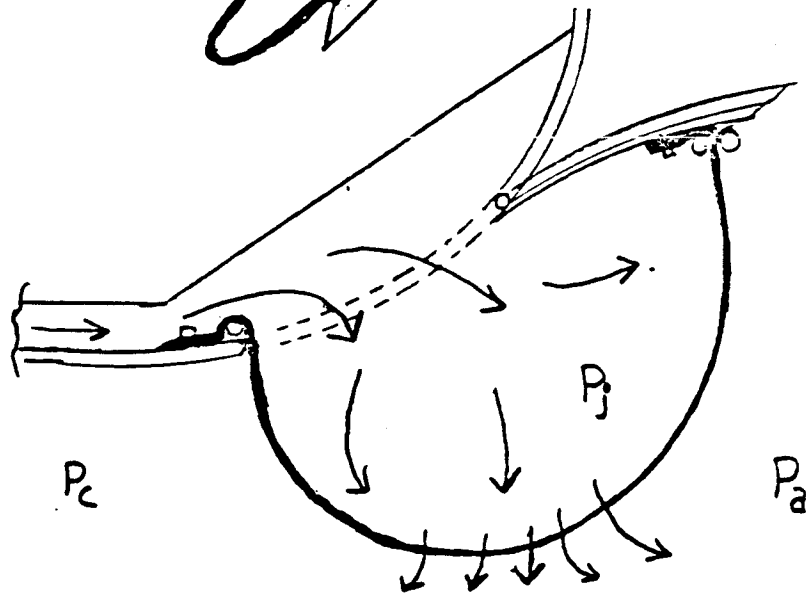
Figure 43. Deployment of the ACLS trunk

Separate Air Supply
Manifold

Bladder

Cross Section

Braking Pillow

Forward

Side Showing Pillow Contact
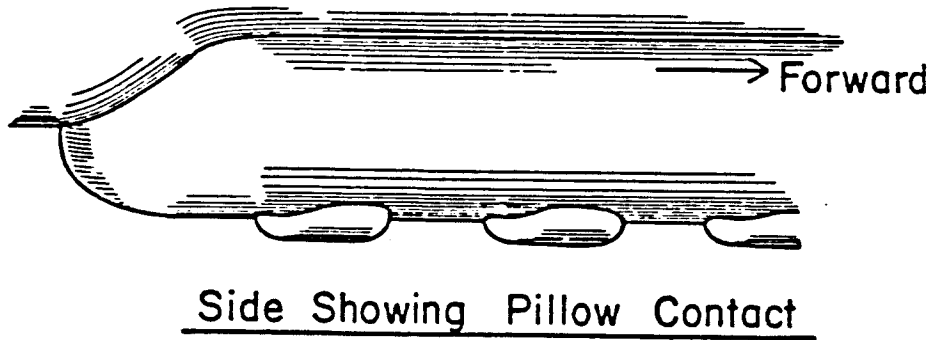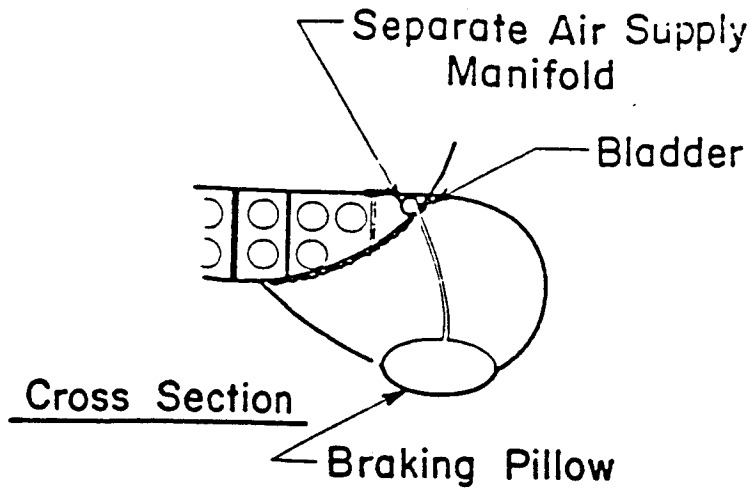
Figure 44. Pillow braking system (ACLS Conf., pg. 228)

MAX
REVERSE
FLOW

-.23
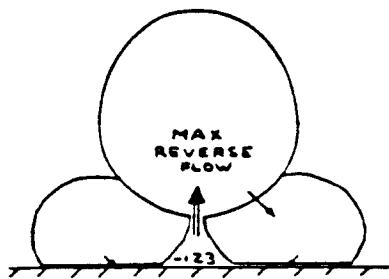
SUCTION BRAKING (1.69)

STOPPING DISTANCE ≈ 398 FT

Figure 45. Suction braking schematic (ACLS Conf., pg. 576)

$A_c = $ ▨

M2-F3

ACLS TRUNK

SIDE

13°

¢

TRUNK PERIMETER

31 ft

UNDERSIDE

13 ft

3.58

NOTE
DIMENSIONS FOR SIZE
REFERENCE ONLY
MCK -1990
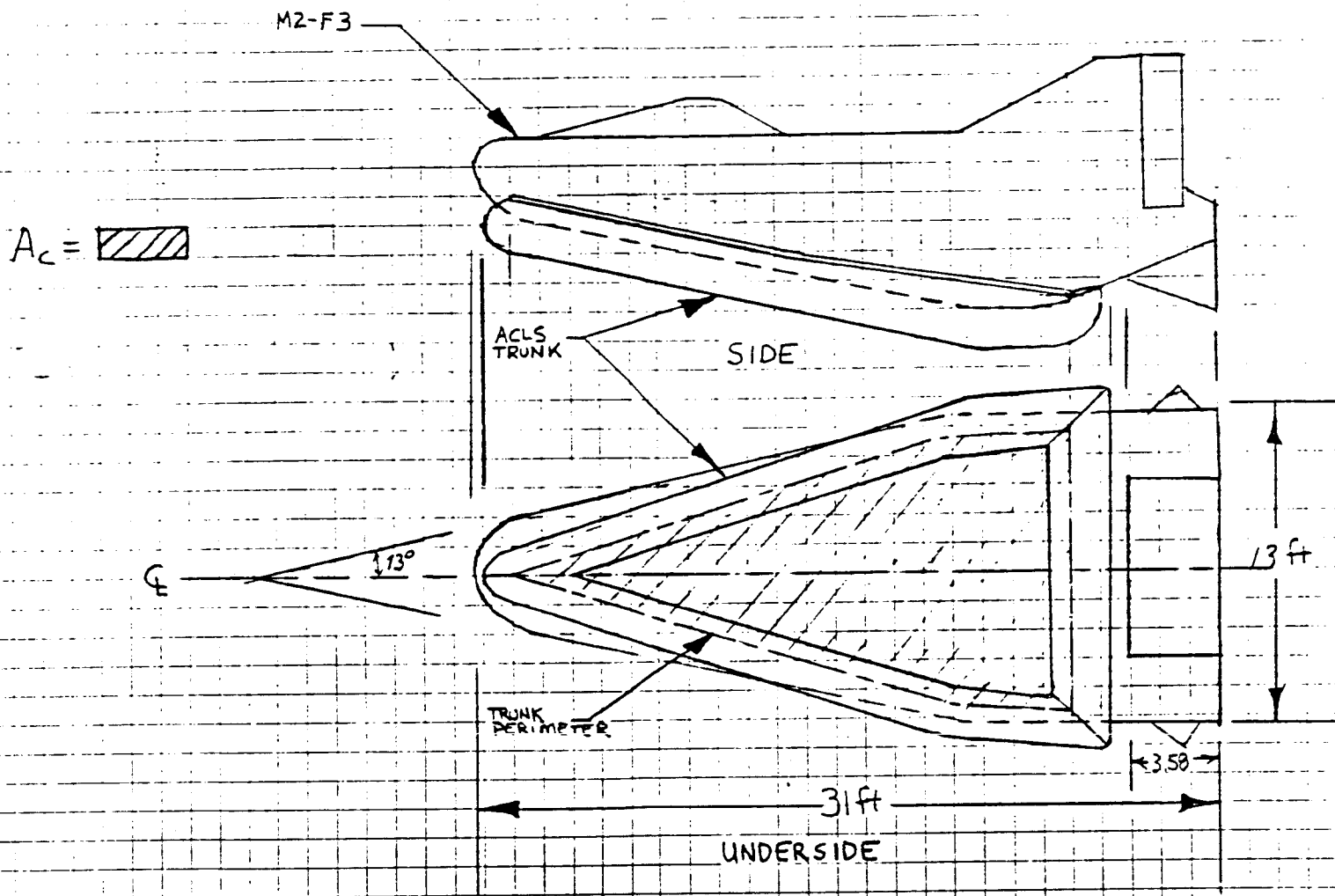
Figure 46. M2-F3 fitted with ACLS
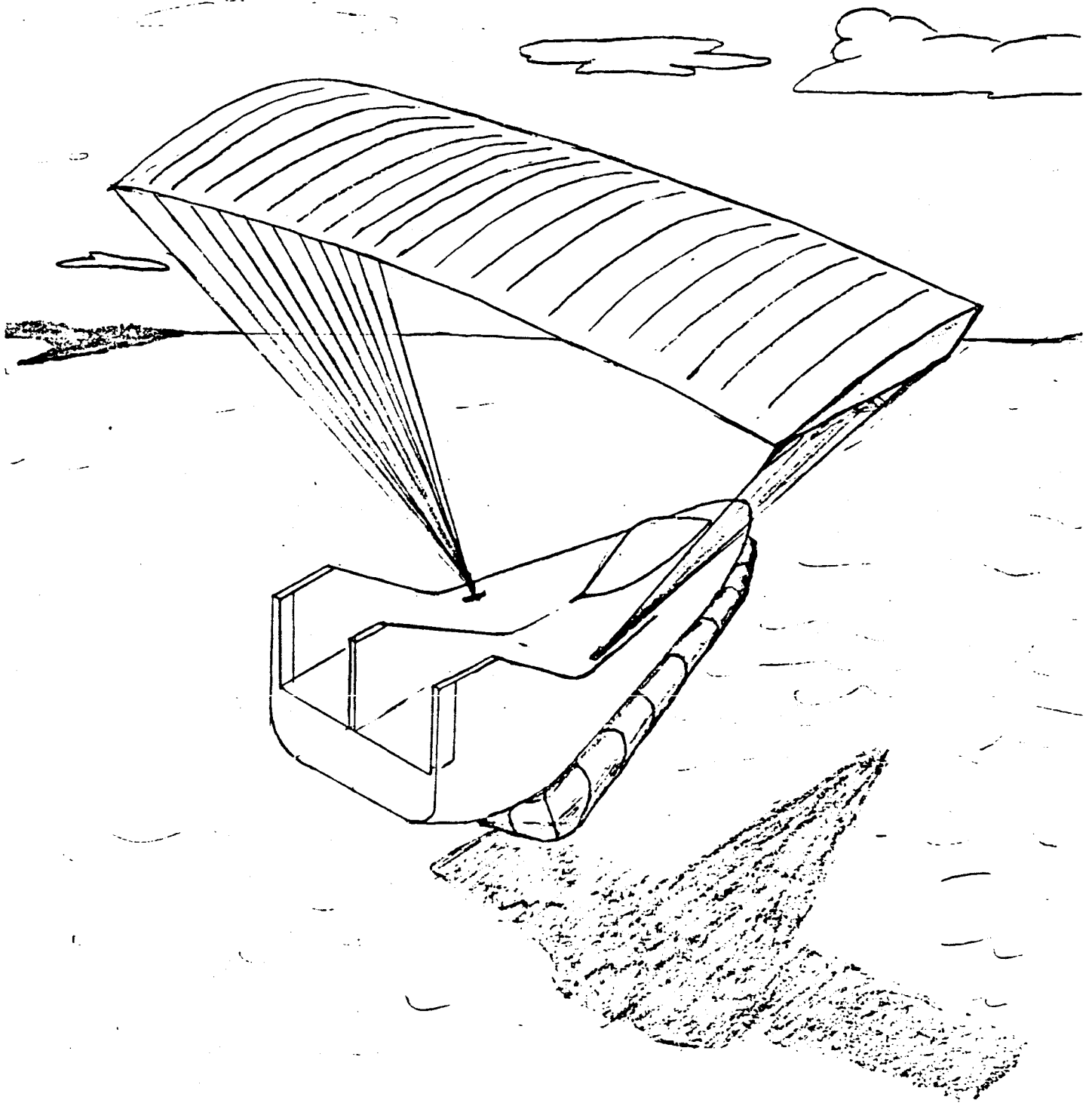
Figure 47. M2-F3 landing with parafoil
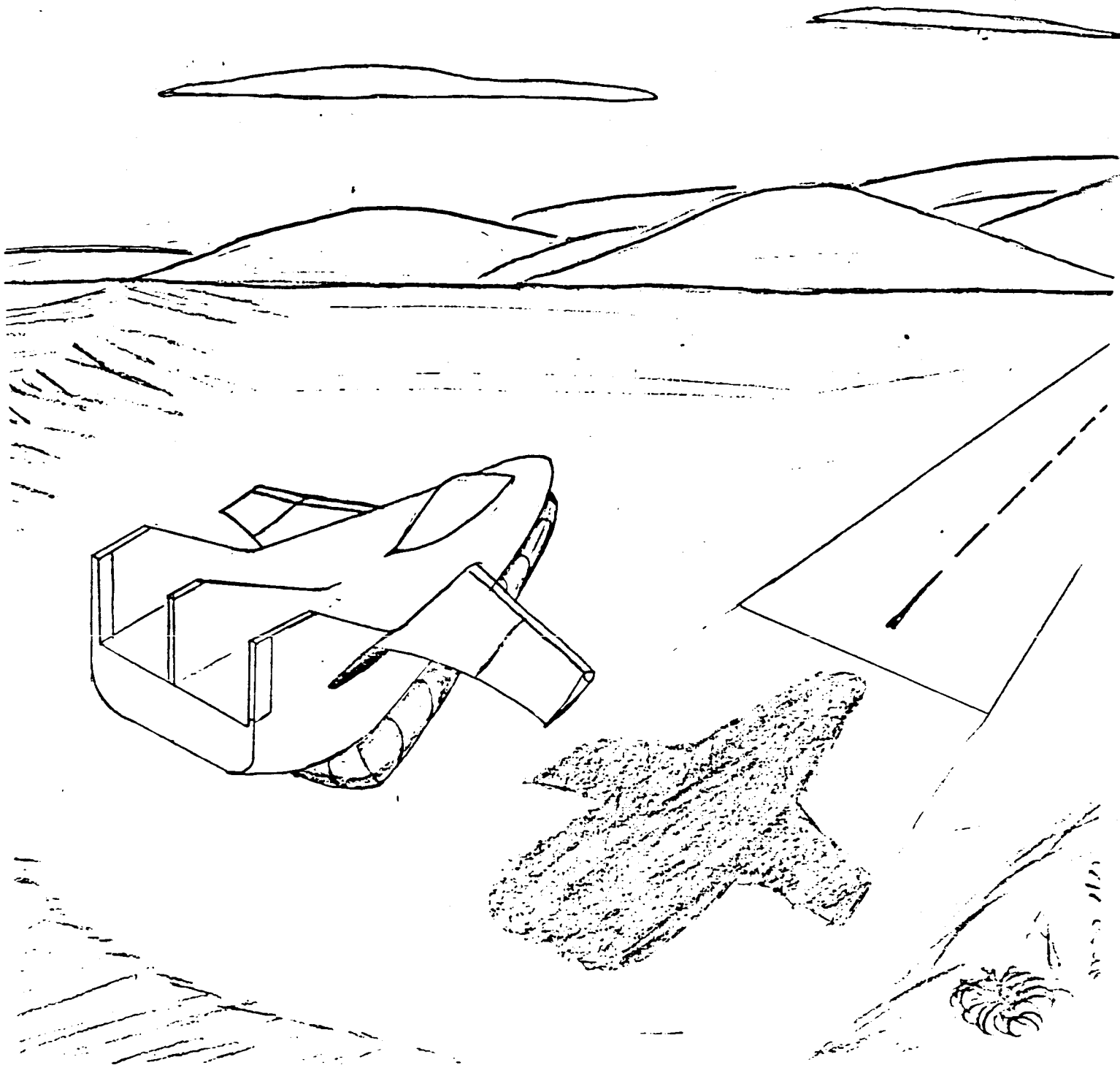
Figure 48. M2-F3 landing with sailwing

97

The computer programs attached were found in Digges (16,261-290) and can be used to determine the cross-sectional shape of the trunk in either the loaded or unloaded mode of operation.

Inelastic Unloaded Trunk Shape

Input Variables:

    a = x coordinate of upper trunk attachment point
    b = y coordinate of upper trunk attachment point
    P_c/P_j = pressure ratio of cushion pressure to trunk pressure
    l = trunk length
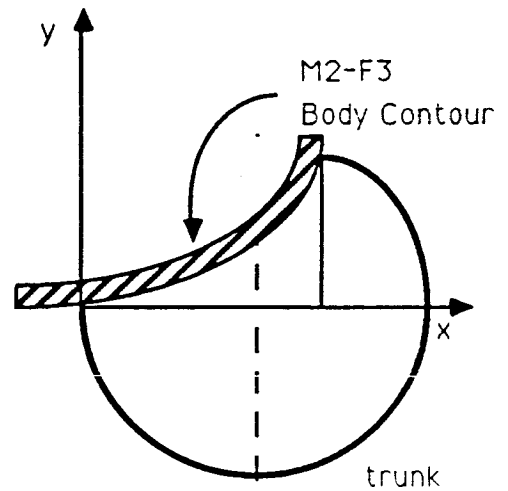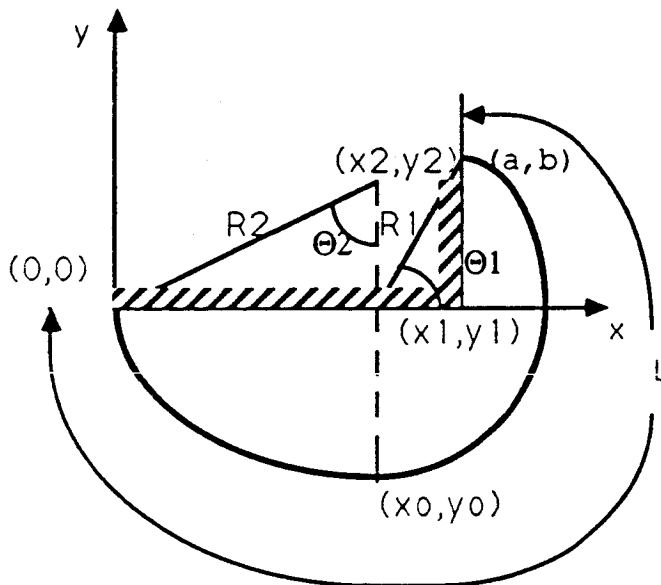
Output Variables:

    R1, R2, X0, Y0, Y1, Y2, ϑ1, and ϑ2.

```
        COMMON /DO/ A,B,PCPJ,L                                              EQT_
        COMMON /DER/ C1,C2,YO,XO,Y1,Y2,TH1,TH2,SGN                          EQT_
        EXTERNAL F                                                          EQT_
        REAL L1,L2,L,LO,LN,LNM1,L3                                          EQT_
        DATA PI/3.1415927/                                                  EQT_
*******************************************************************         EQT_
****   TOL IS A RELATIVE TOLERANCE ON LBAR          *****                   EQT_
*******************************************************************         EQT_
        TOL = 3.0E-5                                                        EQT_
1       READ(5,10) A,B,PCPJ,L                                               EQT_
10      FORMAT(4E20.4)                                                      EQT_
        WRITE(6,11) A,B,PCPJ,L                                              EQT_
11      FORMAT(1H0///4H A = ,E16.4,10X,4HB = ,E16.4,10X,8HPC/PJ = ,E16.4,   EQT_
     +    10X,4HL = ,E16.4)                                                 EQT_
*******************************************                                 EQT_
**   FIX SIGN ON SQUARE ROOT **                                            EQT_
*******************************************                                 EQT_
        SGN = 1.0                                                           EQT_
        IF (PI*SQRT(A**2+B**2)/2.0 .LT. L) SGN = -1.0                       EQT_
                                                                            EQT_
*******************************************                                 EQT_
**   RO EQUALS INITIAL GUESS FOR R1. **                                    EQT_
*******************************************                                 EQT_
        RO = SQRT(A**2 + B**2)*(1.0 +10.0**(-6))/2.0                        EQT_
        RN=RO                                                               EQT_
*******************************************                                 EQT_
**   CALCULATE K-TH VALUE OF R AND OTBAIN LBAR**                           EQT_
*******************************************                                 EQT_
        DO 68 K=1,1000                                                      EQT_
*******************************************                                 EQT_
**   SUBROUTINE F COMPUTES  LBAR  -L**                                     EQT_
*******************************************                                 EQT_
2       PLN = F(RN)                                                         EQT_
        LN = PLN +L                                                         EQT_
*******************************************                                 EQT_
** IS R NEGATIVE OR IS LBAR (R) COMPLEX. IF SO R(K+1)=(R(K+1)+R(K))/2**     EQT_
** (THIS OCCURS WHEN R(K)IS TOO SMALL)                       **             EQT_
*******************************************                                 EQT_
        IF (PLN .NE. 10.**15 .AND. RN .GT. 0.) GO TO 4                      EQT_
        IF (K .EQ.1) GO TO 70                                               EQT_
        RN = (RN +RNM1)/2.0                                                 EQT_
        GO TO 2                                                             EQT_
4       IF (K.EQ. 1) GO TO 5                                                EQT_
*******************************************                                 EQT_
** DETERMINE IF SOLUTION HAS BEEN BOUNDED.  IF SO SET BOUNDS AND CALL**     EQT_
** MUELLER SUBROUTINE.  IF NOT COMPUTE R(K+1) USING NEWTON'S FORMULA **     EQT_
*******************************************                                 EQT_
                                                                            EQT_
        IF ( SIGN(1.,L-LN).NE. SIGN(1.,L-LNM1)) GOTO 100                    EQT_
5       LNM1 = LN                                                           EQT_
                                                                            EQT_
*******************************************                                 EQT_
** SUBROUTINE DF COMPUTES LBAR'(R)**                                        EQT_
*******************************************                                 EQT_
```

```
        DLN = DF(RN)
        R1 = RN
*********************
** TOLERANCE TEST **
*********************

        IF (ABS(LN-L) .LT. TOL*ABS(L)) GO TO 110
        RNM1 = RN
        RN = RN -(LN-L)/DLN
63      CONTINUE
70      WRITE(6,71)
71      FORMAT(17H1 RO COMPLEX ....     )
        STOP
100     IF (RN .GT. RNM1) GO TO 105
        DUM = RN
        RNM1 = DUM
105     WRITE(6,104)
104     FORMAT(1H0,7HMUELLER)
        CALL RTMI( R1,LN,F,RNM1,RN,TOL     ,2000,IER)
        IF (IER .EQ. 0) GO TO 110

        WRITE(6,106) IER,R1,LN
106     FORMAT(1H1,10HIER EQUAL   ,I2,5X,4HSTOP,2E25.6)
        STOP
110     R2 = R1/(1.- PCPJ)
        X07 =X0/A
        L1 =R1 *TH1
        L2 = R2 *TH2
        L3 = 0.0
        WRITE(6,55) R1,R2,X0,Y0,Y1,Y2,TH1,TH2
55      FORMAT(1H0,5HR1 = ,E16.4,10X,5HR2 = ,E16.4,10X,5HX0 = ,E16.4,10X,
     +  5HY0 = ,E16.4,/1X,5HY1 = ,E16.4,10X,5HY2 = ,E16.4,10X,
     +  6HTH1 = ,E15.4,10X,6HTH2 = ,E15.4////////////)
        GO TO 1
        END
```

```
      FUNCTION F (R1)                                              FTNC
      COMMON /CO/A,B,PCPJ,L                                        FTNC
      COMMON /DER/ C1,C2,Y0,X0,Y1,Y2,TH1,TH2,SGN                   FTNC
      REAL L                                                       FTNC
      DATA PI/3.1415927/                                           FTNC
                                                                   FTNC
C**************************************************************    FTNC
C** IF R(K) IS SUCH THAT L-BAR WILL BE COMPLEX, THE VALUE OF**     FTNC
C** F= LBAR -L IS SET TO 10 **15                          **      FTNC
C**************************************************************    FTNC
      R2 = R1/(1.0-PCPJ)                                           FTNC
      C1 = (R1-B-R2)/ A                                            FTNC
      C2 = A/2.0 +(B**2)/(2.0*A)-(R1*B)/A
      ASQ = (2.0*R2+2.0*C1*C2)**2 - (4.0*C2**2)*(C1**2+1.0)
      IF (ASQ.LT.0.0) GO TO 25                                     FTNC
      SQ = SQRT(ASQ)                                               FTNC
      Y0 = (-2.0*(R2+C1*C2)+SGN *SQ)/(2.0*(C1**2+1))               FTNC
                                                                   FTNC
      X0 = C1*Y0+C2                                                FTNC
      Y1 = Y0+R1                                                   FTNC
      Y2 = Y0+R2                                                   FTNC
      TH2 = ATAN(X0/Y2)                                            FTNC
      IF( Y2 .EQ. 0.) TH2 = PI/2.0                                 FTNC
      IF(TH2 .LT. 0.0) TH2 = TH2 + PI                              FTNC
20    PSI = PSI + PI                                               FTNC
21    TH1 = PSI + PI/2.0                                           FTNC
      F = R1*TH1+R2*TH2-L                                          FTNC
                                                                   FTNC
C**************************************************************    FTNC
C** IF VALUE OF VARIABLES ON EACH ITERATION IS DESIRED, REMOVE**   FTNC
C** THE * ON THE TWO WRITE STATEMENTS BELOW.              **      FTNC
C**************************************************************    FTNC
                                                                   FTNC
*     WRITE(6,22) R1,R2,TH1,TH2,Y0,ASQ,C1,C2,PCPJ,X0,Y1,Y2,A,B,F   FTNC
      RETURN                                                       FTNC
23    PSI = PI/2.0                                                 FTNC
      GO TO 21                                                     FTNC
25    F = 10.0**15                                                 FTNC
*     WRITE(6,22) R1,R2,TH1,TH2,Y0,ASQ,C1,C2,PCPJ,X0,Y1,Y2,A,B,F   FTNC
22    FORMAT(1H0/(7E18.5))                                         FTNC
      RETURN                                                       FTNC
      END                                                          FTNC
```

```fortran
      FUNCTION DF(R1)
      COMMON /DER/ C1,C2,YO,XO,Y1,Y2,TH1,TH2,SGN
      COMMON /CO/ A,B,PCPJ,L
      REAL K
      K = 1.0 - PCPJ
      DC1 = (K-1.0)/(K*A)
      DC2 = -B/A
      X = R1 /K + C1*C2
      Y = C1**2 +1.0
      DX = 1.0/K +C1*DC2 + C2*DC1
      DY = 2.0*C1 *DC1
      Z = -SGN *SQRT(X**2 - Y*C2**2)
      DZ = (1.0/ (2.0*Z))*(2.0*X*DX - (2.0*Y*C2*DC2*C2**2*DY))
      DYO = (1.0/Y**2)*(-Y*(DX+DZ)+(X+Z)*DY)
      DXO = C1*DYO+YO*DC1+DC2
      DY1 = DYO + 1.0
      DY2 = DYO + 1.0/K
      S = B-Y1
      T = A-XO
      DST = (1.0/T**2)*(-T*DY1 + S*DXO)
      DXDY2= (1.0/Y2**2) * (Y2*DXO -XO*DY2)
      DPSI = DST/(1.0 + (S/T)**2)
      DTH2 = DXDY2 / (1.0+(XO/Y2)**2)
      DTH1 = DPSI
      DF = R1 *(DTH1 +DTH2/K)+ TH1 +TH2/K
      RETURN
      END
```

102 of poor quality watermark

```
**********************************************************************RTM
*                                                                  *RTM
*          SUBROUTINE RTMI                                          *RTM
*                                                                  *RTM
*                                                                  *RTM
*       PURPOSE                                                     *RTM
*          TO SOLVE GENERAL NONLINEAR EQUATIONS OF THE FROM FCT(X)=0 *RTM
*          BY MEANS OF MUELLER-S INTERATION METHOD.                 *RTM
*                                                                  *RTM
*                                                                  *RTM
*       USAGE                                                       *RTM
*          CALL RTMI (X,F,FCT,XLI,XRI,EPS,IEND,IER)                 *RTM
*          PARAMETER FCT REQUIRES AN EXTERNAL STATEMENT             *RTM
*                                                                  *RTM
*                                                                  *RTM
*       DESCRIPTION OF PARAMETERS                                   *RTM
*          X       - RESULTANT ROOT OF EQUATION FCT(X)=C.           *RTM
*          F       - RESULTANT FUNCTION VALUE AT ROOT X.            *RTM
*          FCT     - NAME OF THE EXTERNAL FUNCTION SUBPROGRAM USED.  *RTM
*          XLI     - INPUT VALUE WHICH SPECIFIES THE INITIAL LEFT BOUND *RTM
*                    OF THE ROOT X.                                 *RTM
*          XRI     - INPUT VALUE WHICH SPECIFIES THE INITIAL RIGHT BOUND*RTM
*                    OF THE ROOT X.                                 *RTM
*          EPS     - INPUT VALUE WHICH SPECIFIES THE UPPER BOUND OF THE *RTM
*                    ERROR OF RESULT X.                             *RTM
*          IEND    - MAXIMUM NUMBER OF ITERATION STEPS SPECIFIED.   *RTM
*          IER     - RESULTANT ERROR PARAMETER CODED AS FOLLOWS     *RTM
*                    IER=0 - NO ERROR,                              *RTM
*                    IER=1 - NO CONVERGENCE AFTER IEND ITERATION STEPS *RTM
*                            FOLLOWED BY IEND SUCCESSIVE STEPS OF   *RTM
*                            BISECTION                              *RTM
*                    IER=2 - BASIC ASSUMPTION FCT(XLI)FCT(XRI) LESS  *RTM
*                            THAN OR EQUAL ZERO IS NOT STATISFIED.  *RTM
*                                                                  *RTM
*                                                                  *RTM
*       REMARKS                                                     *RTM
*          THE SPROCEDURE ASSUMES THAT FUNCTION VALUES AT INITIAL   *RTM
*          BOUNDS XLI AND XRI HAVE NOT THE SAME SIGN.  IF THIS BASIC *RTM
*          ASSUMPTION IS NOT SATISFIED BY INPUT VALUES XLI AND XRI, *RTM
*          THE PROCEDURE IS BYPASSED AND GIVES THE ERROR MESSAGE IER=2.*RTM
*                                                                  *RTM
*       SUBROUTINEA AND FUNCTION SUBPROGRAMS REQUIRED               *RTM
*          THE EXTERNAL FUNCTION SUBPROGRAM FCT(X) MUST BE FURNISHED *RTM
*          BY THE USER.                                             *RTM
*                                                                  *RTM
*       METHOD                                                      *RTM
*          SOLUTION OF EQUATION FCT(X)=0 IS DONE BY MEANS OF MUELLER-S *RTM
*          ITERATION METHOD OF SUCCESSIVE BISECTIONS AND INVERSE    *RTM
*          PARABOLIC INTERPOLATION, WHICH STARTS AT THE INITIAL BOUNDS *RTM
*          XLI AND XRI.  CONVERGENCE IS QUADRATIC IF THE DERIVATIVE OF *RTM
*          FCT(X) AT ROOT X IS NOT EQUAL TO ZERO.   ONE ITERATION STEP *RTM
*          REQUIRES TWO EVALUTIONS OF FCT(X).  FOR TEST OF SATISFACTORY*RTM
*          ACCURACY SEE FORMULAE (3,4) OF MATHEMATICAL DESCRIPTION. *RTM
*          FOR REFERENCE, SEE G. K. KRISTIANSEN, ZERO OF ARBITRARY  *RTM
*          FUNCTION, BUIT, VOL. 3 (1963), PP.205-206.               *RTM
**********************************************************************RTM
          SUBROUTINE RTMI(X,F,FCT,XLI,XRI,EPS,IEND,IER)
*       PREPARE ITERATION
          IER=0
          XL=XLI
```

```
        XR=XRI                                                          RTM
        X=XL                                                            RTM
        TCL=X                                                           RTM
        F=FCT(TOL)                                                      RTM
        IF(F)1,16,1                                                     RTM
1       FL=F                                                            RTM
        X=XP                                                            RTM
        TOL=X                                                           RTM
        F=FCT(TOL)                                                      RTM
        IF(F)2,16,2                                                     RTM
2       FR=F                                                            RTM
        IF (SIGN(1.,FL)+SIGN(1.,FR))25,3,25                             RTM
*       BASIL ASSUMPTION FL*FR LESS THAN 0 IS SATISFIED.                RTM
*       GENERATE TOLERANCE FOR FUNCTION VALUES.                         RTM
3       I=0                                                             RTM
        TOLF=100.*EPS                                                   RTM
*       START ITERATION LOOP                                            RTM
4       I=I+1                                                           RTM
*       START BISECTION LOOP                                            RTM
        DO 13 K=1,IEND                                                  RTM
         X=.5*(XL+XR)                                                   RTM
        TOL=X                                                          2RTM
        F=FCT(TOL)                                                      RTM
        IF(F) 5,16,5                                                    RTM
5       IF (SIGN(1.,F)+SIGN(1.,FR))7,6,7                                RTM
*       INTERCHANGE XL AND XR IN ORDER TO GET THE SAME SIGN IN F AND FR RTM
6       TOL=X                                                           RTM
        XL=XR                                                           RTM
        XR=TOL                                                          RTM
        TOL=FL                                                          RTM
        FL=FR                                                           RTM
        FR=TOL                                                          RTM
7       TOL=F-FL                                                        RTM
        A=F*TOL                                                         RTM
        A=A+A                                                           RTM
        IF (A-FR*(FR-FL))8,9,9                                          RTM
8       IF (I-IEND)17,17,9                                              RTM
9       XR=X                                                            RTM
        FR=F                                                            RTM
*       TEST ON  SATISFACTORY ACCURACY IN BISECTION LOOP                RTM
        TOL=EPS                                                         RTM
        A=ABS(XR)                                                       RTM
        IF (A-1.)11,11,10                                               RTM
10      TOL=TOL*A                                                       RTM
11      IF (ABS(XR-XL)-TOL)12,12,13                                     RTM
12      IF (ABS(FR-FL)-TOLF)14,14,13                                    RTM
13      CONTINUE                                                        RTM
* END OF BISECTION LOOP                                                 RTM
* ERROR RETURN                                                          RTM
        IER=1                                                           RTM
14      IF (ABS(FR)-ABS(FL))16,15,15                                    RTM
15      X=XL                                                            RTM
        F=FL                                                            RTM
16      RETURN                                                          RTM
*       COMPLIANCE OF ITERATED X-VALUE BY INVERSE PARABOLIC INTERPOLATIO RTM
```

ORIGINAL PAGE IS
OF POOR QUALITY

```
17        A=FR-F                                                    RT:
          DX=(X-XL)*FL*(1.+F*(A-TOL)/(A*(FR-FL)))/TOL               RT.
          XP=X                                                      RT.
          FP=F                                                      RTM
          X=XL-DX                                                   RT
          TOL=X                                                     RT
          F=FCT(TOL)                                                RTM
          IF (F)13,16,18                                            RT
*         TEST ON SATISFACORY ACCURACY  IN ITERATION LOOP           RTM
18        TOL=EPS                                                   RTM
          A=ABS(X)                                                  RTM
          IF (A-1.)20,20,19                                         RT.
19        TOL=TOL*A                                                 RTM
20        IF(ABS(DX)-TOL)21,21,22                                   RT
21        IF(ABS(F)-TOLF)16,16,22                                   RTM
*         PREPARATION OF NEXT BISECTION LOOP                        RT.
                                                                    RTM
22        IF (SIGN(1.,F)+SIGN(1.,FL))24,23,24                       RT
23        XR=X                                                      RTM
          FR=F                                                      RT
          GO TO 4                                                   RT
24        XL=X                                                      RT
          FL=F                                                      RTM
          XR=XP                                                     RT
          FR=FP                                                     RT
          GO TO 4                                                   RT
*         END OF ITERATION LOOP                                     RT
                                                                    RT
*         ERROR RETURN IN CASE OF WRONG INPUT DATA                  RT
25        IER = 2                                                   RTM
          RETURN                                                    RT
          END                                                       RT
```

Inelastic Loaded Trunk Shape

Input Variables:

- a = x coordinate of upper trunk attachment point
- b = y coordinate of upper trunk attachment point
- P_c/P_j = pressure ratio of cushion pressure to trunk pressure
- l = l1 + l2 + l3 (trunk length)
- Y0 = y coordinate of lower most point (Note: Y0 < 0, from unloaded trunk program).
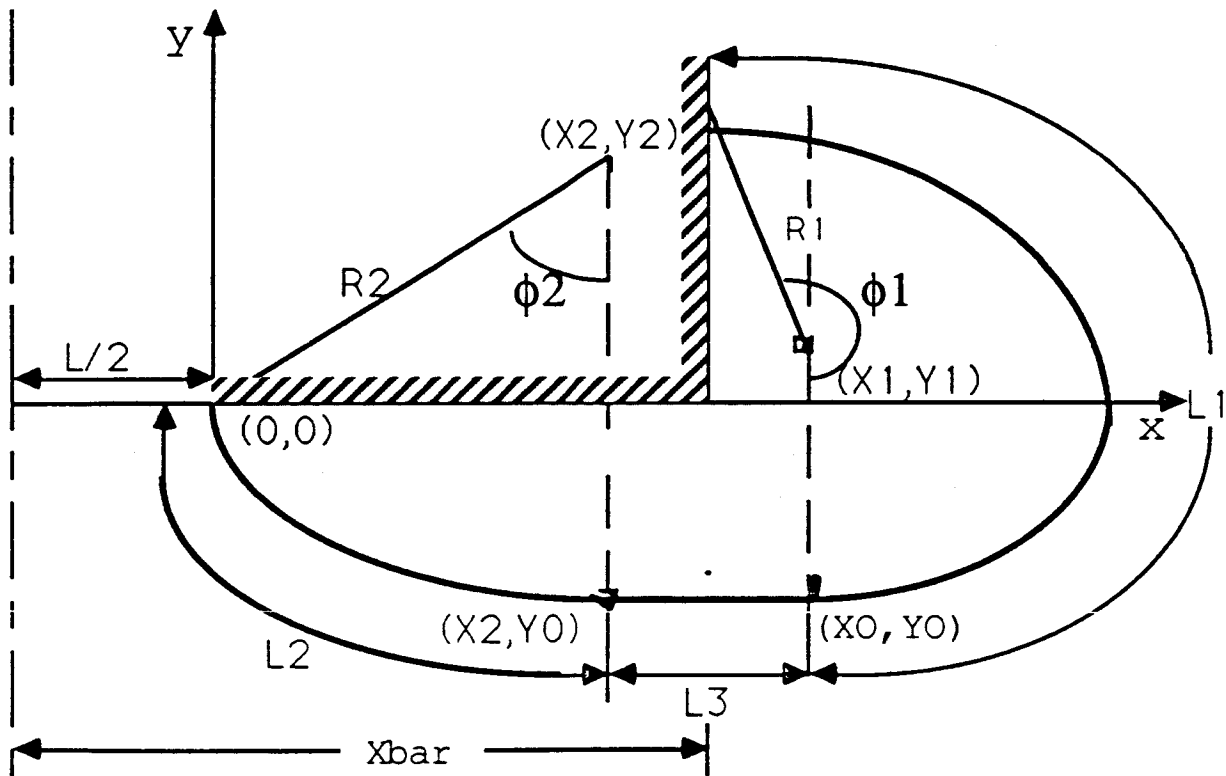
Output Variables:

R1, R2, ϕ1, ϕ2, Y1, Y2, l1, l2, X1, X2, and Xbar (distance to center line of vehicle).

```
      COMMON/CQN/PCPJ,YO,L,A,B,TH1,TH2,X1,X2,Y1,Y2,PSI,SIGN,T,L4      ACLC
      REAL L,LN,L4,L3,L1,L2                                            ACLC
      EXTERNAL F,G                                                     ACLC
      PI=3.1415697                                                     ACLC
*****************************************************************************  ACLC
*     TOL IS THE TOLERANCE ON LBAR, CAN BE CHANGED.                   ACLC
*****************************************************************************  ACLC
      TOL=3.E-5                                                        ACLC
105   READ(5,1)A,B,PCPJ,L,YO                                           ACLC
1     FORMAT(5E15.4)                                                   ACLC
*****************************************************************************  ACLC
*     RO EQUALS INITIAL GUESS FOR R1.                                 ACLC
*****************************************************************************  ACLC
      RO=(B-YO)*(1.0+10.0**(-6))/2.0                                   ACLC
      WRITE(6,2)                                                       ACLC
2     FORMAT(1H1)                                                      ACLC
      RNM1 = AMAX1(-YO*(1.-PCPJ)/2.,(B-YO)/2.)                         ACLC
*****************************************************************************  ACLC
*     FIX SIGN ON SQUARE ROOT.                                        ACLC
*****************************************************************************  ACLC
      SIGN=1.                                                          ACLC
*****************************************************************************  ACLC
*     SUBROUTINE CALLED TO OBTAIN L4.                                 ACLC
*****************************************************************************  ACLC
      T=F(RNM1)                                                        ACLC
*****************************************************************************  ACLC
*     DETERMINE WHETHER X1 IS GREATER OR LESS THAN A.                 ACLC
*     IF GREATER SIGN IS POSITIVE.                                    ACL
*     IF LESS SIGN IS NEGATIVE.                                       
*****************************************************************************  ACLC
      IF(L.LT.L4) GO TO 100                                           ACLC
*****************************************************************************  ACL
*     CONDITION X1 GT A.   COMPUTE UPPER BOUND ON R.          *       ACL
*****************************************************************************  ACL
      AQR=AQRT(A**2+B**2)                                             ACL
      RN=L/(2.0*PI)+SQR/4.0                                           ACL
      IF(SQR.LE.2.*L/PI) GO TO 3                                      ACL
      RN=L/PI                                                         ACL
      DO 5 I=1,30                                                     ACL
      RN=10.*RN                                                       ACL
      IF(RN*SIN(L/2.*RN).GE.SQR/2.) GO TO 3                          ACL
5     CONTINUE                                                        ACL
      WRITE(6,7)                                                      ACL
7     FORMAT(1H0,12H UPPER BOUND)                                     ACL
      R1=0.0                                                          ACL
      GO TO 4                                                         ACL
*****************************************************************************  ACL
*     USE MUELLER'S METHOD TO COMPUTE R SUCH THAT TOLERANCE     *     ACL
*     ON LBAR IS SATISFIED.  (MUELLER ROUTINE CALS SUBROUTINE F TO  *  ACL
*     COMPUTE LBAR = F(B)-L )                                        ACL
*****************************************************************************  ACL
3     CALL RTN(R1,LN,F,RNM1,RN,10.0E-5,50,IER)                        ACL
      IF(IER.EQ.0) GO TO 4                                            ACL
      WRITE(6,11) IER                                                 ACL
11    FORMAT(1H1,14HMUELLER FAILED ,I5)                               ACL
```

```
      R1=0                                                            ACLC
4     R2=R1/(91.-PCPJ)                                                ACLC
      L3=X1-X2                                                        ACLC
      XPAR=(X1+X2)/2.0                                                ACLC
      L1=R1+TH1                                                       ACLC
      L2=R2+RH2                                                       ACLC
      AJ=(TH2+R2**2)/2.-(X2+Y2)/2.-L3*YC+(TH1*R1**2)/2.0+            ACLC
     1  (X1-A)*Y1+((X1-A)*(B-Y1))/2.0                                ACLC
      WRITE(6,500)A,B,PCPJ,YC,L                                       ACLC
500   FORMAT(1HJ,4HA = ,F8.3,14X,4HB = ,F8.3,14X,7HPCPJ = ,F8.5,11X, ACLC
     1 5HYO = ,F8.3,13X,4HL = ,F8.3///)                             ACLC
      WRITE(6,501)R1,R2,LN,TH1,TH2                                    ACLC
501   FORMAT(1HO,5HR1 = ,F8.3,13X,5HR2 = ,F8.3,13X,5HLN = ,F8.5,     ACLC
     1 13X,6HTH1 = ,F8.4,12X,6HTH2 = ,F8.4///)                       ACLC
      WRITE(6,502)Y1,Y2,L1,L2                                         ACLC
502   FORMAT(1HO,5HY1 = ,F8.4,13X,5HY2 = ,F8.4,13X,5HL1 = ,F8.4      ACLC
     1 13X,5HL2 = ,F8.4///)                                          ACLC
      WRITE(6,503) X3AR,AJ,L3                                         ACLC
503   FORMAT(1HO,7HXBAR = ,F6.4,11X,5HAJ = ,F8.2,13X,5HL3 = ,F8.4)   ACLC
      GO TO 105                                                       ACLC
***************************************************************        ACLC
*     CONDITION X1 LESS THAN A.  COMPUTE THE VALUE OF R SUCH THAT  *   ACLC
*     X1 = A.  THIS VALUE OF R GIVES THE MAXIMUM VALUE OF L        *   ACLC
*     POSSIBLE UNDER THE RESTRICTIONS X2 LT X1, X1 LT A            *   ACLC
***************************************************************        ACLC
100   SIGN = -1.                                                      ACLC
      RN=(A**2+B**2+YO**2-2.*YO*B)/(2.*(B-YO))                        ACLC
      IF(X2.LE.A) GO TO 111                                           ACLC
      SIGN= 1                                                         ACLC
      WRITE(6,505)                                                    ACLC
505   FORMAT(1HO,129HCONDITION X2 GT X1 AND X1 LT A NOT SOLVED BY THIS ACLC
     1 PROGRAM.  EITHER THERE IS NO SOLUTION OR A BETTER GUESS FOR R  ACLC
     1 IS REQUIRED.)                                                  ACLC
***************************************************************        ACLC
*     USE MUELLERS METHOD TO COMPUTE FINAL UPPER BOUND ON X        *   ACLC
*     WHICH IS THE CONDITION THAT L3 = 0. (MUELLER ROUTINE         *   ACLC
*     CALLS SUBROUTINE G)                                          *   ACLC
***************************************************************        ACLC
111   CALL RTMI(R1,LN,G,RNM1,RN,1C.CE-6,2000,IER)                    ACLC
      IF(IER.EQ.0) GO TO 201                                          ACLC
      WRITE(6,111)IER                                                 ACLC
      GO TO 4                                                         ACLC
201   RN=R1                                                           ACLC
      GO TO 3                                                         ACLC
      END                                                             ACLC
                                                                      ACLC
      FUNCTION F(R1)                                                  ACLC
                                                                      ACLC
      COMMON/CCM/PCPJ,YC,L,A,B,TH1,TH2,X1,X2,Y1,Y2,PSI,SIGN,T,L4     ACLC
      REAL L,L4                                                       ACLC
      DATA PI/3.1415927/                                             ACLC
***************************************************************        ACLC
*     IF R(K) IS SUCH THAT L-L4K WILL BE COMPLEX, THE VALUE        *   ACLC
*     OF F = L3AR -L IS SET TO 10**15                              *   ACLC
***************************************************************        ACLC
```

```
         R2=PI/(1.0-PCPJ)                                              ACLS
         A1=-Y0**2-2.0*R2*Y0                                           ACLS
         IF(A1.LT. -10.**(-4)) GO TO 45                                ACLS
         IF(A1.LT.0.) A1=0                                             ACLS
         X2=SQRT(A1)                                                   ACLS
         Y2=R2+Y0                                                      ACLS
         TH2=ATAN(X2/Y2)                                               ACLS
         IF(Y2.EQ.0.0) TH2=PI/2.                                       ACLS
         IF(TH2.LT.0.) TH2=TH2+PI                                      ACLS
         L4=(PI*(P-Y0))/2.0+TH2*R2+ABS(A-X2)                           ACLS
9        A2=-(Y0+R1-B)**2+R1**2                                        ACLS
         IF(A2.LT.-10.**(-4)) GO TO 50                                 ACLS
         IF(A2.LT.0) A2=0.                                             ACLS
         IF(A2.LT.0.0) GO TO 50                                        ACLS
         X1=A+SIGN*SQRT(A2)                                            ACLS
         Y1=R1+Y0                                                      ACLS
         T=(B-Y1)/(A-X1)                                               ACLS
         PSI=ATAN(T)                                                   ACLS
10       IF(A-X1.GE.0.) GO TO 10                                       ACLS
         TH1=PI/2.+PSI                                                 ACLS
         F=TH1*R1+TH2*R2+ABS(X1-X2)-L                                  ACLS
*****************************************************************       ACLS
*        IF VALUE OF VARIABLES ON EACH ITERATION IS DESIRED, REMOVE  *  ACLS
*        C ON FOLLOWING WRITE STATEMENT.                             *  ACLS
*****************************************************************       ACLS
         WRITE(6,51)R1,TH1,X1,A,X2,L4,F                                ACLS
51       FORMAT(15H FUNCTION F R1,F3.4,5X,3HTH1,F8.4,5X,2HX1,F8.4,5X,   ACLS
        1 1HA,F8.4,5X,2HX2,F8.4,5X,2HL4,F8.4,5X,1HF,F3.4)              ACL
         RETURN                                                        ACLS
45       F=10.0**15                                                    ACLS
         WRITE(6,103)                                                  ACLS
103      FORMAT(1H0,12HCOMPLEX IN F )                                  ACLS
         RETURN                                                        ACLS
50       F=10.0**15                                                    ACLS
         WRITE(6,103)                                                  ACLS
         RETURN                                                        ACLS
         END                                                           ACLS
         SUBROUTINE RTMI(X,F,FCT,XLI,XRI,EPS,IEND,IER)                 ACLS
*        PREPARE ITERATION                                             ACLS
         IER=0                                                         ACLS
         XL=XLI                                                        ACLS
         XR=XRI                                                        ACL
         X=XL                                                          ACL
         TOL=X                                                         ACL
         F=FCT(TOL)                                                    ACL
         IF(F)1,16,1                                                   ACL
1        FL=F                                                          ACL
         X=XR                                                          ACL
         TOL=X                                                         ACL
         F=FCT(TOL)                                                    ACL
         IF(F)2,16,2                                                   ACL
2        FR=F                                                          ACL
         IF (SIGN(1.,FL)+SIGN(1.,FR))25,3,25                           ACL
*        BASIC ASSUMPTION FL*FR LESS THAN 0 IS SATISFIED.              ACL
*        GENERATE TOLERANCE FOR FUNCTION VALUES.                       ACL
```

```
3         I=0                                                          ACLS
          TCLF=100.*EPS                                                ACLS
*         START ITERATION LOOP                                         ACLS
4         I=I+1                                                        ACLS
*         START BISECTION LOOP                                         ACLS
          DO 13 K=1,IEND                                               ACLS
           X=.5*(XL+XR)                                                ACLS
          TOL=X                                                       IACLS
          F=FCT(TOL)                                                   ACLS
          IF(F) 5,16,5                                                 ACLS
5         IF (SIGN(1.,F)+SIGN(1.,FR))7,6,7                             ACLS
*         INTERCHANGE XL AND XR IN ORDER TO GET THE SAME SIGN IN F AND FR  ACLS
6         TOL=X                                                        ACLS
          XL=XR                                                        ACLS
          XR=TOL                                                       ACLS
          TOL=FL                                                       ACLS
          FL=FR                                                        ACLS
          FR=TOL                                                       ACLS
7         TCL=F-FL                                                     ACLS
          A=F*TOL                                                      ACLS
          A=A+A                                                        ACLS
          IF (A-FR*(FR-FL))8,9,9                                       ACLS
8         IF (I-IEND)17,17,9                                           ACLS
9         XR=X                                                         ACLS
          FR=F                                                         ACLS
*         TEST ON  SATISFACTORY ACCURACY IN BISECTION LOOP             ACLS
          TOL=EPS                                                      ACL
          A=ABS(XR)                                                    A
          IF (A-1.)11,11,10                                            ACL
10        TOL=TOL*A                                                    ACLS
11        IF (ABS(XR-XL)-TOL)12,12,13                                  ACLS
12        IF (ABS(FR-FL)-TOLF)14,14,13                                 ACLS
13        CONTINUE                                                     ACLS
* END OF BISECTION LOOP                                                ACLS
* ERROR RETURN                                                         ACLS
          IER=1                                                        ACLS
14        IF (ABS(FR)-ABS(FL))16,15,15                                 ACLS
15        X=XL                                                         ACLS
          F=FL                                                         ACLS
16        RETURN                                                       ACLS
*         COMPLIANCE OF IERATED X-VALUE BY INVERSE PARABOLIC INTERPOLATIONACLS
17        A=FR-F                                                       ACLS
          DX=(X-XL)*FL*(1.+F*(A-TOL)/(A*(FR-FL)))/TCL                  ACLS
          XP=X                                                         ACLS
          FP=F                                                         ACLS
          X=XL-DX                                                      ACLS
          TOL=X                                                        ACLS
          F=FCT(TOL)                                                   ACLS
          IF (F)16,16,13                                               ACLS
*         TEST ON SATISFACORY ACCURACY  IN ITERATION LOOP              ACLS
18        TOL=EPS                                                      ACLS
          A=ABS(X)                                                     ACLS
          IF (A-1.)20,20,19                                            ACLS
19        TOL=TOL*A                                                    ACLS
20        IF(ABS(DX)-TOL)21,21,22                                      ACLS
```

```
21         IF(ABS(F)-TOLF)16,10,22                          ACLS
*          PREPARATION OF NEXT BISECTION LOOP               ACLS
                                                            ACLS
22         IF (SIGN(1.,F)+SIGN(1.,FL))24,23,24              ACLS
23         XR=X                                             ACLS
           FR=F                                             ACLS
           GO TO 4                                          ACLS
24         XL=X                                             ACLS
           FL=F                                             ACLS
           XR=XP                                            ACLS
           FR=FP                                            ACLS
           GO TO 4                                          ACLS
*          END OF ITERATION LOOP                            ACLS
                                                            ACLS
*          ERROR RETURN IN CASE OF WRONG INPUT DATA         ACLS
25         IER = 2                                          ACLS
           RETURN                                           ACLS
           END                                              ACLS
```

Appendix II - Calculation of Flow Velocity Exiting the Cushion
Perimeter

Using the assumption of continuity of the flow from the cushion to
the outside, the ground jet velocity may be found from Bernoulli's
Equation.

$$V_c^2/2 + P_{c1}/\rho = V^2/2 + P/\rho$$

By allowing the cushion pressure, P_c, to be equal to the gage
pressure, $P_{c1}-P$, where P is the atmospheric pressure, and also
assuming the velocity within the air cushion, V_c, to be zero, the
flow velocity is given by

$$V = S \ d \ \sqrt{(2 \ P_c)/\rho}$$

Conversions: 1 slug = 1 lbf s^2/ft

1 lbf = (1 lbm)(32.2 ft/s^2)

1 Hp = 550 ft lbf/s

ACRV Braking and Landing
Final Report
Spring Semester 1990

Group Davis

Group Members

Tim Pickenhiem   Chris Davis

Amy Delessio   Brian Hartman

Russ Morris   Jeff Palmer

Aerospace 401B

April 30, 1990

ABSTRACT

A conceptual design of the braking and landing system for the Assured Crew Return Vehicle (ACRV) has been completed. In accordance with the requirements specified in the System Performance Requirements Document (SPRD), the main goal stressed in the design of a braking and landing system for the ACRV was to create a safe, reliable, and expedient method for returning crew members of the Space Station Freedom to Earth in the event of the National Space Transportation System (The Space Shuttle) unavailability. In order to approach the design of the ACRV braking and landing system in a systematic manner, the landing sequence was broken into three main segments, de-orbit, upper atmospheric braking, and lower atmospheric braking. Before studying the three separate segments of braking and landing, a body with an L/D of 1.0 and a ballistic parameter of between 55 and 75 lbf/ft^2 was chosen for the shape of the re-entry vehicle. By analyzing the equations of motion for the vehicle, and optimizing the method of moving from Space Station orbit to 400,000 ft (with a flight path angle of -4°), a value for the optimum ΔV and corresponding mass of propellant was determined. With these initial conditions for flight at 400,000 ft, an approximate velocity was generated for the vehicle. During this phase of flight, maximum heating will also occur, and these effects were found to occur at roughly 200,000 ft which is also the point of maximum g's. This analysis has also led to the criteria for heat shield materials needed on the lower surface of the craft. The final phase of flight will be with the use of parachutes. Due to the fact that the lifting body effects slow the vehicle down to approximately mach 0.4 by 30,000 ft, supersonic parachutes are not needed. Instead, two conical ribbon drogue parachutes are deployed first (at an altitude of approximately 30,000 ft). These in turn, help to deploy the pilot chutes for the three main canopies which will allow the ACRV to land in the water at approximately 25 ft/sec.

TABLE OF CONTENTS

INTRODUCTION

The Assured Crew Return Vehicle (ACRV) for the Space Station Freedom must provide a reliable, safe, and expedient rescue in the event of an emergency. One important aspect of the performance of the ACRV will be its ability to brake and land safely and proficiently. The main objective is the design of a reliable and safe re-entry vehicle which employs a braking and landing system that minimizes g-forces and thermodynamic heating while maximizing internal volume.

Important factors in the design of spacecraft subsystems are geometry, stability, and reusability. The vehicle structure should be simple, able to move through the atmosphere on a stable trajectory, and provide adequate heat protection.

Up to this point, various conventional re-entry shapes have been considered, as well as some new concepts. Each of these new ideas was briefly studied, but rejected because their shape was not stable or had excessive heating problems. Previous concepts for re-entry vehicles which range from ballistic types (L/D≈0) to glider types (L/D≈1.5) were also considered. Ballistic types offer reduced heating problems but have limited or no maneuverability. Glider types offer maneuverability but have excessive heating problems[1].

A lifting body, with an L/D of 1.0, which is a compromise between these two general concepts (ballistic and glider types), was decided upon. It will offer both maneuverability and reduced heating problems through its lifting body effects and aerodynamic shape. The lifting body concept would aide in the braking of the ACRV through the atmosphere, due to its lift-producing abilities. Previous lifting bodies (M1,M2) also have a good volumetric efficiency as well as reduced g-loads and heating problems[2].

The research was divided into three main sections: de-orbit from the space station to the upper atmosphere, braking through lifting body effects, and final braking through parachute drag devices. The initial de-orbit phase extends from the space station to the upper limit of the atmosphere. For this phase, the trajectory the ACRV follows was defined.

---

[1] McShera, John T., Jr., and Lowery, Jerry L., "Static Stability and Longitudinal Control Characteristics of a Lenticular-Shaped Re-entry Vehicles at Mach Numbers of 3.5 and 4.65," NASA TMX-763, March 1963.

[2] Cerimele, Chris, "Aero Trades," Johnson Space Center, Advanced Programs Office, September, 1986.

The final conditions of this trajectory, at the upper limit of the atmosphere, were used as the initial conditions to compute velocity profiles for the re-entry phase. Several guidance and control systems used for this phase were also investigated. The final braking phase involved the investigation of several types of parachutes and many of their characteristics, such as size, deployment velocity, coefficient of drag, stability and material. Heating effects on possible heat shield materials were also studied in order to aid in the design of an efficient thermal protection system.

RE-ENTRY TRAJECTORY DETERMINATION

The de-orbit phase of the ACRV re-entry consists of the region between the Space Station altitude and the approximate edge of the atmosphere (400,000 ft.). Important considerations in this phase of flight include: mass of propellent for velocity changes, final velocity at the point of entry into the atmosphere, and flight path angle for entry into the atmosphere. The amount of velocity change and therefore propellant mass is governed by target conditions at the edge of the atmosphere.

In order to fully define this phase of the vehicle entry, an analysis of two different methods of de-orbit was conducted with the following initial and target conditions:

Initial conditions: Space Station has a circular orbit at approximately 225 n.mi. altitude

Entry conditions: At 400,000 ft., the ACRV should reach a target flight path angle between -1 and -5 degrees, with a velocity no greater than 26,000 ft./s

Based on values for the M1 and M2 re-entry vehicles, it has been approximated that the shape of the ACRV will have a ballistic coefficient defined as:

$$\frac{W}{C_dA} = 50 \rightarrow 75 \left(\frac{lbm}{ft^2}\right)$$

It will have a lift to drag ratio of approximately 1.0. Under these two design parameters the initial trajectory will have a flight path angle, γ, of -4 degrees at 400,000 ft in order to keep maximum deceleration less than 4 g's[3].

The first de-orbit method considered included two velocity changes, one at the Space Station to alter the vehicle's speed, and one at the edge of the atmosphere. The second method involved only one change in velocity at the Space Station's altitude.

The complete analysis in contained in Appendix A and the following is a summary of the results.

An estimate of the required velocity change at space station altitude that would achieve the desired flight path angle (γ) at 400,000 ft shows that the spacecraft must enter the trajectory from the space station at 7.3646 km/sec. This gives a velocity change at burn of 0.2944 km/sec from space station speed of 7.659 km/sec (at 225 n.mi.). This velocity change will be executed parallel to the space station flight path ($\beta = 0°$). The percentage of total mass of the ship required for propellant (assuming $I_{sp} = 300$ sec) would be 9.5% for the single burn.

This trajectory will set up acceptable re-entry variables to keep deceleration below the maximum limit. However, the arc the ACRV will cover from 225 n.mi. to 65.79 n.mi. (400,000 ft) is 63.55° ($\emptyset_1$, Figure A1). The time of flight for this trajectory is approximately 16.5 minutes. This is due to the low eccentricity of the flight path. Total downrange distance covered from the space station to touchdown is 80° ($\emptyset_2$, Figure A1). This is approximately 5333 miles downrange distance.

The downrange distance can be shortened by making the first part of the trajectory steeper in one of two ways. The first method would be to make two burns. One burn at the space station's altitude that changes the velocity and another at 400,000 ft that changes the flight path angle to the one desired. The second method involves one burn. This burn would change the velocity and flight path angle of the ACRV at space station altitude in order to achieve the desired flight path angle at 400,000 ft.

Figures A.3 to A.6 show the results of a computer analysis for each of the two methods. The first two graphs show the trade off between the propellant part of the total mass and time of flight. As seen from these

---

[3]Cerimele, Chris, "Aero Trades," Johnson Space Center, Advanced Programs Office, September, 1986.

two graphs, the two burn method (marked corr.) consistently requires more propellant than the one burn method (marked Angle), leading to a conclusion that the one burn method would be the best way to reduce the time of flight.

The second two graphs show the trade off between entry velocity at 400,000 ft and time of flight for each of these two methods. As shown by these graphs, the two burn method is the best at reducing the re-entry speed at 400,000 ft.

UPPER ATMOSPHERIC BRAKING

The second phase of entry consists of the region from the beginning of the atmosphere (approximately 400,000 ft.) to the point at which some sort of auxiliary braking device such as drogue chutes or supersonic parachutes could be deployed. This region of the re-entry trajectory is of extreme importance due to the fact that maximum deceleration loads, heating rates and stagnation heating temperatures are most likely to occur here as the vehicle is falling into the regions of higher density in the atmosphere.

Aerodynamic braking was chosen as the means by which the ACRV could be designed to decelerate within this region of the atmosphere. The amount of aerodynamic braking achieved by a vehicle is dependent upon the lift forces, drag forces, and the ballistic parameter of the vehicle (W/C_DA). All these parameters are, in turn, dependent on the vehicle shape.

Various conventional re-entry vehicle configurations were considered for the ACRV, ranging from ballistic types $(L/D \approx 0)$ to glider types $(L/D \approx 1.5)$. The ballistic configurations in general were found to offer very limited maneuverability and also experience rather large deceleration forces during re-entry. Glider types, on the other hand, offer a large range of maneuverability and lower g-loads than the ballistic types; however, heating problems are more severe for these types of vehicles.

Some other, non-conventional configurations were also considered for the shape of the ACRV during the "brainstorming" process. One of the first designs considered was a ballistic type in the shape of a funnel. A hole in the center of the vehicle would allow air to pass through the center as well as around the outside of the vehicle. The advantage of such a design lies in the net drag force created by exposing a large surface area to the freestream direction thus braking the vehicle during descent. Unfortunately, the increased surface area would also present insurmountable design problems in the area of aerodynamic heating, since both inside and outside surfaces of the funnel would be subject to large amounts of heating. Consequently, the design was not considered any further.

The other non-conventional configuration considered was a wedge-shaped gliding vehicle know as a wave rider. The property which makes the wave rider a desirable shape for a re-entry vehicle is its ability to produce a large lift force at hypersonic speeds. A large lift force is

5

beneficial in two ways. First of all, the lift force aids in the deceleration of the body as it falls to the Earth since the force acts in the upward direction. Secondly, the lift force allows the body to follow a shallow trajectory, thus reducing the g-forces experienced by the crew. Stagnation heating proved to be one crucial design problem with the wave rider. The large number of sharp edges required to produce such high lift would result in very large stagnation temperatures. The second and most serious problem with the wave rider design was that along with the maneuverability and excellent flight characteristics of the vehicle shape would come the need for an experienced, healthy crew member to fly the vehicle. For this particular mission, the ACRV must be operated by a deconditioned crew as specified in the SPRD.

Instead of concentrating on one of these particular designs, the shape chosen for the ACRV was that of a semi-lifting body, a compromise between the characteristics of gliding and ballistic vehicle shapes. It was chosen in an attempt to combine the best characteristics of the two extreme cases.

Aerodynamic Parameters

Throughout the first stages of the design process, emphasis was placed on determining the shape of the ACRV and then attempting to justify that shape by determining the L/D and ballistic coefficient of that shape. Anderson[4] has shown that the aerodynamic performance of a re-entry vehicle depends mainly on these two parameters. This approach was later abandoned due to the difficulty of determining these parameters based solely on the vehicle's shape. Instead, the shape of the ACRV was chosen to represent a vehicle with aerodynamic characteristics lying between those of the M1 and M2 lifting body designs previously developed by NASA.

A three-view drawing of the vehicle is shown in Appendix E with the estimated vehicle dimensions. Based on these dimensions, a total vehicle volume of 1,480 ft^3 has been calculated along with a vehicle weight in the range of 12,000 - 15,000 pounds.

---

[4]Anderson, John D., Hypersonic and High Temperature Gas Dynamics, McGraw-Hill Book Company, New York, 1989.

An L/D of approximately 1.0 was chosen $_\wedge^{in}$ an effort to provide sufficient inherent braking force through the upper regions of the atmosphere without exceeding the maximum g-loads specified by the SPRD.

The ballistic parameter of the ACRV was chosen to lie in the range of 55 - 75 lb/ft^2. These values were chosen based on values for the M1 and M2 lifting bodies. Instead of designing the exact ballistic parameter for the vehicle, an analysis was carried out for a range of ballistic parameters as discussed in the next section.

Lifting Body Analysis

In order to fully define the behavior of a re-entry vehicle with given aerodynamic properties, the equations of motion of a typical re-entry configuration had to be derived and solved numerically. The complete derivation of the equations of motion for a lifting re-entry vehicle are shown in Appendix B. Segments of the derivation are taken from both Anderson[5] and Regan[6] with the main equations based on the derivation given by Anderson.

The derivation was carried out for a simple gliding re-entry vehicle such as the one shown in the force diagram shown below.
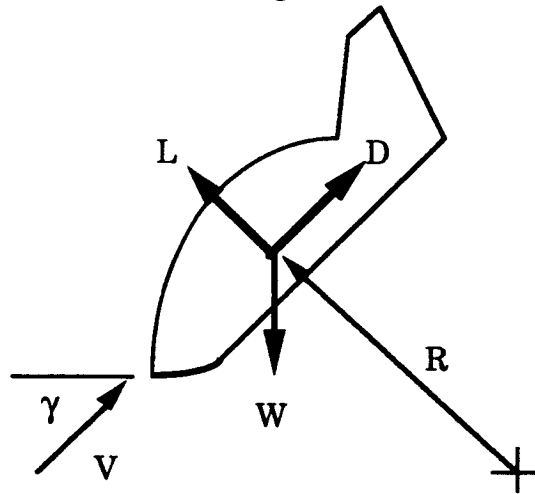
Figure 1: Force Diagram for Re-entry Vehicle

Assuming the vehicle has no propulsive force, Newton's second law may be applied in directions both perpendicular and parallel to the flight path of the vehicle. Summing forces in these two directions gives the following two basic equations of motion which are found in Anderson[7]:

$$L - W \cos \gamma = -\frac{m v^2}{R} \qquad (1)$$

$$W \sin \gamma - D = m \frac{dv}{dt} \qquad (2)$$

[5]Anderson, John D., Hypersonic and High Temperature Gas Dynamics, McGraw-Hill Book Company, New York, 1989.

[6]Regan, Frank J., Re-entry Vehicle Dynamics, American Institute of Aeronautics and Astronautics, Inc., New York, 1984.

[7]Anderson, John D., Hypersonic and High Temperature Gas Dynamics, McGraw-Hill Book Company, New York, 1989.

Equation (1) is found by summing forces perpendicular to the flight path of the vehicle and setting the resultant force equal to the centripetal acceleration which results from the curvature of the vehicle's flight path. Equation (2) is found by summing forces along the flight path of the vehicle and setting the resultant equal to the mass of the vehicle times the transverse acceleration experienced during re-entry.

Equations (1) and (2) may be rewritten in terms of the vehicle lift-to-drag ratio (L/D) and Ballistic parameter. These two quantities, along with the velocity during re-entry are relevant to the analysis of the ACRV design. The previous analysis of the first phase of the re-entry has designated a range of flight path angles and initial entry velocities for the atmospheric portion of the re-entry analysis. Appendix B shows the method by which equations (1) and (2) were manipulated in order to solve for the velocity of the re-entry vehicle as a function of altitude, utilizing the initial conditions at the edge of the atmosphere, the ballistic parameter, and the lift to drag ratio of the vehicle.

In order to accurately design for the third phase of re-entry, the velocity and Mach number of the vehicle were needed at various altitudes. With a range of initial conditions, and a range of aerodynamic parameters, a range of altitudes for deployment of an auxiliary braking device could be determined.

The equations of motion developed in Appendix B were integrated using a fourth-order Runge-Kutta algorithm. The result is a velocity altitude map as shown in figure 2 on the next page. All curves were calculated for an L/D of one.
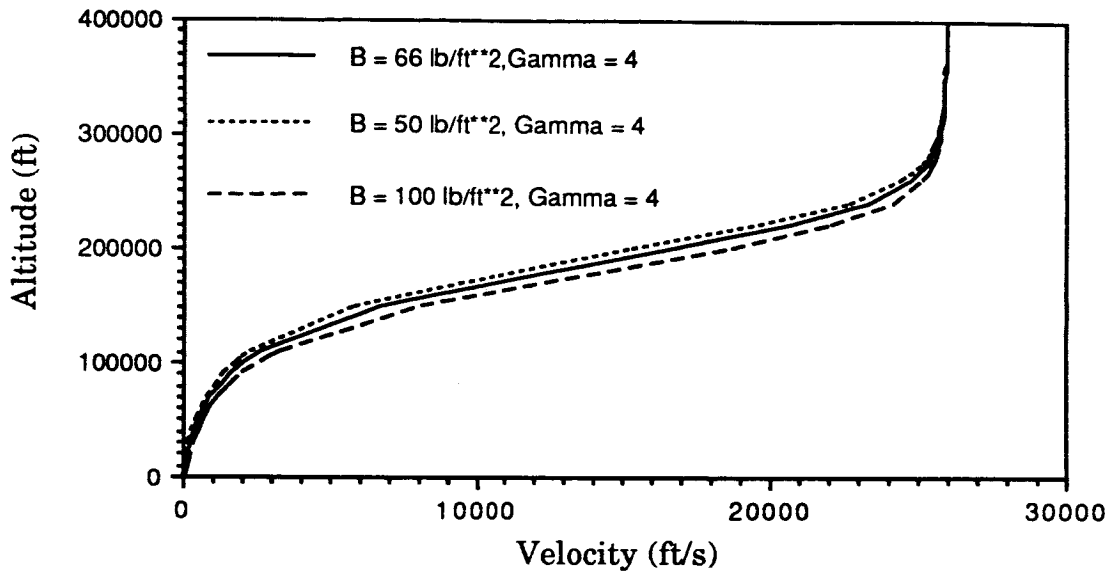
Figure 2: Velocity Altitude Map

The velocity altitude maps generated from the vehicle's equations of motion show that atmospheric effects are nearly negligible around 400,000 feet. There is nearly zero deceleration for the first 100,000 feet, but as the vehicle falls deeper into the denser regions of the atmosphere, atmospheric effects begin to become dominant. The plot shows that the maximum deceleration occurs between 250,000 and 150,000 feet. The ballistic parameters chosen for the velocity altitude map were chosen to give a range of curves based on values given for the M1 and M2 lifting bodies designed by NASA.

The basis of the analysis of the lifting body braking was to determine the effectiveness of the lifting body design in decelerating the vehicle. The choice of the braking system for the lower atmosphere hinged on the conditions at the end of the second phase of entry. Different choices for braking systems depend on whether or not the flow is supersonic or subsonic.

Specific results for the lifting body analysis are summarized in Table 3 on the next page.

Table 3: M=1.0 as a Function of Ballistic Coefficient

Ballistic Coefficient (lb/ft^2)	Altitude where Mach Number = 1.0 (ft)
55	70,000
75	65,000
100	50,000

No provisions were made in the derivation for any type of control systems during the re-entry. During the actual re-entry process, some type of control system (such as those discussed in the next section) would be used to control the attitude of the vehicle during re-entry. These equations are meant to serve as a guide in determining the altitude at which a secondary braking system could be deployed, depending on the type of system chosen for use in the design.

Control Systems

During the second phase of re-entry, where the vehicle's aerodynamic characteristics are very important, stability and control must be maintained before the final phase, where another braking system (parachutes) will be used to land the vehicle. The vehicle must be both statically and dynamically stable during re-entry.

Once the vehicle has reached the sensible atmosphere (H = 400,000 ft.) a guidance system must be used to maintain the trajectory within certain boundaries. If the velocity is to high at a high altitude, the vehicle will skip out of the atmosphere. In fact, there is only a specific range of velocities at which the ACRV must travel, in order to successfully enter the atmosphere[8]. In addition to these boundaries, there are heating and acceleration limits that the vehicle could exceed if it enters the atmosphere too steeply[9]. Various guidance methods that will regulate the aerodynamic

---

[8]Wingrove, Rodney C., "Atmosphere Entry Guidance and Control," Control, Guidance and Navigation of Spacecraft, NASA SP-17, December, 1962.
    [9]Ibid.

11

forces so that the ACRV's trajectory will not exceed these operating boundaries can be used and are discussed below.

Two categories of guidance systems are 1) guidance predicted capabilities and 2) guidance using a nominal trajectory. The second category requires that the state variables (i.e., vertical velocity, circumferential velocity, altitude, and downrange distance) of the most desirable nominal path be precomputed and stored on board[10]. Since the ACRV must be able to leave the Space Station at any time, it would be impossible to predict on which trajectory it will be re-entering the atmosphere. Therefore, the variables of this trajectory could not be precomputed and stored on board. For this reason, this guidance system would not be useful in controlling the ACRV's re-entry and is not further considered.

The first category of guidance systems mentioned above, guidance using predicted capabilities, does not require a stored nominal trajectory since it is capable of predicting possible future trajectories. Using this method, the vehicle will have the choice of several paths to follow, within its maneuvering capability, so that it reaches the desired or satisfactory destination without exceeding the heating and acceleration limits. A preferred destination is either the Pacific or Atlantic Ocean, so as to minimize recovery time. Landing in the Gulf of Mexico is not preferred due to its proximity to Cuba and the presence of oil platforms. As the ACRV is re-entering, and the trajectories are being predicted, the one that would reach a preferred destination would be chosen and followed.

Two types of methods that can be used for this guidance system using predicted capabilities are 1) "fast time" solution and 2) approximate "closed-form" solution of the equations of motion. The disadvantage of this second method, the "closed-form" solution, is that it is limited to the use of only a certain desired trajectory profile since all state variables are not taken into account in the solution of the possible trajectories. Since the ACRV's guidance system must have the capability of predicting all possible trajectories since it could essentially be entering the Earth's atmosphere on

---

[10]Wingrove, Rodney C., "Atmosphere Entry Guidance and Control," Control, Guidance and Navigation of Spacecraft, NASA SP-17, December, 1962.

12

any trajectory after it leaves the Space Station, this closed form method, with its limited capabilities, is not further considered.

The first method, fast time solution, offers the flexibility of predicting all possible trajectories and the ability to predict range, deceleration, heating, etc. It has also been studied for automatic control. Automatic control will be necessary for the ACRV, in case all crew members are injured and unable to the pilot the system. For the fast time prediction method, the differential equations of motion are solved by integration on the on board computer and possible future trajectories are predicted. The information needed to make these predictions is:

1.   Four measured state variables (i.e., vertical and circumferential components of   the velocity, altitude, and downrange distance)

2.   Two vehicle parameters (i.e., lift to drag ratio (L/D), ballistic coefficient $(W/C_L S)$).

The solution of the differential equations with the above information can predict future values of the state variables along the trajectory. In addition, constraints such as heating loads, acceleration loads, maximum skip altitudes and vehicle range capability can be incorporated into the solution so that the ACRV can follow a near optimum trajectory[11].

For automatic control, iteration is used to determine a desired trajectory. If a desired destination is not achieved in the first computation of the solution of the equations of motion, the computations are repeated until a trajectory is found that will reach the destination. Considerations of this iterative process may also include constraints on heating and acceleration[12].

This fast time prediction method is advantageous, as compared to the others methods previously mentioned, because of its ability to account for all possible flight conditions and also calculate range, deceleration, and heating values[13]. The main disadvantage of this system, however, is that the predictions must be made every few seconds for a vehicle that has rapidly changing trajectory conditions. The on board computer must   be

[11]Wingrove, Rodney C., "Atmosphere Entry Guidance and Control," Control, Guidance and Navigation of Spacecraft, NASA SP-17, December, 1962.

[12]Ibid.

[13]Ibid.

able to rapidly solve the equations of motion for this method to provide 'fast time' predictions.

AERODYNAMIC HEATING

The successful return of the ACRV through the Earth's atmosphere depends largely on its ability to withstand the aerodynamic heat transfer to the structure of the vehicle. Excessive local heating of the entry vehicle is a serious problem that must be anticipated and accounted for in the design of the thermal protection. The ACRV will experience the greatest temperatures as it re-enters the Earth's atmosphere due to the ions in the upper atmosphere. For this reason, the ACRV should be designed so that a minimum amount of surface area will be exposed during re-entry. A blunt body (lifting body shape) fulfills this requirement, as compared to a sharp nosed vehicle.

Since the lower surface of the ACRV will be subject to the most heating effects, it will require the most thermal protection. Unlike previous re-entry vehicles (Gemini\Apollo), which were designed to complete only a single mission, the ACRV's thermal protection system will be designed for extended duration in space and perhaps multiple re-entries. The only vehicle currently using a multiple re-entry thermal protection system is the Space Shuttle.

An effective thermal protection system is essential for a successful ACRV mission for three important reasons:

- •Protection of vehicle
- • Capability of several re-entries
- •Protection of crew and internal equipment

The materials used for thermal protection depend on estimates of the heating expected during re-entry maneuvers. An analysis of heating effects for the ACRV is necessary to find applicable materials.

During atmospheric entry, the magnitude of the aerodynamic heating depends upon the precise chemical composition of the upper atmosphere, the vehicle's velocity, and viscous shock wave structure around the vehicle. The development of a computational method to simulate the entire viscous shock layer structure requires prediction of the shape of the embedded shock waves, as well as the bow shock wave around the vehicle. This requires a complex computational scheme ~~involving~~ involving

14

extensive research, experimentation, and theoretical solutions. A simple mathematical model has been developed to evaluate the heating characteristics of different material properties. The model uses an over-all heat balance to simulate a thermal protection material[14]. The model considers both radiant and aerodynamic heating, radiant cooling and heat storage.

The aerodynamic heating experienced by the vehicle is due to the kinetic energy of the vehicle being exchanged for the thermal energy. Radiant heating is a function of the vehicle's distance from heat sources and the view factor from the vehicle to Earth. The primary sources of heat upon the vehicle is from the Sun and the Earth. The rate at which a body radiates thermal energy (radiant cooling) is found by the Stefan-Boltzmann law. The stored heat gives the temperature response of a material to a given heat input. These are all combined in a computer program to form a one-dimensional heat balance equation that is numerically integrated along with trajectory equations of motion to determine the heating and temperature response of a material as a function of time (see Appendix C). Figures 2C to 14C show the results of a computer analysis for a multi-layered material used for thermal protection during re-entry. Figure 2C is the resultant trajectory and inertial g-force loading for a constant flight path angle throughout the re-entry process. As seen from this graph, the g force's increase dramatically between the altitudes of 150,000 and 250,000 feet. Figure 3C shows the results of limiting inertial g-forces experienced by the vehicle by adjusting flight path angle as shown in Figure 4C. This figure also shows the velocity of the vehicle as a function of time. The heating rate experienced by the vehicle is given by figure 5C. As shown by the graph , the heating rate is the greatest at the same time g-forces are greatest, leading to a conclusion that this is the most critical part of the entire re-entry process. Figures 6C through 13C show the heating aspects of a multi-layered material. Figure 6C serves as a basis for heating analysis. Figures 7C and 8C show the results of changing mass

---

[14]Bursey, C.H. Jr., et al., "A Study of the Thermal Kill of Variable Organisms During Mars Atmospheric Entry," Thermal Design Principals of Spacecraft and Entry Bodies: Progress in Astronautics and Aeronautics, Vol. 21, Academic Press, New York, 1969.

15

or specific heat of the material. Figures 9C through 11C show the effects that thermal conductivity has on heating temperatures throughout the layers of the material used for thermal protection. Figure 12C shows the effect of reducing the mass of the outer layer of material while keeping the other layers mass constant. Figure 13C shows the effect of reducing the mass of the layers of material other than the outer layer. Figure 14C shows the effect that emissivity has on the temperature experienced by the outer layer of material of the heat shield.

The results of this analysis has led to several conclusions. The greatest influence on the heating through the layers of the heat shield is the mass (or specific heat). A inadequate amount of mass or specific heat causes the high temperatures of re-entry to reach the interior of the vehicle. The next important aspect of re-entry materials is in the emissivity. As seen from the graph, a low emissivity causes exterior heating temperature to rise significantly. Therefore, a heat shield used for a re-entry vehicle should have the following qualities.

a) High Mass and/or high specific heat
b) High Emissivity
c) Low thermal conductivity

LOWER ATMOSPHERIC BRAKING

The proposed ACRV design will not possess any type of controlled gliding or powered flight capabilities due to the complexity of such systems and the requirement of being operated by a conditioned crew. Because of this, the ACRV will require an external braking system to further slow the vehicle after re-entry. This braking system will be employed once the ACRV reaches a Mach number of approximately 1.5. We feel a parachute system can be used to effectively slow the vehicle down to acceptable landing speeds. The parachute system will be detailed in this section.

In choosing a parachute system, the drag characteristics (C_D), wake stability, and reliability of the chutes are of chief concern. Weight, stowability, size, deployment velocity, and materials must also be considered. Various types of parachutes and deployment techniques have been investigated. In general, the design consists of first deploying two conical ribbon drogue parachutes at supersonic speed. This will be followed by a cluster of three triconical canopy parachutes, which will carry the vehicle to landing. In developing this parachute design, we investigated various supersonic and subsonic parachute types and configurations. Before detailing the proposed braking scheme, the different ideas we considered are briefly discussed.

The initial concern in braking the ACRV was to provide an adequate supersonic braking ability. Many tests have been done on supersonic parachutes, however, they have not been used in practice on any modern re-entry vehicle. Most tests were performed on ballistic bodies weighing about 2/3 of the ACRV. There are many types of supersonic parachutes: conical ribbon, hemisflo, hyperflo, and cup/cone to name a few. All have possibilities, but some possess more desirable performance attributes than others. The cup/cone parachute (also called guide surface parachute) is a drag device designed to handle the shocks generated by the shroud lines and parachute by "swallowing" them (see Figure D1). Its design keeps the shock attached to the chute. This allows the flow to pass through the chute, as opposed to going around it due to a detached bow shock. These parachutes were tested and found to be stable at speeds up to Mach 3.0. Unfortunately, deployment problems, due to the complexity of the chutes design, are a drawback. Also, the cup/cone parachute only performs well

over a limited range of Mach numbers (M=1.5 to about M=3.0). These disadvantages were too significant in our opinion, thus this configuration was eliminated from the list of acceptable choices.

Hyperflo parachutes are similar in design to the cone part of the cup/cone parachutes with the addition of rear cross skirting (see Figure D2). These parachutes were tested in Mach ranges from 2.3 to 6.0 and proved stable. However, these tests were conducted behind a symmetrical forebody, and the resulting drag coefficient was on average around 0.3 across the above mentioned Mach range. Although these parachutes are stable in the above test conditions, the current design will not be a symmetric body, and other parachutes provide higher drag coefficients in harsher flow regimes. Additionally, as it approaches Mach numbers below 2.0, it encounters inflation problems.

Hemisflo parachutes are elongated ribbed structures (sometimes called gore parachutes) that are very porous and thus more stable (see Figure D3). These parachutes operate well in supersonic flow regimes above Mach 1.7 but tend to collapse as the Mach number decreases below that level. Also, the drag coefficient seems to drop steadily above Mach 2.0 indicating the optimum operational Mach Number is approximately 1.7-2.0. For the current design, a larger operation envelope is desired, therefore, the hemisflow configuration was also decided against.

Of all the supersonic parachutes considered, the conical ribbon parachute (see Figure D4) provided the widest range of desirable attributes. Figure D5 compares the C_D of conical ribbon, hemisflo, and hyperflo chutes to Mach number. The conical ribbon parachute provides the greatest C_D of all the chutes below M=1.5. It also provides comparable drag above M=1.5, up to about M=3.0. Tests show that if this device is deployed far enough behind the payload, it experiences little or no inflation problems. Also, the drag area (and thus C_D) remained constant over a wider Mach number range than the before mentioned parachutes. Stable performance at and below the sonic condition is very important. The conical ribbon parachute performs well in supersonic flight as well as the initial phase of subsonic flight. These parachutes are very porous, and with slight modifications in porosity near the center of the parachute, any oscillation problems can be controlled. The optimum material for construction of this type of parachute is Kevlar, which is light, flexible, and

very strong. The conical ribbon parachute would require 1-inch-wide Kevlar webbing for the main structure and the suspension lines.

Although the conical ribbon parachute would perform well in the supersonic and very high subsonic regime, it is not used in our parachute system. The natural braking capability of the ACRV due to its lifting characteristics causes the vehicle to slow down well into the subsonic region without any external braking system. Thus, the design does not use any external supersonic braking system. If a supersonic parachute was required on a vehicle such as this, however, a conical ribbon parachute would perform well. Additionally, devices such as wedge fins or tractor rockets might be used to deploy the supersonic parachutes[15].

The first stage of our parachute braking system is a set of two conical ribbon drogue parachutes, each with a 16.5 ft. diameter. These two parachutes are deployed at about 25,000 to 30,000 feet. This corresponds to a speed of approximately 300 to 350 ft/sec. Table 4 shows some calculated velocities as a function of altitude for the ACRV. These were generated using the program mentioned in the Lifting Body Analysis section.

Table 4:   Calculated velocities of the ACRV as a function of altitude.

Altitude (ft)	Velocity (ft/sec)
31,000	383.62
30,000	370.43
29,000	357.53
28,000	344.92
27,000	332.60
26,000	320.55
25,000	308.77
24,000	297.26

---

[15]Peterson, Carl W., et al., "Design and Performance of a Parachute for Supersonic and Subsonic Recovery of an 800-lb Payload," Sandia National Laboratories, Albuquerque, New Mexico, December 1986.

The ACRV will be well into the subsonic regime, so no supersonic parachutes are necessary. The two drogue parachutes slow the ACRV effectively until larger, final descent parachutes are deployed. The primary purpose of the drogue parachutes is to slow the vehicle more quickly and reduce the speed at which the final descent parachutes are deployed. The size of the drogue chutes was chosen based on previous designs[16].

At about 10,000 to 13,000 feet, the second stage of the parachute system is activated. A cluster of three 88 foot diameter triconical canopy parachutes are deployed using a small pilot parachute for each one. The pilot parachutes effectively guide the large canopies into their inflated configuration. The suspension lines for the large canopy parachutes are about 85 feet in length. Appendix D develops these results in detail. Both the drogue parachutes and the final descent canopy parachutes are deployed at appropriate altitudes and dynamic pressures using pressure sensors, such as a mortar deployment system[17]. These large triconical canopy parachutes would slow the vehicle to a landing velocity of 25 ft/sec. This is an acceptable landing speed for the water landing the ACRV will be making.

Overall, the parachute system design can be summarized as follows:

- Two conical ribbon drogue parachutes deployed at about 30,000 ft
- Three 88 ft diameter triconical canopy parachutes for final descent deployed at about 13,000 ft
- Small pilot parachutes used for deploying each of the large canopy parachutes
- 85 ft suspension lines for the large canopy parachutes
- Pressure sensing deployment mechanism to deploy parachutes at proper altitude

This plan should prove to be effective, reliable, and simple.

---

[16]Cerimele, Chris, et al., "A Conceptual Design Study of a Crew Emergency Return Vehicle" Johnson Space Center, Advanced Programs Office, August 1988.
[17]Cerimele, Chris, et al., "A Conceptual Design Study of a Crew Emergency Return Vehicle" Johnson Space Center, Advanced Programs Office, August 1988.

Types of Landing Schemes

All possible landing schemes for the ACRV may be divided into two distinct categories: water or land. There are some key advantages and disadvantages to both types of landing methods. Both of these landing methods as well as the design decision are discussed below.

Land

Returning the ACRV directly to land has some very important advantages. First, in the case of a medical emergency, the crew member(s) could be transported very close to a medical center by the ACRV. This would increase the chance of survival for a seriously injured crew member. The time of the mission would also be shorter compared to a landing made in the water. The major drawback to landing on the land is that a much more complex vehicle is required. A very high degree of control is needed to land successfully. An experienced pilot could be used to land the vehicle, but this would violate the requirement of having a completely unconditioned crew on board. A sophisticated computer controlled automatic pilot could also be implemented. This would add a great deal of complexity to the vehicle. Automatic controls to land the ACRV might not be too difficult, but the vehicle would need to have many control surfaces and capabilities. This would greatly increase the number of failures or problems the ACRV might encounter. Finding a suitable place to land is more difficult on the ground than in the water. Most medical facilities are located in areas with adverse landing conditions. A large open area would be the safest place to land, but it might also be extremely far away from the closest medical facility. This type of problem defeats the original purpose of landing on the ground.

Water

The main advantage of a water landing is that the complexity of the vehicle's design can be reduced. This type of vehicle is more suitable to operation by a deconditioned crew. The amount of control during the final stage of the mission is reduced significantly, so the vehicle's design can be much simpler. The reduction in the complexity of the vehicle leads to a more reliable design. A disadvantage of a water landing is the increased distance from the medical facility. Nearly all water landing sites will be

21

further from a medical facility than ground landing sites. This, in turn, leads to increased transfer time from the vehicle to a medical facility. Also, it may not be desirable to subject the vehicle to a water environment.

Justification for Water Landing

After analyzing both the advantages and disadvantages of both landing schemes, the decision was made to implement a water landing as the final stage in the ACRV's braking and landing system. There is a distinct tradeoff between transfer time from the vehicle to the medical facility and complexity of the design. While a water landing may generate a longer rescue process, it can still be accomplished with an unconditioned crew and a simple, more reliable design. These last two criteria are specified for the ACRV's mission. Many water landing sites are within a reasonable distance from a medical facility. There is also a larger margin for error in landing location for a water landing as well. Additionally, if the ACRV is not involved in a medical emergency mission, then the time taken to rescue the crew is not as critical. The decision to use a water landing was made due to the decreased complexity and increased reliability of the vehicle.

Recovery Considerations

Several recovery aids will be needed to recover the ACRV and its crew. These include a stabilizing floatation device, detection devices (a flashing light, fluorescein dye, and a sarah beacon) and a mobile recovery unit (water and air vehicles). All of these recovery aids have been successful in recovering Apollo and Mercury capsules.

The stabilizing floatation device, inflatable air bags or floatation collar, will keep the ACRV stable while it is in the water. This device could be either implemented into the ACRV and designed to deploy upon impact, or attached to the ACRV by the rescue crew, when they arrive. Although this area was not thoroughly researched, it would be more desirable if the ACRV will be equipped with this device, so that the rescue crew would use less recovery time. Since the ACRV has been determined to be buoyant, this device will not be used to keep the ACRV afloat, rather it will aid in keeping the ACRV from tipping over when it begins to rock in the water.

22

The detection devices will allow the recovery unit to locate the ACRV when it lands and determine its exact position. In the event of a major catastrophe on The Space Station Freedom which seriously injures crew members, the ACRV must be capable of returning to Earth and being recovered at any time, day or night. If the ACRV returns to the Earth at night time, a flashing light would aid in detecting the spacecraft. This would be set to activate upon impact and should be designed to have a lifetime of at least 12 hours. By the time this 12 hour time limit is expired, it will be day time again. The lifetime could be extended, if deemed necessary, since for the Mercury, the flashing light's lifetime was 24 hours[18].

The second detection device that would aid in locating the ACRV is fluorscein dye. This green-colored dye would be ejected at impact and permeate the surrounding water. This dye would help the aerial recovery unit detect the floating ACRV. This dye should be visible for about 6 hours, which is the length of time the Mercury capsules used[19].

The third detection device that should be used is the sarah beacon. This emits radio signals which notifies nearby rescue units of the ACRV's exact location. This device enables helicopters to be dispatched to retrieve the ACRV.

Although the detection devices are very important in locating the ACRV, the success of recovering the ACRV depends on the rescue vehicles. In case the ACRV overshoots its landing target, a highly mobile rescue unit is desirable. This rescue unit will consist of military ships and helicopters. The helicopter will tow the ACRV to the ship, lift the ACRV out of the water and maneuver it onto the ship's deck. This deck must be large and strong enough to support the ACRV.

Depending on the proximity of the ACRV to a rescue ship, it may be more time efficient for the ship to move to the ACRV's landing location. The helicopter will meet the ship at the landing location, attach a cable to the ACRV, pick it up, and transport it to the ship's deck. However, if the ship is not in close proximity of the ACRV, it would take less recovery time if the helicopter first flew to the

[18]Swenson, Loyd S. Jr., et al, This New Ocean: A History of Project Mercury, Scientific and Technical Information Division, Office of Technology Utilization, NASA, Washington, D.C., 1966.

[19]Swenson, Loyd S. Jr., et al, This New Ocean: A History of Project Mercury, Scientific and Technical Information Division, Office of Technology Utilization, NASA, Washington, D.C., 1966.

ACRV's landing location and attached a cable to it. The helicopter would then tow it to the ship and transport it to the ship's deck.

CONCLUSIONS

A conceptual Design for a Braking and Landing system for the ACRV was completed by separating the in-flight braking into three main sections. These three stages include the first phase of re-entry from the space station to the edge of the atmosphere (roughly 400,000 ft.), the second phase from the edge of the atmosphere to the point where auxiliary braking is employed, and the third phase in which the vehicle is decelerated by the auxiliary braking device. Computational analysis of the first two phases has resulted in an approximate velocity profile which will aid in determining precisely the type of deceleration system needed and the altitude of deployment. Approximate values have been obtained through solutions of the vehicle's equations of motion for the optimum ΔV and corresponding mass of propellent for a de-orbit burn which would place the vehicle at 400,000 ft. with a flight path angle of $-4°$ and initial velocity of 26,000 ft/s. Utilizing these initial conditions, an approximate velocity profile was created for a vehicle with an L/D of 1.0 and Ballistic parameter between 55 and 75 lbf/ft^2.

Among the guidance systems researched for use in the ACRV system were a system of guidance predicted capabilities and guidance using a nominal trajectory. The guidance predicted capability system appears to be the best solution for use with the ACRV system since it offers the ability to control a large variety of possible trajectories and the capability of maintaining automatic control if the 'fast time' solutions of the vehicle's equations of motion are used.

Through a detailed analysis, the maximum heating during re-entry was found to occur at roughly 200,000 ft, the point where maximum deceleration occurs. Research on the heating effects on possible heat shield materials has shown that a heat shield used for a re-entry vehicle should have the following qualities.
    a) High Mass and/or high specific heat
    b) High Emissivity
    c) Low thermal conductivity

Several types of parachute braking systems were investigated, including both subsonic and supersonic parachutes. Since the ACRV will decelerate to a velocity corresponding to Mach 1.5 by aerodynamic braking alone, the parachute braking system was designed to first deploy a conical

25

drogue chute followed by three 88 foot diameter main chutes each deployed by its own pilot chute. This combination of parachutes was designed to brake the ACRV to a water landing with an impact velocity of approximately 25 ft/s.

A more detailed analysis of such topics as heat shield materials and parachute deployment as well as landing impact load spikes is suggested. Overall, this concept for a braking and landing scheme should prove to be reliable, simple, and effective, all of which are very important to the safe, speedy return of the Assured Crew Return Vehicle.

BIBLIOGRAPHY

Agrawal, Brij N., The Design Geosynchronus Spacecraft, Prentice-Hall Inc., Englewood Cliffs, NJ, 1986.

Anderson, John D., Hypersonic and High Temperature Gas Dynamics, McGraw-Hill Book Company, New York, 1989.

Bate, Roger R., et al., Fundamentals of Astrodynamics, Dover Publications, Inc., New York, 1971.

Berndt, Rudi J., and Babish, Charles A., III, "Supersonic Parachute Research," Proceedings of Retardation and Recovery Symposium, Flight Accessories Laboratory Aeronautical Systems Division Air Force Systems Command Wright-Patterson Air Force Base, Ohio, May, 1963.

Bursey, C.H. Jr., et al., "A Study of the Thermal Kill of Variable Organisms During Mars Atmospheric Entry," Thermal Design Principals of Spacecraft and Entry Bodies: Progress in Astronautics and Aeronautics, Vol. 21, Academic Press, New York, 1969.

Cerimele, Chris, "Aero Trades," Johnson Space Center, Advanced Programs Office, September, 1986.

Cerimele, Chris, et al., "A Conceptual Design Study of a Crew Emergency Return Vehicle" Johnson Space Center, Advanced Programs Office, August 1988.

Ertel, Ivan D., et al, The Apollo Spacecraft: A Chronology, Volume 4, Scientific and Technical Information Office, NASA, Washington, D.C., 1978.

Knacke, T.W. and Hegele, A.M., "Model Parachutes: Comparison Test of Various Types," USAF Report MCREXE-672-12D, Jan. 1949.

McShera, John T., Jr., and Lowery, Jerry L., "Static Stability and Longitudinal Control Characteristics of a Lenticular-Shaped Re-entry Vehicles at Mach Numbers of 3.5 and 4.65," NASA TMX-763, March 1963.

Parkinson, Leslie R., Aerodynamics, The Macmillian Company, New York, 1944.

Peterson, Carl W., "The Aerodynamics of Supersonic Parachutes," Sandia National Laboratories, Albuquerque, New Mexico.

Peterson, Carl W., et al., "Design and Performance of a Parachute for Supersonic and Subsonic Recovery of an 800-lb Payload," Sandia National Laboratories, Albuquerque, New Mexico, December 1986.

Regan, Frank J., Re-entry Vehicle Dynamics, American Institute of Aeronautics and Astronautics, Inc., New York, 1984.

Swenson, Loyd S. Jr., et al, This New Ocean: A History of Project Mercury, Scientific and Technical Information Division, Office of Technology Utilization, NASA, Washington, D.C., 1966.

Tipler, Paul A., Physics, Worth, New York, 1982.

Wingrove, Rodney C., "Atmosphere Entry Guidance and Control," Control, Guidance,and Navigation of Spacecraft, NASA SP-17, December, 1962.

APPENDIX A

Objective: Analysis of Velocity, Mass and Time Requirements to satisfy
entry conditions at 400,000 ft.

Initial Conditions: Space Station has a circular orbit at approximately 225
n. mi. altitude.

Entry Condition: At 400,000 ft., the ACRV should have a Flight Path Angle
between -1 and -5 degrees and a velocity no greater than
26,000 ft./sec.
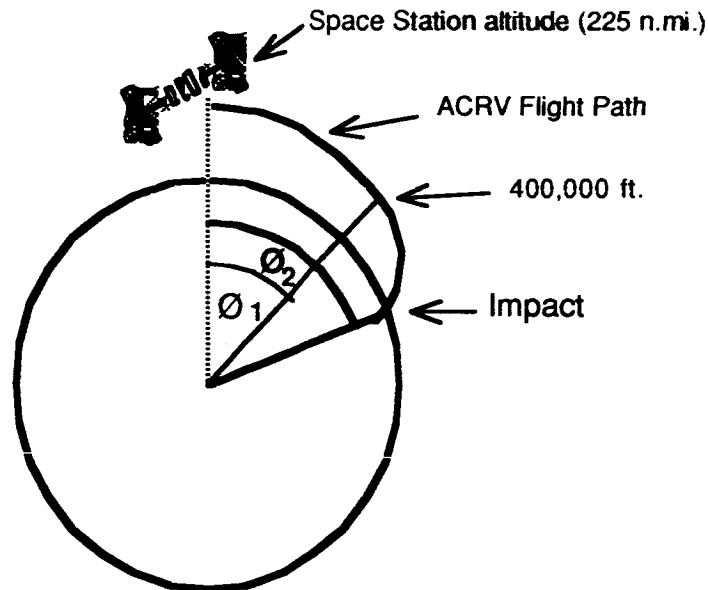
Figure A1: Simplified Flight Path of the ACRV

The above figure shows the flight path of the ACRV from station to impact.
$\emptyset 1$ is the difference in true anomaly from station departure to the entry point at
400,000 ft.. $\emptyset 2$ is the difference in true anomaly from station departure to point of
impact.

ACRV

Local Hortizontal

β=-4° Flight Path Angle

Flight Path

EARTH
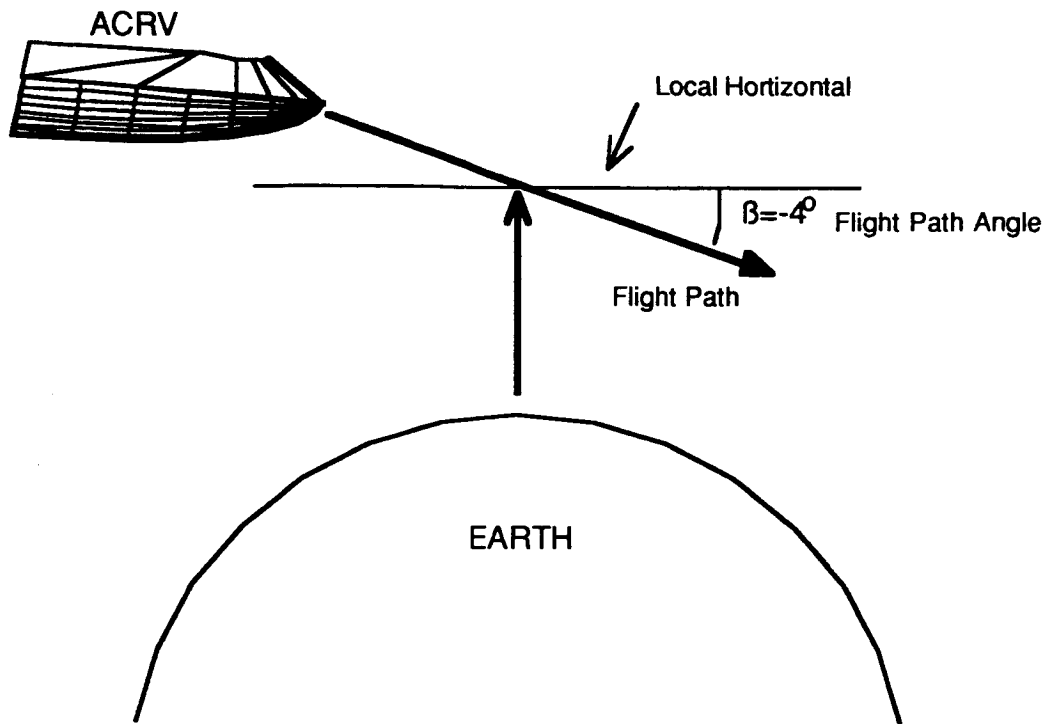
Figure A2: Definition of Flight Path Angle

Two methods of changing the velocity that would achieve the desired flight path angle at 400,000 ft. have been explored using computer calculations. The first involves two burns in order to de-orbit the ACRV. One at space station altitude changes the speed of the ACRV and another at 400,000 ft. changes the flight path angle to the one desired. The second method involves one burn. This burn would change the speed and direction of the ACRV at Space Station altitude in order to achieve the desired flight path angle at 400,000 ft without any additional burns.

METHOD ONE:

Assumptions: Burn #1: Changes Speed of Craft Only.
                Burn #2: Changes Flight Path Only.

Burn #1:

Any speed change will have to have at least a magnitude of 0.08546 km/s. This is the velocity necessary to place the ACRV on an elliptical orbit with a perigee of 400,000 ft. above the surface of the Earth. The program calculates the energy, angular momentum, eccentricity, true anomaly, and semi-major axis

30

length of the new orbit for a given velocity change. The eccentric anomaly and time since perigee are necessary in the analysis and are found by the equations:

$$\tan(E/2) = \tan(\emptyset/2)\,[(1-e)/(1+e)]^{1/2} \quad \text{and} \quad t = (E - e\sin E)[(a^3/\mu)^{1/2}]$$

where: E = eccentric anomaly t = time since perigee

$\emptyset$ = true anomaly e = eccentricity

a = semi-major axis length μ = gravitational coefficient

With the above information, the resultant velocity, flight path angle, true anomaly, and time since perigee are calculated for the orbit at an altitude of 400,000 ft. The true anomaly and time since perigee information is used to compute the total amount of flight time to reach 400,000 ft and the amount of distance covered in the same amount of time.

Burn #2:

With the major orbital dynamics part of the computation done, the program then computes the amount of velocity change in order to correct the current flight path angle to one that is desired for re-entry without changing forward velocity. This involves using the law of cosines in the form:

$$\Delta V = 2\ V_2\ \sin(\beta_d - \beta_2)$$

where: ΔV = change in velocity V_2 = velocity of orbit at 400,000 ft.

β_d = desired flight path angle β_2 = flight path angle of orbit at
                                                400,000 ft.

The total amount of velocity change is derived from adding the velocity changes for burn one and burn two. With this total velocity change known, the amount of propellant mass as a part of the total mass of the space craft can be found. Using the relationship:

$$Mp = 1 - \exp[\Delta V_t/(I_{sp} \times g)]$$

where: Mp = propellant part of Total Mass ΔV_t = total velocity change

I_{sp} = specific impulse g = acceleration of gravity.

The two burn calculations have been derived for the minimum value for the initial burn up until the necessary propellant mass portion exceeded 50% of

31

total mass. This was done for a range of desired flight path angles at 400,000 ft. between -1 and -5 degrees. Results of this part of the computer analysis are shown in the graphs as either two burn data or correction data.

METHOD TWO:
Assumptions:
      One Burn: Changes Velocity and Flight Path Angle of Craft.

This method assumes that one burn is necessary for the desired flight path angle at 400,000 ft. This burn changes the speed and the flight path angle of the ACRV at space station altitude. The total amount of velocity change at this point is found by:

$$\Delta V = [\ V_1{}^2 + V_c{}^2 - 2\,V_1\,V_c\cos(\beta_1)\ ]^{1/2}$$

where: ΔV = total velocity change V_1 = velocity after burn
               V_c = velocity of circular orbit β_1 = flight path angle

The analysis involved using the flight path angle at the burn as the independent variable to find the resultant velocities necessary to achieve the desired flight path angle at 400,000 ft.

The necessary computations for this are:

Conservation of Angular Momentum : $V_1\,r_1\cos(\beta_1) = V_2\,r_2\cos(\beta_2)$

Conservation of Energy : $(V_1{}^2/2) - (\mu/r_1) = (V_2{}^2/2) - (\mu/r^2)$

where: V_1 = velocity after burn r_1 = radial location of burn
               V_2 = velocity at 400,000 ft. r_2 = 400,000 ft. plus Earth radius
               β_1 = flight path angle at burn β_2 = flight path angle at 400,000 ft.
               μ = gravitational coefficient of Earth

Since, the only values unknown in the above equations are V_1 and V_2, and there are two equations, the values of V_1 and V_2 can be found.

The resulting equations are:

$$V_1{}^2 = 2\,\mu\,[\;(1/r_1) - (1/r_2)\;]/\;[\;1 - (r_1{}^2\,\cos^2(\beta_1))/(r_2{}^2\cos^2(\beta_2))]$$

and

$$V_2 = [r_1\,V_1\,\cos(\beta_1)\;]/[r_2\,\cos(\beta_2)]$$

This information is used to compute the true anomaly, time since perigee , total flight time, etc., as in the first method. The total velocity change is computed using the law of cosines from above and is used to calculate the propellant part of the total mass.

The one burn calculations have been made from the initial flight path angle of zero degrees to values no greater than -5. Values less than -5 lead to re-entry speeds greater than 26,000 ft/sec. Results of this part of the computer analysis are shown in the graphs as either a one burn maneuver or Angle data.
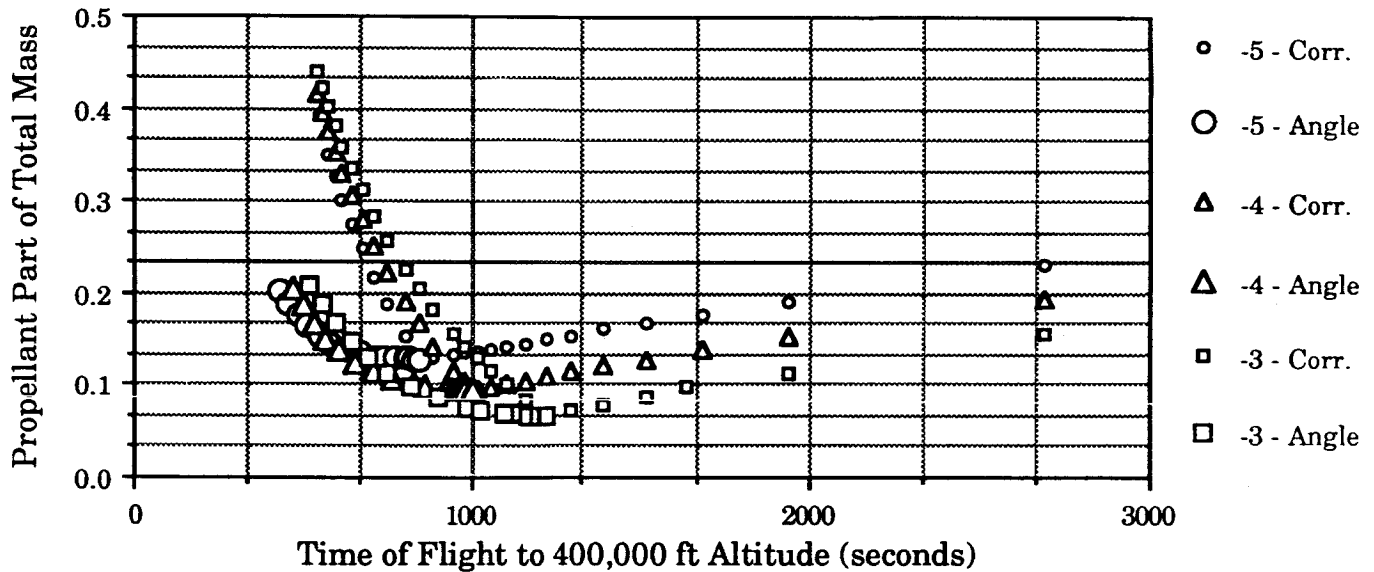
Figure A3:   Graph of Propellant as Part of Total Spacecraft Mass .vs. Total Time
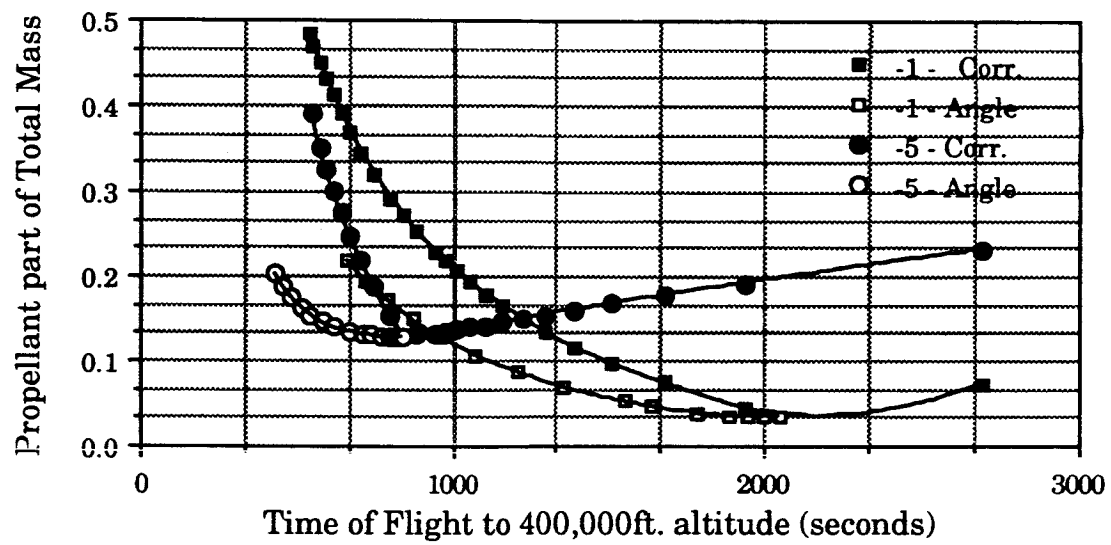
Figure A4:   Graph of Propellant as part of Total Spacecraft Mass .vs. Time of Flight
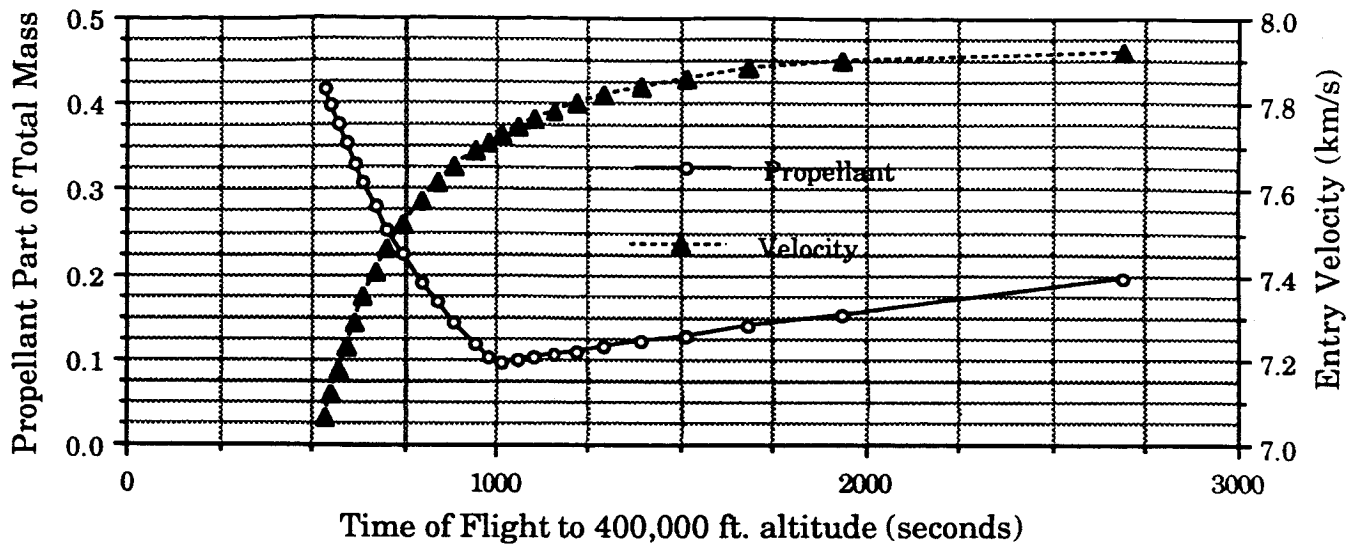
Figure A5: Graph of Entry Velocity at 400,000 ft. for an Entry Flight Path
            Angle of -4° and a Two Burn Velocity Change
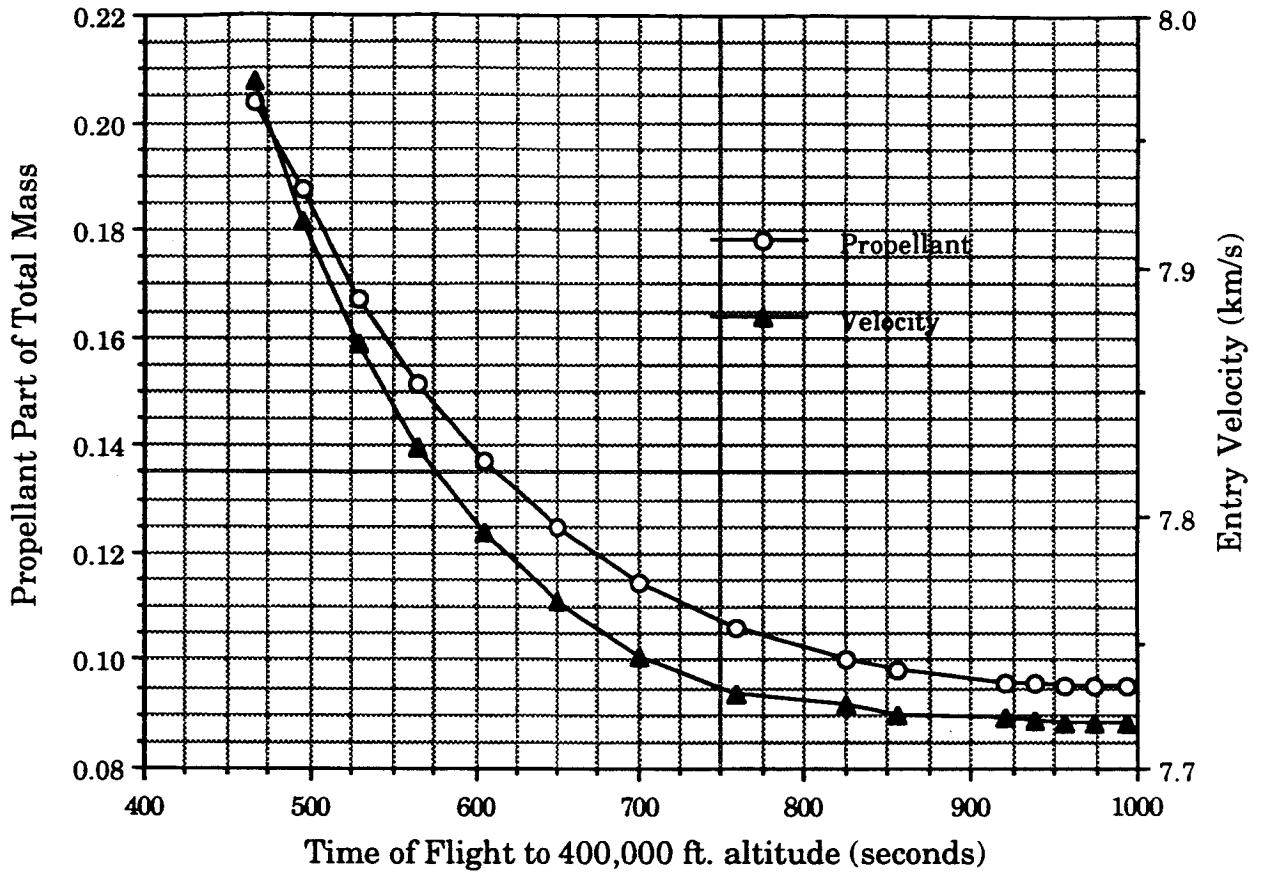
Figure A6:   Graph of Entry Velocity at 400,000 ft. for a Entry Flight Path
Angle of -4°
and a One Burn Maneuver

The atmospheric model chosen for use in the solution of the equations of motion of the ACRV was taken from Regan[20]. It relates the density at any point in the atmosphere to the density at sea level by an exponential relationship as follows:

$$\rho = \rho_0 \, e^{(-h/H)}$$

The force diagram used is shown in Figure B1 below.
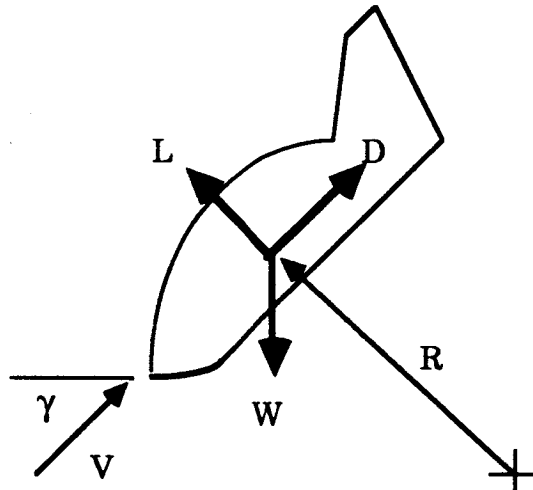
Figure B1: Force diagram

Summing forces perpendicular to the flight path and setting the resultant equal to the mass of the vehicle times the centrifugal acceleration gives:

$$L - W\cos \gamma = -m \, \frac{v^2}{R}$$

but,

$$L = C_L \frac{1}{2} \rho v^2 S$$

therefore, substituting in for L and dividing both sides by W gives:

$$\left(\frac{C_L S}{W}\right) \frac{\rho v^2}{2} = \cos \gamma - \frac{1}{g} \frac{v^2}{(R_e + h)}$$

where R_e is the radius of the earth and h is the altitude.

[20]Regan, Frank J., Re-entry Vehicle Dynamics, American Institute of Aeronautics and Astronautics, Inc., New York, 1984.

The quantity $W/C_L S$ is defined as the ballistic parameter, ß. By substituting   for the ballistic parameter and the atmospheric model above for the density, the equation becomes:

$$\frac{\rho_o e^{-(h/H)}\, V^2}{2\beta} = \cos\ \gamma - \frac{V^2}{g(R_e+h)}$$

Solving this equation for the velocity will give the velocity as a function of the ballistic parameter, the flight path angle, and the altitude.

$$V^2\left[\frac{\rho_o e^{-(h/H)}}{2\beta} + \frac{1}{g(R_e+h)}\right] = \cos\ \gamma$$

$$V = \left[\frac{g(R_e+h)\,2\,\beta\cos\ \gamma}{2\beta + g(R_e + h)\,\rho_o e^{-(h/H)}}\right]^{\frac{1}{2}}$$

In order to incorporate the initial conditions into the problem, a first order differential equation was found for dV/dt and this equation was integrated using a Runge-Kutta fourth-order algorithm.

If we let

$$A = \left[g\left(R_e + h\right)\rho_o e^{-h/H} + 2\beta\right]$$

$$B = \left[2\beta g\cos\ \gamma\right]$$

$$C = \left[2\beta g\cos\ \gamma\left(R_e + h\right)\right]$$

$$D = \left[g\left(R_e + h\right)\rho_o\left(\frac{-1}{H}\right)e^{-h/H}\right]$$

$$E = \left[g\,\rho_o\,e^{-h/H}\right]$$

then after taking differentials the equation of motion becomes:

$$\frac{dV}{dh} = \frac{1}{2}\sqrt{\frac{A}{C}}\left[\frac{A*B - C*(D+E)}{A^2}\right]$$

Regan[21] gives the variation of the flight path angle with velocity as:

$$\frac{dV}{V} = \left[\frac{C_L}{C_D}\right]^{-1} d\gamma$$

[21]Regan, Frank J., Re-entry Vehicle Dynamics, American Institute of Aeronautics and Astronautics, Inc., New York, 1984.

38

Dividing both sides by dh gives:

$$\frac{d\gamma}{dh} = \frac{1}{V}\left[\frac{C_L}{C_D}\right]\frac{dV}{dh}$$

This equation was integrated along with the differential equation for the velocity in the Runge-Kutta algorithm. The result is a profile of the velocity as a function of altitude called a velocity altitude map.

This section is a brief description of a simple re-entry model which analyzes g-force loading and surface heating for given re-entry conditions.

•*Initial Conditions* : At an altitude of 400,000 feet, the ACRV has a flight path angle between -1 and -5 degrees and a velocity no greater than 26,000 ft/sec.

•*Ending Conditions* : The ACRV is either at an altitude or velocity where parachutes can be deployed to further slow the vehicle down.

•*Important Considerations* : The g-forces should be limited to approximately 3 g's and the surface temperature should not exceed 4000° R, due to material limits.

The development of a simple re-entry model began with the process of deriving a trajectory profile. A trajectory profile relates the altitude and velocity of the ACRV with time. The basis for all trajectory profiles derived by this simple re-entry model is from the velocity - altitude map in the lifting body analysis of this report.
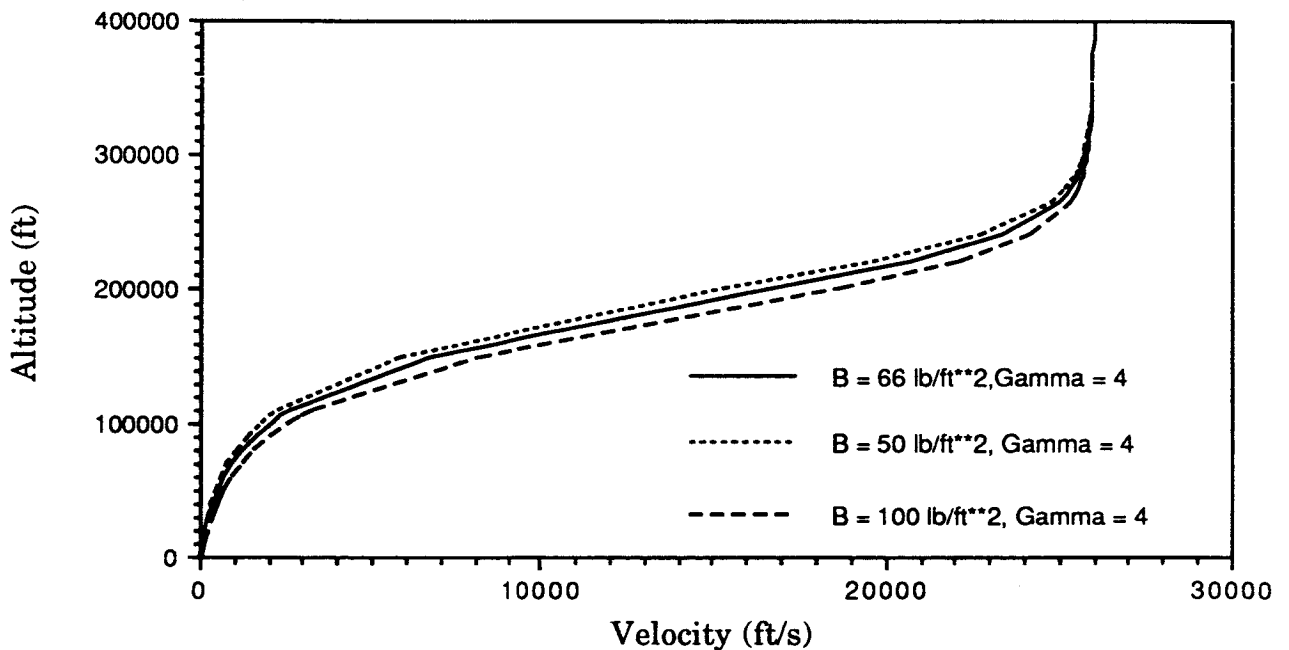
Figure C1: Altitude - Velocity Map

As shown in Figure C1, the velocity of the ACRV varies with altitude for different ballistic coefficients. The information from this graph (i.e. the information from the computer model for atmospheric braking) was integrated into a computer program that generates the different aspects of the ACRV flight conditions as a function of time. The important effects derived directly from this analysis include: the altitude, velocity, and g-forces versus time for different flight path angles.

After setting up the appropriate initial conditions, the program computes the change in altitude from the ACRV's velocity and flight path angle for a given amount of time. The subsequent decrease in altitude is followed by the program using the values from Figure C1 to compute the new velocity at the new altitude. The program then computes the new change in altitude to follow the previous change in velocity and so on. This process continues at a constant flight path angle until the desired parachute altitude is reached.

At the same time that the program computes the changes in altitude and velocity, it also computes the g-forces that the ACRV experiences. The g-forces are found by computing the amount of deceleration that is present in one interval of time.

Preliminary results of the program have shown that a constant flight path angle throughout the re-entry process has some undesirable aspects. As shown in Figure C2, the g-forces reach relatively high values halfway through the flight. After a significant decrease in forward velocity, the constant flight path angle causes the velocity to approach zero asymptotically in the last several thousand feet resulting in an extremely long flight time. A method is needed to limit g-forces and to increase the velocity at the last several thousand feet.

Further computer analysis revealed that the g-force problem could be overcome by adjusting the flight path angle in order to avoid exceeding 3 g's during any part of the re-entry process. A subroutine was designed to accomplish this and to record the change in flight path during the entire re-entry process (see Figure C3).

The heating aspect of the re-entry was added to the analysis after the trajectory profile was such that the g-forces were within required limits and the

41

trajectory agreed with much of the literature on the subject[22]. The heating equations were added to the program in a way as to allow comparison of several different material properties at the same time.

•The heat balance used is defined by:

Atmospheric Heating + Radiant Heating = Emitted Heat + Stored Heat [23]

The equation used to simulate the aerodynamic heating is given by[24]:

$$q = \frac{rV^3 \alpha_e}{2g_0 J}$$

where
α_e = Accommodation coefficient, dimensionless
ρ = Atmospheric density (lbm/ft^3)
V = Velocity of the Vehicle (ft/s)
g_0 = gravitational conversion factor, 32.2 ft/s^2
J = Joules's constant for mechanical equivalent of heat, 778 ft.lb/Btu

The accommodation coefficient is used to specify the ability to exchange energy. As shown above, the aerodynamic heating is a direct function of atmospheric density. For purposes of simplifying analysis, the atmospheric density model used was the U.S. Standard Atmosphere.

---

[22]Cerimele, Chris, et al., "A Conceptual Design Study of a Crew Emergency Return Vehicle" Johnson Space Center, Advanced Programs Office, August 1988.

[23]Bursey, C.H. Jr., et al., "A Study of the Thermal Kill of Variable Organisms During Mars Atmospheric Entry," Thermal Design Principals of Spacecraft and Entry Bodies; Progress in Astronautics and Aeronautics, Vol. 21, Academic Press, New York, 1969.

[24]Ibid.

The equation used to estimate the radiant heating is given by[25]:

$$\text{Radiant Heating} = A_e\,\alpha_s\,\overline{S} + A_s\,F\,\sigma\,T_e^4\,\alpha_{ir}$$

where:

A_e = Exposed surface area, ft^2

A_s = Total surface area, ft^2

α_s = Absorptivity of material in infrared range

α_{ir} = Absorptivity of material in solar range.

F = View Factor from vehicle to Earth.

$\overline{S}$ = Solar constant for Earth, Btu/ft^2 sec

T_e = Surface temperature of Earth, ^oR

σ = Stefan-Boltzmann constant, 4.75×10^{-13} Btu/ft^2 sec $^oR^4$

The equation used to estimate the emitted heat is given by[26]:

$$\text{Emitted Heat} = A_s\,\mathcal{E}_m\,\sigma\,T_s^4$$

where:

$\mathcal{E}_m$ = Emissivity of material, dimensionless

T_s = Temperature of outer vehicle material

Just prior to entry, the vehicle has an equilibrium temperature based on incident and emitted radiant energy. This will serve as the initial temperature for the analysis.

The stored heat equation is given by[27]:

$$\text{Stored Heat} = M_s\,C_p\,\partial T_s/\partial t$$

where:

M_s = Mass of the vehicle's heat shield, lb$_m$.

C_p = Specific Heat of material, Btu/lb ^oR

t = Time, sec.

---

[25]Bursey, C.H. Jr., et al., "A Study of the Thermal Kill of Variable Organisms During Mars Atmospheric Entry," Thermal Design Principals of Spacecraft and Entry Bodies: Progress in Astronautics and Aeronautics, Vol. 21, Academic Press, New York, 1969.

[26]Ibid.

[27]Ibid.

The equation used to simulate heat transfer for multiple layers of materials is given by[28]:

$$m_i c_i \, (\partial T_i / \partial t) \; = \; -C_{ij}(T_i - T_j) - \sigma R_{ij}(T_i^4 - T_j^4)$$

where: $m_i c_i$ = Thermal Capacity at node i

T_i, T_j = Temperatures of nodes i and j

$\partial T_i / \partial t$ = Rate of temperature variation of node i

C_{ij} = Conductive coupling between nodes i and j

R_{ij} = Radiative coupling between nodes i and j

The above equations form a one-dimensional heat balance which is numerically integrated along with the trajectory equations of motion to determine the heating and temperature response as a function of time.

The results of the program were produced in order to determine the effects of different material properties such as thermal capacity, thermal conductivity, and emissivity. The effects of different thicknesses and masses of material used in the layers of the material are considered by this model.

The values used as a basis for material properties are[29]:

Specific Heat $C_p = 1.0$ Btu/lb $^\circ$F   (equivalent to H_2O)

Thermal Conductivity $K = 0.3$ Btu in/h ft^2 $^\circ$F (equivalent to corkboard)

Emissivity $\varepsilon = 0.8$

Mass of a layer $M_1 = 200$ lb$_m$

The variation of these properties with time was not considered in this model and only serve as a basis for comparison (see Figure C6).

[28]Agrawal, Brij N., The Design Geosynchronus Spacecraft, Prentice-Hall Inc., Englewood Cliffs, NJ, 1986.

[29]Tipler, Paul A., Physics, Worth, New York, 1982.
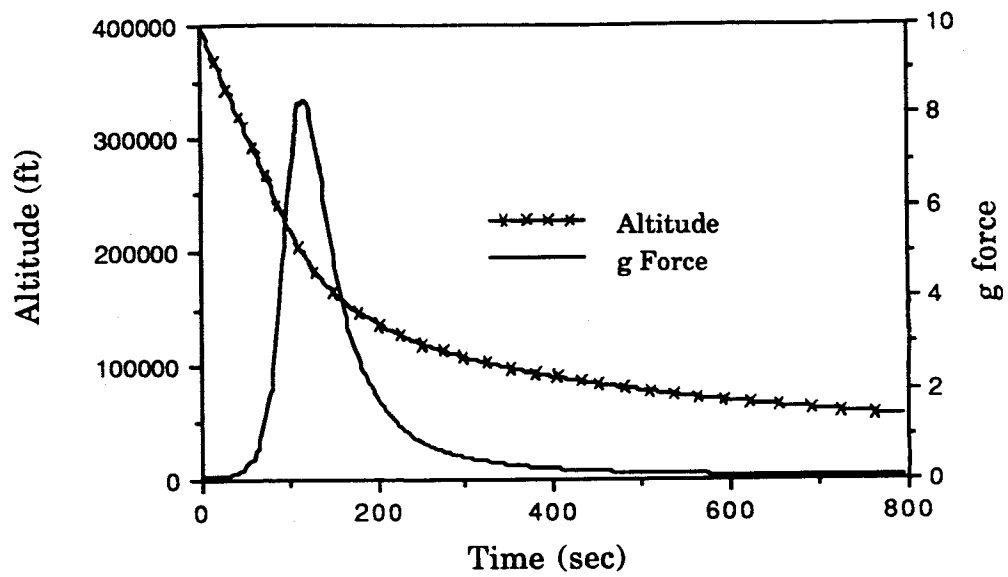
Figure C2: Trajectory Profile During Re-Entry for Constant Flight Path Angle
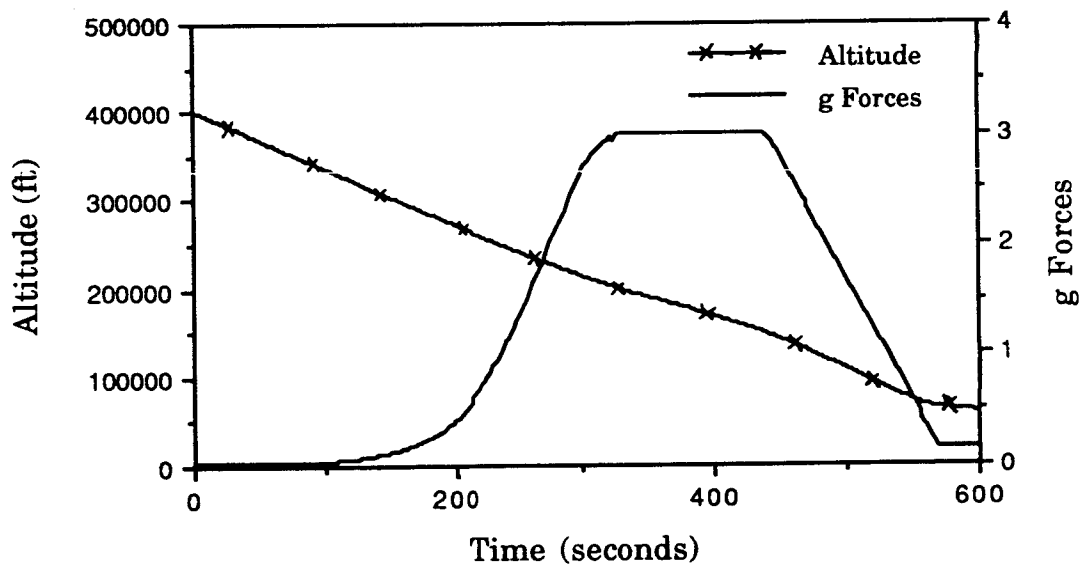
Figure C3: G Force and Altitude vs. Time for a Varying Flight Path Angle
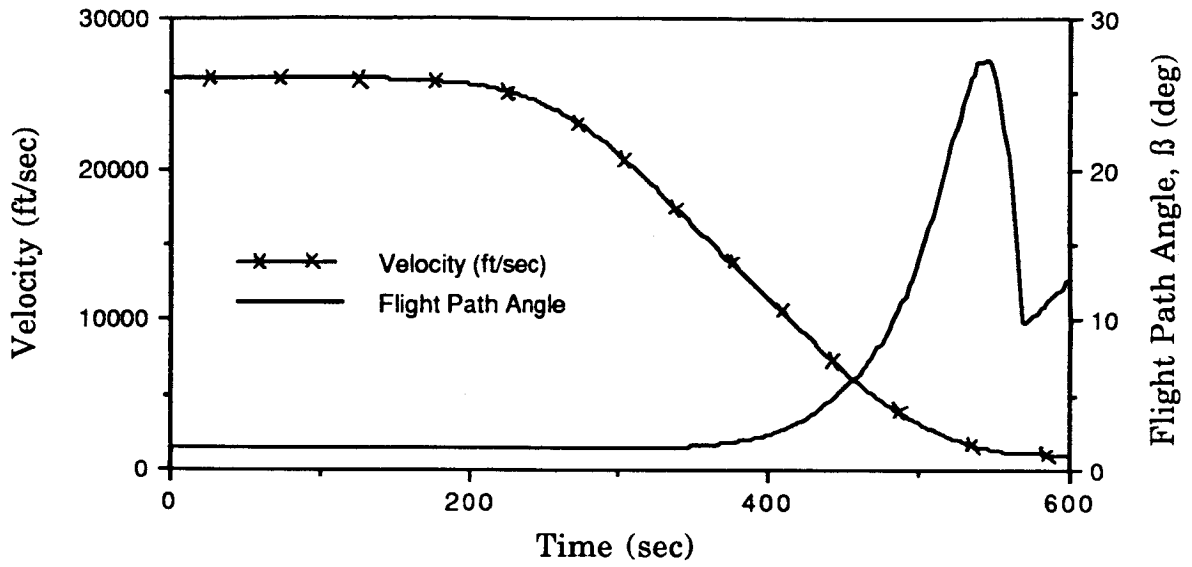
Figure C4: Velocity vs. Time & Flight Path Angle vs. Time
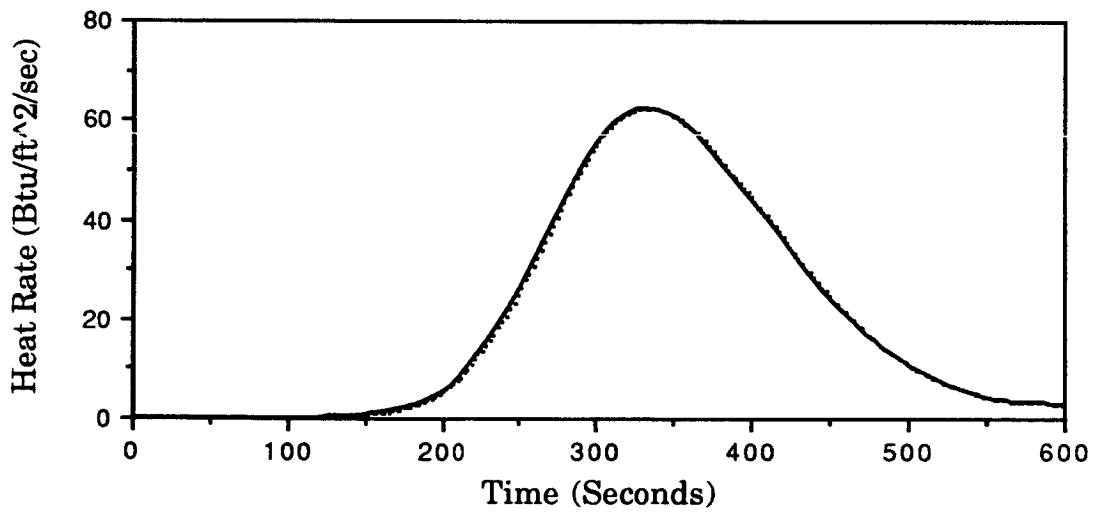
Figure C5: Heat Rate vs. Time
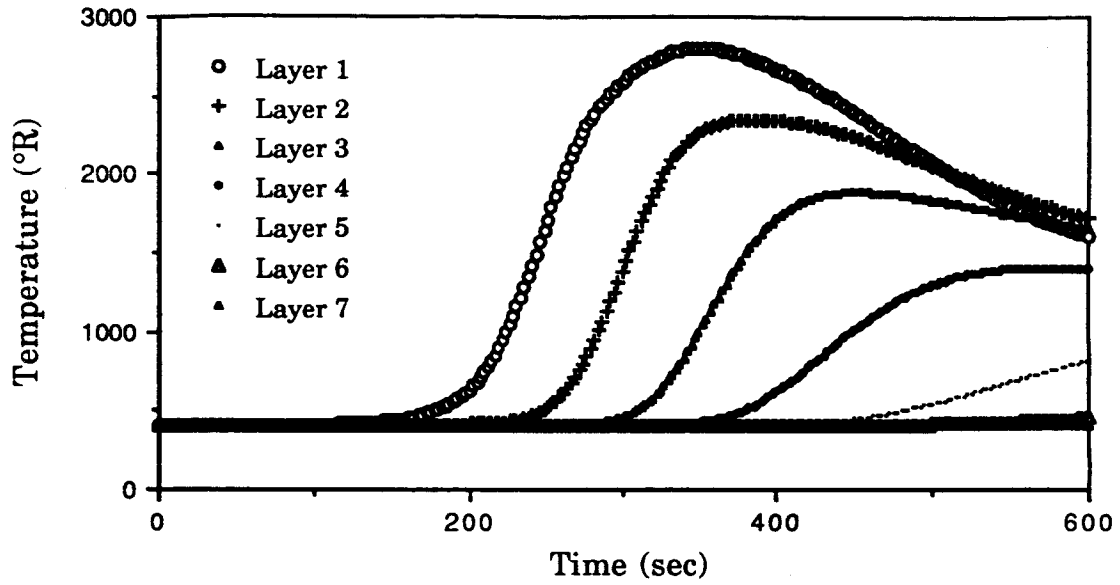
Figure C6: Temperature Response of Multi-layered Heat Shield
(Normal Case)
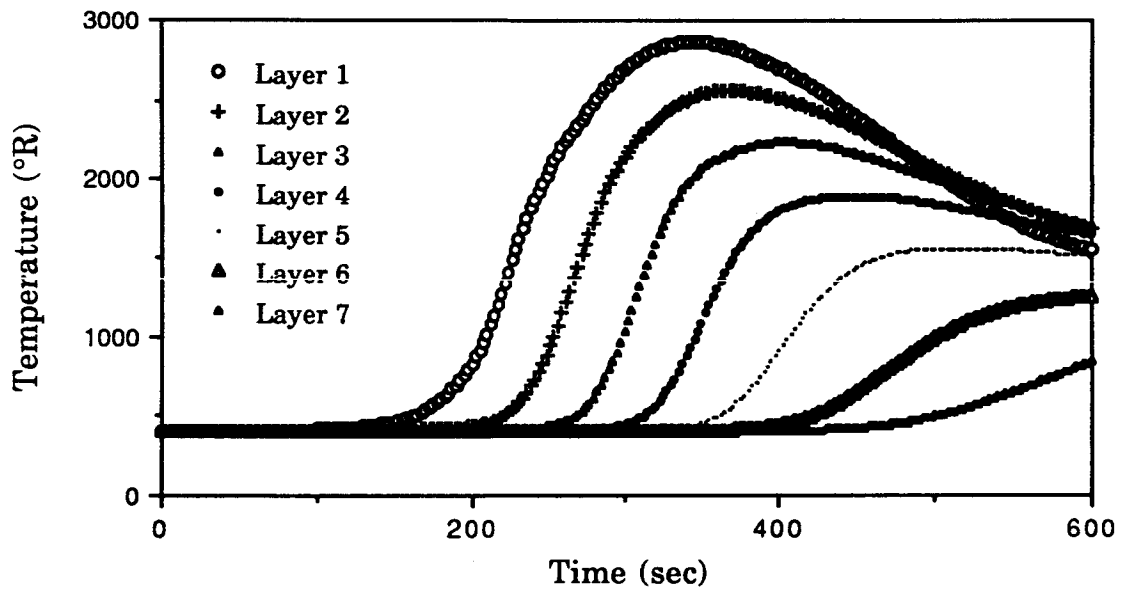
Figure C7: Temperature Response of Multi-layer Heat Shield
(50% Reduction in Specific Heat of Material)

47
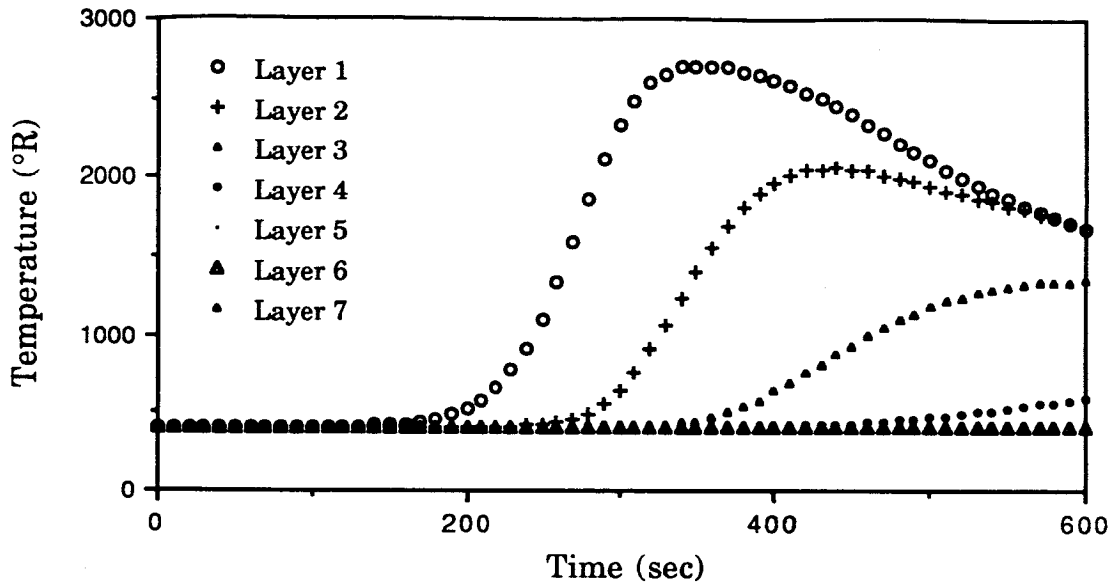
Figure C8: Temperature Response of Multi-layered Heat Shield
(100% Increase in Specific Heat of Material)
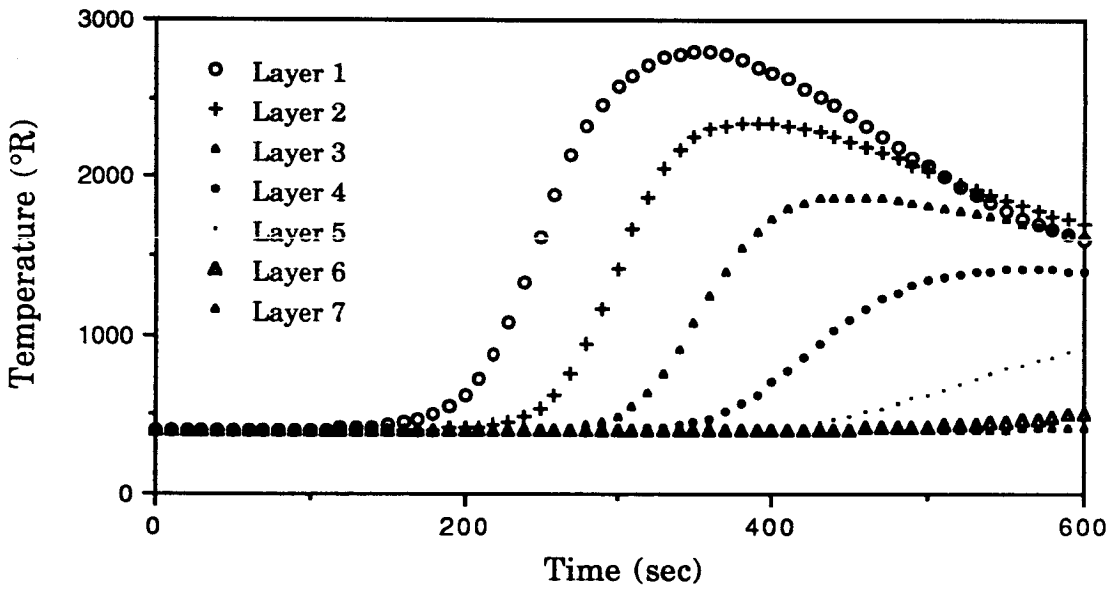
Figure C9: Temperature Response of Multi-layered Heat Shield
(100% Increase in Thermal Conductivity)

48
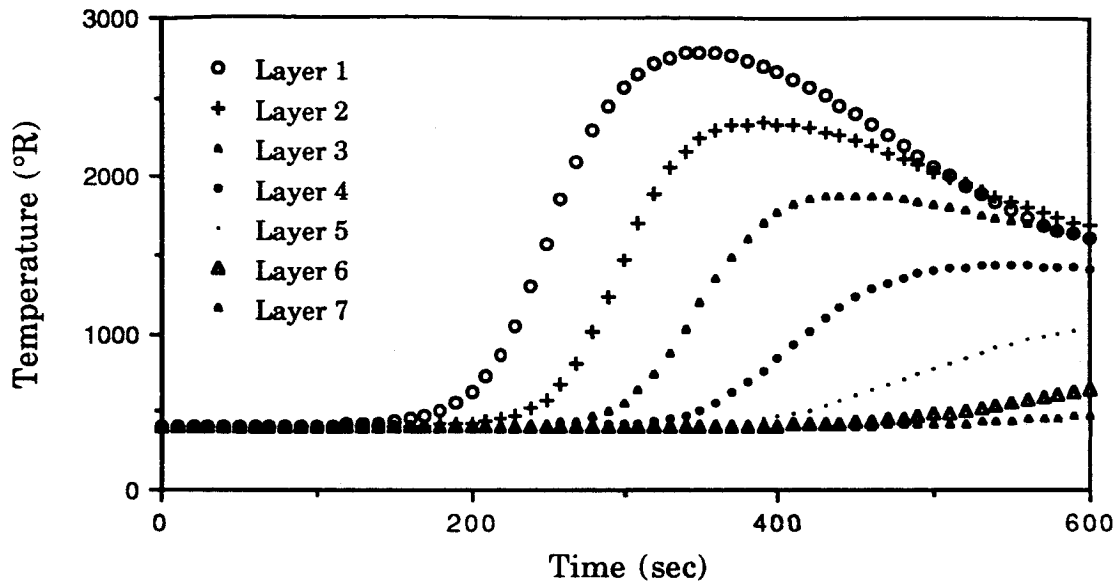
Figure C10: Temperature Response of Multi-layered Heat Shield
(300% Increase in Thermal Conductivity)
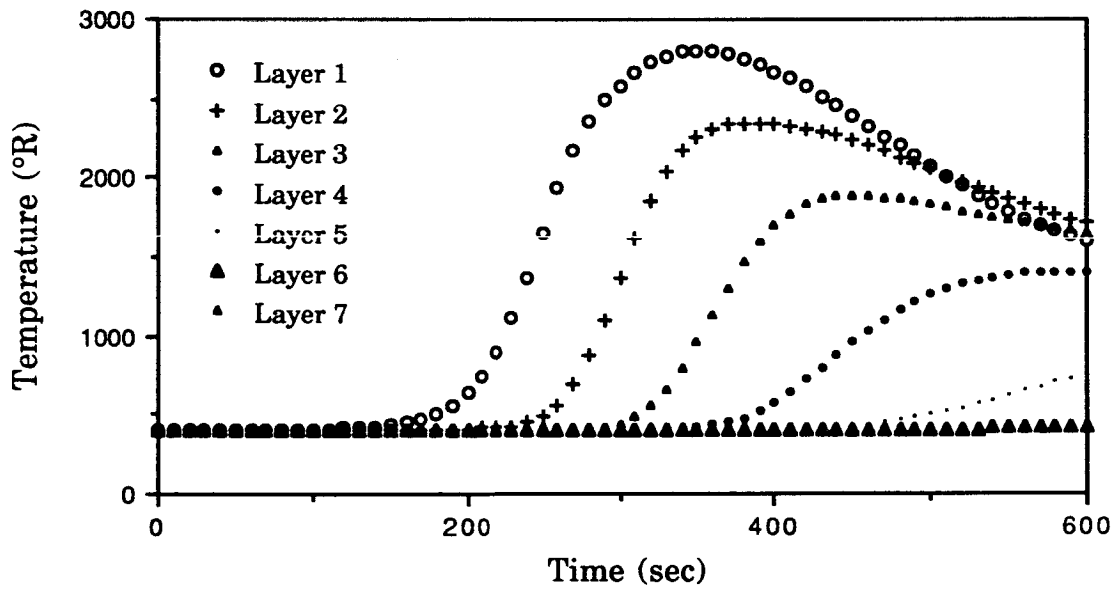
Figure C11: Thermal Response of Multi-layered Heat Shield
(50% Reduction in Thermal Conductivity)
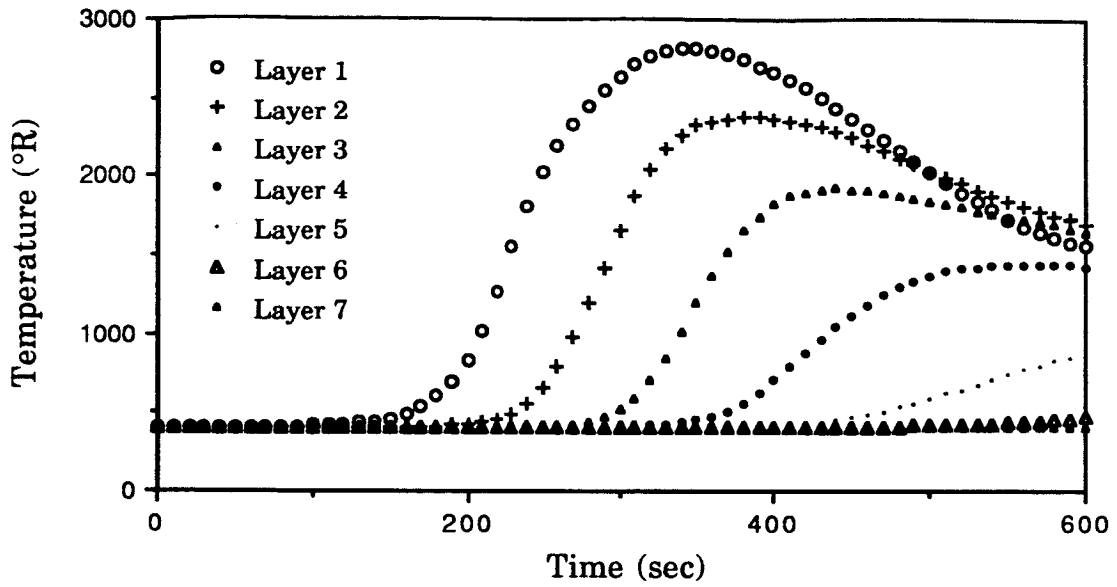
Figure C12: Temperature Response of Multi-layered Heat Shield
(for Reduction in Mass for First Layer)
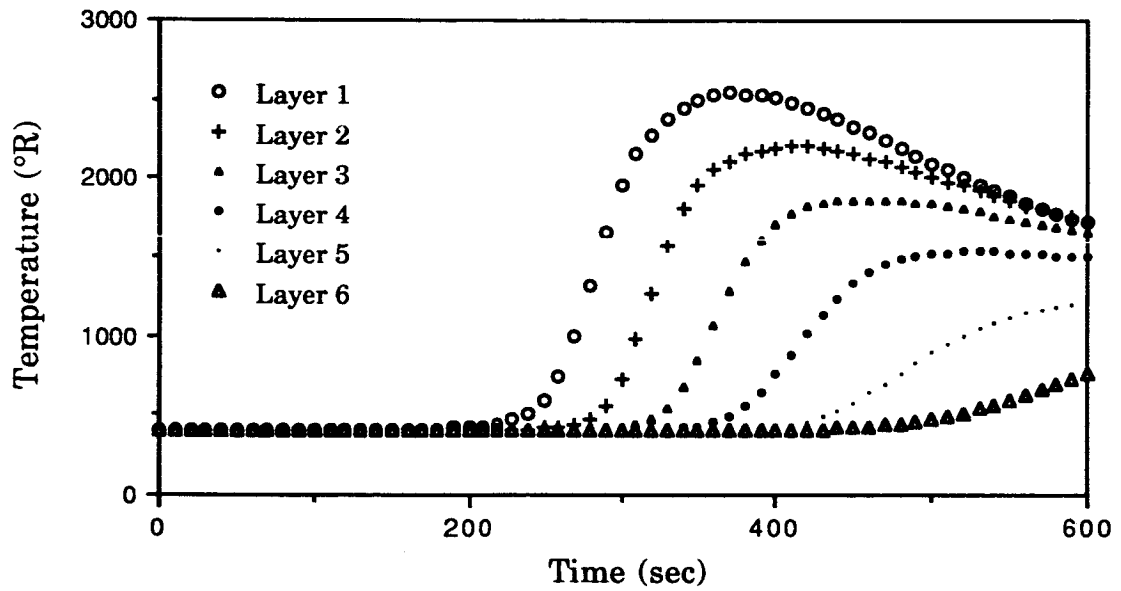
Figure C13: Temperature Response of Multi-layered Heat Shield
(for Reduction in Layers Behind the First)

50
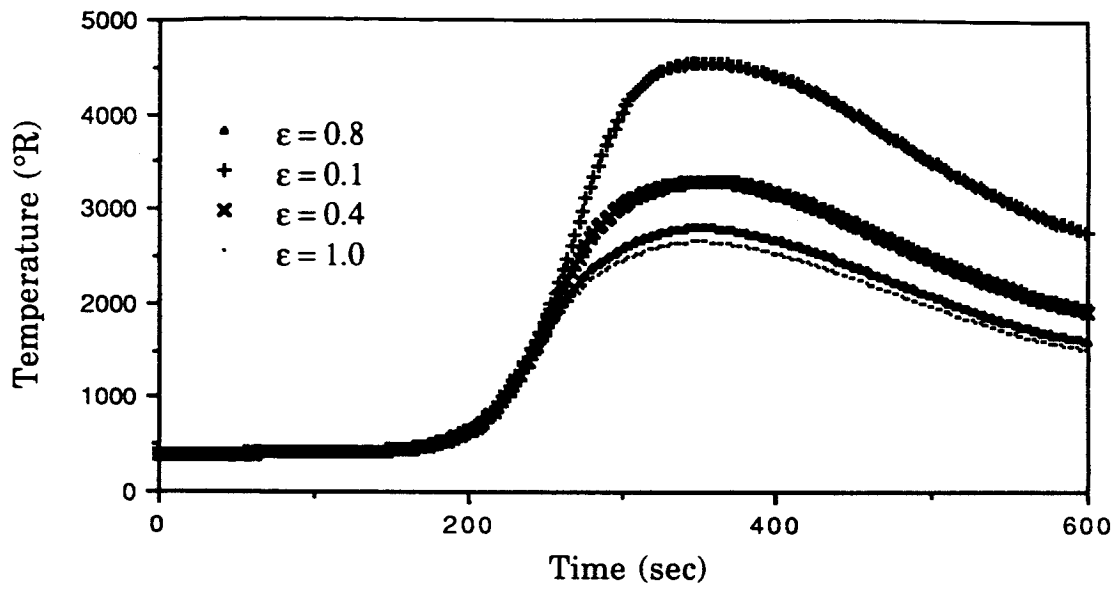
Figure C14: Effect of Heat Shield Emmisivity on Temperature Response

APPENDIX D
DETERMINATION OF PARACHUTE PARAMETERS[†]

Finding parachute diameter:

$$D = C_{Do}\, S_o\, q \qquad \{1\}$$

D = Drag (lbs)

C_{Do} = Drag coefficient of parachute based on canopy surface area

S_o = Canopy surface area (ft^2)

q = Dynamic pressure, $\frac{1}{2}\rho V^2$ (lbs/ft^2)

- For a given parachute (with its unique C_{Do}), S_o can be determined by letting D = Weight of payload and V = landing velocity.

$$D_o = \sqrt{\frac{4}{\pi} S_o} \qquad \{2\}$$

D_o = Nominal diameter of parachute {uninflated} (ft)

- Canopy diameter is thus defined from the surface area. If a cluster of parachutes is to be used, then canopy surface area, S_o must be divided by the number of parachutes in the cluster before computing D_o for each parachute.

$$D_c = \left\{\frac{D_c}{D_o}\right\} D_o \qquad \{3\}$$

D_c = Constructed diameter of the canopy {inflated}

$\left\{\dfrac{D_c}{D_o}\right\}$ = Parachute inflation parameter

- Canopy diameter is now determined.

[†] Based on analysis given in NWC-TP6575, Chapter 5, "Parachute Characteristics and Performance."

Finding length of parachute suspension lines:

$$D_B = \sqrt{\frac{4\,S_B}{\pi}}$$ (4)

D_B = Forebody diameter

S_B = Forebody surface area under parachute

- Forebody diameter is found from the forebody surface area.

$$L = 4\,D_B$$ (5)

L = length of parachute suspension lines

- L is calculated from the forebody diameter.

Example Calculation:

Parachute diameter:

Solving (1) for S_0 with:

D = Weight = 12,000 lbs

$\rho = 0.002378$ slug/ft^3

V = Landing velocity = 25 ft/sec

C_{D_0} = 0.88 for triconical parachute

$\Rightarrow$ $S_0 = 18,350.03$ ft^2

Divide this canopy surface area into three smaller parachutes.

$\Rightarrow$ $S_0 = 6,116.67$ ft^2 for each parachute

Using (2), solve for D_0.

$\Rightarrow$ $D_0 = 88.25$ ft

Now, $\left\{ \dfrac{D_c}{D_0} \right\} = 0.90$ for triconical parachute, so using Eq. (3), solve for D_c.

$\Rightarrow$ $D_c = 79.42$ ft

53

Thus, a cluster of 3 triconical parachutes, each with a nominal (uninflated) diameter of 88.25 ft would be sufficient.

Suspension line length:

Eq.

Solving (4) for D_B with $S_B = 360.7$ ft^2:

$$\Rightarrow \quad D_B = 21.43 \text{ ft}$$

Eq.

Solving (5) for L, the suspension line length:

$$\Rightarrow \quad L = 85.72 \text{ ft}$$

Thus, the length of the parachute suspension lines would be 85.72 ft.

Various Supersonic Parachutes:
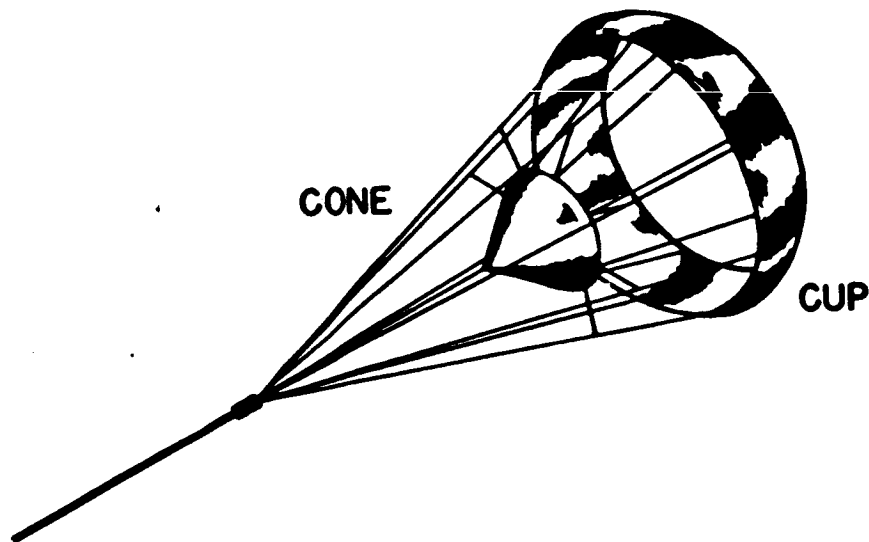
Figure D1: Cone-Cup Parachute Concept
(from Bernot, R.J. and Babish, C.A., 1962)
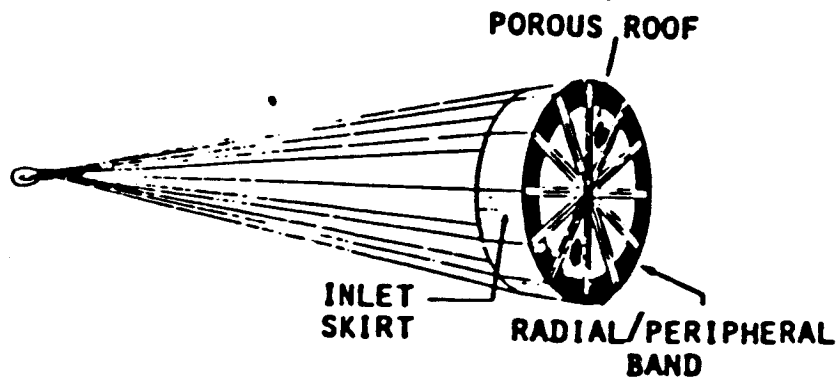
Figure D2:   The Hyerflo Parachute

(from Bernot, R.J. and Babish, C.A., 1962)
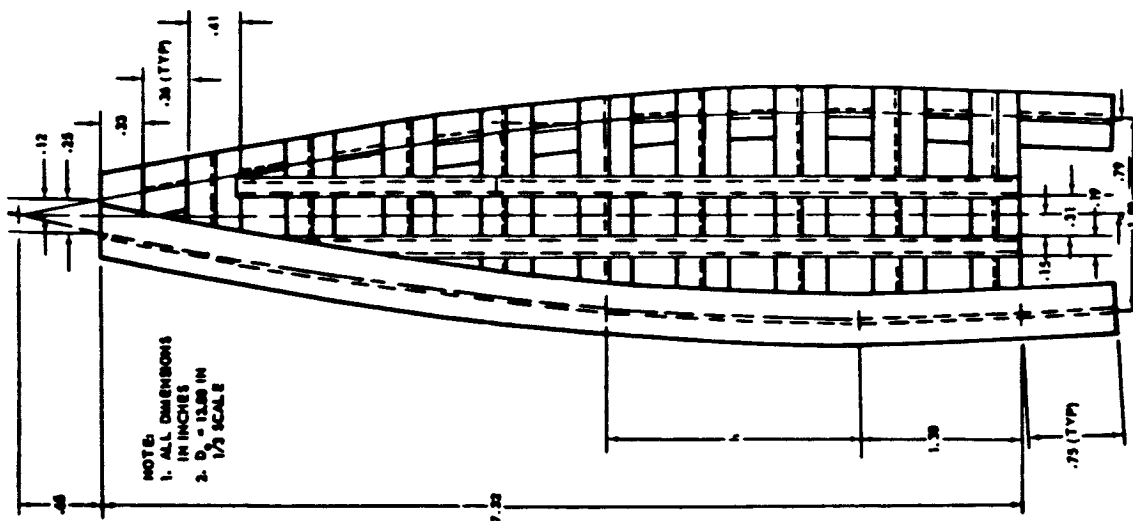
Figure C3:   Hemisflo Parachute Example

(form Buckner, J.K., 1962)

55

Figure D4:   Conical Ribbon Parachute Example

(from Buckner, J.K., 1962)
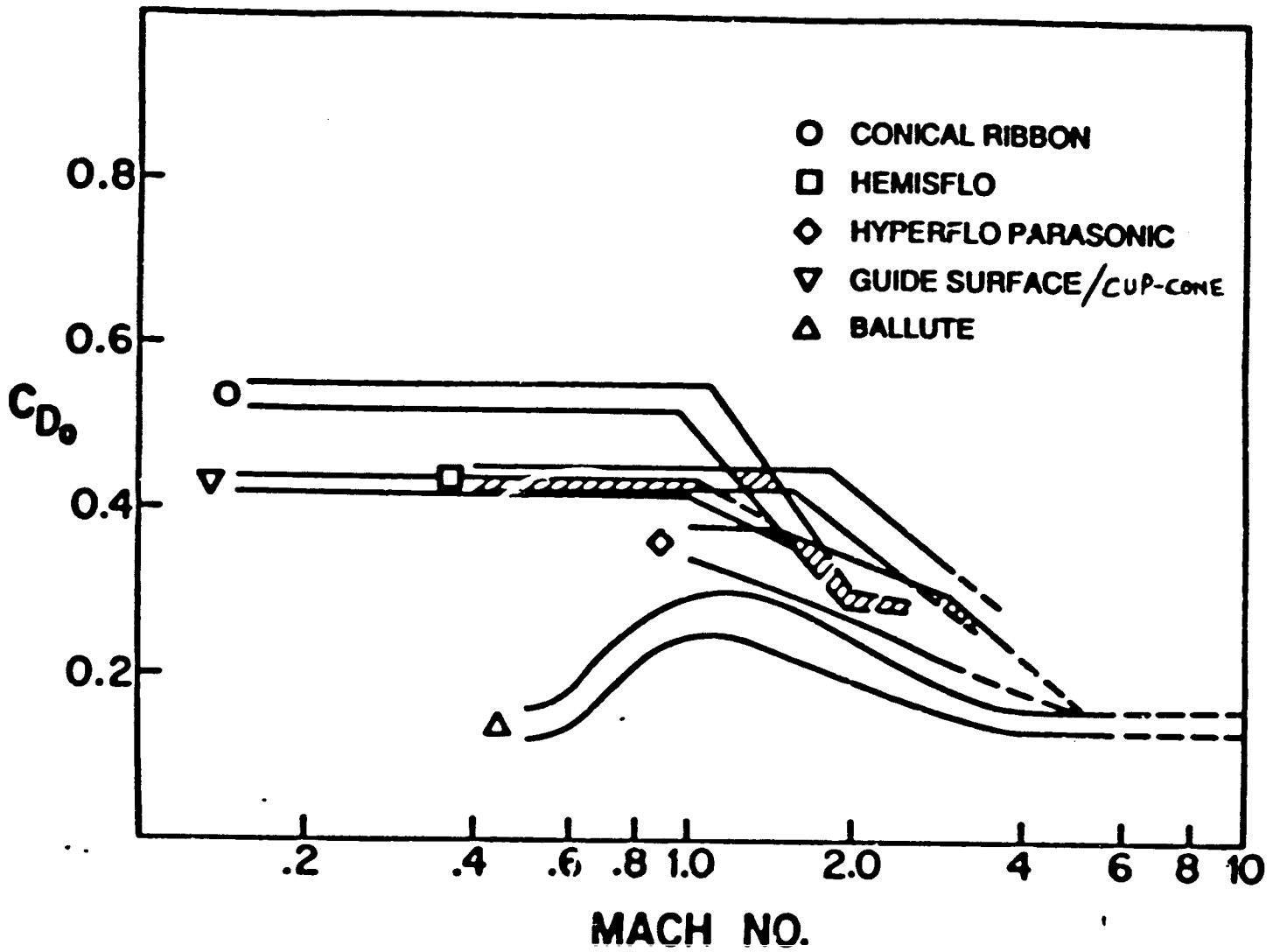
Figure D5: **DRAG COEFFICIENT C_{D_0} VS MACH NUMBER OF INFLATABLE AERODYNAMIC DECELERATORS**

(FROM PETERSON, C.W. , 1986)
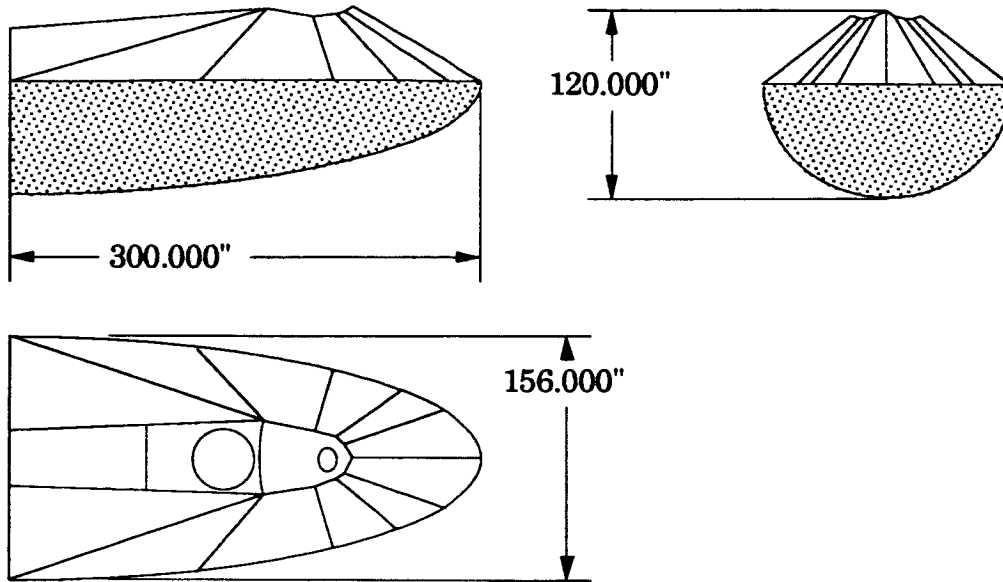
Figure E1:   Three View of Proposed Design

A PRELIMINARY INVESTIGATION OF AN ACRV BRAKING AND LANDING SYSTEM

Jeff Draper - Group leader

Dana Bowersox

Pat McGivern

John Milchuck

Karen Strouse

ACKNOWLEDGEMENTS

1.0 ABSTRACT

The Assured Crew Return Vehicle (ACRV) plays a vital part in securing the safety of the space station crew. Its mission is to provide a means of escape for the crew in the case of an emergency on the station. Proper operation of all ACRV subsystems is vital to its mission. The braking and landing subsystem of the ACRV is discussed in this report.

Once the ACRV has commenced its re-entry trajectory, an epoxy resin heat shield will protect it through atmospheric heating. Next, drogue parachutes will be deployed to stabilize the craft to ready it for parawing release. The parawing will give the system a lift-to-drag ratio of about 2.3 which will allow a wider choice of landing sites. Once the ACRV drops to about 10,000 ft., the heat shield will be discarded and will be decelerated by parachutes to land safely in the ocean. The ACRV itself can land on almost any available runway, but the preferred option is a military base due to the longer runways and better emergency medical support facilities.

TABLE OF CONTENTS

LIST OF SYMBOLS

A = Area

ACRV = Assured Crew Return Vehicle

AFE = Aeroassist Flight Experiment

ASTV = Aeroassist Space Transfer Vehicle

BP = Body Point

Cd = Drag Coefficient

Cl = Lift Coefficient

C_p = Specific heat at constant pressure

C_r = Char rate (mils/sec)

D = Drag

D_o = Nominal Parachute Diameter

ERE-1359 (RDGE) = Resorcinol diglycidyl ether

F = Adjustment factor for off-pitch planes

H_D = Decomposition enthalpy

H_g = Gas enthalpy

H_s = Stagnation point enthalpy

H = Free stream enthalpy

H_w = Wall enthalpy

IML = Inner Mold Line

L = Lift

NMA = Methyl norbornene-2,3-dicarboxylic anhydride

N_{uD} = Nusselt number

P_r = Prandtl number

P_s = Atmospheric pressure

R = Ellipsoid radius

R_e = Reynolds' Number

S = Wetted Area

S_t = Stanton number

SPRD = System Performance Requirements Document

T = Absolute temperature

T_{RE} = Radiation equilibrium temperature

TPS = Thermal Protection System

4

W	= Weight
g	= Acceleration of gravity
h	= Altitude
h	= Average convection coefficient
k	= Thermal conductivity of air
k_c	= Char thermal conductivity
m	= Mass
$\dot{m}_g$	= Gas mass loss rate
$\dot{q}_{BLK}$	= Blockage convective heating rate
$\dot{q}_{CHEM}$	= Chemical heating rate
$\dot{q}_{tot}$	= total heating rate
$\dot{q}_c$	= Convective heating rate
$\dot{q}_r$	= Radiative heating rate
$\dot{q}_{rr}$	= Reradiation heating rate
$\dot{q}_u$	= Recirculation zone heating rate
$t_{200°C}$	= Time for ablator to reach 200°C
$t_{1000°C}$	= Time for ablator to reach 1000°C
v_e	= Entry speed
v_∞	= Free stream velocity
x	= Ellipsoid position (ft)
x_{AFE}	= Aeroassist Flight Experiment Coordinate System
α	= Angle of Attack
γ_e	= Re-entry angle
θ	= Glide path angle
θ_t	= Time
ρ	= Density
ρ_m	= Density of ablator
ρ_∞	= Free stream density
σ	= Boltzman constant = 5.67×10^8 W/m^{2}k^4

LIST OF FIGURES AND TABLES

Table   Page

2.0 MISSION

The Assured Crew Return Vehicle (ACRV) will be an integral part of the space station rescue facilities. The primary mission of the ACRV is to return astronauts to Earth from the Space Station FREEDOM should an emergency arise. Scenarios where the ACRV might be required include emergency medical situations beyond the capabilities of the on-board medical personnel, catastrophic failure of space station systems, or failure of all manned space station rendezvous craft. In order to bring the ACRV crew safely back to Earth, a braking and landing system must be utilized.

There are many issues that must be considered during the design of the ACRV braking and landing system. Among them are the size constraints of the vehicle, the type and shape of heat shield used, the control of the vehicle at high and low altitudes, the type of landing the vehicle will execute, and the type of landing gear the ACRV will use.

The design requirements the ACRV must meet include an indefinite service life of not less than thirty years and the ability to maintain a quiescent state for the majority of that time. It must also be capable of being operated by a minimally trained crew with minimal ground support. Entry accelerations must be limited to four g's in the x direction, one g in the y direction and half a g in the z direction (see Figure 1). In the case of a medical emergency, one healthy crew member must accompany the injured person. For the healthy person, the impact acceleration limits are:[1]

15 g's with an impulse of 3 g-seconds in the x direction
10 g's with an impulse of 1 g-second in the y direction
5 g's with an impulse of 0.5 g-second in the z direction

8

For the injured person, the impact acceleration limits are:

10 g's with an impulse of 2 g-seconds in the x direction

3 g's with an impulse of 0.3 g-seconds in the y direction

2 g's with an impulse of 0.2 g-seconds in the z direction
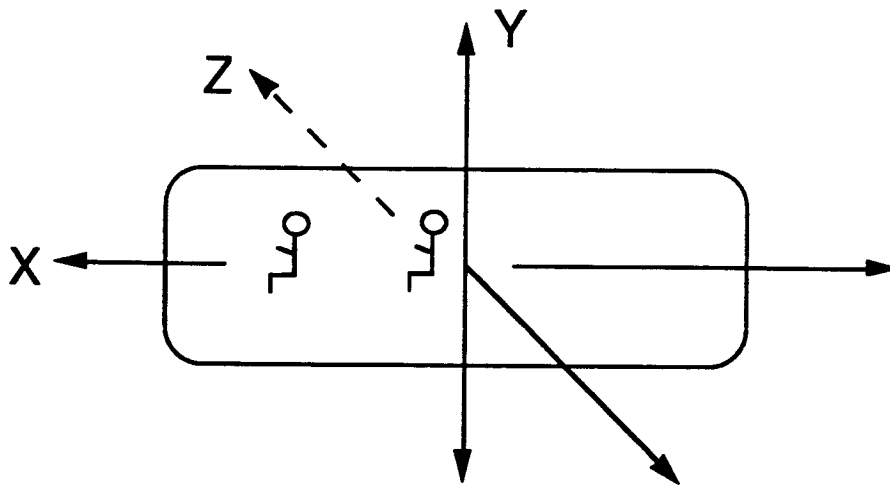
Figure 1: Axes directions for G-forces

3.0 DESIGN OPTIONS

Several braking and landing systems were considered before the present design was chosen. Winged lifting bodies, aerial retrieval, retro-rocket braking, and water landings were all considered at some point in the design process.

Initially, a winged lifting body similar to the North American X-15 was investigated. Although the space shuttle is the next generation of this type of vehicle, this amount of complexity is not required for the ACRV to complete its mission.

Aerial retrieval, although proven successful with a modified C-130 aircraft, was too complicated for this mission. The ACRV would have to be caught with a large hook hanging from the C-130. The main problems with this were the large moments experienced by the ACRV and the high potential for disaster if the connection failed.

Retro rockets were considered for a time to be the main deceleration device. Even though retro rockets will still be used in the ACRV design for separation from the space station, and deorbit control, the fuel cost (in weight and dollars) was too great for use as the primary decelerator.

Before enough evidence could be found to support a parawing ground landing, a water landing was an alternative landing choice. Depending on ground conditions and the nature of the emergency, mission controllers had the option of landing either on the ground or in the water. Land landings, although a bit more complex, are preferable to water landings since recovery forces are not needed and medical facilities are more accessible. Once it was demonstrated that the parawing gave the ACRV enough range to choose a suitable landing site, the water option was discarded altogether and the present system was chosen.

4.0 DESIGN DESCRIPTION

Once the decision is made to disengage the ACRV, the crew will
have two hours to actually depart from the space station. During this
time, the best landing site will be chosen, with weather being the main
consideration. The crew will then have six hours to position the craft for
deorbit, attain a semi-ballistic re-entry, and finally land at the
predetermined site.

The landing procedure includes parachute deployment and heat shield
separation at 15 km, and parawing deployment at 12 km. The parachute
deployment has a dual function. It provides enough drag to allow the heat
shield and the ACRV to separate. Once this separation is complete, the
parachute system helps slow ~~down~~ the ACRV ~~is vertical and horizontal~~
~~velocity~~. The heat shield also has a parachute system. After the heat
shield separates from the ACRV, it deploys a parachute that allows it to
land safely in the ocean.

After the ACRV has been decelerated by the parachute system, the
parawing is deployed. The parawing is used to make a controlled descent
for a safe landing at a pre-chosen landing site. The complete sequence is
shown in Figure 2.

To accomplish the described mission, the braking and landing design
incorporates a three chute conical ribbon system, a two-lobed flexible
parawing, and a detachable, modified ellipsoid heat shield (based on the
AFE Aerobrake.[13]) attached to an independent ACRV design. The ACRV will
be modified to include retractable landing gear for a rolling touchdown.
The parachutes and the parawing will be constructed of Kevlar and the
heat shield will be composed of a lightweight metal alloy structure
covered with a composite ablative material consisting of RDGE cured with

Parachutes deployed and
heat shield discarded at
15 km, 257.7 m/s.

De-orbit Initiation
120 km, 8 km/s.

Parawing Deployment

Heat shield lands
in ocean

ACRV Lands
on runway

Earth
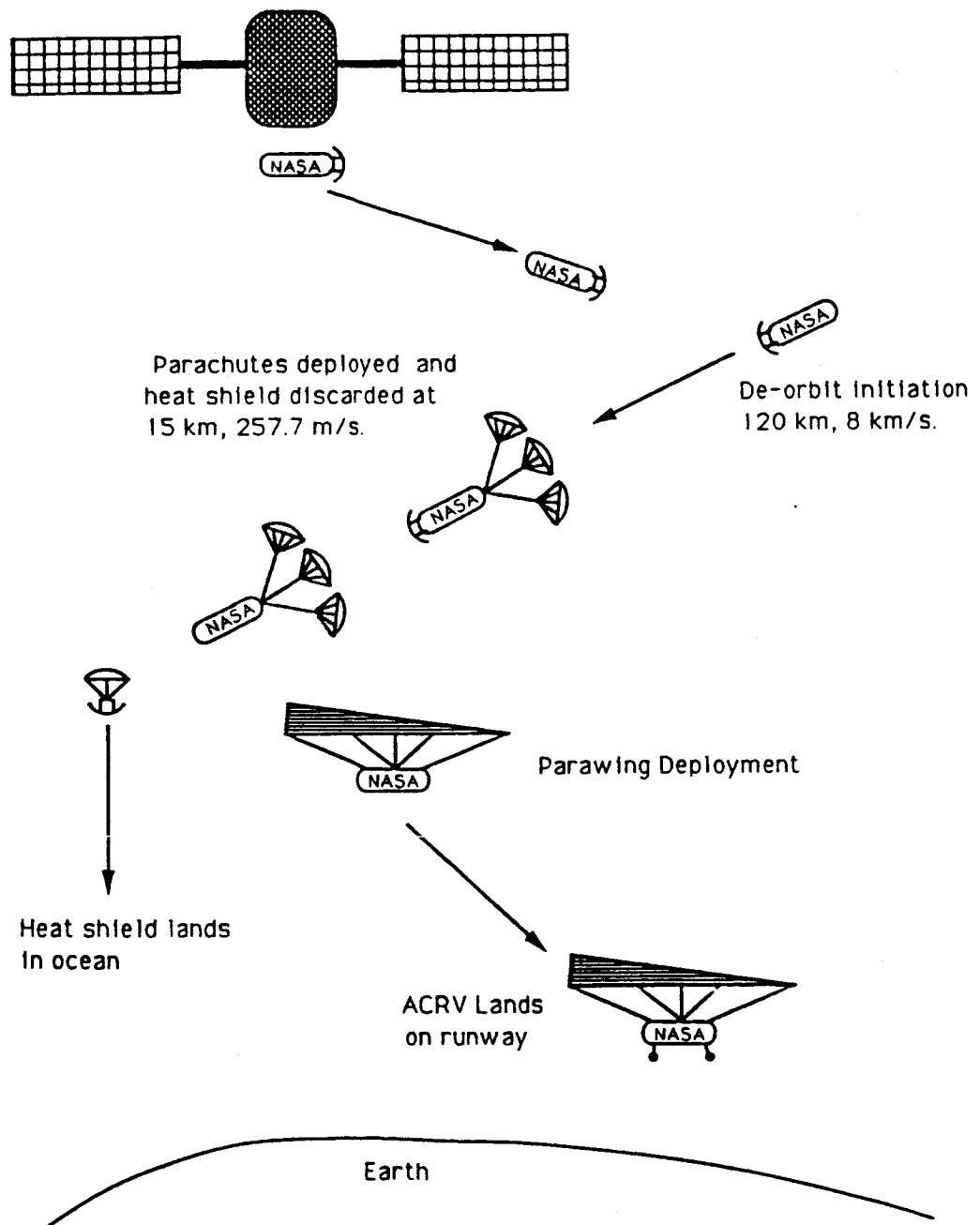
FIGURE 2: Braking and Landing Sequence

NMA. The landing gear will be based on a Learjet 24 & 25 series landing gear[29], and will be modified in a fashion similar to the Space Shuttle's to protect it from the space environment.

Several assumptions have been made in creating this design.

1. The ACRV can attain the desired orbital angle of inclination before reentry is initiated.
2. The vehicle weight is approximately 15,000 lbs (6804 kg).
3. The vehicle can be guided to within 60 km. of the landing site before parawing deployment.

5.0 RE-ENTRY

There are three major types of ballistic re-entry: the pure ballistic re-entry, the skip-ballistic re-entry, and a hybrid lifting-ballistic re-entry. The pure ballistic re-entry ignores any lift forces the vehicle produces and depends completely on the entry slope γ_e, and b, where b = (A*Cd)/W. For the pure ballistic re-entry, the Cd is assumed to be constant during the re-entry phase.[2] Consulting the study by Professor H. Buning's design team[2], it can be seen in Figure 3 that the calculated maximum decelerations for two values of γ_e and b exceed the requirements for the ACRV medical mission.[1]

	$\beta=.0001$	$\beta=.001$
$\gamma_e = -1°$	-7.8 g	-7.5 g
$\gamma_e = -2°$	-8.0 g	-8.1 g

FIGURE 3: Ballistic Re-entry g-forces

If the entry slope is numerically greater than -1°, the vehicle will skip off of the atmosphere and re-entry will not occur.

The advantages of a pure ballistic re-entry include:

1. simplicity due to the minimal maneuvering required
2. speed of re-entry (unlike other re-entry types, the pure ballistic re-entry requires no velocity vector changes and,

14

therefore, is the fastest method for deorbit.)

The disadvantages of a pure ballistic re-entry, not including the high g-forces mentioned earlier *are*

1. the inability to maneuver to correct errors in the re-entry trajectory

2. a limited landing window due to the lack of maneuverability

The second major ballistic re-entry type is the skip-ballistic. In this method, the vehicle's lift is used to help create the trajectory. As the vehicle enters the atmosphere, the magnitude of the velocity begins to decrease due to aerodynamic friction, and the direction of the velocity is changed due to the lift created by the vehicle. By changing the velocity vector in a specified direction, the vehicle exits the atmosphere and re-enters an Earth orbit. While the vehicle is out of the atmosphere, it is cooled through thermal radiation.[2] The vehicle then re-enters the atmosphere and repeats the maneuver until the *speed* is small enough that the vehicle cannot escape the atmosphere. At this point, the vehicle assumes a pure ballistic re-entry.

The two main advantages of the skip-ballistic re-entry are:

1. the reduced heating of the vehicle

2. the increase in downrange allowed by the re-entry

The main disadvantages of the skip-ballistic re-entry are:

1. increase in re-entry time over pure ballistic

2. large g-forces involved (the vehicle still enters ballistically and therefore is still subjected to ballistic g-forces)

3. repeated g-forces due to multiple atmospheric re-entries.

15

The third type of ballistic re-entry is the hybrid lifting-ballistic re-entry. By modifying the vehicle shape to increase the L/D, the vehicle's lifting vector direction can be controlled, which helps to decrease the velocity and increase the size of the landing footprint. By increasing the L/D, the maximum g-forces experienced are decreased when the vehicle follows a linear path. If the vehicle deviates from a linear path due to a banking maneuver, the maximum g-forces experienced rise due to the loss of vertical lift.[2] Banking is the term used to describe a directional change during re-entry. This is used to further decelerate the vehicle.

By using a shallow re-entry angle, the vehicle will experience a lower maximum deceleration, larger crossrange and downrange, and will require a shorter burn for re-entry to occur. Figure 4 shows how the lifting-ballistic re-entry improves the maximum deceleration g-forces over the pure ballistic re-entry for an initial re-entry altitude of 120 km and an initial re-entry velocity of 8 km/s. From this it can be seen that the g-forces are within the limits set by the ACRV requirements.[1] Figures 5 through 7 show the pertinent data, in graphical form, for a lifting-ballistic reentry with $\gamma = -2.0^\circ$ for the ACRV. This data was calculated using the Re-entry Characteristics Program found in Appendix A. This program, which is written in Fortran-77, uses a fourth order Runge-Kutta subroutine to numerically calculate the velocity, altitude, re-entry angle, and heating rates on the heat shield as a function of time.

g (deg)	V max G (km/s)	G's max	Alt max G (km)	Reentry Time (sec)
-1	2.61	2.42	43.23	6331
-2	3.97	2.53	49.00	771
-3	3.25	2.88	45.17	611

FIGURE 4: Lifting-Ballistic Re-entry Parameters
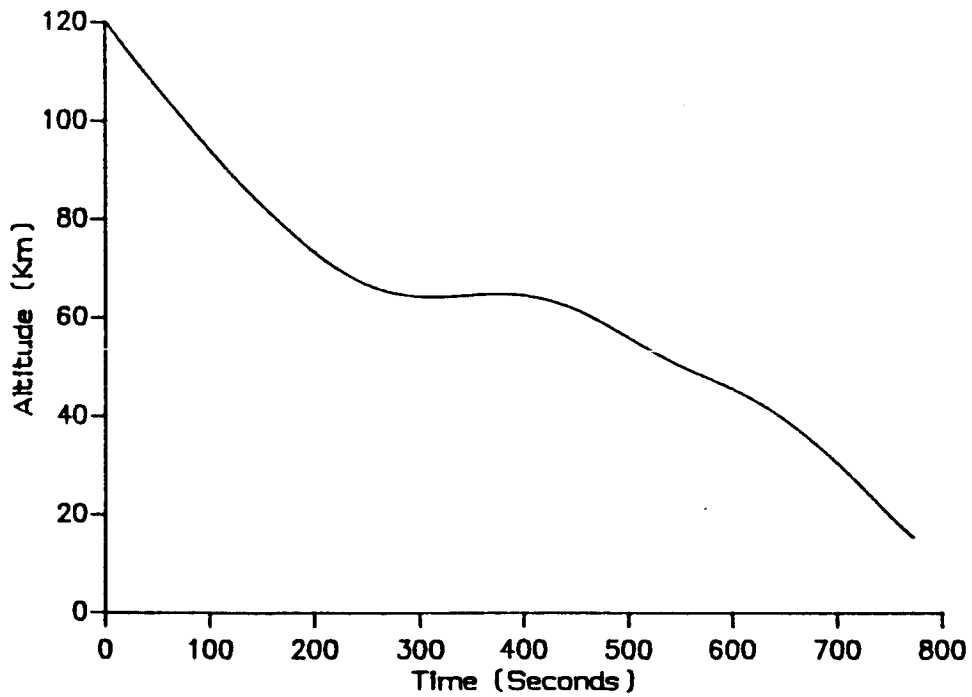
FIGURE 5: Altitude vs. Time for ACRV Re-entry
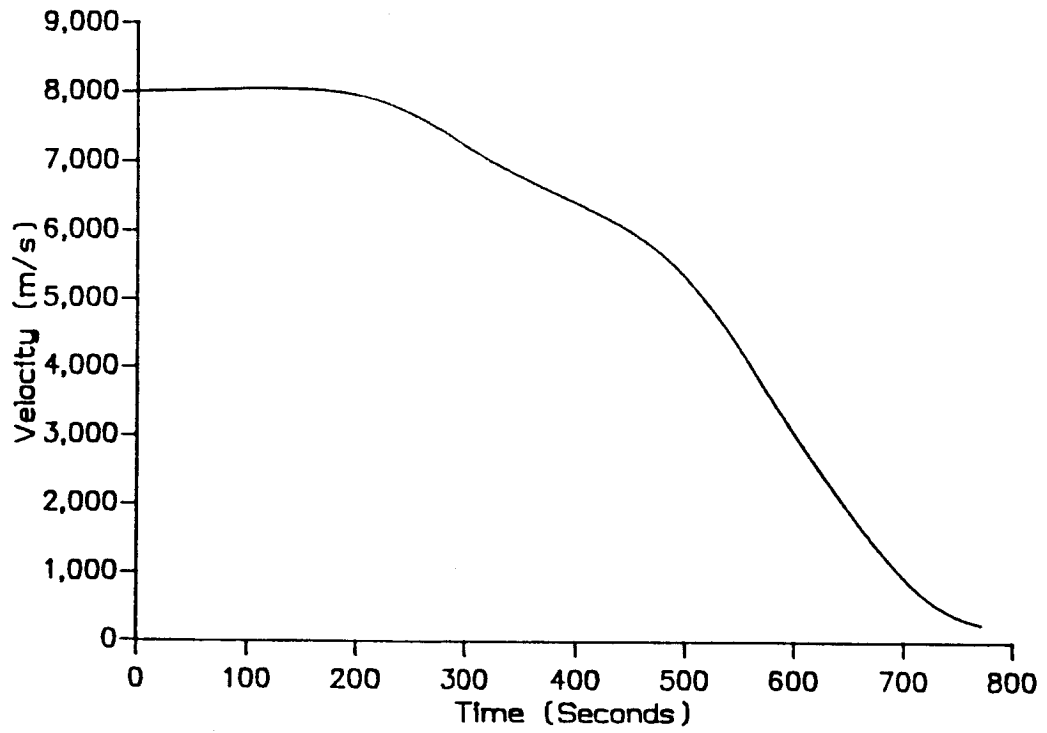
FIGURE 6: Velocity vs. Time for ACRV Re-entry
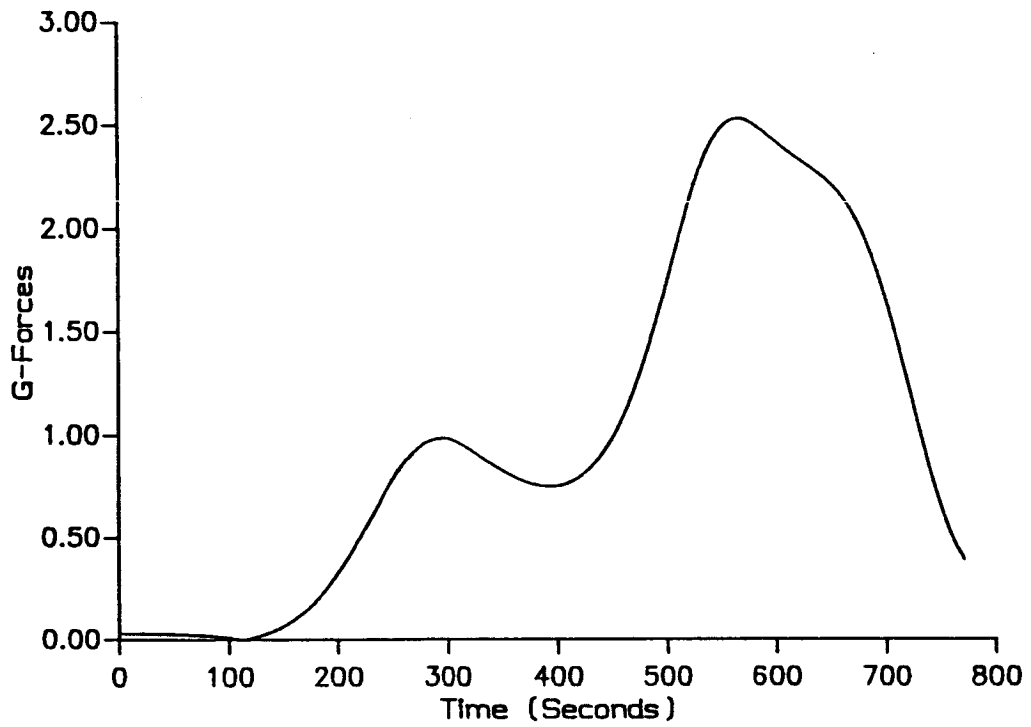
FIGURE 7: G-forces vs. Time for ACRV Re-entry

18

In summary, advantages of the hybrid lifting-ballistic re-entry are:

1. decreased maximum decelerations
2. increased crossrange and downrange
3. increased maneuverability

The disadvantages of the lifting-ballistic re-entry are:

1. large probability of error in re-entry trajectory due to high
    sensitivity to small changes in the re-entry angle.
2. increased re-entry time due to the lift generated and the
    banking and turning in the maneuver

Another re-entry type uses a lifting body. A lifting body presents
the most flexible means of crew return because of its ability to free
itself from a ballistic trajectory. By being able to produce lift, a lifting
body is not only more controllable but also offers the advantage of
reducing g-forces on the crew. Other advantages of this concept are:

1. a more flexible re-entry trajectory
2. wide choice of landing sites
3. the ability to change landing sites in the event of weather
    changes or mechanical malfunctions

The benefits of this concept would make it appear that lifting bodies
are the best overall re-entry vehicle type. However, several
disadvantages inherent to the concept have to be considered. These are:

1. increased expense due to vehicle size
2. increased complexity due to the amount of controls needed
3. heavy protection needed against heating on re-entry due
    to increased drag from a lower re-entry angle

19

For return with healthy crew members, the pure ballistic re-entry could be used, but the ACRV must also be designed for use with injured or sick crew members. The g-forces specified by NASA in the SPRD for the medical mission are much lower than the g-forces that the pure ballistic re-entry creates, precluding its use. The skip-ballistic re-entry is also discarded for the same reasons, in addition to the frequent atmospheric exits and entries exerting considerable forces on the vehicle. The lifting body re-entry is better than both the pure and skip-ballistic re-entries because the g-forces created by this method are well within the limits set by NASA, but because of the complexity of the control systems and the body shape needed, it is also discarded.

It becomes apparent that the hybrid lifting-ballistic re-entry method is better suited for the ACRV mission than the other three. It is much simpler to use than a lifting body re-entry, and it has much lower g-forces than the other ballistic re-entry types.

6.0 SUBSYSTEMS

There are six major subsystems included in the braking and landing system design, which are the heat shield, the parachutes, the parawing, the landing gear, the strut design, and the control systems.

HEATSHIELD

As the ACRV enters the Earth's atmosphere from space, it will have a significant amount of kinetic energy. Initially, a shock wave will form at the nose of the vehicle causing an increase in its temperature. Moving further into the atmosphere, the ACRV's speed will be reduced by the braking force of the atmosphere. This kinetic energy will be converted into heat on the ACRV. The control or severe reduction of this heat transfer is a main concern in the design process to safely return the vehicle to Earth.

There are basically two ways of diverting large amounts of heat away from the vehicle: composite tiles such as those found on the space shuttle or an ablative heat shield similar to the one used on the Apollo capsule. The main advantage of selecting tiles as a thermal protection system is their reusability; however, since this design of the ACRV incorporates an expendable heat shield, the reusability advantage of the tiles becomes insignificant. The choice of an expendable heat shield was made after analyzing the various effects of heating on the type of re-entry. Although heating is excessive for ballistic re-entry, it does not occur for an extended period of time which reduces the total heat transfer rate. Therefore, a ballistic type re-entry was chosen with an expendable heat shield to reduce weight after the heating effects become insignificant.. Since tiles were eliminated as a possible heat shield material, the other solution is an ablative heat shield.

Ablation is an orderly heat and mass transfer process in which a large amount of thermal energy is expended by sacrificial loss of surface region material. Heat from the re-entry is absorbed, blocked, and dissipated. These mechanisms are shown in Figure 8 for an ablating glass fiber-reinforced phenolic resin composite used on the Gemini capsule.[2] They involve heat conduction into the material substrate, thermal storage by the material's heat capacity, material phase changes such as melting and vaporization, convection and chemical reactions. These energy absorbing processes occur automatically, control surface temperature, and restrict inward flow of heat.
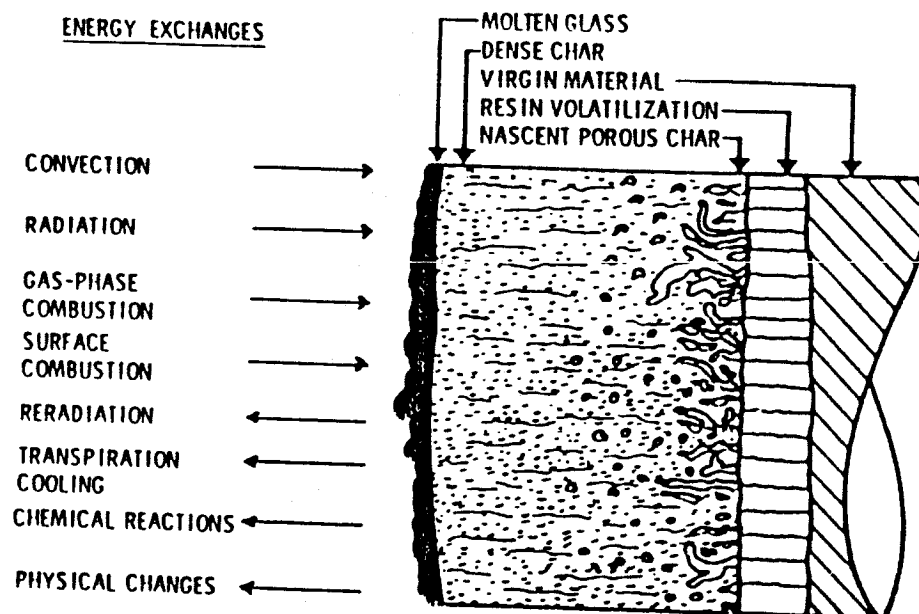
FIGURE 8: Energy Dissipation of an Ablating Phenolic-Glass Composite
(D'Alelio, G. F. Ablative Plastics)

The ablation material can be composed of several different composites. One type of ablative material frequently used in very high temperature re-entry vehicles is polymers. Polymers are used because of the critical need for weight economy in aerospace applications and the frequent inability of other engineering materials to satisfy all the design requirements. To date, polymeric composites have successfully provided environmental protection for hypersonic flight vehicles such as missile nose cones, orbital entry data capsules, lifting and non-lifting manned vehicles, winged spacecraft, and planetary atmospheric probes.[3]

Various classes of polymeric materials have been utilized for ablative thermal protection. The optimum design of a polymeric heat shield strongly depends on the particular mission for which it is intended. Selecting the right polymer that will satisfy a wide range of operational system requirements is dependent on detailed thermal, chemical, and mechanical aspects of the time-dependent environment. Another aspect important to the mission is cost. Because most of the polymeric materials used in present ablative thermal protection systems were originally developed for other purposes, their costs have been relatively low. For example, branched polyphenylene resin which was originally sold for $2300/lb now costs about $100/lb because of improved plant production and increased use.[2] However, some high performance polymers still tend to be expensive and involve large manufacturing process costs. Designing with these materials is justified when the system requirements are critical, weight is of the utmost importance, and/or the part is reasonably small, as in the case of the ACRV's heat shield. Therefore, the goal is to design a heat shield composed of a polymer which satisfies the mission requirements and is reasonably priced.

Because weight is major design consideration, low-density ablators were studied. The two most important characteristics of a heat shield material are its overall heat capacity and its ability to form substantial amounts of strong carbonaceous char. The char is formed as a compound due to the high temperature. Table 1 lists three commonly used ablators and their composition.[2] Reviewing this table, one can see that the epoxy-novolac resin with the lowest density and high specific heat to absorb energy would be the optimal choice. This same compound was used on the

Material composition	Phenolic-25%, phenolic microspheres-25%, nylon powder-50%	Epoxy-novolac-38%, phenolic microspheres-44%, silica fibers-9%, glass fibers-9%	Silicone-66%, microspheres: phenolic-16%, glass-10%, quartz fibers-7%, silica powder-1%
Density, lb/ft^3	37	24	42
Tensile strength, psi	1000	640	167
Tensile elongation at failure, psi	0.9	2.9	5.0
Tensile elastic modulus, million psi	0.125	0.040	0.005
Specific heat, Btu/lb-°F	0.38	0.46	0.37
Thermal conductivity, Btu/hr/ft^2/°F/ft	0.07	0.04	0.07
Thermal expansion coefficient, 10^6 in/in/°F	30.5	17.1	44.0

Table 1: Properties of Low-Density Ablators
(D'Alelio, G. F., Ablative Plastics)

Apollo capsule. As shown, the epoxy-novolac resin satisfies the requirement of a high heat capacity; however, it lacks the appropriate char yield for the mission. There are several reasons why the formation of a strong char layer is essential. First, aerodynamic considerations often require that the dimensional configuration of the heat shield be maintained. Second, the char itself is a good insulator by virtue of its heat capacity. Because of the recent advancements in polymers, several epoxy resins that have the low density of the epoxy-novolac resin and higher char yields were researched.

Several resins are listed in Table 2 in the order of increasing char yield and overall ablative performance.[2] The indicated break shows where two and threefold improvements or greater are observed. One can progress from a subliming or clean melt-type ablator to a high char yield ablator by simply going from top to bottom of Table 2. In the ablative testing of the high-char yield resins, none performed better than RDGE.

Ablator	Trade name	Chemical type	Supplier
Low-char ablators	ERL-4201	Cycloaliphatic	Union Carbide
	Epon 871	Aliphatic	Shell Chemical
	ERLA-0100	Cycloaliphatic	Union Carbide
	Epon 828	Bisphenol-A-epichlorohydrin condensate	Shell Chemical
	KER 997A	Polyglycidyl ether of orthocresolformaldehyde novolac	CIBA
	Kopox 170	Polyglycidyl ether of polyhydroxy terphenyl	CIBA
	DEN-438	Polyglycidyl ether of phenolformaldehyde novolac	Dow Chemical
	ERE-1359	Resorcinol diglycidyl ether	CIBA
	Kopox 171	Triglycidyl ether of trihydroxy biphenyl	CIBA
Char-forming ablators	Epon 1031	Tetraglycidyl ether of tetraphenylene ethane	Shell Chemical

(left margin: Increasing ablative performance)

Table 2: Effect of Epoxy Resin Structure on Ablative Performance
(D'Alelio, G. F., Ablative Plastics)

25

Another important design choice is the curing agent that will be used with the resin. Table 3 gives the ablative performance of various curing agents with RDGE.[2] The best curing agent in terms of char forming is NMA. Figure 9 shows the back face temperature (the temperature of the structure below the virgin polymer) as a function of time for three resins cured with different agents. The melt, or sublime-type ablator such as Teflon, shown as an aliphatic epoxide in the figure, is noted for high erosion rates, but extremely low thermal conductivity, hence low back-face temperature rise until burnthrough. Therefore, the design of the ACRV's heat shield needs a higher char forming resin with less emphasis on back-face heating.

Also shown in Figure 9 is the advantage of an NMA-cured epoxide resin to the conventional phenolic used on the Apollo capsule. For a given type of reinforcement, the phenolic and epoxy resin will differ in the thermal conductivity. Because the epoxy resin has a lower thermal conductivity, a twofold increase in thermal protection is present. Therefore, the resin with the best curing agent in terms of char-yield and thermal protection would be RDGE with NMA. Thus, the ablator used on the Apollo made up of 38% Epoxy novolac, 44% phenolic microspheres, 9% silica and 9% glass fibers, will be replaced with 38% RDGE, 44% NMA, and 9% silica and 9% glass fibers for the ACRV design.

After selecting RDGE cured with NMA, three characteristics that determine the ablator's effectiveness were investigated: its percent weight of the ablator loss, char rate, and insulation time. Shown in Figure 10 is a thermogram of RDGE cured with NMA and cured with two other Dielser-Alder adducts (a type of chemical bond).[12] It interesting to note how the thermal degradation is controlled over a wide temperature range

Ablator	Abbreviation	Chemical name	Supplier
Low-char ablators	TETA	Triethylene tetramine	Eastman Organic
	MPDA	m-Phenylene diamine	Eastman Organic
	DADPS	p,p'-Diamino diphenyl sulfone	Shell Chemical
	MD	p,p'-Methylene dianiline	Allied Chemical
	THPA	Tetrahydrophthalic anhydride	Baker
	TMA	Trimellitic anhydride	Amoco
	BF₃MEA	Boron trifluoride monoethyl amine	Shell Chemical
	BTCD	3, 3', 4, 4'-Benzophenone Tetracarboxylic dianhydride	Gulf Oil Corp.
Char-forming ablators	NMA	Methyl norbornene-2, 3-dicarboxylic anhydride	Allied Chemical

Increasing ablative performance.

Table 3: Effect of Epoxy Resin Curing Agent Structure on Ablative
Performance
(D'Alelio, G. F., **Ablative Plastics**)
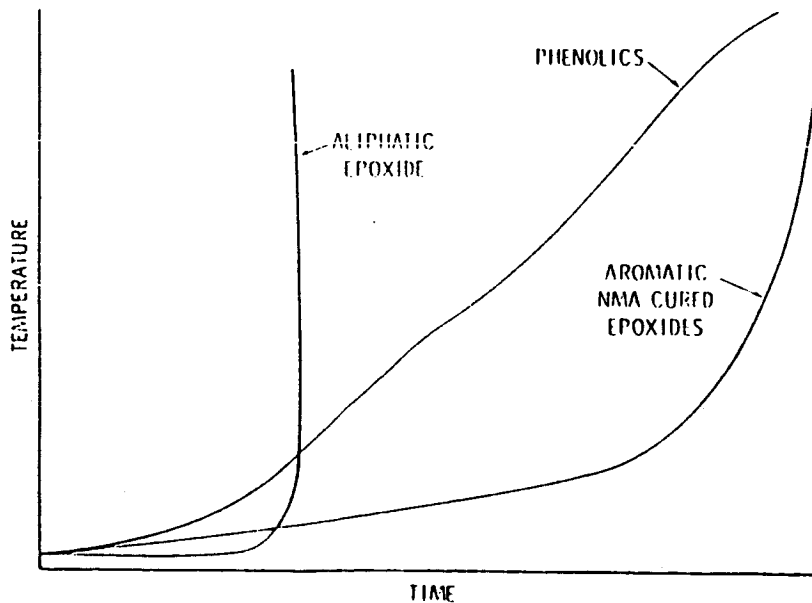
Figure 9: Typical Time-Temperature Curves for Ablating Materials
(D'Alelio, G. F., Ablative Plastics)

27
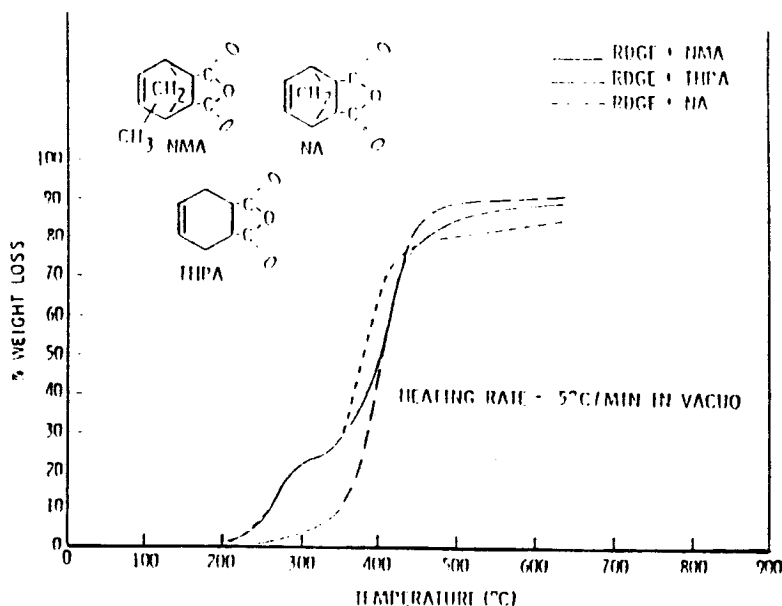
FIGURE 10: Thermograms of resorcinol diglycidyl ether cured with several
Diels-Alder adducts
(D'Alelio, G. F., Ablative Plastics)

from the initiation of degradation to the point where the rate of weight

loss is approaching zero. The char rate (C_R) is given as the rate of

recession of the pyrolsis zone into the virgin polymer. These two regions

are shown in Figure 11[12]. The char rate for RDGE cured with NMA and

several Dielser-Alder adducts is shown in Figure 12[12]. The $t_{200°C}$ and

$t_{1000°C}$ shown in Figure 12 are the times required for a thermocouple,

embedded 0.9525 cm behind the original front face, to sense the

temperatures of 200°C and 1000°C. Therefore, a large $t_{200°C}$ or $t_{1000°C}$

is desirable because it will take a significant amount of time to reach

that temperature resulting in a better blockage of the heat transfer. Note

that RDGE cured with NMA has the highest $t_{200°C}$. Table 4 shows various

28
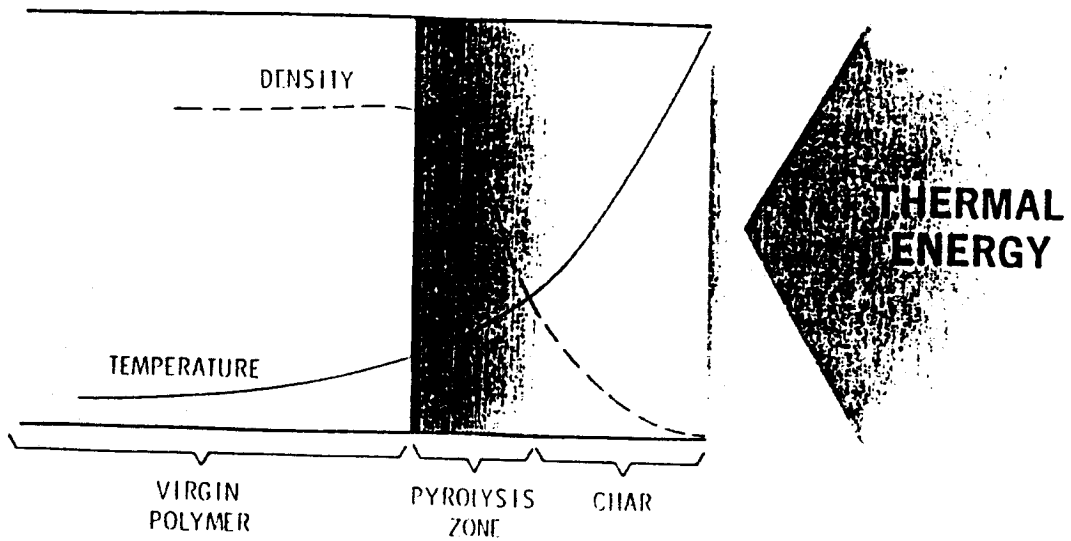
FIGURE 11: Typical temperature and density profile in a charring ablative body
(D'Alelio, G. F., Ablative Plastics)
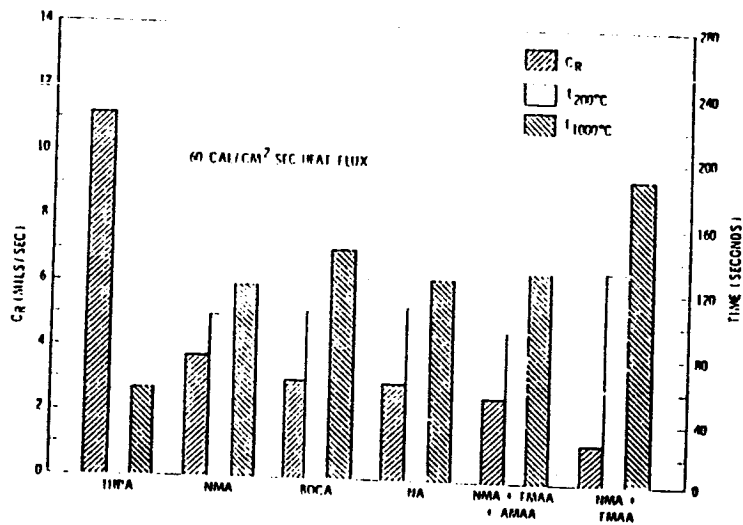
FIGURE 12: Ablative performance data for resorcinol diglycidyl ether cured with several bridged Diels-Alder adducts (20% SiO_2)
(D'Alelio, G. F., Ablative Plastics)

$$\underset{O}{\overset{/\ \backslash}{CH_2}}-CH-CH_2\left[-R-CH_2-\underset{OH}{\overset{|}{CH}}-CH_2----\right]_{\overline{n}}R\ \underset{O}{\overset{/\ \backslash}{CH_2}}-CH-CH_2$$

R	Chemical name	% Char at 700°C (NMA-cured)	$t_{200°C}$ (sec)
(1) Nature of the aromatic nucleus			
(a)	Diglycidyl ether of hydroquinone	14	86.0
(b)	Diglycidyl ether of p, p'-biphenol	15	86.0
(c)	Diglycidyl ether of 1,5-naphthalene diol	18	85.0
(2) Position of attachment of the glycidyl group			
(a)	Diglycidyl ether of hydroquinone	14	86.0
(b)	Resorcinol diglycidyl ether	10	100.6
(a')	Diglycidyl ether of 2,7-naphthalene diol	11	44.0
(b')	Diglycidyl ether of 1,5-naphthalene diol	18	85.0
(c')	Diglycidyl ether of 1,6-naphthalene diol	17	63.0

TABLE 4: Effect of Epoxy Resin Structure on Char Formation
(D'Alelio, G. F., Ablative Plastics)

glycidyl groups and their attachments.[12] Note that RDGE has the largest $t_{200°C}$ and the lowest percent char at 700°C indicating a good ablator.

The question of weight and cost must be addressed. The RDGE ablator's density is 400.55kg/m^3, less than that for the Apollo ablator. Based on a vehicle the size of Apollo, it would have a weight between 400 kg and 450 kg. Although the ACRV weight is larger, the RDGE ablator is still significantly lighter than most polymers. In terms of cost, the justification of using a polymer that can satisfy the weight and thermal requirements has already been presented. Although the cost of the RDGE ablator (approximately $200/lb) is significantly higher than other polymers due to its innovative design, the benefits far outweigh the cost.[2]

The structural integration of the heat shield is shown in Figure 13.[2] The double wall composite is used in most heat shield designs where high reliability is of the utmost importance. The integrated wall is a lightweight structure because the heat shield and load-bearing substrate are combined into a single unit, without the use of an adhesive bond to join them together. For the ACRV heat shield design, the integrated wall will be used, because safety is increased due to the disintegration of fewer bonding agents. After considering the type of ablator and its connection to the substructure, the shape of the heat shield was studied. The design chosen was from the Aeroassist Flight Experiment Aerobrake (AFE) and is shown in Figure 14.[13] The AFE vehicle, to be launched and recovered by the space shuttle, will collect atmospheric entry aerothermodynamic environment data for future Aeroassist Space Transfer Vehicle (ASTV) designs as shown in Figure 15.[14] This shape was selected because the design incorporates a reduced heating rate with its modified ellipsoid

31

Composite Construction

Integrated Wall

Single Wall Composite

Double Wall Composite

Labels: Ablator, Bond, Substructure, Honeycomb, Fibrous Insulation, Honeycomb Pressure Shell
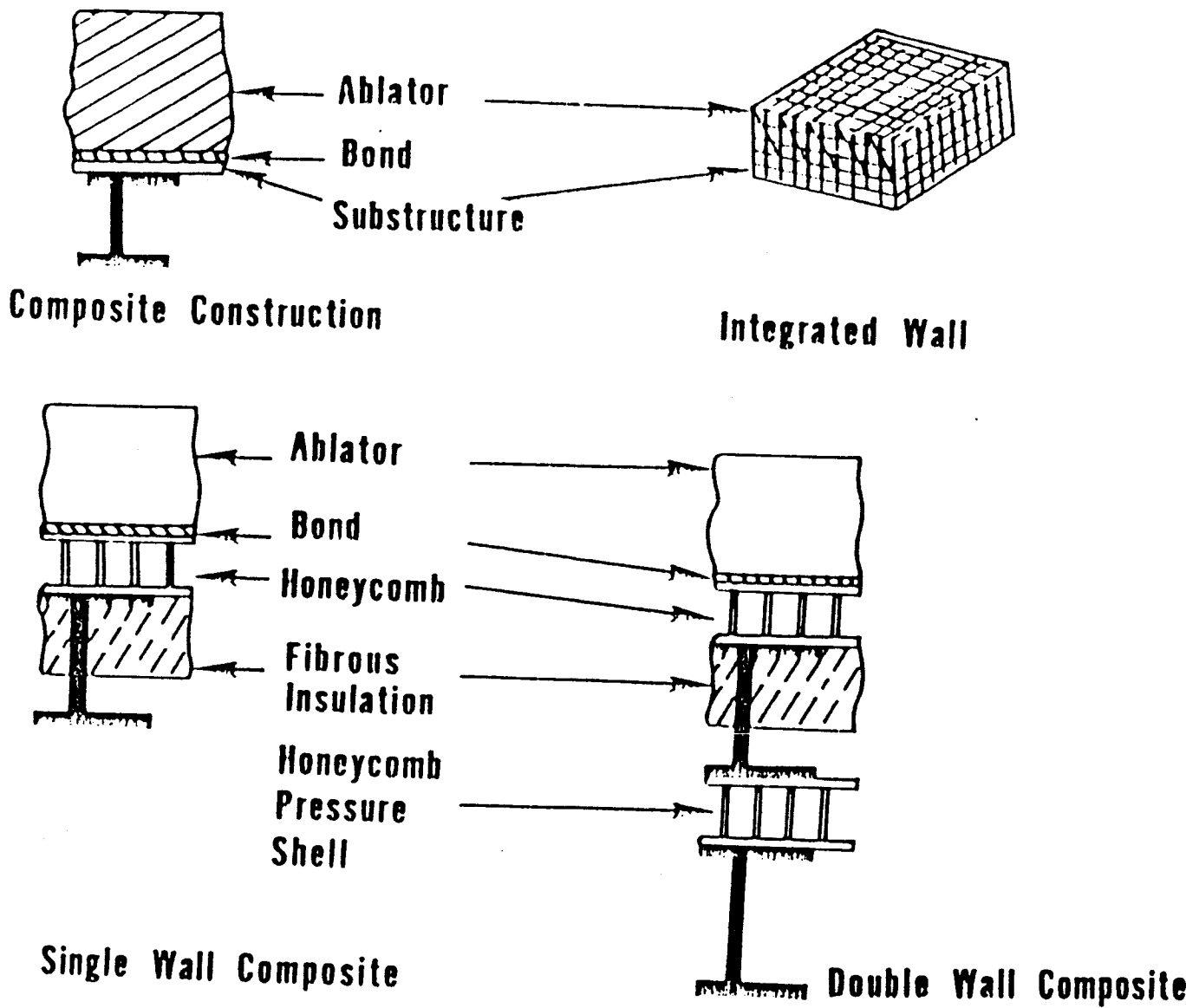
Figure 13: Ablative Heat Shield Constructions
(D'Alelio, G. F., Ablative Plastics)
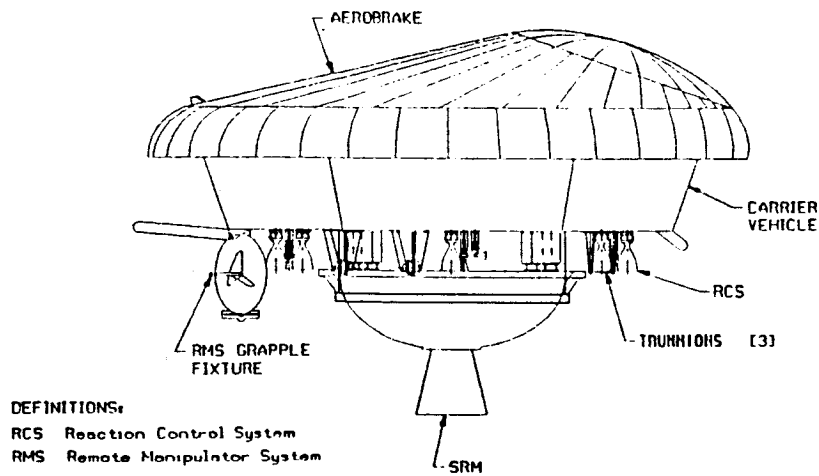
FIGURE 14: AFE Aerobrake

(Curry, D. M., 'Program Requirements for the AFE Aerobrake')
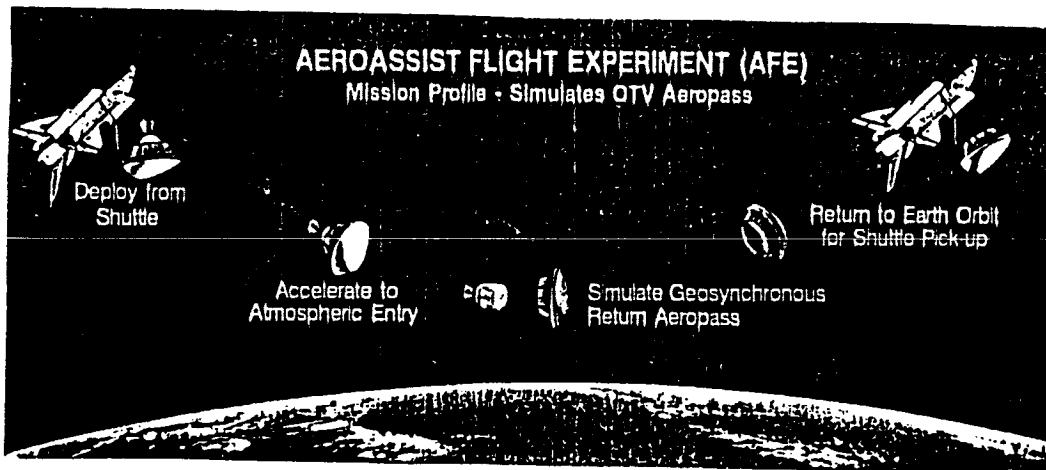
FIGURE 15: AFE Mission Profile

(Colovin, J. E., 'Development of AFE Aerothermodynamic Data Book')

33

base and because of its ease of integration into the space shuttle's cargo bay as shown in Figure 16.[13] The AFE coordinate system (x_{AFE}) shown in Figure 16 is useful when orienting the Aerobrake to the ACRV or to the space shuttle. The origin of this coordinate system is located 2.54 m below the center of the circle formed by intersecting the cone and skirt section as shown in Figure 16. The three views of the AFE vehicle are shown in Figure 17 which shows an overall diameter of 4.2672 m and depth of 0.9144 m.[15] Note that the body point (BP) numbers given on the AFE in Figure 17 are reference points used for heating analysis.

The baseline design of the Aerobrake heat shield structure is a conventional aluminum skin and stringer construction as shown in Figure 18.[13] Basically, the structure consists of an aircraft-type skin, a stringer, a rib, and a frame construction. The three skin areas are shown Figure 18. Skin area 1 is the ellipsoid nose part of the aerobrake where maximum heating occurs during re-entry, skin area 2 is the elliptical cone section of the Aerobrake, and skin area 3 is the skirt of the Aerobrake. The skin is riveted onto the structure in these three basic geometric areas and serves as the inner mold line (IML) for the thermal protection system. The 60° angle of the ellipsoid part as shown in Figure 18 is important because it determines the 1.8923 m base dimension. The aluminum structure has a maximum use temperature of 176.67°C.

To design an ablator with a certain thickness to reduce the back-face temperature on the aluminum to less than 176.67°C, a knowledge of the heating rates encountered on the re-entry trajectory is required. The trajectory is a function of vehicle configuration and weight as well as its
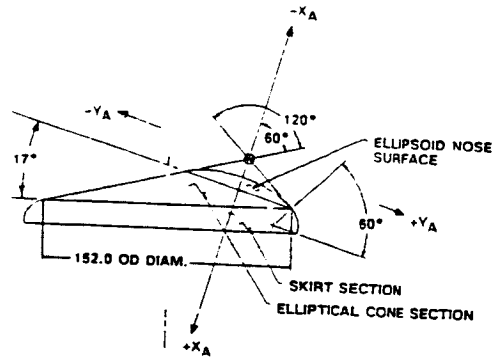
(a) Aerobrake (X_A) coordinate system.
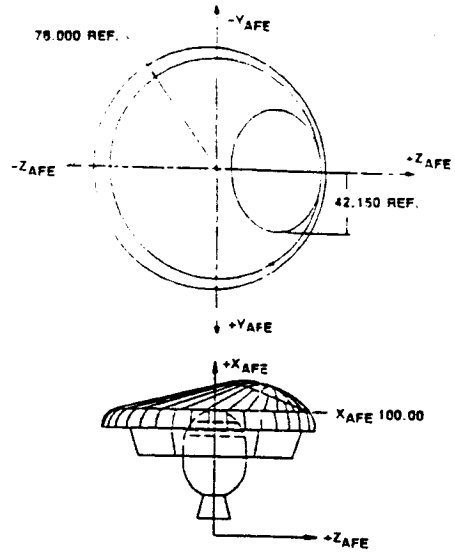
(b) AFE (X_{AFE}) coordinate system.
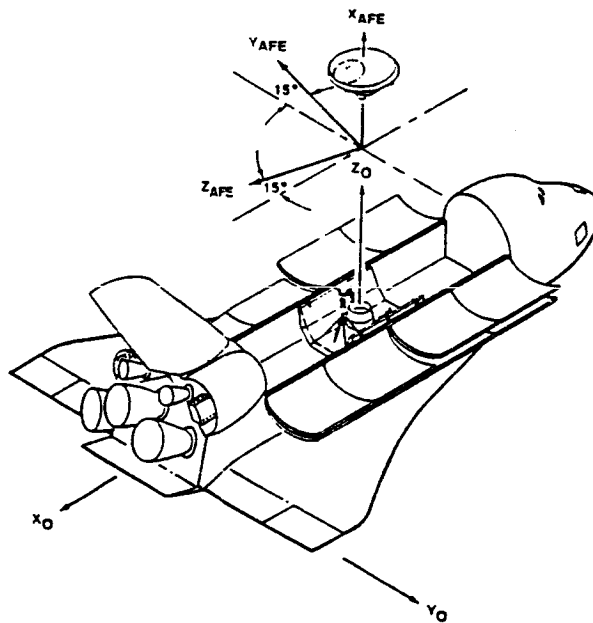
(c) Orbiter (X_O)/AFE(X_{AFE}) coordinate system relationship.

FIGURE 16: Aerobrake/AFE/Orbiter coordinate system relationship
(Curry, D. M., 'Program Requirements for the AFE Aerobrake')

35
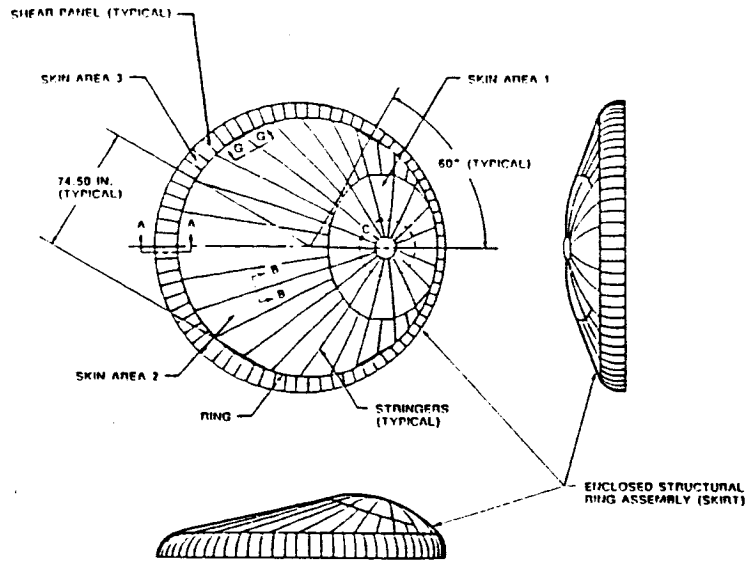
FIGURE 17: AFE Vehicle configuration
(Bouslog, S. A., 'Aerobrake Heating Rate Sensitivity Study for the AFE')
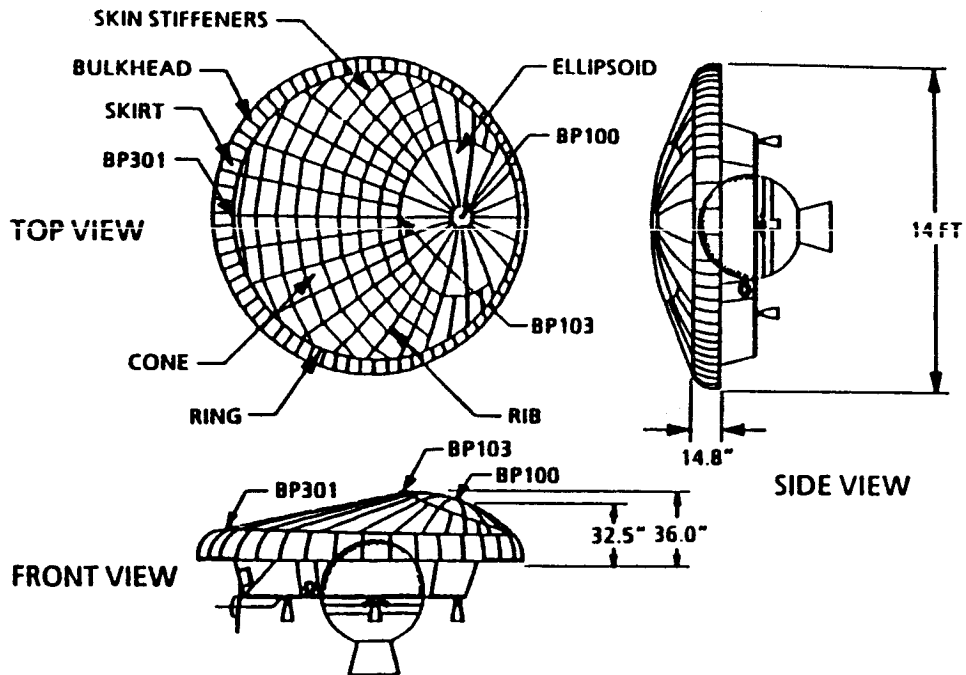
FIGURE 18: Aerobrake Structural Configuration
(Curry, D. M., 'Program Requirements for the AFE Aerobrake')

initial entry angle and speed. Figure 19 shows the predicted aero-thermodynamic environment of the stagnation region on an Apollo-type configuration.[16] The diameter of 4.2 m of the vehicle is similar to the AFE heat shield diameter of 4.2672 m. The range in entry speeds in Figure 19 was chosen to include entries from Earth orbit to a returning Mars mission. The trajectories were chosen so that peak heating occurs at an altitude of 61 km. The lower curve represents the dependence of convective heating rate on entry speed. The upper curve includes the contribution from the radiation of the species in the shock layer. Radiation becomes more dominant at higher speeds. Also note that in Figure 19 the thermodynamic state of the gas in the boundary layer, as characterized by the stagnation point pressure and temperature, is indicated along the abscissa.[16]
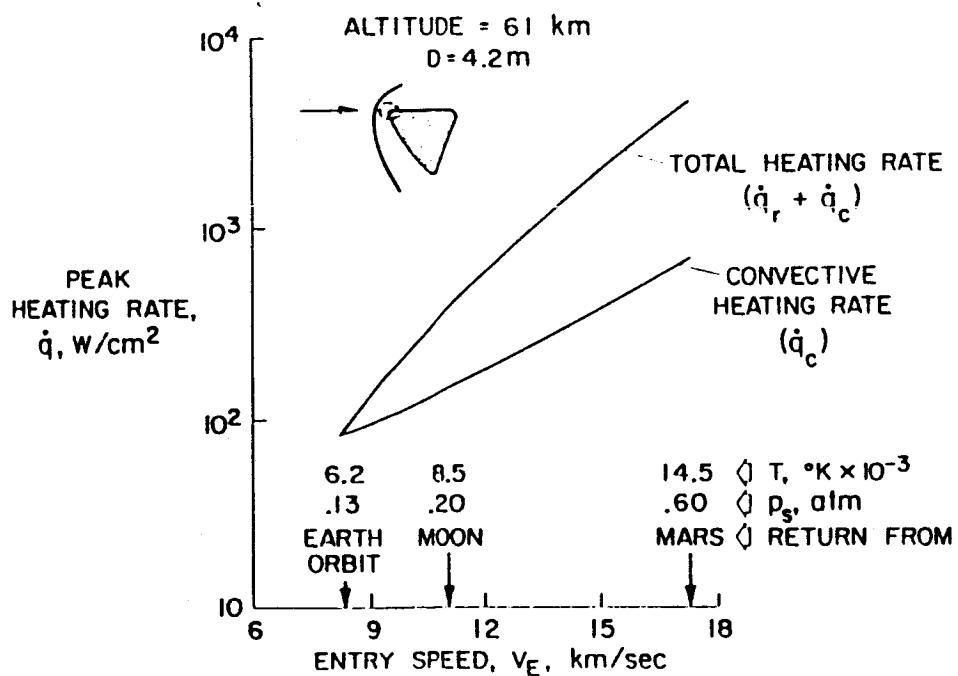
FIGURE 19: Aerothermodynamic environment encountered by a manned spacecraft during entry into the Earth's atmosphere
(D'Alelio, G. F., Ablative Plastics)

A more thorough analysis of the aerothermodynamic environment on the AFE was conducted. This analysis depends on the ACRV's calculated velocity as a function of time as shown in Figure 6. These heating rates were investigated for the stagnation region, since this area is critical. From Re-entry Aerodynamics, the convective heating in the stagnation region is found to be:

$$\dot{q}_{conv,lam} = 21(\rho_\infty/R)^{1/2}(v_\infty/1000)^3(1-H_W/H_S) \qquad (1)$$

or

$$\dot{q}_{conv,lam} = 4/x^{.2}(\rho_\infty/\rho_{SI})^{.8}(v_\infty/1000)^3(1-H_W/H_S) \qquad (2)$$

where $\dot{q}$ is in units of $BTU/ft^2 sec$, ρ of $slug/ft^3$, R and x of ft, and v_∞ of ft/sec.[20] These equations are based upon Newtonian impact theory, isentropic relations, and experimental results. The laminar equation is valid until an altitude of 25 km where continuum or boundary layer flow effects take place. Below this point, the turbulent equation must be used. Figure 20 shows the regions of gas dynamics as a function of free-stream Reynolds number.[14] Also shown is the free-stream Mach number and trajectories for the space shuttle, the AFE, and a Mars return vehicle as a function of free-stream Reynolds number. The ACRV trajectory closely resembles the STS-5 trajectory in Figure 20 which does enter the continuum flow field at the lower altitudes. The R and x in equations 1 and 2 are part of a polar coordinate system shown in Figure 21 where R = 5.6 ft for the stagnation region. Also, the H_W/H_S in equations 1 and 2 can be assumed to be equal to 0.1 from Newtonian impact theory. These equations were incorporated into the Re-entry Characteristics Program in Appendix A which gives the convective heating rate as a function of time
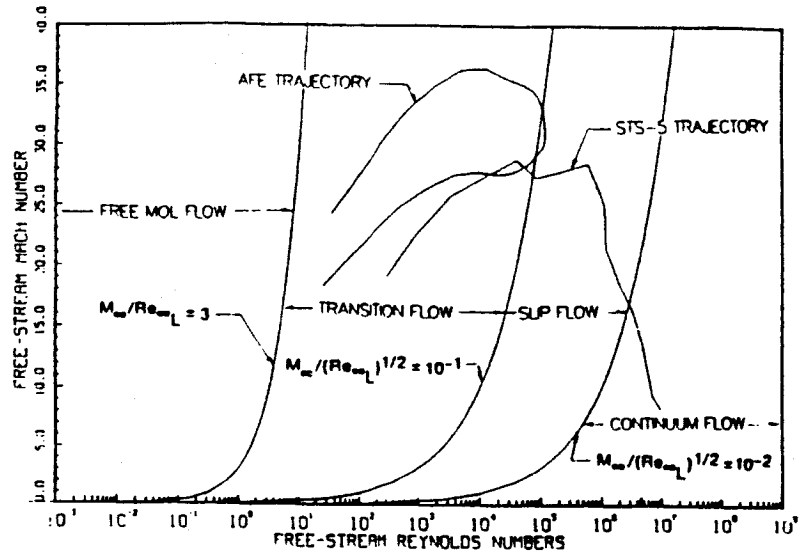
FIGURE 20: Regimes of Gasdynamic Mach Numbers
(Colovin, J. E., 'Development of AFE Aerothermodynamic Data Book)
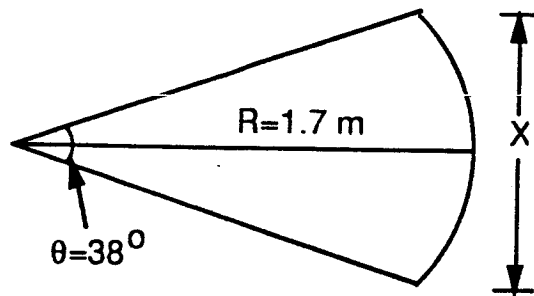
FIGURE 21: Stagnation Region Polar Coordinate System

39

at the stagnation region. The maximum value occurs 271 seconds into the trajectory and is 696.75 kW/m^2. These values are shown in Figure 22.

For the radiative heating rate at the stagnation region, Reference 20 presents a semi-empirical curve-fit equation:

$$\dot{q}_{rad} = 7.5 \; R \; s^{1.5}(v_\infty/10,000)^{12.5} \qquad (3)$$

where v_∞ is in ft/sec and R in ft. The s in the equation is a curve-fit constant with the following values:

s	h
0.0003685	>60.96 km
0.0015	60.96< h < 45.72 km
0.0170	< 45.72 km

This equation was programmed into the Re-entry Characteristics Program. The $\dot{q}_{conv}$ as a function of time is shown in Figure 22. The maximum radiative heating rate occurred 111 seconds into the trajectory and is 626.02 kW/m^2. One interesting point on the graph occurs at 450 seconds, where there is a sudden increase in $\dot{q}_{rad}$. This can be attributed to an inconsistency in the curve fit values for s.

The total heating rate, which is the sum of $\dot{q}_{conv}$ and $\dot{q}_{rad}$, is also shown in Figure 22 as a function of time. The maximum total value is 1047.62 kW/m^2 which occurs at 231 seconds at an altitude of 69 km.

Once the maximum total heating rate in the stagnation region is determined, the maximum surface temperature on the heat shield can be found by the following equation:

$$\dot{q}_{tot} = \dot{q}_{rad} + \dot{q}_{conv} = h(T_s - T_\infty) + \varepsilon\sigma(T_s^4 - T_\infty^4) \qquad (4)$$

where $\varepsilon = 0.9$ for RDGE and most ablative polymers. The average

convection coefficient, h, can be found through the following equations

$$N_{uD} = hD/k \qquad (5)$$

$$N_{uD} = CRe_D{}^m P_r{}^{1/3} \qquad (6)$$

where D = 4.2672 m, C = 0.027, m = 0.085, and for the altitude of maximum heating k = 0.02 W/m-K, P_r = 0.737, and Re_D = 40,000. The Nusselt number equation is for a circular cylinder in a cross flow where C and m are curve-fit constants. The above equations give an average convection coefficient of 10.1444 W/m^2-K. This value ,combined with the temperature of air at 69 km (216.66 K), can be put into equation (4) to yield a maximum surface temperature of 2119.0 K
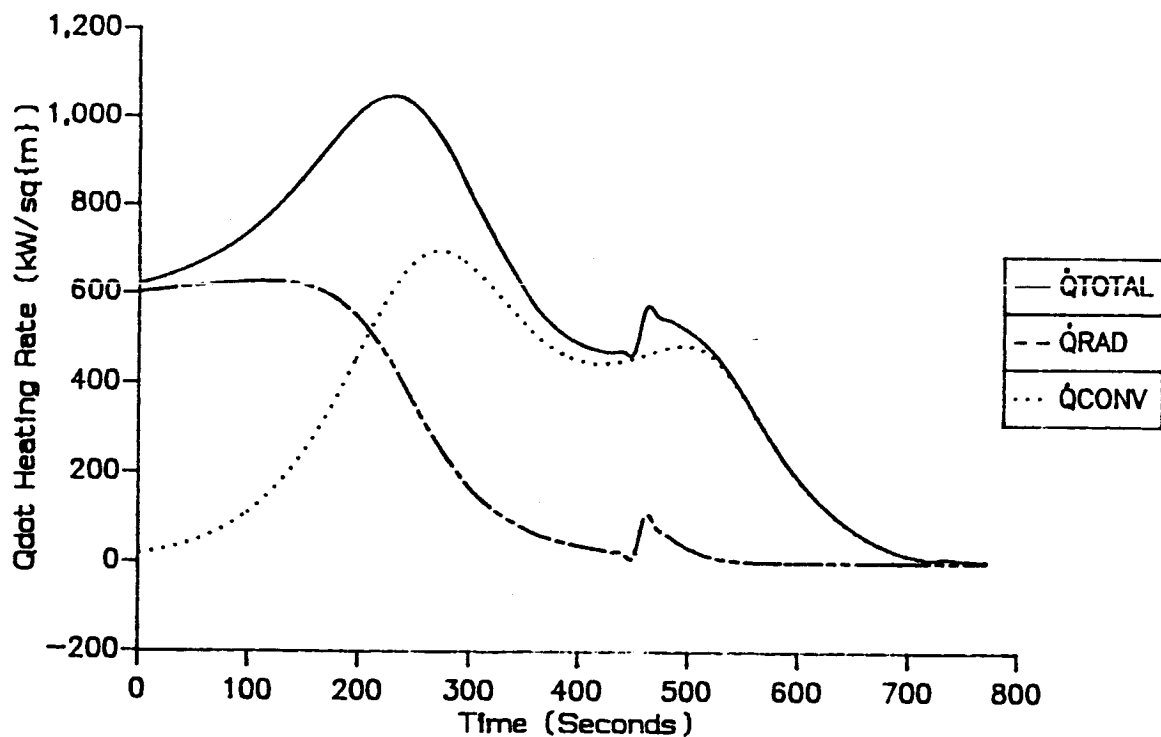
FIGURE 22: Stagnation Heating Rates for a Re-entry Angle of -2.0 degrees

The thickness of the ablator in the stagnation region can then be found for the maximum total heating rate by knowing the maximum surface temperature and the limiting back face temperature which is designed to be 93.33°C. The governing equations for determining a typical charring ablator have been well documented. Through the use of a typical control volume and the one-dimensional form of the conservation of energy equation, the thickness of the ablator can be determined from the following equation.[16]

$$\rho C_p (\partial T / \partial \theta_t) = \partial / \partial x (k \{\partial T / \partial x\}) + m_g (\partial H_g / \partial x) + (\partial \rho_s / \partial \theta_t) H_D \quad (7)$$

The terms in the above equation are respectively time rate of change of stored energy, conduction, flow of chemical energy, and the time rate of change of decomposition energy. Since the coefficients of this equation are all temperature dependent, the resulting equation is nonlinear. Also, an initial boundary condition which must be satisfied is the conservation of the heating rates:

$$\dot{q}_r + \dot{q}_c - (\dot{q}_{rr} + \dot{q}_{BLK} - \dot{q}_{CHEM}) = (k_c \{T / x\})_s \quad (8)^{[16]}$$

where $\dot{q}_{rr}$ is the reradiation from the high-temperature surface, $\dot{q}_{BLK}$ is the blockage of the convective heating by the action of the transpired vapors, and $\dot{q}_{CHEM}$ is the energy generated by chemical reactions such as combustion or sublimation. Because of the complex mathematical nature of this equation, a simpler approximation is used where $\dot{q}_{rr}$, $\dot{q}_{BLK}$, and $\dot{q}_{CHEM}$ are assumed to be negligible. Thus the equation reduces to:

$$k_c \{T / x\} = \dot{q}_r + \dot{q}_c \quad (9)$$

The k_c term in this equation represents the effective thermal conductivity of the ablator since it varies throughout the thickness of the ablator. For RDGE, the effective thermal conductivity is 4.811 J/(m-s-°F).[16] With the

above assumptions, the thickness at the stagnation region for the RDGE ablator was found to be 4.318 cm.

The integration of the ablator thickness of the Apollo command module with the rest of the heat shield substructure is presented in Figure 23.[19] This is a similar design to the ACRV where the ablator thickness is only 4.318 cm. The bond line where the ablator is connected with the brazed stainless steel substructure was described in an earlier section. A fibrous insulator with a density of 56.11 kg/m^3 and a maximum temperature of 371°C is used in the insulation section. The prescribed ablator thickness at the stagnation point will limit the temperature on the aluminum honeycomb substructure shown in Figure 23 to less than 93.3°C as needed by design constraints. For other areas on the heat shield base, the ablator thickness is decreased because of the smaller radiation equilibrium surface temperature.
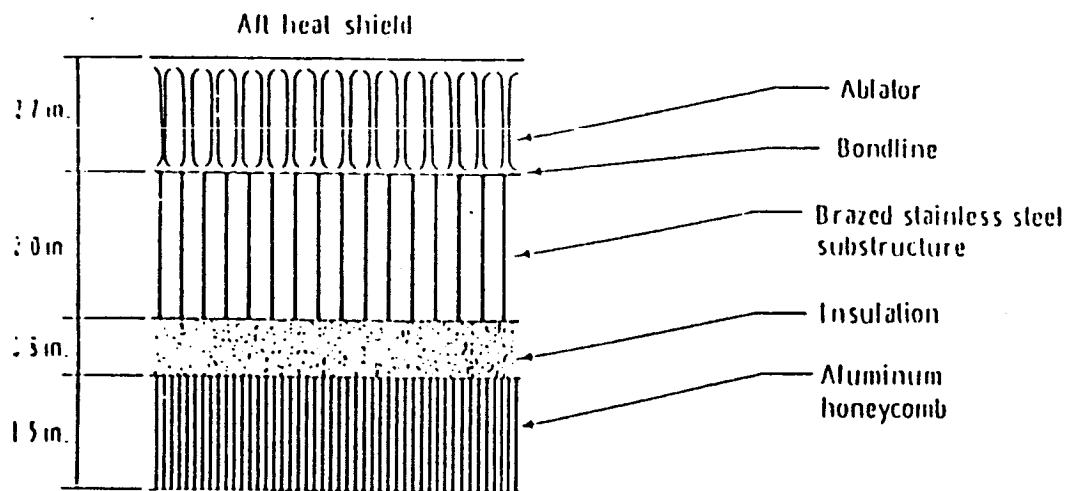
FIGURE 23: Structural arrangement of Apollo TPS
(St. Leger, Leslie G., 'Apollo Experience Report Thermal Protection Subsystem)

43

In addition to the base region of the AFE, another major design concern was the convective heat transfer around the heat shield and its possible effects with the ACRV behind it. The following analysis has been used in investigating this phenomena.

In the hypersonic flow regime, the wake flow in the AFE base region consists of three types of flow fields as shown in Figure 24.[21] The laminar boundary layer separating near the trailing edge of the aerobrake skirt forms a shear layer (region 3 in Figure 24) which wraps around the carrier vehicle and meets at the so called "neck" of the wake. In-board of this shear layer is the wake recirculation flow (region 4 in Figure 24) and this is where the ACRV will be. The flow field outboard of the shear layer is called the local flow (region 2 in Figure 24). Region 2 contains the locally expanded flow and has the highest heating environment, however, since the ACRV will be in region 4, the heating rates in that area are very important. The thermal environment for this wake re-circulation zone has been measured on other blunt nosed flight vehicles and in wind tunnel tests. The observed results were:

1. The heating rates measured on the separated flow region over the conical section of the Apollo command module in flight is one to two percent of the stagnation point heat rate as calculated by the Kemp and Riddell empirical formulation.[22]

2. During low L/D AFE wind tunnel tests conducted in Mach 10 air, the heating rates in the recirculation zone were measured to be about 1.5 percent of the measured stagnation point heating rate.[23]

An independent methodology was developed to generate the wake recirculation zone heating environment for the AFE using Viking flight and

44

wind tunnel data. The Stanton number in the base circulation region is plotted as a function of free-stream Reynolds' number in Figure 25.[21] A least square fit resulted in the following equation.

$$S_t = 4.020 \times 10^{-3}(R_e)^{-0.152} \qquad (10)$$

Once this is known, the heating rate on the AFE in this region can be calculated. During the entire re-entry, the recirculation heating rate using the above empirical correction is less than 2 percent of the stagnation point heating. All of these results support the current design parameter of 2 percent of the reference AFE stagnation point heating rate in the recirculation zone. Therefore, a heating rate of about 2 percent is insignificant and will pose no problems on the ACRV.

In summary, the heat shield will employ the AFE Aerobrake design with an ablator composed of RDGE cured with NMA. The maximum heating rate on this heat shield is 1047.62 kW/m^2 with a radiation equilibrium temperature at the stagnation point of 1845.85°C. The 4.318 cm thick ablator at this area will assure that the aluminum substructure does not exceed its 176.67°C maximum operating temperature. Finally, the convective heat transfer around the heat shield will have little impact on the ACRV.

The effects of storing this heat shield in space for significant amounts of time needs to be further investigated. Also any possible communication effects that would occur during the re-entry needs to be studied.
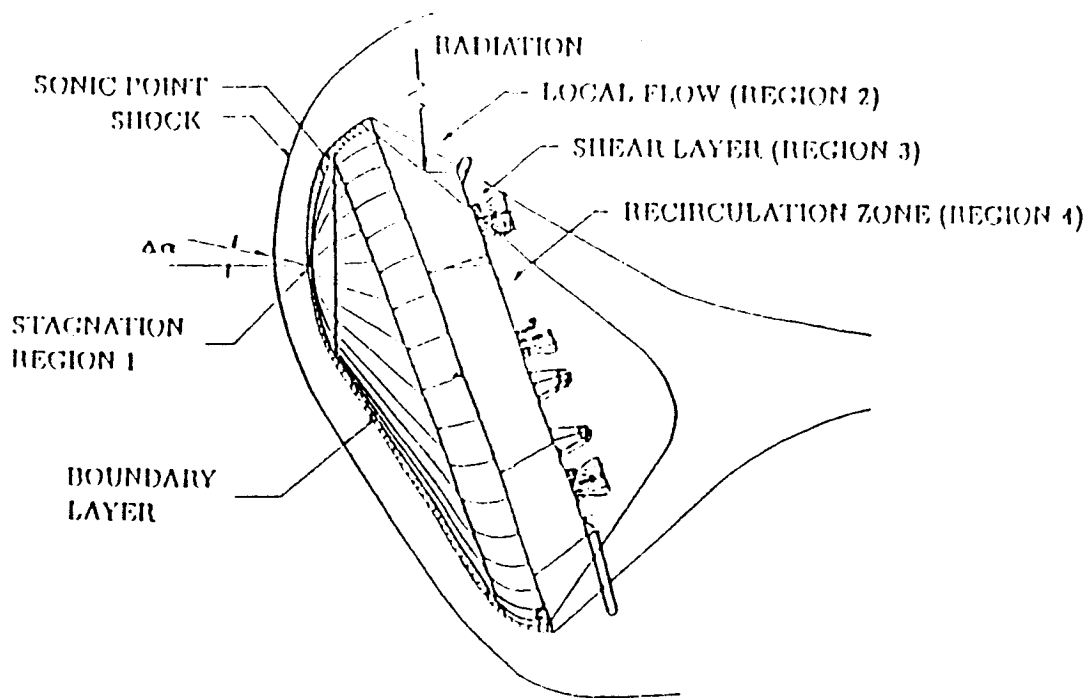
FIGURE 24: Schematic of the Flow Field Around the AFE during Aeropass
(Sambamurthi, J., 'Engineering Methodology to Estimate the Aerodynamic
Heating to the Base of the AFE')
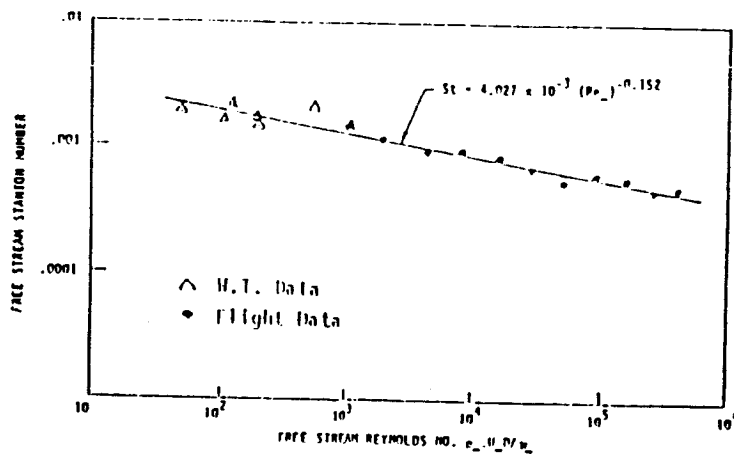
FIGURE 25: Correlation of Flight and Wind Tunnel Base Heating
Measurements on VIKING Configuration
(Sambamurthi, J., 'Engineering Methodology to Estimate the Aerodynamic
Heating to the Base of the AFE')

46

PARACHUTES

A parachute system will be used for both high altitude stabilization of the ACRV prior to parawing deployment and for the deceleration of the heat shield after it has separated from the craft. Figure 26 shows the operational envelope, as of 1985, for parachute operation. This may not apply directly to our high altitude application since this system is used
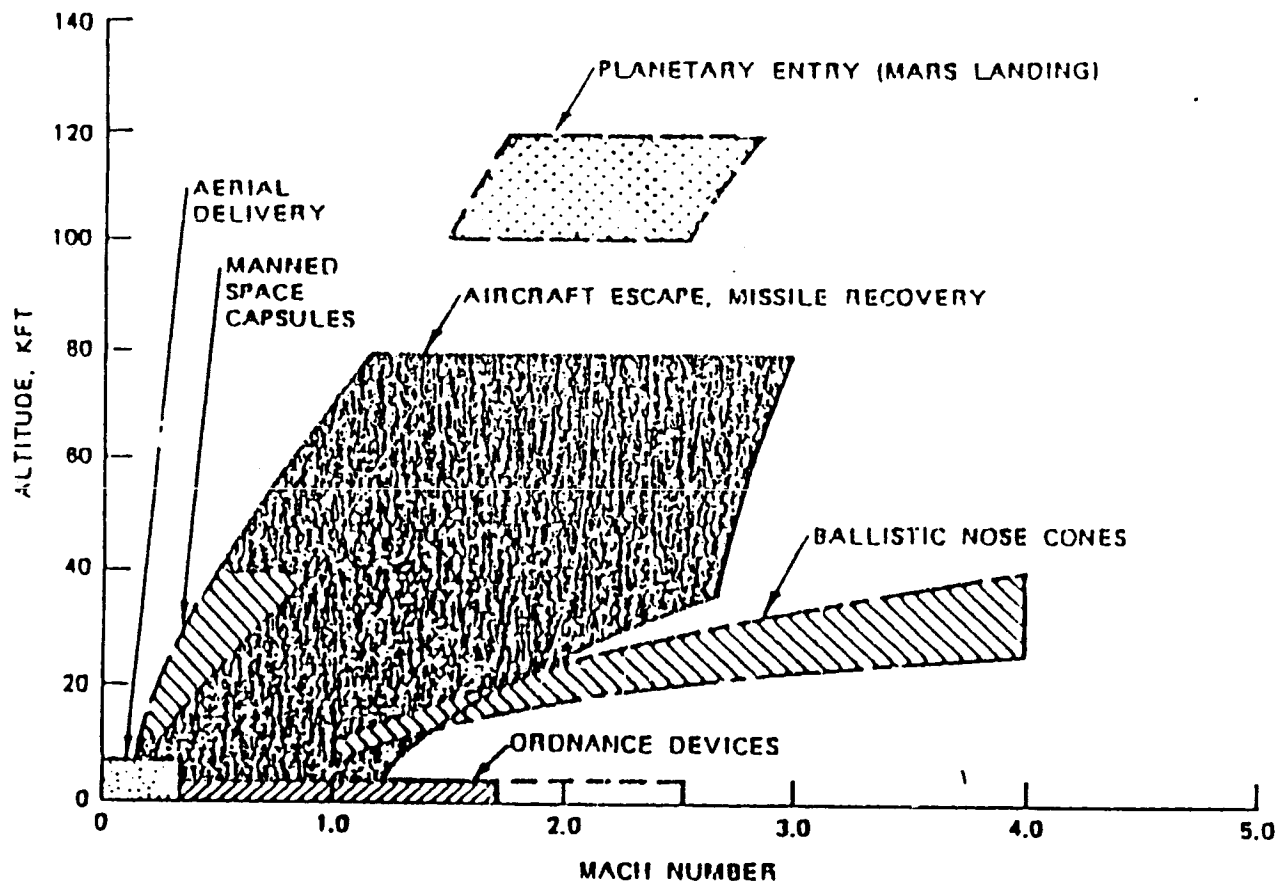
FIGURE 26: Parachute Operational Envelopes
(Knacke, T. W., Parachute Recovery Systems Design Manual)

only to stabilize the ACRV, not to decelerate it significantly. By the time the heat shield is ejected, it should be well within this operational envelope.[5]

Some important criteria to consider when selecting the type and size of the parachutes are: weight, volume, inflated shape, drag coefficient, stability characteristics, and inflation time.[4] Due to the stabilization requirements, high drag type parachutes were eliminated from consideration. The types of chutes that were considered for this mission were: the conical ribbon (with varied porosity), the ribbon (hemisflo), and the ballute (see Figure 27).[5]

TYPE	CONSTRUCTED SHAPE		INFLATED SHAPE $\frac{D_p}{D_o}$	DRAG COEF C_{D_o} RANGE	OPENING FORCE COEF C_x (INF MASS)	AVERAGE ANGLE OF OSCILLATION, DEGREES	GENERAL APPLICATION
	PLAN	PROFILE $\frac{D_c}{D_o}$					
FLAT (FIST) RIBBON	⊙	------ 1.00	0.67	0.45 TO 0.50	~1.05	0 TO ±3	DROGUE, DESCENT, DECELERATION, OBSOLETE
CONICAL RIBBON	⊙	0.95 TO 0.97	0.70	0.50 TO 0.55	~1.05	0 TO ±3	DESCENT, DECELERATION, 0.1 < M < 2.0
CONICAL RIBBON (VARIED POROSITY)	⊙	0.97	0.70	0.55 TO 0.65	1.05 TO 1.30	0 TO ±3	DROGUE, DESCENT, DECELERATION, 0.1 < M < 2.0
RIBBON [1] (HEMISFLO)	⊙	0.62	0.62	0.30[1] TO 0.46	1.00 TO 1.30	±2	SUPERSONIC DROGUE, 1.0 < M < 3.0
BALLUTE		0.51	0.51	0.51[1] TO 1.20	~1.05	<±1	STABILIZATION, DROGUE, 0.8 < M < 4

FIGURE 27: Slotted Parachute Characteristics
(Knacke, T. W., Parachute Recovery Systems Design Manual)

48

The ballute gives a low angle of oscillation, has a typical C_d ranging from 0.5 to 1.2, and is good up to Mach 4. The only problem is its lack of accepted use. The conical ribbon, which is similar in angle of oscillation and opening force, has a C_d of about 0.6, and is good up to Mach 2. The ribbon hemisflo has a C_d of 0.4, low angle of oscillation, and is used up to Mach 3.[5] For both parachute systems, the conical ribbon parachute was chosen due to its reliability and prior use on space missions (Apollo).

Kevlar-29 aramid will be used instead of nylon, which was frequently utilized in the past. This will result in a weight and volume reduction of 50-60%. Kevlar also provides a higher tensile strength and lower peak loads.[6] To reduce loads even further, a skirt parachute reefing system will be used (Figure 28). It consists of reefing rings attached on the inside of the canopy, where the suspension lines are connected. The reefing line runs through each reefing ring as well as several reefing line cutters. It is the reefing line that actually restricts the opening of the canopy. Each reefing cutter has a cutter knife with a highly reliable pyrochemical device which is set off by pulling cords connected to the suspension lines, when the canopy is stretched. After a predetermined time, (on the order of a few seconds) the reefing line is cut and the chute opens to the next reefing stage, or to its full diameter.[5]

Two other considerations in designing a parachute system are the length of the suspension lines and the porosity. Long suspension lines will increase the drag coefficient by increasing the inflated diameter of the canopy. Increasing the porosity will decrease the drag coefficient and produce a highly stable parachute.[5] For the application of the high
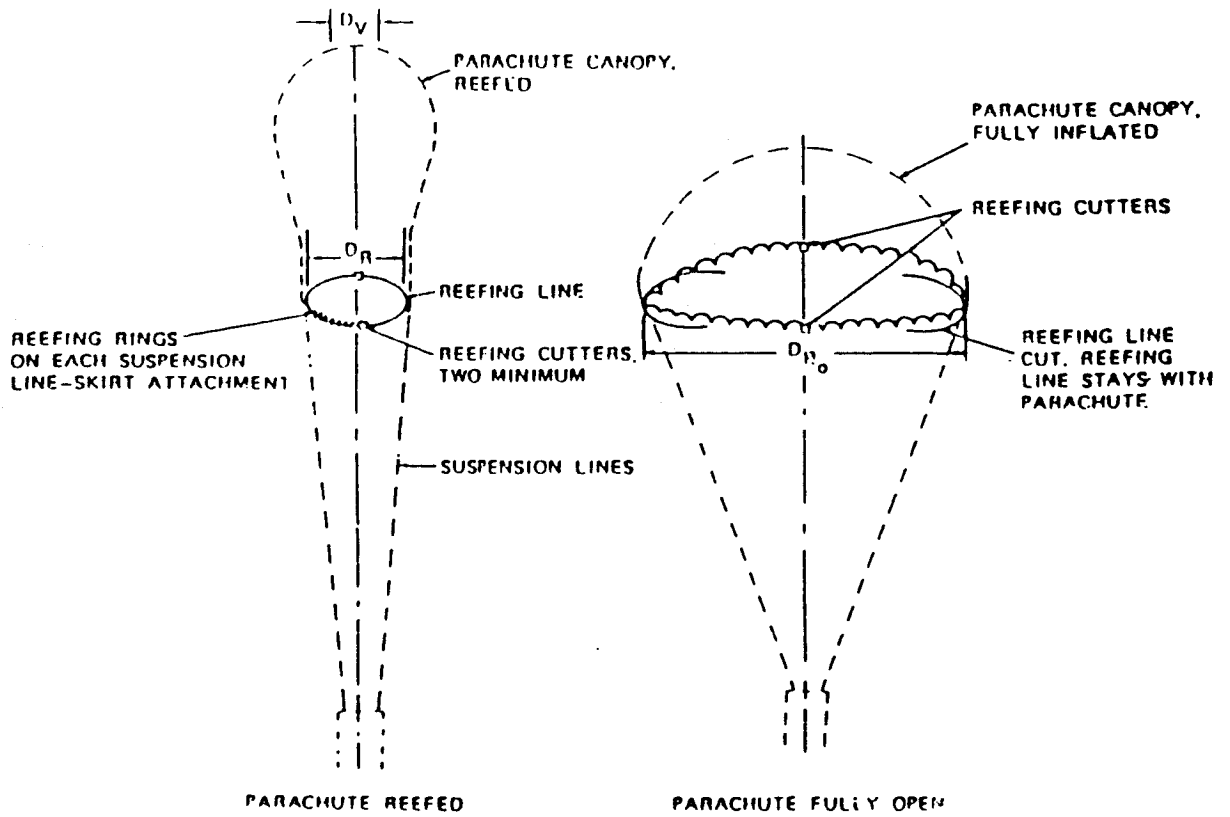
LEGEND

D_R • DIAMETER OF REEFING
LINE CIRCLE, REEFED

D_{R_o} • DIAMETER OF REEFING
LINE CIRCLE, FULLY OPEN

D_V • VENT DIAMETER

FIGURE 28: Parachute Skirt Reefing
(Knacke, T. W., Parachute Recovery Systems Design Manual)

50

altitude stabilizer for the ACRV, the best combination of the above two criteria is long suspension lines and a high degree of porosity for better stabilization.

The main parachute system for the ACRV consists of a cluster of three conical ribbon parachutes. The main advantage of clustering is the reduced probability of a catastrophic systems failure.[5] Each chute will be deployed by its own pilot chute. The pilot chutes are fired from a mortar which forces chutes out the nose cap and pulls out the pilot chutes (see Figure 29). The pilot chutes have a D_o = 2.00 m.[6]
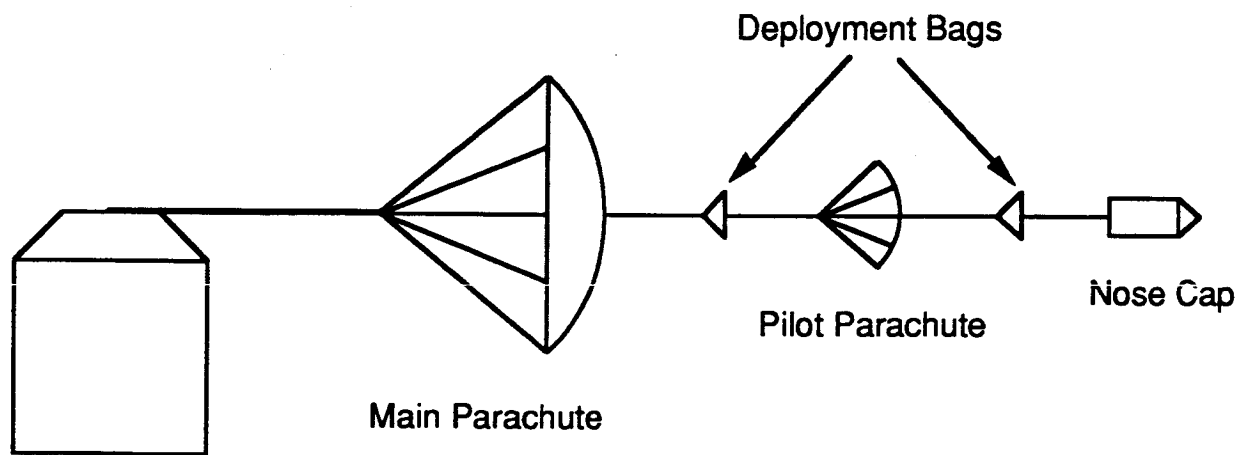
FIGURE 29: Parachute Deployment System
(Buning, H., Project Aneas: A Feasibility Study for Crew Emergency Return Vehicle)

The total surface area needed to properly slow down the ACRV is 304.6 m^2 over the entire cluster. Dividing this number by three gives the surface area needed for each parachute, 101.5 m^2. This is calculated using the following inequality which guarantees that the drag from the parachutes will be high enough to allow separation of heat shield and ACRV.

$$(1/2)SC_d > 9.139 \ m^2 \tag{11}$$

This gives each 20° conical chute a surface area of 101.5 m^2 and a D_0 of 11.4 m, where D_0 is calculated using:

$$D_0 = (4S/\pi)^{1/2} \tag{12}[5]$$

These calculations are based on a drag coefficient of 0.60, an average range for a conical ribbon parachute.[5] The (inflation projected) diameter for each chute is 8.0 m. This system will still complete the mission if one parachute fails to open. Forty suspension lines, each with a length of 20 m, will be used on all three parachutes. Since this length places the parachute at least four forebody diameters away, forebody wake effects are negligible. The porosity of each parachute with a drag coefficient of 0.6 is 27%.[5]

Canopy filling time at supersonic speeds is constant because the parachute operates behind a normal shock.[5] Exact filling time was not calculated because it depends on the degree of reefing. The loads on the ACRV will determine the amount of reefing needed.

To determine stresses in this type of parachute, the reader is referred to CANO, a computer program for determining stresses in slotted canopies. CANO will be presented in Chapter 8 of the Naval Weapons

Center Parachute Recovery Systems Design Manual when it is completed.[5]

The same type of conical ribbon parachute will be used to decelerate the heat shield, once it is blown away from the rest of the ACRV. The heat shield system has only one main parachute (deployed with the same pilot chute described for the ACRV system) to reduce the complexity since redundancy is far less important. The area for this chute is determined by using the following equation:

$$dv/dt = g - C_d S \rho v^2 / 2m \qquad (13)[6]$$

where v = 8.7 m/s and dv/dt = 0.0 because the drag force of the parachute is equal to the gravitational force. A nominal diameter of 14.28 m (inflated diameter of 10.0 m) is needed to slow the heat shield to an end velocity of 8.7 m/sec. The chute will also have twenty-five suspension lines with a length of 25 m. One reefing stage will be used with the degree of reefing to be determined.

Figure 30 shows the parachute configuration in the heat shield. A thin .635 cm aluminum protection plate will be welded to the struts. This plate is located 38.1 cm from the surface of the ACRV. The parachute package (mortar, pilot chute, and main chute) will rest on the protection plate and will be connected to the struts by a D-ring and Kevlar rope. The effect of space exposure on this parachute needs to be investigated further.

The approximate weight breakdown for the ACRV parachute system is[6]

3 main chutes	91 kg
3 pilot chutes	7 kg
Total	98 kg

Top View
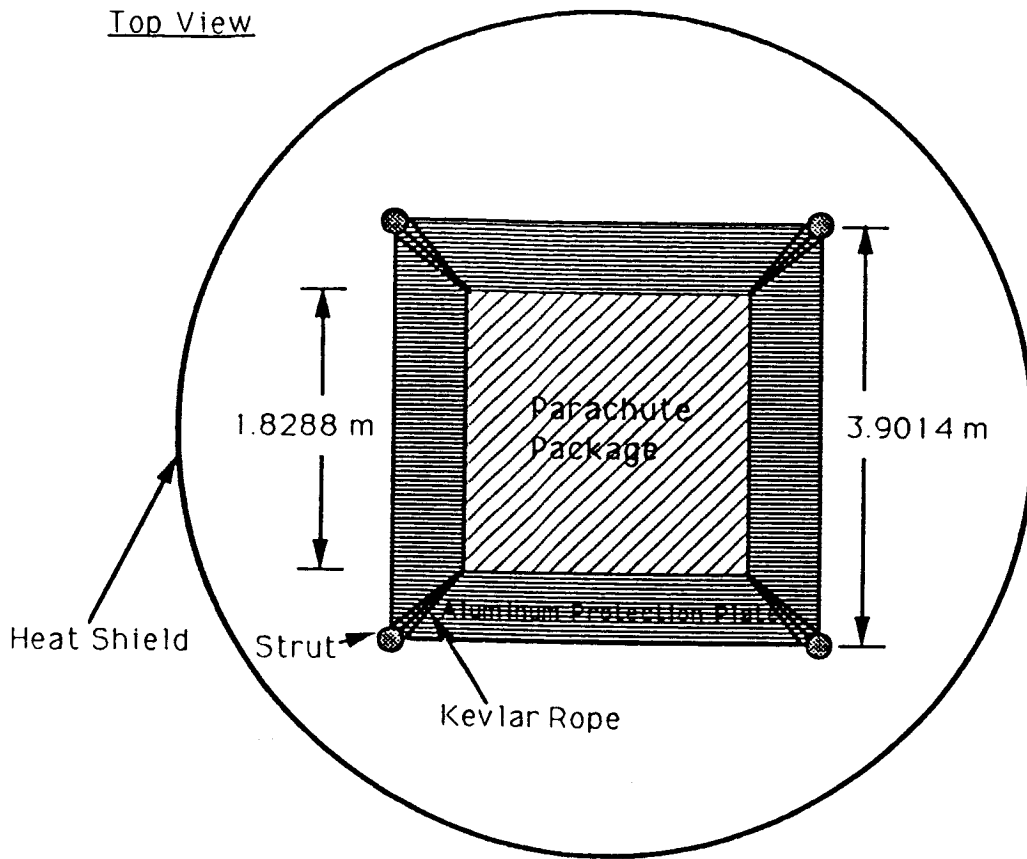
Cut-away Side View
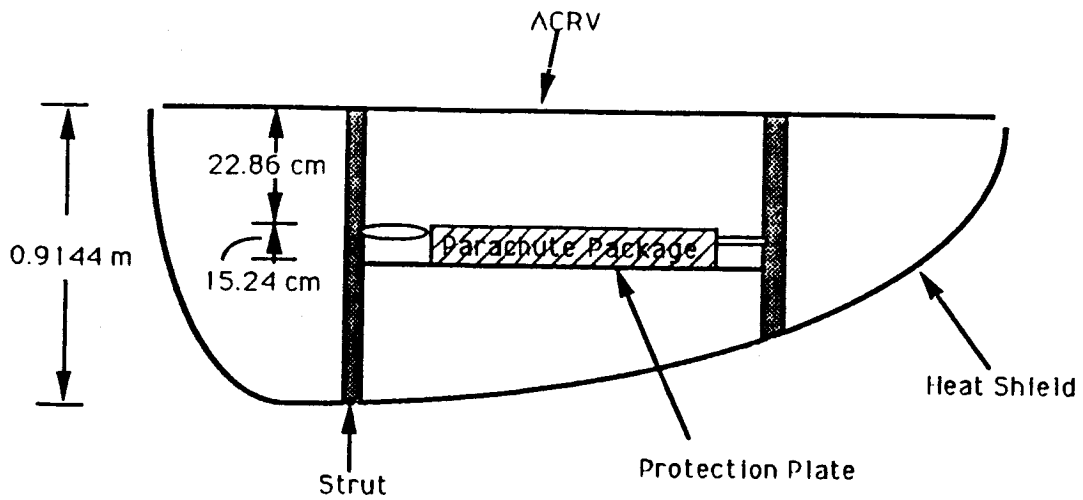
FIGURE 30: Heat Shield Parachute System Configuration

54

Which is about 1.5% of the total ACRV mass. The packing volume breakdown is approximately[6]

3 main chutes	0.107 m^3
3 pilot chutes	$0.008 \text{ m}3$
Total	0.115 m^3

The heat shield system has a weight of[6]

main	30 kg
pilot	5 kg
Total	35 kg

which is approximately 8% of its total weight. It will also have a packing volume on the order of 0.0384 m^3.

PARAWING

The parawing plays a major role in the ACRV braking and landing system. It is responsible for helping to slow the ACRV descent and for landing the vehicle safely. Several design and control areas were investigated for the parawing: The size and structure, the deployment timing, the control method, and the materials to be used.

The size of the wing can be determined from the L/D desired and the landing impact restrictions. To keep the landing under the G-value specified in the SPRD, the vertical velocity must be less than 9 m/s.[6] To calculate the necessary area, the following equations hold for motion in the Earth's atmosphere.[1]

$$L = (1/2)rV^2 S C_L \qquad (14)$$

$$D = (1/2)rV^2 S C_D \qquad (15)$$

At touchdown, the maximum L/D is desired. From Figure 31, for the parawing:

$$a = 44^o$$
$$C_L = 1.0$$
$$C_D = 0.45$$

For the ACRV, using a worst case scenario to ensure that the landing forces are less than the set limits, the lift coefficient is assumed to be zero, and, assuming that the nose of the ACRV is a flat plate with $S = 14.3$ m^2, $C_D = 1.28$. Using equations (14) and (15), at V=50 km/hr., the wing area required is 513.206 m^2. The velocity used was chosen because it is low enough to allow the ACRV to land on any landing strip that can support it s weight while avoiding excessive braking. This velocity is also high enough to keep the wing area from becoming too large to manage.

To calculate C_D for the system, the drag of the parawing, shroud lines and the ACRV must be considered.[18] Table 5 summarizes these values. Since L/D = C_L/C_D, the L/D for the ACRV is 2.11 at touchdown.

The sink rate is the vertical velocity of the ACRV. As specified earlier, this must be less than 9 m/s. It is known that tan θ = D/L.[11] Therefore, θ = 25.38^o. The sink rate, in m/s, is obtained from:

$$V_{sink} = V \sin \theta \qquad (16)[11]$$
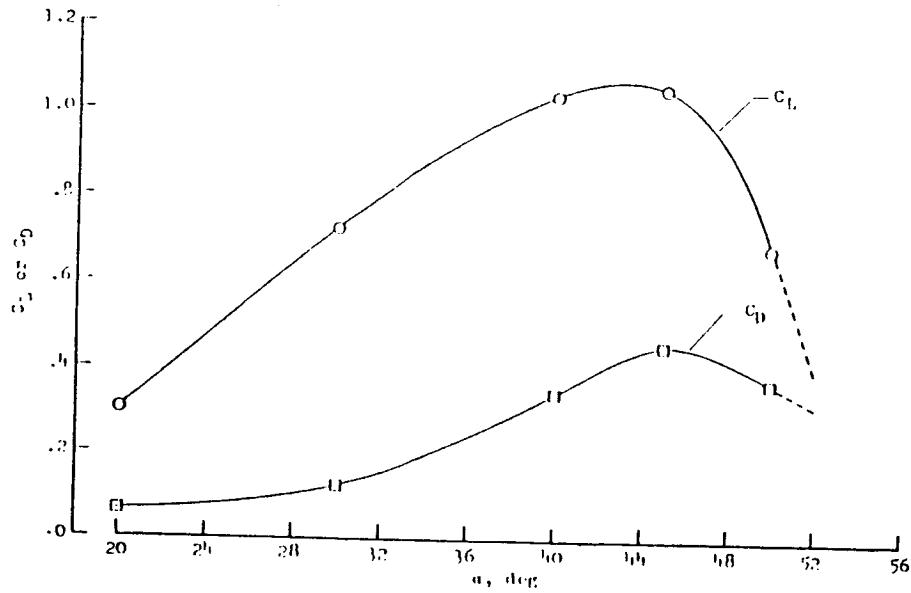
FIGURE 31: Subsonic Lift-Drag Characteristics of a Parawing
(Hatch, Howard G. 'An Analytical Investigation of the Loads, Temperatures, and Ranges Obtained During the Recovery of Rocket Boosters by means of a Parawing')

Body	Drag(N)	C_D	C_L
Parawing	27,286	0.45	1.0
Shroud Lines	216	1.00	0.00
ACRV	2,163	1.28	0.00
System	29,665	0.4473	1.0

TABLE 5: Parawing Lift and Drag Coefficients

57

This gives a sink rate of 5.95 m/s, which is well under the specified value.

One problem that may be encountered in using a parawing is wing instability. ~~Since~~ *because* the wing is flexible, it may not keep its form well. One way to make the parawing more rigid is to use a metal frame to support the wing, but this requires a tremendous amount of space and adds mass. Another method of controlling wing flutter is the use of inflated ribs along the keel and edges of the parawing. These ribs are tapered for aerodynamic purposes. By starting the ribs as points at the nose of the parawing and expanding to a diameter of one meter at the tail, the aerodynamics of the wing can be preserved and the stability improved. A similar design was created by F. Rogallo.[27] By making these ribs out of Kevlar 29 aramid[29], they will provide a strong, lightweight structure weighing 86.18 kg.

Another problem is rib inflation. One method of inflation is to use the velocity of the ACRV to force air into the ribs, but this would cause stability problems that are difficult to solve. Another method is to use compressed gas, preferably CO_2 due to its inability to combust. By incorporating a compressed gas storage container into the ACRV and attaching a feed line to each of the ribs by running them along the parawing shroud lines, the ribs can be easily inflated to a desired pressure. By incorporating one-way valves into the ribs, the gas can easily be retained. More research on this system will definitely be required.

The use of the twin-triangular parawing, or two-lobed parawing as it is more commonly called, at a landing velocity of 50 km/hr will necessitate a panel area of 256.6 m^2. By using a nose angle of 21° for

58

each panel, the parawing will have the dimensions shown in figure 32. The twin-triangular parawing will be used because it was proven effective in the Mercury program parawing test flights.[10] For the design described, the parawing mass will be 598.38 kg, and the shroud line mass will be 16.8 kg, for a total mass of 615.18 kg.
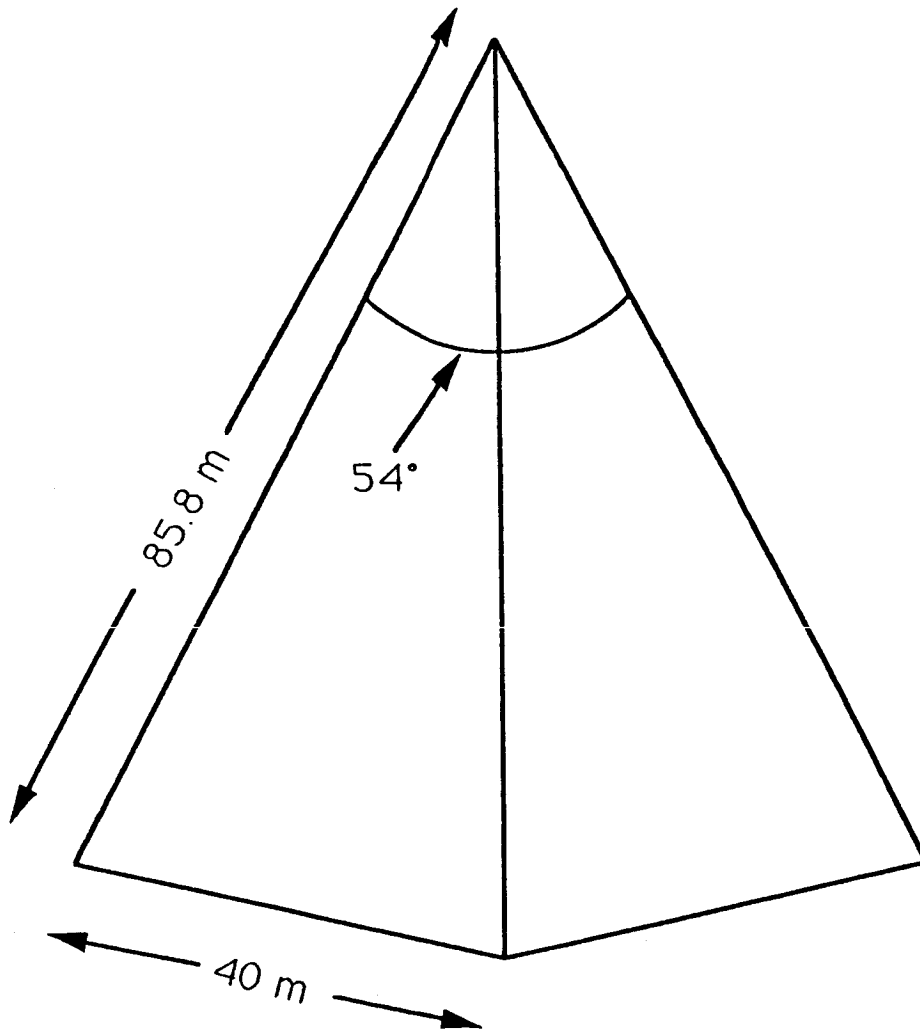
Figure 32: Parawing Dimensions

The deployment of the parawing is another important factor in designing the braking and landing system. Three methods of parawing deployment have already been tested at Langley Research Center.[10] Two of the methods tested were designs involving covers over the parawing, and the third method was a gas charged tube ejection. Because of the size of the wing being considered, the gas tube method was rejected due to the size of the tube needed and the amount of gas required for successful deployment.

The two cover designs are the cover-eject and the cover-retract methods. The only difference between the two methods is the final disposition of the cover. The cover-eject method incorporates a protective cover over the parawing that is blown off just prior to deployment of the parawing. As the name suggests, the cover-retract method uses a retractable cover that stays with the vehicle after the parawing deployment. Since the cover-retract method allows the re-use of all the components in the system, it will be used. Figure 33 shows the parawing package complete with cover, and Figure 34 shows the parawing fully deployed from the package. The cover is a rollaway cover which opens with electric motors. The whole package is attached to the top surface of the ACRV. The parawing will be deployed from the package by ejecting a pilot parachute which will then begin to deploy the parawing. The parawing will be reefed in order to lower the g-forces associated with its deployment. This reefing procedure will take approximately 30 seconds and will expand the parawing from a sharp wedge shape to its final shape.

The physical deployment of the parawing and the orientation of the vehicle are shown in Figure 35. This method was developed for the

Parawing

Shrouds shown are from
one side of parawing only

Parawing Deployment Packages
Attaches to ACRV Along This
Surface

Parawing Deployment
Package
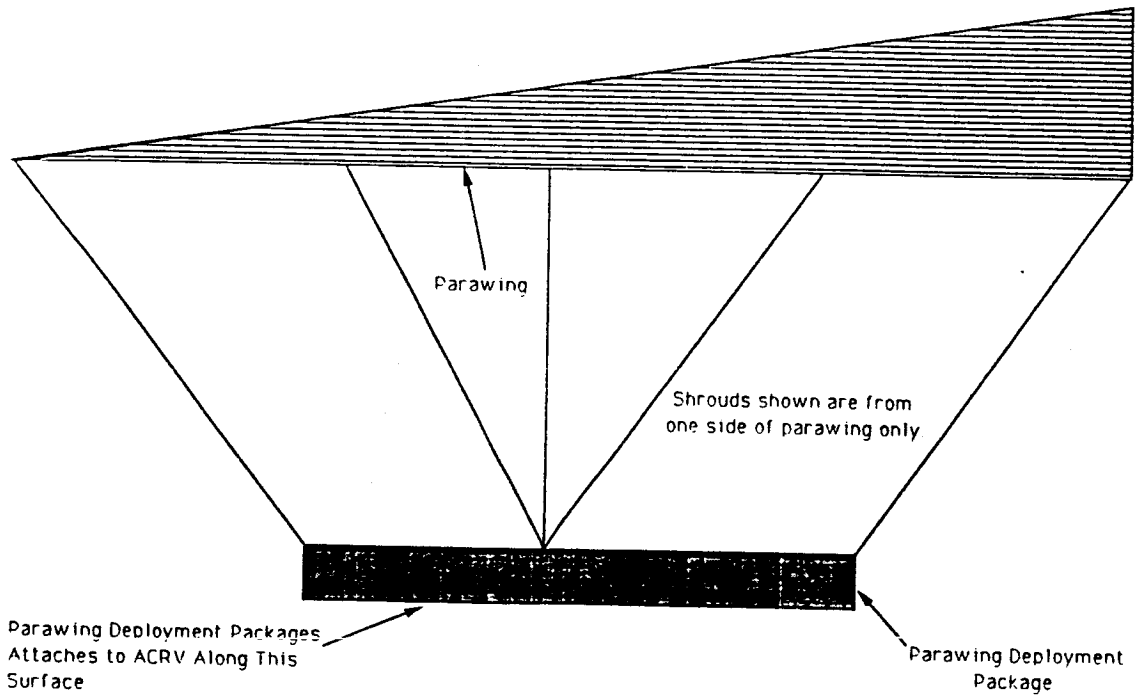
FIGURE 33: Parawing Cover System
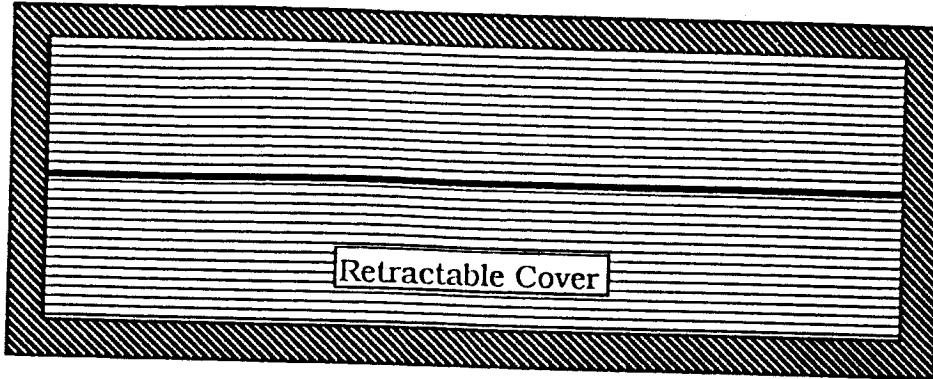
Top View; Cover Closed
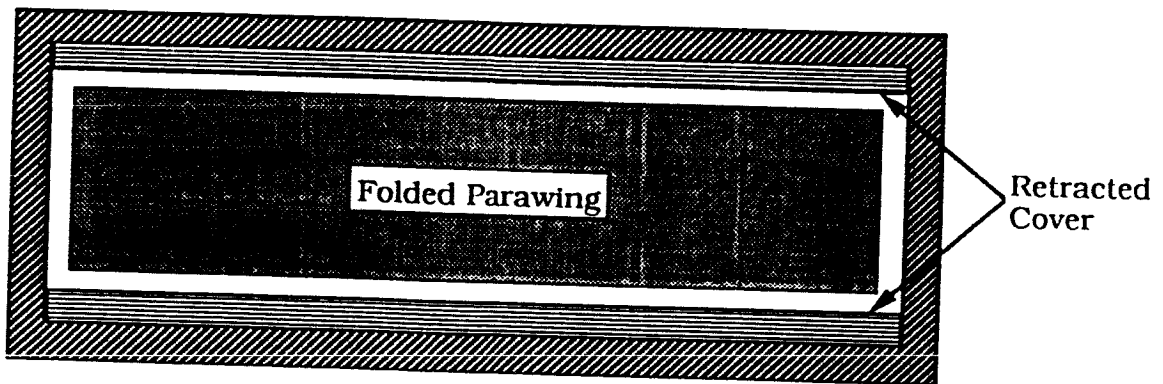
TopView; Cover Retracted
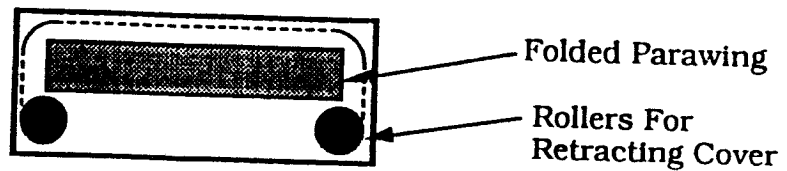
Side View; Cutaway

FIGURE 34: Fully Deployed Parawing
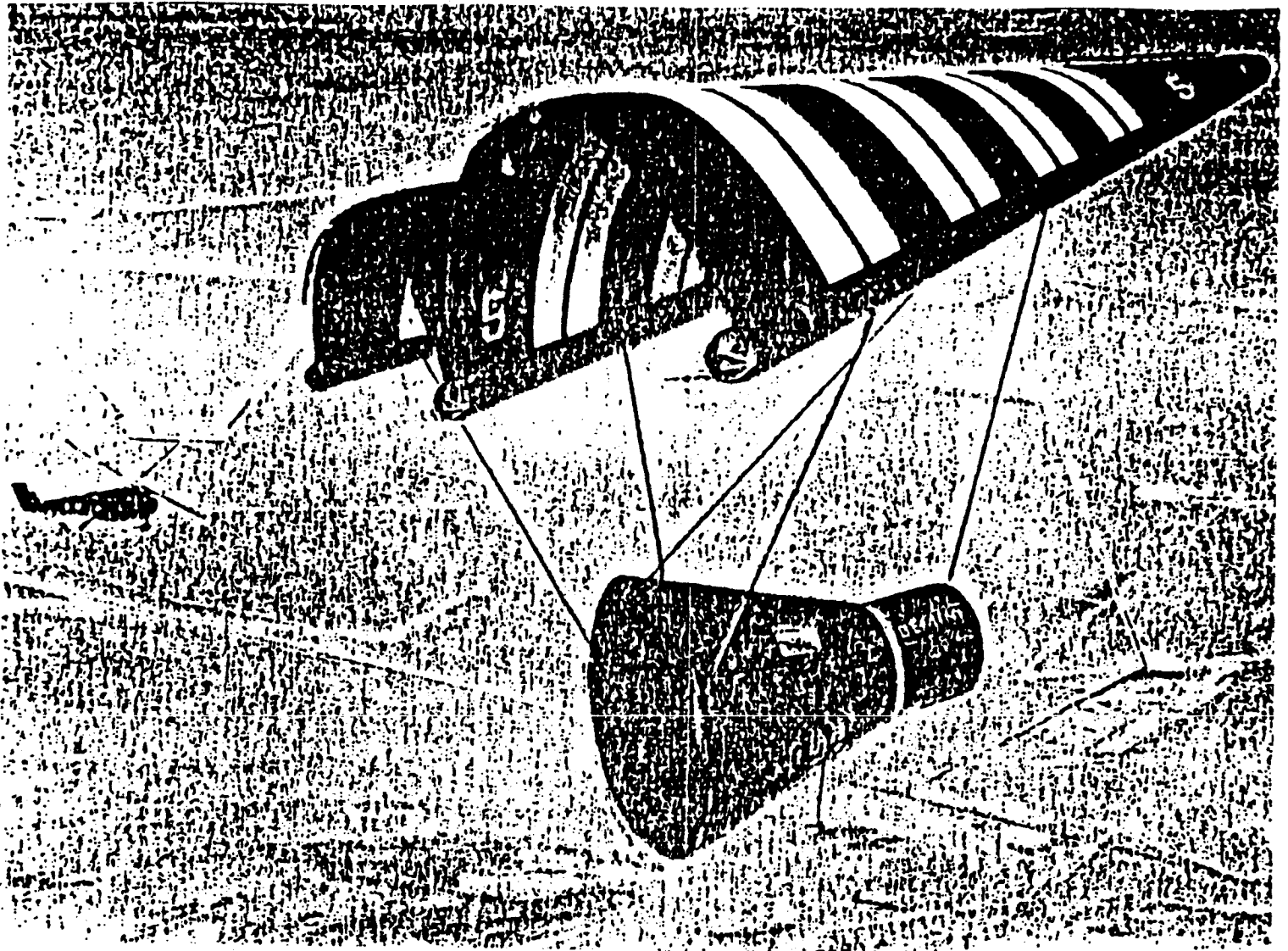
FIGURE 35: Gemini Paraglider Landing System
(Rogallo, Francis M., 'Preliminary Investigation of a Paraglider')

63

Mercury program and has already been tested.[11] By orientating the ACRV with the vehicle suspended lengthwise under the parawing, the vehicle C_d can be significantly reduced, enhancing the wing performance.

The parawing must also be capable of being controlled to adjust the angle of attack and the flight heading. Using twelve Kevlar shroud lines attached to the wing at the points shown in Figure 36, the wing can be suspended above the ACRV. Seven computer controlled high-torque servo motors on the ACRV will control the length of the shroud lines, enabling the vehicle to be maneuvered. The military has many small electric servo motors presently in use that fit the needs of the mission, but the specific model has not been chosen.

Upon touchdown, the parawing is no longer useful as a lifting device and is no longer needed. Instead of discarding the parawing and deploying a parachute braking system, it can be tilted back and used as a ground deceleration device to slow the vehicle during rollout.

The material chosen for the parawing is Kevlar-29 aramid 3-ply[30] and the material chosen for the shroud lines is braided Kevlar-29 aramid.[30] The properties for Kevlar-29 aramid are shown in Tables 6 & 7. Kevlar-29 aramid was chosen over Mylar and a woven steel cloth due to it's excellent strength and light weight. By using 15.22 mm diameter shroud lines, the ACRV will be able to undergo a 25 G static loading force before line failure. This value was chosen because it is higher than most humans can safely tolerate. The safety factor was also chosen to allow for dynamic loading. The dynamic material properties for braided Kevlar-29 aramid could not be located. This shroud line diameter is only preliminary and, when more data on dynamic loading becomes available, the diameter will most likely be reduced.
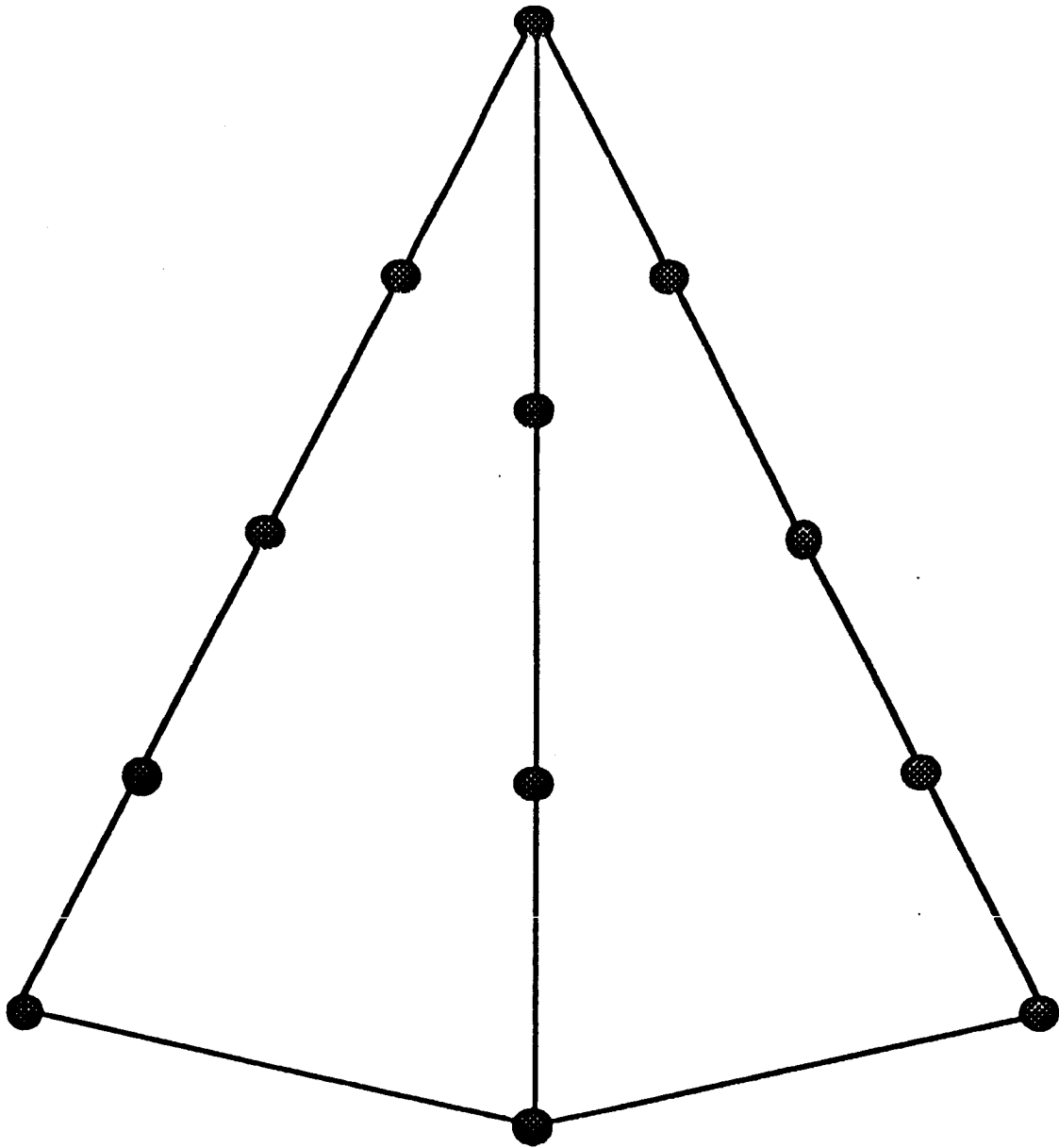
FIGURE 36: Shroud Line Attachment Points

65

BRAID	Diameter in. (mm)	Weight lb/100 ft (kg/100 m)	Break Strength lb (N)
KEVLAR* 29 Aramid	5/8 (15.9)	10.3 (15.3)	34,000 (151 300)
DACRON* Polyester	5/8 (15.9)	14.0 (20.8)	13,000 (57 850)
KEVLAR 29	2 (50.8)	136 (202)	277,000 (1 232 650)
DACRON	2 (50.8)	126 (187)	106,000 (471 700)
Nylon	2 (50.8)	106 (158)	117,000 (520 650)
WIRE ROPE (7 x 19)			
KEVLAR 29	1/2 (12.7)	8.0 (11.9)	25,000 (111 250)
Galvanized Steel	1/2 (12.7)	45.8 (68.2)	22,800 (101 460)

*Du Pont registered trademark

TABLE 6: Typical Rope Properties ('Characteristics and Uses of Kevlar 29 Aramid')

Fabric	Weight oz/yd^2 (g/m^2)	Thickness 10^{-3} in (mm)
KEVLAR 29	9.8 (333)	30 (0.76)
KEVLAR 29 (3 ply)	29.4 (998)	85 (2.16)
KEVLAR 29 (Felt)	27.0 (917)	105 (2.67)
Fiberglass	8.4 (285)	12 (0.30)
Fiberglass (8 ply)	67.2 (2282)	85 (2.16)
Asbestos	40.8 (1386)	90 (2.29)

*Du Pont registered trademark.

TABLE 7: Typical Fabric Properties ('Characteristics and Uses of Kevlar 29 Aramid')

66

LANDING GEAR

In preparation for the final descent of the ACRV, the landing gear will be lowered from the underside of the craft once the parawing has been deployed. There are two basic types of landing gear that could be used on the ACRV. These are externally mounted landing gear and internal or retractable landing gear. For this mission, the gear must be as compact and lightweight as possible in order to meet size and weight constraints placed on it by the space shuttle cargo bay during its initial ascension to orbit. If the gear is external, it must be housed to protect it from the heating effects and re-entry forces encountered during the ACRV's descent. The housing required will add weight to the landing gear package, and will also require additional volume, which is crucial for any space mission. The external housing must also protect the landing gear from the space environment and allow the landing gear to freely deploy during descent. If the gear is internal, it also adds weight and volume to the ACRV due to the deployment mechanisms and support structures. This method provides a savings in external volume due to the absence of the landing gear on the underside of the craft, but it also takes valuable room in the interior of the ACRV. This method is more desirable for the mission since the landing gear for a 6500 kg vehicle is relatively small, light-weight, and does not require a large volume. Also, since the landing gear must be stored and protected for up to four years, internal storage will provide better protection than an external housing if its compartment is properly insulated.

Landing gear weight prediction is primarily affected by: design landing weight, hardness of landing surface, landing speed, braking requirements, and load deflection characteristics.[24] Weight

considerations should be made for rolling stock (wheels, tires, and brakes), structure, and controls for the landing gear depending on the nature of the mission. For the ACRV, a weight estimation of approximately 226.80 kg is used for retractable landing gear weight based on a vehicle weight of 6500 kg. This estimate is found from Figure 37.

Retractable landing gear packages are well developed in the aeronautical industry and therefore, a new design will not be necessary. For use in space, the landing gear must be modified so that it can withstand space environment outgassing effects. Outgassing occurs in a vacuum, ~~such as outer space~~, when the liquid and solid molecules in a material are converted to gaseous molecules which leave the material and cause it to lose its original properties. To avoid outgassing, no hydraulic systems will be used in the landing gear. Mechanical systems, sprayed with a protective resin to avoid outgassing effects, will be used.

For the ACRV, a compatible landing gear design based on weight estimations is the Learjet landing gear shown in Figures 38 and 39.[29] The two rear components of this tripod landing gear have a volume of $0.566m^3$ when housed, a vertical height of 0.9144 m, and deploy from the center of the craft to the sides. The forward gear deploys from the middle of the craft toward the front. For the Learjet, which weighs 6350.29 kg, the landing gear has a total weight of 277.15 kg. As mentioned, this gear must be modified by using mechanical locking mechanisms as opposed to hydraulic systems. The landing gear will be controlled electronically from the ACRV or from a ground uplink. To provide impact cushioning, the method of shock suppression in the shaft of the gear will be a spring system as opposed to a hydraulic shock system. The ACRV's landing gear will be modified using systems similar to the Space Shuttle's to make it

The graph shows axes labeled "LANDING GEAR WEIGHT - LB." (vertical, ranging from 100 to 100 000) and "$K_{LG} W_L$" (horizontal, ranging from 1000 to 1,000,000).

The equation displayed on the graph reads:

$$\text{L.G. WEIGHT} = 0.046 \, K_{LG} W_L$$
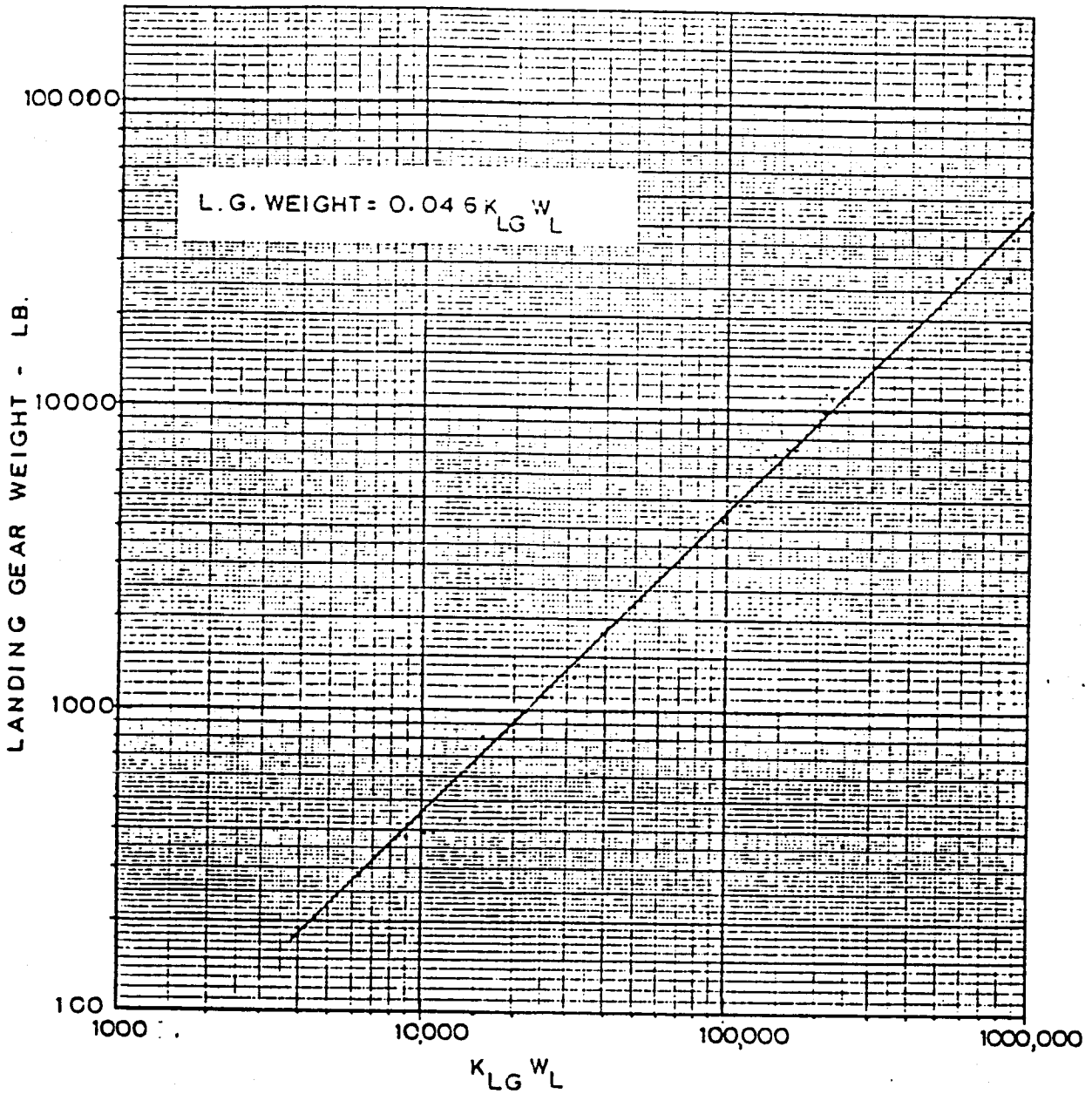
FIGURE 37: Landing Gear Weight-Method 1
(Currey, Norman S., Landing Gear Design Handbook)

69

Actuator Boot

Gear Extension Port

Nose Gear Actuator

Hydraulic Hose

Shuttle Valve

Gear Down and Locked Switch

Emergency Air Pressure Hose

Gear Retraction Port

Nose Wheel Steering Actuator

Bearing Plate

Bearing

Nose Gear Strut

Air Valve

Bearing Plate

Door Pushrod

Bearing

Trunnion Pin

Trunnion Pin Bolt

Uplatch Spacer

Uplatch Roller

Nose Gear Uplatch
Switch Striker

Chined Tire
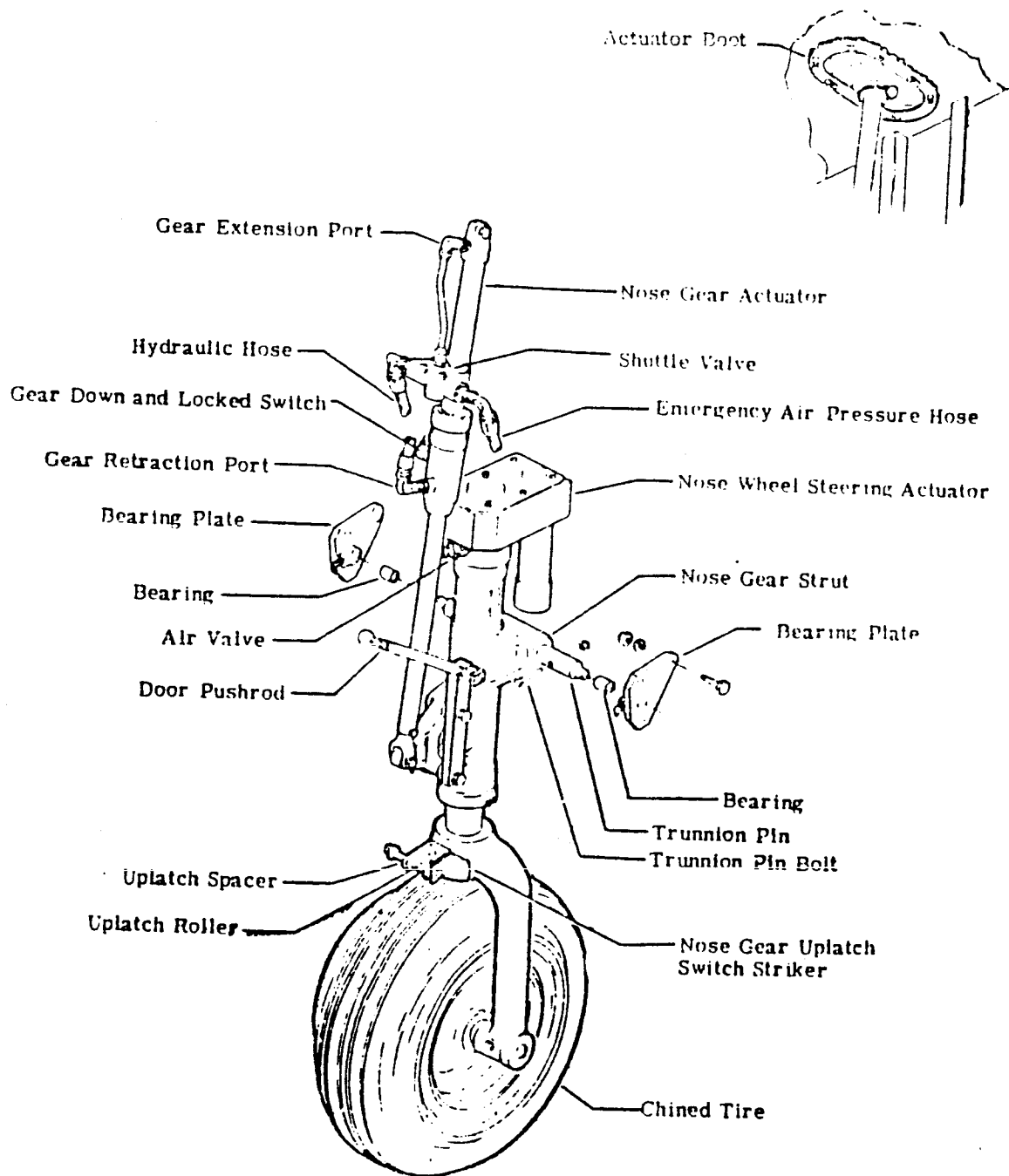
FIGURE 38: Learjet 24 & 25 Nose Landing Gear Installation
(Currey, Norman S., Landing Gear Design Handbook)

70

Aft Trunnion Pin — Shim
— Washer
— Strut
— Shim
Spar No. 7 —

✳ Shim as required to obtain 0. 002 (+0. 003/-0. 001) inch between shim and washer.

✱ Peel shim as required to maintain 1. 295 (+0. 010/-0. 000) inch dimension.

──── B ────

Main Gear Strut (Ref)
— Switch Actuator
— Switch Bracket
Switch Striker —
Upper Torque Arm —
Squat Switch — (LH LSW23, RH LSW 24)

──── A ────

— Washer
Aft Trunnion Pin —
B —
— Outboard Brake Pressure
Aft Trunnion Pin Bolt —
— Inboard Brake Pressure
Shim
Downlock Switch (LH LSW7, RH LSW8) —
— Forward Trunnion Pin
Strut
— Upper Torque Arm
Pillar —
Spacer —
A
— Outboard Door Link
Hydraulic Pressure Gear Extension
Washer —
Retaining Washer —
Nut —
Cotter Pin —
Hydraulic Pressure Gear Retraction —
Main Gear Actuator —
Lower Torque Arm —
Forward Trunnion Pin Bolt
Torque Arm Bolt —

FIGURE 39: Learjet 24 & 25 Main Landing Gear Installation
(Currey, Norman S., Landing Gear Design Handbook)

71

usable in space. Also, all of the landing gear must be sprayed with a protective resin to avoid outgassing during its service lifetime.

The landing gear and its compartment will require a volume of approximately 0.556 m^3 for the ~~back~~ *main* gear and 0.5097 m^3 for the ~~forward~~ *nose* gear, which will not significantly enlarge the ACRV if it is designed properly. The twin doors to each ~~rear~~ *main* landing gear will each have a 30.48cm width and will open using a small mechanical motor. The doors will be made of the same material as the vehicle itself and will be insulated to protect it from thermal extremes and space conditions. The craft will be approximately 0.9144 m from the ground at touchdown so that the tail does not drag while landing.

The tires for the landing gear must be made so that they will be usable without service after years of inactivity. Therefore, tires should be tubeless or solid to help prevent any air leakage during storage. These tires will also be coated so that they do not experience significant outgassing effects. Little is known about long-term effects of outgassing on rubber but again the space shuttle landing gear design will be helpful when considering the ACRV landing gear design in more detail.

STRUT DESIGN

The struts used to connect the ACRV to the heat shield must be strong enough to support the heat shield during re-entry and must be protected from any heating effects. Since the heat shield will be blown away from the ACRV, a method was devised to decouple the struts from the ACRV. This has been done successfully for the solid rocket boosters on the space shuttle using pyrotechnic bolts in the linkage that explode at a designated time during ascent. A similar method will be used for the

ACRV. Since the heat shield will be attached for an extended period of time, pyrotechnic bolts will be used since they have been proven highly reliable regardless of their inactive period.

There are many materials that can be used to design the struts depending on the specifications involved. For this design, it was determined that a maximum force of approximately 7.076×10^9 kg will be distributed across the heat shield during re-entry. Using Aluminum 2014 which has an ultimate tensile and compressive strength of 482.63 MPa in the -T6 condition[25], it is determined that a four strut mounting system with a factor of safety of at least two when using a 1.36×10^6 kg force per strut, can be designed as shown in Figure 40.

The design using the Aluminum 2014 provides an inexpensive and highly reliable method for designing the struts. Four struts will provide stability between the ACRV and the heat shield during re-entry. Buckling in these columns will not be a factor since the material thickness of the cylinder is 4.064 cm and also because the heat shield parachute casing will provide additional support. The material will also be coated with a resin that will resist outgassing effects for at least a four year period.

Composite materials can also be used for this design, but they will be more costly to develop. The entire Aluminum 2014 design proposed here will weigh approximately 36.287 kg which is relatively small compared to the entire weight of the craft, and the struts themselves will be very easy to design.

Again referring to Figure 40, pyrotechnic separation bolts join the 15.24 cm top struts to the bottom struts which attach to the
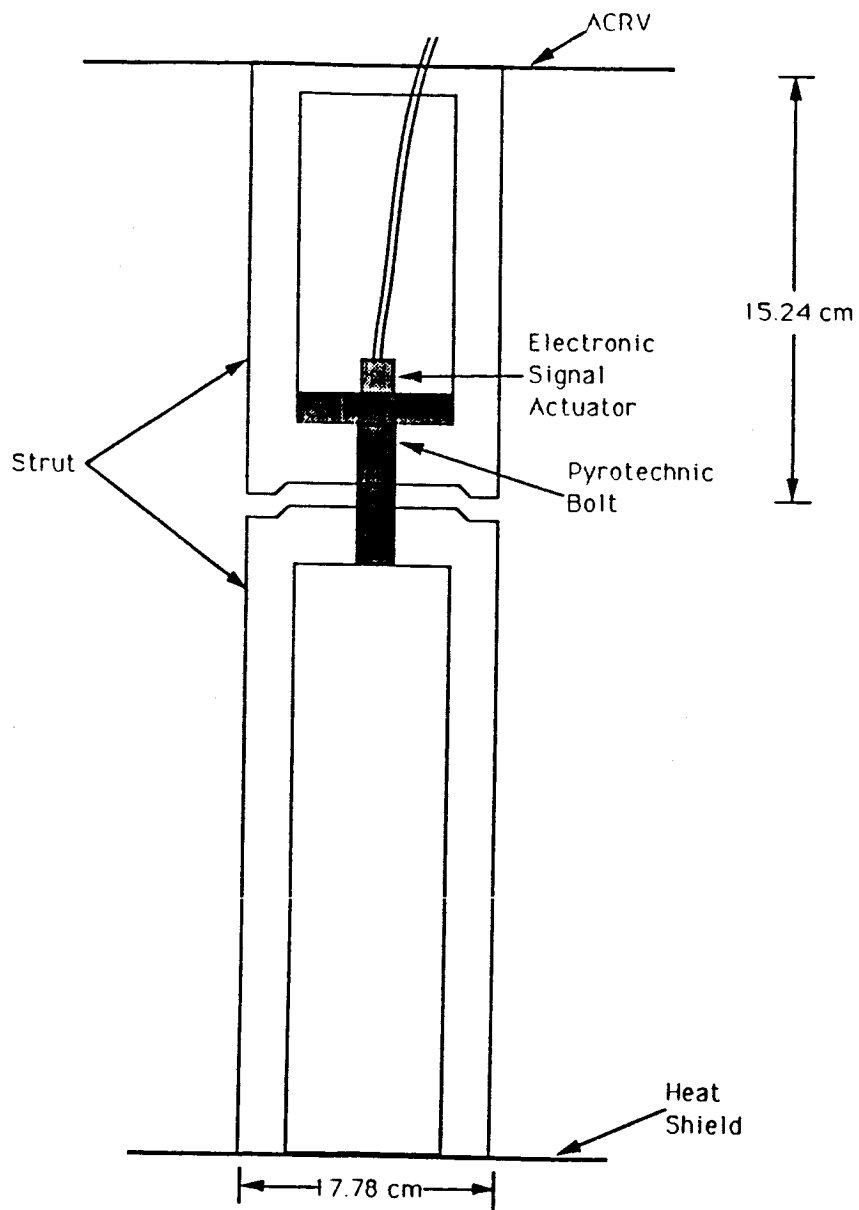
FIGURE 40: ACRV Strut Design

74

heat shield. These bolts are made of high grade steel similar to the separation bolts on the Viking Mars orbiter/lander.[26] Each will have a maximum shank diameter of 3.81 cm which can support any tensile stresses encountered since the tensile strength is 1034.2 MPa per bolt. Due to the design of the struts, any compressive load will be transferred through the aluminum support columns without affecting the bolts. The bolts will be activated by an electric signal given by either the ACRV crew or ground control when detachment of the heat shield is desired.

The struts will be attached to the ACRV and the heat shield by pin joints. Spherical bearings in each strut's clevis ends permit rotation to avoid bending loads. A clevis end is a U-shaped joint with a pin bolt passing through holes at both ends to allow rotation of the fastened components.[26] The electronic detonation cord will run past the pin joints, inside the column, and attach to the top of the bolt.

CONTROL

Directional control of the ACRV will be accomplished by remote radio communication from ground based operations. Two separate channels are available to accomplish this, one being via Tracking and Data Relay Satellites (TDRS), and the other being by direct ground uplink. TDRS transmissions will be used while the ACRV is still in orbit to determine the necessary deorbit path. Once the ACRV has entered the atmosphere it will be within range of ground transmitters at the landing site and can be controlled similarly to a Remotely Piloted Vehicle (RPV). RPV's are frequently used by NASA and the military and their control systems are well documented.

Directional control of the craft with the parawing deployed will be

accomplished by varying the center of gravity of the ACRV with respect to the parawing. Servo motors attached to the shroud lines will control line lengths which in turn will change the center of gravity. A study involving this type of control, using a direct line of sight radio-controlled model, was performed and proved that this type of craft could be effectively controlled.[28] More information on the actual radio transmitters and the frequencies needs to be obtained.

6.0 CONCLUSIONS AND RECOMMENDATIONS

A braking and landing system design has been developed for the ACRV. This design includes atmospheric re-entry starting at 120 km and a re-entry angle of -2°. The vehicle will be protected during the heating phase by an off center ellipsoid ablative heat shield based on the AFE Aerobrake. At an altitude of 44 km, three 20° conical ribbon parachutes, each with a nominal diameter of 11.4 m, will be deployed to stabilize and decelerate the ACRV enough to allow the heat shield to separate safely. The heat shield is attached to the ACRV by four hollow, cylindrical, aluminum struts. It will be separated from the craft by activating four pyrotechnic bolts each with a diameter of 3.81 cm. The heat shield will then descend to the ocean using its own 20° conical ribbon parachute of 14.28 m nominal diameter. A 513.206 m^2 Kevlar parawing is then deployed and the vehicle descends to Earth. The landing gear, modified from a Learjet, is deployed just before touchdown. The ACRV then touches down and rolls to a stop.

Due to time constraints, the design team was unable to fully investigate the following aspects of this design and makes these recommendations for further study. The effects of space storage on materials and systems must be evaluated to ensure the integrity of the braking and landing system. The degree of reefing and the opening forces for the parachute and parawing systems must be studied to determine optimal deployment methods. Servo motor design, control systems, and stability must be analyzed to determine the best combination for controlling the parawing. Communications and ground uplinks for braking and landing control systems must be finalized to ensure a safe landing.

REFERENCES

1. Stone, Dennis A., 'Crew Emergency Rescue Vehicle; System Performance Requirements Document', NASA Publishing, Houston, TX, 1988.

2. D'Alelio, G. F. and Parkes, John A., Ablative Plastics, Marcel Dekker Inc., New York, 1971, pg. 6.

3. Kratsch, K. C., and Hearne, L., 'Thermal Performance of Heat Shield Composites During Planetary Entry.' in Engineering Problems of Manned Interplanetary Exploration, AIAA, New York, 1963.

4. Poynter, Dan, The Parachute Manual - A technical Treatise on Aerodynamic decelerators 3rd Ed., Para-Publishing, Santa Barbara, Ca., 1984.

5. Knacke, T. W., Parachute Recovery Systems Design Manual, Chapters 1-5, NWC TP 6575, Aerosystems Department, Naval Weapons Center, July 1985.

6. Buning, H., Project Aneas: A Feasibility Study for Crew Emergency Return Vehicle, Technische Hogeschool Delft, Netherlands, 1988.

7. Bernard, J. W., 'Space Shuttle Program Solid Rocket Booster Decelerator Subsystem', NASA-CR-178576, Sept. 1985.

8. Currey, Aircraft Landing Gear Design: Principles and Practices, AIAA Educational Series, 1988.

9. Hatch, Howard G. and McGowan, William A. 'An Analytical Investigation of the Loads, Temperatures, and Ranges Obtained During the Recovery of Rocket Boosters by means of a Parawing' NASA TN-D-923, 1960.

10. Rogallo, Francis M., Lowry, John G., Croom, Delwin R. and Taylor, Robert T., 'Preliminary Investigation of a Paraglider', NASA TN D-443, 1960.

11. Aerospace 306 Class notes, PSU, Spring 1989.

12. Fleming, G. J., 'Prediction of Heat Shield Performance in terms of Epoxy Resin Structure,' Ablative Plastics, Marcel Dekker, Inc., New York, 1971, pp. 205-225.

13. Curry, D. M. 'Program Requirements for the Aeroassist Flight Experiment (AFE) Aerobrake', JSC-22962, Revision A, NASA Lyndon B. Johnson Space Center, Houston, Texas, May 1989.

14. Colovin, J. E., Mueller, S. R., Rochelle, W. C., and Troy, P. C., 'Development of AFE Aerobrake Aerothermodynamic Data Book', Paper 89-1734, presented at AIAA 24th Thermophysics Conference, Buffalo, New York, June 12-14 1989.

15. Bousley, S. A., Colovin, J. E., Mueller, S. R., Troy, P. C., Rochelle, W. C., 'Aerobrake Heating Rate Sensitivity Study For the Aeroassist Flight Experiment (AFE)', Paper 89-1733 presented at AIAA 24th Thermophysics Conference, Buffalo, New York, June 12-14, 1989.

16. Vojvudich, Nick S., 'Hypervelocity Heat Protection - A Review of Laboratory Experiments', Ablative Plastics, Marcel Dekker, Inc., New York, 1971. pp. 41-68.

17. Murray, A. L., 'Further Enhancements of the BLIMP Computer Code and User's Guide', AFUAL -TR-88-3010, June 30, 1988.

18. Bertin, John J., and Smith, Michael L., Aerodynamics for Engineers, Prentice Hall, New Jersey, 1989.

19. St. Leslie, G., and Pavlosky, James E., 'Apollo Experience Report Thermal Protection Subsystems', NASA TM X-1778, 1971.

20. Harkey, Wilbur, Re-entry Aerodynamics, AIAA Education Series, 1988.

21. Sambamurthi, J., Seaford, M., and Warmbrod, J., 'Engineering Methodology to Estimate the Aerodynamic Heating to the Base of the Aeroassist Flight Experiment Vehicle', paper 89-1732 presented at AIAA 24th Thermophysics Conference, Buffalo, New York, June 12-14, 1989.

22. Lee, D., and Goodrich, W., 'Aerothermodynamic Environment of the Apollo Command Module During Suborbital Entry', NASA TN D-65792, April, 1972.

23. Hair, L. M., and Engel, C. D., 'Aerothermal Test Data of Low L/D Aerobrake Orbital Transfer Vehicle at Mach 10', Remtech RTR 069-1, April, 1983.

24. Curry, Aircraft Landing Gear Design: Principles and Practices, AIAA Education Series, 1988.

25. Design Reference Manual, D-BN-0012, Engineering Division, NASA, Houston, TX, 1968.

26. Space Shuttle News Reference, NASA.

27. Rogallo, Francis M., 'Paraglider Recovery Systems', for presentation at IAS meeting on Man's progress in the Conquest of Space, St. Louis, MO, April 30, May 1-2, 1962.

28. Hewes, Donald E., 'Free-Flight Investigation of Radio-Controled Models with Parawings', NASA TN D-927, Sept. 1961.

29. Currey, Norman S., Landing Gear Design Handbook, Lockheed Publ. Marietta Ga., 1982.

30. 'Characteristics and Uses of Kevlar 29 Aramid', DuPont, Sept. 1976.

APPENDIX A

```
**********************************************************************
*                                                                    *
*     PROGRAMMER   :   JEFFREY B. DRAPER                             *
*                                                                    *
*       THIS PROGRAM SOLVES THE FIRST-ORDER DIFFERENTIAL EQUATIONS   *
*     NEEDED TO FIND VELOCITY AND ALTITUDE AS FUNCTIONS OF TIME FOR  *
*     THE ACRV'S REENTRY TRAJECTORY USING THE RUNGE-KUTTA FOURTH ORDER *
*     SUBPROGRAM CREATED BY DR. R. G. HELTON.  THE PROGRAM ALSO FINDS *
*     THE HEATING RATES ON THE HEAT SHIELD AS A FUNCTION OF TIME.    *
*                                                                    *
**********************************************************************
*                                                                    *
*     NOMENCLATURE:                                                  *
*                                                                    *
*      CD = DRAG COEFFICIENT                                         *
*      CL = LIFT COEFFICIENT                                         *
*       D = DRAG (N)                                                 *
*      LI = LIFT (N)                                                 *
*       M = MASS OF ACRV (KG)                                        *
*      MU = GRAVITATIONAL CONSTANT (KM**3/M**2)                      *
*   QCONV = CONVECTIVE HEATING RATE (W/M**2)                         *
*    QRAD = RADIATIVE HEATING RATE (W/M**2)                          *
*      RE = AVERAGE EQUATORIAL RADIUS OF EARTH (KM)                  *
*     RHO = ATMOSPHERIC DENSITY (KG/KM**3)                           *
*   RHOSL = ATMOSPHERIC DENSITY AT SEALEVEL (KG/KM**3)               *
*      HS = SCALING FACTOR (KM)                                      *
*      HT = HEIGHT ABOVE EARTH'S SURFACE (KM)                        *
*       S = WETTED AREA OF ACRV  DURING RE-ENTRY (KM**2)             *
*   SIGMA = CONSTANT FOR RADIATIVE HEATING                          *
*    X(1) = VELOCITY (KM/S)                                          *
*    X(2) = RE-ENTRY ANGLE (RADIANS)                                 *
*    X(3) = RADIAL DISTANCE FROM EARTH'S CENTER (KM)                 *
*    TIME = TIME (SECONDS)                                           *
*                                                                    *
*     ALL OTHER VARIABLES ARE FOR PROGRAMMING PURPOSES              *
*                                                                    *
**********************************************************************

      REAL CL,CD,D,G,H,HS,HT,LI,MU,QCONV,QRAD,RE,RHOSL,S,TIME
      REAL X(3),XDOT(3),TEMP(3),G1(3),G2(3),G3(3),G4(3)
      INTEGER IER,L,NDIM,NVAR


      CD=1.15
      CL=0.322
      H=1.0
      HS=7.163
      L=10
      MU=398600.47
      NDIM=3
      NVAR=3
      RE=6378.139
```

81

```fortran
      RHOSL=1.225E9
      S=1.43E-5
      TIME=0
      X(1)=3.0
      X(2)=-0.0350
      X(3)=6498.139


C    THIS SECTION SETS UP THE PROGRAM TO RUN THE RK-4 SUBROUTINE

      OPEN(UNIT=4,FILE='ACRV DATA A',STATUS='NEW',FORM='FORMATTED')
      OPEN(UNIT=3,FILE='HEAT DATA A',STATUS='NEW',FORM='FORMATTED')

      WRITE(4,10)'TIME ','VELOCITY','ALTITUDE','ANGLE','G-FORCES','DRAG'
      WRITE(4,10)'(SEC)',' (KM/S) ','  (KM)  ','(RAD)',          ',' (N)'
      WRITE(3,11)'TIME ',' QCONV  ','  QRAD  ',' QTOTAL '
      WRITE(3,11)'(SEC)','KW/SQ(M)','KW/SQ(M)','KW/SQ(M)'

10    FORMAT(2X,A5,4X,A8,5X,A8,4X,A5,4X,A8,6X,A4)
11    FORMAT(2X,A5,2X,A8,2X,A8,2X,A8)

      WRITE(4,*)' '
      WRITE(3,*)' '

      WHILE(X(3)-RE.GT.15)DO

      G=MU/(X(3)**2)
      HT=X(3)-RE
      RHO=RHOSL*EXP((-HT)/HS)
      D=0.5*RHO*(X(1)**2)*S*CD
      LI=0.5*RHO*(X(1)**2)*S*CL

*******************************************************************
*                                                                 *
*  THIS SECTION CALCULATES CONVECTIVE AND RADIATIVE STAGNATION POINT *
*   HEATING RATES                                                 *
*                                                                 *
*******************************************************************
      IF(HT.GT.25)THEN
       QCONV=214638.3543*SQRT((1.9403E-12*RHO)/5.0)*(X(1)*3.2884)**3
      ELSE
       QCONV=28959.143*(RHO/RHOSL)**0.8*(X(1)*3.2884)**3
      ENDIF
      IF(HT.GT.60.96)THEN
       SIGMA=0.0003685
      ELSE
       IF(HT.GT.45.72)THEN
        SIGMA=0.0015
       ELSE
        SIGMA=0.0170
       ENDIF
      ENDIF
      QRAD=475974.12*SIGMA**1.5*(X(1)*0.32884)**12.5
```

82

```
      CALL RK4(X,XDOT,TIME,H,NDIM,NVAR,TEMP,G1,G2,G3,G4,IER,D,LI,G)
      IF (IER.EQ.1) THEN
        WRITE(4,100)
        STOP
      ENDIF

      IF(L.EQ.10)THEN
        L=1
        D=D*1000

        WRITE(4,20)TIME,X(1),X(3)-RE,X(2),ABS(XDOT(1)*1000/9.81),D.
20      FORMAT(1X,F5.0,5X,F8.5,4X,F8.2,4X,F6.3,5X,F6.4,4X,F9.2)
        D=D/1000

        WRITE(3,30)TIME,QCONV/1000,QRAD/1000,(QCONV+QRAD)/1000
30      FORMAT(1X,F5.0,2X,F8.2,2X,F8.2,2X,F6.2)

      ELSE
        L=L+1
      ENDIF

      ENDWHILE

      WRITE(4,25)
25    FORMAT(' ',1X)
100   FORMAT ('ERROR:   NVAR>NDIM')
      CLOSE(UNIT=4)


      END
```

✿✿✿✿✿✿✿✿✿✿✿✿✿✿✿✿✿✿✿✿✿✿✿✿✿✿ SUBROUTINES ✿✿✿✿✿✿✿✿✿✿✿✿✿✿✿✿✿✿✿✿✿✿✿✿✿✿

```
✿      SUBROUTINE RK4                                          ✿

      SUBROUTINE RK4(X,XDOT,TIME,H,NDIM,NVAR,TEMP,G1,G2,G3,G4,IER,D,LI,
     aG)
✿✿✿✿✿✿✿✿✿✿✿✿✿✿✿✿✿✿✿✿✿✿✿✿✿✿✿✿✿✿✿✿✿✿✿✿✿✿✿✿✿✿✿✿✿✿✿✿✿✿✿✿✿✿✿✿✿✿✿
✿      INTEGRATES A SET OF FIRST-ORDER DIFFERENTIAL EQUATIONS ✿
✿         USING A RUNGE-KUTTA FOURTH-ORDER METHOD             ✿
✿                                                            ✿
✿      AUTHOR :  R. G. MELTON                            ●    ✿
✿      REVISED:   2/18/88                                     ✿
✿✿✿✿✿✿✿✿✿✿✿✿✿✿✿✿✿✿✿✿✿✿✿✿✿✿✿✿✿✿✿✿✿✿✿✿✿✿✿✿✿✿✿✿✿✿✿✿✿✿✿✿✿✿✿✿✿✿✿

      DIMENSION X(NDIM),XDOT(NDIM),TEMP(NDIM)
      DIMENSION G1(NDIM),G2(NDIM),G3(NDIM),G4(NDIM)
      REAL D,LI,G
      IF (NVAR .GT. NDIM) THEN
        IER=1
```

```fortran
          RETURN
        ELSE
          IER=0
        ENDIF
        CALL VALUE(X,XDOT,TIME,NDIM,NVAR,D,LI,G)
        DO 100 I=1,NVAR
          G1(I)=H*XDOT(I)
100     CONTINUE
        DO 200 I=1,NVAR
          TEMP(I)=X(I)+G1(I)/2
200     CONTINUE
        CALL VALUE(TEMP,XDOT,TIME+H/2.,NDIM,NVAR,D,LI,G)
        DO 250 I=1,NVAR
          G2(I)=H*XDOT(I)
250     CONTINUE
        DO 300 I=1,NVAR
          TEMP(I)=X(I)+G2(I)/2.
300     CONTINUE
        CALL VALUE(TEMP,XDOT,TIME+H/2.,NDIM,NVAR,D,LI,G)
        DO 350 I=1,NVAR
          G3(I)=H*XDOT(I)
350     CONTINUE
        DO 400 I=1,NVAR
          TEMP(I)=X(I)+G3(I)
400     CONTINUE
        CALL VALUE(TEMP,XDOT,TIME+H,NDIM,NVAR,D,LI,G)
        DO 450 I=1,NVAR
          G4(I)=H*XDOT(I)
450     CONTINUE
        DO 500 I=1,NVAR
          X(I)=X(I)+1/6.*(G1(I)+2.*(G2(I)+G3(I))+G4(I))
500     CONTINUE
        TIME=TIME+H
        RETURN
        END


*       SUBROUTINE VALUE                                              *

        SUBROUTINE VALUE(X,XDOT,TIME,NDIM,NVAR,D,LI,G)

*********************************************************************
*                                                                   *
*     THIS SUBROUTINE CREATES THE VALUES OF X AND XDOT USED         *
*  IN THE RK4 SUBROUTINE.                                           *
*                                                                   *
*********************************************************************

        REAL D,G,LI,M,X(NDIM),XDOT(NDIM)
        M=6803.8865
        XDOT(1)=(-G)*SIN(X(2))-D/M
        XDOT(2)=(X(1)/X(3))*COS(X(2))-(G/X(1))*COS(X(2))+(LI/(M*X(1)))
        XDOT(3)=X(1)*SIN(X(2))

        RETURN
        END
```

84

ORIGINAL PAGE IS
OF POOR QUALITY

TIME (SEC)	VELOCITY (KM/S)	ALTITUDE (KM)	ANGLE (RAD)	G-FORCES	DRAG (N)
1.	8.00032	119.72	-0.035	0.0331	34.17
11.	8.00353	116.93	-0.034	0.0324	50.54
21.	8.00666	114.17	-0.034	0.0316	74.33
31.	8.00971	111.46	-0.033	0.0306	106.07
41.	8.01264	108.79	-0.033	0.0293	157.91
51.	8.01544	106.16	-0.032	0.0278	228.21
61.	8.01806	103.58	-0.032	0.0258	327.83
71.	8.02045	101.04	-0.031	0.0232	468.09
81.	8.02254	98.54	-0.031	0.0197	663.95
91.	8.02423	96.09	-0.030	0.0151	935.53
101.	8.02540	93.69	-0.029	0.0089	1309.43
111.	8.02585	91.34	-0.029	0.0007	1820.50
121.	8.02535	89.04	-0.028	0.0103	2512.57
131.	8.02359	86.79	-0.027	0.0248	3440.31
141.	8.02015	84.59	-0.027	0.0440	4675.44
151.	8.01454	82.46	-0.026	0.0689	6288.61
161.	8.00611	80.40	-0.025	0.1011	8379.10
171.	7.99407	78.41	-0.024	0.1418	11039.70
181.	7.97750	76.50	-0.023	0.1927	14363.48
191.	7.95534	74.69	-0.022	0.2547	18429.50
201.	7.92648	72.98	-0.021	0.3284	23281.47
211.	7.88979	71.40	-0.019	0.4128	28796.36
221.	7.84431	69.95	-0.017	0.5064	34932.64
231.	7.78931	68.64	-0.015	0.6055	41427.15
241.	7.72453	67.50	-0.013	0.7048	47916.78
251.	7.65034	66.54	-0.011	0.7971	53938.46
261.	7.56776	65.75	-0.009	0.8757	59036.51
271.	7.47842	65.15	-0.007	0.9361	62918.78
281.	7.38436	64.71	-0.005	0.9743	65325.13
291.	7.28776	64.44	-0.003	0.9901	66252.44
301.	7.19072	64.30	-0.001	0.9858	65852.00
311.	7.09502	64.28	0.001	0.9653	64389.80
321.	7.00191	64.34	0.002	0.9344	62264.75
331.	6.91222	64.45	0.002	0.8974	59755.98
341.	6.82627	64.60	0.002	0.8580	57110.46
351.	6.74416	64.74	0.002	0.8210	54656.89
361.	6.66538	64.84	0.002	0.7892	52574.95
371.	6.58937	64.89	0.001	0.7640	50961.65
381.	6.51535	64.87	-0.001	0.7477	49957.88
391.	6.44244	64.75	-0.002	0.7407	49597.96
401.	6.36964	64.52	-0.004	0.7448	49988.74
411.	6.29578	64.17	-0.006	0.7611	51212.98
421.	6.21964	63.69	-0.009	0.7904	53310.27
431.	6.13973	63.07	-0.011	0.8365	56541.49
441.	6.05438	62.32	-0.013	0.9000	60930.95
451.	5.96171	61.45	-0.015	0.9837	66668.38
461.	5.85965	60.46	-0.018	1.0897	73883.44
471.	5.74590	59.36	-0.020	1.2201	82715.06
481.	5.61802	58.18	-0.021	1.3753	93188.44
491.	5.47370	56.95	-0.023	1.5528	105121.56
501.	5.31111	55.70	-0.023	1.7440	117941.88
511.	5.12943	54.45	-0.024	1.9408	131113.31

85

TIME (SEC)	VELOCITY (KM/S)	ALTITUDE (KM)	ANGLE (RAD)	G-FORCES	DRAG (N)
521.	4.92854	53.22	-0.024	2.1321	143882.94
531.	4.71013	52.06	-0.024	2.2981	154938.38
541.	4.47746	50.97	-0.023	2.4248	163366.75
551.	4.23483	49.95	-0.023	2.5059	168751.81
561.	3.98676	49.00	-0.023	2.5409	171091.00
571.	3.73740	48.09	-0.024	2.5368	170807.31
581.	3.48993	47.20	-0.025	2.5076	169030.13
591.	3.24638	46.29	-0.028	2.4610	166115.63
601.	3.00760	45.32	-0.033	2.4114	163097.06
611.	2.77363	44.29	-0.039	2.3630	160256.81
621.	2.54407	43.15	-0.046	2.3209	157941.69
631.	2.31841	41.91	-0.056	2.2833	156052.75
641.	2.09633	40.54	-0.067	2.2464	154343.25
651.	1.87825	39.07	-0.081	2.2012	152229.88
661.	1.66528	37.49	-0.097	2.1412	149326.31
671.	1.45924	35.80	-0.118	2.0610	145318.56
681.	1.26269	34.02	-0.143	1.9499	139579.06
691.	1.07854	32.16	-0.176	1.8090	132287.31
701.	0.90982	30.22	-0.217	1.6384	123605.00
711.	0.75907	28.20	-0.271	1.4455	114163.81
721.	0.62813	26.12	-0.339	1.2368	104564.31
731.	0.51788	23.99	-0.425	1.0251	95703.31
741.	0.42798	21.82	-0.528	0.8226	88274.13
751.	0.35658	19.64	-0.646	0.6454	82940.75
761.	0.30100	17.51	-0.769	0.4994	79457.75
771.	0.25772	15.44	-0.889	0.3914	77646.00

TIME (SEC)	QCONV KW/SQ(M)	QRAD KW/SQ(M)	QTOTAL KW/SQ(M)
1.	18.54	601.29	619.83
11.	22.56	604.32	626.88
21.	27.38	607.29	634.67
31.	33.13	610.19	643.32
41.	39.97	613.00	652.97
51.	48.08	615.69	663.77
61.	57.67	618.23	675.90
71.	68.95	620.56	689.52
81.	82.16	622.62	704.79
91.	97.57	624.31	721.89
101.	115.47	625.51	740.97
111.	136.17	626.02	762.19
121.	159.95	625.64	785.59
131.	187.09	624.06	811.16
141.	217.93	620.92	838.85
151.	252.41	615.75	868.16
161.	290.77	607.99	898.76
171.	332.79	597.04	929.82
181.	378.07	582.21	960.28
191.	425.94	562.86	988.79
201.	475.16	538.48	1013.63
211.	523.90	508.82	1032.71
221.	570.53	474.06	1044.58
231.	612.78	434.84	1047.62
241.	648.28	391.39	1040.67
251.	674.83	348.35	1023.18
261.	691.00	304.58	995.59
271.	696.75	262.87	959.62
281.	692.29	224.59	916.88
291.	679.12	190.60	869.72
301.	659.17	161.22	820.38
311.	634.56	136.34	770.90
321.	607.70	115.55	723.25
331.	580.14	98.31	678.44
341.	553.09	84.03	637.12
351.	528.10	72.20	600.30
361.	505.88	62.31	568.19
371.	486.74	53.97	540.71
381.	471.14	46.86	518.00
391.	459.00	40.71	499.71
401.	450.46	35.33	485.79
411.	445.47	30.55	476.02
421.	443.63	26.26	469.89
431.	445.29	22.37	467.65
441.	449.60	18.80	468.40
451.	456.15	15.54	471.68
461.	464.09	103.09	567.18
471.	472.41	80.95	553.35
481.	479.66	61.34	541.00
491.	483.97	44.52	528.49
501.	483.06	30.71	513.76
511.	475.53	19.99	495.52

87

C-5

TIME (SEC)	QCONV KW/SQ(M)	QRAD KW/SQ(M)	QTOTAL KW/SQ(M)
521.	460.38	12.22	472.60
531.	436.81	6.98	443.79
541.	405.74	3.73	409.47
551.	369.25	1.87	371.12
561.	329.81	0.88	330.70
571.	289.89	0.40	290.29
581.	251.60	0.17	251.77
591.	215.99	0.07	216.06
601.	183.85	1.02	184.87
611.	155.14	0.37	155.52
621.	129.73	0.13	129.86
631.	107.24	0.04	107.28
641.	87.35	0.01	87.36
651.	69.77	0.00	69.78
661.	54.44	0.00	54.44
671.	41.34	0.00	41.34
681.	30.41	0.00	30.41
691.	21.66	0.00	21.66
701.	14.93	0.00	14.93
711.	10.01	0.00	10.01
721.	6.57	0.00	6.57
731.	10.15	0.00	10.15
741.	7.28	0.00	7.28
751.	5.36	0.00	5.36
761.	4.08	0.00	4.08
771.	3.21	0.00	3.21

PRELIMINARY SUBSYSTEM DESIGNS

for the

ASSURED CREW RETURN VEHICLE

(ACRV)

Final Report Vol. II

Department of Aerospace Engineering
Pennsylvania State University
University Park, PA

PENNSTATE

ABSTRACT

This report comprises a series of design studies concerning the Assured Crew Return Vehicle (ACRV) for Space Station *Freedom*. Study topics, developed with the aid of NASA/Johnson Space Center's ACRV Program Office, include: a braking and landing system for the ACRV, ACRV growth options, and the design impacts of the ACRV's role as a medical emergency vehicle.

Four alternate designs are presented for the ACRV braking and landing system. Options presented include: ballistic and lifting body reentries; the use of high-lift, high-payload aerodynamic decelerators, as well as conventional parachutes; landing systems designed for water landings, land landings, or both; and an aerial recovery system. All four design options presented combine some or all of the above attributes, and all meet performance requirements established by the ACRV Program Office.

Two studies of ACRV growth options are also presented. Use of the ACRV or a similarly designed vehicle in several roles for possible future space missions is discussed, along with the required changes to a basic ACRV to allow it to perform these missions optimally. The outcome of these studies is a set of recommendations to the ACRV Program Office describing the vehicle characteristics of the basic ACRV which lend themselves most readily to be adapted for use in other missions.

Finally, the impacts on the design of the ACRV due to its role as a medical emergency vehicle were studied and are presented herein. The use of the ACRV in this manner will impact its shape, internal configuration, and equipment. This study included: the design of a stretcher-like system to transport an ill or injured crew member safely within the ACRV; the compilation of a list of necessary medical equipment and the decisions on where and how to store it; and recommendations about internal and external vehicle characteristics which will ease the transport of the ill or injured crewman and allow for swift and easy ingress/egress of the vehicle.

This report is divided into three volumes. Volume I contains the four braking and landing proposals, volume II contains the two growth options studies, and volume III contains the single medical mission impact study.

VOLUME II

ACRV GROWTH OPTIONS

Growth options are the future missions which an ACRV or a similar vehicle might undertake. A study of ACRV growth options includes investigating proposed or suggested future missions in space to determine whether an ACRV-based vehicle might be able to perform or contribute to these missions. Once this preliminary investigation is done, the modifications to the ACRV to enable it to perform these missions optimally are determined, and these modifications are then used to recommend the vehicle characteristics of the basic ACRV which lend themselves most readily for adaptation in these future missions. A growth options study is essential for good design in this sort of circumstance, where planning for the future now could mean saving many dollars tomorrow due to the availability of a vehicle which can be easily modified to perform many tasks.

Two of the seven project groups participating in this program chose to examine growth options for the ACRV. The two groups were able to determine some fundamental characteristics of an ACRV by knowing about its mission and by examining the System Performance Requirements Document (for example, the structure of the ACRV must be designed to take the high stresses of an atmospheric reentry). From these characteristics, they were able to perform a growth options study. In addition, both groups examined a more detailed aspect of the ACRV growth options. The two final reports for these project groups are included in the following sections.

ACRV

GROWTH OPTION

DESIGN STUDY

A Design Project For Aerospace 401
April 30, 1990

The Pennsylvania State University

Design Team:
Richard P. Barton
Eric J. Bell
Dave Brzenchek
John R. Cohrac, Group Leader
Michael Di Labio
Darryl E. Hummel
Eileen P. Morgan

ABSTRACT

This report investigates possible growth options for the Assured Crew
Return Vehicle (ACRV), and presents a detailed design study for a lunar
crew transfer, a mission derived from the ACRV. There are two sections to
this report: the first section discusses possible growth options derived
from the ACRV, while the second section provides a preliminary design for
the lunar mission. Included in the first section is a brief description of all
growth options considered and the rationale for selecting which growth
options are the most compatible with the ACRV. This is followed by a
detailed analysis of the most promising growth options and a discussion of
their basic mission requirements. An analysis is presented of the
numerical method employed to determine which of the remaining growth
options is the optimum choice for an in-depth design effort. From this
analysis it was concluded that the most feasible options were international
rescue, space station crew/cargo rotation, a lunar ACRV and the lunar crew
transfer mission. To accommodate these missions and other growth
options, this report recommends to the ACRV Program Office that a
modular ballistic design for the ACRV be developed, with two hatches and
a detachable heat shield. In the second section of this report, the pursuit
of a detailed design included development of a mission scenario and
calculation of required velocity changes and mass estimates. The specific
phases of the mission are discussed, and the requirements of vehicle
subsystems are investigated. The results of preliminary work indicate that
the lunar mission represents a promising growth option for the ACRV, and
therefore deserves further consideration.

TABLE OF CONTENTS

LIST OF TABLES

LIST OF FIGURES

FOREWORD

This report was written to make recommendations to the ACRV Program Office regarding future use of Space Station Freedom's Assured Crew Return Vehicle. It presents the methods and conclusions from a design project that investigated ACRV growth options for the 1989/1990 academic year as part of Aerospace 401, a spacecraft design course at the Pennsylvania State University. This effort was completed with the invaluable guidance and support of NASA and the Aerospace Engineering Department at Penn State. Special thanks go to Dr. Robert G. Melton, Dr. Roger C. Thompson, and Jay Burton for their assistance.

LIST OF ACRONYMS

ACRV - Assured Crew Return Vehicle

ECLSS - Environmental Control and Life Support System

ECTV - Earth Crew Transfer Vehicle

EVA - Extra-Vehicular Activity

GEO - Geosynchronous Earth Orbit

LCTV - Lunar Crew Transfer Vehicle

LEO - Low Earth Orbit

NSTS - National Space Transportation System

OMV - Orbital Maneuvering Vehicle

OTV - Orbital Transfer Vehicle

SDI - Strategic Defense Initiative

SS - space station

SSF - Space Station Freedom

I. ACRV GROWTH OPTIONS

Introduction

This study was initiated in September of 1989. Its purpose has been to devise growth options for the Assured Crew Return Vehicle (ACRV) on Space Station Freedom (SSF). The ACRV will serve as a back-up to the National Space Transportation System (NSTS), providing a means of evacuation from SSF in the event of a medical emergency, a station-wide catastrophe or the inability of the NSTS to perform crew rotation$\leq$ The return flight of the ACRV is to be fully automated, with few selected manual operations for its deconditioned crew, and should require only minimal ground support.

In light of limited funding for the space station and other future space operations, it is desirable to design an ACRV that can be adapted to perform beyond the requirements of its basic mission. The purpose of this study is to devise and analyze a number of growth options applicable to the ACRV in an effort to mold recommendations as to the optimal configuration of the basic vehicle for future growth. Over twenty-five growth options were considered, ranging from satellite repair missions to interplanetary exploration. Each growth option was evaluated on its compatibility with the ACRV and the extent to which the ACRV would need to be modified to perform the given mission; feasibility and timeliness of the growth options

-1-

were the two primary factors in this evaluation. After much scrutiny, several options remained, and a numerical method was developed to select the most viable ones. Presented in the following section is the evaluation of growth options for the ACRV which led to the detailed design of the Lunar Crew Transfer Vehicle (LCTV), a derivative of the ACRV.

OPTIONS CONSIDERED

Presented below are the ideas for the ACRV growth options that evolved out of group meetings and brainstorming sessions. Some of the ideas have been discarded due to major limitations or significant incompatibilities with the ACRV. Options requiring more detailed analysis are shown below, but the discussion on their compatibility is discussed later.

The following is a list of the proposed ideas that were considered in the initial stage of the project:

Planetary Supply	SSF Cargo Rotation	*Tour Ship*
Mars Mission	*Asteroid Deflector*	*Energy Collector*
International Rescue	*Debris Collector*	*OMV/OTV*
Asteroid Mining	*SDI Missions*	*Lunar Mining*
GEOshack	*Orbital Construction*	*Lunar SS*
Lunar Transfer	*Mars SS*	*Scientific Lab*
SSF Crew Rotation		

* Items in italics were discarded due to basic incompatibilities
(discussed below)

Some of the options were discarded based on the fact that they will never be required to reenter Earth atmosphere (even so much as to descend to low Earth orbit via an aerobraking maneuver). The reason for discarding

these options is simply that the vehicle would be _structurally_ over-designed and

therefore would be inefficient for such a mission. Options discarded based

on this factor include: lunar space station, Mars space station, greenhouse

retrieval, energy collector, orbital construction vehicle, and the asteroid

deflector. The scientific lab was dropped since SSF already satisfies this

need. Although the tour ship is an attractive option for those who could

afford it, any time relatively close to the present does not seem to support

the implementation of such a craft. Until recently, the SDI-related

missions were a possibility, but the current trend toward peaceful

relations between the United States and the U.S.S.R. suggests funding

would not be present for such an endeavor. It is for this reason that the

option is no longer _under_ consideration. The OMV/OTV missions would be

redundant, since they shall be accomplished in dedicated vehicles. Finally,

asteroid mining lies far in the future, and current proposals for asteroid

mining do not use a craft for transportation of the material; instead, the

mined ore is propelled via some sort of mass driver and received at an

orbiting construction station.

Detailed Description of Promising Options

This section provides a brief description of the ~more~ promising growth options. Each mission is described in terms of required life support (length in days), propulsion, reentry, crew size, cargo capacity, mission support, and external activity. The description presented for each option is intended to specify the mission scenario that will occur, as well as give information on the aspects of the mission that rely heavily on the ACRV design. This information culminates in a feasibility analysis and matrix that will give a basis for which options will be pursued.

GEOshack

The GEOshack is a spacecraft designed to retrieve or repair spacecraft in geosynchronous orbit. The need for such a spacecraft is justified by the fact that many satellites in geosynchronous orbit (GEO) are nearing ~the end of~ their life expectancy. The life of a satellite is ~generally based on~ often limited by propellant or power supplies. Servicing of these satellites has been identified as a potential mission for the late 1990's. The reason for repairing and refueling of the satellites is quite simply that there is already a large number of them in orbit, and the cost for replacing a satellite is large compared to the cost of refurbishment. The GEOshack's lifetime has been set at 25-30 years and will provide a permanent base for GEO operations. The mission duration is to be a few days and it is to be supported by an

ORIGINAL PAGE IS
OF POOR QUALITY

aerobraking space transfer vehicle based at SSF. (Ref. 1)

Requirements

Life Support:	12 days/shirtsleeve environment
Propulsion:	must deliver 20,000 lb to GEO (return empty) ;
Earth Reentry:	possibly; will require aerobrake (return LEO, Crew Module)
Crew Size:	3
Cargo Capability:	yes
Mission Support:	no
External Activity:	manipulator arms and possibly EVA

Lunar Transfer Missions

President Bush has decided that after the SSF, the next logical step in American space exploration is to return to the Moon to stay. An international symposium on the Space Station outlined future space operations and also considered lunar activity to be forthcoming (see Figure 1). A necessary component for lunar base operations is a crew transfer vehicle that could bring people to and from the base in a routine manner, as well as providing an Assured Crew Return scenario should the need arise. This Lunar Assured Return mission must be SSF- independent to provide for the worst case scenario, should SSF be non-operational for any reason. This emergency mission would be very similar to the original mission of the ACRV once LEO is achieved (i.e. satisfy the information contained in the ACRV Performance Requirements Document, Ref. 2).

Requirements

Life Support:	3-4 days/shirtsleeve environment
Propulsion:	Sufficient to provide for round-trip to the Moon
Earth Reentry:	yes
Crew Size:	4
Cargo Capability:	possibly
Mission Support:	minimal (required)
External Activity:	none

Mars Mission

A manned mission to Mars is expected to occur in the first half of the twenty-first century (Ref. 3). Several proposals for this mission call for a small crew transfer vehicle. One proposal by the Martin Marietta Astronautics Group uses an Earth Crew Transfer Vehicle (ECTV). The ECTV is a small crew vehicle (8 people) that is 'ejected ' from the Mars Mother-ship on its return from Mars. An aerobrake-aerocapture design is utilized to slow the vehicle down in the Earth's atmosphere. The ECTV will return to the SSF or directly to the Earth.

Requirements

Life Support:	1-2 days/shirtsleeve environment
Propulsion:	Sufficient to provide orbital transfer and precise attitude control
Earth Reentry:	possibly
Crew Size:	6-8
Cargo Capability:	none (minimal)
Mission Support:	limited
External Activity:	none

Asteroid Mining

"The use of near-Earth resources, obtained from the Moon and other nearby asteroids, will be essential..." B. M. French, NASA Headquarters (Ref. 4)

The need and desire for exploration of near-Earth resources (from the Moon and from nearby asteroids) is agreed upon by many influential people in the space industry. An exploitation mission would involve sending spacecraft to an asteroid, collecting resources, then returning the material to the Earth (most probably to an orbiting processing station). This would be accomplished by either actually collecting the material or breaking a part of the asteroid off and "strapping" rockets on it (Ref. 5).

As of 1985, less than 50 of the nearly 200,000 Earth approaching asteroids had been analyzed. Of these, it is estimated that only 100 are suitable for exploitation (Ref. 5). Currently no significant 'asteroid analysis' research effort is under way. Even if an object was chosen for mining, sending a human there is unlikely. NASA has already begun preliminary planning for this type of mission and it does not include a manned mission. Due to the length of such a mission (about 6 months) robotic devices are much more feasible (Ref. 5). Also there is danger of contamination (Ref. 4), which would require an additional mission length for any quarantine that would be imposed.

Requirements

Life Support:	none
Propulsion:	extensive
Earth Reentry:	aerobraking
Crew Size:	6-8(none likely)
Cargo Capability:	yes
Mission Support:	minimal
External Activity:	manipulator arms/tools

International Rescue

With the U.S.S.R. already having an established human presence in
space, and other countries soon to follow suit (Japan and Europe)

it would be beneficial to have some sort of international rescue

vehicle available in case of an emergency on any manned spacecraft or

station. A modified ACRV would be ideal for such a mission, because it already

possesses all the necessary tools for a rescue mission. The only additional

items necessary would be an international docking hatch, and possibly an

increased amount of fuel and attitude control systems for an extended

rescue operation.

Requirements

Life Support:	1-3 days/shirtsleeve environment
Propulsion:	Sufficient to provide orbital transfer and precise attitude control
Earth Reentry:	yes
Crew Size:	6-8
Cargo Capability:	none

Mission Support: minimal
External Activity: none

SSF Crew and Cargo Rotation

The ACRV is already intended to provide return emergency journeys for SSF crew members back to the Earth's surface. It is for this reason that a crew rotation mission would be supported. Also feasible is the simple redesign of the internal area of the vehicle such that it would be capable of supporting cargo transport to and from SSF.

Requirements

Life Support: 1-2 days/shirtsleeve environment or none
Propulsion: Sufficient to provide orbital transfer and
                   precise attitude control
Earth Reentry: yes
Crew Size: 6-8/none
Cargo Capability: for cargo missions only
Mission Support: limited
External Activity: none

Planetary Supply

A planetary supply mission would simply be a cargo transfer of necessary supplies to and from a lunar outpost and/or possibly a Mars outpost. This would involve the addition of a cargo module or a ~~revision~~ redesign of the ACRV's internal space.

Requirements.

Life Support:	minimal
Propulsion:	sufficient for the mission (lunar or Martian transfer)
Earth Reentry:	aerobrake
Crew Size:	none
Cargo Capability:	yes
Mission Support:	limited
External Activity:	none

Analysis of Promising Options

In order to quantify compatibility of the growth options with the mission and design of the basic ACRV, a method of analysis based on numerical ratings was devised. All options, including the basic mission, were rated on a scale from one to five in several categories: life support, propulsion, reentry, crew size, cargo, mission support, external support/activity, and need/timeliness. The ACRV was rated as a three for all options. Values less than three suggested that the ACRV is over-designed for the option, and values greater than three gave a representation of how much the option requires *in* excess of the basic ACRV requirements.

Each criterion was given a percent rating to indicate a relative importance or "weight" (e.g. reentry is a crucial part of the mission and a large determining factor in design, so it is rated at 25%). Then a sum of the deviation for the ACRV is calculated based on the following formula:

$$\text{Deviation} = \sum_{1}^{n} (3 - x_i) W_i$$

W_i = the weighting of category i
x_i = number rating for category i
n = the number of categories

Table 1 gives ratings for categories, Table 2 shows weights and

explanations for each category (reentry, cargo, etc.), and Table 3 shows the growth option compatibility matrix. Figure 2 is a bar chart summarizing Table 3. Using this method of analysis, growth options with deviation values less than one were considered to be viable options deserving further study.

Table 1: Category Ratings

Life Support :
  1 - none/minimal
  2 - 0 to 12 hours
  3 - 12 to 48 hours (ACRV)
  4 - 2 to 10 Days
  5 - greater than 10 days

Propulsion :
  1 - none
  3 - orbit, attitude control, and deorbit (ACRV)
  4 - GEO excursion
  5 - The Moon and planets

Earth Reentry :
  1 - no reentry
  2 - entry to LEO (aerobrake)
  3 - reentry to surface (ACRV)

Crew Size :
  1 - 0
  2 - 1 to 5
  3 - 6 to 8
  5 - greater than 8

Cargo Capability :
  2 - none
  3 - minimal (ACRV)
  4 - supplies for extended journey
  5 - payload extensive, cargo only

Ground Support :
  1 - totally self contained
  3 - minimal ground support (ACRV)
  5 - totally ground controlled

External Activity :
  3 - none
  4 - manipulator arm or EVA
  5 - manipulator arm and EVA

Timeliness/Need :
  1 - already in production
  3 - Contemporary ACRV
  4 - within ACRV system life
  5 - within the next 50 years

Table 2: Category Weights

Life Support	10%	important but easy to adjust
Propulsion	10%	again easily adjusted
Earth Reentry	25%	major ACRV requirement
Crew Size	10%	important but semi-flexible
Cargo Capability	5%	easily adjusted, not very important
Mission Support	5%	not real important
External Activity	10%	some additional design necessary
Timeliness/Need	<u>25%</u>	extremely important
Total	100%	

Table 3: Growth Option Matrix

ACRV	life support	propulsion	reentry	crew	cargo	ground support	external activity	need and timeliness	Deviation from ACRV
	3	3	3	3	3	3	3	3	0.000
weighting percent	0.1	0.1	0.25	0.1	0.05	0.05	0.1	0.25	
Asteroid Mining	1	5	2	1	5	5	5	4.5	1.625
GEOshack	5	4	2	2	4	1	5	3	1.000
International Rescue Vehic	3	3.5	3	3	2	3.5	4	3	0.225
Lunar Missions									
Transfer Vehicle	4	5	3	2	3.5	3	3	3.5	0.550
ACRV	4	5	3	2	3.5	3	3	3.5	0.550
Mars mission	3	5	2.5	3	4	1	3	5	0.975
Space Station Freedom									
Crew Rotation	3	3	3	3	2	4	3	3	0.100
Cargo Rotation	1	3	3	1	5	5	3	3	0.600
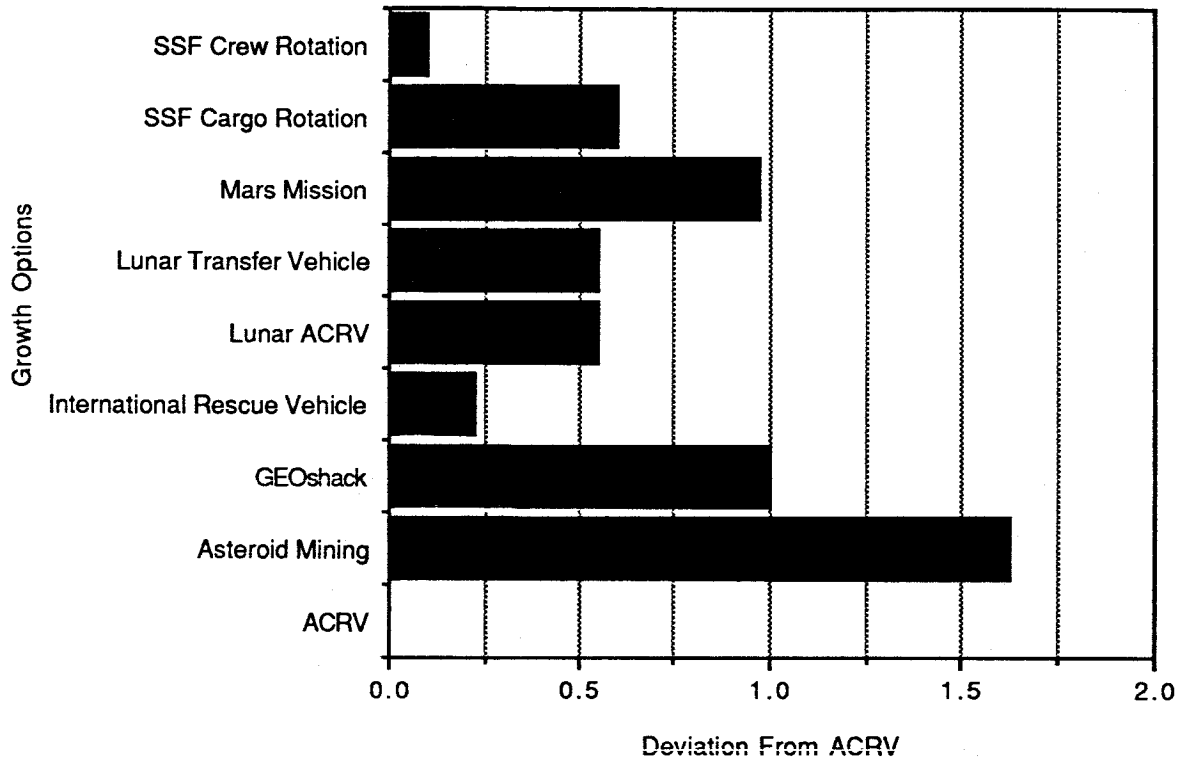
Figure 1: Growth Option Deviation

Conclusions

The growth options matrix (table 3) suggests that nearly half of the growth options considered show a significant deviation from the ACRV design. Many of the options could be eliminated primarily due to the need and timeliness of the option; e.g. the prospect of regular asteroid mining or a space tour ship is not likely to occur within the system lifetime of the ACRV and therefore basing these vehicles on the ACRV would be using 30 year old technology. As can be seen in the matrix, there are five growth options which show little deviation from the ACRV. The SSF crew rotation option is almost identical to the basic crew return mission and therefore shows minimal deviation (see earlier). Using the ACRV as a cargo carrier for the SSF is also a promising growth option, requiring only minor modifications to the crew module for carrying supplies. An international rescue mission is a natural and relatively simple extension of the basic purpose of the ACRV design as a return vehicle. It is recommended that this growth option be incorporated into the original ACRV design. Another option which warrants further study in relation to the ACRV, is manned interplanetary exploration. It is possible that an ACRV type vehicle could provide some assistance with certain manned phases of an interplanetary mission.

II. LUNAR CREW TRANSFER

Introduction

The establishment of a lunar base is among the primary future
missions
~~directions~~ of the space program. Once operational, it can be used for low

gravity experiments and research into planetary geological development

and the history of the solar system; a lunar base would also permit noise

free radio astronomy, as well as atmosphere-free optical astronomy.

Oxygen from the lunar soil could be utilized for propulsion and life support

systems on the Moon and in space operations. In addition, a lunar base

will help develop colonization technology and will support manned travel

throughout the solar system. To be permanently manned, a major

requirement of the lunar base will be the routine and cost-effective

rotation of its inhabitants. It is also necessary to provide for an emergency

escape from the base. A lunar crew transfer vehicle (LCTV) that is a

derivative of the ACRV will provide a reliable means of meeting both

transportation needs at a low design cost.

A detailed design study was initiated to develop an LCTV using the

ACRV as a starting point. Prior to establishing the needs of the LCTV, the

constraints and limitations of its mission must be known; these were

determined by first defining the Lunar Crew Transfer Mission and the

required velocity changes for each of its phases. Mass estimates and a

general vehicle configuration were determined, and the subsystem requirements were investigated. Particular consideration was given to propulsion, heat transfer, aerobraking and life support. The level of research to date is discussed in the following sections, followed by conclusions and recommendations for the continued development of the lunar crew transportation system as a growth option of the ACRV.

Mission Scenario and Descriptions

The primary objective of the lunar crew transfer mission is to transfer a crew of four replacement personnel with supplies from a Low Earth Orbit (LEO) to an existent lunar base and subsequently return four members of the lunar personnel to Earth. In addition, the mission accomplishes a second objective in that it provides a means of evacuation from the lunar base in the event of an emergency. The mission consists of six phases and utilizes several reusable vehicles, in particular the ACRV.

PHASE 1:   The object of this phase is to deliver a reusable lunar landing assembly into a 200 km. circular lunar orbit. The assembly consists of a docking device, full propellant tank, and lunar lander. This vehicle will be launched from . SSF (Ref. 6) in LEO and will arrive at the prescribed lunar orbit. The assembly will be used later in Phases 3 and 4.

PHASE 2:   Phase 2 involves the transfer of a crew of four with supplies to the Moon. This will be accomplished by attaching the modified ACRV to a reusable transfer vehicle which will carry sufficient propellant for the outbound and inbound legs of the journey. This combination

of ACRV and transfer vehicle, or Lunar Crew Transfer

Vehicle (LCTV), will rendezvous *in* lunar orbit with the

lunar landing assembly.

PHASE 3:   Upon its arrival in lunar orbit, the ACRV will detach from

the transfer vehicle and attach itself to the lunar landing

assembly. The lunar lander will carry propellant

sufficient for descent and ascent from the lunar surface.

These combined vehicles will descend and, utilizing

retrorockets, land at the lunar base. The crew and

supplies will then be transferred to the base. It is

assumed that several of these ACRV/Lunar Lander

combinations will be stationed at the lunar base at all

times (one combination for every four members of the

lunar personnel). These will serve as evacuation

vehicles in the event of an emergency at the lunar base.

PHASE 4:   The ACRV/ Lunar Lander combination will then remain

at the base and serve as one of these evacuation vehicles.

The lunar personnel who are returning to Earth will

board one of the ACRV/Lunar Lander combinations

already at the base and return to the 200 km. circular

lunar orbit. This phase effectively allows for the rotation of ACRV/Lunar Landers at the lunar base.

PHASE 5:   The ACRV will then detach from the lunar landing assembly and reattach to the transfer vehicle, once again forming the LCTV. The Lunar Lander will have used the majority of its propellant and will remain in its orbit around the Moon. The LCTV will depart from its lunar orbit and return to an orbit in LEO.

PHASE 6:   The final phase of the mission involves returning the lunar personnel to the Earth's surface. Once again, the ACRV will detach from the transfer vehicle, but will then connect itself to an ablative heat shield which will be waiting in orbit . The ACRV will descend through the atmosphere, deploying parachutes and perhaps retro-rockets to slow the craft. The ACRV will then splash down in the ocean. The transfer vehicle will return to the space launching station, where it will be refueled for subsequent missions.

Following the first execution of the mission, Phase 1 must be modified. Since the lunar landing assembly is permanently maintained in its circular lunar orbit, a new assembly need not be sent for each execution of the mission. Instead, a filled propellant tank will be sent to the lunar landing assembly. This tank will dock with the assembly and resupply the lander with sufficient propellant for its tasks. This propellant tank could possibly carry sufficient propellant for more than one refueling of a lunar landing assembly.

Required Velocity Changes

Estimation of the required Delta V's for transfers between LEO and the lunar surface was divided into two segments: the Delta V's needed for the transfer between the Earth and lunar orbit and the Delta V's required for transfer between the lunar orbit and lunar surface.

A Hohmann transfer was used to approximate the required Delta V's for an Earth orbit-to-lunar orbit transfer and a lunar orbit-to-Earth orbit transfer. For a transfer between a 400 km Earth orbit and a 200 km lunar orbit, the necessary Delta V was calculated to be approximately 3.9 km/sec. A 400 km Earth orbit was selected since it is approximately the proposed Space Station's orbit. A 200 km lunar orbit was chosen since Apollo used roughly the same orbit. This first Delta V estimation (along with estimated vehicle mass) enabled the calculation of a rough estimate of the required propellant.

A better Delta V approximation was obtained by analyzing Apollo Delta V data. For a transfer from Earth orbit (400 km altitude) to lunar orbit (200 km altitude), the following Delta V's were required:

Table 4A: Delta V's from Earth to Moon

Trans-lunar injection	3.155 km/sec
Mid-course correction	0.060 km/sec
Lunar-orbit insertion	0.915 km/sec

The total Delta V necessary for an Earth orbit-to-lunar orbit transfer is approximately 4.13 km/sec. For a return trip (same altitudes), the required Delta V's were found to be:

Table 4B: Delta V's From Moon to Earth

Trans-Earth injection	0.915 km/sec
Mid-course correction	0.060 km/sec
Earth-orbit insertion	negligible

The total Delta V required for a lunar orbit-to-Earth orbit transfer is approximately 0.975 km/sec. This second Delta V estimation for Earth-lunar orbital transfers enabled the calculation of a more accurate propellant requirement.

Apollo data was utilized for Delta V requirements of transfers between the lunar surface and lunar orbit. For a lunar descent (200 km altitude), the Delta V required is 2.165 km/sec. For a lunar ascent (200 km altitude), the Delta V required is 1.92 km/sec. This Delta V data will provide an adequate approximation for the LCTV.

It is seen from the previous data that an Earth-orbit to lunar-surface transfer requires much more propellant than a return trip from the lunar surface. The total Delta V for an Earth orbit-to-lunar surface transfer is approximately 6.295 km/sec. For a lunar surface-to-Earth orbit transfer, the required Delta V is approximately 2.895 km/sec.

Gross Mass Estimation

Rough estimations were made for the mass of the vehicles and the required propellant. To determine these rough estimations, the LCTV system was modeled after the Apollo missions of the 1960's and 1970's. (Ref. 7) The Apollo vehicle was chosen because its mission is so similar to the LCTV.

Because of the similarities in missions, the LCTV will have many of the same components that the Apollo mission had: a Command Module (the LCTV), a Service Module (the Transport Vehicle), and a Lunar Lander. Not only will the component functions be similar, but the component designs will also be similar.

This similarity was utilized in the rough mass estimations, since the Apollo vehicles were scaled to suit the size requirements of the LCTV. However, the Apollo vehicles and the LCTV are not identical. Mission requirements of the LCTV, such as reusability, demand a more rugged and durable design. A more rugged design is often indicative of a heaver vehicle. On the other hand, advancements in materials and technology would make the vehicle lighter and improve its performance.

Without performing a detailed study of the vehicles and their individual subsystems, it is difficult to make a specific mass determination. Because this is only a first approximation, the scaling of the Apollo vehicle is a reasonable method.

Approximations for the LCTV were based on the following Apollo 11 Command Module data:

length = 10.6 ft

maximum diameter = 12.8 ft

habitable volume = 210 ft^3

weight with astronauts = 13,090 lbs

number of astronauts = 3

These numbers were proportionally increased to the following for the LCTV:

number of people = 4

volume occupied per person (based on the Apollo data) = 70 ft^3/person

additional cargo space = 60 ft^3

total internal volume = 340 ft^3

Mass estimation:

$$\frac{\text{mass of the ACRVT}}{\text{internal volume of the ACRVT}} = \frac{\text{mass of the Apollo C.M.}}{\text{internal volume of the Apollo C.M.}}$$

approx. mass of the LCTV = 21,190 lbs = 9625 kg

The service module and the landing module of the Apollo missions were utilized in the mass estimations for ascent and descent. The propulsion systems from the Apollo missions were used for the LCTV. No

scaling factor was used; the only change was in the amount of propellant used (which is determined in Appendix A).

Other Apollo data:

Service Module mass (dry) = 5600 kg

Lunar Descent Vehicle mass (dry) = 2760 kg

Also taken from the Apollo missions were the total changes in velocity needed for each phase of the mission:

LEO to lunar orbit: DV=4130 m/s

lunar descent: DV=2165 m/s

lunar ascent: DV=1920 m/s

lunar orbit to L.E.O.: DV=975 m/s

The Rocket Equation was used to determine the mass of propellant required for each phase of the mission:

$$Mp=Mi(1-exp(\frac{-\Delta v}{I_{sp}g})$$

Mp=mass of propellant

Mi=total mass of vehicle before the DV

I_{sp}=specific impulse of the propulsion devices

g=gravitational acceleration at the Earth's surface

Appendix A uses the Rocket Equation and the data from the Apollo missions to perform the mass estimations. The mass breakdown of each phase of the Lunar Mission is presented in Table 4c. The breakdown of the mission vehicles is as follows:

LCTV	9,625 kg
Lunar Lander	2,760 kg
Transport Vehicle	5600 kg

The mass of the LCTV is questionable for two main reasons. The first reason is that a linear scaling of the Apollo capsule was made to determine the LCTV mass. Because of technological advancements and differences in the mission, the relation between the two vehicles may not be linear. The linear approximation was used because it is impossible to account for new technology and mission dissimilarities without doing a detailed vehicle and mission analysis.

The second reason is that the LCTV may use retrorockets when slowing down within the Earth's atmosphere. Retrorockets are heaver than the reaction control propulsion system used on the Apollo vehicle and retrorockets require extra propellant. To determine the effects that retrorockets would have on the LCTV, an evaluation first has to be made as to whether retrorockets are required. If they are required, a further evaluation of what type of rockets and their degree of use needs to be made before the weight of this system can be obtained. Even with the question of retrorockets and technology, the scaling appears to be a good first approximation.

The mass approximations presented in Table 5 show each phase of the mission as it is currently configured. A key assumption made in the mission scenario is that propellant will be available at the locations where

it is needed. The Transport Vehicle will receive its propellant in LEO so that the propellant doesn't have to be launched with the LCTV from the Earth's surface. The same assumption is made about the Lunar Lander; propellant will be available in lunar orbit and on the lunar surface.

Table 5: Lunar Mission Mass Distribution By Phase

Phase	Mission	Mass to be Transported	Mass of Required Propellant	Total Mass of Phase
Phase 1	The Transport Vehicle transports the LCTV, the Lunar Lander and descent propellant, and the return trip propellant from LEO to a lunar orbit.	56,923 kg	127,834 kg	184,757 kg
Phase 2	The Transport Vehicle transports the LCTV and the return trip propellant to lunar orbit.	14,503 kg	32,570 kg	47,073 kg
Phase 3	The Lunar Lander transports the LCTV to the lunar surface from lunar orbit.	12,385 kg	39,660 kg	52,045 kg
Phase 4	The Lunar Lander returns the LCTV from the lunar surface to lunar orbit.	12,385 kg	31,856 kg	44,241 kg
Phase 5	The Transport Vehicle transports the LCTV from lunar orbit to LEO.	15,225 kg	4,878 kg	20,103 kg
Phase 6	The LCTV separates from the Transport Vehicle and reenters the Earth's atmosphere.	9,625 kg	N/A	N/A

Space Station Operations and Support

The lunar crew transfer mission requires a facility in LEO for housing and maintenance of the lunar landing assembly and support for Phase 1. This facility can be either: A) an extension of the space station Freedom, or B) a separate launch station.

A. Space Station Freedom as a Baseline of Operations

For each standard rotation of lunar base personnel, the Space Shuttle will be used to transport the fresh lunar crew from Earth to the space station. Since the Shuttle launch schedule is subject to stringent commitment criteria and subsequently many delays, the lunar crew may be delivered to LEO and then be required to wait at the space station until a window opens for a lunar mission. For routine LEO to lunar missions, an optimum launch window occurs at approximately 9 day intervals. (Ref. 6) Therefore, there will be a need for an additional habitat module on the space station to accommodate at least 4 transient base personnel and 2 to 4 permanent crew members to assist with lunar mission on-orbit operations. These additional permanent space station crew members will be dedicated to the lunar base transportation system and will be responsible for monitoring all lunar traffic at the space station. Between lunar sorties, they will service and refuel the lunar vehicle and its boosters, and test/monitor its subsystems (this may require EVA). The

Environmental Control and Life Support System (ECLSS) of the additional habitat module will be the same as that of the space station, and there will be crew access to at least one ACRV for emergency return to Earth.

B. Autonomous LEO Launch Facility

Another option for lunar transport is to have a separate facility in LEO as a baseline for lunar missions in order to limit interference with the operation of the space station. One proposal considers a Space Transportation Node as a baseline in LEO, which includes a habitat module, a fuel depot and a large hanger to house reusable Orbital Transfer Vehicle's (OTV), lunar landers, fuel storage tanks, and other lunar spacecraft. The rationale for a facility separate from the space station is that "frequent traffic noise, cg changes, intensive servicing, visiting traveler commotion, extensive storage allotments, precise launch schedule commitments, contamination problems and unavoidable mechanical movements," make a lunar baseline "unacceptably incompatible with users in the space station supporting microgravity science applications." (Ref. 6) It is assumed for this report that there will be a dedicated launch facility in LEO, whether it be autonomous or an extension to the space station. The LCTV must therefore have environmental control and life support systems and communications systems that are compatible with this baseline facility.

Life Support, Communications and Control

While docked with the space station, the lunar crew transfer vehicle will draw from the power and life support system of the space station habitat module. Prior to departure from LEO, equipment checkout and preparations can be conducted in a shirt-sleeve environment. The transfer vehicle should be capable of a pressurized transfer of some or all of its four crewmen. It is recommended that the LCTV have two hatches: one for normal entry and egress when docked with the space station, and one for emergency exit as well as routine exits to both lunar and Earth surfaces. At launch and during any maneuvers within close proximity of the station, it is recommended that the crew be in space suits, in case of a loss of ECLSS or a need for an emergency evacuation. Once clear of the station, the crew can spend a majority of the trip in a shirt-sleeve environment.

To minimize the structural weight resulting from the pressure-resistant walls of the spacecraft, the crew transfer vehicle will be normally pressurized to about 5 psi (1/3 of sea level atmospheric) and maintained at 25 degrees C. At this internal pressure, other forces such as acceleration and impact govern the structural weight. (Ref. 8) Also, to reduce initial LCTV mass, water (drinking and wash) can be generated from fuel cells that combine hydrogen and oxygen; however, as a back-up, some water will be stored in an auxiliary 4 gallon tank prior to launch. Urine will be

vented directly overboard as in the Apollo spacecraft, while solid waste will be stored in containers with a germicide to kill bacteria. Water and oxygen regenerative subsystems can save as much weight as 18 lb/man-day; however, the ECLSS of the LCTV is already somewhat more complex than that of the ACRV, and it is more cost-effective to minimize the complexity of the transition from ACRV to crew transfer vehicle. The following table lists the minimum requirements for a semi-closed life support system, and can be used for initial estimates for the ECLSS of the 4 man, 5 day lunar crew transfer mission:

Table 6: ECLSS Requirements and Products (Ref. 8)

Requirements

Metabolic oxygen	2.0 lb/man-day
Drinking water	8.0 lb/man-day
Hygiene water	12.0 lb/man-day
Food	1.3 lb/man-day

Waste Production

Carbon dioxide	2.25 lb/man-day
Water vapor (perspiration and exhale)	5.5 lb/man-day
Waste wash water	12.0 lb/man-day
Urine	3.2 lb/man-day
Feces	0.35 lb/man-day
Metabolic heat	12,000 BTU/man-day

The communications subsystem of the lunar crew transfer vehicle should provide voice, television, telemetry, tracking and ranging communication with an Earth station. Voice communications with the space station will also be necessary for launching, docking and close proximity maneuvers. The communications subsystem should be capable of transmitting biomedical data on any injured or ill crew members to Earth; this is to allow the control center to determine if an abort of the current mission is necessary, and to prepare for the injured member's return (in the case of an ACRV mission). Another vital part of the communications system of the lunar crew return vehicle is a beacon to locate and recover the spacecraft after reentry.

Control of the lunar crew transfer vehicle will be automated using its on-board computer in conjunction with Earth-based mission control for a majority of its maneuvers. LEO prelaunch operations, launch control and space station rendezvous will be managed by Earth-based mission control with on-site operators at the space station. This is due to the large number of personnel required; they can be afforded on Earth (as opposed to the space station). For sensitive manipulations at or around the space station, such as final vehicle approach and closure, the vehicle is best observed on the space station and control is more direct from the space station operators. (Ref. 9) In case of an emergency malfunction of the on-board system and back-up, or a communications blackout, the pilot of the crew

transfer vehicle can take over the flight controls. Manual control may also be required for unusual lunar operations and for final approach to the lunar surface. Therefore, the flight controls, guidance and navigation systems and displays must be within reach of the pilot in his seated position.

Reentry Considerations

Before reentering the Earth's atmosphere, the ACRV will need to turn around so that the blunt end supporting the heat shield enters first. This allows the pressure of the atmosphere to push against the heat shield causing the craft to slow down. The heat shield is also used to protect the spacecraft and crew members from the extremely hot temperatures of reentry. The heat shield, during a normal reentry, will reach a temperature of 4200 ° F, while the temperature in the cabin will remain at about 80 ° F. During reentry, the ACRV must be at a certain angle to achieve a successful landing. If the angle is too shallow, the craft will deflect off the atmosphere and head back into space. On the other hand, if the angle is too steep, the friction between the atmosphere and the spacecraft will produce such a great amount of heat that the craft will burn up.

After reentering the atmosphere, the ACRV will descend to Earth. At 23,330 ft. the ACRV will release special parachutes called drogues. The drogues will slow down the ACRV and steady it if it is wobbling. At 10,500 ft. the three main parachutes are released and the retrorockets are fired. The combination of parachutes and retrorockets will slow the descent of the ACRV down to about 12 feet per second upon impact (Ref.10). This speed of impact is slow enough to assure a soft and safe landing for an ill or injured crew member.

After splashdown, the ACRV will be turned upright by a system composed of three 20-cubic-foot airbags and an electric inflation pump. This will prevent flooding of the main compartment by keeping the ACRV upright in the water. A flotation collar will also be used to keep the craft afloat until recovery.

For safety, there will be post landing water survival equipment on board. This will consist of a four-man life raft, a 12 hour duration dye marker packet , an extra 18 hours of additional dye marker for security, and two radio beacons and transmitters. The 12 hour dye packet will be deployed on impact for locating the crew. The rescue/recovery forces will then dispatch to the landing site and recover the crew and ACRV. They will transport the crew to the appropriate medical or debriefing facility and the ACRV to the appropriate servicing facility.

We have chosen a water landing over a land landing for many reasons. The reasons that were considered for the mode of landing of the ACRV mission were the constraints on trajectory, landing accuracy, and landing systems. The following analysis of some of the problems was made and led to the preference for water landing:

- If certain systems on board the ACRV should fail, the spacecraft can land as far as 500 miles from the prime recovery area. This contingency can be provided for at sea, but serious difficulties

might be encountered on land.

- Because the time and location of the landing is unknown, weather forecasting for the landing zone (on land) will be unpredictable. This could result in serious injury to the crew and/or damage to the spacecraft.

- If the ACRV should tumble during descent, the possibility for serious damage to the spacecraft is far less for water landings.

- On land, there are obstacles such as rocks and trees that might cause serious damage to the spacecraft.

- After reentry, the ACRV will be extremely hot. Landing on water will cool the spacecraft quickly and minimize ventilation problems.

- The requirements for control during reentry are less stringent in a sea landing, because greater touchdown dispersions can be allowed.

- Because most contingencies require a landing at sea anyway,

the choice of water as the primary landing surface will alleviate some constraints in the spacecraft design.

The principal disadvantages of the land recovery mode are the possibility of landing in an unplanned area and the degree of impact involved if a problem arises with the landing system. The principal disadvantages of the water recovery mode are the establishment of suitable landing areas in the southern hemisphere and the apex-down flotation problem. This problem , however, is taken care of by using an inflatable device to upright the spacecraft after splashdown. On the basis of our analysis, it was determined that land impact problems would be so severe that they require abandoning this mode as a primary landing mode. Even in water landings there may be impact damage which would result in leakage *in* the capsule. However, in land landings, it is highly probable that the spacecraft's impact limit would be surpassed. As recommended for the Apollo program, we have also chosen that the Earth landings be primarily on water for the ACRV missions. This is primarily based on the advantage of the softer impact conditions and the operational flexibility afforded by ocean landing (Ref. 10).

Atmospheric braking is used to decelerate spacecraft by dissipating their great kinetic energy. Because most of this energy is disposed of in the wake of the spacecraft, only about 1% is transmitted to the vehicle as

heat. Even such a small percentage results in severe heating conditions. Spacecraft heating is largely determined by the way the vehicle enters and travels through the atmosphere. Steep entries result in high heating rates. Shallow entries result in lower heating rates, but the time of entry is longer and the spacecraft experiences a greater heat pulse (the time integral of the rate). Figure 2 shows the heating rates and pulses of various vehicles (Ref. 11).
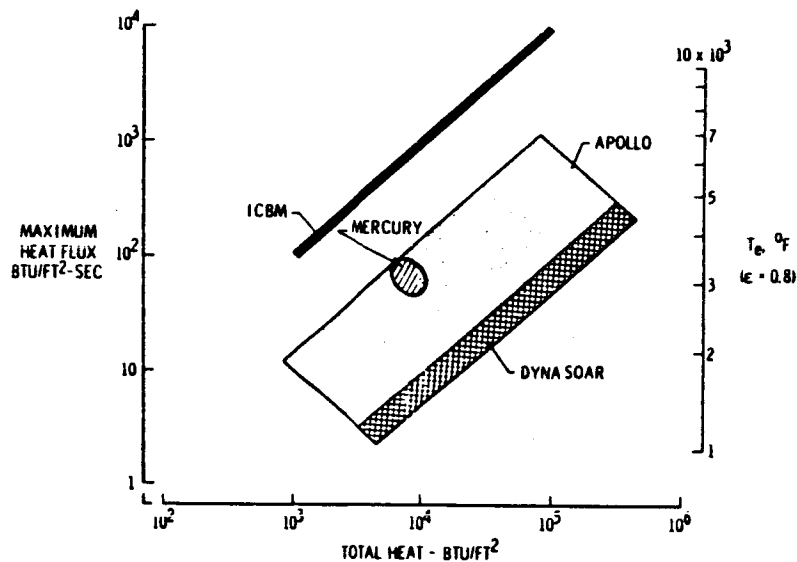
Figure 2: Heat Loads of Entry Vehicles (Ref. 11)

The ACRV will be exposed to atmospheric heating when descending to the Earth's surface and when aerobraking through the Earth's atmosphere to achieve Earth orbit. Because of the similarity in size, weight, L/D ratio and mission requirements, the heating rates of the ACRV can be closely represented by those of

- 42 -

the Apollo reentry spacecraft. The ACRV must withstand heating

rates of 1500 Btu/ft^{2}s, a total heat pulse of 100,000 Btu/ft^2, and

maximum temperatures of 6000°F (Ref. 11). These estimates are

for the descent from Earth orbit to the Earth's surface. The

heating rates, total heat pulse and maximum temperatures are

somewhat lower, depending on the braking time and deceleration,

for aerobraking into Earth orbit.

An efficient method of shielding the ACRV from

atmospheric heating must be found by exploring the various types

of heat shields. Re-radiative systems employ high temperature

resistant materials to withstand the high heating rates. Carbon

has the highest known heating rate resistance of 800 $Btu/_{ft}2$ and

maximum temperature resistance of 6000 F. Clearly, this type of

heat shield would not suffice for use on the ACRV. Heat sink

systems overcome the material limitations of re-radiative systems

by utilizing a thick slab of material that conducts and stores excess

heat from the surface that cannot be re-radiated. The maximum

practical value for heat stored is about 1000 $Btu/_{lb}$. Because the

total heat pulse imposed on the ACRV would be nearly

100,000 $Btu/_{ft}2$, an extremely large mass of heat sink material

would be necessary to protect the vehicle, rendering this system

impractical. Ablative systems overcome the limitations of both the above systems by utilizing materials with low conductivity on the external portion of the shield. While keeping the interior relatively cool, steep heat gradients develop in the external material, and its surface would exceed its melting temperature. This surface would then char, leaving a carbonaceous residue. Pyrolysis of the resin system in the external material would then penetrate into the low conductivity material and release gaseous products through the porous char. It is extremely advantageous to have large amounts of hydrogen as a product of the pyrolysis since hydrogen, having a high specific heat, would absorb much of the surface heat. Ablative systems are extremely efficient, and can disseminate up to roughly 6000 $^{Btu}/_{lb}$. An ablative system will be utilized on the ACRV. Figure 3 gives estimates of the characteristics of several heat shields (Ref. 11).

As shown in Figure 4, the section of the Apollo capsule subject to the most severe heating conditions sustained a peak heat flux of 1,500 $^{Btu}/_{ft^2s}$ and a total heat pulse of 100,000 $^{Btu}/_{ft^2}$. Because the nature of the Moon to Earth growth option is similar to the Apollo mission, the reentry speed of the proposed ACRV would be similar to that of the Apollo capsule.
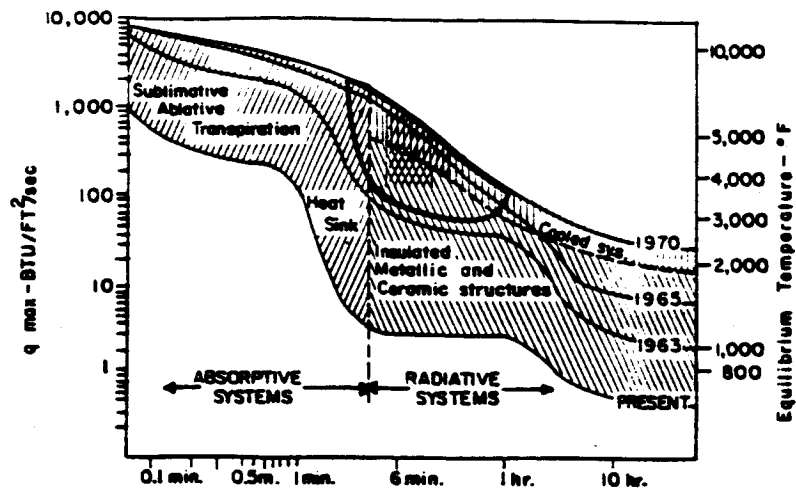
Figure 3: Characteristics of Several Heat Shields (Ref. 11)
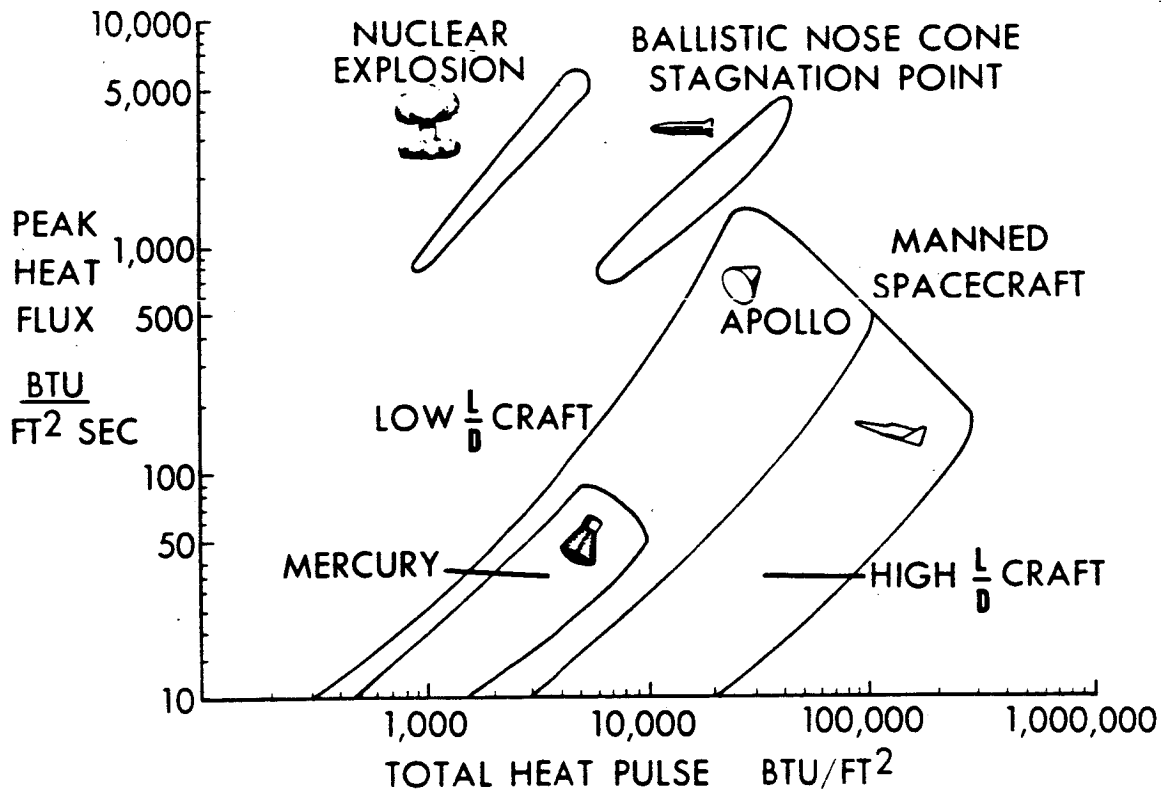
Figure 4: Thermal Environment Associated With
Various Entry Vehicles (Ref. 12)

- 45 -

The ACRV would not decelerate quite as fast as the Apollo vehicle, and would sustain a lower peak heat flux and a higher total heat pulse. Still, the Apollo heating characteristics provide a good preliminary estimate of ACRV heating (Ref. 12).

For ease of design, maintenance and serviceability, the ACRV's heat shield was determined to be cast as one piece, as on the Apollo capsule. Several proposals have been suggested for fold-out shields to provide more surface area for deceleration. These designs are intended mainly for aerobraking in the low-density upper atmosphere. One of the proposed growth options intends for the ACRV to aerobrake in the atmosphere and then enter Earth orbit. Because the ACRV must be designed for the most severe heating conditions it could sustain, the heat shields are being designed primarily with Earth atmospheric entry and surface landing in mind.

Figure 5 gives estimates on the type and weight density of ablative systems available that are able to sustain ranges of maximum heat flux and total heat. Given the heating characteristics of the proposed ACRV, a charring ablator would be needed that has a weight density of roughly 20 $^{lb}/_{ft^2}$. Because the heat shield surface would be approximately 180 ft^2, the
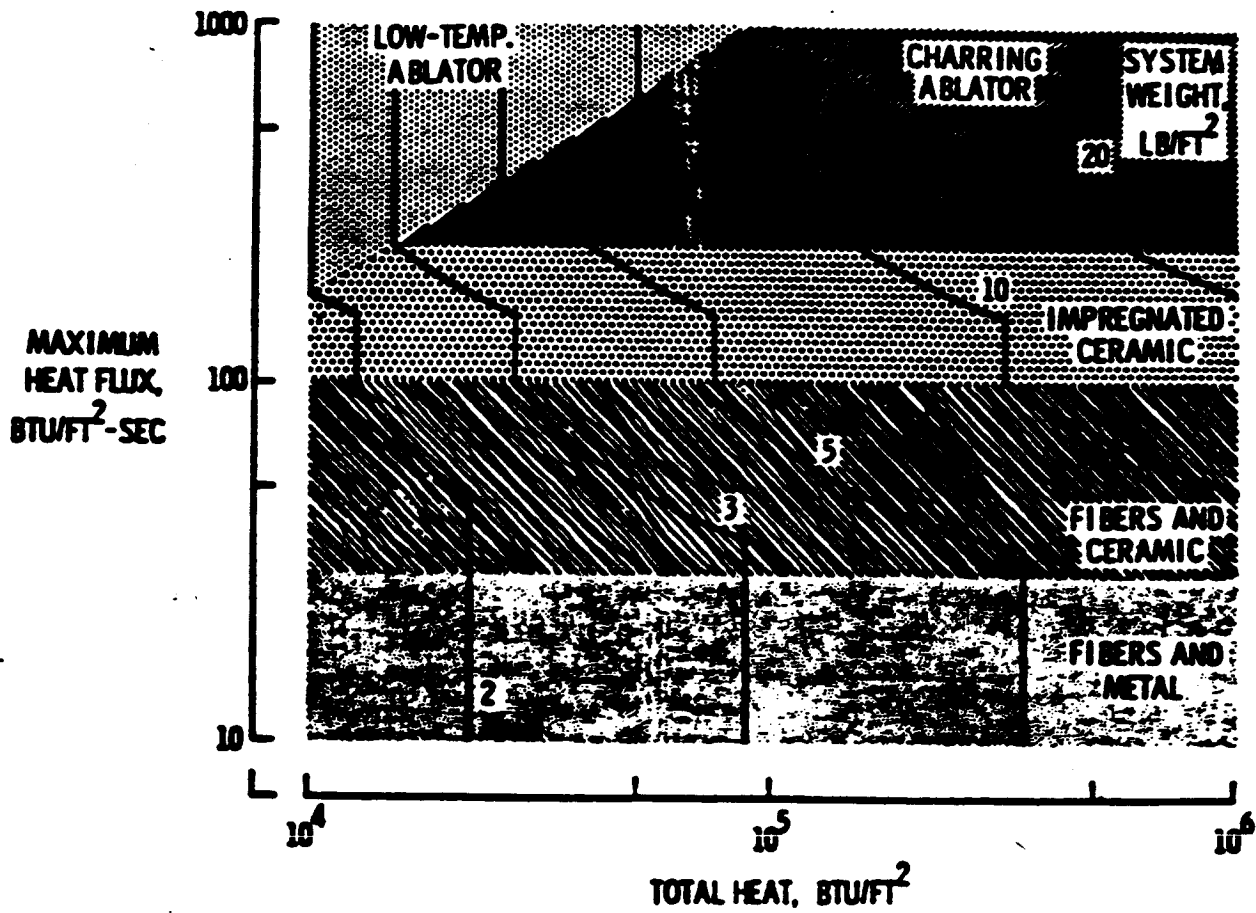
Figure 5: Ranges of Efficient Application
of Thermal Protection Systems (Ref. 11)

required ablator system would weigh roughly 3,500 pounds. In the case of a removable heat shield, this does not take into account the weight of the heat shield structure. A removable heat shield would yield greater efficiency for other missions planned for the ACRV that would not require heat shielding. In addition, if only aerobraking were needed to achieve orbit, a more efficient aerobrake could be attached to the ACRV. If a removable heat shield was needed, the shield structure was estimated to weigh approximately 12 $^{lb}/_{ft}2$. The shield structure in addition to the ablative system would weigh approximately 5,500 pounds (Ref. 11).

Conclusions and Recommendations

The lunar missions discussed in this report show strong potential as viable growth options for the ACRV. It is recommended that an autonomous launch facility be available in LEO for the refueling and support of all spacecraft associated with lunar crew transfer. Initial calculations of the required velocity changes and mass estimates indicate that an ACRV could be utilized for lunar missions. These missions would require the use of additional propulsion modules and minor modifications to life support, communications and other subsystems of the ACRV. A more comprehensive analysis of the lunar crew transfer mission is required for a detailed design of the LCTV; this vehicle is contingent upon the final ACRV design.

FINAL REMARKS

Of all the growth options considered, the following missions are the most compatible with the ACRV: international rescue, space station crew/cargo rotation, lunar ACRV and lunar crew transfer. To accommodate these and other growth options, it is recommended that the ACRV be modular in design, with a ballistic body, two hatches and a detachable heat shield. Using a modified ACRV to provide crew transfer for a lunar base is a viable growth option deserving further study.

The ACRV could play a number of different roles in the future of manned and unmanned space activities, and therefore should be designed with growth options in mind.

REFERENCES

1.   GEOshack Proposal Team Space Design Competition for AIAA

2.   <u>Crew Emergency Return Vehicle System Performance Requirements Document</u>, November 9, 1988, NASA, London B. Johnson Space Center, Houston, Texas.

3.   "OEXP (Office of Exploration) Exploration Studies Technical Report," Roberts, B. B., Bland, D., NASA, FY 1988 Status Report, Manned mission to an asteroid:

4.   "Planetary Exploration Through Year 2000," by the Solar System Exploration Committee of the NASA Advisory Council, 1986.

5.   "Design Study for Asteroidal Exploitation," C. Adams, J. Blissit, D. Jarrett, R. Sanner, K. Yanagawa, August 1985, Massachusetts Institute of Technology.

6.   Kahn, Taher Ali, et. al., "Space Transportation Nodes Assumptions and Requirements: Lunar Base Systems Study," Eagle Engineering, April 18, 1988.

7.   <u>Lunar Flight Handbook, Vol II,</u> Martin Co., Baltimore, MD, 1963.

8.   Sharpe, Mitchell R., <u>Living in Space: The Astronaut and His Environment</u>, Doubleday and Co., Inc., Garden City, NY, 1969.

9.   Weidman, Deene J., "Space Station Accommodations for Lunar Base Elements: A Study," NASA, October 1987.

10. Morse, Mary Louise and Jean Kernahan Bays ed., <u>The Apollo Spacecraft: A Chronology, Vol. II, Nov. 8, 1962 - Sept. 30, 1964</u>.

11. Haser, Peter E., <u>Aerodynamically Heated Structures,</u> Cambridge, MA, July 25, 1961.

12.	Faget, Maxime A., Paul E. Purser and Norman F. Smith, <u>Manned Spacecraft: Engineering Design and Operations,</u> Fairchild Publications, New York, 1964.

substituting into the Rocket Equation and itterating for Mp yields:

$$Mp = 4878 \text{ kg}$$

This is the required propellant for the return trip from lunar orbit.

The next phase to be analysed is Phase 3, the descent of the Lunar Lander and the LCTV from lunar orbit to the lunar surface. This phase is analysed next because Phase 1 transports propellant for the initial descent of the lander and so Phase 1 must know the required propellant mass for the descent stage.

Phase 3

Transfer of the LCTV, by the Lunar Lander, from lunar orbit to the lunar surface. Except for when the Lunar Lander is initially transfered to lunar orbit, it is assumed that the lander will acquire all necessary propellant, for the descent stage, in lunar orbit.

The Lunar Lander is based on the descent stage of the Apollo lander so, as with the Transfer Vehicle, the Isp of the Apollo propulsive system needs to be determined.

Apollo 11 Lunar Lander Descent Stage Data
         dry weight=2760 kg
         propellant weight=8838 kg
         descent delta V=2165m/s

from the Rocket Equation

$$I_{sp} = \left\langle \ln\left(1 - \frac{Mp}{Mi}\right)\right\rangle^{-1} \left\langle \frac{-\nabla v}{9}\right\rangle = 153.57 \text{ seconds}$$

determining the propellant for the descent from lunar orbit to the lunar surface.
         delta V=2165 m/s
         Mi=M(LCTV)+M(Lunar Lander, dry)+M(required propellant)
         Mi=9625+2760+Mp=12385 kg+Mp

the Rocket Equation:

$$Mp = M_i\left(1 - \exp\left(\frac{-\Delta v}{(I_{sp})(g)}\right)\right)$$

substituting into the Rocket Equation and itterating for Mp yields:

$$Mp = 39660 \text{ kg}$$

This is the required propellant for the trip
from lunar orbit to the lunar surface.

Phase 4

The transfer of the LCTV, by the Lunar Lander, from the lunar surface to the lunar orbit. In this phase it is assumed that the Lunar Lander will take on the propellant required for the phase on the lunar surface.

The Isp of the Lunar Lander was developed for Phase 3.

         Isp=153.57 seconds

determining the propellant for the ascent from the lunar surface to lunar orbit.

> delta V=1920 m/s
> Mi=M(LCTV)+M(Lunar Lander, dry)+M(required propellant)
> Mi=9625+2760+Mp=12385 kg+Mp

the Rocket Equation:

$$Mp = Mi\left(1 - \exp\left(\frac{-\Delta v}{(Isp)(g)}\right)\right)$$

substituting into the Rocket Equation and itterating for Mp yields:

Mp=31856 kg

This is the required propellant for the trip from the
lunar surface to the lunar orbit.

Phase 1

The Transfer Vehicle transfers the LCTV, the return trip propellant, the Lunar
Lander, and propellant fot the Lunar Landers initial descent to the lunar surface.
It was assumed that the propellant required for this phase of the mission can be
obtained in LEO.

The Isp of the Transfer Vehicle was developed for Phase 5.

> Isp=357.22 seconds

determining the propellant for the trip from LEO to lunar orbit.

> delta V=4130 m/s
> Mi=M(LCTV)+Mp(return trip propellant)+
>   M(Lunar Lander, dry)+Mp(lunar descent propellant)
> Mi=9625+4878+2760+39660+Mp=56923 kg+Mp

the Rocket Equation:

$$Mp = Mi\left(1 - \exp\left(\frac{-\Delta v}{(Isp)(g)}\right)\right)$$

substituting into the Rocket Equation and itterating for Mp yields:

Mp=127,834 kg

This is the required propellant for the trip from LEO to lunar orbit

Phase 2

Phase 2 is identical to Phase 1 except that the Lunar Lander is already in lunar
orbit. The Transfer Vehicle needs only to transport the LCTV and the return
trip propellant from LEO to lunar orbit.

The Isp of the Transfer Vehicle was developed for Phase 5.

> Isp=357.22 seconds

determining the propellant for the trip from LEO to lunar orbit.
> delta V=4130 m/s

Mi=M(LCTV)+Mp(return trip propellant)+Mp
Mi=9625+4878+Mp=14503 kg+Mp

the Rocket Equation:

$$Mp=Mi\left(1-exp(\frac{-\Delta v}{(Isp)(g)}\right)$$

substituting into the Rocket Equation and itterating for Mp yields:

Mp=32570 kg

This is the required propellant for the trip from LEO to lunar orbit

Phase 6

The LCTV separates from the Transport Vehicle and reenters the Earth's
atmosphere. The LCTV, like the Apollo Command Module, has a Reaction Control
Propulsion System built into its' structure so that the LCTV will require no
extra propellant to enter the Earth's atmasphere. If retrorockets are used in slowing
the LCTV, an analysis of what type of rockets will be required and how much the
rockets will slow down the LCTV is necessary before propellant mass estimations
can be made.

ACRV
Growth Options
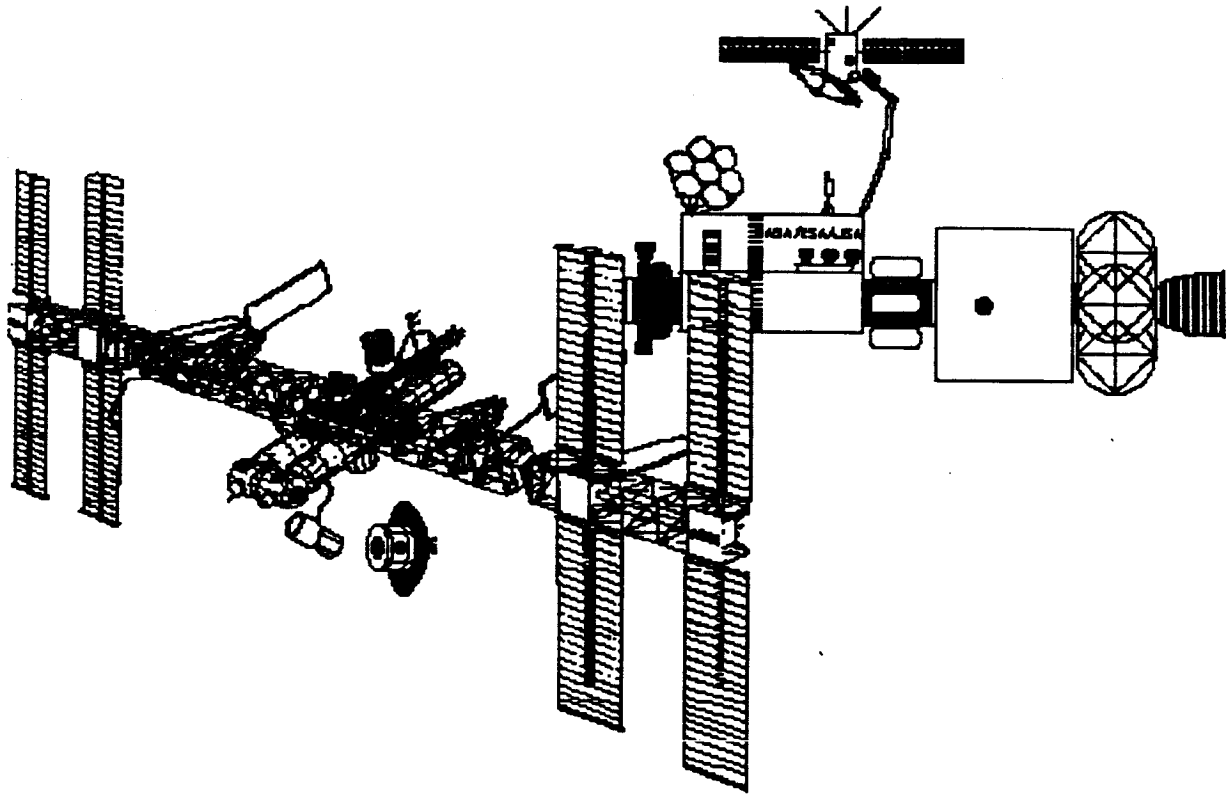
Aerospace 401
Final Design Project

NASA/USRA/Penn State

Completed: 1 May 1990

Group Members:

Tom Hill   Mike Williams
Mark Keller   Chris Livingstone
Chuck Frey   Scott English
            Dan McCusker

Abstract

Since the beginning of the manned space program, the National Aeronautics and Space Administration (NASA) has been committed to assured crew return for U.S. astronauts. Currently, NASA is developing an Assured Crew Return Vehicle (ACRV) for Space Station *Freedom*. The baseline mission for the ACRV is crew return in the event of a medical emergency or station catastrophe. *or NSTS shutdown* The ACRV program presents NASA with the opportunity to design a vehicle not only for crew return, but one that could accomplish a variety of other missions, or *growth options*. In this report, several possible growth options for the ACRV are proposed. ~~Proposed growth options include~~: Shuttle and International Rescue, Crew Transfer, Cargo Transfer, Satellite Boost, Satellite Servicing, Lunar Operations, and Ground-Based Missions. Several different methods of accomplishing these growth options are discussed: the mission specific ACRV, the multi-mission ACRV, and the modular ACRV. Recommendations are made for the baseline ACRV design that will allow it to accomplish the growth options discussed. After extensive research, it was determined that the modular ACRV is the most efficient design for accomplishing all of the proposed growth options. It is therefore recommended that the ACRV be ballistic in shape, and be designed so that the systems and structure are modular. An analysis of possible systems and add-on modules is also included for the modular ACRV design.

Table of Contents

List of Figures

List of Tables

ii

I. INTRODUCTION

Since the beginning of the manned space program, the National
Aeronautics and Space Administration (NASA) has been committed to
assured crew return for U.S. astronauts. During the Mercury and
Gemini programs, the capsule's first orbit assured re-entry into
the atmosphere. The early Apollo missions to the Moon were flown
in a "free return" trajectory where the capsule could circle the
Moon and return to Earth automatically. The Skylab missions had
an Apollo capsule docked at the station whenever a crew was
aboard. Today the Space Shuttle, or National Space Transportation
System (NSTS), has a high level of redundancy built into the
critical subsystems to assure the safe return of the crew.

Space Station *Freedom*, now being designed by the United States
and other countries, has special needs to assure crew return.
Unlike other manned spacecraft, this permanent orbiting facility
cannot ~~inherently return its crew to Earth~~ *enter the Earth's atmosphere*. Currently, NASA is
developing an Assured Crew Return Vehicle (ACRV) which will be
docked at *Freedom* to allow the crew to return to Earth. Three
primary missions are identified for the ACRV: (1) space station
emergencies, (2) crew related medical emergencies, and (3) NSTS
unavailability. The ACRV program also presents an opportunity to
accomplish a variety of other missions, while at the same time
providing assured crew return for *Freedom*.

Expanding the ACRV's basic mission is practical for many
reasons. First, expansion will allow NASA to combine several
programs currently under development with the ACRV program,
thereby decreasing long run costs. Also, a multi-mission ACRV

1

would allow the space station system to be more flexible, giving the crew a utility vehicle capable of handling unforeseen contingencies, and perhaps lowering *Freedom's* dependence on the space shuttle.

In this report, several growth options (missions to be carried out by a modified ACRV) are presented. Then, the preliminary research on a modular ACRV is presented. A Modular ACRV entails the connection of different modules to the return vehicle, allowing the ACRV to accomplish various missions. However, in its normal state (no attached modules), the ACRV would be able to carry out the primary mission of the system--crew return. For the mission and modular ACRV analysis, it is assumed that at least three ACRV's will be available for use at Space Station Freedom. One of the primary missions of the ACRV is to provide an emergency escape route in the event of a space station catastrophe. Therefore, it is imperative that two ACRV's be docked and ready at the station at all times. A third ACRV will be utilized to conduct the growth options, *missions*.

II. GROWTH OPTIONS

This section of the report explains, in detail, the growth options that were considered. First, the importance of each mission is discussed and then a mission is outlined. Finally, the systems necessary to accomplish this mission are described. Reasons will also be given for discarding several growth options proposed in preliminary studies. At the end of this section, the growth options and mission requirements will be summarized in a matrix format.

II.A. Shuttle and International Rescue.

During the 1990's and into the early 21st century, manned space flight activities -- by the United States, Soviet Union, and other nations -- are expected to increase substantially. The probability of life-threatening contingencies will be an ever-increasing concern in space system development and operation. If an accident should occur while a spacecraft is in orbit, it is imperative to have a space vehicle capable of assuring the safe return of its crew, whether they be American or international astronauts. The ACRV is a vehicle capable of performing this in-orbit rescue operation.

A space shuttle or international rescue mission would begin by preparing the ACRV and launching it from *Freedom*. It may be necessary to perform orbital transfers to rendezvous with the troubled vehicle. The transfer will generally take place within the current manned spaceflight envelope -- orbital altitudes of 185-740 km, and orbital inclinations of 5-58 degrees. After

completing the rendezvous, the crew will be transferred to the rescue vehicle either by docking or by Extravehicular Activity (EVA), depending upon the circumstances of the rescue. Upon the completion of the crew transfer, the ACRV would then return directly to Earth or to the space station, where the crew would receive medical treatment if necessary.

In order for the ACRV to conduct a shuttle or international rescue mission, many modifications must be made. Life support and propulsion systems of the ACRV must be extended and many structural changes are necessary. Since the National Space Transportation System (NSTS) has a maximum crew capacity of 8 personnel, and assuming a 2 man crew aboard the ACRV to assist in the rescue, the life support system must be able to provide for a maximum of 10 personnel for up to 2 days. The time is a direct result of the large orbital transfers necessary for the ACRV to successfully cover the manned space flight envelope.

Rendezvous with a vehicle in orbit requires matching the inertial position and velocity defined in terms of orbital plane, altitude, and phasing. Rendezvous requirements are relatively simple and economical for two vehicles in the same orbital plane. Since orbital rate varies inversely with altitude, an altitude range of 185 - 740 km gives a relative phasing control range of 24 degrees per hour, allowing correction of the worst phasing mismatches in less than 16 hours (not including the time for planning the maneuvers). However, rendezvous requirements are much more complex for two vehicles in different orbital planes. The ACRV must have large maneuvering capabilities to rendezvous with a second vehicle.

Many space vehicles such as the NSTS, Hermes, Soyuz and MIR all

4

operate within an orbital inclination range of 5 - 58 degrees. Since *FREEDOM* has an orbital inclination of 28.5 degrees, the ACRV must be able to perform orbital plane changes of at least 30 degrees. It has been calculated, that a propellant mass fraction of 2.91 is required for the ACRV to accomplish these orbital transfers, rendezvous with a disabled vehicle, and successfully return the crew to Earth or *Freedom* (see Appendix A for a description of mass fractions).

The rescue vehicle must have the structural capability to accommodate either type of crew transfer, docking or EVA. For a docking transfer, the ACRV must be equipped with a docking module; this module should be capable of docking with any manned spacecraft, foreign or domestic. For an EVA transfer, the ACRV should be equipped with a remote manipulator arm to aid in moving the disabled spacecraft near the ACRV, and an airlock to provide the crew with easy access to space. If the ACRV is not equipped with an airlock, the crew cabin must be capable of depressurizing and repressurizing in order to accommodate astronauts in space suits or in Personal Rescue Systems. Smaller systems such as lights and cameras would also be very useful in performing a rescue.

II.B.   CREW TRANSFER.

Although this mission would not be needed until more than one space station is built, crew transfer between two space stations or between the Earth and a space station, could be easily accomplished by a modified ACRV. With the recent developments in world politics, the possibility of international exchange of crews may become an important factor in future space operations.

Crew transfer between space stations, would begin at the sending station. The transfer crew would board the ACRV, and undock. The ACRV would then make the necessary orbital changes to rendezvous and dock with the receiving station. Depending on the specific mission, the ACRV could return to the original station either empty or carrying another crew.

Another possible mission is a crew transfer between a space station and the Earth. This mission would be similar to the ACRV crew return mission. The crew would enter the ACRV and undock from the space station. The crew of the ACRV would choose the appropriate landing site, and make the necessary de-orbit maneuvers.

These missions will require approximately 24 hours of life support for 2 to 8 crew members. To make the necessary orbital maneuvers, propellant mass fractions of 0.3 to 17.0 will be required. Also, an international docking adapter would make crew transfer between international vehicles more convenient.

II.C. CARGO TRANSFER.

The future of manned spaceflight depends upon the ability to resupply space station provisions, refurbish life support systems, and deliver medical supplies. The possibility of international cooperation in the near future will make the cargo transfer mission of prime importance for manned space operations. If the ACRV were capable of cargo transfer, then vehicles like the NSTS and Soyuz would spend less time performing this task, allowing them to accomplish more important scientific missions.

The cargo transfer mission between space stations is very similar to the crew transfer mission. The cargo would be loaded

at the sending station and the ACRV would undock. The ACRV would make the required orbital changes to rendezvous and dock with the receiving station. Once the cargo is unloaded, the ACRV would return to the sending station. This mission could be accomplished either through the use of a manned ACRV or an unmanned ACRV, which is controlled by a ground station or one of the space stations involved.

Heavy cargo transportation may require propellant mass fraction values as high as 20.2; therefore, large fuel tanks and engines will be necessary. Extra cargo space will also be necessary; this could be accomplished by removing seats from the interior of the ACRV or adding cargo pods to the outside.

II.D.   Satellite Boost.

The are many satellites in orbit at the present time that have depleted fuel supplies and can no longer make orbit changes. Several satellites are in decaying orbits and will be lost if they are not boosted to safer altitudes. The ACRV could be used to correct the orbit of a satellite that does not have its own *operational* propulsion system.

A typical satellite boost mission will begin by having the guidance and control computers on the ACRV determine the optimum launch window to rendezvous with the satellite; this could also be done by ground based or space station based systems and uplinked to the guidance computers. A two man crew will then enter the ACRV, separate from the space station, and insert the vehicle into the transfer orbit. When the ACRV has rendezvoused with the satellite, the crew will exit the vehicle and attach a support structure to it; this support structure will be used to connect

7

the satellite to the ACRV. The satellite's orbit may then be
changed, using the ACRV$_\wedge$. *as a booster* Once the satellite is in its new orbit
and the support structure has been removed, the ACRV will return
to the space station.

To accomplish this mission, there are several requirements for
the ACRV design. First, large inclination or altitude changes may
be necessary if the satellite is in a polar or geosynchronous
orbit; the propellant mass fractions range from 4.41 to 20.9,
depending on the mission. Secondly, the ACRV will need to
depressurize, allowing its crew to exit, and then repressurize
when they have finished. Lastly, and most important to this
mission, a support structure will have to be designed to connect
the ACRV to the satellite. Several support structures could be
built to handle satellites with different shapes; the appropriate
one could be attached to the ACRV before it leaves the station.

II.E.   Satellite Servicing.

The Satellite Servicing mission is one of the most important
missions for the ACRV; it will allow the aging fleet of satellites
that are in orbit to be refueled and repaired, thus extending
their useful lifetime. This will provide a substantial economic
benefit for NASA, because they will not have to replace every
satellite when it needs only minor repair or its power supply is
exhausted. Once the space station and ACRV become operational,
the space shuttle would not have to be launched every time there
is a problem with a satellite.

A typical mission for Satellite Servicing would begin with the
ACRV detaching from the space station. It would then perform
orbital maneuvers to rendezvous with the satellite. The ACRV

should be capable of reaching orbits ranging from 160-42,000 km with inclinations of 0-90 degrees. Once the vehicle gets to the required orbit, it must approach the disabled satellite so that repairs may be performed. The ACRV crew must then either repair the satellite on location or return it to the space station for major repairs. After repairing the satellite, the ACRV will return ~~the satellite~~ *it* to its original orbit.

~~Since~~ *Because* the satellites that the ACRV will repair have many different orbital inclinations and altitudes, propulsion requirements for the ACRV will be *a* large; it has been calculated that a propellant mass fraction of 3.3 to 20.2 will be required for this mission. The exterior structure of the ACRV will have to be designed to accommodate a manipulator arm*s* that can capture satellites of different shapes and sizes without damaging them. It will also need an airlock, or the ability to depressurize; this will allow the crew to perform *an* EVA to service satellites.

In addition to the external changes to the basic ACRV, the satellite servicing mission will require some internal changes as well. Space-suited crew members must be able to move within the ACRV; all controls inside the ACRV must be larger and spaced to compensate for the decreased dexterity of spacesuit gloves. The life support system will have to accommodate 1-3 people for 7 or 8 days.

II.F.   Lunar Operations.

The ACRV has a projected lifetime of thirty years; this makes it a likely candidate to aid in the establishment of a manned lunar base in the early 21st century. The ACRV could be used to transport supplies, scientific equipment, and personnel to and

9

from the moon to support this base. Also, in the event of a major
catastrophe, the ACRV could be used as a rescue vehicle.

The lunar mission would originate at *Freedom*. One possible
plan would use the ACRV as a strap-on command module placed on top
of a cargo container and an engine. Fuel tanks could be fastened
to a detachable rack mounted on top of the structure. The ACRV
and its associated add-on subsystems would leave the space
station, exit Earth-orbit, and enter a lunar parking orbit. The
ACRV would then rendezvous with a tug (a spacecraft conducting the
actual cargo transfer), making the lunar mission simpler and more
feasible. Since the rendezvous will take place in orbit, the ACRV
will not be required to land on the Moon. This will significantly
reduce fuel requirements and remove the need for landing gear.
Once the cargo has been transferred, the fuel rack attached to the
ACRV will be left in lunar orbit. Another fuel rack, already in
lunar orbit, will be connected to the ACRV for the return trip.
The use of this detachable rack will reduce the amount of
propellant stored at the space station since it will only have to
carry propellant for a one-way trip. If a large-scale lunar base
is in operation, hydrogen and oxygen could be mined from lunar
rocks to supply the propellant needed. A lunar rescue is another
mission for which the ACRV could be used. In the event of a major
catastrophe at a lunar facility (where the lunar rescue vehicle
was damaged or destroyed), the ACRV could be used as an emergency
rescue vehicle to evacuate all lunar personnel.

Because the velocity changes that are required for a lunar
mission are so high, a tremendous amount of fuel will be needed.
Also, life support should be able to sustain 6-8 crew members for
up to two weeks.

10

II.G. Ground Based ACRV Missions.

An ACRV capable of adapting to an Expendable Launch Vehicle (ELV) will be more useful than one which is not. An ELV-adapted ACRV would be capable of carrying out its operations during a period of NSTS inactivity, and could provide support (resupply, personnel transfer, etc.) for *Freedom* without interfering with the NSTS mission schedule. An ELV-adapted ACRV could also carry out other growth option missions without the support of the space station, thus allowing the ACRV to be injected directly into the orbit necessary for a particular mission.

Possible support missions for the space station could include ground-based cargo transfer, as well as personnel transfer to and from the station. A cargo transfer mission could be either manned or unmanned. If the mission were to be manned, part of the interior of the ACRV must be adapted to cargo carrying. Cargo racks (for solid supplies) or tanks (for liquids) would replace some of the normal seating positions. The craft would then lift off and ascend into orbit. Once the ACRV separates from the booster, the crew would guide it toward the space station and dock. An unmanned cargo ACRV would be capable of carrying more payload, (because more personnel space could be converted to cargo) but would require ground control in its chase and docking maneuvers.

The personnel transfer mission is similar to the manned cargo supply mission, but it does not require conversion of the ACRV interior. For crew rotation, the ACRV would be capable of carrying up to 8 crew members to the station by launch on an ELV. The craft could then be used to return members of the crew to Earth.

Another mission which could be supported by the ground-based ACRV would be shuttle and international rescue. In this scenario, the ACRV would be launched after an emergency situation has been declared, the crew would insert the vehicle into the proper orbit and rendezvous with the disabled space craft. Once the ACRV has rendezvoused with the troubled ship, the mission plan is similar to that in the previous section describing a Space and International Rescue.

The ground-based rescue mission sounds promising, however, there are several problems which would limit its usefulness. The first is a time factor. Current space launches take months or years to plan and carry out; in a space rescue mission, action must be taken immediately to prevent loss of life. Even if contingency plans existed for such a mission, the vehicle would have to be ready for flight at all times, with a rescue crew on duty and ready to fly within hours of notification. Although the monumental logistical problems of supporting such a mission seem to decrease its feasibility as a potential use for the ACRV, the mission is possible.

The ACRV will require only minor changes to its basic design so that it can be launched by an ELV. One important addition to the ACRV which would be required is an escape system like that used in early U.S. manned space flights. Such a system must be capable of removing the ACRV and its cargo from a dangerous situation involving the launcher (such as an explosion).

ELV changes are required because all ELV's which are in use today in the United States are not man-rated. Other nations with space programs that are supportive of the US do not have man-rated capability as yet, but they are working on the required systems.

Although the Soviets have several man-rated launchers, a recent congressional resolution bars the use of Soviet vehicles for US programs.

II. H. Discarded Growth Options.

There were several missions that were proposed during the initial design procedure that are not detailed in this final report. Some of the missions that were proposed but later eliminated were a space debris collection vehicle, a temporary living habitat, a station repair vehicle, a Mars mission, and a scientific payload platform. The reasons that these missions were not investigated varied.

The space debris collection vehicle would have been used to collect and dispose of, or recycle, errant pieces of space hardware and useless material. This is an important mission, since there are literally thousands of pieces of debris now in orbit that could pose serious safety and navigation problems. The orbiting debris ranges in size from small flecks of paint to discarded hand-tools to ~~burned-out hulks of old~~ inactive satellites. This mission was not pursued because a debris collection would require ~~enough~~ so many specific types of hardware (manipulator arm(s), cutting tools, disposal and recycling bins) that it would probably be better to design a dedicated vehicle for the task. It was decided that this mission was sufficiently different from the other missions in terms of goals and capabilities to preclude its immediate inclusion in the growth options of the ACRV; a robot vehicle, under ground control, could perform the mission significantly better than a manned vehicle.

Another mission that was proposed but not pursued further was

13

the possibility of using the ACRV as a station repair and work pod. Because the space station will need to be repaired and serviced, or at least require preventive maintenance, a vehicle capable of repairing the station would be useful. Also, if any vehicle or payloads were assembled in orbit, it would be convenient if astronauts could work in a shirt-sleeve environment while they assembled the object in question. This mission was not developed further because a work or repair ACRV would have to be much smaller than the original design in order to maneuver into the small spaces that would have to be serviced. Also, if the ACRV was used for repairing or assembling other vehicles or the space station, it would need to use cold gas jets to maneuver, to avoid damaging the station or the object being assembled. Again, the original ACRV would be too big to effectively move around without extensive modifications to its cold gas jet systems. A dedicated vehicle could perform this mission significantly better than a modified ACRV.

President Bush has proposed a manned Mars mission by the end of the century, therefore it was proposed that the ACRV could be used as a living or command module for the Earth-Mars transfer vehicle, or as a combined command and living module for a human-piloted cargo vehicle. The vehicle configuration would be similar to the configuration for the lunar operations ACRV. The Mars mission is going to be expensive, and any possible use of an off-the-shelf vehicle like the lunar missions ACRV could be a very useful alternative to designing, building and testing another vehicle. Nevertheless, this idea was dropped because the extensive modifications to the ACRV that would be necessary before the mission could be performed were beyond the scope of this project.

14

The last mission that was proposed, but not included, was the scientific payload mission. The ACRV could be used as a workbench where experiments could be mounted. The ACRV could then stay near the station, or travel farther away to avoid any interference with the equipment. This mission was not considered in the final analysis because it was felt that it was more cost effective to use an inexpensive unmanned vehicle as opposed to making expensive modifications to the ACRV.

It is unfortunate that not all of the proposed missions could be completely investigated, but some of the ideas were infeasible from the beginning. Also, to make the task more manageable, it was decided to concentrate on the seven most promising missions.

II.I. Matrix Description.

A matrix was developed to describe and summarize the various growth options. A matrix format was chosen because of the convenience in grouping similar mission requirements. The final format chosen three major areas of investigation for each ACRV design explored. The three areas selected are propulsion requirements, life support requirements, and structural changes.

The above categories are the column headings of the matrix; the missions that are to be accomplished are the row headings. In the various cells that make up the matrix, there will be a number, letter, or a few words that represent various changes necessary to adapt the vehicle to a specific mission.

In the propulsion column, the number that appears is a propellant mass fraction. This represents the amount of fuel, in kilograms, that the vehicle will need, per kilogram of spacecraft. For example, if the number 0.23 appears in the matrix, then 0.23

15

kilograms of fuel will be needed for each kilogram of the vehicle's dry mass. Thus, the percentage of the vehicle that must be fuel is m/(1+m). In this case, the mass percentage is 18.7%. The fuel calculations were performed assuming that Hohmann and Hohmann-like transfers were used; they represent the worst case value for the mission. In many instances, the actual amount of fuel needed for a given mission will actually be lower than the number in the matrix. All calculations assumed that hydrogen and oxygen were used as a fuel/oxidizer mix, with a specific impulse of 330 sec. A brief description of the computer program used to generate the mass fractions is included in Appendix A.

The number that appears in the life support column is the number of man-days of life support needed to perform each mission. Such life support will include things like water, food, air, heating, and waste disposal facilities. No attempt to determine an actual mass of the life support consumables or equipment was made. This table assumes that a backup, or reserve, of one and a half times is included. For example, if a mission is expected to last for 5 days with a crew of two (resulting in 10 man-days of supplies), the ACRV will carry 25 man-days of consumable supplies.

In the structural column, the specific systems or subsystems that will have to be changed or added to complete the mission are listed. For example, the cargo transfer mission has the phrase 'adjustable interior' written in, which means that extensive modifications to the interior of the ACRV are necessary to carry the cargo; this could be in the form of removing the seats and filling the inside with supplies. Any description with parentheses, (), means that the item in question would be useful, but is not critical in performing the mission. For example, the

Satellite Repair mission has the words 'hatch' and '(airlock)' in the structural changes column. This means that a hatch will be necessary to complete the mission, and that an airlock would be helpful, but not necessary.

The major reason that the matrix form was used was to make it easier to group the missions in terms of their propellant usage, their life support requirements, their structural modifications, and the special subsystems that need to be added.

II. J. Matrix Term/Abbreviation Explanation

Abbreviations	Description/definition
Adjustable Interior	- Allows seats to be moved in order to increase volumetric storage
Airlock	- Allows EVA without depressurizing main cabin
Dom	- Domestic (ie. - NASA compatible systems)
ELV Capability	- Hardware which will allow the ACRV to be launched by an expendable launch vehicle
External	- Rescue mission in which vehicles can not dock, requires space suits for both the rescuers and rescuees
GEO	- Geosynchronous Orbit (for purposes of this report, 36,000 km altitude)
Hatch	- Allows crew to exit into space environment, includes depressurizable cabin, assumes no airlock
Int'l	- International (ie. - systems not necessarily compatible with NASA)
Int'l Docking Adapter	- Allows the ACRV to dock with many different spacecraft

Landing Gear	-	Struts, supports, etc., which will allow a moon landing
LEO	-	Low Earth Orbit (for purposes of the report, 180-700 km altitude)
Link-up	-	Rescue mission in which the rescue vehicle may dock with the damaged vehicle, allowing transfer without spacesuits
Lrg	-	Cargo which must be stored outside the ACRV and is more than one ACRV mass but less than 3.
MID	-	Middle range orbit (for purposes of the report, 4,600 km altitude)
Repair	-	ACRV travels to satellite and fixes it on location
Return	-	ACRV travels to satellite and returns it to space station
Satellite Grappler	-	Device which will allow hook-up to different satellites
Sht'l	-	Space shuttle orbiter
Sml	-	Cargo which can be placed inside the ACRV

II.K ACRV Mission Design Matrix

Mission	Fuel Req't	Life Support	Structural Change Requirements/Supplements
Crew Return	.23	20	None
STS + Int Rescue			
– Sht'l Link–up	2.91	50	10 person capability (docking adapter)
– Sht'l External	2.91	50	(Airlock), hatch, space suited individuals, 10 pers.
– Int'l Link–up	2.91	50	Int'l docking adapter, 8 person capability
– Int'l External	2.91	50	(Airlock), hatch, space suited individuals, 8 pers
Satellite Boost			
– LEO – LEO	4.405	20	Satellite grappler
– LEO – MID	8.01	20	Satellite grappler
– LEO – GEO	20.2	20	Satellite grappler
Satellite Repair			
– LEO–Repair	3.31	30	(Airlock,Remote manipulator arm) Hatch,Handholds,Satellite grappler
– LEO–Retrieval	4.45	30	(Airlock,Remote manipulator arm) Hatch,Handholds,Satellite grappler
– MID–Repair	6.3	30	(Airlock,Remote manipulator arm) Hatch,Handholds,Satellite grappler
– MID–Retrieval	8.01	30	(Airlock,Remote manipulator arm) Hatch,Handholds,Satellite grappler
– GEO–Repair	16.9	30	(Airlock,Remote manipulator arm) Hatch,Handholds,Satellite grappler
– GEO–Retrieval	20.2	30	(Airlock,Remote manipulator arm) Hatch,Handholds,Satellite grappler
Lunar Operations			
– Simple	13.8	140	Cargo hard points
– Mid–range	16.32	140	Cargo hard points (Landing gear)
– Advanced	36.3	140	Cargo hard points (Landing gear)

Figure 1A – ACRV Mission Matrix

Mission	Fuel Req't	Life Support	Structural Change Requirements/Supplements
Crew Transfer			
Int'l LEO	2.91	80	(Int'l docking adapter, Airlock) Hatch
Int'l MID	6.3	80	(Int'l docking adapter, Airlock) Hatch
Int'l GEO	16.9	80	(Int'l docking adapter, Airlock) Hatch
Dom LEO	.38	80	(ELY Adaptability)
Dom Mid	1.77	80	(ELY Adaptability)
Dom GEO	16.9	80	(ELY Adaptability)
Cargo Transfer			
Sml-Int'l-LEO	4.405	80	(Int'l docking adapter) Adjustable interior
Sml-Int'l-MID	8.01	80	(Int'l docking adapter) Adjustable interior
Sml-Int'l-GEO	20.2	80	(Int'l docking adapter) Adjustable interior
Sml-Dom-LEO	.84	80	Adjustable interior (ELY Adaptability)
Sml-Dom-MID	2.43	80	Adjustable interior "
Sml-Dom-GEO	20.2	80	Adjustable interior "
Lrg-Int'l-LEO	5.5	80	Structural hard points
Lrg-Int'l-MID	9.72	80	Structural hard points
Lrg-Int'l-GEO	23.24	80	Structural hard points
Lrg-Dom-LEO	.727	80	Structural hard points ELY
Lrg-Dom-MID	3.089	80	Structural hard points "
Lrg-Dom-GEO	23.24	80	Structural hard points "

Figure 1B - ACRV Mission Matrix (continued)

20

III.   METHODS OF ACCOMPLISHING MISSIONS

After the growth options were analyzed, it was necessary to group them in terms of which missions were compatible. One logical criterion for determining compatibility is to compare the systems that would be needed to complete each mission. By doing this, it was possible to determine what configuration of the ACRV would be most useful in terms of the number of alternative missions it could perform. Three possible designs that could complete these missions will now be discussed.

III. A.   Mission Specific ACRV's.

One possible option that was developed was not grouping the missions at all. This would correspond to tailoring an ACRV for each mission. This way, every vehicle could complete the mission it was called upon to perform, since it would have been optimally designed for that particular mission. Examples of systems found on mission specific ACRV's include: engines designed specifically for cargo transfer, or a manipulator arm built into an integrated structure for the satellite servicing mission. The principal drawbacks to this idea are cost and primary mission goals.

Obviously, a large fleet of specialized vehicles, each of which can do one job very well, would be an expensive undertaking. Each vehicle would need to be extensively designed and tested. If there were no budget constraints, this would be the optimum solution, because each vehicle would be perfect for the job it was designed to do. Unfortunately, it is unrealistic to follow this course of action.

Another stumbling block to this approach is that the primary mission of the ACRV -- crew return -- would have a reduced priority compared to each secondary mission during the design procedure. This would, in effect, result in a diverse fleet of vehicles capable of performing a primary mission, such as satellite servicing or cargo transfer, and also capable of performing a secondary mission of crew return; however, crew return is the primary mission of the ACRV.

III. B.   Multi-Mission ACRV's.

A second approach is to group missions according to their projected modifications to the baseline ACRV, and thereby determine common requirements. To do this, a grouping plane was developed to describe the different changes. The grouping plane, Figure 2a, is a two-dimensional graph that plots projected changes in life-support and fuel on the vertical axis, and projected structural changes on the horizontal axis. These particular vehicle subsystems were chosen because they would change the most for different vehicle designs. The fuel and life-support were grouped together since, for the most part, using more fuel indicates a longer trip which will require more life-support.

The diagram that was developed has several rectangles plotted. These rectangles correspond to mission envelopes that represent the ranges of structural and propulsion/life support modifications necessary for the completion of each mission. Once these mission envelopes were defined, it was possible to group the missions together into 3 larger categories, Figure 2b. The large categories represent possible vehicle designs that could accomplish all of the sub-missions enclosed. The three designs

developed were the low-range ACRV (ACRV-L), the mid-range ACRV (ACRV-M), and the extended-range ACRV (ACRV-X).

The advantage to this method of design is that a large number of overly-specialized vehicles do not have to be built; a smaller number of utilitarian designs can be used instead. While the ACRV designed for each envelope would not be ideally suited for every mission in its envelope, it is much more flexible than the previous (ungrouped) method because each vehicle can perform a variety of missions.

The basic ACRV (ACRV-L) envelope is at the lower left of the grouping diagram. This design would be capable of performing the primary mission of crew return in the event of a medical emergency or station catastrophe. It would also be capable of performing LEO crew transfers, shuttle and international rescues, and some light cargo carrying missions. The vehicle would be reentry capable, and would not require any modifications to perform its three sub-missions. The vehicle would have small engines and fuel tanks, and limited life-support capabilities. The ACRV-L would never spend more than a day or two away from the space station.

The mid-range vehicle design (ACRV-M) would be a utility design, capable of performing many missions in LEO and mid-range orbits, and have some limited GEO capabilities as well. The ACRV-M would be used to perform the LEO to mid-range crew and cargo transfers, satellite repair and retrieval, and satellite boost missions. The ACRV-M should also be appropriate for limited GEO activities, such as GEO satellite repair, but not retrieval, due its fuel constraints. It would also be capable of operating away from the space station for several days. The ACRV-M should, in emergency situations, perform the basic ACRV missions also, but

23

not as well as the ACRV-L. It is unknown at this time how difficult it would be to perform a rescue mission with this vehicle design. The ACRV-M would have larger engines and/or fuel tanks than the ACRV-L, as well as extended life-support capabilities, and possible add-on systems. Such add-on systems might include manipulator arms, deployable solar arrays, and detachable cargo modules. If the ACRV-M is to perform rescue missions, it must be reentry capable as well.

The third vehicle design, the ACRV-X, would be a heavy-work vehicle, capable of delivering large payloads to GEO or the moon. The ACRV-X would be used to perform the GEO satellite retrieval and repair missions, the GEO cargo missions, and also the lunar operations. The ACRV-X would not be capable of completing any rescue missions, and it would not be reentry capable. The ACRV-X could possibly perform any of the ACRV-M missions as well. The ACRV-X would be an upgraded version of the mid-range vehicle, with much larger fuel tanks, extended range life-support, deployable solar arrays, manipulator arms, or other systems that may be necessary. It would be capable of missions lasting as along as two weeks.
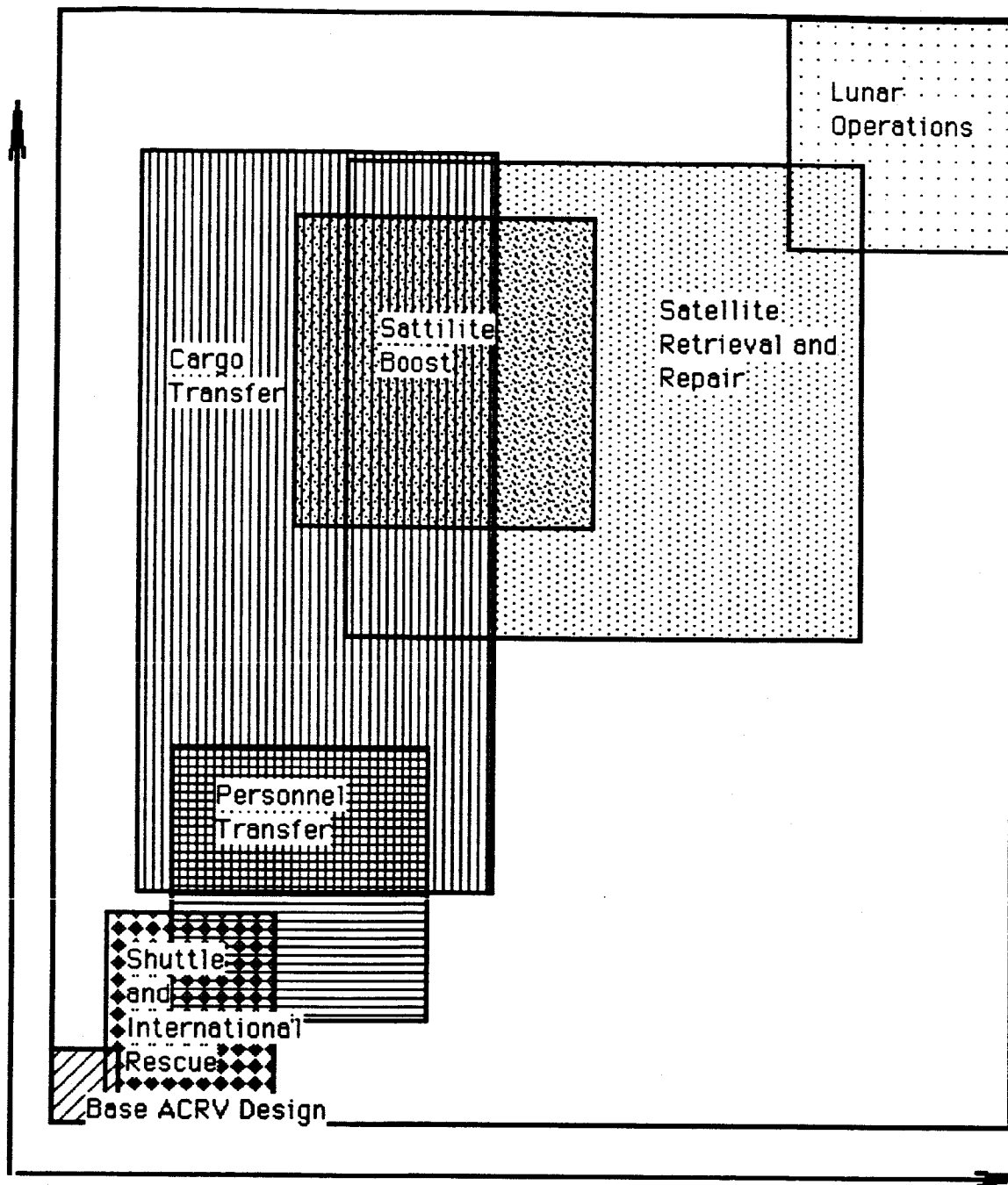
Figure 2a - Grouping Plane showing required changes in life-support and structural changes.

25
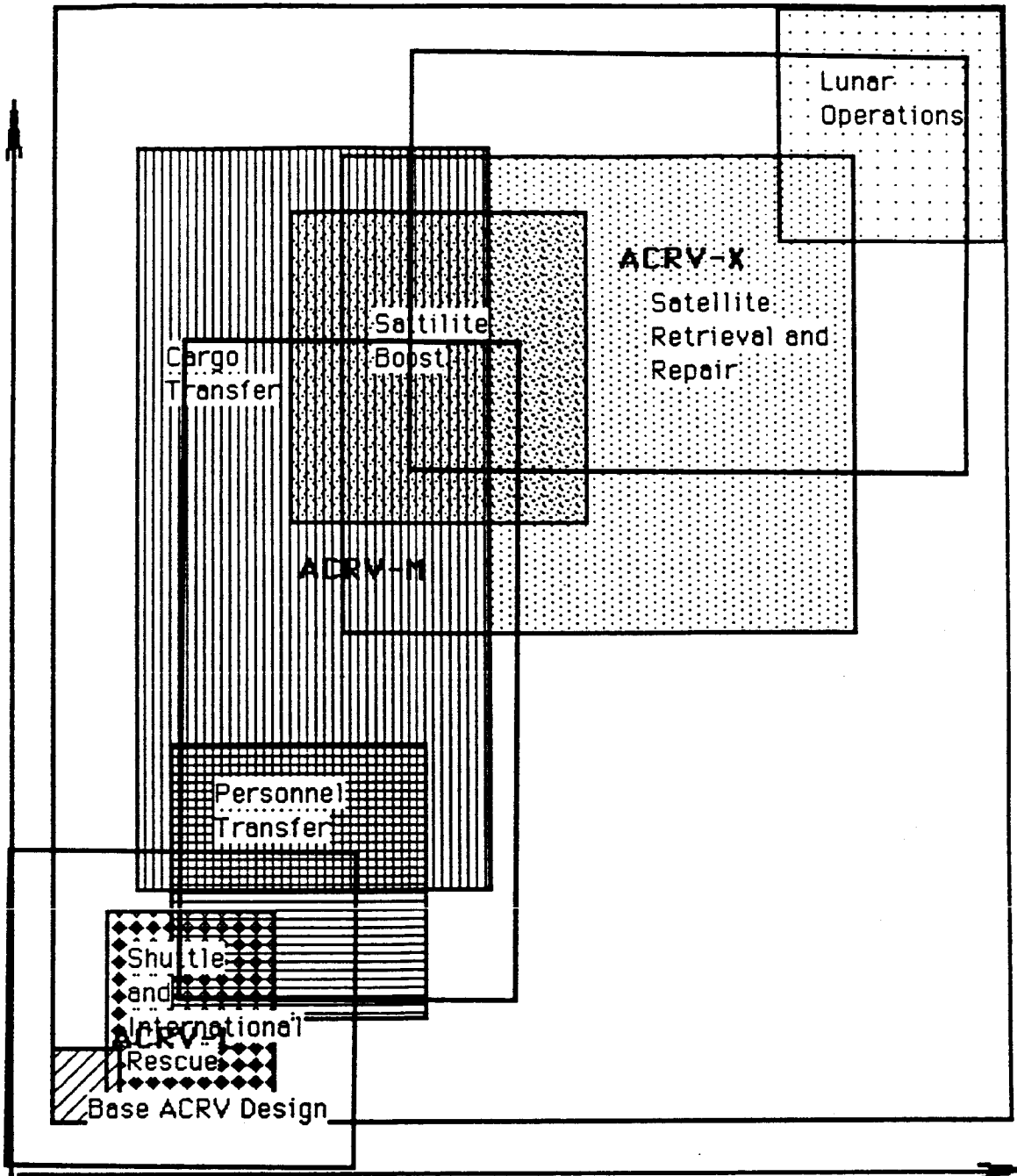
Figure 2b - Grouping Plane with overlay showing how various multi-mission ACRV's would adapt to different missions

III. C. Modular ACRV Design.

The method of expanding ACRV growth options that has the greatest potential, and the possibility for the most problems, is modularity. Modularity entails a system of modules which could be attached to the ACRV. Connecting different modules would allow the ACRV to accomplish various missions, while in its normal state (no attached modules) it would be able to carry out the primary mission of the system -- crew return.

While the concept of a modular spacecraft may be new, many of the essential first steps have already been taken. In past space missions that required more than one craft (Apollo moon missions, Gemini/Agena missions), two spacecraft which were not originally connected (Apollo CSM-LM, Gemini capsule-Agena target) docked and supported one another. Support could be in the form of electrical power, computer communication and actual commands which would be sent from one craft to the other.

NASA has recently begun research into a craft which has some of the features of a modular-designed ACRV. The Space Transfer Vehicle (STV) is planned to be an evolutionary craft which will be able to handle a wide range of missions. Such missions include Geosynchronous satellite transfer, planetary probe launch, and later, manned operations including support of a moon base. The STV project proves that NASA considers evolutionary, expandable spacecraft important to the future of space exploration.

The modular design offers many advantages over other solutions to the multi-role ACRV problem. The first advantage to a modular design consideration is ease of development. The design of the basic ACRV could be changed slightly to allow future expansion. This modified ACRV could be placed into service at *Freedom* with a

27

C-6

minimum delay ~~time~~ compared to placing an ACRV into operation without such modifications. The ease of development would also lead to a lower cost for an expansion-modified ACRV over an ACRV which was designed to carry out multiple missions.

Keeping expansion options outside the ACRV in the form of modules also decreases the complexity of the ACRV itself. For example, an ACRV which is designed to rescue members of a space shuttle crew would have to carry several systems which a basic ACRV would not need, such as: A depressurizable crew section, a larger crew section (to allow space-suited individuals freedom of motion) and the ability to carry ten people (including rescuers and rescuees). Obviously, the shuttle rescue ACRV would be much more complex than an ACRV devoted simply to crew return.

Modularity also allows the ACRV to adapt to other, perhaps future, missions which have not been planned or are not necessary yet. In order for the expandable ACRV to handle a new mission, all that is required is another module that is compatible with the ACRV system. This expandability will assure the ACRV's place in the future of space flight.

The modular ACRV is not a perfect solution to the multi-mission problem, however. There are several difficulties which must be addressed before this option can be considered beyond preliminary concepts. Module breakdown is a problem which could render an ACRV useless for a particular mission. The ACRV mission modules will require extensive crew handling in the space environment. The techniques needed for this type of handling have not yet been developed. Due to this lack of experience, module breakdown may become a problem in the ACRV system, because the crews will not have the experience needed to repair them in space.

Another concern for the expandable ACRV is changeover time. To use a previous example, if an ACRV-M designed for rescue purposes, was called upon to perform its mission it could leave the space station in a short time, since it only requires minor preparation. The modular ACRV would require assembly time to prepare the vehicle for the mission, which could result in loss of life.

The modular ACRV would also require more support from *FREEDOM* than a basic ACRV. A major concern would be storage space for the many modules that would be necessary; this extra material stored at the station will serve to complicate maneuvers around the station, and may contribute to the problem of space debris.

To change the basic ACRV to an expandable spacecraft, several adjustments will be required. These may seem formidable, but they are small when compared to the changes required to give the ACRV the ability to carry out two or more missions.

Structural connectors will be required to secure the modules together. They will be required to handle complex loadings without releasing, but should be easy to disassemble when required. The connectors will need to be very simple in design and require little maintenance.

Computer connections will allow the ACRV to communicate with its additional parts. The interfaces will need to connect and disconnect easily, as well as provide a constant link between the ACRV and its modules.

Fluid, air, and electrical connections will also be required to allow the ACRV to support the modules which are attached to it, or the modules to support the ACRV. Again, the connectors must be simple, and allow easy connection/disconnection.

The modularity concept entails several different modules that

can be attached to the ACRV during missions requiring advanced features. Three attributes of each module will be discussed: the physical characteristics, importance, and applications in different missions.

The most important module for the ACRV will be the propulsion module. This module will be used in every mission with the exception of the medical/crew return mission. The module will consist of a liquid-fueled engine with a high specific impulse.

An extended life-support module will also be employed for almost every mission of the ACRV. This module will include the necessary air, food, and water requirements for the crew. The life-support module will need to be directly connected to the main cabin of the ACRV so that the food and water systems will be accessible by the crew.

An airlock module may be added to the ACRV for crew transfer, satellite repair, and shuttle rescue. It will allow the ACRV to pick up space-suited crew members from a spacecraft that has sustained damage. It will also allow ACRV crew members to leave the spacecraft to repair satellites while some crew members remain in the ACRV in a shirt sleeve environment. The airlock will have to be attached directly to the main hatch of the ACRV and will also have to be connected to the life-support module to gain access to an air supply.

The satellite retrieval and repair missions will require the ACRV to have a satellite capture module. The device will resemble a variation of the manipulator arm used on the space shuttle.

A docking adapter would be useful for international and shuttle rescue, crew transfer, and cargo transfer. This will be a simple module that attaches to the main hatch of the ACRV and allows it

to dock with other vehicles to transfer crew members and supplies.

The landing gear module may need to be attached to ACRV for the lunar operations mission. This module will be connected to structural hard points on the ACRV if it is to actually land on the moon.

IV.   RECOMMENDATIONS

The purpose of using the ACRV to accomplish other missions is to save NASA the expense, both monetarily and technically, of designing many new vehicles. The ACRV has a design lifetime of 30 years, with characteristics which would allow it to perform several valuable missions during that period. The ACRV will be more useful in the future if growth options are considered during its early design phase. In this section, several recommendations will be offered for the basic design of the ACRV.

Any structural shape should be able to perform the growth options that have been discussed. Preliminary research done by this design team and others shows that a ballistic vehicle will be the most efficient. A lifting-body does possess better re-entry and landing qualities, but the cost of building and maintaining such a structure far outweighs these benefits. Also, it will be much easier to adapt a ballistic vehicle to the exterior modifications that will be necessary for the growth options.

The reusability of the ACRV exterior has not been extensively researched. Protective tiles, like those on the NSTS, could be used to protect the vehicle on re-entry; however, these tiles must be able to withstand the harshness of the space environment for a much longer time than previous thermal protection systems. They will be exposed to debris and micrometeoroids, as well as structural loadings from extended missions the ACRV performs; the tiles may crack or fall off, becoming useless on re-entry. The heat shielding will also add mass to the ACRV that must be carried around on extended missions; this could become very expensive in

terms of propellant. Therefore, it is recommended that the heat shield be removable. A removable heat shield will solve both the storage and mass problems. When the ACRV is performing one of the growth option missions, the heat shield could be removed and stored so that it is protected from incidental impacts; if the vehicle then needed to re-enter, the heat shield could be replaced intact. The reduced mass from removing the heat shield would allow extra cargo or propellant to be carried on extended missions.

(A) Preliminary study suggests that the structure of the ACRV be designed so that extra equipment or modules could be attached to the exterior of the vehicle. The ACRV and its related systems must be carried to *Freedom* aboard the Space Shuttle, so there is a limit on how big they may be, unless the vehicle is to be assembled in orbit. One way to avoid assembling major portions of the vehicle in orbit is to assemble the pieces on the ground, and then boost these modules to *Freedom's* orbit so that they may be attached in orbit. This way, most of the assembly takes place on the ground, with only minimal construction in orbit.

The basic ACRV mission may be accomplished with a passive life-support system. The researched growth options may have mission times up to two weeks in length for a crew of two to four. A mission of this length will need an active life-support system that can process waste gasses produced by the crew. It is therefore recommended that an active life-support system be installed in the ACRV. It would be much easier to install such a system now than to replace a passive one later; preliminary research has shown that the increase in mass will not be extensive. It would also be advisable that this life-support system be

33

designed so that it could be augmented from extra supplies stored in exterior modules.

The basic ACRV mission will have to be performed by a deconditioned crew, so many of the piloting and guidance tasks will be accomplished by the onboard computer; this system could be quite powerful. The growth options will require many of the same guidance and control methods employed in the basic mission, but each mission will have to be programmed on an individual basis. Therefore, the ACRV computer should be modular in design. The computer could be designed such that a "black box" could be programmed with the information necessary to accomplish a mission. These boxes could be programmed at the space station for each specific mission and then plugged into the ACRV main computer; this is done today for the navigation systems on US strategic bombers. The computer will also have to communicate with the exterior additions that may be added to the ACRV for the growth options. This could be accomplished by providing exterior ports that connect the main computer to the electronic systems in the modules, and then adding another "black box" to the main computer that would run the module's systems.

V.   MODULAR ACRV

V.A.   Baseline Design for a Modular ACRV

The ACRV systems have been examined to determine which ones
need to be augmented for longer missions. These systems must have
the capability to be expanded. The expansion could take the form
of adding supplies (such as air, food, or water), allowing access
to the modules (such as crew travel between the baseline ACRV and
any expansions), or providing augmented control (such as computer
commands and/or status). The systems which will be affected are
shown in Figure 3 below.
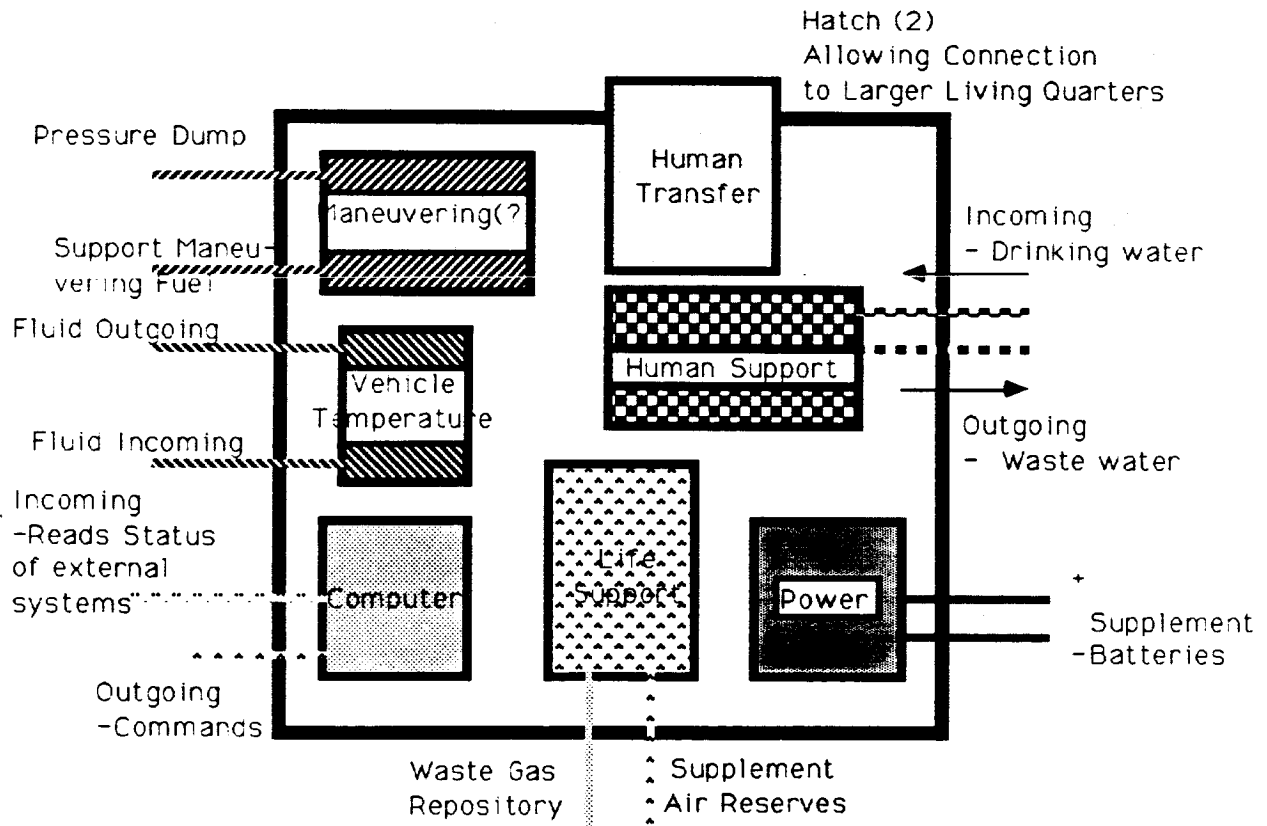
Figure 3 - System diagram showing systems which would require
connection to external modules for support in long ACRV missions.

All modular systems will have one (or more) of their connectors exposed to space while the ACRV is in the baseline configuration. Therefore, all ports on the ACRV must have a valve system which will not allow fluid or air flow when the module is disconnected.

It has already been stated that for optimum performance, the ACRV should have a ballistic shape. Research has shown that the unsymmetrical shape of a lifting body ACRV would make the module system difficult to implement. This report concentrates on a ballistic vehicle, because this design is simpler to analyze and is more readily adaptable to the modular design. In Figure 4, one possible configuration for the lifeboat ACRV is presented; the shape of the command section is arbitrarily drawn (any ballistic body is acceptable).

Top View

- Heat Shield
- Flotation Collar
- Parachutes
- Hatch/Station Attachment Point

Side View

- Hatch/Station Attachment Point
- ACRV Command Section
- Flotation Collar
- De-Orbit Engines (2)

Bottom View

- Heat Shield (Tile or Ablative)
- De-Orbit Engines
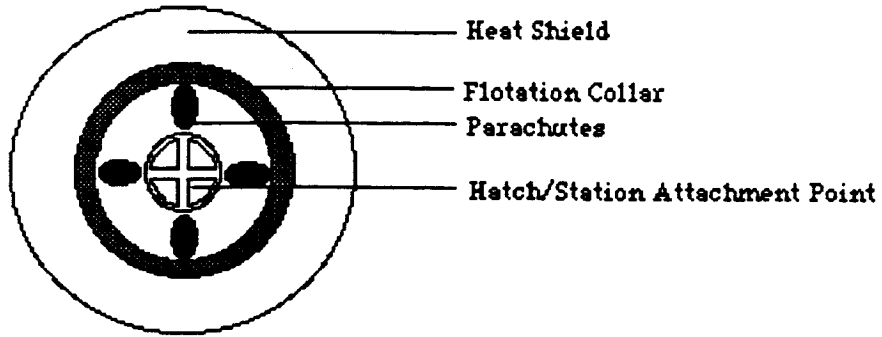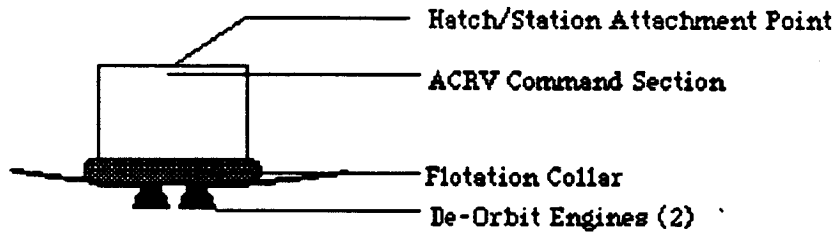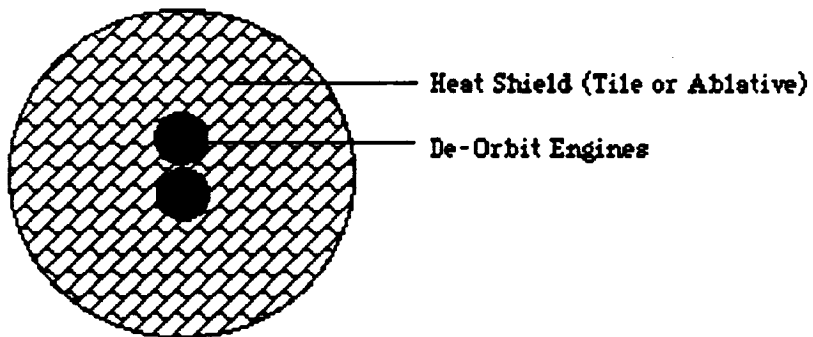
Figure 4 - Suggested Design for an ACRV which would be ready for conversion into a modular mission ACRV.

V.B.   Overall Configuration.

Several factors were considered in order to formulate the best design for a modular ACRV. Some of these included command section configuration, hatch and station attachment points, system expandability, structural support, module arrangement, engine capability and fuel tank capacity. Once these design factors were analyzed, it was concluded that many modifications need to be made to the baseline ACRV design in order to perform the growth option missions.

Three different preliminary designs for the modular ACRV were developed, and are shown in Figures 5-7. The major external components that may be added ~~or modified~~ to the baseline ACRV, depending on the design, are the larger liquid rocket engine, propellant tanks & truss supports, pressurized connecting tunnel, modules & supporting truss, and maneuvering thrusters.

The first design for the modular ACRV, shown in Figure 5, involves the placement of the support modules in a hexagonal array around the central ACRV command section. This configuration allows two, three, four or six modules to be used symmetrically. The fuel tanks and the main engine are mounted to the rear of the command section. Multi-member trusses should be used to support both the propellant tanks and modules and also to connect these components to the command section. The main hatch (station attachment point), should remain the same as in the baseline ACRV (i.e. built into the nose of the command section). Although this configuration is quite simple, it would require that the baseline ACRV command section contain numerous hatches so that all modules could be accessed easily.

38

The second design of the modular ACRV is shown in Figure 6. this design includes a pressurized connecting tunnel which will be attached between the command section and truss structure supporting the propulsion system. Two or four modules will be positioned radially around the connecting tunnel. Four pressure doors will be built into the tunnel allowing the modules to be accessed. This connection scheme requires only two hatches in the baseline ACRV -- one in the front for station attachment, and one in the rear to connect with the pressure tunnel. A multi-element truss will be used to connect the pressurized tunnel to the propulsion platform. This truss structure will transfer the thrust force from the engine to the rest of the vehicle. Once again, multi-member trusses will be used to support and connect the propellant tanks and modules to the vehicle. Smaller extended life support tanks will be attached to the exterior of the tunnel between the modules and the command section.

To minimize the number of hatches built into the baseline ACRV, a third configuration for the modular ACRV, shown in Figure 7, was developed. In this design, the modules are positioned in front of the command section instead of behind. This design allows the use of an ACRV with only one hatch. This hatch (station attachment point), will allow the pressurized tunnel to connect to the command section without the use of another entrance. The tunnel will have four radially-spaced pressure doors and a hatch at its tip which can attach to the station. Small life-support tanks will be mounted on the lower half of the connecting tunnel between the command section and the various modules. Also, a set of small maneuvering thrusters will be connected to the end of the connecting tunnel. The propellant tanks and main engine are

located to the rear of the vehicle. Multi-member trusses will be used to support and connect the fuel tanks and the modules to the ACRV.

Although only three different configurations of the modular ACRV have been considered, current research has shown that the third design, presented in Figure 7, is the best choice due to its simplicity and effectiveness. Figure 7 also requires the least number of changes applied to the original ACRV.

ACRV Side View

Hatch/ Station Attachment Point

ACRV Command Section

Modules (3 or 6)

Support Truss

Fuel Tanks

Main Engine

ACRV Front View

Modules

ACRV Command Section

Hatch

Support Truss
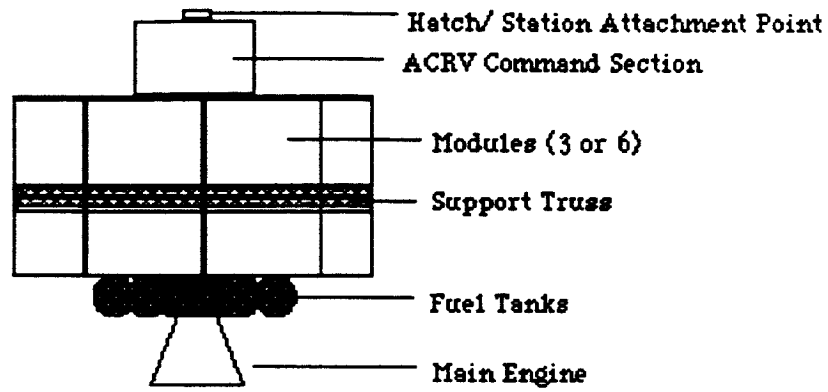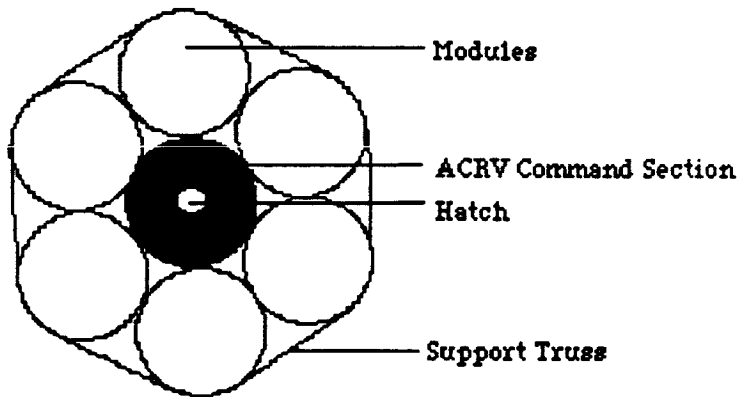
Figure 5 - First design considered for modular ACRV system. Discarded due to added complexity required on baseline ACRV.
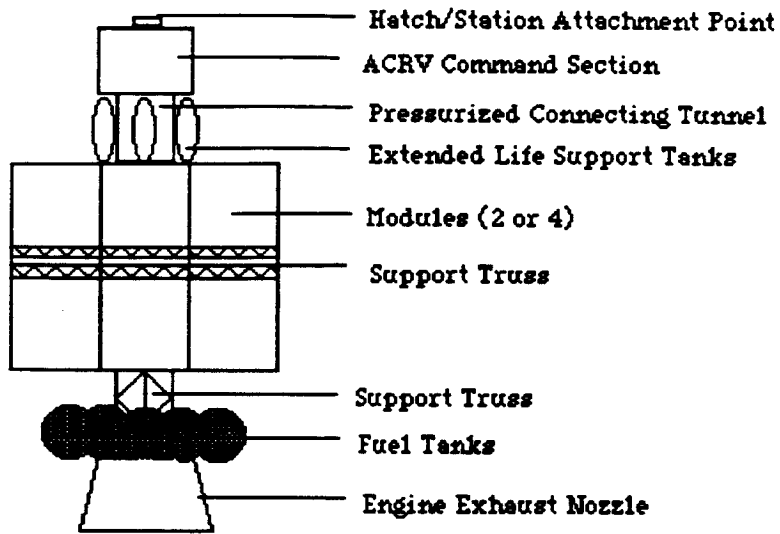
Cross Section to Show Detail
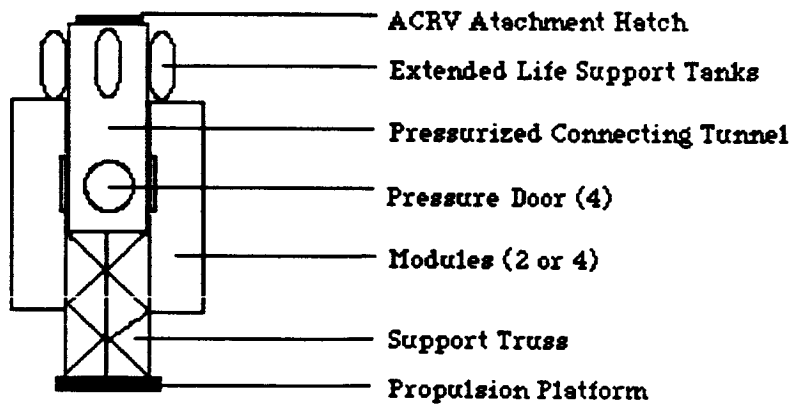
ACRV Rear View
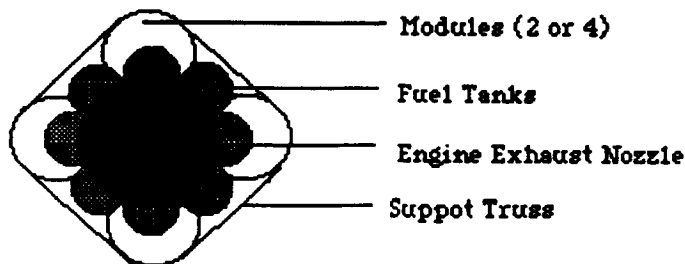
Figure 6 - Modular design consideration #2. Also Discarded due to
excessive change to lifeboat ACRV

Modular ACRV Design III

ACRV Front View

Heat Shield
Connecting Tunnel and Maneuvering Jets
Modules (2 or 4)

ACRV Side View

Connecting Tunnel and Maneuvering Jets

Modules (2 or 4)

Extended Life Support Modules
Pressurized Connecting Tunnel
ACRV Command Section

Fuel Tanks and Support Truss

Engine Exhaust Nozzle

ACRV Cross Section Detail

Maneuvering Jets
Connecting Tunnel
Modules (2 or 4)
Pressurized Connecting Tunnel
Pressure Doors (4)
Extended Life Support Tanks

ACRV Rear View

Heat Shield

Propellant Tanks and Support Truss

Engine Exhaust Nozzle

Figure 7 - Final configuration of modular ACRV.

43

V.C.   Propulsion.

The primary mission of the ACRV is the station evacuation-medical emergency mission. The baseline ACRV propulsion system must be able to perform a de-orbit burn from Space Station *Freedom's* orbit, which involves a comparatively small change in velocity. The vehicle must also sit in readiness at *Freedom* for months or years before it may be required to perform this mission. Therefore, it is reasonable to assume that a solid rocket engine would be best for this mission. The engine would be affixed to the bottom of the heat shield with some form of pyrotechnic bolts, so that when it has burned all of the propellant it may be discarded. This would insure that small pieces of the engine would not flake away during reentry and damage the heat shield, and the aerodynamic characteristics of the vehicle will not be adversely affected. For reasons of safety, it may be necessary to include a second engine in case of a ~~miss-fire~~ *failure*. Each engine should be able to be ignited separately, and each one should be capable of making the de-orbit burn.

The modular ACRV design will need a significantly larger, more versatile propulsion system. Research has shown that the only practical type of engine for growth options is a liquid bi-propellant engine. Some preliminary estimates for the amount of propellant needed, the size and weight of the propellant tanks, and the required thrust have been determined, based on some simplifying assumptions. These assumptions are:

1) All orbital maneuvers are considered impulsive, as long as the burn time is less than 10% of the orbital period. Ideally, the burn time should be as small as possible to approximate an impulsive burn. This leads to extremely high

44

thrusts and accelerations, which are unhealthy for the crew
and cargo, and also require prohibitively large engines. The
relationship between the impulsive velocity change required
(ΔV_{imp}) and the actual, non-impulsive velocity change
required (ΔV_{act}) is

$$\Delta V_{act} = \Delta V_{imp}\left[1 + \frac{\mu T^2}{24\, r^3}\right]$$

where μ is the gravitational parameter of the Earth, T is the
time period during which the velocity change is
accomplished, and r is the instantaneous distance to the
Earth's center.

2) The propellant used is a slightly fuel-rich mixture
(slightly more fuel per oxidizer than that of a stoichiometric
combustion) of liquid hydrogen and oxygen, stored externally in
spherical tanks. Although liquid hydrogen is extremely light
(specific weight 0.07), and, therefore, requires huge storage
tanks, it has a very high specific impulse when burned with
oxygen. Because of the problems associated with hydrogen and
oxygen (storage, boil-off, safety) an alternative propellant
was investigated. Mono-methyl hydrazine and nitrogen tetroxide
are very easy to store, fairly dense, and are hypergolic (i.e.
they ignite on contact). This combination has one drawback in
the form of a lower specific impulse than the hydrogen-oxygen
mixture.

3) The propellant tank mass is approximately 5% of the
propellant mass that it carries. This is the same ratio as
the mass fraction of the Space Shuttle external tank. The
ACRV will not experience the high launch stresses or
aerodynamic loadings that the space shuttle tank must face,

45

so this is a conservative estimate which may actually be reduced, or justified as a factor of safety. Empty tanks will not be discarded in flight, both to save money and to avoid a navigation hazard. Good estimates for cryogenic storage facilities (refrigerators and insulation) were not readily available and have not been included in this figure.

4) For these preliminary estimates, the propellant combinations were assumed to have a vacuum I_{sp} of 450 and 313 seconds, corresponding to hydrogen-oxygen and MMH-N_2O_4, respectively. These numbers were determined by examining the Space Shuttle technical specifications for the main engine (hydrogen-oxygen) and the orbital maneuvering system (MMH-N_2O_4).

Using these assumptions, the computer program MASSCALC FORTRAN includes a method of estimating the tank mass, and also determines the longest possible burn time (10% of the orbital period) for the maneuver to be considered impulsive. The program must have the following quantities as input: the destination orbital radius and inclination, as well as the amount of mass to be picked up or dropped off at the destination orbit, and the specific impulse. The results of these computer runs are summarized in the following table.

Key- ΔV_1 -Velocity difference to insert into transfer orbit, km/sec

ΔV_2 -Velocity difference to exit transfer orbit, km/sec

ΔV_i -Velocity difference for inclination change, km/sec

a_{max} -Maximum acceleration required, m/sec

46

XC$_{Drop}$ -Mass fraction of cargo to leave in destination
orbit.

XC$_{Pick}$ -Mass fraction of cargo to pick up in destination
orbit.

XP$_{450}$ -Mass fraction of propellant; I$_{sp}$ = 450 sec.

XP$_{313}$ -Mass fraction of propellant; I$_{sp}$ = 313 sec.

LEO -Low Earth orbit, 520 km.

MID -Mid range Earth orbit, 10000 km.

GEO -Geosynchronous orbit, 35600 km.

Table 1-- Estimated Mission Characteristics

Mission	ΔV1	ΔV2	ΔVi	Amax	XCDrop	XCPick	XP450	XP313
SS-Int'l Rescue	0.106	- - -	- - -	0.19	0.00	0.00	0.056; Isp= 200sec	
SS-Int'l Rescue	0.046	0.045	1.968	3.45	0.00	0.20	1.832	3.102
LEO Boost	0.046	0.045	1.986	3.45	0.75	0.00	1.912	3.426
MID Boost	1.433	1.149	1.292	2.60	0.75	0.00	4.012	8.211
GEO Boost	2.413	1.460	0.793	4.38	0.75	0.00	6.453	15.438
LEO Repair	0.046	0.045	1.986	3.45	0.00	0.00	1.490	2.710
MID Repair	1.433	1.149	1.292	2.60	0.00	0.00	3.199	6.813
GEO Repair	2.413	1.460	0.793	4.83	0.00	0.00	5.250	13.258
LEO Retrieval	0.046	0.045	1.986	3.45	0.00	0.75	2.612	4.176
MID Retrieval	1.433	1.149	1.292	2.60	0.00	0.75	4.762	8.961
GEO Retrieval	2.413	1.460	0.793	4.83	0.00	0.75	7.203	15.797
Lunar Mission	3.092	0.829	0.045	5.62	1.35	0.00	6.830	15.423
Lunar Mission	3.092	0.829	0.107	5.62	1.35	0.00	6.830	15.423
LEO Crew	0.046	0.045	1.986	3.45	0.20	0.00	1.632	2.902
LEO Crew	0.046	0.045	1.986	3.45	0.00	0.20	1.832	3.102
MID Crew	1.433	1.149	1.292	2.60	0.20	0.00	3.390	7.198
MID Crew	1.433	1.149	1.292	2.60	0.00	0.20	3.590	7.398
GEO Crew	2.413	1.460	0.793	4.83	0.20	0.00	5.636	13.644
GEO Crew	2.413	1.460	0.793	4.83	0.00	0.20	5.836	13.844

The values in the previous table were generated using several assumptions:

1) The Space Station moves in a perfectly circular orbit, with r=360 km. All destination orbits are perfectly circular.

2) Only two-burn Hohmann transfer ellipses are used.

3) All transfers have a 30^0 inclination change except lunar missions. The basic lunar mission has an inclination change of 5^0, and the extended mission has a change of 12^0.

4) Inclination changes are done in the outer orbit at the same time the Hohmann transfer burn is conducted.

5) The propellant mass fraction is defined in terms of the dry mass of whatever part of the vehicle makes the whole trip; i.e. if a vehicle of mass M carried mass C of cargo, the reported propellant mass fraction is in terms of M, not (M+C).

As can be seen from the previous table, the most demanding missions, in terms of propellant expenditures and required thrust, are the GEO and lunar missions. GEO missions have large velocity changes to insert into a transfer orbit, and, because most geosynchronous satellites have an orbital inclination of 0^0, there are large velocity changes required to change the orbital inclination. The lunar missions require large velocity changes to insert into the transfer orbit, but, if the missions are planned correctly, little or no inclination change is necessary.

The last subject that needs to be addressed is the choice of engines. When choosing the proper type of engine for the ACRV

missions, it was discovered that there was no one particular kind that was best for all missions. It is entirely possible that the best way to perform the various missions would be to use several different engines, each one with a different mass and maximum thrust. One important consideration for choosing the engines was the possible use of gimballing systems. If a gimballed engine is used, the placement and masses of the modules is less critical, since a gimballed engine can compensate for minor differences in the location of the center of mass of the vehicle. Another important consideration is whether or not an engine is rated to carry humans. The following table (Table 2) lists only two man-rated systems; the Space Shuttle Main Engine, and Space Shuttle Orbital Maneuvering System. The other engines are included to indicate trends in engine characteristics. The Olympus RCS engine is currently being developed by ESA as a reaction control and orbit circularizing engine; it is included here to show possibilities for attitude control. An estimate of the reaction control authority for the vehicle will require a specific vehicle design, including masses and moments of inertia.

Table 2 - - Rocket Engine Characteristics

Engine Type	RL-10	LE-5	HM-60	SS-ME	SS-OMS	Olympus RCS
Max Thrust (kN)	67	103.5	1025	2130	26.7	0.490
Vacuum Isp (sec)	444.	448	430	455	313	308
Mixture Ratio	5.0	5.5	5.1	6.0	1.65	1.64
Comb. Pressure (MPa)	3.2	3.7	10	20.7	0.86	0.69
Expansion Ratio	40	140	106	77.5	#	150
Burn Time (sec)	450	370	500	520	+	+
Mass (kg)	132	255	1100	3065	#	2.8

= unavailable, + = variable

Many of the missions discussed could be performed by a cluster of 2 LE-5 engines, or perhaps 3 RL-10 engines. Both of these combinations will give a thrust of about 200,000 Newtons, and have comparatively low mass. For the more advanced missions, it might be desirable to use a larger engine, like the HM-60, which has less mass than a cluster of smaller engines delivering the same thrust. It is also assumed that by the time the ACRV and its family of expansion modules is built, engine technology will have advanced enough to scale some of the engines up or down to meet the mission needs and still have the same thrust to weight ratio.

V.D.   Modules.

To perform the growth options discussed earlier, several modules are required. To begin the analysis, the specific needs for each mission were examined, and separated into distinct categories. The categories were then grouped together to lower the number of modules required. Modules that were investigated include: a Cargo Module, a Passenger Module, a Work Module, an Extravehicular Activity (EVA) Module, and an Extended Power Module. Several other necessary attachments (an attachment is a system which does not require its own module, but may be necessary for a mission) such as a docking adapter and a satellite support structure, were also studied.

The basic design for each module is a circular cylinder that is 2.5 meters in diameter by 7.5 meters long; it is based on a structure being developed by the ERNO Raumfahrttechnik G.m.b.H. Corporation for use with the Space Station. The modules will be designed to be pressurized, but will have the ability to operate unpressurized. The interior of this basic structure will be

designed to accommodate the specific module.

The Cargo Module will be used to carry supplies, equipment, fuel and other small payloads from Space Station *Freedom* into different Earth orbits or to the Moon. The interior structure will be able to accommodate solid payloads, mounted on racks, as well as fuel and other liquids stored in tanks. An exterior hatch may be put on the cargo module so that astronauts can access the cargo while performing an EVA.

The Passenger Module will be used to transfer crews between *Freedom* and other manned space vehicles or the Moon. Basically, the interior of a pressurized Cargo Module will be redesigned to carry passengers; seats and other amenities will be added to make the flight as comfortable as possible. To prevent an overload of the ACRV life support system, this module will carry its own life support system and supplies.

The Work Module will be needed when the ACRV is on a repair or recovery mission. It will be used to capture disabled satellites and spacecraft, as well as for performing minor maintenance on these vehicles. A remote manipulator arm, lights, and closed-circuit cameras will be mounted onto the exterior of this module. The interior will provide a shirt-sleeve environment for the astronauts to work in.

The EVA Module is closely related to the Work Module; it will be used when an astronaut needs to leave the ACRV to work on another spacecraft. This module will carry spacesuits, a Manned Maneuvering Unit (MMU), and other equipment necessary for an EVA mission. An airlock will also be mounted onto this module; this will allow astronauts to enter and leave the ACRV without depressurizing the entire vehicle.

51

The ACRV missions including these growth options may last anywhere from one day to three weeks. A mission to Geosynchronous orbit or the Moon will require much more power than can be supplied by the baseline ACRV. The Extended Power Module will carry power cells, or possibly retractable solar panels, to provide power for long duration missions. This module could also carry supplemental life support supplies.

There are two other items that are necessary to complete the remaining growth options. First, a docking adapter for the airlock will be needed if the mission involves Soviet spacecraft. The docking adapter would be similar to the device used in the Apollo-Soyuz Mission to accommodate the differences in docking mechanisms. Secondly, a satellite support structure should be designed to hold a satellite during orbital operations. This attachment is to allow the ACRV to move satellites into different orbits, or bring them back to *Freedom* for repair.

All six of the previously mentioned growth options may be accomplished using two to four modules similar to the ones just described. The Shuttle and International Rescue mission will require the Work module (if a manipulator arm will be needed to grapple a disabled vehicle), the docking adapter (so that the ACRV can dock if possible), and the EVA module (in case docking is not possible). A passenger module may also be taken to add extended life support.

The Cargo Transfer mission will require one or more Cargo Modules. The number of Cargo Modules carried will be determined by the amount of supplies being carried. An EVA module may also be necessary if the Cargo Transfer is to take place externally. Similarly, the Crew Transfer will carry multiple Passenger

Modules, depending on how many people are being moved. The docking adapter is an option on both of these missions.

The Satellite Boost and Satellite Service missions will both require the Work Module and the EVA Module. The Work Module will be used to capture the satellite, and provide the necessary equipment to repair it. The EVA Module is necessary, because an astronaut might be required to perform an EVA if the satellite can not be repaired with the manipulator arm. The Satellite Support Structure will also be required if the satellite is to be moved to a different orbit.

The Lunar Operations mission is a very diverse mission and may require all of the modules at one time or another; the Extended Power Module will definitely be required for every lunar mission. The modules that are required, or that are optional, for each of the Growth Options are summarized in Table 3.

Table 3
Modules Required for Specific Missions

	Cargo Module	Passenger Module	Work Module	EVA Module	Docking Adapter	Sat. Support Structure	Extended Power Module
Shuttle & Int'l Rescue		O	X	X	X		
Cargo Transfer	X,M			O	X		
Crew Transfer		X,M			X		
Satellite Boost			X	X		X	O
Satellite Service	O		X	X		O	O
Lunar Operations	O,M	O,M		O	O		X

Legend:
X - Module necessary
M - Multiple modules possible
O - Module optional

V.E.   Module Connection

The modular ACRV will need several types of connectors at each interface between modules. Connectors required include: structural, fluid, and electrical.

The first and most important of these connectors is the structural connections. These connectors will have to withstand stresses due to acceleration of the ACRV. In addition, the structural connectors must be easily engaged and disengaged by spacesuited individuals or an automated system. Therefore, the connectors must be able to function with a fairly high degree of positioning error when connecting to the target module.

Research into structural connectors has lead to the discovery of one which suits the needs of a modular spacecraft. The connector is currently under development at NASA, and is shown in Figure 8.

Type I structural connector
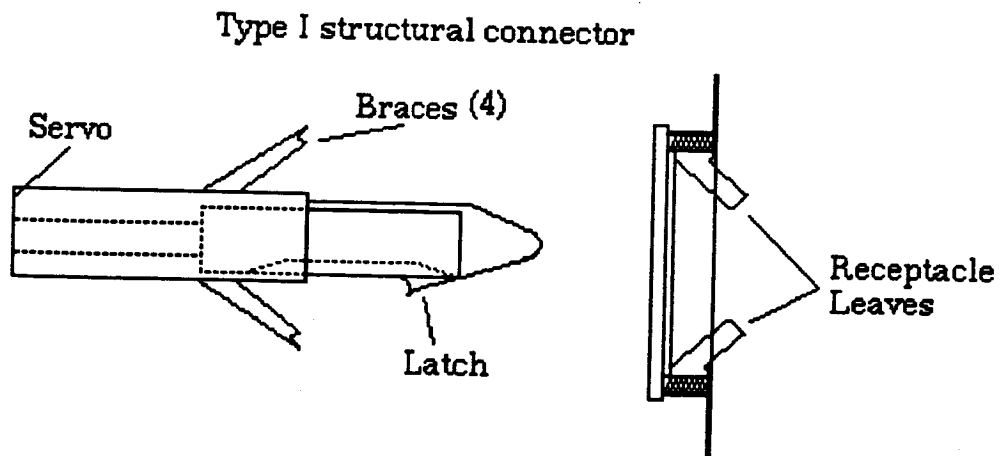
Figure 8 -   Modular structural connector researched for use with the Multimission Modular Spacecraft.

The connector is a plug and receptacle docking system that can withstand the stress of a multi-mission spacecraft. The system consists of a long cylindrical plug that tapers to a pointed end. This plug has a spring loaded latch approximately midway between the base of the plug and the point. The receptacle on the target module has a large open end that tapers to a smaller circular opening that the plug fits snugly into. When the plug is inserted into the receptacle, the spring loaded latch catches the leaf of the tapered receptacle. Once the latch has passed the leaf, the plug is pulled back into the base and the receptacle is pulled tightly against the braces of the plug. The large open end of the receptacle and the tapered point of the plug allow for quite a large margin of error when engaging the system. This is necessary because the modules will be connected in a 0 g environment by spacesuited workers who will have limited manual dexterity. However, once the spring loaded hook is in place and the receptacle is pulled in, the system holds the two modules in place with great accuracy. Three plug and receptacle systems will be used on each of the modules to insure that the interfaces between modules are stable and accurate so that the fluid and electrical hook-ups can be engaged.

The fluid connections between modules will also be borrowed from existing NASA technology. After the structural connection has been completed, the fluid connection will be made either manually or by an automated system that will engage the fluid connector. It is very important that the structural connector align the modules with a high amount of accuracy. This is due to the fluid connection device being researched for use on the modular ACRV, which requires an axial approach accuracy of ±3 degrees.

The electrical connections will then be made using a floating nut system researched for use on other modular spacecraft. This system allows an axial mismatch of $\pm$ 0.20 inches and a large angular misalignment at the start of engagement. These characteristics make the floating nut system very useful for the ACRV because the errors for engagement are large enough that the hook-ups can easily be made in a 0 g environment.

V.F.   Storage of ACRV Modules

Many considerations must be taken into account in storing the modular ACRV. Among these are the size and shape of the modules and the truss structure connecting them, the large mass of fuel that will be needed for the missions, the amount of power needed to recharge the ACRV's systems after a mission, and cost. Keeping preliminary designs that have been considered in mind, possible areas of storage have been examined. The two storage areas under investigation are directly on Space Station *Freedom* and on a co-orbiting platform.

Storage of the modules directly on the initial phase of the space station would take place near the shuttle docking area at one of the four resource nodes. The ability to permanently store the modules and truss structure in this area will greatly depend on the size and mass of these components. Interference with shuttle operations and station controllability concerns, limit space available for module storage on the initial phase of Space Station *Freedom*. Completion of the space station's dual-keel configuration, creating more truss space, will make storage more feasible. The expanded station provides more available space for storage, with the most probable areas for storage on either end of

57

the keel.

Storing the modular ACRV on a co-orbiting platform is a feasible alternative to storage directly on the station. NASA's 1989 Long-Range Program Plan calls for a co-orbiting platform for additional payloads to be built soon after the station. Another platform could be built in close proximity to the station for storage of ACRV modules. For a mission other than that of station escape, the baseline ACRV would undock from Space Station *Freedom* and rendezvous with the platform. The mission ACRV would then be assembled.

A co-orbiting platform would minimize the following: disruption of normal space station operations, the space used and equipment required on Space Station *Freedom*, and the possible danger of fuel storage. Necessary considerations in this storage method are the increased cost, increased overall orbit-keeping difficulty and the recharging of the ACRV's systems. Recharging of the ACRV could be done by power generation on the platform or by power from Space Station *Freedom*.

Both on station and co-orbiting *storage locations* are feasible methods of storing ACRV modules. Although problems would arise in both methods, they are not insurmountable. Further research in size, shape, mass and power requirements of the ACRV and its systems is necessary to lead to a decision on which storage method is most feasible.

V.G.   Example Mission

Once the modular ACRV system is on line, several missions which require extensive planning and materials (such as a satellite rescue made by the space shuttle) will become commonplace. In

this section, a satellite servicing mission will be described as it would be accomplished by the modular ACRV. In addition to the text description, preliminary sketches of the system appear in Figures 9 and 10.

When it is determined that there is a satellite in need of repairs or resupply, the ACRV will leave its docking port on the space station and move to either the transportation node, or the co-orbiting module storage area. There, astronauts will remove the heat shield and install the propulsion module. Next, the ACRV will dock with its connecting tunnel and the modules required for the mission, (in this case, the work module and the EVA module).

Once all connections have been made and systems have been checked out, the ACRV will fire its main engine and transfer to the *disabled* satellite's orbit. The ACRV will approach the satellite, and grapple it with its manipulator arm. If necessary, astronauts will then leave the ACRV to conduct repairs on the satellite. When the satellite is functioning again, or it has been decided to return the satellite to *Freedom* for more extensive repairs, the ACRV will again fire its main engine and return to the space station.

When the ACRV arrives at the station, it will be able to dock with *Freedom* upon its arrival, due to the hatch located on the connecting tunnel. Later, the system can be stripped down to the basic ACRV, and it can be returned to its normal duty.

Conceptual Drawings for
Modular ACRV
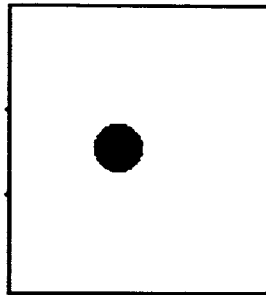
ACRV with Heat Shield Separated
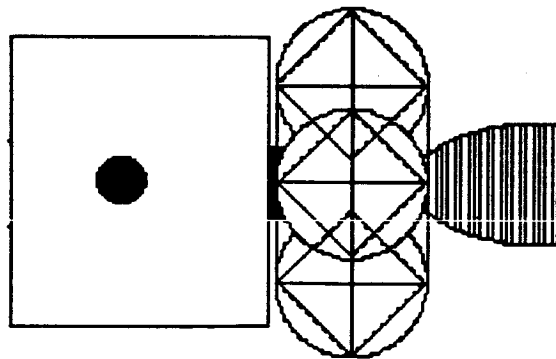
ACRV After Engine Module Connection

Figure 9 - Preliminary design drawings of modular ACRV

Conceptual Drawings for Modular ACRV (Cont'd)
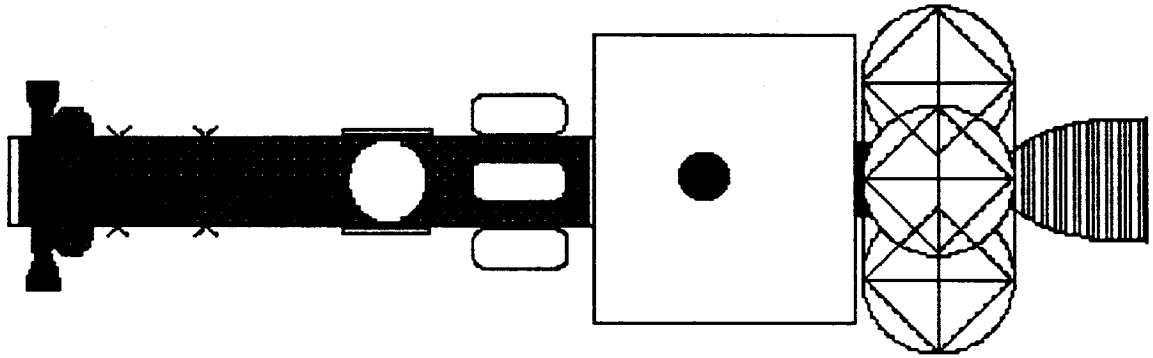
Connecting Tunnel Added
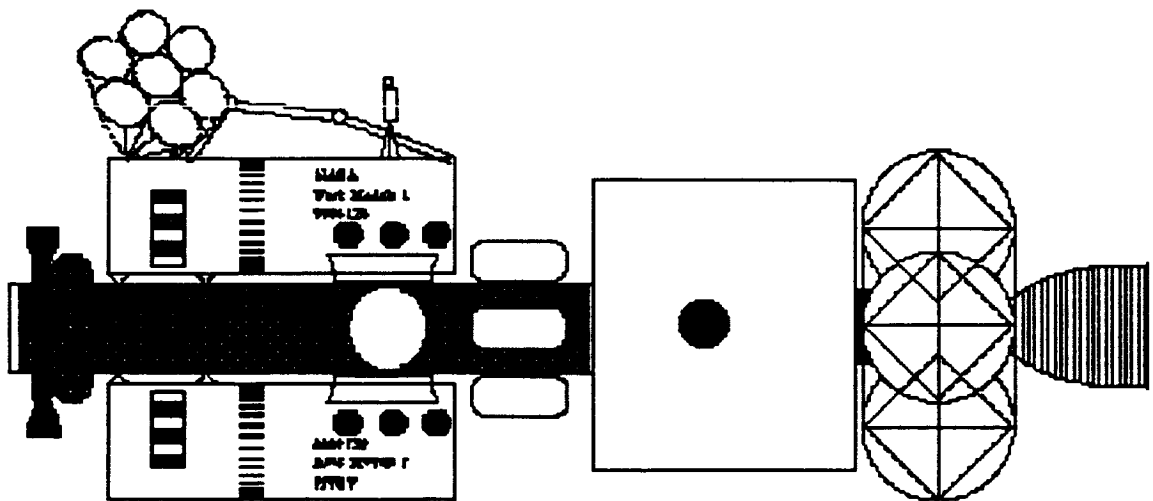
Assembly Complete. Airlock and Work Module Included to
Allow Work on a Disabled Satellite

Figure 10 Preliminary design drawings of modular ACRV (cont'd)

VI.   Conclusions

In order to allow the ACRV to take an active part in space operations other than its primary purpose, it must be designed to accomplish other missions. The extra missions will give the ACRV added flexibility and utility; both of which are highly important in this time of reduced space funding. This increased flexibility will lengthen the useful life of the ACRV, and the decreased need for other vehicles will allow funding to be diverted to other ACRV missions.

The growth options that were recommended include: shuttle and international rescue, crew transfer, cargo transfer, satellite boost, satellite servicing, lunar operations, and ground based ACRV missions. These growth options have been determined to be seven of the most useful missions for the future of the space station and other manned space activities.

Further research lead to the discovery of three primary methods of accomplishing growth options, and it was decided that the expandable ACRV would be the best method. The expandable or modular ACRV would be able to carry out several missions by attaching different modules to the normal ACRV. This would greatly increase the flexibility and range of the spacecraft. Modularity also keeps the main purpose of the ACRV, crew return, in focus. When the ACRV is in its normal state (no attached modules), crew return is easily accomplished.

When all monetary and design considerations are taken into account, growth options become a very important part of the ACRV program. Economic and structural factors also dictate that the

modular craft is the most feasible method of accomplishing missions beyond the scope of the normal ACRV. The modular ACRV is the way to maximize the usefulness of the ACRV while minimizing the overall cost.

VII.   REFERENCES

1. Hill, et al "ACRV: Growth Options" NASA/USRA/Penn State
    University-sponsored study.   11 December 1989

2. Timnat, N.W., "Advanced Chemical Rocket Propulsion",
    London, England, 1987

3. "Assured Crew Return Capability for Space Station Freedom:
    CERV", NASA, Lyndon B. Johnson Space Center, Houston,
    Texas, 1989

4. Assured Crew Return Capability (ACRC) Study (NAS-17900)
    Performed By: Eagle Engineering/LESC
    Funded By: NASA
    1988

5. Space Station *Freedom* Media Handbook, NASA Public
    Affairs Office, April, 1989

6. Study of in-orbit Servicing of Columbus Elements by ALV,
    Executive Summary.   (ERNO-Raumfahrttechnik GMBH,
    Bremen, West Germany)

7. "Design of Geosynchronous Spacecraft" Agrawal, Brij.
    Harcort, Brace, and Johanovich.   New York, NY 1988

8. "Fundamentals of Astrodynamics", Bate Mueller and
    White.   Dover Publications Inc., New York, NY 1971

9. "History of Manned Spaceflight" Baker, David.   Crown
    Publishers, Inc. New York, NY 1985

10. Orbital Spacecraft Resupply Systems: Volume 4 - Extended
    Study
    Results: Final Report
    Performed By: Rockwell International
    Funded By: NASA
    1987

11. "Numerical Analysis" Burden and Faires, McMillian
    Publishing, Inc. New York, NY 1985

Appendix A - Program MASSCALC Description

The various ACRV missions that were proposed had very different fuel requirements. To calculate the fuel necessary for a given mission, a computer program, called MASSCALC FORTRAN was developed. In order for MASSCALC to run, the following input parameters are required: the initial orbit that the ACRV starts from, the specific impulse of the fuel used, the final destination orbit, the difference between the initial and destination orbit inclination angles, the amount of mass that will be left in the destination orbit, and an initial guess for the upper limit of the fully loaded vehicle mass (both expressed as a fraction of the ACRV mass). The program will return the changes in velocity that will be required, as well as the mass of fuel that will be needed, expressed as a fraction of the dry mass of the ACRV vehicle. The final mass fraction of the fuel is determined by a bisection numerical method.

The matrix that was developed in this study lists small and large cargo and satellite operations. Small was defined as anything with a mass of less than 1 ACRV mass, and large is anything with a mass of more than 1 ACRV mass, but less than 2 *times the* ACRV masses. The program was written assuming that Hohmann or Hohmann-like transfers are made, and all fuel is burned quickly enough that the velocity changes can be considered impulsive. For the present, continuous thrust will be ignored.

```
        PROGRAM MPCALC                                              IMP  01
* PROGRAM ASSUMES THAT FUEL IS OPTIMIZED HYDROGEN/OXYGEN (ISP=360)   IMP  02
* ASSUMES THAT FUEL TANK PRESSURE IS 6.8E5 PA                        IMP  03
* ASSUMES FACTOR OF SAFETY 1.2                                       IMP  04
* ASSUMES INITIAL ORBIT 360 KM (6738KM)                              IMP  05
        REAL ISP,MU,MP1,MP2,MP12,MP22,M,MPI,MPI2,MACRV               IMP  06
        DATA MU/3.986E5/,RHO/430.0/,RC1/6738/,FS/1.2/                IMP  07
        PRINT*,'ENTER FINAL ORBIT'                                   IMP  08
        READ*,RF                                                     IMPC 09
*       PRINT*,'ENTER INCLINATION CHANGE'                            IMP  10
*       READ*,THETA                                                  IMP 011
*       PRINT*,'ENTER MASS OF CARGO TO BE LEFT IN DESTINATION ORBIT IN AC IMPC 12
*    + RV MASSES'                                                    IMP 013
*       READ*,XM                                                     IMP 14
*       PRINT*,'ENTER ACRV MASS IN KG'                               IMPC 15
*       READ*,MACRV                                                  IMP 017
        PRINT*,'ENTER ISP'
        READ*,ISP
        THETA=30.0/57.28                                             IMP  18
        OPEN (UNIT=6,FILE='LEO 313',STATUS='UNKNOWN')
        VC1=SQRT(MU/RC1)                                             IMP 20
        VC2=SQRT(MU/RF)                                              IMP 21
        E=(RF-RC1)/(RF+RC1)                                          IMP 22
        AM=(RC1+RF)/2.0                                              IMPC23
        P=AM*(1-E**2)                                                IMPC024
        H=SQRT(P*MU)                                                 IMP 25
        VT1=H/RC1                                                    IMP 26
        VT2=H/RF                                                     IMP 27
        DV1=(VT1-VC1)*1000.0                                         IMP 28
        DV2=(VC2-VT2)*1000.0                                         IMP 29
        DVI=VC2*SIN(THETA/2.0)*1000.0                                IMP 30
        DVI2=SQRT(DV2**2+DVI**2)
        IF (RC1.GT.RF) THEN                                          IMP 31
         DV1=-DV1                                                    IMP 32
         DV2=-DV2                                                    IMP 33
        ENDIF                                                        IMP 34
        ISP=ISP*9.8                                                  IMP 19
        DO 10 I=1,200
         XM=I/50.0
        A=35                                                         IMP 35
        B=0                                                          IMP 35
99      C=(A+B)/2.0                                                  IMP 36
        M=C                                                          IMP 37
        MP1=M*(1-EXP(-DV1/ISP))                                      IMP 38
        M=M-MP1                                                      IMP 39
        MP2=M*(1-EXP(-DVI2/ISP))                                     IMP 40
        M=M-MP2                                                      IMP 41
        M=M-XM                                                       IMP 44
        MP12=M*(1-EXP(-DVI2/ISP))                                    IMP 47
        M=M-MP12                                                     IMP 48
        MP22=M*(1-EXP(-DV1/ISP))                                     IMP 49
        M=M-MP22                                                     IMP 50
        IF (M.GT.1.01) THEN                                          IMP 51
         A=C                                                         IMP 52
        ENDIF                                                        IMP 53
```

```
        IF (M.LT.0.99) THEN                                    IMP00540
         B=C                                                    IMP00550
        ENDIF                                                   IMP00560
        IF ((M.LT.1.01).AND.(M.GT.0.99)) GO TO 15              IMP00570
        GO TO 99                                                IMP00580
15      XP=(C-1.0-XM)                                           IMP00590
        XFT=0.0327*FS*XP                                        IMP00600
        WRITE (6,1001) XM,XP+XFT
10      CONTINUE
1001    FORMAT(2F10.4)
        END                                                     IMP00770
```

PRELIMINARY SUBSYSTEM DESIGNS

for the

ASSURED CREW RETURN VEHICLE

(ACRV)

Final Report Vol. III

Department of Aerospace Engineering
Pennsylvania State University
University Park, PA

PENNSTATE

ABSTRACT

This report comprises a series of design studies concerning the Assured Crew Return Vehicle (ACRV) for Space Station *Freedom*. Study topics, developed with the aid of NASA/Johnson Space Center's ACRV Program Office, include: a braking and landing system for the ACRV, ACRV growth options, and the design impacts of the ACRV's role as a medical emergency vehicle.

Four alternate designs are presented for the ACRV braking and landing system. Options presented include: ballistic and lifting body reentries; the use of high-lift, high-payload aerodynamic decelerators, as well as conventional parachutes; landing systems designed for water landings, land landings, or both; and an aerial recovery system. All four design options presented combine some or all of the above attributes, and all meet performance requirements established by the ACRV Program Office.

Two studies of ACRV growth options are also presented. Use of the ACRV or a similarly designed vehicle in several roles for possible future space missions is discussed, along with the required changes to a basic ACRV to allow it to perform these missions optimally. The outcome of these studies is a set of recommendations to the ACRV Program Office describing the vehicle characteristics of the basic ACRV which lend themselves most readily to be adapted for use in other missions.

Finally, the impacts on the design of the ACRV due to its role as a medical emergency vehicle were studied and are presented herein. The use of the ACRV in this manner will impact its shape, internal configuration, and equipment. This study included: the design of a stretcher-like system to transport an ill or injured crew member safely within the ACRV; the compilation of a list of necessary medical equipment and the decisions on where and how to store it; and recommendations about internal and external vehicle characteristics which will ease the transport of the ill or injured crewman and allow for swift and easy ingress/egress of the vehicle.

This report is divided into three volumes. Volume I contains the four braking and landing proposals, volume II contains the two growth options studies, and volume III contains the single medical mission impact study.

VOLUME III

ACRV MEDICAL MISSION

The medical mission of the ACRV is the mission that arises if a Space Station crewmember becomes ill or injured and requires time-critical medical treatment beyond the capability of the Space Station's facilities, and the Shuttle cannot respond in time to transport the crewmember. This mission places special restrictions on the ACRV design, because the ACRV Program Office has decided that it should be a design requirement that the ACRV is able to perform this mission within twenty-four hours of the decision to make the trip, and the portion of that time spent in transit cannot exceed six hours. Additionally, there are different impact impulse requirements for healthy and ill or injured crew. For the purpose of this analysis, it was determined that the ACRV itself only met the restrictions for healthy crewmembers, and that special equipment was necessary to protect the ill or injured occupant.

The assignment for the one project group that performed this study was to assess the impacts that the medical mission makes on the ACRV. This mission will impact the shape, internal configuration, and equipment of the entire vehicle. Additionally, the group was asked to design the actual stretcher-like system for transporting the crewman safely. Their final project report is included in the following section.

MED-ACRV

Final Design Report

Aerospace 401
Spacecraft Design

April 30, 1990

Group: Nixon

Group Leader
Robert Nixon

Partners
Christopher Bauer
William Elliott
Mark Guman
Jay Kerosetz
Mike Xenakis

ABSTRACT

The necessity for safe crew return via the Assured Crew Return Vehile (ACRV) in the case of medical emergency has brought forth the need for a stretcher system capable of operating in microgravity and during re-entry. This report is based on extensive research of state-of-the-art paramedical and industrial technologies. The system has two components: (1) a sub-stretcher consisting of an immobilization device called a vacuum splint, and (2) a permanent base structure inside the ACRV. Medical concerns, specifically re-entry accelerations and microgravity physiological effects, are presented as justifications for certain design decisions. A lifting body is preferred as the ACRV shape because of the reduced G-forces incurred by an injured crew member. A spring-damper model was developed to determine the characteristics of a shock absorption system to satisfy the System Performance Requirements Document (SPRD) specifications for injured crew members. Methods of restraint, or attaching the sub-stretcher to the base, are also discussed. In addition, life support equipment and necessary first aid supplies are listed and their location in the ACRV is described. The possibility of multiple stretchers on one ACRV and a preferable vehicle layout (the domino configuration) are also investigated. Finally, an argument for a large top hatch on the ACRV is offered to expedite evacuation of a patient by Search and Rescue (SAR) forces.

TABLE OF CONTENTS

LIST OF FIGURES

INTRODUCTION

"Since the beginning of the manned space program NASA has been dedicated to Assured Crew Return Capability (ACRC)."[1] This policy along with NASA's commitment to a permanently-manned space station, suggests the necessity for a space-based return vehicle. For this reason, NASA is currently designing an Assured Crew Return Vehicle (ACRV) to perform the following functions: (1) transport crew members to Earth in a medical emergency, (2) evacuate crew members in the case of a space station catastrophe, and (3) return crew members to Earth in case of unavailability of the Shuttle. This report is centered on the first function, the medical mission of the ACRV. The medical mission requires a means of transporting the injured crew member safely back to Earth, while maintaining the patient's condition.

The general approach for the development of such a system was to examine present-day medical emergency care and transportation. This led to the investigation of ambulance and helicopter services as well as search and rescue procedures. The aim was to adapt or improve upon techniques and technology used in modern emergency medicine for the possible scenarios requiring the use of the ACRV.

The main focus was on the design of a medical unit that included life-support and immobilization equipment that would effectively keep the patient stabilized until medical facilities were reached on Earth. Elements that may affect the condition of the patient, such as the environment of space, flight re-entry and impact, were of primary interest as well. The design was divided into four main areas: medical concerns, stretcher design, medical equipment, and vehicle configuration. The requirements and guidelines specified by NASA for the medical mission are presented first and will be referred to later. A short description of the evolution is presented for those areas involving actual design considerations.

DESIGN SPECIFICATIONS

Certain design specifications were established by NASA in the System Performance Requirements Document(SPRD).[2] The requirements summarized below concern the medical mission of the ACRV and will be referred to throughout this document.

In the event of a medical emergency or accident, a 24 hr period is needed for mission planning before the patient can be transported to Earth. Six hours was the constraint set for the transportation time. This six hour period is divided into 3 sections:

- 3 hrs from ingress to landing
- 1 hr from landing until crew recovery
- 2 hrs to transport the patient to a health care facility

During the flight the incapacitated crew member will be positioned in a seat especially designed for accommodating the ill/injured crew member. It is recommended that the patient be placed in a supine position from the hips-up. The seat will include any special life-support features or equipment. In addition, the ACRV will be equipped with an emergency medical kit. The following constraints were provided for re-entry accelerations referenced to the coordinate system shown in Figure 1,

$$+ \text{X direction} \leq 4 \text{ G's}$$
$$+ \text{Y direction} \leq 1 \text{ G}$$
$$+ \text{Z direction} \leq .5 \text{ G's}$$

In addition the threshold accelerations for impact of the $ACRV_X$ are

	Healthy crew member	Injured crew member
+ X direction	<= 15 G's	<= 10 G's
+ Y direction	<= 10 G's	<= 3 G's
+ Z direction	<= 5 G's	<= 2 G's

and

~~This table gives~~ the restrictions for impulses that can be incurred[3] *are*

	Healthy crew member	Injured crew member
+ X direction	<= 3 G-sec	<= 2 G-sec
+ Y direction	<= 1 G-sec	<= .3 G-sec
+ Z direction	<= .5 G-sec	<= .2 G-sec

Spin stabilization is not recommended because of the ~~limited resistance~~ *effects upon* ~~of~~ the human body. A healthy person can tolerate between 5-8 rpm. Nausea, vomiting and disorientation may occur above these spin rates. An injured person would ~~be able to withstand even lower spin rates.~~ *feel the effects to a much greater degree.*[4]

MEDICAL CONCERNS

The two major medical concerns associated with the return of the ACRV are the accelerations involved in re-entry and landing, and the physiological effects caused by re-adaptation to a 1-G environment. Each possible ACRV design (i.e., glider-type, Apollo-type, and ballistic-type) will experience a different type and magnitude of acceleration due to its shape and method of re-entry. These accelerations will also be imposed on the crew members. The physical condition of the crew at the time of return will also affect their capacity to withstand the accelerations and their ability to adapt to an environment with gravity.

Accelerations

Crew member tolerance of re-entry forces depends upon several factors, including magnitude, duration and direction of the force. For example, spacecraft re-entry involves a force applied over a longer duration, but with a relatively small magnitude, compared to the sudden, large impact force associated with landing. The possible medical complications which may accompany large acceleration forces are interference with circulation, impedance of respiration, and movement/deformation of internal organs. For humans, the most

3

dangerous type of stress is the $-G_z$ (footward acceleration) where the blood is forced away from the brain toward the feet. The body is most resistant to $+G_x$ forces (forward acceleration), thus suggesting that the ACRV crew members should be positioned so that the major component of the entry and landing G-forces act through the $+G_x$ axis (See Figure 1).

Although a healthy crewmember can withstand large accelerations, high G-forces can result in severe consequences for an injured or ill crewmember. Some illnesses will be too severe for ACRV transportation because of this fact. Some examples are acute heart attacks/angina, untreated pneumothorax, and acute anemia. In these cases, treatment of the injured crewmember in the Health Maintenance Facility (HMF) on the space station would be safer than the risk of return in the ACRV (unless the station itself experiences a catastrophic emergency). Illnesses that would allow for a return on a high G vehicle (8 to 11 G_x) are acute psychotic reactions, kidney stones, and some burns, however, at these levels there is still some risk of symptoms such as: decrease in hemoglobin saturation and effects on cardiovascular and other body systems under high G force.

Rotational acceleration, such as in spin stabilization, if used, may be harmful to crew members in an ACRV. Although healthy crew members may withstand ~~small~~ low spin rates, it is likely that they can still experience nausea, vomiting, and disorientation. Injured crew members would almost always be unable to withstand spin rates of more than a few RPM. Another consideration is the fact that only one or two crew members will be located near the axis of rotation. Crew members farther from the spin axis will experience significantly larger rotational accelerations. ~~So,~~ Consequently, spin stabilization is not recommended during re-entry in the case of a medical emergency.

Tolerance to impact acceleration (landing) in the $+G_x$ direction is fairly high if the force is a short or impulsive force. For extremely brief periods (0.2 sec), humans can tolerate 20 G_x and this tolerance is higher if the person is restrained properly. The limits for maximum impact G's and impulse were given above in the design specification section. As ~~seen~~ indicated, a 15 G impact acceleration with a 3 G-sec impulse is the restriction for a healthy individual, while an injured person is allowed to encounter 10 G's over a 2 G-sec impulse. These requirements

4

show the need for additional protection for the injured person, such as an impact attenuating (shock absorbing) mechanism for the stretcher.

Physiological Effects

Upon returning to Earth's gravity after staying in a microgravity environment for extended periods of time, the human body is subject to three basic changes: (1) orthostatic intolerance due to cardiovascular or fluid/electrolyte changes, (2) neurovestibular changes, and (3) musculoskeletal changes. These processes are important in considering the overall ACRV scenario because even if a "healthy" crew returns to earth from the space station, he/she may be physically unable to perform actions which may be necessary during the rescue procedure.[5]

During decreases in atmospheric pressure, an existing air embolism in the body can change in size and further aggravate the patient's condition. The embolism could lodge in any organ of the body, producing a loss of blood flow to that organ. Treatment for such an emergency is to place the patient in a recompression chamber. Under normal conditions, in the event of an embolism, the patient has to be transported to a chamber as soon as life support is started, usually by air transport such as a helicopter. Placed in the helicopter at one atmosphere, and raised in altitude to a lower pressure, the embolism will increase in size and usually produce more damage. Once the patient is returned to the original pressure, treatment can begin. For the ACRV, there will be an increase from vacuum to atmospheric pressure, which will constrict an existing embolism. For this reason, the danger of an embolism does not apply and a preventive system is not necessary.

STRETCHER DESIGN

Stretcher Design Evolution

Several configurations for the stretcher were considered. One design ~~involves~~ consists of a stationary base within the ACRV supplemented by a portable sub-stretcher which can be attached to the base quickly and easily. The main advantage of this configuration is that the patient can be transported quickly from the Space Station Medical Facility to the ACRV and from the ACRV to a rescue vehicle on Earth.

Another possib~~ility~~ le design that was considered is a system that includes a means of rotating the stretcher on the ACRV to accommodate the various orientations of the spacecraft upon re-entry, approach, and touchdown. From the SPRD, an injured crew member is permitted to withstand the maximum G-force (10 G) in the G_x direction (see Figure 1). This direction, called "eyeballs in", could continually be adjusted to coincide with the direction of maximum force experienced. This system could rotate the patient about all three axes. Although it has some advantages, the size and weight of such a system would be enormous and impractical for the ACRV.

Another possibility involves a reduction in the number of rotational axes to two. The ACRV will perform re-entry in a specified attitude, and the rotation about the third axis will not be necessary. This system consists of the stretcher mounted on a set of four vertical tracks which extend from the floor of the ACRV to the ceiling, where a top hatch will allow for easy removal from the vehicle. One feature of this design is its capacity to include two stretchers on the same set of tracks. Each of these stretchers will enable the victim to be rotated about the head-to-toe axis and the waist axis (which extends from the right side to the left side of the victim's waist). This idea was abandoned because of the inability to support and dampen the stretcher(s) and the instability that will accompany a track system. This system is also too massive to be used on the ACRV.

The possibility of using a pressure suit was also considered. This suit would be similiar to the ones used for the Apollo mission. The suit would be like a sleeping bag, to fit any size patient. It would be able

6

to hold the pressure inside at a constant value or adjust slowly if there was a fluctuation in outside pressure. The suit would be temperature-controlled which could assist the treatment of shock. Oxygen could be admitted into the unit for total oxygenation treatment of the patient. The unit could be used for isolation of the patient in a hazardous material accident or radiation emergency. The purpose of the suit is not to cure the patient, but to maintain patient status and prevent any further injury. The development of such an isolation unit would involve many sub-systems, such as environmental and pressurization control, and would be fairly bulky and cumbersome. Limited environmental control will already be a feature of the ACRV (shirt-sleeve conditions), so the suit does not offer a significant advantage. Something simpler needed to be examined.

The floor-based design is the best option for the ACRV because of its relative simplicity, adaptability and space optimization potential (see Figure 2). This configuraton ~~entails~~ *compr.sed of* a base stretcher that is permanently attached to the ACRV, which houses the necessary life-support equipment and damping systems. A detachable sub-stretcher will be used to immobilize the incapacitated crew during the entire transport period, from the HMF on the *Space Station* to a medical facility on Earth.

Sub-Stretcher

The design chosen for optimal performance and mission completion is the floor-based configuration with the portable sub-stretcher (see Figure 3). This sub-stretcher first consisted of a modified Stokes stretcher because of its light weight and durability. A better device, though, is a commercially available product called a vacuum splint (see Figure 4). This is basically a bag filled with flexible beads and air. The patient would be immobilized in the vacuum splint for the entire trip. The splint is wrapped around the victim and is conformed to the shape of the body. Openings for monitoring equipment leads and IV tubing will not reduce the effectiveness of this device as an immobilizer. When the patient is positioned properly on the splint, the air is evacuated, conforming the airtight shell to the shape of the body. The

7

beads are forced together to form a "cast" hard matrix. The specific vacuum splint researched, called Evac-U-Splint, is also able to withstand extreme temperature fluctuations. It is fully washable and can be sterilized, making it a viable component of the reusable ACRV.[6] It is recommeded that a larger more durable version of this type splint be used, and that it be equipped with reinforced clamps and straps for turbulent re-entry and landing.

After the patient is immobilized in the vacuum splint and transported to the ACRV, he/she will be restrained to the base section of the stretcher.

Restraints

There are many methods of securing the sub-stretcher to the base. Several different types of restraint were considered. Some are conceptual ideas and others are based on modern restraining devices. One method of restraint is the use of adjustable straps. Several straps could be attached and located at various positions along the body, depending on the type of injury. On an ambulance, stretcher straps are usually located at the chest, abdomen, upper thighs, and lower legs. The straps will be padded to lessen the possibility of aggravating the patient's condition. They will be held tight by buckles, clips, or velcro. The latter is preferable because of its ease of attachment and detachment.

A net of thick stretchable blanket is ~~one~~ *another* possible restraining device. This net ~~will~~ *could* be stretched over the entire body and be connected to the base of the stretcher. A foam pad could be placed in between the victim and the blanket to further secure the patient and allow for some cushioning during turbulent periods. This blanket will be easily removable if emergency medical attention is required during transport. Velcro or a zipper will accomplish this task.

Any combination of the above methods could be used to secure the patient. Figure 5 shows some examples. Figure 5-A shows straps only being used to secure the patient. Figure 5-B illustrates the use of the blanket and Figure 5-C shows straps used in conjunction with the foam blanket to further insure the immobilization of the injured crew

8

member. The sub-stretcher will be connected to the base using three to five straps. These will be adjustable allowing for tightening or loosening when desired, similar to a seat belt in a car. The base stretcher will have heavy-duty links positioned along the edges to attach the straps.

Base Section

The base section of the stretcher is a permanent fixture on the ACRV and will have several functions (see Figure 6). These include, a *acting as* shock absorber for the patient, a cabinet for life support and emergency equipment, and a storage area for first aid supplies (bandages, tape, drugs, etc.). The top surface of the base will be recessed to accept the portable stretcher. Foam padding approximately an inch thick will provide some additional cushioning. When in place, the appropriate restraining device will be applied to secure the sub-stretcher to the base.

Shock Absorption

The SPRD specifies an impact acceleration tolerance for healthy crew members of 15 G and 10 G for injured crew members. This requires a device or system to reduce the acceleration experienced by the patient from 15 to 10 G or less. To perform this function a damping system was considered, either an of energy absorption mechanism, or spring-damping system.

A crushable honeycombed material was examined as a means of energy absorption. This is a network of homogeneous cellular blocks or pads constructed of various material such as aluminum, paper, or high strength plastic laminates (like fiberglass or polyurethane). This material could be placed under the base section of the stretcher either in a layer or in "pods" at each corner. The honeycomb would have to be constructed to deform only under impact loads, not during re-entry, and to function at different weights, *of the occupants.* The weight differential could be solved by using two different types of materials or different cell sizes. Nevertheless, crushable materials were abandoned as a means of

9

shock absorption, because of the difficulty in developing an effective model. The analysis necessary to determine a relationship between average crushing stresses and specific energies for various materials to maximum impact G's and impulse limits, proved to be too complex and required too many assumptions. Additionally, a honeycomb structure would be usable only once, requiring replacement after each use. Instead, the base stretcher was modeled as a spring-mass damping system.

The stretcher, including the sub-stretcher and crewmember, was modeled as a single mass. A spring-damper combination was connected in parallel to the single mass. Three restrictions were set on the model: (1) insure the maximum acceleration experienced is less than 10 G's, (2) the impulse is less than 2 G-sec, and (3) the displacement of the stretcher is no more than .5 meters. This stroke length was considered reasonable when compared to the 1 meter displacement used for Apollo. The general equation for the motion of this type of system for an applied *step function* ~~impulse~~ is:

$$x(t) = e^{-\sigma t}[A \cos(w_d t) + B \sin(w_d t)] + f/k \qquad (1)$$

where,

σ = damping factor = $c/2m$

w_d = damping frequency

f = impulse loading

k = spring constant

t = time

The impulse load is the maximum loading that could be experienced by the mass, which is 15 G's. The damping frequency and factor are determined from the mass, m, the spring constant, k, and the damping constant, c. The constants A and B are determined from the boundary conditions on the system. A computer program was developed to determine what values of k and c complied with the above specifications. The derivation of the equations used in the computer programs is shown in the Appendix along with the computer program itself. A plot was generated from the solutions of Eqn (1). This provided a region or envelope of values of k and c that might be used in a spring-damper combination that would

10

satisfy the conditions above. This was done for two different cases of the mass, 100 kg and 150 kg. It was assumed that the stretcher itself and equipment would be approximately 50 kg, and a possible "mass" range of injured members from 50 kg (110 lb) to 100 kg (220 lb). Another assumption was that the initial velocity of the mass (stretcher) was 7.62 m/s (25 ft/s) at impact, which is a conservative estimate. The results are shown in Figures 7 & 8. By noting where the graphs overlap, an acceptable region of values will be found. These values can then be used to select shock absorbers already developed commercially.

Storage

A secondary function of the base section is housing the medical equipment components and first aid supplies (Figure 9). These items are discussed in the "Medical Concerns" section of this report. Life support equipment will be located in the base to provide proximity to both the patient and the attending crew members. The lead wires for the heart monitor and pacemaker along with the respirator line and mask will pass from the components at the side to the top surface as needed. If possible, all such lines should be on spring loaded reels to avoid unnecessary slack and tangling.

The first aid supplies and drugs will also be stored below the patient in the base. During re-entry and landing, movement will be severely restricted among the crew, so these items must be readily available.

MEDICAL EQUIPMENT

A list of medical equipment considered is provided below. The different types of equipment are described. In some cases, components are excluded from the ACRV design; to minimize weight, only essential units will be included. Recommendations for improvement or adaptation to microgravity are also provided.

11

Life-Support Equipment

Oxygen Administration Equipment

An approved administration unit should be installed. The regulator should be easy to connect. The flowmeter should have a calibrated gauge or dial with range of 0 to 15 Liters per minute (LPM) in calibrated increments. The devices should maintain accurate readings and calibrations under all operations and should be unaffected by temperature conditions. The prevention of oxygen leakage into the cabin should be a concern during any operation. Provisions for rapid transfer to ground unit administration equipment should also be considered.

Airway Protection Equipment

Airway adjuncts for patients experiencing respiratory difficulty or airway obstruction will be needed onboard the craft. The following equipment will be necessary for assuring a patient airway. About half a dozen disposable endothracheal tubes, with the laryngoscope and blades, would help with the insertion of tubes, be lightweight and be easy to store. A lighted stylet is suggested for easier insertion of the endotracheal tube. Magill forceps for removal of obstructions should be included with the intubation kit. A method for securing the tube in place after insertion and during movement of the patient or during reentry is necessary.

Some type of ventilator is needed to provide respiratory support for the intubated patient. The unit could be electrical or powered by compressed gases. The unit will have to be adjustable to provide total ventilation support for normal respirations and hyperventilation. Since respiratory support has to be maintained throughout transport, the unit will have to be totally automatic, because the attendant will not be able to operate the unit during re-entry.

Equipment will be necessary to provide supplemental oxygenation of the patient at low LPM, without intubation, but consideration of higher concentrations of oxygen in the cabin of the vehicle should be included due

12

to potential fire risk. Some type of mask that would re-cycle the expired air is a consideration.

Suction Equipment

Suction of airway obstructions or fluids which could block the air passage is needed prior to and/or during re-entry. Obstructions can be removed with a hand operated unit that is commercially available (see Figure 10). Fluids that require continuous suction, such as through a nasogastric tube, would require constant maintenance by an electrical or gas powered unit. The whistle tip and tonsil tip suction catheter, along with a supply of nasogastric tubes should be available. The system should provide a free flow of air of at least 20 LPM and achieve a minimum of 300 mm Hg (11.811 inches) vacuum within four seconds after the suction tube is clamped closed. A vacuum control and a shutoff valve, or combination thereof, should be provided to adjust vacuum levels, and to discontinue aspiration instantly.

Heart Monitor

The assessment of the cardiac muscle is necessary before, during and after re-entry. Equipment would include electrocardiographic monitor/defibrillator/pacemaker (see Figure 11). A three lead ECG monitor will operate through three common chest leads. The defibrillator/pacemaker will operate through a chest and back lead. The entire unit will have to be able to interpret the ECG, provide automatic defibrillation or synchronized cardiovertion, or pacing of the cardiac muscle if necessary. The unit should be capable of working independently, or being remotely controlled from Earth, or manually controlled by an attendant within the vehicle. Recording and storage of all information of the unit's operations throughout treatment would be useful. The unit should operate through a power source such as battery during flight. Lithium batteries may provide meet the these requirements of long shelf-life without loss of power.

13

Blood Pressure and Pulse Rate Equipment

Blood pressure and pulse rate are important vital signs for any ill patient. The pressure and rate can be obtained through the same equipment. A blood pressure cuff can be inflated with any substance as long as it is correctly calibrated to read in mm of mercury. The pulse can be obtained through a lead in the cuff. This system should be self-sufficient and require little maintenance.

Fluid Infusion Devices

The standard intravenous catheters, tubing and bags would need to be revised for use in zero gravity conditions. Present day administration of drugs is introduced via needles to the IV tube through a thin rubber "y" injection site. The problem lies in the difficulty of fitting the needle into the small aperture provided. Instead, a lurelock configuration should be used. A lurelock is a syringe without a needle that has serrated edges that allow the syringe to be locked into an adaptor on the IV tubing. A valve on this adaptor would prevent flow into the syringe and a cap would be used to keep the tip of the syringe clean and sanitary. Since gravity cannot be used as a means of administering IV fluids, a spring-loaded IV-pusher would be used to perform the same function. The flow of the IV can be changed by the stiffness of the spring and by flow restrictors on the IV tubing. IV fluid can generally be stored at room temperatures and must be kept from excessive heat. The IV fluid is used to maintain the same volume of fluid in the body in the case of loss of blood. The fluid dilutes the existing blood. There is currently in development a blood substitute that would be capable of carrying oxygen and could be stored like IV solutions. If this product is developed in the near future, it would be a valuable tool for any medical emergency and increase the chances of survival for an injured crewmember.

14

Waste Products

A urinary catheter with temperature sensor ~~will~~ _could_ assist monitoring or perfusion of the kidney function and also monitor the core body temperature. It is not really a necessary medical component for the short amount of time the vehicle is in flight.

Drugs

The following drugs are generally used in emergency medicine. Recommended by paramedics, these drugs should be available on the ACRV. The dosages will have to be determined depending on the individual cases and circumstances.

1. albuterol
2. aminophylline
3. atropine sulfate
4. bretylium
5. dexamethasone sodium phosphate
6. diazepam
7. diphenhydramine hcl
8. dobutamine
9. dopamine
10. epinephrine hcl
11. furosemide
12. glucagon
13. **hydrocortisone sodium succinate**
14. **intravenous electrolyte solutions**
    a. **dextrose**
    b. **lactated ringer's**
    c. **sodium chloride**
15. isoproterenol hcl
16. lidocaine hcl
17. meperidine
18. metaproterenol
19. morphine sulfate

15

20. naloxone hcl

21. nitroglycerin sublingual tablets

22. procainamide

23. sodium bicarbonate

24. terbutaline

25. verapamil

Immobilization Equipment

For spinal immobilization, a vacuum splint that is large enough to encompass the entire body would provide support for the spine, yet provide for the immobilization of the body in various positions. This device also provides support on both sides of the patient. The vacuum splint can come in smaller sizes to supply extremity immobilization. The use of a traction splint is useful for the relief of pain in a femur fracture, but the extremity has to be extended straight to be used. For cervical spine immobilization, cervical collars are needed; many such items are available on the commercial market. For extremity fractures, a splint known as the "Sam" splint is very useful and practical. It is small, lightweight, waterproof, molds easily to any extremity and is functional at any temperature.

Pneumatic Anti-shock Garments

The use of Medical Anti-Shock Trousers (MAST) for this application has to be considered. The use of these anti-shock trousers (or "balloon pants") in zero gravity may not be beneficial. MASTs are inflated to displace internal body fluid of the lower extremities and abdomen into the thoracic cavity and brain for treatment of shock. Again zero gravity has to be considered; during reentry, the lower body is planned to be in a supine position. Circulation should be enhanced by the reclined position of the victim. MASTs hold the body from the waist down in a straight configuration. The MAST will also require a pump and monitoring of the pressure. The vacuum splint used as the sub-stretcher will perform the same function as MAST. For these reasons, the trousers are not part of the ACRV design.

16

Blood Monitoring

A device to check a patients blood-glucose *and* oxygen saturation would be helpful in evaluation of the patient's condition during a medical emergency; But this equipment is not necessary during the descent. It would most likely be needed onboard the space station.[8]

Modifications & Suggestions

Coming from the Space Station's medical facility, the patient will have a portable respirator and IV unit upon reaching the ACRV. "Standard IV units depend on a gravity drip and the fact that air bubbles rise to the top--neither of which happens in microgravity. To meet this challenge, a positive pressure IV pump has been developed, along with an air/fluid separator, both of which have been tested in short zero-gravity sessions aboard NASA's KC-135 jet."[9] If these devices are proven reliable, their implementation is suggested. If not, a newly-marketed "IV-Push Pressure Infusor" can be used. This spring-driven unit delivers a constant pressure on the bag, simulating the pressure of gravity which would be created if the bag were one meter above the patient. "The IV-Push may rest on the cot between the patient's feet or be strapped to the patient, thus reducing set-up time and making the patient extremely mobile, even in air evacuation."[10]

The information from the monitoring equipment (respiration rate, pulse rate, and blood pressure) will be sent by telemetry to the on-duty physician at Johnson Space Center. In addition, it is suggested that at least two crew members should be trained to a level of Emergency Medical Technician, Class II (This would require approximately 250 hours of training). They will be sufficiently trained in the administration of oxygen and drugs. They can also observe auxiliary signs. These include pupil dilation and capillary refill, which involves pinching an extremity and measuring the time it takes for blood to return. Their observations can also be sent to Johnson Space Center via telemetry, and the NASA M.D. can advise treatment accordingly.

Changes to the supplemental oxygen supply mechanism may be necessary. The ACRV cabin atmosphere will be similar to that of the Earth in composition, but the supplemental supply may be pure oxygen. In the event of leakage from nasal prongs or standard medical oxygen masks, fire could result from the presence of the extra oxygen. A tightly fitting aviation mask is the solution to this problem, because it will prevent the oxygen from contaminating the cabin atmosphere.[11]

For the purpose of safe transport back to Earth, paramedics stress trauma-prevention. All of this equipment serves to treat causes and symptoms of trauma. It is assumed that the patient will be stable before transport. The equipment chosen will sustain a patient's condition until proper medical attention can be applied on Earth. Although extra medical training is recommended for a number of crew members, the equipment will be easy to operate, to allow for a deconditioned crew.

After the patient is attached to the base section of the stretcher, he/she can be "hooked up" to any of the life support components as needed. The following units will be stored below the patient in the base section and will be available if necessary: Pacemaker/Heart Monitor(ECG)/ Defibrillator, Respirator, Oxygen Supply (6 hrs.), and Aspirator (Suction Unit). NASA has compact versions of most of these components in a portable pack aboard the Space Shuttle, all of which are battery-powered.

Battery power is listed as a requirement in <u>Considerations for Medical Transport from Space Station</u>.[12] To constantly remain charged, conventional batteries will have to be stored on the space station, preferably near the ACRV entrance. The medical equipment will be stored on the ACRV in the base section of the stretcher. The use of lithium batteries could be a practical cure to the problem of maintaining battery charge. Lithium batteries are sealed when manufactured and they remain fully charged for extended periods of time. When the ACRV has to be used, the seals to the lithium batteries can be broken to provide full power.

18

VEHICLE CONFIGURATION

Shape Determination

The physical shape of the ACRV is obviously the most critical factor in determining G-force magnitude. Three cases are discussed: a lifting body which imparts 1-2 G's, an Apollo type vehicle (semi-ballistic) which induces 3-4 G's, and a ballistic vehicle such as GE's Moses which produces from 8-12 G's accelerations during re-entry. Restrictions given by the SPRD for the ACRV allow only 4 G's in +X direction, 1 G in the +Y direction and .5 G's in the +Z direction. These specifications narrow the field of the selection for the appropriate vehicle between the lifting body and the semi-ballistic configuration. Figure 12 shows the G's incurred during re-entry for various shaped vehicles versus the lift to drag (L/D) ratio of each. This graph further emphasizes the need for a vehicle with an L/D of 0.5 or higher to be able to meet this standard. Because of the large accelerations associated with the ballistic-type design, it is not recommended for the medical mission of the ACRV. The Apollo-type design, although not ideal for medical transport, could be an adequate configuration choice. The problem lies in the fact that this type of vehicle would not allow for patient access during flight, thus requiring that the patient's condition remain stable until landing. In the Apollo-type vehicle, the crew members, especially the injured crew members, would have to be positioned carefully to reduce the possible detrimental effects of re-entry G's. A Shock-absorbing seat/stretcher would have to be used to lessen the effects of landing impact forces.

In considering the many possible causes of medical complications which may occur during the ACRV's return to earth, the best design, from a medical standpoint, is the glider-type ACRV due to the low re-entry G-forces and impact forces. This vehicle will also make it possible for attending crew members to have access to the patient almost continuously. With either design, efficient and organized Search and Rescue (SAR) forces are needed, since readaptation to earth's gravity may limit the physical ability of the returning crew members.

19

Interior Configuration

The ACRV should be equipped with a large top hatch. In the event of a water landing, this means of egress would prevent water from entering the interior of the vehicle. In microgravity, the orientation of the hatch for ingress is not a critical factor. A top hatch is necessary, though, to create an easy method of evacuation of an immobilized crew member with a traumatic injury. The transportation to a hospital will be via helicopter because of its simplicity and speed. When transferring the patient from the ACRV to the rescue helicopter, a winch cable can simply be lowered through the top hatch, attached to the sub-stretcher after the restraints are removed, and the patient can be hoisted out.

Guide rails will be used to keep the stretcher from swaying as it is lifted out of the ACRV (see Figure 13). These will be approximately one foot in length. When not in use, these guide rails will stay flush against the ACRV ceiling, one at each of the four corners of the top hatch. During egress, a simple pivot hinge will lock the rails perpendicular to the ceiling. Their purpose is to control the immobilized patient after he/she is out of reach of the ACRV crew and prevent further injury or damage to the vehicle.

The floor-based design was judged the best option for the ACRV because of its relative simplicity and its minimal size and weight. Because the capacity to transport two injured crew members on one ACRV would be advantageous, the idea of a double-sized base stretcher with room for two sub-stretchers was introduced. It was reasoned that the costs of added weight, added size, and added complexity would be at least balanced by the increased capacity of two stretchers. Manipulation of basic shapes, such as seats and stretcher, found on the ACRV were used to generate generic floor plans for the ACRV. Floor plans were made for two possible exterior shapes, semi-ballistic and lifting body (see Figures 14 - 16). With the semi-ballistic configuration, the feasibility of two stretchers was investigated. The results suggested that one or two seats may have to be sacrificed to create the needed room. This is an unacceptable disadvantage when combined with the extra weight and complexity, so the idea was abandoned.

In the __Crew Emergency Return Vehicle Preliminary Man-Systems Study__, the 6-man domino configuration obtained the highest rating for "volumetric efficiency and overall people packing issues." It also had the best rating for ease of ingress and egress. The Johnson Engineering Corporation, contracted by NASA to perform the study, assumed the presence of a top hatch to obtain its ratings. For these reasons, the 6-man domino configuration is recommended as the layout for the ACRV, whether it be a ballistic design or the pressure vessel of a lifting body design. The 6+2 domino is similar and could be used if an eight-man capacity is necessary, but the two extra seats above the other six will inhibit evacuation considerably.[13]

CONCLUSION

The *preliminary* design of the stretcher system for the ACRV was ~~carried out~~ *completed* under several general criteria: reusability for cost-effectiveness, simplicity of design for a deconditioned crew. and the ability to comply with the specifications for an injured crew member listed in the SPRD. Investigation into modern paramedical equipment and procedures led to the final design of the stretcher. Existing devices were either improved or adapted to microgravity *conditions* before incorporation into the system.

In order to compensate for the SPRD specification differences between healthy and injured crew members, a simple computer model was developed to find a range of suitable "c" and "k" values needed to accomodate a patient range between 50 kg and 100 kg. These ranges can be used to size a set of four shock absorbers, which will reduce the impact forces to below 10 G and impulse below 2 G-sec.

Life support equipment, such as a defibrillator, heart monitor, pacemaker, suction unit, and oxygen supply will be housed directly under the patient in the base section of the stretcher to allow for easy accessibility. For the same reason, first aid supplies, such as bandages, tape, disinfectants, and the list of drugs presented in the "Medical Equipment" section of this report, will also be stored in a compartment that is close to both the patient and the attending crew member.

The vacuum splint was chosen as the sub-stretcher because of its simplicity of use and its effectiveness as an immobilizer. The splint is open down the middle area where the chest appears, so monitoring and diagnostic equipment will not be affected. When the splint is evacuated, it becomes very rigid, but it maintains a cushioning property. When combined with padding and a heavy-duty shock absorption system, the vacuum splint will keep an injured crew member safe and comfortable during transport.

Conventional restraining techniques will be used to attach the sub-stretcher to the base. These must be strong, simple to use, and quickly attachable and detachable.

22

The ACRV should have a top hatch to allow for an easy egress when Earth is reached. Search and Rescue (SAR) forces will use a helicopter to hoist the patient out of the ACRV. Guide rails attached to the interior's ceiling guide the patient through the top hatch safely. The 6 Man Domino configuration would provide for optimum evacuation capability when coupled with a top hatch.

REFERENCES

[1] Crew Emergency Return Vehicle Pamphlet, NASA.

[2] System Performance Requirements Document (SPRD), NASA, Nov 9, 1988.

[3] SPRD, p. 21.

[4] "Considerations for Medical Transport from Space Station via ACRV," NAG 9-270/1, December, 1989, p. 15.

[5] "Medical Concerns for A Crew Emergency Rescue Vehicle," P. Santy and J. Boyce, January 15, 1987.

[6] "Evac-U-Splint," Hartwell Medical Corporation, San Marcos, CA.

[7] "Recovery Systems Design Guide," Irvin Industries, Inc., December, 1978.

[8] Murray Peterson, Paramedic, Ritenour Health Center, University Park, PA.

[9] "First Aid for Freedom," R. Spangenburg and D. Moser, Ad Astra, January, 1989, p. 44.

[10] "DynaMed Emergency Care Products Catalog-1990," Carlsbad, CA, p. 144.

[11] "Considerations for Medical Transport from Space Station via ACRV," NAG 9-270/1, December, 1989.

[12] "Consideration for Medical Transport," NAG 9-270/1.

[13] Crew Emergency Return Vehicle Preliminary Man-Systems Study, Design Edge, Houston, Texas, April 15, 1988.

Other Sources

JEMS - Journal of Emergency Care & Transportation- Oct., 1989, p. 35.

"Medical Products, Inc.," Milwaukee, WI, September, 1989.

APPENDIX I

- G$_z$

- G$_y$

+ G$_x$

- G$_x$

+ G$_y$

+ G$_z$
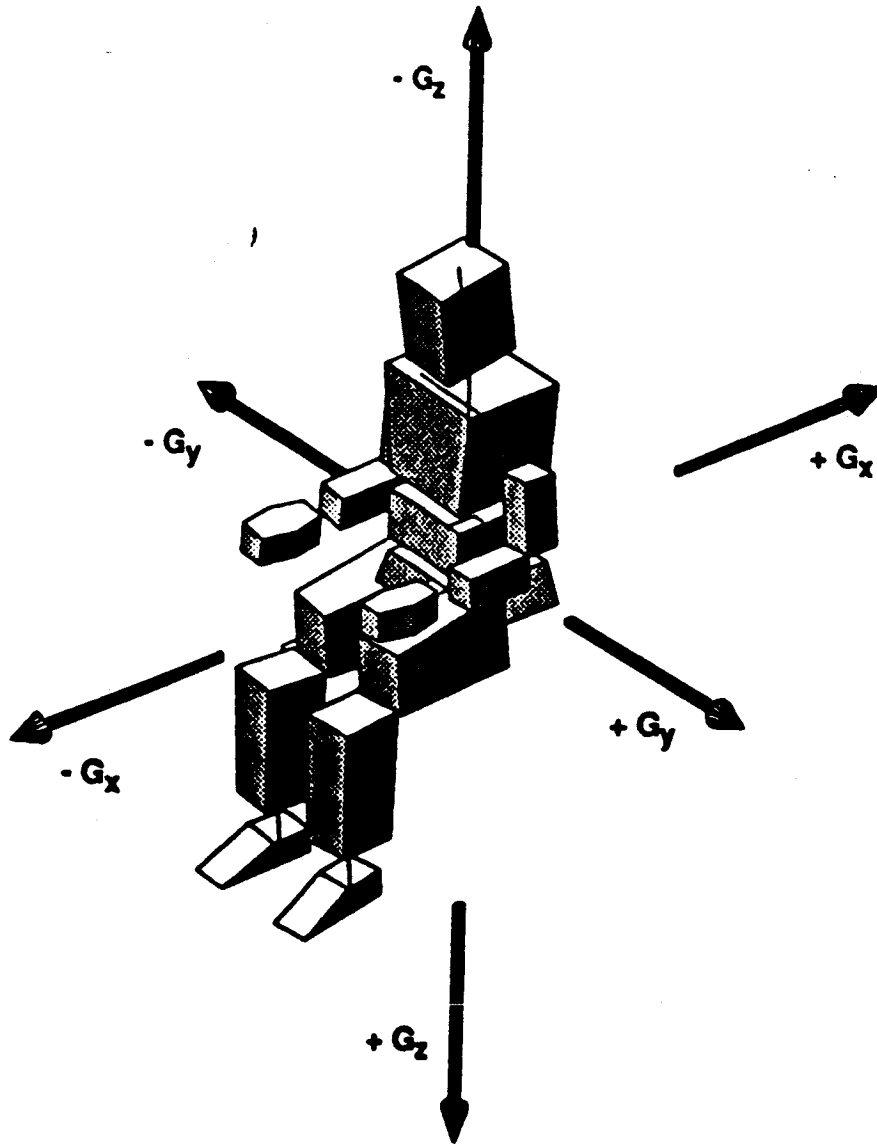
From Crew Emergency Return Vehicle Preliminary Man-Systems Study;
Design Edge, Houston, TX, p. A-2.

Figure 1: Acceleration Vector Convention

Linear Motion	Acceleration Description	Physiological Displacement
Forward	Forward Accel.	+Gx
Backward	Backward Accel.	-Gx
Upward	Headward Accel.	-Gz
Downward	Footward Accel.	+Gz
To right	R. Lateral Accel.	-Gy
To left	L. Lateral Accel.	+Gy

25
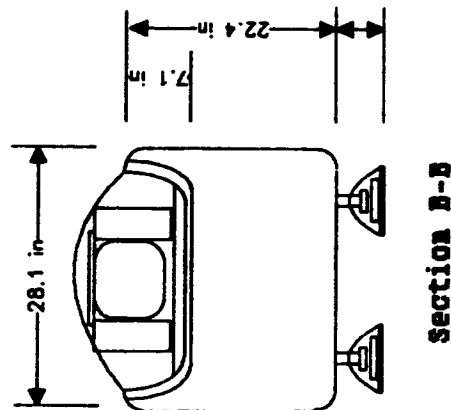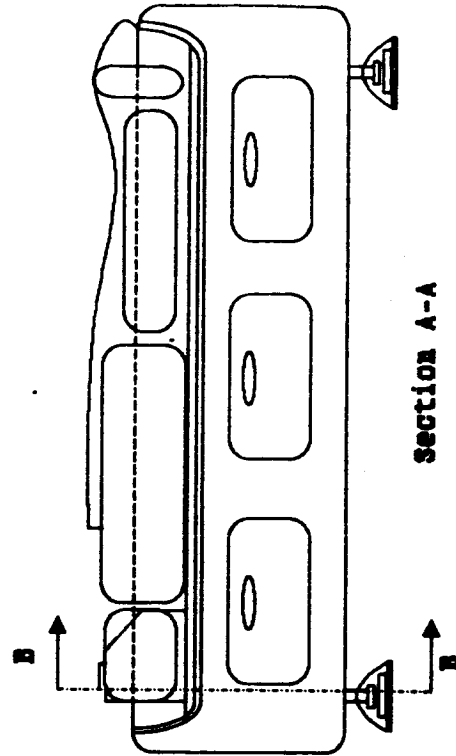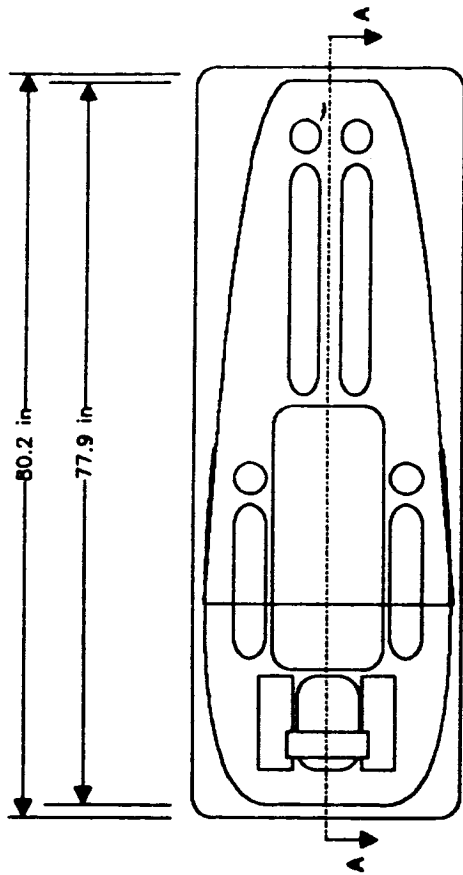
Figure 2: Entire Stretcher Configuration

80.2 in

77.9 in

Section A-A

Section B-B

22.4 in

7.1 in

28.1 in

26.7 in.

78.8 in.

7.5 in.
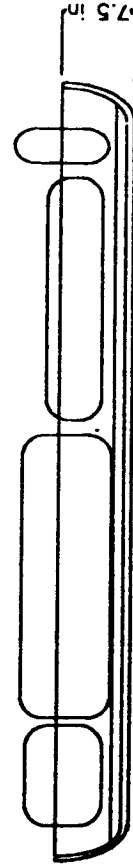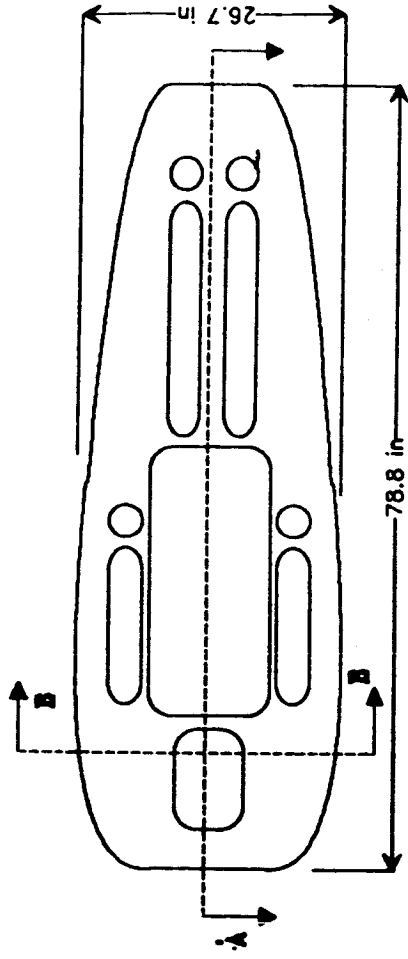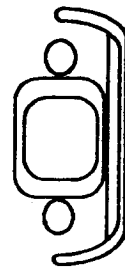
Section A-A

Section B-B

Figure 3: Sub-stretcher Configuration

27
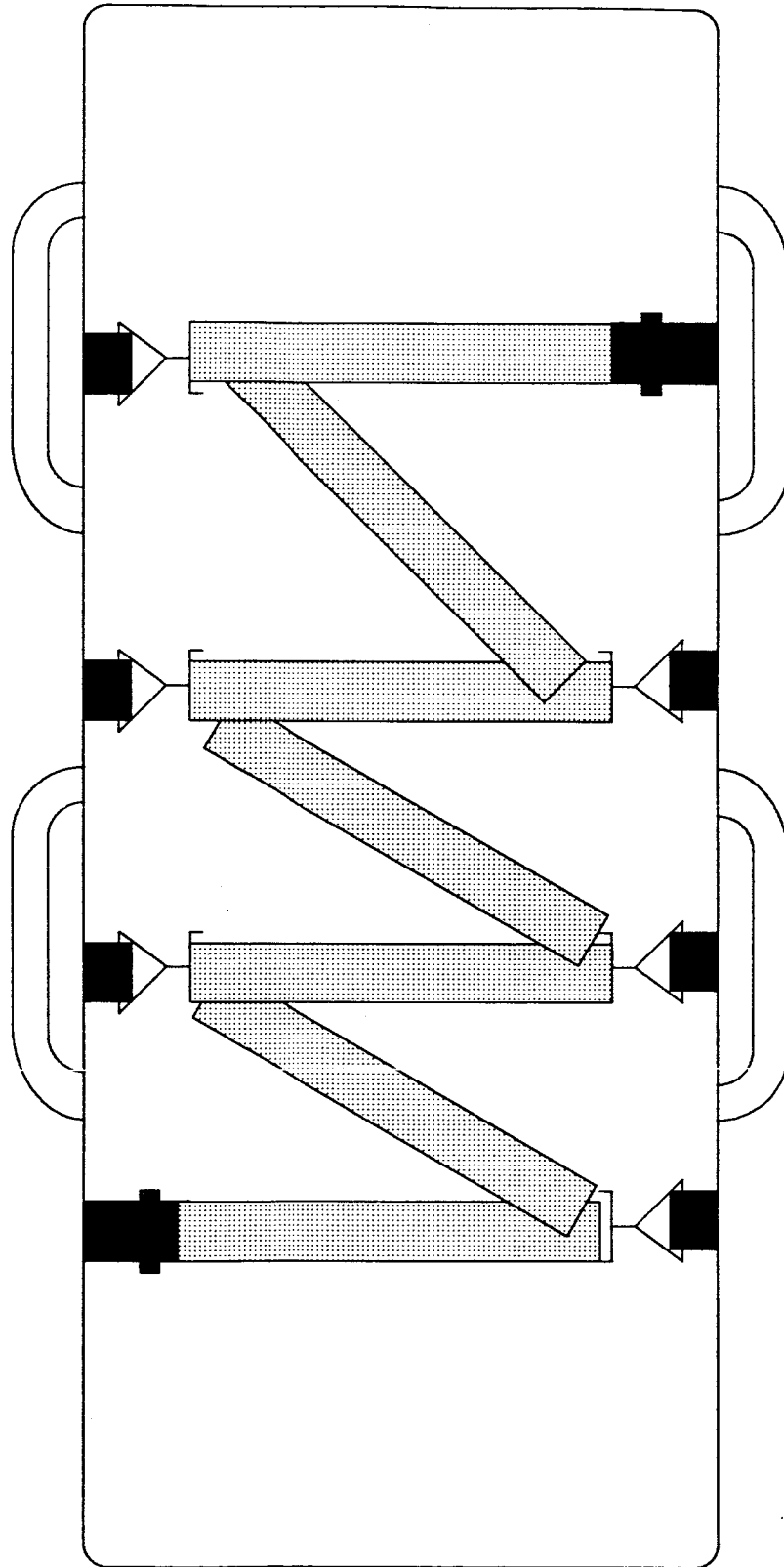
EVAC-U-SPLINT®

Figure 4: Vacuum Splint

28
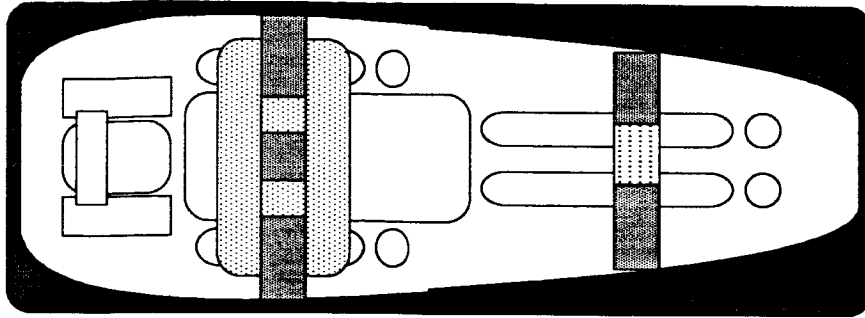
5-A
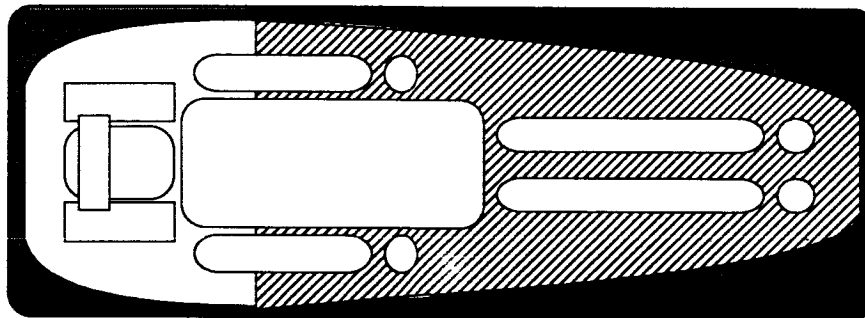
5-B
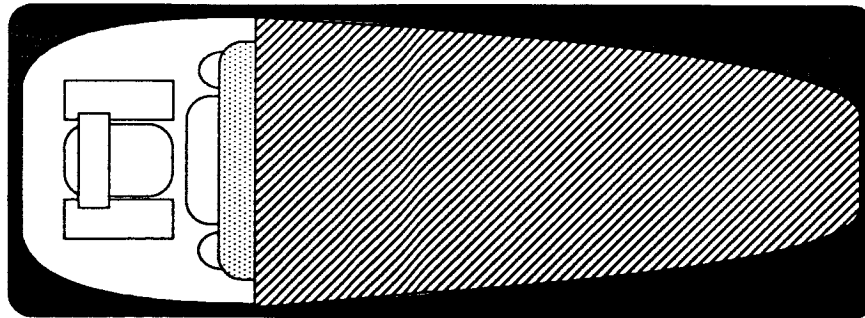
5-C

Figure 5: Restraining Devices

SUB-STRETCHER

BASE STRETCHER

STORAGE COMPARTMENT

SPRING

RUBBER DAMPER
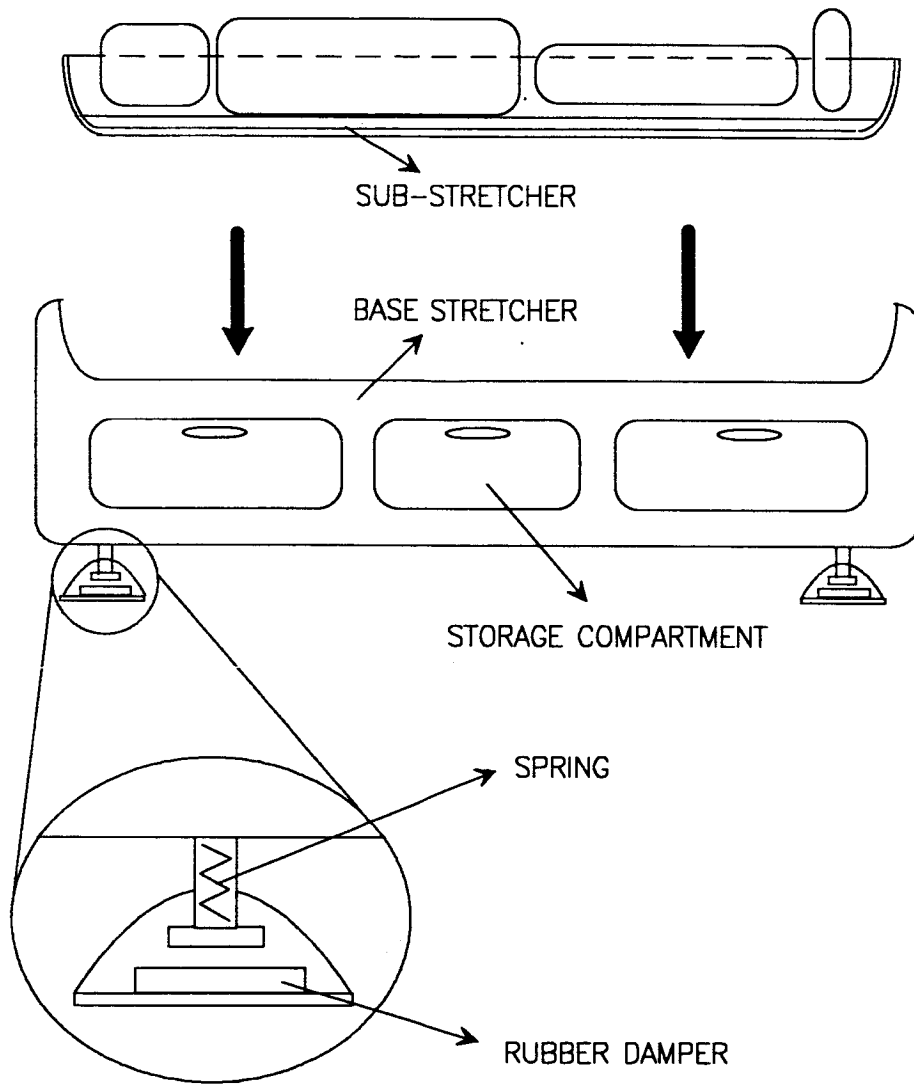
Figure 6: Base Structure

30
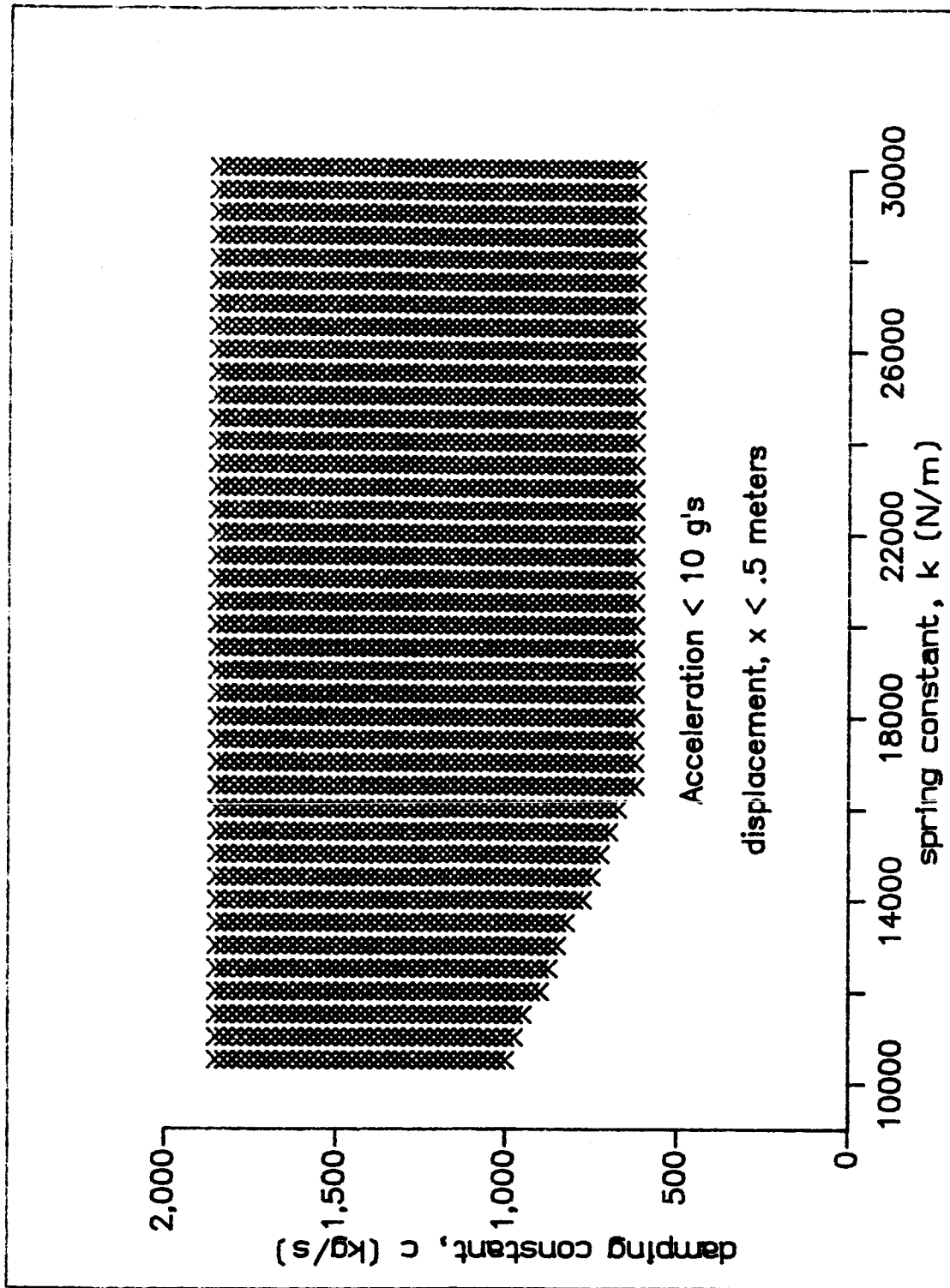
Figure 7. Spring-damper envelope for mass = 100 kg
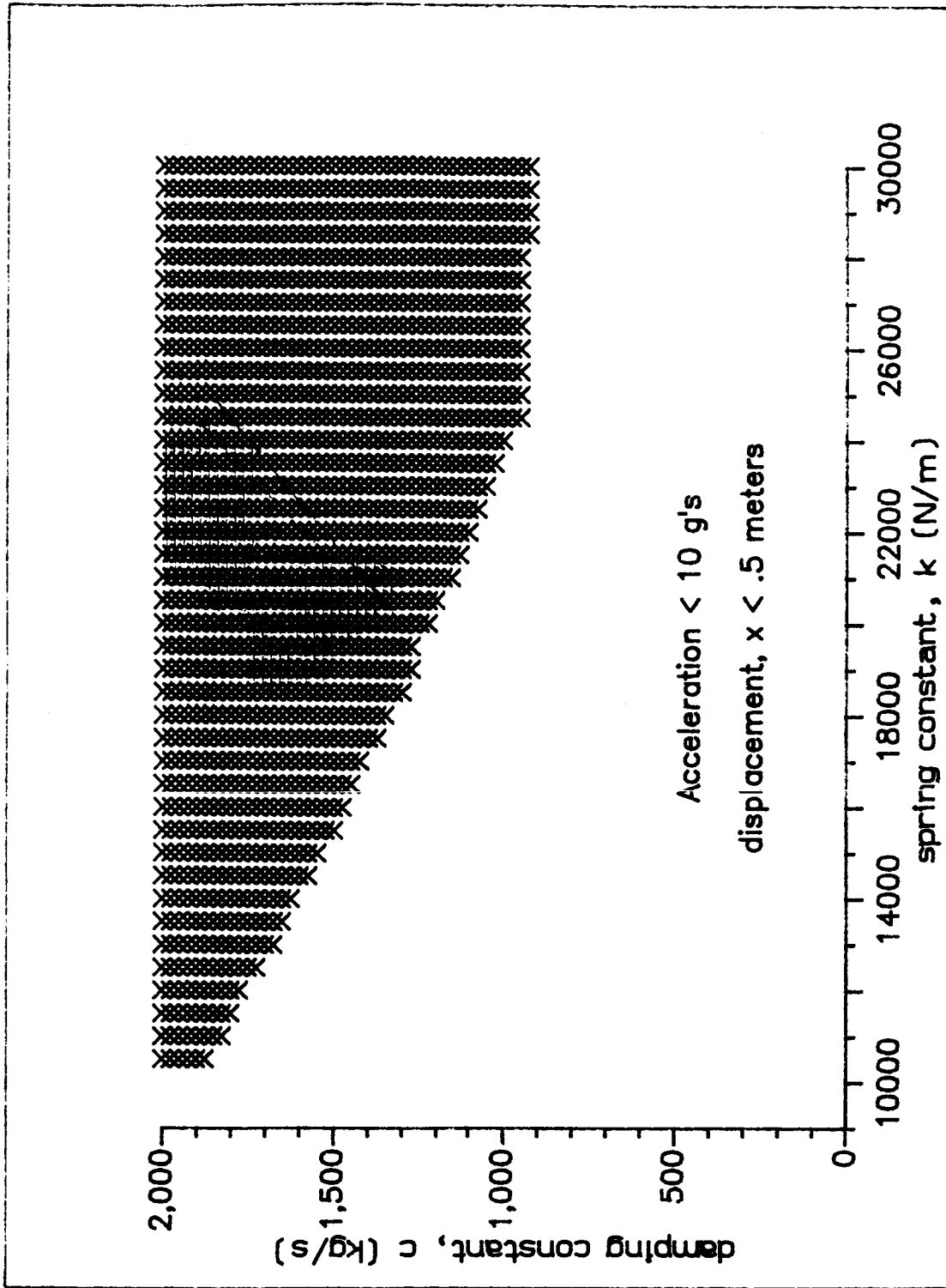
Figure 8. Spring-damper envelope for mass = 150 kg

Acceleration < 10 g's

displacement, x < .5 meters

spring constant, k (N/m)

damping constant, c (kg/s)

32

BATTERY PACK

MISCELLANEOUS EQUIPMENT

OXYGEN SUPPLY
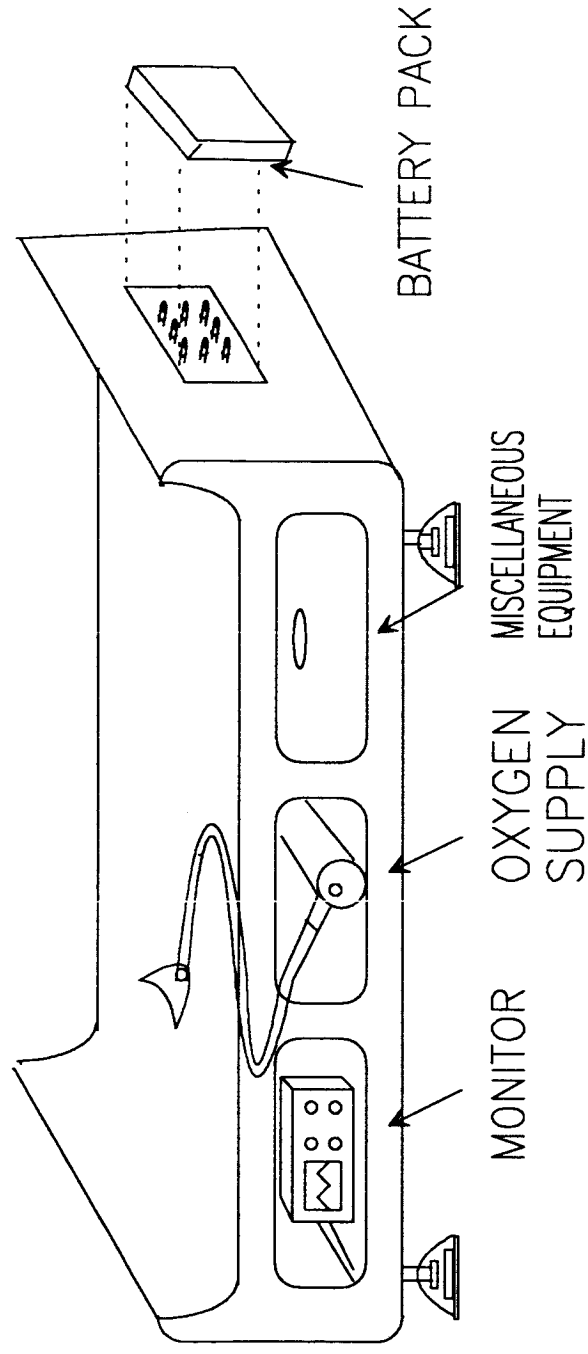
MONITOR

Figure 9: Base Stretcher Storage

33
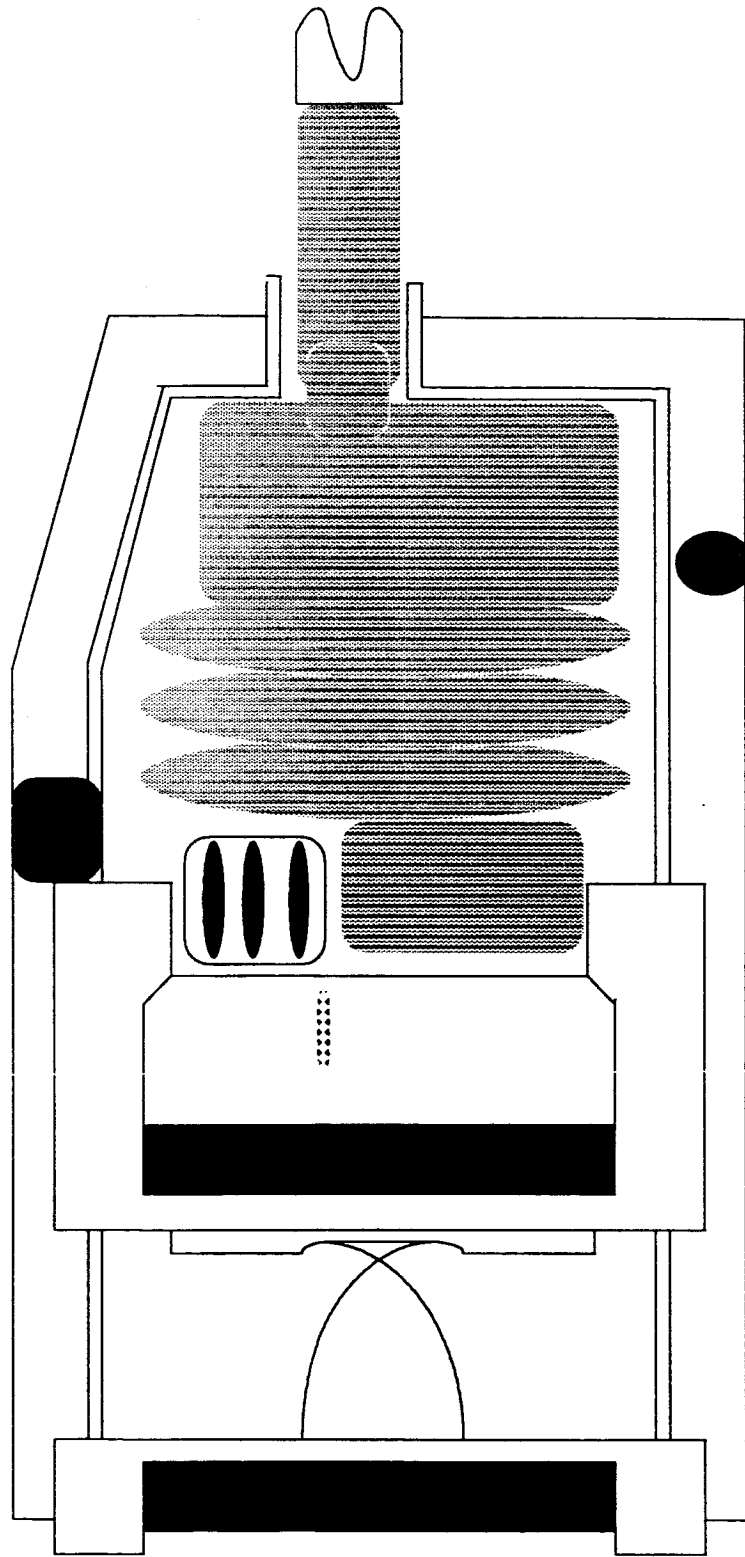
Figure 10: Hand Suction Unit

34
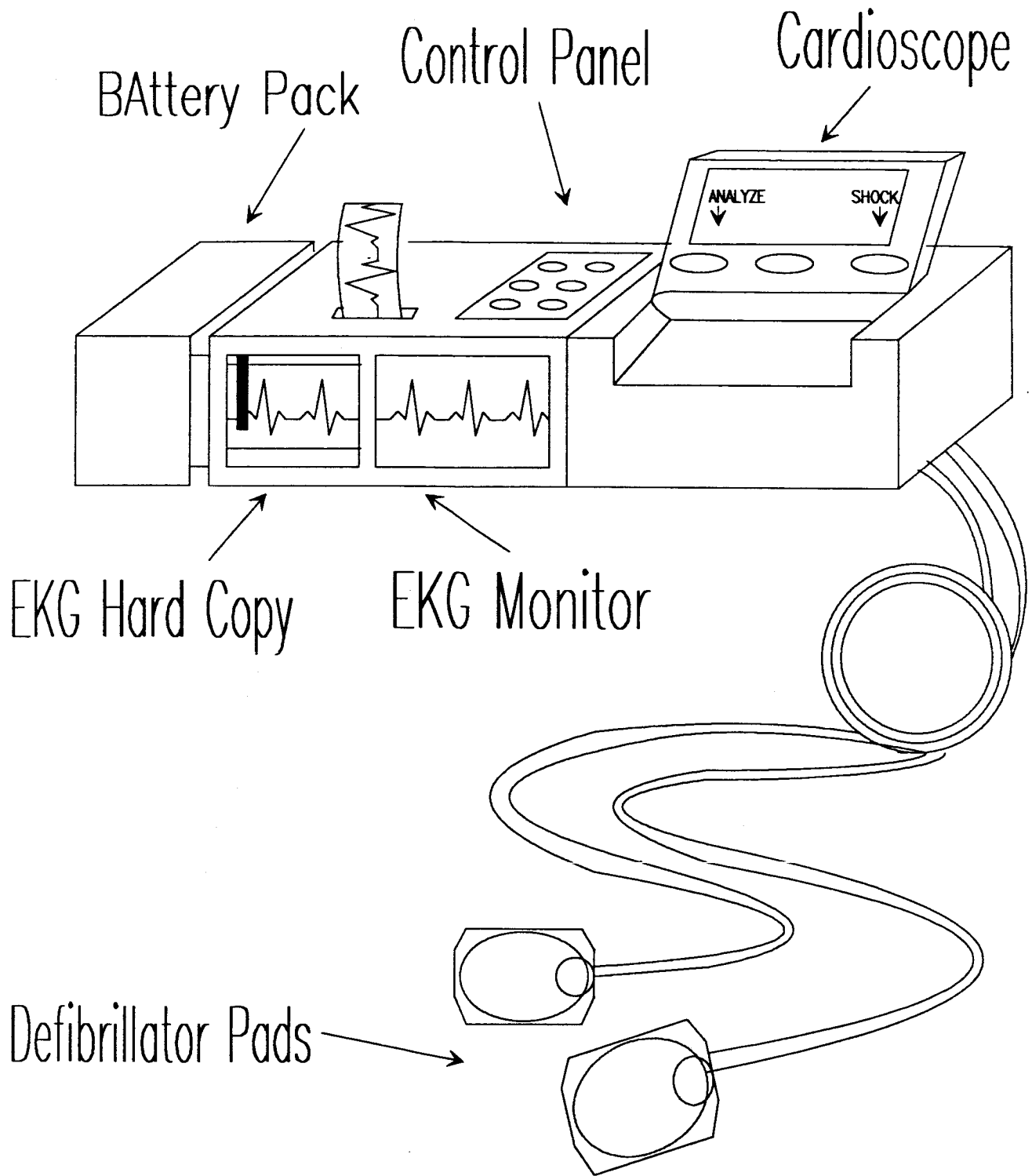
Figure 11: Monitor/Defibrillator/Pacemaker
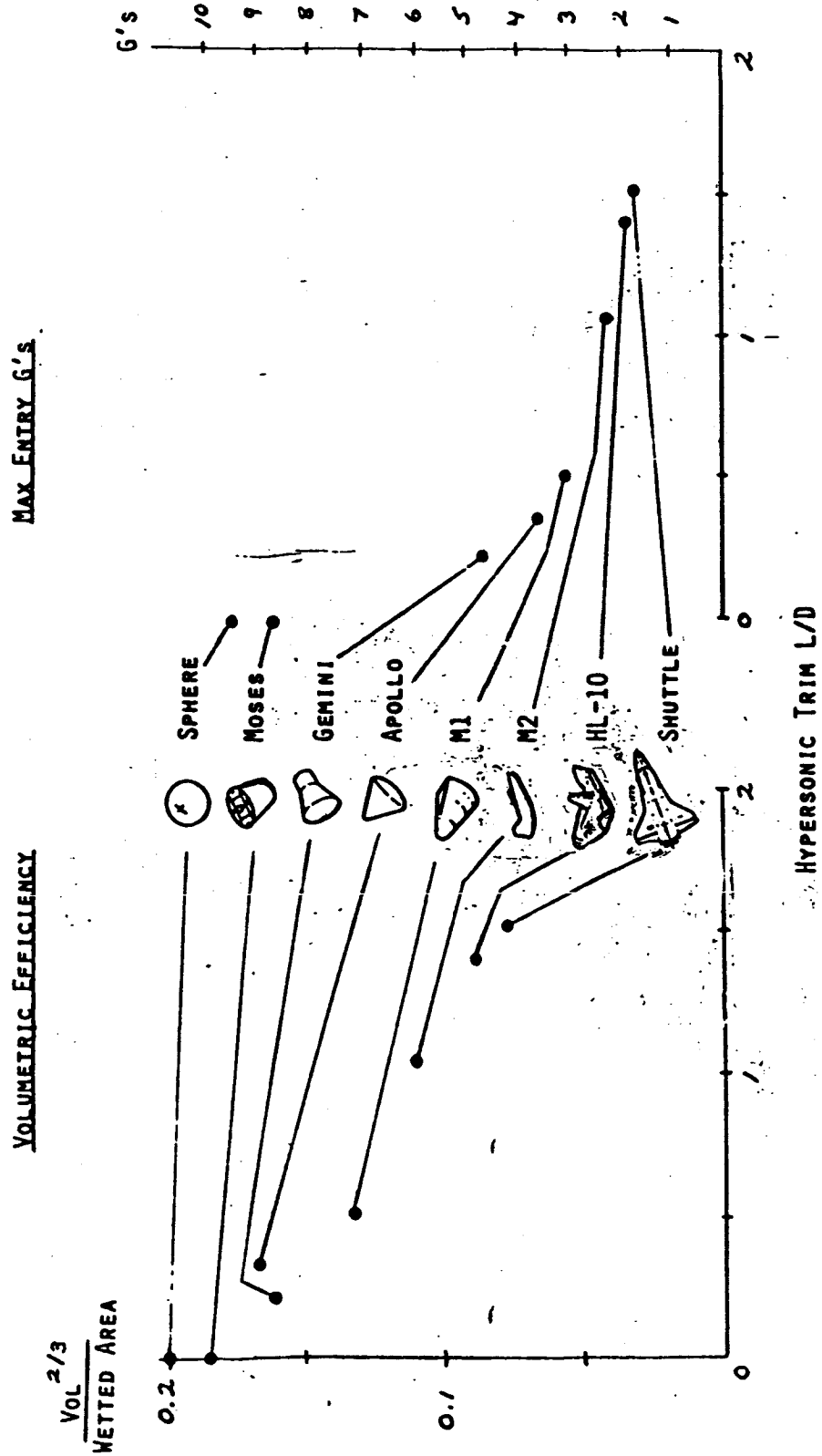
Figure 12: L/D to Re-entry G's
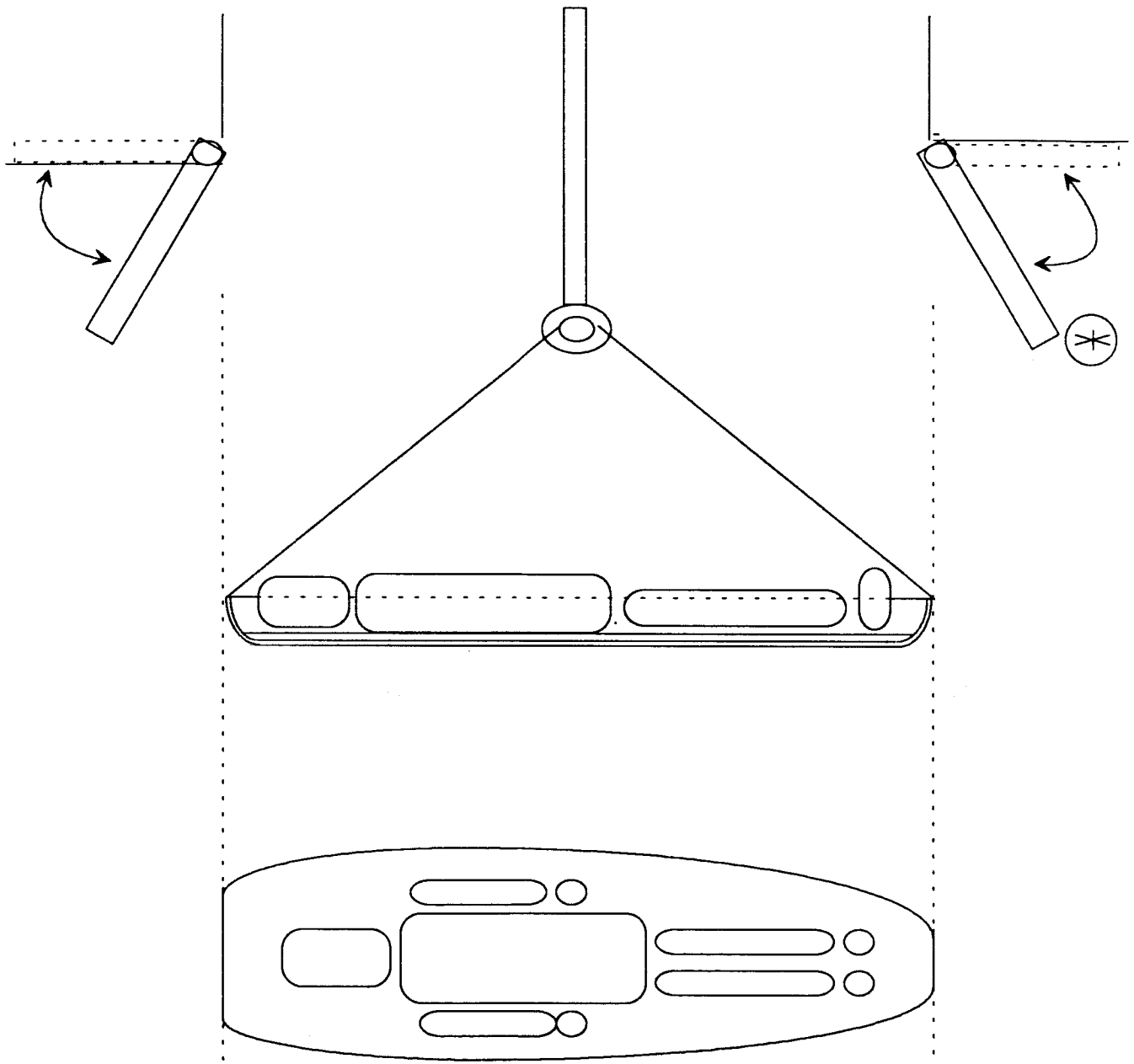
Note: Guide Rail System which is lowered from a position set into the ceiling of the ACRV to lock into place in order to help maneuver the stretcher through the hatch.

Figure 13: Guide Rails
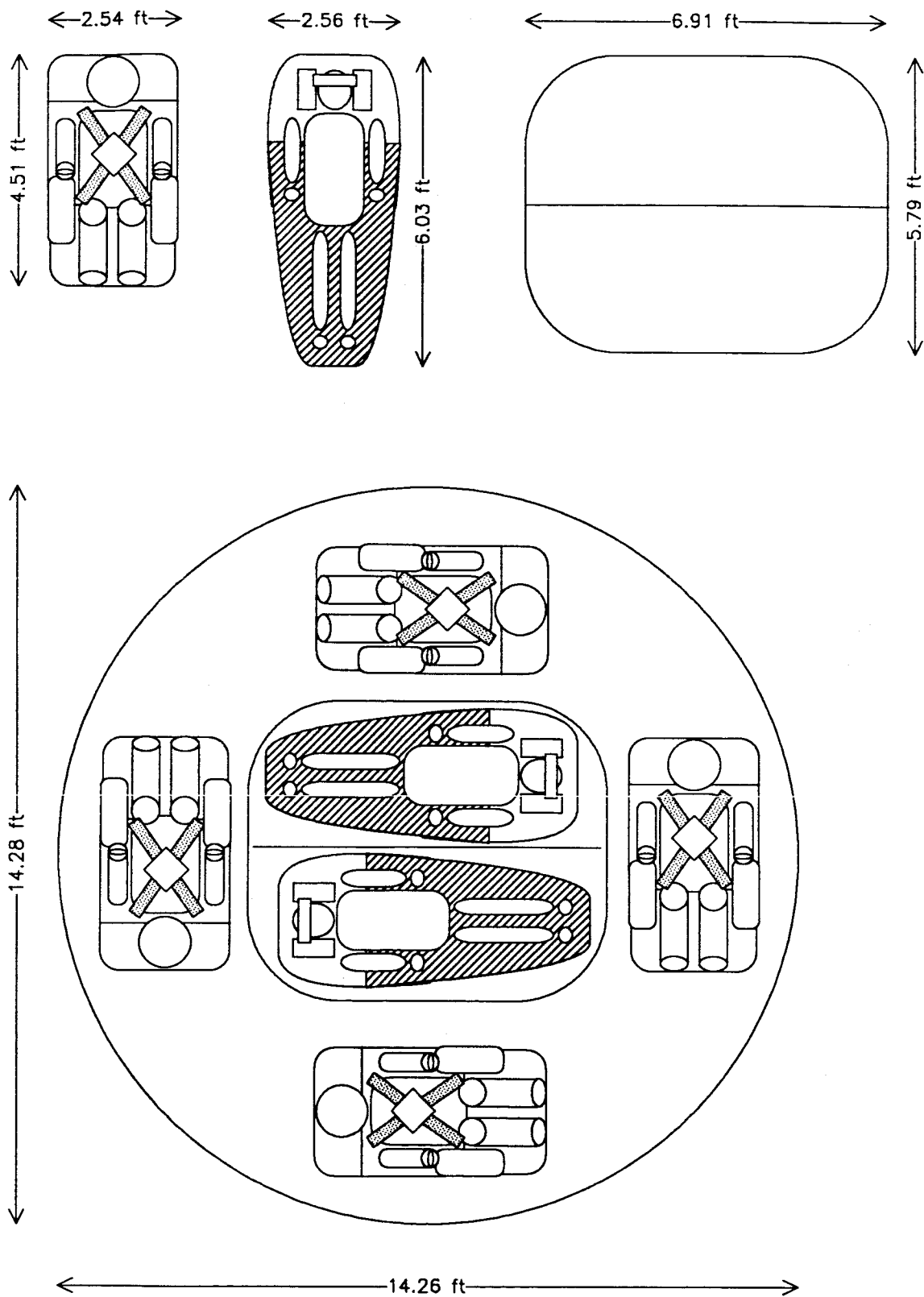
Figure 14: Semi-ballistic : View 1

14.43 ft

2.86 ft

14.44 ft
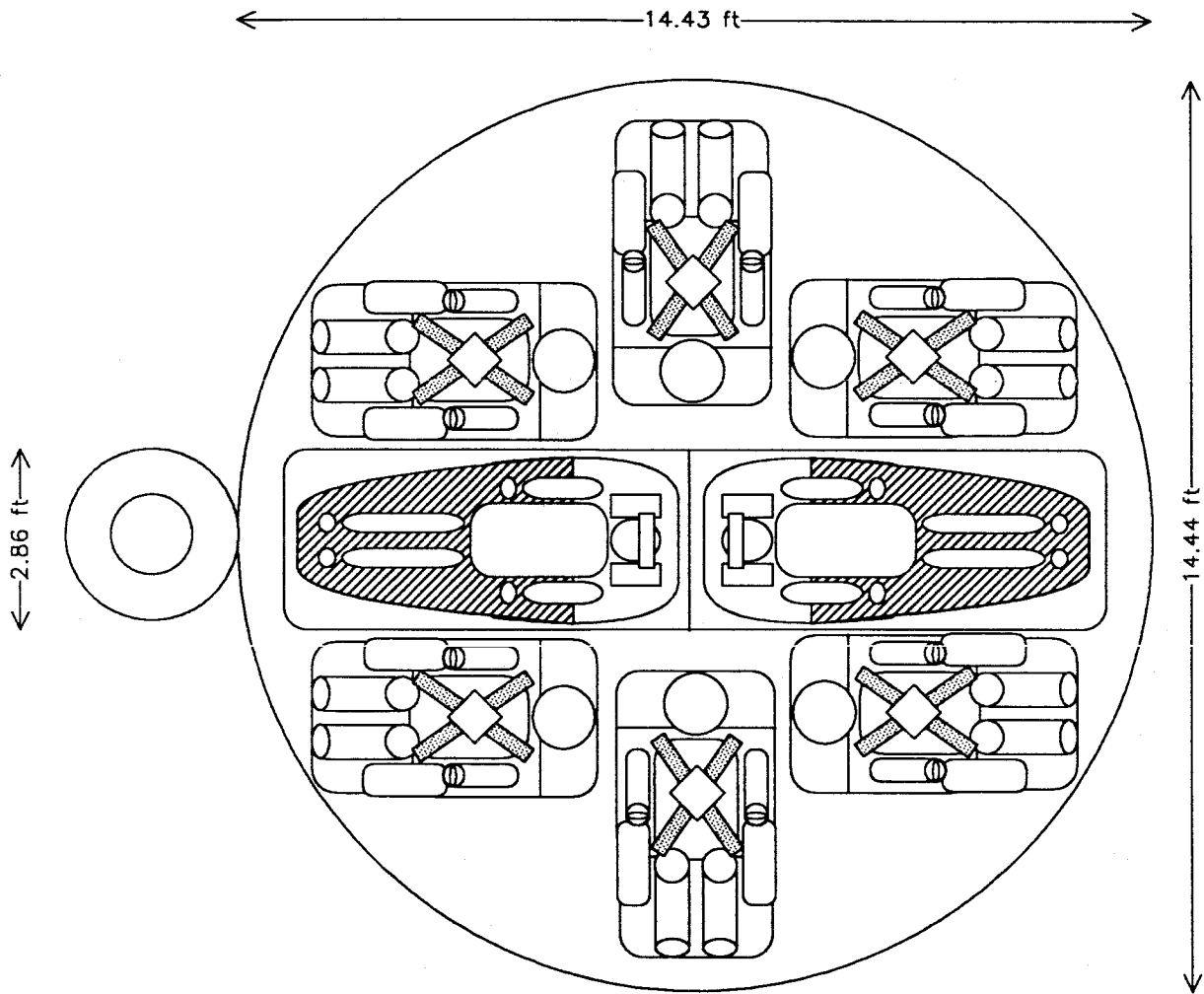
Figure 15: Semi-ballistic : View 2
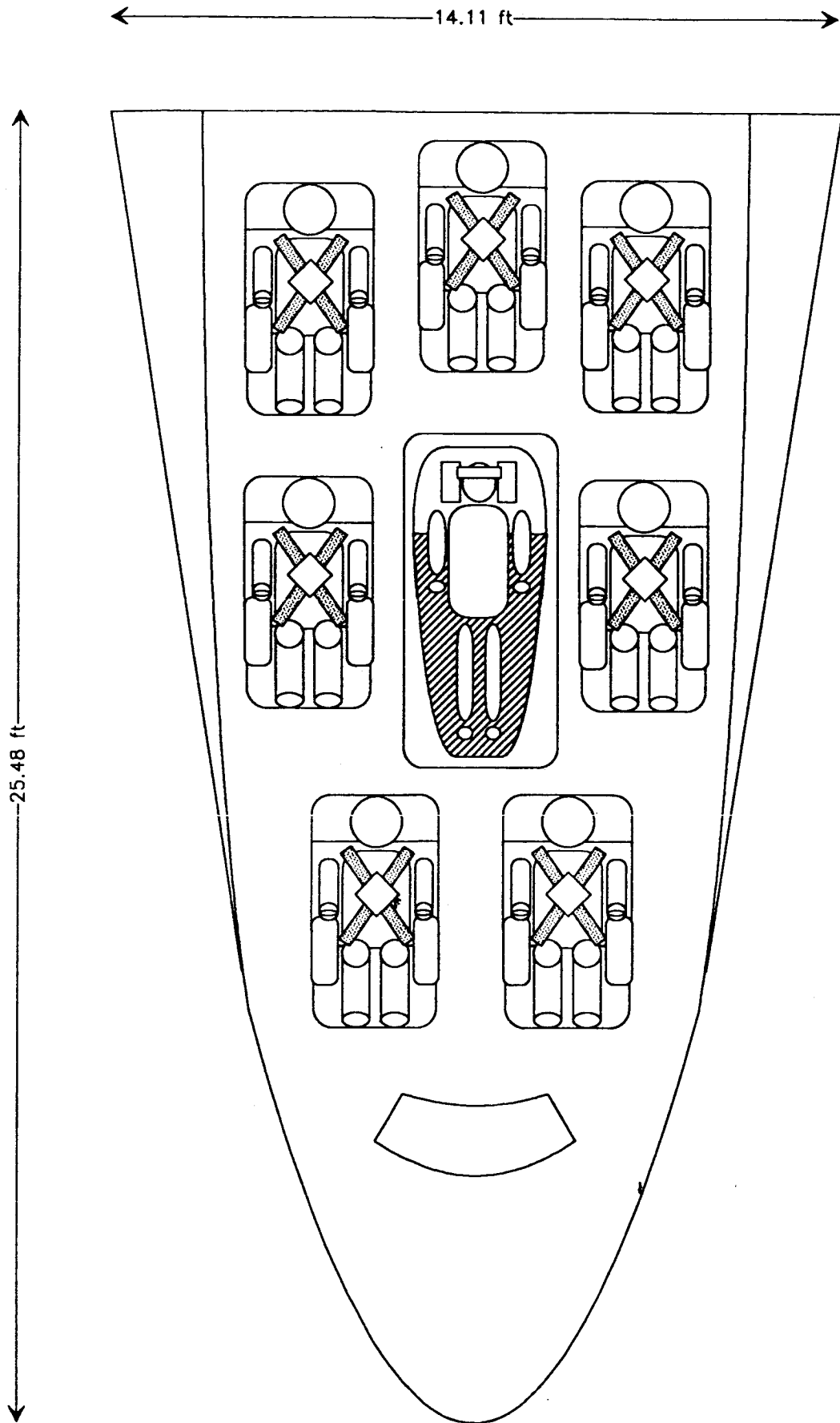
Figure 16: Lifting Body

40

APPENDIX II

DERIVATION OF EQUATION FOR SPRING-DAMPER SYSTEM

$F(t) = 15g u(t)$
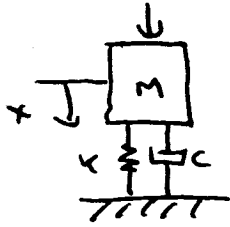
$x(t) = x_h(t) + x_p(t)$

$x_h(t) = e^{-\sigma t} [A \cos \omega_d t + B \sin \omega_d t]$

$x_p(t) = 15g \cdot m/k$

$$x(t) = e^{-\sigma t} [A \cos \omega_d t + B \sin \omega_d t] + \frac{15gm}{k} \qquad (1)$$

BOUNDARY CONDITIONS:

$$x(0) = 0 \qquad \dot{x}(0) = 7.62 \, m/s \, (25 \, ft/s) = V_i$$

APPLY BOUNDARY CONDITIONS TO (1)

$$x(0) = 0 = A + \frac{15gm}{k} \qquad \Rightarrow \qquad A = -\frac{15gm}{k}$$

$$\dot{x}(t) = -\sigma e^{-\sigma t} [A \cos \omega_d t + B \sin \omega_d t]$$
$$+ \omega_d e^{-\sigma t} [-A \sin \omega_d t + B \cos \omega_d t]$$

$$\dot{x}(0) = V_i = -\sigma A + \omega_d B$$

$$\Rightarrow B = \frac{V_i + \sigma A}{\omega_d}$$

$$x(t) = e^{-\sigma t} [A \cos \omega_d t + B \sin \omega_d t] + \frac{15gm}{k} \qquad (2)$$

WHERE

$$A = -\frac{15gm}{k} \qquad B = \frac{V_i + \sigma A}{\omega_d}$$

$$\sigma = \frac{c}{2m} \qquad \omega_d = \omega_n \sqrt{1 - \zeta^2} \qquad \omega_n = \sqrt{\frac{k}{m}} \qquad \zeta = \frac{c}{2\sqrt{km}}$$

$$= \omega_n \zeta$$

41

TAKE 2ND TIME DERIVATIVE OF (2) TO GET ACCELERATION

$$\dot{x}(t) = e^{-\sigma t}\left[-\sigma(A\cos\omega_d t + B\sin\omega_d t) + \omega_d(-A\sin\omega_d t + B\cos\omega_d t)\right]$$

$$\ddot{x}(t) = -\sigma e^{-\sigma t}\left[-\sigma(A\cos\omega_d t + B\sin\omega_d t) + \omega_d(-A\sin\omega_d t + B\cos\omega_d t)\right]$$

$$+ e^{-\sigma t}\left[-\sigma\omega_d(-A\sin\omega_d t + B\cos\omega_d t) + \omega_d^2(-A\cos\omega_d t - B\sin\omega_d t)\right]$$

$$= e^{-\sigma t}\left[\sigma^2(A\cos\omega_d t + B\sin\omega_d t) + \sigma\omega_d(A\sin\omega_d t - B\cos\omega_d t)\right]$$

$$+ e^{-\sigma t}\left[\sigma\omega_d(A\sin\omega_d t - B\cos\omega_d t) - \omega_d^2(A\cos\omega_d t + B\sin\omega_d t)\right]$$

$$\boxed{\ddot{x}(t) = e^{-\sigma t}\left[(\sigma^2 - \omega_d^2)(A\cos\omega_d t + B\sin\omega_d t) + 2\sigma\omega_d(A\sin\omega_d t - B\cos\omega_d t)\right]}$$

```
C*******************************************************************SHO*
C  THIS PROGRAM WILL FIND AN ENVELOPE OF VALUES OF K AND C FOR A SPRING *SHO
C  MASS-DAMPING SYSTEM FOR CERTAIN RESTRICTIONS. INITIAL ACCELERATION,  *SHO
C  IMPULSE AND DISPLACEMENT ARE CALCULATED AND COMPARED TO RESTRICTIONS *SHO
C  IF THESE VALUES FALL WITHIN THE RESTRICTIONS THEN THE VALUES OF K    *SHO
C  AND C ARE PUT INTO A DATA FILE                                       *SHO
C*******************************************************************SHO*
C                                                                    SHO
        REAL K,C,M,G,VI,SIG,WN,ZETA,WD,A,B,STEP                      SHO
        REAL FACT,ACC(1000),T                                       SHO
        INTEGER I,N,J,I,P                                           SHO
        CALL CMSF( FILEDEF 8 DISK ACCEL DATA A ,IERROR)             SHO
        CALL CMSF( FILEDEF 9 DISK TIME DATA A ,IERROR)              SHO
                                                                    SHO
C  SET VARIBLES                                                     SHO
                                                                    SHO
        N = 40                                                      SHO
        C = 100                                                     SHO
        M = 100                                                     SHO
        G = 9.81                                                    SHO
        VI = 7.62                                                   SHO
                                                                    SHO
C  LOOP EXECUTION  DETERMINATION OF INITIAL ACCELERATION ,IMPULSE AND SHO
C  DISPLACEMENT OF MASS FOR VARIOUS VALUES OF K AND C.              SHO
                                                                    SHO
        DO 70 L=1,80                                                SHO
          K = 10000                                                 SHO
          WRITE(6,*) C,K                                            SHO
          DO 80 J=1,N                                               SHO
            K = K + 500                                             SHO
            SIG = C/(2*M)                                           SHO
            WN = SQRT(K/M)                                          SHO
            ZETA = C/(2*SQRT(K*M))                                  SHO
            IF (ZETA .GT. 1.0) GOTO 80                              SHO
            WD = WN*SQRT(1-ZETA**2)                                 SHO
            A = -15.*G*M/K                                          SHO
            B = (VI+SIG*A)/WD                                       SHO
            T = 0.0                                                 SHO
            STEP = .001                                             SHO
                                                                    SHO
C  ACCELERATION DETERMINATION                                       SHO
                                                                    SHO
            DO 5 I=1,500                                            SHO
              T = T + STEP                                          SHO
              FACT1 = A*COS(WD*T)+B*SIN(WD*T)                       SHO
              FACT2 = A*SIN(WD*T)-B*COS(WD*T)                       SHO
              ACC(I)= EXP(-SIG*T)*((SIG**2-WD**2)*FACT1+(2*SIG*WD*FACT2) SHO
              IF (ACC(I) .LT. 0.0) THEN                             SHO
                  GO TO 80                                          SHO
              END IF                                                SHO
              IF (ACC(I) .LT. 0.0) GO TO 15                         SHO
            CONTINUE                                                SHO
                                                                    SHO
C  IMPULSE CALCULATION                                              SHO
```

ORIGINAL PAGE IS
OF POOR QUALITY

43

```fortran
        Z = (T/STEP)
        SUM = 0.0
        DO 10 P=1,Z
          AVE = ABS(F+ACC(P+1))/(2*9.81)
          AREA = AVE*STEP
          SUM = SUM + AREA
          WRITE(P,110) P,P*STEP,SUM
        CONTINUE

C   DISPLACEMENT CALCULATION

        T1 = STEP*Z
        X=EXP(-SIG*T1)*(A*COS(WD*T1)+B*SIN(WD*T1))-A
        CHECK = ACC(1)/9.81

C   CHECK FOR RESTRICTIONS

        IF (SUM .LT. 2.0 .AND. CHECK .LT. 10.0 .AND. CHECK .GT. 0.0
     -  .AND. X .LT. .5)THEN
          WRITE(8,120) C,K,CHECK,SUM,X
        END IF
      CONTINUE
      C = C + 25
      CONTINUE
110   FORMAT(' ',1X,F6.3,2X,F9.4)
110   FORMAT(' ',2X,I3,2X,F6.3,2X,F8.4)
120   FORMAT(' ',2X,F6.1,2X,F7.1,2X,F8.4,2X,F7.4,2X,F6.3)
      STOP
      END
```